RADIATION TRANSPORT IN SCALE INVARIANT OPTICAL MEDIA

BY

ANTHONY DAVIS

A thesis submitted to the Faculty of Graduate Studies and Research in partial fulfillment of the requirements for the degree of Doctor of Philosophy

Department of Physics
McGill University
Montréal, Canada
February 1992

ISBN 0-315-74934-2

À celles qui m'ont accompagné
sur le chemin de la solitude.

L'ÉTRANGER

« Qui aimes-tu le mieux, homme énigmatique, dis ?
ton père, ta mère, ta sœur ou ton frère ?
– Je n'ai ni père, ni mère, ni sœur, ni frère.
– Tes amis ?
– Vous vous servez là d'une parole dont le sens m'est resté jusqu'à ce jour inconnu.
– Ta patrie ?
– J'ignore sous quelle latitude elle est située.
– La beauté ?
– Je l'aimerais volontiers, déesse et immortelle.
– L'or ?
– Je le hais comme vous haïssez Dieu.
– Eh ! qu'aimes-tu donc, extraordinaire étranger ?
– J'aime les nuages... les nuages qui passent... là-bas... là-bas... les merveilleux nuages ! »

Charles Baudelaire,
tiré du SPLEEN DE PARIS
(Petits Poèmes en Prose, I)

ABSTRACT – *RÉSUMÉ*

RADIATION TRANSPORT IN SCALE INVARIANT OPTICAL MEDIA

We focus primarily on the bulk response to external illumination of conservatively scattering thick inhomogeneous media (or simply "clouds") which are exactly or statistically scale invariant; these radiative properties are compared to those of homogeneous media with the same shapes and masses. Also considered are the ensemble-average responses of multifractal distributions of optical thicknesses and the closely related spatially averaged responses obtained within the "independent pixel" approximation to inhomogeneous transfer. In all cases, the nonlinearity of the radiation/density field coupling induces systematic and specific variability effects. Generally speaking, the details of the scattering process and of the boundary shape affect only prefactors whereas "anomalous" scaling exponents are found for extreme forms of internal variability which, moreover, are different for different physical transport models (e.g., kinetic versus diffusion approaches). Finally, detailed numerical computations of radiation flows inside a log-normal multifractal illustrate the basic inhomogeneous transport mechanism of "channeling."

TRANSPORT DU RAYONNEMENT EN MILIEU OPTIQUE INVARIANT D'ÉCHELLE

On étudie principalement les réponses globales à l'illumination externe de milieux optiques hétérogènes épais qui sont exactement ou bien statistiquement invariants d'échelle; ces propriétés radiatives sont comparées à celles de milieux homogènes de même forme et masse. Aussi considère-t-on les réponses moyennes pour des distributions multifractales d'épaisseurs optiques, celles-ci sont étroitement liées aux réponses obtenues dans l'approximation au transport hétérogène par les "pixels indépendants." Dans tous les cas de figure, la nature non-linéaire du couplage entre les champs radiatifs et de densité induit des effets de variabilité systématiques et spécifiques. En général, les détails de la fonction de phase ou de la forme précise du milieu n'influencent que les préfacteurs alors que l'exposant caractéristique devient "anormal" pour les formes extrêmes d'hétérogénéité; il dépend alors également du choix de modèle physique du transport (e.g., méthodes cinétiques versus diffusives). Finalement, le mécanisme élémentaire de transport hétérogène ("channeling") est illustré par des calculs numériques détaillés du champ radiatif à l'intérieur d'un multifractal typique.

TABLE OF CONTENTS

Abstract – *Résumé* i
Table of Contents ii
List of Figures v
Prelude vi
Contributions to Original Scholarship xi
Manuscripts and Authorship xii
Acknowledgements – *Remerciements* xiii

Chapter Zero: INTRODUCTION 1
0.1. Theoretical and Observational Motivations 1
0.2. A Survey of the Literature from the Scaling Viewpoint, followed by our Main Results 6
0.3. A Detailed Overview of this Thesis 13
Notes and Bibliography for Chapter 0 19

Chapter One: TECHNICAL PRELIMINARIES, DEFINITIONS AND CONVENTIONS 25
1.0. Orientation Conventions 25
1.1. (Optical) "Medium," or (Cloud) "Model" 26
1.2. "Scale Invariant," or "Scaling" (both Simple- and Multiple-) 27
1.3. (Physical) Radiation "Transport Model," or "-Theory" 28
1.4. (Radiative) "Response," or "-Property," and its Scaling 32
1.5. (Cannon's Radiative) "Channeling" and/or (Stephens') "Mode-Coupling" 33
Notes and Bibliography for Chapter 1 37
Figures for Chapter 1 39

Chapter Two: THE BASIC RADIATIVE EFFECTS OF SPATIAL VARIABILITY, THE DIFFUSION PICTURE 40
2.1. On the Effect of Shape in Horizontally Extended Homogeneous Media (and an Interpretation in Terms of Internally Variable Media) 43
2.2. On the Effect of Shape in Horizontally Bounded Homogeneous Media (and the Irrelevance of Comparison with Plane-Parallel Media) 48
2.3. On the Effect of Internal Structure (and a Tentative Quantification of "Channeling") 56
Notes and Bibliography for Chapter 2 70

Chapter Three: DISCRETE ANGLE RADIATIVE TRANSFER, ELEMENTS AND CONNECTIONS 73
3.1. DA Phase Functions and Transfer Equations 74
3.2. The Simplest DA Systems: Orthogonal Beams 77

3.3. The Second Order Formulation for Orthogonal DA Systems, Their Relation to Diffusion 82

3.4. "Independent Pixels" and/or Scattering Media with Random Optical Thicknesses 87

3.5. DA Similarity Theories and the Singularity of the Diffusion Limits 91

Notes and Bibliography for Chapter 3 96

Chapter Four: THICK HOMOGENEOUS AND FRACTAL MEDIA, RADIATIVE SCALING PROPERTIES 100

4.1. Homogeneous Squares, Cubes and Beyond 101

4.2. Deterministic Monofractal Media (Sierpiński Gaskets) 105

4.3. The Transition from Normal to Anomalous Radiative Scaling 107

4.4. On the Mechanisms Involved in Anomalous Radiative Behaviour 114

Notes and Bibliography for Chapter 4 126

Figures for Chapter 4 130

Chapter Five: RADIATIVE PROPERTIES OF MULTIFRACTALS, AN ASYMPTOTIC ANALYSIS 135

5.1. Simple Scaling Properties of Direct Transmittance 136

5.2. Multiple Scaling Properties of Total 1-D Transmittance 140

5.3. Summary and Discussion of Multifractal Radiative Scaling Properties 141

5.4. Multifractal Independent Pixels, A Case Study 143

Notes and Bibliography for Chapter 5 147

Figures for Chapter 5 149

Chapter Six: RADIATIVE TRANSFER IN A MULTIFRACTAL, A NUMERICAL EXPERIMENT 150

6.0. The Structural Properties of the Optical Density Field 153

6.1. The Optical Parameters, Boundary Conditions and Independent Pixel Responses 157

6.2. Validation of the Numerics, Monte Carlo and Relaxation Compared 160

6.3. The Two-Dimensional Internal Radiation Vector Fields 162

6.4. The One-Dimensional Exiting Radiation Fields 166

6.5. The Spatially Unresolved Radiation Fields 169

Notes and Bibliography for Chapter 6 173

Figures for Chapter 6 177

Chapter Seven: CONCLUSIONS 194

7.1. Physical Discussion 194

7.2. Meteorological Implications 201

7.3. Future Directions 203

Notes and Bibliography for Chapter 7 206

Cadenza 208

APPENDICES 211

Appendix A: ELEMENTS OF CONTINUOUS ANGLE RADIATIVE TRANSFER THEORY 212

A.1. Radiative Transfer: A Formalism for Arbitrary Dimensionality 212

A.2. Non-Local and Non-Linear Aspects: Direct Transmittance and Photon Propagation 217

A.3. Local and Linear Aspects: Sources and Similarity Theory 221

A.4. Diffuse Reflection/Transmission Problem: Boundary Conditions and Overall Responses 228

Notes and Bibliography for Appendix A 236

Appendix B: TWO SIMPLE TECHNIQUES IN NUMERICAL TRANSFER, APPLICATIONS TO MULTIFRACTALS AND ORTHOGONAL BEAMS 241

B.1. Direct Monte Carlo Simulation 242

B.2. Finite Differencing Followed by Relaxation 246

Notes and Bibliography for Appendix B 252

Figures for Appendix B 254

Appendix C: SCALE INVARIANT MODELLING TOOLS IN TURBULENCE THEORY 255

C.1. Turbulent Cascade Processes, Power-Law Structure Functions and Spectra 256

C.2. Fractal Sets as Models for the "Support" of Turbulence 261

C.3. Multifractal Measures as Models for Turbulent Dissipation Fields 267

C.4. Multiple Scaling of the Statistical Moments and the Dual Codimension Function 274

C.5. Continuous Cascades and Universal Multifractals 282

C.6. Passive Scalar Advection by Homogeneous Turbulence 285

Notes and Bibliography for Appendix C 288

Appendix D: DIFFUSIVE TRANSPORT, THE RADIATION CONNECTION 292

D.0. Radiative Energy and Momentum Flux: Conservation Equations for Scattering Media 294

D.1. The Radiative Hydrodynamic Limit: Eddington's Approximation as a Closure in Direction Space 296

D.2. The "Diffusion Domain" of Real Clouds: Recent Observations by King, Radke and Hobbs 299

D.3. The Classical Similarity Relations: Their Interpretation in Terms of Correlated Random Walks 302

D.4. Diffusion in Homogeneous Media: The Standard Scaling Properties 305

D.5. The Power of Formal Analogy: Transposing Results to/from Another Field 309

D.6. Diffusive "Channeling" in Inhomogeneous Media: Examples of Normal and Anomalous Scaling 313

Notes and Bibliography for Appendix D 320

Appendix E: THE STATISTICAL APPROACH TO RADIATIVE TRANSFER 324

E.1. Phase Space Flows and Boltzmann's Equation 325

E.2. Linear Transport Theory 1, The Case of Neutrons 327

E.3. Linear Transport Theory 2, Generalization to Photons 329

Notes and Bibliography for Appendix E 331

LIST OF FIGURES

Fig. 1.1: Inter-connections of the various radiation transport theories used in this thesis.

Fig. 1.2: A schematic illustration of the two basic types of "channeling" event that can occur within the framework of diffusive (radiation) transport.

Fig. 4.1: CA transmittance and albedo for homogeneous squares with various g values.

Fig. 4.2a: Isotropic CA and DA transmittance and albedo for homogeneous squares.

Fig. 4.2b: Same Fig. 4.2a but for cubes, with the "C1" phase function added.

Fig. 4.3: Determination of the albedo exponent for squares.

Fig. 4.4a: Generation of a deterministic monofractal cloud model in d=2.

Fig. 4.4b: Deterministic monofractal used as prototypical medium permeated by holes of all sizes.

Fig. 4.5: Transmittance versus spatially averaged optical thickness for the horizontally periodic cloud with a $D = \log_2 3 \approx 1.585$, $d = 2$ elementary cell.

Fig. 4.6: Responses for the isolated fractal cloud.

Fig. 4.7: Plotting technique described in text for the determination of R_∞ and v_R.

Fig. 5.1: A special microcanonical cascade model for both density and optical thickness.

Fig. 5.2: A diagram of the (γ_1,γ_2) plane showing the three different regions that characterize the scaling of the optical thickness and direct transmission. The straight line corresponds to $c'(0)=c(0)=K_{Td}(1)=0$, and the curved line to $K(1)=0$.

Fig. 6.0: Generation of a random multifractal cascade field in d = 2 spatial dimensions.

Fig. 6.1: Linear grey-scale map of the orders of singularity for the adopted log-normal multifractal density field.

Fig. 6.2: Theoretical $c(\gamma)$ codimension function the cascade process illustrated in fig. 6.1.

Fig. 6.3a: Exceedance set for $\gamma = \gamma_1 = +C_1 = 0.5$.

Fig. 6.3b: Same as Fig. 6.3a but for $\gamma = \gamma_{1/2} = 0$.

Fig. 6.3c: Same as Fig. 6.3a but for $\gamma = \gamma_0 = -C_1 = -0.5$.

Fig. 6.4: (a) Column-averaged densities and corresponding orders of singularity, (b) "independent pixel" responses (direct and total transmittances) for the thinner cloud.

Fig. 6.5: (a) Same as Fig. 6.4a but for row-averages, (b) row-averaged internal fields of total radiance.

Fig. 6.6: DA radiance fields in eigen-vector decomposition for $\bar{\tau}$ = 12.2: (a) J, (b,b') $F_{y,z}$, and (c) X.

Fig. 6.7: Same as Figs. 6.6a,b,b',c but for $\bar{\tau}$ = 195.

Fig. 6.8: (a) Monte Carlo DA reflectance R(y) and transmittance T(y) fields and (b), (c) their respective power spectra, for $\bar{\tau}$ = 12.2.

Fig. 6.9: Same as Figs. 6.8a,b,c but for $\bar{\tau}$ = 195.

Fig. 6.10a: Relaxation DA reflectance R(y) and transmittance T(y) fields, for $\bar{\tau}$ = 12.2.

Fig. 6.10b: Apparent absorbance A(y) = 1 - [R(y)+T(y)] corresponding to Fig. 6.10a.

Fig. 6.11: Histograms of the singularities of R(y) for the five different values of $\bar{\tau}$.

Fig. 6.12: Overall transmittancies of the multifractal cloud for the five different optical thicknesses and three different methods of calculation.

Fig. 6.13: Order-of-scattering decompositions of the transmittance at $\bar{\tau}$ = 12.2.

Fig. 6.14: Order-of-scattering decompositions of the reflectance at $\bar{\tau}$ = 12.2.

Fig. B.1: Propagation in an inhomogeneous DA(2,4) Monte Carlo simulation.

Fig. B.2: Iteration in a simple DA(2,4) finite difference scheme.

PRELUDE

"[...] the greatest sculptures can be viewed—indeed, should be viewed—from all distances since new aspects of beauty will be revealed in every scale."
Henry Moore's answer to S. Chandrasekhar's question as to 'how should one view sculptures: from afar or nearby?'

My first encounter with radiative transfer happened, as a matter of course, during my astronomically oriented M.Sc. at U. of Montreal, in '77-'79. It was a little bit like a love-at-first-sight and I somehow incorporated its non-equilibrium features into my life-style: I subsequently took a (seemingly) random walk through (mainly) teaching-related jobs through the early '80s. At mid-decade, my professional life was becoming a little fuzzy, at least that much was clear about it! By then I was then easily convinced that I should geophysically "recycle" my astrophysical experience.[1] This appealed to my environmentally friendly political ideas and lead me (almost) straight to the Ph.D. program at McGill. Over five academic years, spanning '86 to '91, I was involved in research into atmospheric scattering but, under numerous influences, the focus of my research project considerably shifted after the first two of those years. It started off with a compulsive investigation of all the angular details on radiances emerging from completely homogeneous models of thin (hazy) atmospheres,[2] possibly overlaying ground with a discontinuity in albedo at a specific scale;[3,4] this work was specifically targeting direct applications to the remote sensing of air quality, and a qualified success was achieved.[5] It ended with an extremely crude treatment of fluxes[6] only inside very

---

[1] This is by no means uncommon and I'm beginning to view certain (radiation-related) aspects of geophysics as "applied" astrophysics, or maybe astrophysics as a school for atmospheric radiation scientists. At the '92 spring meeting of AGU (in Montreal), I happened on three ex-comrades-in-arms from the struggle for survival in (pure) astrophysics, lost for a decade! It was as pleasurable as unexpected. Counting myself, there were three early drop-outs from the Ph.D. program in (astro)physics at U. of Montreal, all of which are now somehow involved in atmospheric radiation. Interestingly, we work in three quite distinct "spheres:" M.C. now studies aurora borealis in the ionosphere, D.T. monitors stratospheric ozone depletion, and A.D. is involved with tropospheric (turbulence dominated) cloud systems; J.-P. A. actually pursued his astrophysical career but is now considering a move.

[2] Royer, A., N. O'Niell, A. B. Davis and L. Hubert, "Comparison of Radiative Transfer Models used to Determine Atmospheric Parameters from Space," *S.P.I.E. Proceedings*, 928, 118–135, 1988.

[3] Davis, A. B., and A. Royer, "Effet de l'environnement dû à la diffusion atmosphérique sur une cible de petites dimensions," *Proceedings of the 11th. Canadian Remote Sensing Symposium*, Canadian Aeronautics and Space Institute, June 22–25, Waterloo (Ont.), Canada, 1988.

[4] Royer, A., A. B. Davis, and N. O'Niell, "Analyse des Effets Atmosphériques dans les Images HRV de SPOT," *Canadian Journal of Remote Sensing*, 14, 80–91, 1989.

[5] O'Niell, N., A. Royer, L. Hubert, J. R. Miller, J. Freemantle, G. L. Austin and A. B. Davis, *Critical Evaluation of Atmospheric Pollutant Parameterization from Satellite Imagery*, Report for the Ontario Ministry of Environment, Toronto (Ont.), Project #349-G, April 1989.

inhomogeneous models of thick (cloudy) atmospheres, (implicitly) overlaying absorbing ground; this work lead to very strong conclusions on the theoretical aspects but with only potential applications to satellite imagery interpretation at present (and, on the longer run, to the improvement of radiation treatment in climate prediction). In short, a complete turnabout in topic, methodology, etc. The overall trend being a constant move towards the most basic physical principles (i.e., theory)—but it is now timely to reverse that trend. No attempt has been made in this thesis to reunify the two phases of the project as described in the above. Is there any point? We already know that the number of "interesting" problems in atmospheric radiation is infinite and, clearly, both of the above topics belong to the more restricted class of (currently) "important" problems. At any rate, the experience is gained, the publications are there to bear witness to this and I fully acknowledge the (moral and financial) support from my previous supervisors/collaborators at CARTEL (Université de Sherbrooke).

I will therefore concentrate only on the work carried out during calendar years '88 to (circa) '91.5. Interestingly, and in spite of the obviously desirable restriction in focus, the present thesis suffered much the same fate as the research project itself: a complete turnabout. The opening remarks of the first draft—a naive attempt to expose both radiative transfer and multifractals on their common ground (viz., probability measures in phase space)—eventually evolved into the last appendix of the final version! Apart from the articles on which a majority of chapters are based, the writing exercise took a half year full time, starting with a skeleton made of this (published) and other (unpublished) material. Major cuts were made, yet there remains a certain amount of partial overlapping and, in a couple of instances, outright redundancy (going from certain portions of the appendices to some parts of the chapters). The final structure was adopted relatively late on, and the intricate internal cross-referencing was carefully monitored, yet some minor errors may have survived; there is little doubt that the whole volume would gain in coherence from a complete overhauling. However, in the meantime, I have come to subscribe entirely to an aphorism (found in a margin note) of Shaun Lovejoy's, my thesis advisor (and mentor-in-all-things-multifractal), '[...] research is an ongoing process which still hasn't achieved the status of solid "knowledge." [...]' which I understand as 'imperfection is our lot (and in fact this keeps us going).' Consequently, it would be borderline dishonest to rewrite the thesis in text-book style. It must be said that Shaun's proofreading of all the major sections of this thesis, all of his suggestions and all of the subsequent discussions proved extremely valuable in every respect.

---

[6] We will see (sect. 3.1) that DA "radiances" are akin to (hemispherical) fluxes and, at any rate, use the same physical units.

A comment on the final structure and adopted style is in order. There has been a deliberate effort to make the thesis as self-contained as possible.[1] This was perceived as particularly important because potential readers can be attracted either from the statistical physics and/or multifractal community with little or no knowledge of radiation transport (especially in the atmospheric context) ... or vice-versa. Indeed, very little cross-fertilization has happened as yet. The net result of this choice is that a large amount of background material to be reviewed accumulated, and this was finally compiled into the various appendices (which collectively rival the main part of the thesis, chap. 2–6, in terms of sheer volume). For guidance, the following flow-chart illustrates the connections between the various chapters and appendices.

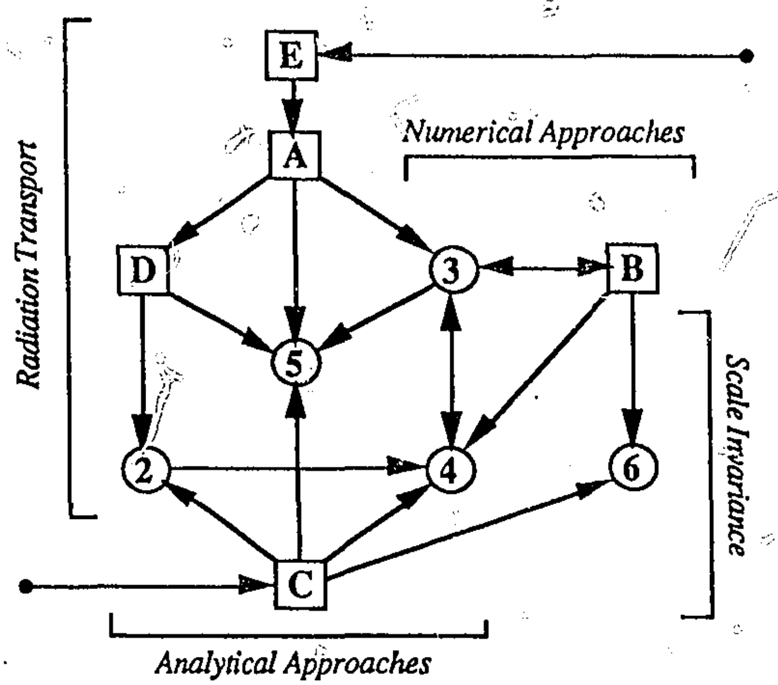

Flow chart illustration of the inter-dependencies amongst the various parts of this thesis. Notice the two "entry points:" respectively, kinetic theory (i.e., molecular chaos and additive processes) by above and multifractals (i.e., multiplicative chaos and turbulent hydrodynamical processes) by below. Interestingly, these "points" are in fact conceptually much closer than they seem since both formalisms rely heavily on probability and measure theory applied to phase spaces. The key is

- A: CA transfer (general theory)
- B: CA and DA transfer (computational aspects)
- C: Fractals and multifractals in turbulence
- D: Diffusion (general theory)
- E: CA transfer (kinetic theory foundations)
- 2: Diffusion (basic inhomogeneity effects)
- 3: DA transfer and IPs (general theory)
- 4: Universal radiative scaling, trivial and anomalous
- 5: Multifractal direct, plane-parallel or IP transmittancies
- 6: Numerical DA transfer through a typical multifractal

[1] To some extent, this is true also of each individual chapter. In many cases, "Introductory Notes" are provided and most of the abbreviations are redefined locally when needed. The better kown abbreviations (r/l.h.s., w.r.t., m.f.p., p.d.f., etc.) are however nowhere speeled out.

A generic equation identification/reference would read "(c.n)" where "c" is the chapter number and "n" the equation's order of occurence in the chapter (sometimes 's and/or letters are appended) whereas reference to the contents of sub-section "p" of sect. "s" of chap. "c" reads "§c.s.p" (no further sub-divisions are used). Furthermore, footnotes are collected at the end of each chapter which makes them less disruptive to the reading. In my opinion, this is the best place for them since they are used to convey information deemed "non-vital" to the problem at hand. This information can range from the odd note of historical interest to a clarification, from extra evidence for some result (even a short proof) to an application of a result. Finally, a specialized bibliography is provided for each chapter, some repetitions will therefore be noticed.

The thesis will be overviewed in the course of the Introduction, so (after our stance on redundancy) we shall not repeat the process here; we point out only that, to use a double musical metaphor, it goes *crescendo* and makes use of a *leit-motiv*. By this we wish to express the fact that it starts, in chap. 2, with rather weak (*pp*) disorder where diffusion is a valid model for radiation transport (with one counter-example at the very end, viz., singular percolating binary mixtures). Chap. 3 is an "interlude," no particular inhomogeneous cloud model is studied since a general purpose transport model takes center stage, namely, discrete angle transfer which is presented as the basic tool we need to cope with the upcoming extreme forms of variability. Sect. 4.1 elaborates on the "theme" of homogeneous horizontally bounded media but, all of a sudden (*sf*), a very intermittent but deterministic monofractal model is introduced in sect. 4.2. Sect. 4.3–4 "recapitulate" the material and an explanation of anomalous scaling from first principles is proposed. This concludes the first "movement." In the second, chap. 5 and 6, the focus is on random multifractals, using respectively analytical and numerical (solo) "instruments." The variability "volume" can hardly be pumped up beyond the level attained in chap. 6 with the introduction of the (*fff*) multifractal model with Gaussian generators. Indeed, it is classified by Schertzer and Lovejoy [*Physica A*, in press] as the 'wildest' and 'hardest' of all (universal multifractals). And the reassuring thing about it all is that we can still recognize the "light-motif" introduced from the outset, namely radiative "channeling." Of course, the symphony is patently unfinished. This is of course not a fatal flaw in itself—famous precedents exist—but many quacks will doubtless be heard as the "measures" go by and the "scales" unfold, until the final, harmonically unresolved chord is struck.

The opening quote was borrowed from Chandrasekhar's *Truth and Beauty - Aesthetics and Motivations in Science* [U. of Chicago Press, 1987]. It was originally intended as a juxtaposition of a symbol of radiative transfer (Chandrasekhar's query) and one of scale invariant stuctures (Moore on sculpture). However, the way I read it now is that interesting sculpture is not scale invariant (at least in a trivial way) ... and this contrasts markedly with our opinion of cloud models, especially from the point of view of radiation. Understandably, the encounter of the famous physicist and sculptor happened at the inauguration of the latter's work that marks the site of the first controled fusion experiment , in front of the Enrico Fermi Institute on the U. of Chicago campus. In this remarkable piece of art—at once heavy and buoyant, threatening and attractive—Moore used a relatively dark material (bronze) to define not so much an outer shape but empty internal spaces, cavities through which bright skylight would shine; adults invariably see skulls and/or atomic mushrooms in this abstract creation but the artist envisaged children playing with/in it [I owe all of this to Prof. Chandrasekhar himself]. I cannot imagine a more true and beautiful metaphor for clouds in general and our fractal models in particular: at once massive and transparent, unconventional yet necessary.

A.D.
Montreal,
14th of February (revised 10th of May) 1992.

CONTRIBUTIONS TO ORIGINAL SCHOLARSHIP

This thesis is made up of a main part (ch. 2–6) followed by an extensive appendix section; on p. viii, there is a tentative graphical display of the next level of internal structure. This way of organizing it makes the separation of the original—but not necessarily highly original—contributions from the prerequisite, background and otherwise ancillary—but not necessarily readily avaivable—material relatively easy. There are only a few exceptions worth mentioning.

On the one hand, the non-original parts of the main section are as follows. Firstly, and most importantly, Shaun Lovejoy must receive full credit for the basic radiative scaling ansatz expressed in eq. (0.1). In sect. 2.1 and §2.3.4, previously existing transport results have been quoted and then simply adapted to the radiation problem; the important result in §§2.3.1–2 on transmittance being boosted by any form of inhomogeneity was more-or-less known but not readily explained in terms of "channeling." The contents of §3.2.1 and §3.3.1 on the basic formulation of "DA(d,2d)" transfer basically reproduce (and, to some extent, were even "lifted" from) previous collaborative work by S.L. and Philip Gabriel (PhD, McGill '88). In the other parts of chap. 3 related to their work on DA fundamentals, there has been at the very least substantial clarification. Finally, P.G.'s continuous angle Monte Carlo results for homogeneous cubes are used in fig. 4.2b.

On the other hand, some CA work that is original (to the best of our knowledge) has been embedded in the appendices because of the logical connections. More precisely, §A.2.3 on the nonlinearly induced necessity of non-exponential average propagation kernels in the kinetic theory of random media and their relation to characteristic functionals, §A.3.3 on the transfer (or any other so-called "linear transport") equation as an "x-gradient/u-anisotropy" balance with a role for $\rho(\mathbf{x})$, and §A.4.2–3 where the various definitions of (overall) albedo are clearly spelled out for horizontally bounded media and the issue of "terminator pathology" is risen (in connection with the reexamination of our previous results on homogeneous squares and cubes). On a more technical note, a new two-dimensional "Henyey/Greenstein-like" model phase function is described in eqs. (A.21b) and (B.5) while, in sect. B.2, we address the "thick cell" problem that arises in all numerical techniques based on finite differencing when applied to extremely variable media. Finally, sections D.2–3 are also new; they respectively comment extensively on King, Radke and Hobbs' [*J. Atmos. Sci.*, 47, 894–907, 1990] recent *in situ* cloud radiance observations, on the one hand, and provide an interpretation of the standard "transport" m.f.p. rescaling in terms of correlated random walks in space that map onto uncorrelated ones on the unit sphere, on the other hand.

MANUSCRIPTS AND AUTHORSHIP†

The faculty of Graduate Studies and Research of McGill University requires that the following text from the Guidelines concerning thesis preparation be cited in full in the introductory sections of any thesis to which it applies.

The candidate has the option, subject to the approval of the Department, of including as part of the thesis the text, or duplicated published text (see below), of an original paper, or papers. In this case the thesis must still conform to all other requirements explained in Guidelines Concerning Thesis Preparation. Additional material (procedural and design data as well as description of equipment) must be provided in sufficient detail (e.g. in appendices) to allow a clear and precise judgement to be made of the importance and originality of the research reported. The thesis should be more than a mere collection of manuscripts published or to be published. It must include a general abstract, a full introduction and literature review and a final overall conclusion. Connecting texts which provide logical bridges between different manuscripts are usually desirable in the interests of cohesion.

It is acceptable for theses to include as chapters authentic copies of papers already published, provided these are duplicated clearly on regulation thesis stationery and bound as an integral part of the thesis. Photographs or other materials which do not duplicate well must be included in their original form. In such instances, connecting texts are mandatory and supplementary explanatory material is almost always necessary.

The inclusion of manuscripts co-authored by the candidate and others is acceptable but the candidate is required to make an explicit statement on who contributed to such work and to what extent, and supervisors must attest to the accuracy of the claims, e.g. before the Oral Committee. Since the task of the Examiners is made more difficult in these cases, it is in the candidate's interest to make the responsibilities of authors perfectly clear. Candidates following this option must inform the Department before it submits the thesis for review.

---

†A footnote referenced in the same way as this one will be placed at the beginning of chapters 2 through 6. It quotes the related publications and roughly describes the responsibility of this author w.r.t. his co-authors within the project related to the topic of that chapter, viewed as a separate entity.

ACKNOWLEDGMENTS – *REMERCIEMENTS*

Above all, I thank Shaun Lovejoy, my main supervisor at McGill University's Physics Department, for the always illuminating guidance and the continual support, especially during the periods of interpersonal and fortunately intermittent turbulence that we were unable to circumnavigate. But I don't think that I ever expected this to be easy either, to paraphrase* R.-M. Rilke, 'only difficult things are really worth doing.' In fact, had the ride through fractal territory been smooth, I probably would have been disappointed, confused to say the least. *Je tiens également à remercier chaleureusement Daniel Schertzer, responsable du (défunt) TURB/CRMD à la Météorologie Nationale à Paris, car sa collaboration lui fût extrêmement précieuse, sinon étroite, tout au long du projet. Et je regrette très sincèrement que certains de ces épisodes "turbulents" ont coincidés avec des problèmes de "transfert" qui n'ont absolument rien de radiatif.*

Over the past decade, Shaun and Daniel have relentlessly promoted fractals and multifractals as a pertinent modelling tool in almost every aspect of atmospheric structure and evolution; they have advocated all forms scale invariance in a field where the notion of characteristic scale has been used for centuries. Only a modern day Cervantes could properly describe their crusade. Their perceptiveness of where the real problems are, their stunningly creative use of simple fractal concepts, their struggle for formalistic coherence, have been a source of inspiration to me and will continue to be for a long time to come. No number of words can ever express how much I have learned from/with them; this thesis as a whole (≈100,000 words) can be viewed as a very modest attempt at this exercise.

I also wish to thank Geoff Austin who was not only instrumental in my admission into the PhD program at McGill but who counselled me in subtle ways throughout the project. I hope I have not failed him in my attempts to "build bridges" between the somewhat abstract theory of multiple scattering in inhomogeneous optical media and the numerical simulations of radiative transfer that we have conducted in scale invariant cloud models, on the one hand, and the observed (or at least observable) radiative properties of real world clouds, on the other hand. *Je tiens à remercier tout particulièrement Alain Royer et Norman O'Niell, tous deux du Centre d'Application et de Recherche en Télédétection (CARTEL) de l'Université de Sherbrooke, pour m'avoir donné l'occasion de travailler dans le domaine de la télédétection de l'environnement (atmosphère incluse); cette expérience m'a sensibilisé au fait qu'en prenant l'astronomie à l'envers—on observe la planète Terre depuis l'espace—elle devient non*

*Letter #7 in Rainer-Maria Rilke, *Briefe an einem jungen Dichter*, Insel, Leipzig, 1929. (Traduction française par B. Grasset et R. Biemel, *Lettres à un Jeune Poète*, Bernard Grasset, Paris, 1937.) Rilke gives examples of some of the "difficult" things that poets "do:" solitude, death, and love. He also defines "difficulty" by its converse, which is to adopt easy (conventional) solutions (attitudes) in the face of adversity.

seulement agréable mais utile. En plus de m'avoir encouragé à entreprendre ce programme de doctorat, ils m'ont proposé un sujet aussi intéressant que difficile sur les aérosols, en relation avec la pollution atmosphérique. Mais les nuages se sont en quelque sorte imposés d'eux-mêmes du simple fait que leur "signal" domine complètement la rétro-diffusion atmosphérique et que, par exemple, l'effet climatologique des aérosols est de loin inférieur à la seule incertitude que nous avons sur celui des nuages (sauf peut-être dans quelques contrées désertiques). Aussi, au cours de cette phase du projet, les échanges que j'ai eu avec L. Charbonneau, J. Freemantle, L. Hubert, et P. Teillet ont été d'un très grand intérêt.

I must acknowledge my direct (i.e., "radiatively involved") collaborators Philip Gabriel (now at CIRA, Colorado State University at Fort Collins), Brian Watson (now back at St. Lawrence University, from his sabbatical at McGill), Régis Borde (during his DEA, plus *service militaire*, in Paris). It was very stimulating to work with every one of them. From the outset, I was hesitant between the Meteorology and Physics Departments at McGill and, to this day, I feel strong connections with both. When focussing on the former, I remember many a fruitful discussion with R. Davies, H. Leighton, T. Warn and P. Yau while several conversations with I. Graham and M. Grant, that turned out to be quite important for me, happened in the latter ... where I finally made my academic nest. It was been a pleasure to progress along side with the likes of Ch. Hooge, Ch. Lardner, D. Lavallée, S. Pecknold, K. Pflug, A. Saucier, P. Silas and Y. Tessier, whether on the highest floor or in the foundations of the Rutherford Physics Building—in a sense, the perfect place to study scattering kernels[1] in a situation where empty space dominates the picture. *Durant mon séjour à Paris en 1990, j'ai apprécié l'interaction plus ou moins formelle que j'ai eu avec J.-F. Geleyn, R. Devaux et P. Gauthier ainsi qu'avec les participants des rencontres plus ou moins mensuelles du "GVaNG," mais plus particulièrement G. Sèze, M. Desbois et L. Smith. Je garderai toujours avec moi le souvenir de la plaisante compagnie de François-"Faf"-Schmitt, Patrick Brenier, ainsi que des étonnants frères Gadjandra et Ravi. Et que dire du café quotidien, systématiquement assaisonné d'une dose quotidienne de discussion politique sous les auspices de Philippe Ladoy (de la "CLIM"), sinon que ce rituel m'a cruellement manqué tout au long de 1991.*

En 1990, j'ai également eu l'occasion de visiter les principales institutions françaises engagées dans la recherche sur le rayonnement atmosphérique et je remercie les organisateurs et/ou les personnes présentes aux discussions qui se sont avérées extrêmement enrichissantes pour moi: J.-Cl. Buriez, M. Herman, Y. Fouquart, J. Lenoble, B. Bonnel, G. Brogniez, D.

[1] "Kern" is (also) "nucleus" in german.

Crétel et F. Parol du LOA (Lille). Et je n'oublie aucunement D. Tanré dont les travaux sur "l'effet d'environnement"—où les flux horizontaux jouent un rôle fondamental—m'a servi avant même le début du doctorat; c'est juste que, malheureusement, nous nous sommes manqués et à Lille et à la NASA (mais entre-aperçus à San Fransisco) en '91. Dans la même veine, je veux exprimer ma reconnaissance à J.-F. Royer et J.-L. Bringuier du CNRM (Toulouse), ainsi que M. Menguzzi du CERFACS (Toulouse, également) qui m'a fait valoir simplement et sans complexes les mérites du super-calcul. During the final stages of this project (1991-92), I had the opportunity to make some very stimulating visits and I want to thank all the people who made them happen and become the encouraging events I now remember: W. Wiscombe, R. Cahalan, A. Marshak, W. Ridgway, and S.-C. Tsay of NASA (Goddard Space Flight Center); D. Steenbergen and H. Barker of AES (at Downsview), as well as L. Garand (at Dorval) and J.-P. Blanchet (now at UQAM); R. Pierrehumbert and H. Yang at U. of Chicago (Dept. of Geophysical Sc.) and, in this last connection, I greatly appreciated Stephanella's natural organizational talents. I thoroughly enjoyed my '92 midwest "tour" and the stops in Iowa City and Milwaukee are thanks to W. Krajewski and A. Tsonis, respectively.

Turning to the technical asssistance that I recieved, I must first mention the extremely generous portions of Cray 2 time that where put at my disposal by Météo-France, of this I am extremely grateful; the support by the personel at the C^2VR was greatly appreciated in several instances. At McGill, the "super-users" of the Sun/Iris workstation network, "Loki" Jorgensen, Mario "Eru" Lacasse and François Bégin, were always extremely helpful when the level of frustration became intolerable—and I confess that my threshold is quite low! *Je suis aussi très reconnaissant à Fred Francis pour l'aide avec les (maudites) bandes magnétiques.*

I recieved financial support in several forms, starting with a three year doctoral scholarship from *FCAR* (*comité "Sciences de l'Environnement"*) which was complemented by a *CARTEL* scholarship. I has also granted a one year PhD scholarship from AES (via NSERC); this support was renewed for another half year in 1991—special thanks to Guy Fenech in this respect. I am deeply grateful to all of these institutions. I also especially acknowledge the *DMN/EERM* at *Météo-France* for the opportunity to be a *Collaborateur Scientifique* at the *CRMD* (Paris) during most of 1990. Finally, I was appointed by Prof. Lovejoy as a research assistant for several months.

Clearly I never would have found the energy to fulfill this project were it not for the comforting presence of my family and friends—old and new—at times of discouragment and I will be so glad to share times of achievement in such very special company. *Un très gros merci à Nelly et à Daniel pour leur chaleureux accueil à Paris et à Georges-Henri, simplement d'être là au bon endroit et au bon moment (à savoir, ici et maintenant).* Last but far from least, I want to express (in my usual clumsy way) the deep gratitude I feel towards the women with whom I shared, over the past five or so years, moments of ecstatic joy and others of intense pain. *Que ce soit de près ou de loin—et le plus souvent, c'était les deux à la fois, sur des plans différents—, dans l'aventure du quotidien ou dans l'aventure sans lendemain, vos générosités sont si manifestes et ma soif si grande. C'est avec un sentiment de tendresse que je vous dédie ce travail avant de céder de nouveau la plume au poète "écorché vif" ... toujours en prose mais cette fois en bien meilleure forme (psychique s'entend, et pour des raisons évidentes).*

LA SOUPE ET LES NUAGES

Ma petite folle bien-aimée me donnait à dîner, et par la fenêtre ouverte de la salle à manger je contemplais les mouvantes architectures que Dieu fait avec les vapeurs, les merveilleuses constructions de l'impalpable. Et je me disais, à travers ma contemplation : « – Toutes ces fantasmagories sont presque aussi belles que les yeux de ma bien-aimée, la petite folle aux yeux verts. »

Et tout à coup je reçus un violent coup de poing dans le dos, et j'entendis une voix rauque et charmante, une voix hystérique et comme enrouée par l'eau-de-vie, la voix de ma chère petite bien-aimée, qui disait : « – Allez-vous bientôt manger votre soupe, s... b... de marchand de nuages ? »

Charles Baudelaire,
tiré du SPLEEN DE PARIS
(Petits Poèmes en Prose, XLIV)

Chapter Zero

INTRODUCTION

0.1. Theoretical and Observational Motivations

0.1.1. Repatriation of Radiative Transfer (Back Into the Realm of Theoretical Physics)

This thesis is concerned with the transport of radiation through inhomogeneous distributions of scattering material that are invariant under scale changing operations. Rewording this with our prime application in mind, we can say that this thesis is about what happens to sunlight when it encounters a cloud (deck), in terms of reflection, transmission, and (in some cases) absorption. We will be looking at clouds as members of families of objects that can be transformed into one another using zooms, i.e., we will model them with simple geometrical shapes and homogeneous (that is, no) internal structure, as well as their far more interesting and realistic fractal and multifractal counterparts. We will seek characterizations of the radiative properties of these "scaling" families of optical media as a whole; in short, we are interested in the exponents related to the radiation transport. This focus on the scaling exponents for the radiative properties of the cloud families allows us to separate radiatively "important" and "unimportant" factors: an "important" factor must be able to affect an exponent. In this respect, we follow the tradition established in the study of nonlinear dynamical systems where the preferred terms are "relevant" and "irrelevant," also used in statistical physics.

Before proceeding to the scale invariant media, we must clarify what we mean by radiation "transport" and "scattering." At the most rigorous level, these concepts should be approached using classical or quantum EM theory and we have indeed learned (in our standard curriculum) that any inhomogeneity in density (hence permeability) scatters waves into all directions, usually in a relatively complicated pattern (cf. Mie theory for plane waves impinging on spheres). In this wave-theoretical framework, multiple scattering theory is extremely difficult, even for scalar waves. Spurred in part by the technologically (even tactically) important problem of propagation of EM waves through turbulence, steady progress has been made, usually at the expense of some approximation such as small scattering angles. This is of course an ongoing and fascinating area of research[1] but, from our point of view, it applies only to the very fine structure of the "direct" beam, as induced by coherence effects.[2] Fortunately, there are many circumstances where the effects of coherence can be disregarded: we simply add scattered energy fluxes as soon as a large number of randomly distributed discrete scattering centers is considered. However, this is reasonable only if the typical distances between these entities are large w.r.t. their typical size and w.r.t. the wavelength of interest, otherwise characteristically wave-like localization phenomena will occur. Again fortunately, there is an *ad hoc* theoretical framework for the description of radiation transport in this intermediate density regime where the wave-like behaviour is not of interest as such; it is of importance only to compute the given scattering and/or absorption cross-sections. This theory is known as "radiative transfer" and it uses macroscopically defined fields that model the fluxes of radiant energy propagating in geometrically defined beams into the various directions.

The connection between radiative transfer and mainstream optics is still unclear; in §1.3.1 (and more so in app. E), we briefly describe the major problems and refer to the relatively small literature on the subject. In sharp contrast to this conceptually uncomfortable situation, radiative transfer is formally identical to neutron transport theory as modelled by a Boltzmann equation with a linear collision kernel (rather than a diffusion equation): the word "neutron" can be replaced loosely[3] by "photon," see app. E for further details (including a mapping of transfer concepts onto those of Markov chain theory). Following a very large community of researchers, we will adopt radiative transfer as our highest level of physical theory for the matter-radiation interaction that we intend to investigate. Curiously, relatively few members of this large community would define themselves as "pure" physicists, more likely as astrophysicists (either observationally or theoretically inclined), as geophysicists (e.g., specializing in remote sensing, meteorology or climate), as engineers or as applied physicists (most probably working on neutron and/or plasma devices) and, in a few cases, as applied mathematicians (usually working with one of the above). Apart from the uncertain position of radiative transfer in the overall structure of theoretical physics, there are many reasons why the physics community *per se* has shown little interest in the subject.

First of all, we must recognize that Chandrasekhar [1950] carried radiative transfer theory to a very high degree of perfection. However, his results apply only to highly symmetrical systems, usually made of homogeneous plane-parallel scattering media. This brings us to the point where we must make a realistic (and sobering) assessment of the status of the theory of inhomogeneous radiative transfer. (Notice that in the above—and throughout this thesis—we do not take "radiative transfer" to be synonymous with "radiation transport," as used in the title; see sect. 1.3 below for the technical distinction.) The most general problem of inhomogeneous radiative transfer through arbitrarily shaped, arbitrarily structured optical media, with arbitrarily complicated phase functions (i.e., differential scattering cross-sections), and arbitrarily distributed sources seems to be fundamentally intractable, analytically speaking. Several general numerical approaches have been developed [e.g.,[4] Cannon, 1970; Stephens, 1986] that go beyond straightforward Monte Carlo simulation which, in turn, can always be used as a calibration[5] tool; however, there will always be practical (CPU time and RAM capacity) limitations in numerical work. This is a rather frustrating state of affairs, given the fundamental importance of radiative (and/or neutron) transfer to our understanding of the structure and evolution of macroscopic systems ranging in size from laser-fused droplets of heavy water to the Universe as a whole with, in between, Tokamaks, A- and H-bombs, single clouds, planetary atmospheres, stars and interstellar clouds, to mention but a few applications. Indeed, radiation—all frequencies combined—is often an active component in the dynamics of these natural or man-made systems. Moreover, radiation is an extremely useful diagnostic tool—virtually the only one available in astronomy—for extracting, without interference, information on the state of the system. However, in order to convert such remotely sensed data into physically meaningful information, we need to know (or, more likely, make an assumption on) the structure of the system viewed as an optical medium. And the real world is obviously made of very inhomogeneous material structures that create, destroy, or simply scatter radiation.

The above situation basically explains why radiative transfer has become more of an engineer's than a physicist's topic: the practical applications are pressing (in particular, coming from the civilian and military nuclear industries) and the kind of breakthroughs (insights) that the pure scientist thrives on are few and far between. Even in the applications to both meteorological and astrophysical problems, radiative transfer plays a central role yet it has become a sub-topic that the dedicated dynamicist has little time to cope with. We believe this situation can be remedied by applying three complementary measures:

1- The general radiative transport problem does not have to be posed in terms that attempt to make it as close as possible to reality (i.e., there is no absolute necessity to work in three spatial dimensions with complicated scattering kernels). This is especially true if we want to learn (understand in depth) something about the inhomogeneity aspects of the problem, if only because we will soon be confronted with our analytical or numerical limitations anyway.

2- Our attitude w.r.t. the kind of inhomogeneity to be studied need not be one of compulsively trying to accommodate the most general case (at least, right away) because, again in a learning process, a few well chosen but specific examples are often enough to anticipate the general principles, to provide guidelines for future research at the very least.

3- Possibly most importantly, we need to take an objective way of deciding (in fact, learning) what is physically important and what is not. This is a necessary step if we want to rethink the basic theory, elaborate alternative models of radiation-matter interaction that target the most important radiative features of the most relevant types of media. In turn, such alternative, more focused theory should lead to improved tools for dynamical modelling as well as for diagnostic applications.

Accordingly, we will (1) systematically seek ways of simplifying the general radiation transport problem, (2) systematically collect examples that are representative of broad categories of media, and (3) systematically use scaling relations to define radiatively important exponents.

0.1.2. Some Current Problems in Terrestrial Atmospheric Radiation

So we cannot solve the most general radiative transfer problem, let alone in the inverse direction where one extracts physical information on a system simply by measuring its radiative properties. Focussing only on terrestrial clouds and sunlight, we are nevertheless compelled to interpret our satellite imagery quantitatively, and we are still committed to constantly improve our weather forecasting skills, in particular, by using remotely sensed data (at the level of the initialization of the numerical model). Unsurprisingly, major atmospheric radiation problems more-or-less directly related to clouds abound. Here is a short line-up where the visible-, near IR- and thermal IR spectral regions each take center stage:

a- Wiscombe *et al.* [1984] summarize in their cloud "albedo paradox" what kind of problem can arise when ideas based on unrealistic models are applied to reality. Stated simply, the paradox is that optical thicknesses obtained from seemingly reasonable liquid water content (LWC) profiles, based on actual field measurements, can reach the hundreds, even for clouds of moderate geometrical thickness. However, in order to obtain consistency between the value of the planetary albedo (≈0.3), and the globally averaged cloud cover (50%), the latter cannot have a mean albedo greater than ≈0.5 [Paltridge and Platt, 1980]. This last value is achieved by homogeneous non-absorbing plane-parallel clouds at optical thicknesses of order 10 only.[6] According to the same models, the observed optical thicknesses lead to albedoes in excess of 0.9, a value very rarely observed. Conversely, the optical thicknesses deduced from satellite observations are too small when the same models are used [Twomey and Cocks, 1982]. We will see that this paradox vanishes once we leave the very artificial case of homogeneous plane-parallel models. Alternative explanations [e.g., Fouquart *et al.*, 1990] call for an amount of absorption that seems to be unsubstantiated, at least at strictly visible wavelengths (≈0.5μm) [e.g., King *et al.*, 1990]. In our opinion, the considerable spread in the observed (apparent) absorptance bears witness more to the presence of internal variability than to the difficulty in conducting simultaneous reflectance and transmittance measurements, which is already considerable.

b- At any rate, much of the attention has now shifted towards the cloud "absorption anomaly" which has been recently reviewed by Stephens and Tsay [1990]. In the energetically important near-IR (that contains one half of the solar irradiance at the top of the atmosphere), there are known and well-understood sources of (true) absorption. There are also reasons to believe that there might be some more, poorly understood sources of absorption such as H_20 dimers or a water vapor continuum formed by the extended "wings" of very remote but numerous spectral bands. Whatever the absorption situation is, scattering is also very much present and, given the systematic (and eventually quite strong) inhomogeneity effects that we observe in the non-absorbing cases, it is unclear whether we are witnessing truly enhanced absorption or just more variability effects, or (worse) a combination of the both. Obviously, the implications on the radiative budget are totally different in the two extreme cases.

c- Finally, we are acutely conscious of the fact that continuous input of (inhomogeneously distributed) solar radiation is quite literally "driving" the dynamics of the atmosphere on all meteorogically defined "scales," from the "micro-" (e.g., slope breeze, convectional instability) to the "synoptic" (e.g., Hadley cells).[7] Simultaneously, the closely related problem of climate prediction has all of a sudden become a major concern for policy makers; these newcomers to atmospheric science are trying very hard to balance economic and political pressures exerted respectively by the typical lobby, representing an industry that still needs fossil fuels (to generate profit), and their constituents, ordinary (voting) people concerned with runaway greenhouse effects and that now demand action, not (more) hot air. Understandably, the politicians want reliable predictions about the climatic effects of human activity but all that they can get for the moment is scientifically sound statements about the uncertainties of climate modelling. It is indeed notorious that climate models are very sensitive to their treatment of cloud backscatter, especially in the visible/near-IR [Ramanathan *et al.*, 1983]. It is still unclear whether the clouds will tend to counter-balance or enhance the warming effect of the various greenhouse gases that are themselves active in the thermal IR; there are semi-empirical as well as theoretical indications that both can happen, at different latitudes [Ramanathan *et al.*, 1989]. The only real consensus is that the uncertainties, on the cloud-factor in particular, are so large that the reliability—even the feasibility—of climate modelling is highly questionable. The ceptics have turned to data analysis and the believers need, amongst other things, better cloud-radiation interaction parameterizations.

We should also mention the problems related to the dependence of albedo and "cloud amount" on satellite resolution which are to be expected in scaling cloud and/or radiation fields [see Gabriel *et al.*, 1988; and references therein]. In response to the challenges posed by these atmospheric radiation problems, we advocate the use a combination of simplified transport models and idealized cloud models (the latter are only required, for the moment, to not be of the homogeneous plane-parallel type). We are aware of the fact that this attitude is in complete opposition to the usual approach in theoretical radiative transfer studies which is to postulate an unrealistically homogeneous and symmetric (usually plane-parallel) cloud model and then to use ever more sophisticated transport schemes. This attitude could be partially justified in times when detailed quantitative information on internal cloud structure was largely inaccessible, but this is no longer the case: for examples of LWC variability, see Tsay and Jayaweera [1984], Stephens and Platt [1987], or Durouré and Guillemet [1990].

0.2. A Survey of the Literature from the Scaling Viewpoint, followed by our Main Results

0.2.1. Inhomogeneous Radiation Transport (Theoretical and/or Computational Approaches)

For reasons tentatively described in the above, there are very few specifically radiative transfer studies in the traditional physics literature. However, transport problems in general have always generated considerable interest in the physics community; a well studied example that is quite relevant to our concern with basic effects of inhomogeneity is the question of diffusion in percolating binary mixtures. This subject has a sub-literature all of its own and we will not even attempt to review it here, rather in §§D.6.2–3 we describe the main results of importance to us (viz., used for radiative purposes in §2.3.4) and thereabouts references are given that contain adequate bibliographical surveys. For the moment, we will focus almost entirely on geo- and astrophysical publications.

For some time, the term "inhomogeneous" atmosphere in the radiative transfer literature was synonymous with a vertically stratified system of atmospheric layers which can be described within the context of plane-parallel geometry; see Lenoble [1977] for an extensive review. There is no doubt that stratification is present in the atmosphere, but ignoring horizontal variability is a very extreme assumption: if strictly applicable, the variability of (visible) satellite imagery would be due only to the random spatial distribution of surface albedo[8] and the deterministic variation of illumination geometry. This simple fact has created the need to better understand "multidimensional radiative transfer." In the circumstances, this expression is rather unfortunate since we want to avoid all possible confusion with the concept of "multiple (fractal) dimensions." This is especially important given the key role of the latter in transfer phenomena and we therefore prefer to use the expressions like "higher-dimensional transfer" or "horizontally inhomogeneous media" (when the directional bearings have been made clear) to characterize this broad field of research. In the upcoming discussion, we will exclude from the outset work on "inhomogeneous" atmospheres where variability is confined only to the vertical; for the purposes of this study, these stratified media exhibit plane-parallel (or one-dimensional) behaviour. Furthermore, in this succinct review, we will mainly be concerned with the simplest of boundary conditions (BCs) that define the so-called "albedo" problem. In essence, these BCs describe the sources and sinks for the (generally conservative) multiple scattering problem: namely, external[9] illumination from above (usually by a uniform collimated beam) and absorbing[10] ground below. Alternatively, we can say that such BCs provide a "forcing" of the flow of radiant energy through the medium. There is a basic dichotomy in the literature which is important to respect (see sect. 0.3 on our main results): horizontally finite cloud models versus their horizontally extended counterparts.[11] We start with the former.

There as been a sustained interest in treating clouds as simple geometrical shapes (usually cubes or cylinders) while maintaining internal homogeneity. See, for example, McKee and Cox [1974], Davies [1976, 1978], Barkstrom and Arduini [1977], Busygin *et al.* [1977], Cogley [1981], Welch and Zdunkowski [1981a], Preisendorfer and Stephens [1984], Stephens and Preisendorfer [1984] for various approaches; see also Crosbie and Dougherty [1985] who compound the difficulties, using laser beam-like illumination conditions in cylindrical media. The basic motivation is always to understand the basic radiative effects of imposing an outer horizontal scale on a system; we approach this essentially homogeneous problem from the scaling point of view in sect. 2.2 and 4.1 of this thesis where we reevaluate the findings of Gabriel [1988], Gabriel *et al.* [1990] and Davis *et al.* [1989, 1990a]. Before leaving this artificial class of internally homogeneous cloud models, we must note the conspicuous absence of fractal (nowhere rectifiable) boundary shapes, either deterministic (like the von Koch curve) or random (like fractional Brownian motion); this contrasts sharply with the fact that these surfaces actually "grow" very much like (convective) clouds do, i.e., by "budding" (as in cauliflower).[12]

Regularly striated systems (one-dimensional horizontal variability at one specific scale, often specified by a sine wave) have always attracted some attention if only because, like our inhomogeneous atmosphere, they offer no outer scale in the horizontal. This can be done either by assigning some purely horizontal variation in optical density (which is easier to approach analytically) or by modulating periodically the upper (or lower) surface of an otherwise homogeneous medium (if a piecewise linear profile is used, this type of medium is easily treated by Monte Carlo techniques). See Weinman and Swartztrauber [1968], van Blerkom [1971], Romanova [1975], Davies [1976], Wendling [1977], Romanova and Tarabukhina [1981], Stephens [1986, 1988a] and Cahalan [1989] for a variety of examples and techniques of solution. By using a multifractal cascade to model the horizontally variable optical thickness, the last author in fact leaves the realm of smooth, deterministic profiles. It is also important to note that Stephens [*ibid.*] offers a much more general formalism but his examples exhibit (deterministic) one-dimensional variability in the horizontal only since this allows him to use an inhomogeneous variant of the "adding/doubling" technique which has proved to be very expedient in plane-parallel applications.

In order to simulate horizontally extended cloud fields more realistically, Busygin *et al.* [1977], Aida [1977], Gube *et al.* [1980], Davies [1984], Kite [1987] (with a comment by Rawlins [1990]), Crétel *et al.* [1989], Barker and Davies [1992a; and other references therein] have arranged the above mentioned homogeneous cloud shapes into periodic or random two-dimensional arrays, with or without clustering, with or without distributed sizes and, when distributed, there is usually a characteristic (or very representative mean) size involved. In step with current observational findings (see below), the last authors use random scaling geometry to define the clustering properties of their clouds; for comparison, they also allow the individual cloudy cells to be of different optical thicknesses, as naturally dictated by their truncated additive model (briefly described in sect. C.2). These purely numerical investigations can be contrasted with the approach that consists of ensemble averaging the (analytical, parameterized, or tabulated) radiative responses associated with the simple homogeneous cloud geometries in an attempt to model the effect of spatial variability. More precisely, one argues that the ensemble averages can be interpreted as spatial averages if one neglects all (net) effects of radiative interaction from cell-to-cell, or cloud-to-cloud (depending on whether one is thinking of a single variable cloud model, or a model for a field of clouds). See, e.g., Busygin *et al.* [1973], Mullaama *et al.* [1975], Ronnholm *et al.* [1980], Welch and Zdunkowski [1981b], and Stephens *et al.* [1991; and (more) references therein] for some examples.[13] In essence, this last approach is very close to what we will come to call "independent pixels." This expression is due to Cahalan [1989] who applies the technique numerically to a (definitely spatial) multifractal distribution of optical thickness in an effort to mimic his results for the albedo field obtained by Monte Carlo simulation (and therefore with horizontal fluxes fully accounted for). For a general discussion of the idea, we refer the reader to sect. 3.3. Davis *et al.* [1991a, or chap. 5] obtain analytical results for multifractals in general, Schertzer and Lovejoy's [1984] "α-model" in particular; a "microcanonical" version of the latter was in fact used, with specific parameter values, by Cahalan [*ibid.*].

All of the above media have horizontal as well as vertical variations in their radiation fields, the latter being largely driven by boundary conditions. Up until now however, the only systems with density gradients in both the vertical and (at least one of the) horizontal directions are those homogeneous ones with a non-planar surface: for instance, collections of spheres [e.g., Davies, 1984] or else slabs supplemented with periodic "turrets" on top [e.g., van Blerkom, 1971; Davies, 1976]. At any rate, relatively little attention has been paid to systems with *bone fide* "internal" inhomogeneity (density fluctuating in all directions).[14] We also note that, within this more general framework, the standard distinction between the one- or two-dimensional cloud array problems (discussed above) and the problems of internal variability (discussed below) is in fact quite artificial since the former can be viewed as a special sub-class of the latter where density is either finite and constant on some given set or null on its complement.

Turning to internally variable media, we find, on the one hand, that Mosher [1979] and Welch [1983] have adopted a deterministic approach to cloud structure respectively built from a (relatively small) number of elementary "blocks" and controlled by the numerical integration of the fluid dynamical equations (at necessarily very moderate Reynolds numbers). On the other hand, Avaste and Vaynikko [1974], Glazov and Titov [1979], Titov [1979, 1980, 1990], and Boissé [1990] have developed analytically a mean field theory applicable to media with two possible values of the density and a spatial distribution generated by a Poissonian (exponentially decorrelating) process. These last idealized media are well approximated by white noise on a grid if the lattice constant is identified with the integral correlation length; such media have been investigated numerically by Welch *et al.* [1980] although they allowed for a continuous (rather than a binary) distribution of density values. Stephens [1988b] also develops an analytical mean field approach based on Reynolds averaging of the transfer equations and the subsequent application of different closures to a two-flux approximation.

All of these authors report relatively small but systematic effects of internal variability on the overall radiative properties of their models; their direction is dictated by the nonlinearity of the radiation-scattering material coupling and it appears to depend only[15] on the choice of radiative property to be monitored (i.e., albedo decreases and transmittance increases). The smallness of the observed differences w.r.t. homogeneity is partly due to the fact that the cloud models are usually taken as quite thin, i.e., not dominated by (effectively isotropic) scattering which means an overall smaller nonlinear coupling between the radiation and density fields. It is also partly due to the relative weakness of the variability of the media. In sharp contrast to this situation, the multiplicative cascade models presented in app. C are designed specifically to mimic the very singular features of extremely high Reynolds number flows: they are characterized by a huge variability (implying, in particular, a very wide range of values), the possibility of diverging statistical moments, a heavy concentration of the "activity" onto very sparse (fractal) sets, hence a correspondingly high degree of intermittancy, and yet long-range (algebraically decaying) correlations. We will return to their radiative properties after an observational justification of their introduction.

0.2.2. Fractal and Multifractal Aspects of the Atmosphere (Observations and Simulations)

There are many theoretical reasons, as well as considerable empirical evidence supporting the idea that, over wide ranges in scale, the statistical properties of clouds are invariant under scale changing operations. Scale invariant (or simply "scaling") systems are associated with power law behaviour and complex fractal structures arise naturally since over the corresponding range, the system has no characteristic size. Theoretically, we expect atmospheric fields, including clouds, to be scaling since the governing dynamical equations have no characteristic length between the outer (planetary) scale and the inner (viscous) scale. Furthermore, the radiative transfer equation introduces no intrinsic scale either since we expect the optical density field itself to obey scale independent spatial statistics. In the following we shall consider observationally based motivations, focussing only on cloud structure and/or radiation fields. In particular, we will leave aside the growing literature on the scaling properties of rain, wind, temperature, and other atmospheric fields in spite of the fact that many of these quantities are clearly related physically to cloudiness); see Schertzer and Lovejoy [1991] for a broader survey.

Empirical (aircraft) energy spectra of cloud liquid water content, such as those obtained by King *et al.* [1981], are scaling (power-law) in form and broadly support the idea that, at least over wide ranges in scale, clouds (as revealed by satellite images) are fractal [Lovejoy, 1982; Rhys and Waldvogel, 1986; Kuo *et al.*, 1988; Welch *et al.*, 1988a,b; Lee, 1989; Sèze and Smith, 1989; Cahalan and Joseph, 1989; Yano and Takeuchi, 1991]. For reviews, see Lovejoy and Schertzer [1986, 1990] or Schertzer and Lovejoy [1988]. Ludwig and Nitz [1986] extend scaling analysis techniques to lidar probings of smoke plumes, as do Durouré and Guillemet [1990] to *in situ* cloud LWC probings, followed by Malinowski and Zawadski [1991]. There have been some reports of scale breaking [Cahalan and Snider, 1989], but these may well be due to the use of monofractal rather than multifractal analysis techniques; see Lovejoy and Schertzer [*ibid.*] for a discussion of this difference as well as a critical reevaluation of previous analyses. In any case, systematic studies of scaling and its limits in the atmosphere still have not been undertaken and the basic issues are still open.

The very least that can be said is that cloud scaling is fairly complex. In this regard, Gabriel *et al.* [1988] analyzed several IR and VIS channel images captured by GOES, over ranges from 8 to 512 km; they found that the intense and weak regions have different scaling exponents, i.e., the clouds (and the underlaying ground) are "multifractal." Schertzer and

Lovejoy [1987] show theoretically that under fairly general circumstances the entire multifractal spectrum or (co)dimension function, can itself be characterized by three parameters which define multifractal "universality classes." Unlike fractal dimensions which provide purely geometric characterizations of sets, these parameters characterize the dynamical generator of the process. Lovejoy and Schertzer [1990] refine the analysis of Gabriel *et al.* [*ibid.*] and estimate the three parameters for IR and VIS (cloud and/or ground surface) radiances which are respectively translated into albedoes and brightness temperatures). The same type of dataset is reanalyzed[17] by Tessier *et al.* [1992] and compared with other types of satellite imagery. A further complexity in the scaling is empirically discussed in Lovejoy *et al.* [1987] (in connection with radar rain fields) showing that the appropriate scale changing operator is not simply a zoom (self-similarity), but involves stratification as well and a new "elliptical" dimension must be introduced; this is not unexpected in presence of a gravitational field and the ensuing convective activity [Schertzer and Lovejoy, 1985]. Moreover, Lovejoy and Schertzer [1985] argue that the relevant scaling should also involve differential rotation due to the presence of Coriolis forces and they illustrate their ideas with quite convincing simulations. This aspect of "generalized scale invariance" (or GSI) has now been validated empirically by scaling cloud "texture" analyses [Pflug *et al.*, 1991; Lovejoy *et al.*, 1992]. In summary, multiple scaling and anisotropy are likely to be fundamental ingredients of realistic cloud models.

0.2.3. Radiation Transport in Fractals and Multifractals (Including Results in this Thesis)

We now resume our discussion of theoretical/computational (rather than empirical) radiative transfer studies at the point where we left it at the end of §0.2.1, viz., in search for cloud models with strong inhomogeneity effects, large enough to explain the cloud "albedo paradox" described in §0.1.2 above at any rate. This challenge is met by Gabriel *et al.* [1986] who obtain numerical results for a random monofractal cascade model—a so called "β-model" (see sect. C.2)—that develops in all three dimensions of space.[18] In comparison, Cahalan [1989] uses only one (horizontal) direction to develop his random multifractal cascade model—of the type known as an "α-model" (see sect. C.3)—with interesting effects induced by this very strong structural anisotropy [Davis *et al.*, 1991a; also sect. 5.4 of the present thesis]. It is important to realize that both of these models are generated by a multiplicative cascade procedure and are therefore very intermittent and singular in nature as well as highly correlated, even the monofractal one.[19]

Lovejoy *et al.* [1989] and Gabriel *et al.* [1990], on the one hand, and Davis *et al.* [1989, 1990a; or sect. 4.2 of this thesis], on the other hand, study a deterministic monofractal model with, respectively, innovative analytical (renormalization) and standard numerical (Monte Carlo) approaches. Their results are somewhat different and the discrepancy is explained by Lovejoy *et al.* [1990] in terms of the adopted methodology. At any rate, these studies are the first to define and to illustrate "anomalous" radiative scaling with reasonably strong numerical evidence of "universal" (phase function independent) behaviour. A detailed discussion of this phenomenon is conducted in chap. 4, on both computational and theoretical grounds. For the moment, we simply let "F" denote some appropriately normalized bulk radiative response to the external illumination, e.g., total transmittance (which is simply the mean flux through the system expressed in units of incident flux). We also let "τ" represent some non-dimensionalized measure of the total mass (or LWC) of the cloud model. For this last parameter, optical thickness—vertically integrated cross-section per unit of volume—is a convenient choice, provided that it is spatially averaged horizontally in inhomogeneous situations. If the scattering is conservative, if the cloud's structure is scale invariant, and if it is optically thick enough (i.e., we require $\tau \gg 1$), then we can confidently anticipate an asymptotic regime with algebraic (or "scaling") behaviour:

$$|F_\tau - F_\infty| \approx h_F \, \tau^{-\nu_F} \qquad (0.1)$$

where ν_F is the universal scaling exponent associated with response F and h_F, a (phase function dependent) prefactor. Naturally, if the cloud model is stochastic, we should be considering ensemble-averaged F's and τ's; in sect. 1.4, we will offer an alternative parameterization of the basic radiative scaling relation in eq. (0.1) that incorporates this possibility, in a "mean field" sense. We will see many applications of such relations throughout this thesis, mainly in chap. 2, 4 and 5.

As a first example, consider transmittance (F=T) which we will often use in practice. The thick cloud limit (T_∞) is naturally 0 and the "standard," or "normal," or "trivial" scaling exponent, associated with homogeneous plane-parallel slabs,[20] is $\nu_T = 1$ while an "anomalous" scaling is characterized by $\nu_T < 1$ hence much higher transmittancies at a given τ and this generically explains the cloud "albedo paradox." As customary, the signs in eq. (0.1) are chosen in such a way that the parameters remain positive. Nevertheless, we can define a similar thin cloud—we should say "haze"—limit (F_0) for $\tau \ll 1$, in which case we expect to find a linear response ($\nu_F = -1$); this is a well-known fact for thin homogeneous systems[21] but we present arguments for its generalization to the most extreme cases of multifractal variability [Davis *et al.*, 1991a; or sect. 5.1–2 of this thesis]. Physically speaking, linear response means that the light particles suffer at most a single scattering within the medium. In contrast, the non-linear regime described above and where the anomalous scaling can eventually be observed is associated with a predominance of highly scattered photons. In fact we can take the multiplicity of scattering as a (stochastic) measure of the non-linearity of the coupling between the radiation and density fields which is of course defined, however less intuitively, by the equations of radiation transport themselves. In this connection, we argue (in sect. 4.4) that "$\tau \gg 1$" is a necessary but not a sufficient condition to obtain strong nonlinear effects such as the anomalous scaling described in eq. (0.1). Indeed, multifractal examples of infinitely massive clouds with no scattering whatsoever are provided in sect. 5.4.

The idea of anomalous scaling exponents and universality in transport phenomena is adapted from the abundant statistical physics literature on conductance (or diffusion) in disordered media, a brief summary of which is presented in app. D (and the results therein are adapted to the radiative problem in chap. 2). The real novelty here is to operate within the theoretical framework of radiative transfer: an exact kinetic theory (and ballistic random walks), not its hydrodynamical limit (and diffusive random walks). Lovejoy *et al.* [*ibid.*; also sect. 3.5] present a similarity-based argument for the universality within the framework of "discrete angle" transfer. Davis *et al.* [1991a, or chap. 5] have since defined and evaluated "mean field" and/or "independent pixel" exponents for multifractal media; in essence, these last exponents capture the statistical scaling effects of nonlinearity that are already present in one-dimensional transfer or, equivalently, do not call for horizontal fluxes.

Finally, Davis *et al.* [1991b, also chap. 6 (and app. B, for the numerical technicalities)] leave aside the determination of new exponents to have a closer look at how radiation flows through a typical multifractal density field with various overall optical masses. Having been carefully validated (at a considerable computational cost), these last results first of all set a precedent against which tentative improvements in numerical transfer schemes can be evaluated; the challenge for approaches based on finite differencing (rather than direct Monte Carlo simulation) is to cope with the very thick cells that naturally arise in any multifractal type of optical medium. Beyond the numerics, these simulations serve as illustrations of the higher-dimensional aspects of the nonlinear radiation/density field coupling (traceable to Cannon's [1970] concept of radiative "channeling") that are at work in particular when anomalous scaling is obtained (sect. 4.3–4). In spite of the very arbitrary choice of internal structure, many specific features of the numerical experiment compare quite favorably with the corresponding observations in real clouds. These quantitative successes are very encouraging for the future of scale invariant cloud modelling. Also encouraging is the fact that our numerical multifractal results in no way conflict with the qualitative understanding of inhomogeneous radiation transport that we develop in chap. 2 with the help of diffusion theory applied to far less realistic but analytically tractable media.

0.3. A Detailed Overview of this Thesis

First of all, we have systematically collected radiation transport theories that are general enough to accommodate any given inhomogeneous scattering optical medium. More precisely, each of these physical models for matter-radiation interaction can be used, for instance, to predict an albedo (or reflectance) and/or an overall flux (or total transmittance), the remainder, if any, yielding absorptance. We restrict ourselves to "general purpose" transport theories—they can be applied to an arbitrary medium—they are therefore readily compared quantitatively, simply by keeping the same medium. We have clarified the interconnections between these theories and organized them in a hierarchy. By order of increasing "ease of manipulation," we have: continuous angle (CA) transfer, discrete angle (DA) transfer, diffusion theory, and "independent pixels" (IPs). For the moment, let it simply be said that

- CA transfer is the standard kinetic-type "linear transport" theory, completely equivalent to neutron transport theory (and reviewed in app. A).
- DA transfer is a special simplifying choice of the "phase function" (scattering kernel) in its CA counterpart (full details to be found in chap. 3).
- diffusion theory is known as "Eddington's approximation" in the radiative literature, and the "hydrodynamic limit" in statistical physics (reviewed in app. D).
- IPs means that the medium is somehow divided into columns that exchange no radiant energy with one another (see sect. 3.4 for specifics).

We better describe, contrast and inter-relate of all of the above approaches in sect. 1.3 (and the above-mentioned sections of the thesis give all the necessary technicalities).

0.3.1. General Theory of Inhomogeneous Radiation Transport (App. A and D, Chap. 2–3)

Within the most general framework (i.e, CA transfer), we have

- established that photon free paths are always longer on average in inhomogeneous situations than in homogeneous ones (with the corresponding average density).
- proposed and exploited a new model phase function that is the two-dimensional counterpart of the celebrated Henyey-Greenstein phase function.
- interpreted the radiative transfer equation for (the important case of) conservative and isotropic multiple scattering as a detailed balance between spatial gradients and directional anisotropies in the radiation field, with (relatively minor) role for density.
- enumerated and contrasted the various definitions in existence for albedo (versus transmittance and, possibly, absorptance) for the case of horizontally bounded media (i.e., "isolated" clouds). Also, the IP approach is shown to be largely irrelevant to these horizontally bounded cases.
- related the "transport" m.f.p. rescaling to the statistics of correlated random walks in space, viewed as images of their uncorrelated counterparts in direction-space.

Focusing primarily on conservative scattering, several analytically-based results have been obtained using the three simpler theoretical frameworks in the hierarchy (DAs, diffusion, and

IPs), often further simplifying the problem at the level of the boundary conditions (this last procedure poses no major problem for horizontally extended media, at least in the case of weak enough variability). These results include:

- generalized similarity relations for DA transfer, where a single phase function parameter is varied, rather than all at once as in the standard theory;
- total transmittance is always increasing when going from IPs to DAs to diffusion, for a given medium;
- the average transmittance of an ensemble of media with various masses (or optical thicknesses) and given structure is always less than the transmittance of the medium with the average mass (due to the convexity of transmittance w.r.t. mass and Jensen's inequality);
- the previous statement also applies to any IP transmittance, as compared to the corresponding mean density transmittance;
- the homogeneous distribution always yields the smallest transmittance, for a given total mass. In particular, we find (horizontally) homogeneous plane-parallel media to be extremal w.r.t. the the decrease of transmission, equivalently, increase of albedo.

The three last results and the one in the above concerning free paths (hence direct transmittance) were previously known but, in our opinion, not well explained. We have underscored the fundamental role of the nonlinear coupling that exists between the radiation and density fields. Furthermore, higher dimensionality is essential to the last result and it is shown to be directly related to Cannon's [1970] "channeling" (see §1.5.1 for a discussion of the author's original definition) and Stephens' [1986] "mode-coupling" (see §1.5.2 for an explanation of this paraphrasing of the author's original analysis). In essence, the authors have used these expressions to describe the basic effects of inhomogeneneity on the flow of radiant energy, respectively in physical and Fourier spaces. This basic fact is illustrated with a novel (closed-form) analytical solution for homogeneous and hollow spheres. The conditions of its extension to CA transfer are also discussed: normal, isotropic or otherwise quite symmetric illumination geometry seems to be required.

Finally, all of the above results seem to generalize (when necessary) to every case of extreme variability and/or (numerical) application of exact boundary conditions to be mentioned in the following. In particular, this indicates that "channeling/mode-coupling" is still at work on a per realization basis in the case of stochastic cloud models. Notice that pure internal variability (hence "channeling") and pure stochasticity (hence Jensen's inequality) both enhance the overall and/or average transmittance, so it is conceptually important to consider them separately, at least at this point in time since we are still trying to positively identify the basic mechanisms at work.

0.3.2. Normal and Anomalous Radiative Scaling Exponents (Chap. 4–5)

In the following, we use the scaling parameterization defined in eq. (0.1).

- Homogeneous Squares, Cubes, Etc.: Contrary to previous claims concerning the scaling of albedo, these media prove, upon closer examination, to be in the same class as other types of horizontally bounded media (e.g., spheres), especially if the albedo is properly defined. Of course, this scaling is "normal" ($\nu_R = \nu_T = 1$), i.e., cloud sides are asymptotically unimportant. This scaling is indeed found to be "universal" (phase function independent) and is the same for both transfer and diffusion theories; recall that IPs are (applicable but) irrelevant here. However, if the apparently simple hyper-cubical media are used, then the beginning of the asymptotic regime is already large in two dimensions and it is pushed to still higher sizes in higher dimensionalities.
- Binary Mixtures on a Grid: In general, the scaling is normal; in the interesting but very special case where an exactly "percolating" fraction of the cells are totally empty (i.e., the "RSN" limit in conductance studies), "anomalous" scaling does occur ($\nu_T < 1$) but only for diffusion, not for transfer, nor IPs.
- Deterministic Monofractal Cascade Field: In this case, we find strong numerical evidence of anomalous scaling for transfer theory too and it is shown to be universal in general. Furthermore, the exponents associated with the various transport theories are all different.
- The Transition from Normal to Anomalous Scaling: These two last results can be explained from first principles, reckoning on the structure of the basic diffusion and transfer equations and the key roles played by singular density values and long-range correlations in conjunction with our understanding of the radiative "channeling" process. In particular, these arguments make clear that the previous result is very likely to be true for otherwise "multiplicative" (i.e., random and/or multifractal) cascade fields too, but doubtful for all "additive" models.
- Random Multifractal Distributions: Analytically estimated exponents for ensemble averaged total plane-parallel transmittance show that the (mean field) radiative scaling can be either normal (homogeneous-like) or anomalous (inhomogeneous-like), depending on whether the small scale limit makes the cloud ever thinner or ever thicker. The same applies to direct transmittance which is normally exponential w.r.t. optical thickness (formally, $\nu_{Td} = \infty$) and for which we find $\nu_{Td} < \infty$, in the thick cloud case. These results can all be interpreted in terms of IP calculations, at least within a specially restricted class of cascade models (that still contains most cases used in the cloud radiation literature).

0.3.3. Numerical Simulation of Transfer Through a Typical Multifractal (Chap. 6, App. B)

Up until now, we have concentrated on spatially unresolved or ensemble averaged responses to external illumination. We now turn to fully resolved radiation fields associated with a specific realization of a random multiplicative cascade sporting Gaussian generators (with standard deviation $\sigma = \sqrt{\ln 2} \approx 0.83$ and centered at $\mu = -\sigma^2/2$, which guarantees that the ensemble average is unit, cf. §C.3.2). After 10 discrete cascade steps with a dividing ratio of 2, this yields an extremely variable log-normally distributed density field on a 1024X1024 grid; the spatial average is ≈ 1.5 but the max-to-min ratio is $\approx 10^{11}$ over the whole field and ratios in the range 2–4 are not rare going from one cell to the next. Finally, the whole field is modulated by a numerical factor $\kappa = 2^k$, with $k = -7(+1)-3$, which at once keeps the average cell relatively thin and the whole cloud relatively thick. This defines a highly non-trivial problem in computational transfer, bearing in mind that we want to see the internal radiation fields in full detail.

- The purely numerical aspects are considerably simplified by opting for an isotropic DA phase function; the problem is then approached in two totally independent ways in order to make sure that the results are reliable (i.e., physical). We can live with unbiased random numerical errors of known magnitude (as in the Monte Carlo method), but we must avoid at all costs contamination by systematic biases (to which finite difference methods are prone, especially in presence of very thick cells). Apart from a straightforward Monte Carlo simulation, a simple finite differencing scheme (followed by relaxation of the sparsely coupled system of difference equations) is used but with the utmost care. The final results of the two methods compare is very satisfactorily. So, on the one hand, we now have an extremely inhomogeneous benchmark medium w.r.t. which different codes can be compared and, on the other hand, we have truly physical results to discuss in the following.
- As expected from the above, the visualizations of the internal radiation fields show "channeling" at work (on all scales observable to the eye), as demonstrated by the way the horizontal and vertical (net) fluxes interplay.
- As expected on general grounds, the component of the radiation field that vanishes when diffusion is a good approximation to transfer becomes very small in the thickest regions and/or clouds. This is quite interesting because very diffusion-like radiance distributions were recently observed in real cloud decks [King *et al.*, 1990].
- As observed in real clouds, we find scaling power spectra for the albedo field, with roughly the same exponent, for all but the smallest scales that are contaminated by Monte Carlo noise (at the expected level).

- Again as with real clouds, comparing the albedo, transmittance and incident flux for each column, one can define an "apparent" absorptance field with roughly the observed range of values (even though not all are positive since the spatial average must identically vanish).
- Also as observed in real clouds, we find smoother albedo fields for the thicker clouds (it naturally saturates) but, simultaneously with this more "homogeneous plane-parallel" appearance, we find stronger "channeling" effects (i.e., greater differences with the homogeneous plane-parallel prediction for the same total optical mass).
- Finally, another predicted effect of "channeling" shows up in the order-of-scattering decompositions of the overall albedo and transmittance. Namely, we find lower reflectance values when compared with the homogeneous case (of equal overall mass) but only for two and more scatterings. In contrast to this higher transmittance values, even at no scattering at all (directly transmitted light). Interestingly, saturation occurs at roughly the same order-of-scattering as in the equivalent homogeneous case. In short, the distributions are displaced towards much lower orders and considerably broadened.

The above results on a single realization of a stochastic cloud model clearly point, on the one hand, to the necessity of improving our numerical techniques in order to reduce the computational costs involved since we eventually want to obtain accurate ensemble-averages and, on the other hand, to the necessity of improving the cloud model itself using Nature as a guide. Finally, we must refine our procedures for comparing CA and DA quantities and explicitly define the appropriate (vectorial, n-point, cross-correlating) scale invariant statistics to quantify the occurrence of "channeling" events in both computerized and *in situ* radiation experiments.

---

[1] For successive reviews of the problem of wave propagation through random media, see Chernov [1960], Tatarski [1961], Frisch [1968], Radio Science [1975], Ishimaru [1978], Chow *et al.*, [1981], and Sornette [1989]; this last author covers the regimes when the (homogeneous, "equivalent medium") diffusion equation should be used as well as the onset of (classical) localization phenomena, also summarized by Anderson [1985] himself. Very interesting pioneer work by Bourret [1962, 1964, 1965, 1966] shows, in particular, that stochastic classical systems where propagation occurs are equivalent to second quantized systems (and the characteristic non-commutation arises bcause of the same kind of nonlinearity that we encounter in §A.2.3 for direct transmittance).

[2] This occurs on scales too small for us to model with radiative transfer, even in theory, due to the necessity of "coarse-graining" of the wave fields (see sect. E.3).

[3] Here, the expression "photon" is not to be understood in the strict QED sense of a single quantum of a given mode of the EM field if only because no coherence effects can be modeled by transfer as such.

[4] We will often return to these two remarkable papers that not only present innovative numerical techniques but, more importantly, give qualitative but precious insight into the basic processes of inhomogeneous transfer.

[5] Indeed, the Monte Carlo method has no systematic bias due to spatial discretization, its only problem is the presence of an intrinsic statistical noise (which is fortunately well understood, see sect. B.1). It therefore provides a bottom line point of reference in terms of accuracy and efficiency: any viable alternative must be faster and/or more precise.

[6] One can use radiant energy conservation $R+T = 1$ in conjunction with, e.g., the diffusion result $R/T = \tau/2\chi$ (see sect. D.4) where τ is the optical thickness and $\chi \approx 1/(1-g)$ is the "extrapolation length" parameter; according to Deirmeinjian's C1 drop size distribution at 0.45 μm, we can take $g \approx 0.85$ for the phase function's "asymmetry factor."

[7] In essence, solar radiation is fueling the atmospheric engine but the thermodynamics are complex, very poorly understood since the solar radiation field can in no way be considered even close to thermal equilibrium with the system; see Essex [1984; and references therein] for some of the fundamental consequences.

[8] Incidentally, inhomogeneous ground reflectance under a homogeneous plane-parallel atmosphere is sufficient to generate horizontal gradients everywhere in the radiation field; this problem has important implications in the field of remote sensing of the environment and many authors, including Malkevich [1960], Otterman and Fraser [1979], Diner and Martonchik [1984], Kaufman and Fraser [1983], and Stephens [1988a] have studied it for different configurations with different methodologies. The same remark applies to non-uniform illumination of the upper boundary. Consider, for instance, the "search-light" problem where an initially very narrow pencil of radiation impinges on a scattering atmosphere (this is of importance, in particular, to lidar sounding of the atmosphere); see Lenoble [1985] for a review and many references, also Crosbie and Koewing [1979] for a sine-wave illumination pattern as well as Weinman and Masutani [1987] for the problem of an isotropic point source. Tanré *et al.* [1981] make an interesting combination of these two types of transfer problems with horizontal gradients driven by only boundary conditions: they use reciprocity to model the "adjacency effect" of inhomogeneous ground using "search-light" problem responses.

[9] For completeness, we should mention the work of several geophysicists and many more astrophysicists concerned with the effects of spatial variability (in more than one direction) of internal (thermal) sources for continuum or otherwise "coherent" transfer, going back at least to Giovanelli [1959]. More recently, we have for example Harshvardan *et al.* [1981], Crosbie and Schrencker [1984], Preisendorfer and Stephens [1984], Stephens and Preisendorfer [1984], and Stephens [1986]. For cases (mainly of astrophysical interest) with a frequency redistribution function that models spectral line (or "incoherent") transfer, see Jones and Skumanich [1980; and references therein].

[10] Some authors, obviously pressed to simulate "typical" remote sensing and radiation budget situations, have started to investigate (numerically) "broken" cloudiness overlaying homogeneous Lambertian [e.g., Welch and Wielicki, 1988] or otherwise [Barker and Davies, 1992b] reflecting ground.

[11] This is an important difference (the media have totally different kinds of support) even though it can be described in terms of BCs in the case of horizontally periodic media. It is important not to think of this dichotomy as a question of BCs because *bone fide* BC differences (e.g., "mixed" versus more standard) normally tend to be quite minor.

[12] See however Mullaama *et al.* [1975] who model the directional effects of cloud top "roughness" by assuming it to be a random Lambertian surface (no multiple scattering is involved).

[13] In particular, the whole mini-literature on "Markovian" media in one dimension only (reviewed and quoted, e.g., by Boissé [1990]) enter this category because none of the fundamentally higher-dimensional effects that interest us primarily can occur. However, other non-trivial effects on the internal fields have been by studied quite rigorously in this type of medium using the analytical methods developed for treating stochastic ODEs (reviewed,

in particular, by van Kampen [1976]). The main groups involved in this research effort are situated at either Lawrence Livermore National Laboratory or the (french) *Commission à l'Énergie Atomique* and one can only wonder how far the higher-dimensional transport—possibly classified, probably mainly numerical—investigations have been carried out in these prestigious institutions.

[14]This is largely due to the fact that some of the techniques used in computational transfer become more involved when density gradients are apt to appear in any direction.

[15]If more sophisticated (continuous angle) transfer theory is used, then illumination conditions also play a role, though mainly in the optically thin regime.

[17]These last authors prefer, for methodological reasons, to study the (finite difference) Laplacian of the albedo field in absolute value or else its absolute gradient; they point out that the main universal parameter (called the Lévy index) is indeed invariant under such operations for simulated cascade fields but here they find, quite understandably, rather different universal parameters than those obtained for the albedo field itself. See sect. C.3–5 for brief descriptions of the different analysis techniques employed by the various authors.

[18]This numerical experiment is described in full detail by Gabriel [1988] while the main results of are also reported by Davis *et al.* [1990a].

[19]*A priori*, such is not the case of the additive models recently proposed by Barker and Davies [1992a]. In order to obtain interesting cloud fields (the authors take the individual clouds to be homogeneous), they must use a truncation, a "zero-crossing set," to restore intermittancy into the system (see sect. C.2–4 for a discussion of similar models used in turbulence theory).

[20]These media have the following two-flux—equivalently, diffusion—transmittance: $T = 1/(1+b\tau)$ and $R = 1-T$, where $b \sim (1-g)$ is as BC/phase function (g is the asymmetry factor), up to an $O(1)$ numerical factor. So $T \sim (1/b)\tau^{-1}$ for $\tau \gg 1$, hence $\nu_T = \nu_R = 1$ in the (thick) cloud limit.

[21]The above yields $R = b\tau/(1+b\tau)$ and $T = 1-R$. So $R \sim b\tau$ for $\tau \ll 1$, i.e., a linear response, hence (formally) $\nu_T = \nu_R = -1$ in the limit of "thin clouds" (a somewhat self-contradictory expression).

Bibliography for Chapter 0

Aida, M., "Scattering of solar radiation as a function of cloud dimensions and orientation," *J. Quant. Spectrosc. Radiat. Trans.*, 17, 303–310, 1977.

Anderson, P. W., "The question of classical localization - A theory of white paint?" *Phil. Mag. B*, 52, 505–509, 1985.

Avaste, O. A., and G. M. Vaynikko, "Solar radiation transfer in broken clouds," *Izv. Acad. Sci. USSR Atmos. Oceanic Phys.*, 10, 1054–1061, 1974.

Barker, H. W., and J. Davies, "Solar Radiative Fluxes for Extensive Broken Cloud Fields," *J. Atmos. Sc.*, 1992a (in press).

Barker, H. W., and J. Davies, "Solar Radiative Fluxes for Broken Cloud Fields above Reflecting Surfaces," *J. Atmos. Sc.*, 1992b (in press).

Barkstrom, B. R. and R. F. Arduini, "The effect of finite size of clouds upon the visual albedo of the earth," in *Radiation in the Atmosphere*, edited by H.-J. Bolle, Science Press Princeton, 188–190, 1977.

Boissé, P., "Radiative Transfer Inside Clumpy Media: The Penetration of UV Photons Inside Molecular Clouds," *Astron. Astrophys.*, 228, 483–502, 1990.

Bourret, R. C., "Propagation of randomly perturbed fields," *Can. J. Phys.*, 40, 782–790, 1962.

Bourret, R. C., "Quantised fields as random classical fields," *Phys. Lett.*, 12, 323–325, 1964.

Bourret, R. C., "Ficton theory of dynamical systems with noisy parameters," *Can. J. Phys.*, 43, 619–639, 1965.

Bourret, R. C., "Stochastic syatems equivalent to second quantized systems: Examples," *Can. J. Phys.*, 44, 2519–2524, 1966.

Busygin, V. P., N. A. Yevstatov, and E. M. Feigelson, "Optical properties of cumulus clouds and radiant fluxes for cumulus cloud cover," *Izv. Acad. Sci. USSR Atmos. Oceanic Phys.*, 9, 1142–1151, 1973.

Busygin, V. P., N. A. Yevstatov, and E. M. Feigelson, "Calculation of the direct, scattered and total solar radiant fluxes and their distribution in cumulus clouds," *Izv. Acad. Sci. USSR Atmos. Oceanic Phys.*, 13, 184–190, 1977.

Cahalan, R. F., "Overview of Fractal Clouds," in *Advances in Remote Sensing (RSRM'87)*, Eds. A. Deepak *et al.*, 371–389, A. Deepak, Hampton (Va.), 1989.

Cahalan, R. F., and J. H. Joseph, "Fractal statistics of cloud fields," *Mon. Wea. Rev.*, 117, 261–272, 1989.

Cahalan, R. F., and J. B. Snider, "Marine stratocumulas structure," *Remote Sens. Environ.*, 28, 95–107, 1989.

Cannon, C. J., "Line Transfer in Two Dimensions," *Astrophys. J.*, 161, 255–264, 1970.

Chandrasekhar, S., *Radiative Transfer*, Oxford University Press, 1950. (Reprinted by Dover, New York, NY, 1960.)

Chernov, L. A., *Wave Propagation in Random Media*, transl. from russian by R. A. Silverman, McGraw Hill, 1960. (Reprinted by Dover, New York, NY, 1967.)

Chow, P. L., W. E. Kohler, G. C. Papanicolaou (Eds.), *Multiple Scattering and Waves in Random Media*, North-Holland, Amsterdam, The Netherlands, 1981.

Cogley, A. C., "Initial results for multidimensional radiative transfer by the adding/doubling method," in *Proceedings of the 4th Conference on Atmospheric Radiation*, Am. Meteorol. Soc., Toronto, June 12-16, 1981.

Crétel, D., M. Herman and D. Tanré, "Fluxes and directional effects of broken clouds," in *IRS'88: Current Problems in Atmospheric Radiation*, edited by J. Lenoble and J. F. Geleyn, pp. 95–98, A. Deepak, Hampton, Va., 1989.

Crosbie, A. L., and R. L. Dougherty, "Two dimensional linearly anisotropic scattering in a finite-thick cylindrical medium exposed to a laser beam," *J. Quant. Spectros. Radiat. Transfer*, 33, 487–520, 1985.

Crosbie, A. L., and J. W. Koewing, *J. Quant. Spectros. Radiat. Transfer*, 21, 573–, 1979.

Crosbie, A. L., and R. G. Schrencker, *J. Quant. Spectros. Radiat. Transfer*, 31, 339–, 1984.

Davies, R., *The three dimensional transfer of solar radiation in clouds*, Ph.D. thesis, 219□pp, Univ. of Wisc., Madison, 1976.

Davies, R., "The effect of finite geometry on three dimensional transfer of solar irradiance in clouds," *J. Atmos. Sci.*, 35, 1712–1724, 1978.

Davies, R., "Reflected solar radiances from broken cloud scenes and the interpretation of scanner measurements," *J. Geophys. Res.*, 89, 1259–1266, 1984.

Davis, A. B., P. Gabriel, S. Lovejoy, and D. Schertzer, "Asymptotic Laws for Thick Clouds, Dimensional Dependence - Phase Function Independence," in *IRS'88: Current Problems in Atmospheric Radiation*, Eds. J. Lenoble and J.F. Geleyn, pp103–106, Deepak Publ., 1989.

Davis, A. B., P. Gabriel, S. Lovejoy, D. Schertzer, and G. L. Austin, "Discrete Angle Radiative Transfer - Part III: Numerical Results and Atmospheric Applications," *J. Geophys. Res.*, 95, 11729-11742, 1990a.

Davis, A. B., S. Lovejoy, D. Schertzer, P. Gabriel, and G. L. Austin, "Discrete Angle Radiative Transfer Through Fractal Clouds," *Proceedings of the 7th Conference on Atmospheric Radiation*, San Fransisco (Ca.), July 23–27, Am. Meteorol. Soc., Boston, 1990b.

Davis, A. B., S. Lovejoy, and D. Schertzer, "Radiative transfer in multifractal clouds," in *Scaling, Fractals and Non-Linear Variability in Geophysics*, Eds. D. Schertzer and S. Lovejoy, Kluwer, Hingham (Mass.), 1991a.

Davis, A. B., S. Lovejoy, and D. Schertzer, "Discrete angle radiative transfer in a multifractal medium," *S.P.I.E. Proceedings*, 1558, 37–59, 1991b.

Diner, D. J., and J. V. Martonchik, "Atmospheric transfer of radiation above an inhomogeneous non-Lambertian ground, I: Theory," *J. Quant. Spectrosc. Radiat. Transfer*, 31, 97–125, "II: Computational considerations and results," *Ibid.*, 32, 279–304, 1984.

Durouré, C., and B. Guillemet, "Analyse des Hétérogenéités Spatiales des Stratocumulus et Cumulus," *Atmos. Res.*, 25, 331–350, 1990.

Essex, C., "Radiation and the irreversible thermodynamics of climate," *J. Atmos. Sci.*, 41, 1986–1991, 1984.

Fouquart, Y., J. C. Buriez, M. Herman, and R. S. Kandel, "The influence of clouds on radiation: A climate modelling perspective," *Rev. of Geophys.*, 28, 145–166, 1990.

Frisch, U., "Wave Propagation in Random Media," in *Probabilistic Methods in Applied Mathematics*, vol. I, pp. 75–197, Ed. A. T. Barucha-Reid, Academic Press, New York, NY, 1968.

Gabriel, P., S. Lovejoy, G.L. Austin, and D. Schertzer, "Radiative transfer in extremely variable fractal clouds," in *Proceedings of the 6th Conference on Atmospheric Radiation*, Williamsburg (Va.), May 12–16, Am. Meteorol. Soc., Boston, 1986.

Gabriel, P., *Discrete angle radiative transfer in uniform and extremely variable clouds*, Ph.D. thesis, 160pp, Phys. Dep., McGill Univ., Montréal, Québec, 1988.

Gabriel, P., S. Lovejoy, D. Schertzer, and G. L. Austin, "Multifractal Analysis of Resolution Dependence in Satellite Imagery," *Geophys. Res. Lett.*, 15, 1373–1376, 1988.

Gabriel, P., S. Lovejoy, A. B. Davis, D. Schertzer, and G. L. Austin, "Discrete Angle Radiative Transfer - Part II: Renormalization Approach for Homogeneous and Fractal Clouds," *J. Geophys. Res.*, 95, 11717-11728, 1990.

Giovanelli, R. G., "Radiative Transfer in Non-Uniform Media," *Aust. J. Phys.*, 12, 164–170, 1959.

Glazov, G. N, and G. A. Titov, "Average solar radiation fluxes and angular distribution in broken clouds," *Izv. Acad. Sci. USSR Atmos. Oceanic Phys.*, 15, 802–806, 1979.

Gube, M., J. Schmetz, and E. Rashke, "Solar radiative transfer in a cloud field," *Cont. Atmosph. Phys.*, 53, 24–34, 1980.

Harshvardan, J. A. Wienman, and R. Davies, "Transport of infrared radiation on cuboidal clouds," *J. Atmos. Sci.*, 38, 2500–2513, 1981.

Ishimaru, A., *Wave Propagation and Scattering in Random Media*, 2 vol., Academic, New York, NY, 1978.

Jones, H. P., and A. Skumanich, "The physical effects of radiative transfer in multidimensional media including models of the solar atmosphere," *Astrophys. J. Suppl.*, 42, 221–240, 1980.

Kaufman, Y. J., and R. S. Fraser, "Different atmospheric effects in remote sensing of uniform and nonuniform surfaces," *Adv. Space Res.*, 2, 147–155, 1983.

King, M. D., L. F. Radke, and P. V. Hobbs, "Determination of the Spectral Absorption of Solar Radiation by Marine Stratocumulus Clouds from Airborne Measurements within Clouds," *J. Atmos. Sci.*, 47, 894–907, 1990.

King, W. D., C. T. Maher, G. A. Hepburn, "Further performance tests on the CSIRO liquid water probe," *J. Atmos. Sci.*, 38, 195–200, 1981.

Kite, A., "The albedo of broken cloud fields," *Q. J. R. Meteorol. Soc.*, 113, 517–531, 1987.

Kuo, K. S., R. M. Welch, and S. K. Sengupta, "Stuctural and textural characteristics of cirrus clouds observed using high spatial resolution Landsat imagery," *J. Appl. Meteor.*, 27, 1242-1241, 1988.

Lee, F. Y. P., "Statistical parameters of a cloud field," in *IRS'88: Current Problems in Atmospheric Radiation*, edited by J. Lenoble and J. F. Geleyn, pp. 91–94, A. Deepak, Hampton, Va., 1989.

Lenoble, J. (Ed.), *Standard Procedures to Compute Radiative Transfer in a Scattering Atmosphere*, NCAR, Boulder, Colo., 1977.

Lenoble, J. (Ed.), *Radiative Transfer in Scattering and Absorbing Atmospheres: Standard Computational Procedures*, A. Deepak, Hampton, Va., 1985.

Lovejoy, S., "The area-perimeter relation for rain and clouds," *Science*, 216, 185–187, 1982.

Lovejoy, S., and D. Schertzer, "Generalized Scale Invariance in the Atmosphere and Fractal Models of Rain," *Wat. Resour. Res.*, 21, 1233–1250, 1985.

Lovejoy, S., and D. Schertzer, "Scale invariance, symmetries, fractals and stochastic simulation of atmospheric phenomena," *Bull. Am. Meteorol. Soc.*, 67, 21–32, 1986.

Lovejoy, S., D. Schertzer, and A. A. Tsonis, "Functional box-counting and multiple elliptical dimensions in rain," *Science*, 235, 1036–1038, 1987.

Lovejoy, S., P. Gabriel, D. Schertzer, and G. L. Austin, "Fractal clouds with discrete angle radiative transfer," in *IRS'88: Current Problems in Atmospheric Radiation*, eds. J. Lenoble and J. F. Geleyn, pp. 99–102, A. Deepak, Hampton (Va.), 1989.

Lovejoy, S., and D. Schertzer, "Multifractals, Universality Classes and Satellite and Radar Measurements of Cloud and Rain Fields," *J. Geophys. Res.*, 95, 2021–2034, 1990a.

Lovejoy, S., A. B. Davis, P. Gabriel, D. Schertzer, and G. L. Austin, "Discrete Angle Radiative Transfer - Part I: Scaling and Similarity, Universality and Diffusion," *J. Geophys. Res.*, 95, 11699-11715, 1990.

Lovejoy, S., D. Schertzer, and K. Pflug, "Generalized Scale Invariance and differential rotation in cloud radiances," *Physica A*, in press, 1992.
Ludwig, F. L. and K. C. Nitz, "Analysis of lidar cross sections to determine the spatial structure of material in smoke plumes," in *Proc. of Smoke Obscurants Symposium*, vol. 10, Harry Diamond Labs, Adelphis, Md., pp. 231–241, 1986.
Malinowski, S. P., and I. Zawadzki, "On the surface of clouds," preprint, 1991.
Malkevich, M. S., "An approximate method of allowing for horizontal albedo changes of the underlaying surface in problems of light scattering in the atmosphere," *Bull. (Isv.) Acad. Sci. USSR, Geophys. Ser.*, no. 2, 1960.
McKee, T. B., and J. T. Cox, "Scattering of visible light by finite clouds," *J. Atmos. Sci.*, 31, 1885–1892, 1974.
Mosher, F. R., *Visible flux across finite clouds*, Ph.D. thesis, 109□pp, Univ. of Wisc., Madison, 1979.
Mullaama, R. Y., M. A. Sulev, V. K. Poldmaa, H. A. Ohvril, H. J. Niylsick, M. I. Allenov, L. G. Tchubakov, and A. F. Kuusk, *Stochastic structure of clouds and radiation fields*, NASA Tech. Transl., TT F-822, 1975.
Otterman, J., and R. S. Fraser, "Adjacency effects on imaging by surface reflection and atmospheric scattering: Cross radiance zenith," *Appl. Opt.*, 18, 2852–2860, 1979.
Paltridge, G. W, and C. M. R. Platt, *Radiative Processes in Meteorology and Climatology*, 318pp, Elsevier North-Holland, New York, NY, 1976.
Pflug, K., Lovejoy, S., and D. Schertzer, "Generalized Scale Invariance and differential rotation in cloud texture," in *Non-linear Dynamics of Structures*, Eds. R. Z. Sagdeev *et al.*, 213–235, World Scientific, Hong Kong, 1991.
Preisendorfer, R. W., and G. L. Stephens, "Multimode radiative transfer in finite optical media, I: Fundamentals," *J. Atmos. Sci.*, 41, 709–724, 1984.
Radio Science, vol. 10, No. 1, Special Issue: Waves in Random Media, 1975.
Ramanathan, V., E. J. Pitcher, R. C. Malone, and M. L. Blackmon, "The response of a spectral general circulation model to refinements in radiative processes," *J. Atmos. Sci.*, 40, 605–630, 1983.
Ramanathan, V., E. J. Pitcher, R. C. Malone, and M. L. Blackmon, "Cloud-radiative forcing and climate: Results from the Earth Radiation Budget Experiment," *Science*, 243, 57–63, 1989.
Rawlins, F., "A note on 'The albedo of broken cloud fields' by A. J. Kite," *Q. J. R. Meteorol. Soc.*, 116, 243–244, 1990.
Rhys, F. S., and A. Waldvogel, "Fractal shape of hail clouds," *Phys. Rev. Lett.*, 56, L784–787, 1986.
Romanova, L. M., "Radiative transfer in a horizontally inhomogeneous scattering medium," *Izv. Acad. Sci. USSR Atmos. Oceanic Phys.*, 11, 509–513, 1975.
Romanova, L. M., and T. M. Tarabukhina, "Light reflection by a sunlit horizontally inhomogeneous cloud," *Izv. Acad. Sci. USSR Atmos. Oceanic Phys.*, 17, 19–26, 1981.
Ronnholm, K., M. B. Baker, and H. Harrison, "Radiative transfer through media with uncertain or variable parameters," *J. Atmos. Sci.*, 37, 1279–1290, 1980.
Schertzer, D., and S. Lovejoy, "On the dimension of atmospheric motions," in *Turbulence and chaotic phenomena in fluids*, ed. T. Tatsumi, Elsevier North-Holland, New York, NY, pp505–508, 1984.
Schertzer, D., and S. Lovejoy, "Generalized Scale Invariance in Turbulent Phenomena," *P.C.H. Journal*, 6, 623–635, 1985.
Schertzer, D., and S. Lovejoy, "Physically Based Rain and Cloud Modeling by Anisotropic, Multiplicative Turbulent Cascades," *J. Geophys. Res.*, 92, 9693–9714, 1987.
Schertzer, D., and S. Lovejoy, "Multifractal simulations and analysis of clouds by multiplicative processes," *Atmos. Res.*, 21, 337–361, 1988.
Schertzer, D., and S. Lovejoy (Eds.), *Scaling, Fractals and Non-Linear Variability in Geophysics*, Kluwer, Hingham (Mass.), 1991.
Sèze, G. and L. Smith, "On quantifying the geometry of statocumulus cloud fields," in *IRS'88: Current Problems in Atmospheric Radiation*, edited by J. Lenoble and J. F. Geleyn, pp. 168–170, A. Deepak, Hampton, Va., 1989.
Sornette, D., "Waves in random media - I: Weak disorder regime," *Acustica*, 67, 199–215, "Waves in random media - II: Coherent Effects and strong disorder regime," *Ibid.*, 67, 251–265, "Waves in random media - III: Experimental situations," *Ibid.*, 68, 15–25, 1989.
Stephens, G. L., "Radiative Transfer in Spatially Heterogeneous, Two-Dimensional Anisotropically Scattering Media," *J. Quant. Spectrosc. Radiat. Transfer*, 36, 51–67, 1986.
Stephens, G. L., "Radiative transfer through arbtrarily shaped media, I: General solution," *J. Atmos. Sci.*, 45, 1818–1835, 1988*a*.
Stephens, G. L., "Radiative transfer through arbtrarily shaped media, II: Group theory and closures," *J. Atmos. Sci.*, 45, 1836-1838, 1988*b*.
Stephens, G. L., and R. W. Preisendorfer, "Multimode radiative transfer in finite optical media, II: Solutions," *J. Atmos. Sci.*, 41, 725–735, 1984.
Stephens, G. L., and C. M. R. Platt, "Aircraft observations of the radiative and microphysical properties of stratocumulus and cumulus cloud fields," *J. Climate Appl. Meteor.*, 26, 1243–1269, 1987.

Stephens, G. L., and S. Tsay, "On the Cloud Absorption Anomaly," *Q. J. R. Meteorol. Soc.*, 116, 671–704, 1990.

Stephens, G. L., P. M. Gabriel, and S.-C. Tsay, "Statistical radiative transfer in one-dimensional media and its application to the terrestrial atmosphere," to appear in *Trans. Theory and Stat. Phys.*, 1991.

Tanré, D., M. Herman, and P.Y. Deschamps, "Influence of the background contribution upon space measurements of ground reflectance," *Appl. Opt.*, 20, 3676–3684, 1981.

Tatarski, V. I., *Wave Propagation in a Turbulent Medium*, transl. from russian by R. A. Silverman, McGraw Hill, 1961. (Reprinted by Dover, New York, NY, 1967.)

Tessier, Y., S. Lovejoy, and D. Schertzer, "Universal Multifractals: Theory and Observations for Rain and Clouds," submitted to *J. Appl. Meteo.*, 1992.

Titov, G. A., "Solar radiation transfer modeling for cumulus cloud conditions," *Izv. Acad. Sci. USSR Atmos. Oceanic Phys.*, 15, 432–436, 1979.

Titov, G. A., "Statistical characteristics of short wavelength solar radiation in the presence of cumulus cloudiness," *Izv. Acad. Sci. USSR Atmos. Oceanic Phys.*, 16, 500–505, 1980.

Titov, G. A., "Statistical description of radiation transfer in clouds," *J. Atmos. Sci.*, 47, 24–38, 1990.

Tsay, S.-C., and K. Jayaweera, "Characteristics of Arctic Stratus Clouds," *J. Climate Appl. Meteor.*, 23, 584-596, 1984.

Twomey, S., and T. Cocks, "Spectral reflectance of clouds in the near infrared: Comparisons of measurements and calculations," *J. Meteorol. Soc. Jpn.*, 60, 583–592, 1982.

van Blerkom, D., "Diffuse reflection from clouds with horizontal inhomogeneities," *Astrophys. J.*, 166, 235–242, 1971.

van Kampen, N. G., "Stochastic differential equations," *Physics Reports (Phys. Lett. C)*, 24, 171–228, 1976.

Welch, R. M., S. Cox, and J. Davis, "Solar radiation and clouds," *Meteorol. Monogr.*, *39*, 1980.

Welch, R. M., and W. G. Zdunkowski, "The effect of cloud shape on radiative characterisitics," *Contrib. Atmos. Phys.*, 54, 482–491, 1981*a*.

Welch, R. M., and W. G. Zdunkowski, "The radiative characteristics of noninteracting cloud fields, I: Parameterization for finite clouds, II: Calculations for cloud fields," *Contrib. Atmos. Phys.*, 54, 258–285, 1981*b*.

Welch, R. M., "Radiation calculations based upon detailed microphysics," in *Proceedings of the 5th Conference on Atmospheric Radiation*, pp 505–506, Am. Meteorol. Soc., Baltimore, 1983.

Welch, R. M., and B. A. Wielicki, "Reflected fluxes for broken clouds over a Lambertian surface," *J. Atmos. Sc.*, 46, 1384–1395, 1988.

Welch, R. M., K. S. Kuo, B. A. Wielicki, S. K. Sengupta, and L. Parker, "Marine stratocumulus cloud fields off the coast of southern California observed by Landsat imagery, 1: Structural characteristics," *J. Appl. Meteor.*, 27, 341–362, 1988*a*.

Welch, R. M., S. K. Sengupta, and K. S. Kuo, "Marine stratocumulus cloud fields off the coast of southern California observed by Landsat imagery, 2: Textural analysis," *J. Appl. Meteor.*, 27, 363–378, 1988*b*.

Weinman, J. A., and M. Masutani, "Radiative transfer models of the appearance of city lights obscured by clouds observed in nocturnal satellite images," *J. Geophys. Res.*, 5565–5572, 1987.

Weinman, J. A., and P. N. Swartztrauber, "Albedo of a striated medium of isotropically scattering particles," *J. Atmos. Sci.*, 25, 497–501, 1968.

Wendling, P., "Albedo and reflected radiance of horizontally inhomogeneous clouds," *J. Atmos. Sci.*, 34, 642–650, 1977.

Wiscombe, W. J., R. M. Welch, and W. D. Hall, "The effects of very large drops on cloud absorption, 1: Parcel models," *J. Atmos. Sci.*, 41, 1336–1355, 1984.

Yano, J.-I., and Y. Takeuchi, "Fractal dimension analysis of horizontal cloud pattern in the intertropical convergence zone," in *Scaling, Fractals and Non-Linear Variability in Geophysics*, edited by D. Schertzer and S. Lovejoy, Kluwer, Hingham, Mass., 1991.

Chapter One

TECHNICAL PRELIMINARIES, DEFINITIONS AND CONVENTIONS

Succinct Overview of this Thesis: We are primarily concerned with the effects of spatial variability on the radiative properties of clouds in the visible part of the EM spectrum (wavelengths ≈0.5 μm, where absorption is negligible) associated with BCs that describe collimated illumination of the (top) boundary. We will be comparing the predictions of different radiation transport theories when applied to various inhomogeneous cloud models (in particular, of the scale invariant type), and find that systematic differences arise from one theory to another, on the one hand, and w.r.t. the very special case of homogeneity, on the other hand. In agreement with Cannon [1970], we view "channeling" as one[1] of the basic mechanism underlying inhomogeneous radiative transport in presence of multiple scattering. In the following, we will define as precisely as possible the terms underlined in the above (respectively, sect. 1.4, 1.3, 1.2, 1.1, and 1.5), right after setting our bearings (sect. 1.0).

1.0. Orientation Conventions

As mentioned above, there is generally a privileged direction in our radiation transport problems: that of the incoming radiance. This will allow us to define a "top" (hence a "bottom") as well as a vertical direction (hence horizontal planes). We will sometimes need to differentiate the vertical and illumination directions; in such cases however, the geometry of the cloud must have some very obvious anisotropy (e.g., the infinite horizontal extension obtained by periodic replication of a finite unit cell). When axes become necessary, we will take the z-axis as vertical, oriented downwards (i.e., following the incoming flux) and coordinates originating at cloud top; this choice is common practice, but not universal, in radiative studies. We will orient the coordinates on our unit sphere, i.e., (propagation) direction space, using the same convention: that is, its "north pole" is at nadir (in the direction of the positive z-axis). This last choice is by no means universal in the radiative literature, it however seems to be more consistent with the kinetic theory foundations of radiative transfer (detailed in app. E): there is no reason to reorient the axes when going from the position part to velocity part of the photon's phase space.

1.1. (Optical) "Medium," or (Cloud) "Model"

For the purposes of radiation studies (at visible wavelengths), we view a "cloud" as a distribution of scatterers within a given region (M) of d-dimensional space ($\Re^d$). This distribution is best described mathematically as a density function of position (**x**) in M (or, more simply, a density "field"): say, $\rho(\mathbf{x})$ with $\mathbf{x} \in M$. The pair $\{\rho(\cdot),M\}$ constitute what we will call the (optical) medium or cloud model and it obviously has two basic attributes: a "support" M (equivalently, a "shape" or "boundary" ∂M, in standard topological notation) and a "structure" described by the non-negative function $\rho(\cdot)$.

The "support" can be either infinite, semi-infinite, or bounded. Infinite media must necessarily be invested with internal sources and, in such cases, we are generally interested in the temporal evolution of a sudden burst of radiant energy and the ensuing random walk statistics of the energy carriers (that we will somewhat abusively call "photons," see app. E and B). The semi-infinite medium can be steadily illuminated at the boundary that lies at finite range and we can ask about its reflection (or "albedo") properties. Bounded media come in two categories: vertically bounded (and, implicitly, horizontally unbounded), and horizontally bounded (and, again implicitly, vertically bounded too). In practice, members of the former class are usually made of an infinite number of replicas of a given member of the latter class laying one next to the other (the horizontal projection of M must then be a shape that tiles $\Re^{d-1}$) and the radiation flows freely from one unit cell to the next.[2] Notice that this arrangement could provide the kind of anisotropy needed to define a "vertical" independently of illumination. We will sometimes talk about "cyclic" (versus "open") horizontal BCs. This is however somewhat misleading since the difference is one of support, not one of BCs at all—in the sense of, say, using the Dirichlet-type versus the mixed-type or a simple change of illumination angle. This possible source of confusion must be clarified from the outset because we are interested in separating the radiatively important and unimportant factors and, with a few subtleties to be explored further on, "support" and "BCs" are in different categories (respectively, important and unimportant[3]).

The "structure" of the medium can be either homogeneous (constant ρ) or inhomogeneous (variable ρ). It is normal practice to require ∂M to be convex and almost everywhere smooth (see app. A) which is not a limitation within the framework of inhomogeneous media because of the option of using null density values. In fact, we can embed a homogeneous medium with an almost nowhere differentiable hence (or otherwise) non-convex boundary in a region with an outer smooth and convex boundary containing complementary empty and filled sub-regions; we thus create a special class of inhomogeneous media that, as it turns out, can teach us something (give us hints) about variability effects in general (see chap. 2 for details). *Bone fide* inhomogeneous media can be either deterministic or stochastic. In the former case, some (hopefully) simple rule for constructing the medium is sufficient (see sect. 4.2 for an example). In the latter case, all of its n-point statistics should, in principle, be specified; the better known 2-point statistic is the auto-correlation function (see sect. 4.4 for details). In practice however, a set of rules that precisely describes the role of randomness is sufficient (see app. C, chap. 2 and chap. 6 for examples); one can always determine the said statistics from the rules anyway (at least numerically). When dealing with stochastic cloud models we will be interested in ensemble-average radiative or structural properties; we will denote such averages (over the "disorder") by angular brackets: $<\cdot>$. Stochastic, deterministic and even homogeneous (but somehow asymmetrical) media all require spatial averages to be taken, for instance, to obtain total mass or bulk responses; we denote these averages with bars: $\bar{\cdot}$. We will meet yet another kind of stochasticity in sect. 1.3 below which is more fundamental since already present in homogeneous (or otherwise deterministic) optical systems.

Independently of the deterministic/stochastic dichotomy, inhomogeneous media come in many flavors ranging from regular, "smoothly varying" (differentiable) ρ-fields to their "extremely variable" (multifractal) counterparts, with the intermediate categories of "irregular" media (non-differentiable but possibly continuous on average) or of "singular" media which can exhibit an arbitrarily wide range (or ratio) of ρ-values but lack the cascade-type (hence highly correlated) structure of multifractals. We will be investigating generic examples from most of these broad categories. Another important factor in inhomogeneous cloud models is the range of scales involved in the variability and just how that affects the various statistics of the density field.

1.2. "Scale Invariant," or "Scaling" (both Simple- and Multiple-)

These adjectives have both extremely broad and very narrow meanings. They can be used to describe anything vaguely related to fractal structures and (usually statistical) power law relations, i.e., they describe systems that exhibit no characteristic length; they can also be applied to families of objects (sets) whose members are exactly self-similar images of one another, i.e., the family is invariant under change of scale ($x \to \lambda^{\pm 1}x$, $\lambda \geq 1$); they can also mean both together ... as in the title of this thesis. Connections with dimensional analysis and similarity theory are obvious and examples are provided in sect. C.1 and C.6. As mentioned above, we are interested in systems that are invariant over a wide range of scales; in theory (e.g., chap. 5), this range can be infinite ($\lambda \in [1,\infty[$) and, in practice (e.g., chap. 2, 4 and 6), this range remains finite but is made as large as possible ($\lambda \in [1,\Lambda]$ with $\Lambda \gg 1$).

In the most interesting (and contemporary) acceptance of scaling concepts, they are applied to fields (rather than sets) and the variability of (range of values taken by) the field quantity is directly related to the range of scales involved; we can distinguish two types of scaling behaviour: simple- and multiple scaling. In simple scaling models, we are usually more interested in absolute differences ($|\Delta\rho|$'s) taken over a scale ($\Delta x = |\Delta x|$) than in the field value itself; they are typically such that

$$|\Delta\rho|_{\lambda\Delta x} \stackrel{d}{=} \lambda^{H} |\Delta\rho|_{\Delta x} \tag{1.0}$$

where "$\stackrel{d}{=}$" means equal in distribution. These models are said to have "stationary increments," and clearly they must be constructed by some "additive" procedure, possibly in Fourier space. We notice that a single exponent arises (some examples are provided in sect. C.2 where the fractal interpretation of H is discussed). In contrast, multiple scaling models have a different scaling exponent for every threshold (λ^{γ}, $\gamma \in \Re$) which is best expressed as

$$\text{Prob}\{\rho_{\lambda} \geq \lambda^{\gamma}\} \sim \lambda^{-c(\gamma)} \tag{1.1}$$

where "~" is used to absorb non-exponential (prefactor) functions of γ as well as slowly varying (log) functions of λ. We refer the reader to sect. C.2–5 for the nomenclature associated with γ and $c(\gamma)$ as well as several mono- and multifractal examples, all constructed with "multiplicative" procedures.

1.3. (Physical) Radiation "Transport Model," or "-Theory"

1.3.1. Kinetic-Type Theories

This expression is used to describe any well-defined way of associating radiation fields to density fields. The "way" usually consists of equations that express some kind of physical conservation law or balance between different features of the radiation field and this necessarily involves the density field, along with the pertinent optical parameters (typically related to elementary cross-sections), plus the appropriate BCs. In Preisendorfer's [1976] words, we want to relate a cloud's "inherent" properties (i.e., its structural and optical parameters) to its "apparent" properties (i.e., the source dependent radiation fields). We are mainly interested in "general purpose" radiation transport theories (i.e., that can accommodate any given density field) and we know of the following four categories that fall into two groups of two. We will proceed from the most general (and difficult to deal with) to the most simple (and easy to use).

- Continuous angle (CA) radiative transfer. This basic model was pioneered by Schwartzchild [1914], standardized by Chandrasekhar [1950], and now routinely connected with particulate-based kinetics, centered on Boltzmann's equation [see, e.g., Mihalas, 1978], but its relation to mainstream optics is still unclear: see Ishimaru [1975] and Barabanenkov [1969] for connections with scalar wave theory, Wolf [1976] and Harris [1965] with EM wave theory. The formal connection with kinetic theory and stochastic processes (app. E) is the most useful conceptually anyway since it firmly establishes the central role of the photon's free path (f.p.) distribution hence, in the inhomogeneous case, the spatial- and/or ensemble-distribution of f.p.-distributions (see sect. A.2). Recall that in homogeneous situations everything is determined by the m.f.p. (and ∂M), but such is not the case in inhomogeneous situations where the m.f.p. becomes a notion which is only local (and is therefore useless by itself). The most interesting (but difficult) problems involve multiple scattering and we are then dealing with random walks (RWs) in random environments (or, at least, environments where the m.f.p. is a non-constant function of space). We will see that these two sources of stochasticity—one additive in nature, one multiplicative (in the multifractal case)—interact in a highly non-trivial fashion. In order to unravel this interaction as best we can, we need a separate notation for the RWs and we have adopted the mathematician's "expectancy:" $\mathsf{E}(\cdot)$. Notice that the RWs are subordinated to the spatial disorder; so $\langle \mathsf{E}(\cdot) \rangle$, or $\overline{\mathsf{E}(\cdot)}$, makes sense but not $\mathsf{E}(\langle\cdot\rangle)$, nor $\mathsf{E}(\bar{\cdot})$; examples of how the different sources of stochasticity/variability can be combined are provided in sect. A.2 (and an application is found in sect. 4.4). The basic construct of CA transfer is the field $I_{\mathbf{u}}(\mathbf{x})$ ($|\mathbf{u}|=1$, $\mathbf{x} \in M$) of radiance propagating into direction $\mathbf{u}$ and we will present (in sect. A.3) a reading of the transfer equation as a balance between $\mathbf{x}$-gradients and $\mathbf{u}$-anisotropy in $I_{\mathbf{u}}(\mathbf{x})$, on the one hand, and $\rho(\mathbf{x})$, on the other hand. We also refer the reader to app. A for the other CA idiosyncrasies related to other parts of this thesis (spherical harmonic expansions, phase functions, similarity, BCs, and various operational definitions of albedo versus transmittance).

- <u>Discrete angle (DA) radiative transfer.</u> This approach can be traced back to Schuster's [1905] two-flux theory, possibly the first theoretical paper ever on multiple scattering. Later generalized by Chu and Churchill [1955] to a six-beam model, the idea was systematically explored by Lovejoy and his co-workers in the late '80s [Gabriel *et al.*, 1986; Gabriel, 1988; Lovejoy *et al.*, 1990; Davis *et al.*, 1990a,b]. DAs are merely a special case of CAs (with δ-like phase functions and radiances) where only finite families of beams are coupled by the scattering processes. The simplification is very welcome when the focus is turned towards the effects of inhomogeneity since at least modest analytical progress is possible (chap. 3) while numerical speed-up is outstanding (app. B, chap. 4 and 6).

In sect. 4.1–2, we make sure that DAs and CAs are sufficiently similar (in the scaling sense of the word) to be considered in the same class of transport models that we will refer to generically as transfer (bearing in mind that they are basically kinetic theories).

1.3.2. Diffusion-Type Theories

Notice our insistence on using "transport" as the most general expression and "transfer" as a more specific case, although we will see that either of the two above models contains both of the two remaining models as special cases, formal limits and/or approximations. We must however beware that, in the literature, "diffusion" is often referred to as "transfer" ... and sometimes vice-versa. This can be partially justified in the more homogeneous applications where all of the theories agree pretty well (e.g., chap. 2, last example in §2.3.4 excluded). In extremely variable media however, they systematically disagree (e.g., last example in §2.3.4, and sect. 4.2) and we are therefore of the opinion that they should be viewed as independent transport theories, each one interesting in its own right. Notwithstanding, the connections between the various theories are also interesting to explore since they help us to understand the reasons for their (dis)agreement as a function of the structural properties of the media (see sect. D.1, D.6, 2.3 and 4.4).

- Diffusion. This is the well-studied "hydrodynamic" limit of kinetic (hence CA transfer) theory (see sect. D.0–1 for a review); in the context of radiation transport, the original idea goes back to Eddington [1916] in homogeneous systems, and Giovanelli [1959] in inhomogeneous systems. Interestingly, the diffusion model can also be reached via DA formalism [Lovejoy *et al.*, 1990; Davis *et al.*, 1990b, 1991; or sect. 3.3] and this is done by operating on the phase function, not on the **u**-distribution of the radiance field (as in the standard approach) since this option has already been implicitly exploited by putting oneself in the DA framework. This is a much simpler model that has attracted far more attention from the physics community at large, probably because it calls for a single scalar field $U(\mathbf{x})$ ($\mathbf{x} \in M$) that represents (radiant energy) density; at any rate, we systematically exploit it in chap. 2 to investigate the basic effects of inhomogeneity. The key concept here is (radiative) "diffusivity" that we will denote $D(\mathbf{x})$ and which is the diffusion theoretical counterpart of both m.f.p.'s and phase functions in (CA or DA) transfer (see sect. D.3 for the connection with correlated RWs). The gradient-anisotropy balance is reflected in the characteristic Fickian law or "constitutive" relation: (net radiative) flux is given by $\mathbf{F} = -D\nabla U$ and, in absence of absorption, we of course have $\nabla \cdot \mathbf{F} = 0$. We will see (chap. 2–4) that, generally speaking, the diffusion and transfer theories make different predictions for transport through extremely variable media but, we maintain a keen interest in both theories not only for theoretical reasons but observational ones also; indeed, King *et al.* [1990] have recently produced strong evidence that diffusion may apply quite well in typical cloud decks (see sect. D.2 for a detailed discussion of their findings). We refer the reader to the final sections of app. D for the standard similarity properties, the non-standard BCs (that should be used in radiative applications), the RWs of "diffusing" particles (not to be confused with photons!), and examples from radiative- and other homogeneous and inhomogeneous applications.

- "Independent pixels" (IPs). This is certainly the simplest possible model for inhomogeneous radiation transport since all higher-dimensional effects are neglected: the radiative flux lines are constrained to be vertical. This can be done in different ways in all of the above theories: CAs call for internal vertically oriented boundaries that are perfect Fresnel reflectors (followed by homogenization inside each sub-domain), diffusion calls for similarly oriented boundaries that are insulating ($F_\perp$=0), and DAs simply call for a phase function with no side-scattering, only in the forward/backward directions. This last approach to IPs yields d uncoupled one-dimensional diffusion equations, one for each spatial direction (although only the vertical one is excited with our usual BCs), so this is essentially another, ultra-simplified diffusion-type theory. A certain number of radiatively independent columns are thus defined, each equivalent to a homogeneous plane-parallel medium, and an analytical solution can therefore be obtained for each one; the IP solution is simply the spatial average of these "pixel-wise" partial solutions. Because of the nonlinear—convex, for transmittance—dependance of the plane-parallel result on (optical) thickness, this last (averaging) operation alone is enough to guarantee a systematic difference between the IP solution and the one that consists in neglecting internal structure altogether (see sect. 3.3 for mathematical details and D.5 for electrical parallels). In practice (computational effort), IPs constitute a kind of compromise between the complete homogenization of the medium and the full-blown d-dimensional inhomogeneous transport; we shall not be surprized to see that this is exactly where the IP answer (say, for transmittance) lies quantitatively also: viz., in between the (analytical) homogeneous plane-parallel result and the (numerical) transfer or diffusion result, at least if the total mass is held constant (see chap. 2–3 for the theory, and chap. 4 and 6 for illustrations). The name that we have retained for this approach was coined by Cahalan [1989] in connection with Landsat imagery simulation with the help of a multifractal cloud model. The technique has however been used in many other circumstances, for its sheer simplicity, e.g., in GCM radiation routine calls, going from one grid point to the next, but also by using the "cloud fraction" concept inside each cell; in absence of further information on sub-cell variability, this use of IPs is more-or-less justified. For an application of IPs to *in situ* cloud radiation measurements, see also King *et al.* [1990]; in this case, the method is far less justified due to the observed variability (see sect. D.2 for more details).

We have listed the four transport theories by order of increasing "user-friendliness," as measured by the degree of understanding we have of inhomogeneity effects which goes more-or-less hand-in-hand with the amount of analytical progress to date. Furthermore, we notice that the number of ways a given physical transport model can be reached is in direct proportion to this (rather subjective) notion, as well as the degree of approximation (using CAs as the benchmark). In fig. 1.1 we present graphically our complete constellation of transport theories with all of the above mentioned inter-connections.

We have deliberately excluded from the above discussion all "non-general purpose" radiation transport theories which can only handle a specific kind of medium. Some of these will however be discussed in relevant part of the thesis (e.g., chap. 4). Amongst these approaches to the multiple scattering radiation problem, we could mention the work of Lovejoy *et al.* [1989] and Gabriel *et al.* [1990] who adapted (real space) "renormalization" ideas to DA transfer on grids; although the general idea may prove more useful, their method applies specifically to the deterministic monofractal medium studied in sect. 4.2 (as well as some less interesting homogeneous cases). Another example is the "mean field" theory developed by Avaste and Vaynikko [1974], Titov [1990], Boissé [1990]—the two latter relying heavily on the former—that applies only to transfer through exponentially decorrelating (hence generally[4] non-scaling) binary mixtures in plane-parallel geometry.

1.4. (Radiative) "Response," or "-Property," and its Scaling

We will use these expressions to designate some simple, scalar measure of the radiation field that is excited by external illumination at a boundary: albedo (or reflectance), transmittance (direct or total), and absorptance (on occasions). The main thrust of this thesis is to investigate the systematic effects of inhomogeneity on these "bulk" properties (which we will also call integrated-, unresolved-, global-, overall-, mean-, or spatially averaged-) in presence of multiple scattering but no absorption. With such tools, we are therefore addressing the cloud "albedo paradox" problem, rather than the cloud "absorption anomaly" problem or the problems related to the spatial variability of radiation fields (see however chap. 6 for a glimpse at simulated fields and sect. 7.3 for our ideas on these exciting subjects). Finally, we can formulate a little more precisely our basic radiative scaling relation (0.1): if there are no characteristic scales in the system (in particular, this implies[5] vanishing absorption), we will have

$$\langle |F_\lambda - F_\infty| \rangle \sim \lambda^{K_F} \tag{1.2}$$

when $\lambda \gg 1$. If furthermore, K_τ in

$$\langle \tau_\lambda \rangle \sim \lambda^{K_\tau} \tag{1.3}$$

is positive, then we are in the thick cloud regime and v_F in eq. (0.1) is equal to $-K_F/K_\tau$. Otherwise, we are in the thin cloud regime, where linear responses can be expected: $v_F=-1$ in (0.1) and $K_F=K_\tau$ in (1.2–3). See chap. 5 for examples of both types of small scale limit.

1.5. (Cannon's Radiative) "Channeling" and/or (Stephens') "Mode-Coupling"

1.5.0. Cannon's Original Idea, in Kinetic Theoretical Jargon and Physical Space

Our main objectives are to define and clearly as possible the effects of density fluctuations on the flow of radiation: (a) on the mean flow (i.e., the previous entry), and (b) on its local features. Generally speaking, the answer to question (a) is that mean fluxes are systematically enhanced but to different extents for the various transport theories. A possible approach to question (b) is to try to identify a basic, universal mechanism by which the radiation fields react to a perturbation in the density field, using the simplest possible situations and seeing just how far we can follow the lead into the more complex cases. With this strategy in mind, we propose "channeling" as the basic radiative reaction to inhomogeneity. This expression was coined by Cannon [1970] and seems to have gained acceptance in the astrophysical literature [Jones and Skumanich, 1980]. Cannon was investigating numerically spectral line transfer through some deterministic two-dimensional arrangement of variable optical density (and/or other optical parameters); as usual in line transfer, he was considering a semi-infinite medium. He noticed the tendency of the radiation to flow 'into the less opaque regions by increased scattering in the regions of greater opacity.' Just how this very natural phenomenon connects with question (a), which corresponds to a very different type of support and source distribution than Cannon's, will be demonstrated analytically within the framework of diffusion in chap. 2 and illustrated with numerical results for DA transfer in chap. 6. For the moment, we will simply clarify Cannon's definition as best we can in the languages adapted to each level in our hierarchy of radiation transport theories, starting with the kinetic-type.

CA transfer is indeed the tool that Cannon himself was working with and his verbatim captures the most fundamental aspect of inhomogeneous transfer theories, namely, the spatially variable free path (f.p.) distribution: 'increased scattering' means smaller f.p.'s, conversely we expect longer f.p.'s in the more tenuous regions but, interestingly, the effects do not cancel on average due to the nonlinearity of f.p.'s probability distribution function with respect to optical density (which is directly related to the astrophysicists' 'opacity,' see sect. A.1). In homogeneous media, f.p.'s are exponentially distributed; in sect. A.2, we show (using characteristic function theory) that average f.p. distributions in inhomogeneous media will always be wider and in chap. 5 we look at the special case of multifractal media and indeed we find algebraic laws. There is however another important and complementary aspect to kinetic "channeling" that is related to the angular part of the transfer problem. Schematically, we can say that the photons are painfully random walking in dense regions and freely streaming in the tenuous ones, from the boundary of one denser domain to another. At these interfaces, we can expect stronger **u**-anisotropy (pointing towards the less dense region) thus driving enhanced **x**-gradients, fluxes away from the dense region appear; see §A.3.3 for an argument for the **u**-anisotropy/**x**-gradient connection from first principles. Inside the denser regions, we can expect more **u**-isotropic (diffusion-like) radiance fields to prevail due to the enhanced scattering (shorter photon f.p.'s). Finally, we expect no fundamental difference to arise when going from CA to DA formulations, the **u**-distribution becomes discrete—it is carried by a finite sub-set of the unit sphere—but simple measures of anisotropy can nevertheless be defined; see, e.g., §3.3.2.

1.5.1. Stephens' Ideas, using Fourier Space and Spherical Harmonic Language

Adopting the slightly more abstract language of spherical harmonic analysis, we can describe **u**-anisotropy quantitatively by adding weight to the higher order modes of the radiance field, viewed as a **u**-distribution. In the following, we will argue that any kind of horizontal fluctuation in the density field will break the spatial symmetry that prevails at homogeneity. We will closely follow the analysis of Stephens [1986] who uses a Fourier space approach to inhomogeneous transfer; accordingly, we will refer to the symmetry-breaking process as "mode-coupling" throughout this thesis (it is used in particular in sect. 2.3). In essence, we view "mode-coupling" as the Fourier space/spherical harmonic counterpart of "channeling," which has natural physical space/unit sphere overtones.

In his basic [1986] paper, Stephens talks about a 'horizontal divergence term' that appears in the horizontally Fourier transformed transfer equation once it is made to look as much as possible like the classical plane-parallel (i.e., 1D) equation. This new term formally looks like an source/sink term but it has a characteristic $\sqrt{-1}$ factor (it is best called a "pseudo-source/sink" term). Furthermore, it is a Fourier space convolution (associated with a simple product in physical space) of density with radiance; if horizontal homogeneity prevails (a δ-function at the origin in the corresponding Fourier space), then the more symmetric 1D formalism is identically retrieved. Upon spherical harmonic analysis of the directional distribution of radiance, Stephens [1988a] notices that[6] 'unfortunately, the [azimuthal] ϕ dependence does not decouple in the more general 2D and 3D transfer problems' due to this same term. The symmetry breaking mechanism is as follows: under the combined mathematical effects of the convolution product and the $\sqrt{-1}$ factor, the <u>non-vanishing wavenumber (horizontal) Fourier modes of the density field will excite non-axisymmetric spherical harmonic modes</u> in direction-space at all scales (wavenumbers), including the largest (vanishing wavenumber). In particular, this means that the overall (spatially averaged) flux will generally be affected, although just how (much) and what parameters of the problem play a role are non-trivial questions that should be the object of future research.

We tentatively summarize this whole Fourier space/spherical harmonic picture with the expression "mode-coupling" although we do not want this to be confused with Stephens' [1988b] description of a hierarchical coupling of scales (spatial Fourier modes) leading to a closure problem. We in fact use a (numerically-based) finding of Stephens' [*ibid.*] to show (in §2.3.2) that the above mentioned effect on the overall flux is apt to be a boost under quite general circumstances, thus confirming our (§2.3.1) diffusion theoretical analysis of "channeling" in physical space.

1.5.2. Implications for Diffusion Theory

Diffusion is a special limit of both CA- and DA transfer, corresponding to radiation fields that can modelled with an "isotropic" component (J) and "dipole" component (**F**), it is therefore quite easy to find the implications of "channeling" in this context. The flux **F** tells us about the mean direction and intensity of the flow of the radiation, as controlled by the multiple scattering (which is taken for granted in this approach, see sect. D.1–3). **F** enhanced by the occurrence of higher radiative diffusivity D (lower density ρ) and/or stronger gradients ($|\nabla J|$), but the second factor is of less interest to us because it is also at work in homogeneous situations. "Channeling" can therefore be described graphically in this context: the pattern of the **F**-lines along with the density field tell the whole story. Fig. 1.2 illustrates the two basic situations of a hypothetical average radiative flow colliding with a positive and a negative density fluctuation. In the former case, the lines are repelled by the dense region (where F decreases); in the latter case, they are attracted into the tenuous region (where F increases). Notice that the total number of lines (hence the mean flux) has increased when going from homogeneity to inhomogeneity; this is a non-trivial effect (investigated in sect. 2.3) that is guaranteed to arise when the total mass is kept constant.

1.5.3. Position with respect to the "Independent Pixel" Approximation

Although some systematic nonlinear effects remain that are traceable to Jensen's inequality for convex functions in functional analysis (see sect. 3.4 for details), the simplicity of the IP approach stems entirely from the postulate of "non-channeling" (only vertical **F**-lines are allowed) and indeed higher dimensionality plays a fundamental role in both of the above descriptions. Indeed, a whole sequence of events is initiated if the IP constraints described above are suddenly relaxed (e.g., side-scattering is "turned-on" in DAs). As stated above (and demonstrated in various ways in various parts of this thesis), the new steady-state configuration will obviously include non-vertical (possibly very convoluted) **F**-lines and an increased overall transmittance, which is proportional to the mean (vertical component) of **F**. In this respect, we can use IPs as a benchmark and define an overall measure of "channeling" as the difference between the IP response and its CA, DA, or diffusion counterpart. In chap. 6, we turn from unresolved- to fully resolved radiation fields in (a specific realization of) a multifractal cloud model, only to find our above description of the basic inhomogeneous transport mechanism confirmed. Other interesting and "channeling-related" effects are also observed; for instance, the powerful smoothing (via multiple scattering) of the features of the density field that increases along with the "level" of "channeling," defined as the "DA minus IP" difference in the (bulk) transmittance. This tells us that the thicker the cloud, the more scattering occurs, the more "channeling" is enhanced (a prerequisite for "anomalous" scaling to occur) but also, and somewhat paradoxically, the more bland the features of the apparent (emerging, remotely measurable) radiation field.

1.5.5. Summary

It is fair to say that "channeling" is above all a pattern, a concept which shows different facets of itself when examined under the different theoretical "spot-lights," as described in the above. We remark that all of the three descriptions we have provided in the above are perfectly compatible with one another, at the highest level in the hierarchy of transport theories: in transfer approaches, one has at once order-of-scattering statistics, flux vector fields and overall responses. In the future, we can expect more precise definitions to arise, or else the concept will evolve into one more precise, with a different name ... either way, we have gained insight. In final analysis, we have adopted the expression because it is intuitively appealing, it conjures up ideas of the fluid-like behaviour of the radiation: it "flows" around obstacles (dense regions), into "valleys" (defined by the more tenuous regions). This is what one expects from any macroscopic continuum-type theory, in sharp contrast with wave-like behaviour that characterizes a microscopic (say, EM) theory of matter-radiation interaction.[7] The fundamental roles of higher dimensionality and of nonlinearity are stressed by this analogy but it should not be pushed to far—or rather, there are subtleties. For instance, the "nonlinearity" is not an attribute of the radiation field itself, the basic equations are linear in this quantity (unlike the Navier-Stokes equations (C.1–2) w.r.t. the Eulerian velocity field); instead, we are talking about the radiation-density coupling (not totally unlike the admixture-velocity coupling in eq. (C.42) for passive scalars which is linear).

[1]The other mechanism identified by Cannon [1970], a more-or-less efficient coupling of the radiation- to the temperature field, is irrelevant to the "albedo" (diffuse reflection/transmission) problems discussed throughout this thesis as it only applies to problems with a specific type of internal source.

[2]The same remark can be applied to the very first that we category mentioned, i.e., infinite media (then M must of course tile $\Re^d$).

[3]This statement applies to the mixed/standard BCs in the important case of horizontally extended atmospheres, the illumination angle problem is not really addressed in this thesis and we suspect it to be far more subtle (see, e.g., §5.4.3). Also, in the extreme case of quasi-grazing incidence, the scaling properties become more complex since the thin cloud fixed points (T_0 and R_0) are both 1/2, instead of 1 and 0, respectively.

[4]There are two scaling limits to this model: infinite and vanishing integral correlation length, corresponding respectively to homogeneity and white noise. Interestingly, the two lead to formally identical equations (hence trivial scaling behaviour).

[5]In homogeneous absorbing systems, one can define a characteristic optical scale (the so-called "diffusion" length scale) and expect associated exponential behaviour (see sect. D.3–4). This scale diverges with vanishing absorption (probability per elementary collision event), leaving only the overall size of the system as a relevant scale in the system to describe the resulting algebraic behaviour. Clearly the same is true in mildly inhomogeneous situations but just how much this picture carries over into extremely inhomogeneous multifractals is an interesting and ("absorption anomaly") relevant question for future research (see sect. 7.3).

[6]Stephens' use of the word 'unfortunately' is very interesting because, in effect, the pseudo-source/sink term will cause the inhomogeneous radiative transferist to have many a head-ache but at the same time it will make his life most interesting.

[7]As pointed out in app. E, the connection between these two aspects of matter-radiation interaction is highly non-trivial.

Bibliography for Chapter 1

Avaste, O. A., and G. M. Vaynikko, "Solar radiation transfer in broken clouds," *Izv. Acad. Sci. USSR Atmos. Oceanic Phys.*, 10, 1054–1061, 1974.

Barabanenkov, Y. N., "On the Spectral Theory of Radiation Transport Equations," *Sov. Phys. JETP*, 29, 679–684, 1969.

Boissé, P., "Radiative Transfer Inside Clumpy Media: The Penetration of UV Photons Inside Molecular Clouds," *Astron. Astrophys.*, 228, 483–502, 1990.

Cahalan, R. F., "Overview of Fractal Clouds," in *Advances in Remote Sensing (RSRM'87)*, Eds. A. Deepak *et al.*, 371–389, A. Deepak, Hampton (Va.), 1989.

Cannon, C. J., "Line Transfer in Two Dimensions," *Astrophys. J.*, 161, 255–264, 1970.

Chandrasekhar, S., *Radiative Transfer*, Oxford University Press, 1950. (Reprinted by Dover, New York, NY, 1960.)

Chu, M. C., and W. S. Churchill, "Numerical Solution of Problems in Multiple Scattering of Electromagnetic Radiation," *J. Chem. Phys.*, 59, 855–863, 1955.

Davis, A. B., P. Gabriel, S. Lovejoy, and D. Schertzer, "Asymptotic Laws for Thick Clouds, Dimensional Dependence - Phase Function Independence," in *IRS'88: Current Problems in Atmospheric Radiation*, Eds. J. Lenoble and J.F. Geleyn, pp103–106, Deepak Publ., 1989.

Davis, A. B., P. Gabriel, S. Lovejoy, D. Schertzer, and G. L. Austin, "Discrete Angle Radiative Transfer - Part III: Numerical Results and Atmospheric Applications," *J. Geophys. Res.*, 95, 11729-11742, 1990a.

Davis, A. B., S. Lovejoy, D. Schertzer, P. Gabriel, and G. L. Austin, "Discrete Angle Radiative Transfer Through Fractal Clouds," *Proceedings of the 7th Conference on Atmospheric Radiation*, San Fransisco (Ca.), July 23–27, Am. Meteorol. Soc., Boston, 1990b.

Davis, A. B., S. Lovejoy, and D. Schertzer, "Discrete angle radiative transfer in a multifractal medium," *S.P.I.E. Proceedings*, 1558, 37–59, 1991.

Eddington, A. S., "On the radiative equilibrium of stars," *Mon. Not. Roy. Ast. Soc.*, 77, 16–35, 1916.

Gabriel, P., S. Lovejoy, G.L. Austin, and D. Schertzer, "Radiative transfer in extremely variable fractal clouds," in *Proceedings of the 6th Conference on Atmospheric Radiation*, Williamsburg (Va.), May 12–16, Am. Meteorol. Soc., Boston, 1986.

Gabriel, P., *Discrete angle radiative transfer in uniform and extremely variable clouds*, Ph.D. thesis, 160pp, Phys. Dep., McGill Univ., Montréal, Québec, 1988.

Gabriel, P., S. Lovejoy, A. Davis, D. Schertzer, and G. L. Austin, "Discrete Angle Radiative Transfer - Part II: Renormalization Approach for Homogeneous and Fractal Clouds," *J. Geophys. Res.*, 95, 11717-11728, 1990.

Giovanelli, R. G., "Radiative Transfer in Non-Uniform Media," *Aust. J. Phys.*, 12, 164–170, 1959.

Harris, E. G., "Radiative Transfer in Dispersive Media," *Phys. Rev. B*, 138, 479–485, 1965.

Ishimaru, A., "Correlations Functions of a Wave in a Random Distribution of Stationary and Moving Scatterers," *Radio Science*, 10, 45–52, 1975.

Jones, H. P., and A. Skumanich, "The physical effects of radiative transfer in multidimensional media including models of the solar atmosphere," *Astrophys. J. Suppl.*, 42, 221–240, 1980.

King, M. D., L. F. Radke, and P. V. Hobbs, "Determination of the Spectral Absorption of Solar Radiation by Marine Stratocumulus Clouds from Airborne Measurements within Clouds," *J. Atmos. Sci.*, 47, 894–907, 1990.

Lovejoy, S., P. Gabriel, D. Schertzer, and G. L. Austin, "Fractal clouds with discrete angle radiative transfer," in *IRS'88: Current Problems in Atmospheric Radiation*, eds. J. Lenoble and J. F. Geleyn, pp. 99–102, A. Deepak, Hampton (Va.), 1989.

Lovejoy, S., A. B. Davis, P. Gabriel, D. Schertzer, and G. L. Austin, "Discrete Angle Radiative Transfer - Part I: Scaling and Similarity, Universality and Diffusion," *J. Geophys. Res.*, 95, 11699-11715, 1990.

Mihalas, D., *Stellar Atmospheres*, 2nd ed., pp. xvii+632, Freeman, San Francisco, CA, 1979.

Preisendorfer, R. W., *Hydrological Optics*, vol. 1, NOAA, PMEL, Hawaii, 1976.

Schuster, A., "Radiation Through a Foggy Atmosphere," *Astrophys. J.*, 21, 1–22, 1905.

Schwartzchild, K., "Diffusion and Absoption in the Sun's Atmosphere," *Sitzungsberichte der Köninglichen Preussichen Akademie der Wissenschaften*, pp1183–1200, 1914. (Reprinted in *Selected Papers on the Transfer of Radiation*, Ed. D.H. Menzel, Dover, New York, NY, 1966.)

Stephens, G. L., "Radiative Transfer in Spatially Heterogeneous, Two-Dimensional Anisotropically Scattering Media," *J. Quant. Spectrosc. Radiat. Transfer*, 36, 51–67, 1986.

Stephens, G. L., "Radiative transfer through arbtrarily shaped media, I: General solution," *J. Atmos. Sci.*, 45, 1818–1835, 1988*a*.

Stephens, G. L., "Radiative transfer through arbtrarily shaped media, II: Group theory and closures," *J. Atmos. Sci.*, 45, 1836-1838, 1988*b*.

Titov, G. A., "Statistical description of radiation transfer in clouds," *J. Atmos. Sci.*, 47, 24–38, 1990.

Wolf, E., "New Theory of Radiative Energy Transfer in Free Electromagnetic Fields," *Phys. Rev. D*, 13, 869–886, 1976.

Figure 1.1: Inter-connections of the various radiation transport models (or theories) used in this thesis. An $\rightarrow$ (or two) from theory X to theory Y means that "Y can be reached from X" as a special (or limiting) case; this can usually be interpreted as "theory Y approximates theory X" in certain circumstances, most of which are spelled out in the various parts of this thesis. Interestingly, each transport theory is uniquely characterized by the number of $\rightarrow$'s it receives and this number is a reasonable measure of its degree of "ease to handle" (on a scale from 0 to 3). The key describes the basic operations to be performed.

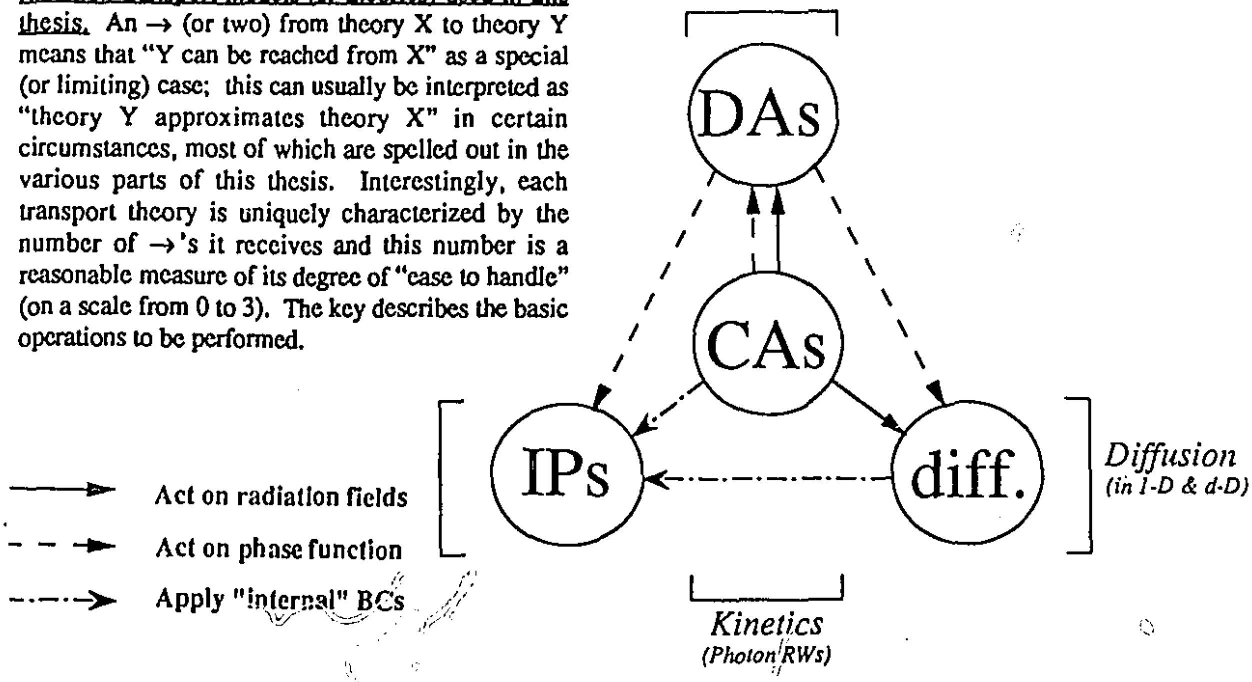

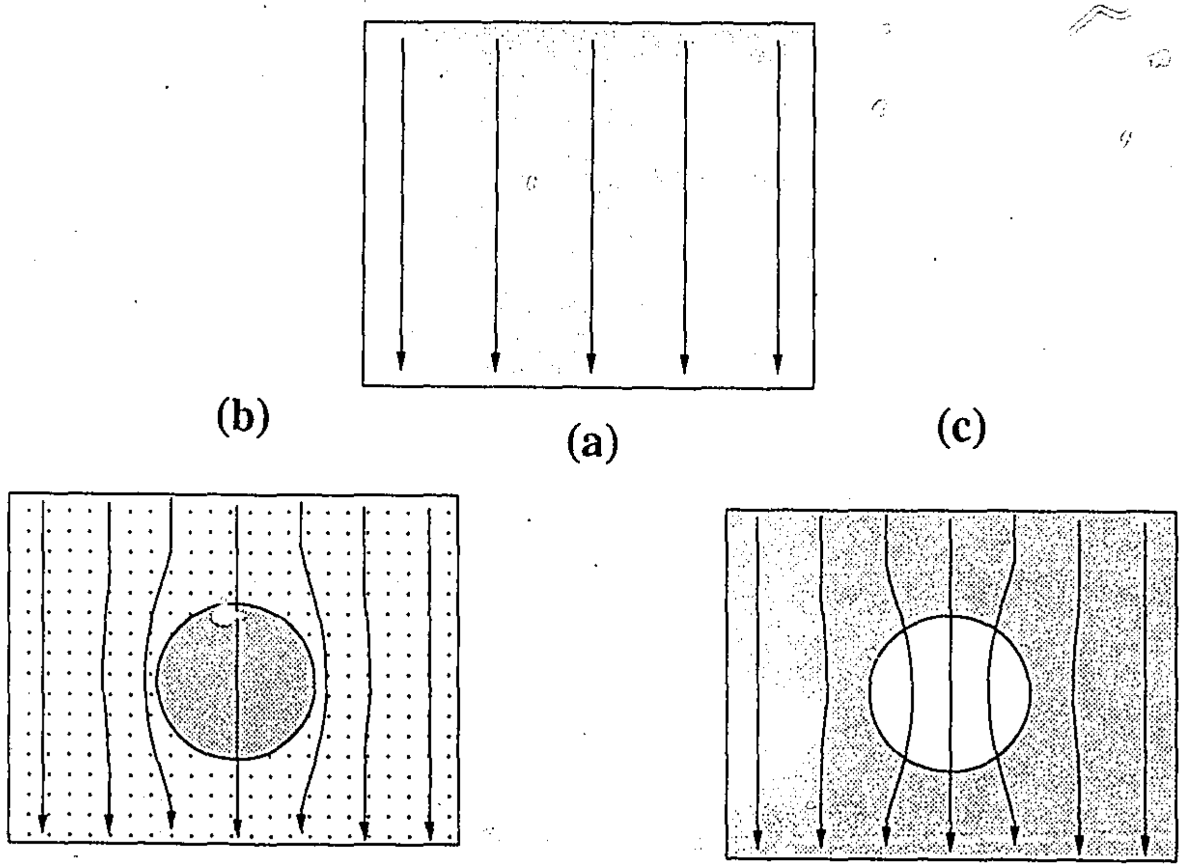

Figure 1.2: A schematic illustration of the two basic types of "channeling" event that can occur within the framework of diffusive (radiation) transport. (a) Reference flux-lines for a homogeneous medium. Notice that more lines are "pulled in" from the sides in the inhomogeneous cases, assuming the total mass is constant (this expresses the fact that the overall flux has increased). (b) The flux-lines tend to be expelled from a region of higher-than-average (optical) density, i.e., the flow is "deflected" by the obstacle. (c) In presence of a negative density fluctuation, the flux-lines are attracted into it, i.e, the flow is "funnelled" through the low density region.

Chapter Two†

The Basic Radiative Effects of Spatial Variability, The Diffusion Picture

Overview and Preliminary Remarks: In this chapter, we use the diffusion model of radiation transport to explore the most obvious effects of spatial variability on the overall radiative properties of clouds in the context of diffuse reflection/transmission via multiple scattering (m.s.). In all circumstances, we underscore the fundamental importance of net horizontal fluxes that play a key role in the ubiquitous phenomenon described by Cannon [1970] as "channeling," tentatively defined in the introductory chapter.

At this point, we take the term "spatial variability" in a rather broad sense. In sect. 2.1, we investigate media that are homogeneous and horizontally extended like their standard plane-parallel counterparts but, having upper and lower boundaries of arbitrary shape, they are more general; in fact these media are best viewed as a special class of internally inhomogeneous media bounded by two horizontal planes. In sect. 2.2, we turn to homogeneous media that are horizontally as well as vertically bounded (and special interest is taken in spherical shapes). Finally, in sect. 2.3, the external shape is no longer of any importance and the systematic effects of internal variability on overall response to illumination are the focus. In the various sections, we use quite different methodologies: formal analogies with electrostatics (sect. 2.1), harmonic analysis using separation of variables (sect. 2.2) and, finally, a perturbation-type approach that parallels Stephens' [1988b] application of a simple "closure" hypothesis to a two-flux theory modified for the most obvious effects of inhomogeneity (sect. 2.3), followed by further harmonic analysis and formal analogies. The basic results are:

* In the first section and following our discussion in sect. D.5 (on horizontally extended homogeneous media), we relax our normal (mixed) boundary conditions (BCs) to their simpler Dirichlet counterparts and find two rigorous inequalities in the mathematical physics literature. Expressed in radiation transport terms, they read: 'for a given boundary shape, transmittances associated with d-dimensional diffusion exceed those corresponding to its "independent pixel" (IP) approximation (where no horizontal fluxes

are allowed),' on the one hand, and 'arbitrarily shaped media (diffusively) transmit more than their plane-parallel counterparts of equal mass,' on the other hand.

* In the second section, we find a closed form solution for the albedo problem of homogeneous spheres (diffusely illuminated by a distant point source) which turns out to be formally equivalent to that obtained in app. D for a (diffusely illuminated) slab. It is argued that every step in the calculation can be transposed to several other shapes that must however be everywhere smooth. This purely mathematical necessity precludes cubes, that are obviously in the same (homogeneous, horizontally bounded) class as spheres from the physical point of view, as shown in sect. 4.1. In this case, a naive application of IP ideas can violate the above inequality and, furthermore, using Dirichlet BCs leads to physically absurd situations (infinite fluxes arise). These findings stress the fact that one cannot quantitatively compare the optical properties of media that do not share the same support (to within a well-defined scale-changing operation).
* In the final section, we show that inhomogeneous media are more than likely to be more transmitting than their homogeneous counterparts with the same outer shape and total mass. This last inequality is illustrated for horizontally bounded media by boring a cavity out of the homogeneous spheres of sect. 2.2 and generalizing the analytical solution to this elementary form of inhomogeneity—the outcome being a prefactor effect in the scaling characterization spelled out in eq. (1.1–2). Finally, horizontally extended media are illustrated with random binary mixtures and the outcome is either a prefactor- or an exponent effect, depending on whether or not the low density cells are in fact completely empty.

Many of the results obtained (analytically and/or by analogy) here will be combined with those obtained (numerically) in the first two sections of chap. 4 for (the analytically intractable) homogeneous cuboids and (the far more interesting) fractal media respectively; we therefore postpone until the end of that chapter, our general discussion of when, why and for which physical transport model (diffusion versus transfer), one can expect to observe "anomalous" radiative scaling.

We restrict ourselves throughout this chapter to conservative steady-state problems, for which diffusion theory makes use of

$$\nabla \cdot \mathbf{F} = 0 \tag{2.1}$$

where $\mathbf{F}$ is the net flux vector. This result is exact as it simply reflects the conservation of radiant energy (see sect. D.1). It must be complemented by the appropriate constitutive relation expressed in this case by Fick's law (for radiation) which reads as

$$\mathbf{F} \propto -\frac{c}{(1-g)\kappa\rho} \nabla U \tag{2.2}$$

where U is radiant energy density but we tend to use $J=cU$ that we will call "total radiance" (somewhat abusively, see sect. A.1). The flux-to-gradient ratio is radiative diffusivity (c is the velocity of light) as is shown in sect. D.2 (and, independently, in sect. 3.3). The usual asymmetry factor, related to the phase function by (A.20), is denoted by "g," while "$\kappa\rho$" designates optical density and we recall that these parameters combine into the so-called "transport" m.f.p. $1/(1\text{-}g)\kappa\rho$. Finally, the proportionality factor in (2.0b) is always $O(1)$ and depends on the details of how the hydrodynamic limit of the radiative transfer equation is taken; for instance, if Eddington's approximation is used (as in sect. D.2), then we find 1/d where "d" is the dimensionality of space. For further details on the connection of the above approximation with standard continuous angle (or "CA") transfer theory (including a discussion of its conditions of validity), similarity relations, boundary conditions, formal analogies, standard (homogeneous) scaling properties, as well as a qualitative description of the idiosyncrasies of inhomogeneous diffusion (including an illustration using random binary mixtures), we refer the reader to app. D where much of this prerequisite and ancillary material has been collected.

In several portions of this chapter (most notably §§2.1.2–3, §2.3.4), we will be exploiting formal analogies of the diffusion approximation (to radiative transfer) with apparently remote transport or polarization[1] problems. In this way, we can cast new light on the fundamental processes of inhomogeneous radiation transport by "recycling" into radiative language existing theorems, in some cases (§§2.1.2–3), and re-interpret precise numerical results, in other cases (§D.6.2 and §2.3.4). The specific field with which we choose to establish a formal connection is determined largely by the (usually) bibliographical source where the result of interest was first established—or, at least, found by this investigator. Moreover, we favour the use of notations that are more-ore-less traditional for the field of research in which the targeted result was originally obtained since this somehow eases our (mental) "visualization" of the process under consideration. At a higher level of abstraction (than we presently wish to work at), all physical systems constrained by a continuity and a constitutive equation—respectively, for a conserved (extensive) thermodynamic quantity and an (intensive) thermodynamic forcing on its flux—are equivalent to one another. In table 2.1, we detail the (electrical) correspondences used somewhere in this chapter. Since we have come to adopt fluid mechanical jargon to describe inhomogeneous radiative "flows" (including Cannon's expression of "channeling" itself), we have added to table 2.1 the formal analogy with the (laminar) fluid dynamics of porous media; for a recent survey of this topic with many geophysical applications, see the recent volume edited and contributed to by Cushman [1990].

Application:	Radiation Transport or Neutronics	Conductors	Capacitors	Flows in Porous Media
Conserved Quantity:	Radiant Energy (or particle number)	Charge (dynamic)	Charge (static)	Mass (of incompressible fluid)
Flux Quantity: f (with $\nabla\cdot f = 0$)	Radiative Flux $\mathbf{F}$	Current Density $\mathbf{j}$	Displacement $\mathbf{D}$	Specific Discharge Rate $\mathbf{Q}$ ($\propto$ velocity)
Field Quantity: F	Energy Density $U = J/c$	Potential ϕ $(\mathbf{E} = -\nabla\phi)$	Potential ϕ	Hydraulic Head H ($\propto$ pressure)
Coupling Coefficient: C (with $f = -C\nabla F$)	Diffusivity $D \approx c/(1-g)\kappa\rho$	Conductivity σ	Permittivity ε	Hydraulic Conductivity K
Constitutive Relation:	$\mathbf{F} = -D\nabla U$ (Fick)	$\mathbf{j} = \sigma\mathbf{E}$ (Ohm)	$\mathbf{D} = \varepsilon\mathbf{E}$ (-)	$\mathbf{Q} = -K\nabla H$ (D'Arcy)
Boundary Conditions:	mixed	[Dirichlet ...	or	... von Neumann]

Table 2.1: The correspondences in formal diffusion analogies.

One can always consider diffusion as an interesting transport theory in its own right but, from our discussion in app. D on the connections between diffusion and radiative (or neutron) transport, we can only expect a good agreement for media that are not too inhomogeneous—this is amply verified and (at least tentatively) explained by the end of chap. 4. Generally speaking, this means that the variability effects that we observe here are weak versions of the kind of effect we can expect from highly irregular optical media such as those modeled with the help of fractals and multifractals that we turn to in the middle of chap. 4. In short, we will tend to find prefactor effects in the following and exponent effects later on but the directions of these effects is the same (higher fluxes) and we strongly suspect that the basic mechanisms involved are also very similar. More precisely, we introduce "channeling" as soon as the upcoming section on a very restricted class of inhomogeneous media (that merely model homogeneous cases with arbitrary shape by introducing internal discontinuities) and we will still be seeing it actively at work in chap. 6 but on a all scales within a typical multifractal density field (this is extremely variable and highly singular).

2.1. On the Effect of Shape in Horizontally Extended Homogeneous Media (and an Interpretation in Terms of Internally Variable Media)

In this section, we make use of the formal analogy existing between the radiative and dielectrical diffusion problems since this is the focus in the early sections of Mossino's [1984] monograph (on isoperimetric problems in mathematical physics) that we will be following in the next two sub-sections. We also recall from our discussion in sect. D.5 that, for weakly variable horizontally extended media (there is no "terminator" in sight, as defined in sect. A.4) that are also relatively thick, we do not need to enforce mixed BCs, the Dirichlet conditions suffice.

2.1.1. *The Extremal Property of Diffusive Transport in Higher Dimensions ("Channeling" versus "Independent Pixels")*

Consider the problem of capacitors of arbitrary shape: a bounded but not necessarily convex (open) domain Ω_0 of $\Re^d$ containing a (closed) cavity H, also of arbitrary shape. We only assume enough regularity of the boundaries ($\partial\Omega_0$,∂H) to allow the definition of normal vectors (almost) everywhere. $\Omega = \Omega_0 \backslash H$ (i.e., the points of Ω_0 that do not belong to H) is then the (open) region of space that constitutes the capacitor *per se*. It is assumed to be uniformly filled with some homogeneous dielectric material—for simplicity, we can take this to be vacuum. The "inner" boundary of Ω (∂H) is maintained at a constant unit potential while its "outer" boundary ($\partial\Omega_0$) is grounded. In Ω, the potential obeys Laplace's equation ($\nabla^2\phi = 0$) and is therefore a harmonic function; in particular, this implies that $0 \le \phi \le 1$ where the equalities are reached on $\partial\Omega_0$ and ∂H respectively. In these circumstances, capacitance is the total charge accumulated on ∂H:

$$C(\Omega) = \int_{\partial H} \mathbf{n}\cdot\nabla\phi \; d^{d-1}\mathbf{x} \qquad (2.3)$$

where we have assumed the normal $\mathbf{n}$ oriented away from Ω.

We first remark that the requirement of boundedness is strictly for convenience: this problem is topologically equivalent to the problem of capacitance developed between two horizontally periodic, non-intersecting hypersurfaces. We also note that, apart from the Dirichlet BCs, the problem is equivalent to that of diffusive radiation transport through a homogeneous medium with (almost everywhere) smooth but otherwise arbitrary upper and lower surfaces. In turn, this problem is equivalent to the one of an inhomogeneous medium (M) contained between two hyperplanes that bound from above and from below a sub-domain (M') with finite density (while M\M' contains optical vacuum). From (2.3) and (D.29), recalling that $\phi \leftrightarrow J$ in formal analogies with both electrostatics and conductance problems, we see that overall flux (or transmittance) can be equated with $\chi C(\Omega)$ where χ is the "extrapolation length," introduced in sect. D.4.

Using the divergence theorem (for the field $\phi\nabla^2\phi$), it can be shown that

$$C(\Omega) = \int_{\Omega} |\nabla\phi|^2 \, d^d\mathbf{x} \qquad (2.4)$$

which is also the total (electrostatic) energy stored in the system. The variational formulation of electrostatics (Dirichlet's principle) tells us that, for given fixed Ω (hence Ω_0 and H) and an arbitrary function $\phi(\mathbf{x})$ supported by Ω that is only required to obey the above conditions on $\partial\Omega_0$ and ∂H, then (2.4) is absolutely minimal when ϕ is harmonic.

We now stretch between $\partial\Omega_0$ and ∂H any number of smooth but otherwise arbitrarily shaped internal boundaries where we require that the fluxes in and out of these boundaries vanish identically[2] $\mathbf{n}\cdot\nabla\phi_i = 0$; in the electrostatic analogy, the electrical field-lines must be tangent to them (i.e., they carry no charges). We have thus divided Ω into a number of regions Ω_i; each one of these now works as an independent capacitor and they are all connected in parallel mode (their $C(\Omega_i)$'s add). But Dirichlet's principle applies to each and every capacitor hence the part of the integral in (2.6b) corresponding to the original (undivided) system's potential exceeds $C(\Omega_i)$. This tells us that its "effective" capacitance, $\Sigma_i C(\Omega_i)$, has been decreased by the subdivision into separate capacitors. The only case where capacitance is unchanged is when the divisions are bundles of electric field lines.[3]

In our radiative analogy, the IP approximation is merely a special kind sub-division—it constrains flux lines to be vertical—and we now see that it necessarily decreases the total transmittance:

$$T_{IP} \leq T_{dif} \tag{2.5}$$

Moreover, the only configurations that remain unperturbed (equality in the above) have perfectly vertical flux lines, viz. plane-parallel slabs. In essence, allowing net horizontal fluxes to arise[4] causes the flux lines to wander away from the vertical and the direction in which they move is not hard to predict. In the above example of homogeneous media with arbitrary boundary geometry, they will "head" towards the nearest boundary, i.e., the radiation is "channeled" towards the nearest exit. In the internally inhomogeneous media that we will encounter in sect. 2.3 (weak but general variability) and in chap. 6 (strong but specific variability), the flux lines "seek" the more tenuous regions and, again, we can talk about "channeling." Finally, we note that the result in (2.5) must not be taken out of context; in particular, horizontal extension (by periodicity) is one of its basic premises and it will have to be re-examined in the case of horizontally finite optical media (which have no capacitor analog, see §2.2.3 below).

2.1.2. *The Extremal Property of Slab Geometry in Higher Dimensions*

We now allow the shape of the internal and external boundaries to change freely but the volume between them must remain unchanged: vol(Ω)=constant, i.e., we are dealing with a given and fixed amount of dielectric. Following (and generalizing) the analysis of Szegö [1930], Mossino [*ibid.*] shows—with some recourse to "rearrangement" theory (in Sobolev function spaces)—that $C(\Omega)$ reaches its absolute minimal value when Ω is a shell contained between two concentric hyperspheres (and their radii are totally determined as soon as the volume of the cavity is also specified). This is a classic example of an "isoperimetric" inequality.[5] The proof is outside the scope of this thesis but it should be noted that it relies on transformations of the solution $\phi(x)$ of the given boundary value problem that are based on Lebesgue's measures and integrals (i.e., decimating ϕ-space, not x-space) which allow for more generality. The unbounded but periodic equivalent of the concentric spheres are of course plane-parallel slabs which therefore appear to be the absolutely optimal geometry in terms of flux reduction or, equivalently, albedo generation. In obvious radiative notations, we have

$$T(\text{slab geometry}) < T(\text{anything else}) \quad (2.6)$$

Finally, we can generalize this result by taking the period to infinity (equivalently, the size of H becomes very large).

Notice that, in the above discussion based on electrostatic-radiative analogies, we have considerably simplified the BCs, not only are they considered Dirichlet but the imposed potential is considered as uniform on ∂H and $\partial\Omega_0$. If we were to be totally consistent with the idea of illumination by a collimated beam, we should modulate the top boundary value by the vertical direction cosine of the local normal vector ($\mu_0(x)$, $x \in \partial H$); this means that boundary values could, in principle, fluctuate from 0 to 1 in the most general case. If the upper boundary has multiple points along a vertical (i.e., $\mu_0(x)$ can become negative), then the "non-illuminated" and the "shaded" parts should receive a null boundary value. Even further complications ensue if we attempt to model the illumination of a boundary point by the diffuse radiation coming out of another; this obviously becomes more important as the boundary shape becomes more convoluted. As argued in sect. A.4, in such cases we are better off moving to the framework of internally inhomogeneous media. (In this case, we are dealing with a restricted class with simple boundary shapes, a constant density in some sub-domain and null values everywhere else.) In other words, our argument remains perfectly valid as long as we limit ourselves to (top) boundaries that are "almost" horizontal ($\mu_0(x) \approx 1$; $x \in \partial H$); the final result then takes on a perturbative flavour, much like our analysis of internal variability (in sect. 2.3 below).

Returning to electrostatics *per se*, we can clearly extend the result (on physical grounds) to boundary shapes that are not necessarily smooth anywhere, in particular, they can be fractals (that are almost nowhere rectifiable but in a uniform and self-similar way, see sect. C.2). This can be seen by visualizing the limit of ever more convoluted (piecewise) smooth surfaces: the electric field (hence charge) at the boundary develops singularities that can only add to the (surface integral) expression for $C(\Omega)$ in (2.3).[6] We strongly suspect that the analogous radiative statement can also be extended, just as the 2nd order but systematic effect predicted by perturbing the internal structure is considerably enhanced when the variability becomes "extreme," i.e., singularities arise in the density field (see, for instance, the example studied in chap. 6).

2.1.3. Summary and the Possibility of Generalization to Arbitrary Internal Inhomogeneity

Summarizing and rephrasing, we have considered the restricted class of media contained between two horizontal planes ($M=\{x\in\Re^d, 0<z<L\}$) that are inhomogeneous in both horizontal and vertical directions but in a restricted way. Density is zero between the upper limiting plane and an upper internal boundary, similarly for the lower case, and the density is uniform in the region (M') between the two arbitrarily shaped, non-intersecting internal boundaries which are horizontally periodic (modulo N). The volume of the unit cell in M' (that we denote M_N') is however held constant, consequently, so is the total (optical) mass of the system. (The region M' of course constitutes the "real" medium but on which it is difficult to apply BCs since its boundaries need not even be rectifiable anywhere.) On the one hand, it has been shown that, apart from unimportant boundary layer effects, IPs yield a smaller transmittance than diffusive transport (with the horizontal fluxes fully accounted for). We will see in the following chapter that these two methods of obtaining an overall transmittance correspond respectively to the "$p\rightarrow0$" and "$p\rightarrow\infty$" limits of "discrete angle" (DA) transfer with orthogonal beams; so the transmittance for finite "p" (i.e., a *bone fide* kinetic approach to the transport problem) is likely to yield an intermediate value since we are dealing with a single-parameter family of transport models. On the other hand, it was shown that the smallest transmittance of all is obtained when the (internal) boundaries are made flat and slab geometry is thus retrieved: we are back to standard homogeneous plane-parallel optical media. Adding the intermediate (highly plausible) inequality, we can collect our results in the following way:

$$T(M'=M) \leq T_{IP}(M') \leq T_{DA}(M') \leq T_{dif}(M') \text{ with } \int_{M_N'} d^dx = \text{const.} \quad (2.7)$$

In the following chapter, we will confirm that IPs, orthogonal DAs and diffusion all yield the exact same result for the very special (ultra-symmetric) horizontally homogeneous plane-parallel medium. We suspect this to be the only situation where such perfect agreement happens whereas (in chap. 4) we will argue that any kind of medium with non-singular internal structure will have the same scaling properties (in the sense of sect. 1.4), irrespective of boundary shape.

Finally, it would be interesting if we could generalize (2.7) from the restricted class of inhomogeneous density fields contained by two horizontal planes to arbitrary internal variability $\rho(x)$ with $x\in M_N$, the elementary cell (of size N) which is to be replicated in all horizontal directions; viz.

$$T(\rho(x)=\text{const.}) \leq T_{IP}(\rho(x)) \leq T_{DA}(\rho(x)) \leq T_{dif}(\rho(x)) \text{ with } \int_{M_N} \rho(x)d^dx = \text{const.} \quad (2.8)$$

In sect. 2.3 below, we present a perturbation-type argument for the "widest" inequality (relating the first and last quantities) for general but weak variability. The leftmost inequality is easily proven on completely general grounds, using Jensen's inequality (see sect. 3.4 for details). However, all we can say about the second (IP-to-DA) inequality is that it is verified by our numerical results for the deterministic fractal media introduced in sect. 4.2 (at all cascade steps), as well as those that pertain to the single realization of a stochastic multifractal investigated in chap. 6 (see sect. 6.5); in fact, we have never seen a violation to date in all of our test-, preliminary- or otherwise unpublished numerical results. This leaves little doubt about the validity of (2.8) within the relatively simple class of transport models we are presently working with. The conditions where we can expect $T(\rho(x)\text{=const.}) < T_{CA}(\rho(x))$ are tentatively discussed in §2.3.2; basically, we should remain in the optically thick cloud regime and use the simplest possible illumination conditions (i.e., normal or diffuse).

2.2. On the Effect of Shape in Horizontally Bounded Homogeneous Media (and the Irrelevance of Comparison with Plane-Parallel Media)

2.2.1. Background, Motivation and Main Results

In this section, we will be presenting and use a (closed-form) solution of the albedo problem for homogeneous spheres within the framework of the diffusion approximation to radiative transfer (that we will generally refer to simply as "diffusion"). This case is of interest for at least two reasons, one more historical and one more pedagogical.

Firstly, the fact that the problem is entirely tractable seems to have been over-looked in the literature. In the heyday of analytical (pre-computer) approaches, Davison[7] [1951] uses various approximations to obtain transfer results concerning the extrapolation length (cf. sect. D.4) for spheres and very long cylinders (lying on their side)—effectively 2-D "spheres"—while Giovanelli and Jefferies [1956] investigate diffusion in several geometries, including spheres and (infinite) cylinders. The latter authors solve the problem completely but they insist on irradiation conditions so arbitrary that their final results are delivered in the form of infinite expansions containing undefined coefficients. We will basically be showing, from first principles, that these series are trivially summable for the simplest albedo problem where illumination comes from a distant point-like source.[8] Since then, high-speed computation has become a primary tool in transfer research and consequently, there has been a natural tendency to use geometries where ray-boundary intersections ("piercing points") are easily determined for the purposes of Monte Carlo simulation: "cylinders" of finite length standing on an end with various sections. For instance, McKee and Cox [1974] worked on "cuboidal" cloud shapes (orthogonal parallelepipeds or, equivalently, cylinders with a rectangular section)—a problem that has since been attacked analytically with a "multi-mode" approach [Preisendorfer and Stephens, 1983]. Within this framework, this problem formally looks enough like one in plane-parallel geometry that the plane-parallel techniques of invariant imbedding can be used to solve it [Stephens and Preisendorfer, 1983]. (In the case of diffusion in spheres, we will be able to take this formal analogy one step further.) In this context, the word "analytical" does not mean that the computer is superfluous; in fact, the encoding of the analytical solution is bound to be far more intricate than a simple Monte Carlo simulator program but, in the end, it will be faster and more accurate. The primary aim of the above analytical approach—and ours—is however not numerical efficiency but to gain insight into the workings of transfer in presence of horizontal fluxes, breaking away from slab geometry, e.g., to what extent can we view the effect of sides as a formal analog of absorption? (Our views on this question are spelled out in sect. A.4.2–3.)

These upright "cylinders" have also attracted the attention of theoreticians versed in Eddington's approximation (or its "δ" variant): circular sections [Barkstrom and Arduini, 1977] and square sections [Davies, 1976, 1978; Davies and Weinman, 1977]. Since these authors are solving a Laplace[9] equation on a finite and regular domain, they can use the standard techniques of separation of variables but these lead, in both cases, to (quite similar) non-trivial eigenvalue problems in order to match the BCs on the sides and on the ends, hence final results that (again) come in the form of infinite eigenfunction expansions. As in the case of exact transfer, these diffusion results are numerically more expedient than Monte Carlo but they are approximate in nature and no longer are expected to be an unconditionally accurate representation of transfer. Returning to homogeneous spheres and infinite cylinders (having gone a complete circle), the former at least have become quite popular as a basic cloud shape in numerical studies of broken cloudiness where they are in direct competition with cubes; these cloud aggregation models can be made of identical individuals or individuals which are either of constant optical density and different sizes or vice-versa with various rules as to their spacings ranging from regular grids to randomly scaling [references in chap. 1]. We propose to fill the gap left in this intensive use of finite homogeneous cloud shapes and show that the simplest of shapes has the simplest of expressions for its transmittance (exactly analogous to a slab), in spite of the manifest presence of net horizontal fluxes.

The second major reason to consider homogeneous spheres is important to the basic logic of this thesis: we are systematically investigating the scaling properties of optical media, moving away from the standard homogeneous slab model one step at a time. A first logical step is simply making the medium not only vertically but horizontally finite. Homogeneous cubes were studied for the same reason but under normal illumination (the simplest, in principle) cubes develop "terminator pathology" (see sect. A.4 for details) hence there is an ambiguity about what we should call albedo, and uncertainties ensue about its scaling properties ('Is it really non-trivial?' see sect. 4.1 for a final analysis, hopefully). By contrast, spheres can be viewed as a generic representative of the only class of bounded homogeneous media of any practical interest (those with "proper" terminators, including cubes under slant illumination) and the whole picture of strictly boundary induced horizontal fluxes can be considerably simplified: from the scaling (exponent) point of view at least, the effect is exactly nil!

Since the radiative problem for homogeneous spheres can be solved with the proper radiative BCs (of the "mixed" type) we can look into the question of how important these are for horizontally bounded media. The answer is (unfortunately) a lot more than for their horizontally extended counterparts and this is an unescapable consequence of the existence of a terminator. Horizontal boundedness also makes IP-type calculations largely irrelevant since near the terminator external (absorbing) and internal (insulating) boundaries become parallel and, in the same vicinity, optical thicknesses vanish slowly (they can dominate the spatial statistics). Finally and possibly most importantly, the methodology of the analytical solution procedure for the homogeneous sphere can be quite easily generalized to the case of an internally inhomogeneous sphere with one radial discontinuity in density (§2.3.3). So we can compare homogeneous spheres with hollow spherical shells (or spheres with a denser core, and all the combinations in between). This gives us a textbook example where we can verify our prediction (§2.3.1) that inhomogeneous media always transmit more that their "homogenized" (equal mass) counterparts with the very same external boundary shape.

2.2.2. *A Detailed Solution for Spherical Media*

Following a proverbial [Harte, 1985] path that needs no further presentation, we consider a spherical cloud in d=3, of radius R, and homogeneous in $\kappa\rho$ (which can be taken as unit for convenience). It was eventually realized that Giovanelli and Jefferies [1956] had obtained partial results towards the analytical formula that we obtain below for the transmittance by such a medium; it was then soon realized that it is in fact easier to start from scratch than to explain their notations. From our point of view, their result is to general to be directly useful since they consider arbitrary illumination conditions (which is a logical choice in neutron transport studies). To make this point even clearer, we will reverse their logic completely, i.e., we start by exploiting the simplifications related to the collimated illumination and the spatial averaging of the radiative responses. Only then do we solve the Laplace equation with the appropriate (mixed) BCs, targeting specifically the features of the solution important to the determination of overall transmittance.

We naturally center the sphere at the origin and use spherical coordinates with the "north pole" (hence z-axis) oriented downwards, following the incident and mean fluxes of radiation (more-or-less) as usual in atmospheric radiation studies. The problem being axi-symmetric, we are only retain interest in coordinates r and θ. We are particularly concerned with the in-coming and out-going fluxes (at $r=R$) as defined in the most general case by eq. (D.28), while here, they are best represented as a Legendre series simply because of the boundary shape (we are not even interested yet if it is a diffusion process going on inside or not!). So we write

$$F^{\pm}(\cos\theta) = \sum_{0}^{\infty} B_n^{\pm} P_n(\cos\theta) \tag{2.8}$$

The lower signs in (2.8) designate known quantities since they specify the BCs for the albedo problem, namely, a unitary collimated flux (coming from a very distant point-source):

$$F^{-}(\cos\theta) = \begin{cases} 0 & 0 \le \theta \le \pi/2 \\ -\cos\theta & \pi/2 \le \theta \le \pi \end{cases} \tag{2.9a}$$

Equivalently, in the harmonic representation defined in (2.8):

$$\begin{cases} B_0^{-} = 1/4 \\ B_1^{-} = -1/2 \end{cases} \tag{2.9b}$$

and, for $n>1$, all the odd contributions vanish identically. Even contributions beyond $n=0$ exist but they will not be of any use in the following since we are interested in the overall responses, not the local fluxes[10] (we return to this question below). In particular, transmittance—according to the (terminator-based) definition in (A.29)—is given by

$$T = \frac{1}{\pi R^2} \int_{0}^{\pi/2} F^{+}(\cos\theta)\ 2\pi R^2 d(\cos\theta) \tag{2.10}$$

and similarly for albedo R with the bounds of the integral moved to $\pi/2$ and π.

The expression for T in (2.10), as well as its counterpart for R, can be considerably simplified by introducing Heaviside's step function (for $\pm\cos\theta$) along with its Legendre expansion:

$$\Theta(\pm\cos\theta) = \sum_{0}^{\infty} \eta_n^{\pm} P_n(\cos\theta) = \begin{cases} 1 & \text{if } \pm\cos\theta \ge 0 \\ 0 & \text{otherwise} \end{cases} \tag{2.11a}$$

Here too, only the first two terms will be of direct interest to us:

$$\begin{cases} \eta_0^{\pm} = 1/2 \\ \eta_1^{\pm} = \pm 3/4 \end{cases} \tag{2.11b}$$

For $n>1$, all the even contributions vanish identically. Eq. (2.10) can then be rewritten and generalized to read

$$\left\{ \begin{matrix} T \\ R \end{matrix} \right\} = 2 \int_0^{\pi} F^+(\cos\theta)\, \Theta(\pm\cos\theta)\, d(\cos\theta) = 2\sum_0^{\infty} \frac{2}{2n+1} B_n^+ \eta_n^\pm \tag{2.12}$$

where the last equality makes use of the orthogonality relation for the Legendre polynomials. From the above discussion, we see that there are in fact only n=0,1 contributions to the (functional) scalar product in (2.12). We can then easily see that

$$\frac{R}{T} = \frac{1}{T} - 1 = \frac{1 - B_1^+/2B_0^+}{1 + B_1^+/2B_0^+} \tag{2.13}$$

In short, all that is required of the solution of the transport problem is the single ratio $B_1^+/2B_0^+$. Notice that the only assumption we have made in the above is the axi-symmetry which is guaranteed by the uniform illumination, on the one hand, and an internal distribution of scattering material that is purely radial, on the other hand. In the following, we assume internal homogeneity and, in §2.3.3 below, we will allow for one radial discontinuity.

Only now do we need to make an assumption about the radiation transport model, which we of course take to be diffusion. We must therefore solve Laplace's equation inside the sphere. For the moment (see §2.3.2 below), we are only interested in the regular part of the general (axi-symmetric) solution in spherical coordinates which is

$$J(r,\theta) = \sum_0^{\infty} \beta_n r^n P_n(\cos\theta) \tag{2.14}$$

where the constants β_n are to be eventually determined by the BCs. The general definition (D.28) of in- and out-going fluxes yields

$$F^\pm(\cos\theta) = \frac{1}{2}[\,1 \mp \chi\frac{\partial}{\partial r}\,]\, J(r,\theta)\,\big|_{r=R} \tag{2.15}$$

when specialized for spherical systems. Recall that the lower signs refer to the (given) BCs assigned to external illumination from a distant source in eq. (2.9a); the upper signs refer to the (required) responses to the said illumination. By substituting the solution (2.14) into the above, we find

$$F^\pm(\cos\theta) \equiv \frac{1}{2}\sum_0^{\infty} [\,1 \mp n\frac{\chi}{R}\,]\, \beta_n R^n P_n(\cos\theta) \tag{2.15'}$$

which, by comparison with (2.8) yields

$$\left\{ \begin{aligned} 2B_0^\pm &= \beta_0 \\ 2B_1^\pm &= [\,1 \mp x\,]\, \beta_1 R \end{aligned} \right. \tag{2.16}$$

where we have let $x = \chi/R$. Using (2.9b) and eliminating the $\beta_{0,1}$ from the eqs. (2.16), we find the required combination of harmonic coefficients:

$$\frac{B_1^+}{2B_0^+} = -\frac{1-X}{1+X} \tag{2.17}$$

Finally, substituting this into (2.13) and simplifying, we find

$$\frac{1}{T} - 1 = \frac{R}{\chi} \tag{2.18}$$

or, as usual (e.g., §D.4.2), $T = 1/(1+R/\chi)$. This result is readily validated by straightforward numerical Monte Carlo simulation, bearing in mind that we are not to expect the same value of χ to apply over the full range of values of R. More precisely, we expect $\chi \to 4/3^-$ for $R \to 0^+$ and $\chi \to 0.7104\cdots$ for $R \to \infty$ which are universal (geometry independent, dimensionality dependent) limits; the latter value also corresponds to the limit of a semi-infinite medium with an up-welling flux (the "Milne problem").[11]

The main focus of this thesis is on overall (or average) radiative responses but there is no reason to limit oneself to this very lowest level of spatial resolution in the above development. The information about illumination conditions in (2.16)—with lower signs—can be complemented up to any arbitrary order in the spherical harmonic expansion and, consequently, all the β_n (internal fields) and B_n^+ (external fields) can be determined. It is not hard either to anticipate the main features of the flux field. The flux lines start, straight down, parallel and equally spaced, on the the upper half of the boundary since that is where the radiation sources are, constantly fueled by the ($\cos\theta$-distributed) external illumination pattern. The same lines end on the lower half of the boundary[12] but they are no longer equally spaced, nor straight, nor parallel; instead, they fan out: all off-axis lines deviate from the z-axis in the direction of the closest part of the non-illuminated lower boundary. In other words, the radiation is "channeled" towards the nearest "exit" (i.e., low density environment) by the onset of horizontal fluxes which build up constantly from the top to the bottom. We will encounter the converse manifestation of diffusive channeling in §2.3.3 below and, being driven by internal density variation, it provides a less trivial example: after creating cavities inside the spheres, the flux-lines will tend to funnel into the empty region where the radiation gets a "free ride" through the medium.

Finally, we would like to know whether the simpler Dirichlet BCs could be applied with comparable success, as we found in the case of slab geometry and strongly argued for in otherwise horizontally extended geometries. The answer is yes but only if we are far more careful than in the above (sect. 2.1) discussion of arbitrary boundary shapes where we applied the same boundary value everywhere on the top (and similarly on the bottom) of the cloud, irrespective of the local orientation of the boundary w.r.t. the incident beam. This "cosine" law was explicitly incorporated into our expression of BCs (2.9a,b), had we not and had we applied (uniform) Dirichlet BCs, we would have found singular fields near the equator (or terminator, $\theta=\pi/2$). In short, the medium would offer no bulk resistance to the radiation (or current) because of all the very short paths available at the equator. As a rule-of-thumb, we should keep to the mixed BCs when dealing with horizontally finite cases and, in horizontally extended cases, we can simplify not only to Dirichlet BCs but to their standard (uniform) format, especially if we are only interested in the simplest radiative properties of the system: for instance, low-order perturbation (not unlike in §2.3.2) or else the leading term for asymptotic scaling behaviour (as in §2.3.4).

2.2.3. *Independent Pixels, Scaling Implications and Generalization to Other Cloud Shapes*

The final closed-form result (2.18) for the transmittance of (homogeneous) spheres has a familiar look to it: if we take L to be the diameter ($R=L/2$), then we retrieve exactly the diffusion result for slab geometry (D.31") as well as the exact result (of sect. 3.4) for transfer in d=1 (where transfer and diffusion are equivalent, see sect. D.2). Since we have the exact same result for a *bone fide* sphere (in d=3) and a segment, or "1-sphere" (in d=1), we can conjecture that the same formula will appear[13] in d=2 (and probably also in d>3). In all cases, the sphere has the same transmittance as the slab defined by the tangent planes at north and south poles.

This brings up an interesting but only apparent paradox. The IP transmittance for spheres in any d>1 is[14]

$$T_{IP} = \overline{T_{d=1}(l)} = \int_0^{2R} \frac{1}{1+l/2\chi}\, dP(l) = \frac{\chi}{R} \ln\left(1+\frac{R}{\chi}\right) \tag{2.19}$$

where l designates the length of a vertical section of the d-sphere. Now T_{IP} is greater than the diffusive transmittance expressed in (2.18). In fact that result corresponds to the minimum value of $T_{d=1}(l)$ (and the maximum $l=L=2R$) and the logarithmic term in (2.19) is due to the relatively numerous small l-values around the equator ($\theta\approx\pi/2$). In essence, we are facing the same kind of problem as above in the discussion of the potential usefulness of Dirichlet BCs in horizontally bounded cases and the answer is the same: we must be more careful (and this applies to all horizontally bounded media, including normally illuminated cubes). This time, we cannot generalize the general (shape-independent) "$T_{IP}\leq T_{dif}$" result obtained at the beginning of this chapter for horizontally extended (or periodic) media to the horizontally bounded counterparts (spheres in particular). This is because, near the terminator, the "open" (or absorbing) external boundary of the medium gets confused with the "no-flux" (or insulating) internal boundaries in the IP approximation. The comparison of the two results is largely irrelevant. In fact, totally wrong conclusions can be drawn by trying to compare quantitatively horizontally finite and extended media like 'horizontal fluxes cause lower transmittancies since $T_{cube}<T_{slab}$ (cf. figs. 4.2a,b)' whereas exactly the opposite

is happening when the media have the same boundaries: transmittancies are generally enhanced when horizontal fluxes arise, necessarily due to internal variability in this case (sect. 2.3). The only way to compare the radiative properties of cubes and slabs quantitatively is to take into account all the light that is directly transmitted through the empty space around the cube.[15] This of course applies to inhomogeneous cases too: given some density field defined on a plane-filling cell in the horizontal, going from "open" horizontal BCs to "cyclical" horizontal BCs (see sect. 4.2, for an example) is far less innocent than going, say, from "mixed" to "Dirichlet" (in sect. 2.1 or even 3.5, in connection with "generalized" DA similarity theory).

Instead of trying to quantitatively compare horizontally bounded and unbounded cases, it is more interesting to notice that the homogeneous diffusive result in (2.18) can probably be generalized to many other cloud shapes, all horizontally bounded in higher dimensionality. All we really require in the calculation that leads to (2.18) is (i) a coordinate system where Laplace's equation can be treated by separation of variables (Morse and Feshbach [1953] enumerate 13 of them in d=3) and (ii) that the boundary of the optical medium is a (necessarily closed) surface were one coordinate remains constant. In particular, the latter condition implies that the boundary is everywhere smooth: cuboids (and rectangular coordinates) are excluded since they are made up of several constant coordinate surfaces, not just one, but ellipses (and elliptical coordinates) of all kinds can certainly be used. Within this class of cloud shapes (and associated coordinate systems), every detail of a solution for the radiative problem in one case can be (conformally) mapped onto another case. We therefore expect to retrieve a final result of the same form as (2.18) in all these cases.

In summary, we have just argued that all homogeneous horizontally bounded media with well-defined terminators have transmittancies that scale inversely with their size and that, if the boundary is furthermore everywhere smooth, the asymptotic regime is approached in the same way as homogeneous slabs do, namely, as in (2.18). This (exponent) is totally independent of the phase function choice which appears nowhere in the above (beyond the natural choice of "rescaled" units of length); the phase function will however influence the prefactor χ (if we insist on using units other than transport m.f.p.'s for the extrapolation length). In the following chapter, we retrieve (analytically) the same scaling for DA transfer through plane-parallel slabs in any dimension w.r.t. their vertical thickness. In chap. 4, we show (numerically) that normally illuminated homogeneous cuboids (in d=2,3) behave like the spheres in both transmittance and reflectance (even in the restricted sense, w.r.t. definition (A.29), of exit through the top only), i.e., that in such media "sides" may be geometrically well-defined (and the terminator ill-defined) but they are asymptotically unimportant as far as radiation is concerned.

2.3. On the Effect of Internal Structure (and a Tentative Quantification of "Channeling")

2.3.1. Homogeneity as an Extremal Property

We have anticipated systematic inhomogeneity effects on the bulk radiative properties in different qualitative ways: perturbed optical path (order-of-scattering) distributions in sect. A.2, and anomalous diffusive random walks in sect. D.6. Quantitative scaling examples of these effects are discussed in §5.1.1 and §D.6.3 respectively. These examples however do not pertain directly to the steady-state albedo problem but rather to initial condition problems for an internal point-source. It is therefore in order to evaluate and analyze, in the most quantitative terms possible, the effect of inhomogeneity on an overall response to illumination: albedo, equivalently, transmittance (or, even more simply, average net flux). The following development has the flavour of a perturbation analysis but does not claim to be a mathematically rigorous expansion[16] in higher order perturbations; rather we show—using Fick's law, BCs and mass conservation—that the linear (1^{st} order) contributions to the correction to "mean field" flux due to inhomogeneity vanish identically and that we are left with nonlinear contributions (of all higher orders in principle), cf. eq. (2.25) below. This is an interesting result but not too surprizing: inhomogeneous transport theory would not be the challenging problem it is were it dominated by linear effects! We then argue that the sign of this correction term is likely to be positive (fluxes increase); in a sense, this is more valuable than a mathematically rigorous result because it forces us to clarify the notion of "channeling" on physical grounds. In fact two arguments are given, one specifically diffusive, the other based on independent research into inhomogeneous radiation transport based on the transfer model. Firstly, we somewhat refine our qualitative discussion of the inhomogeneous diffusion equation in §D.6.1; more precisely, we ask 'how do the "pseudo-source/sink" terms (that appear along with density fluctuations) affect the geometry of the flux-lines?' Secondly, we turn to a closure hypothesis introduced by Stephens [1988b] in order to accommodate a simple form of inhomogeneity in a modified two-flux scheme based directly on the inhomogeneous CA transfer equation made to look formally like its plane-parallel counterpart after spherical harmonic analysis and horizontal Fourier transformation [Stephens, 1988a]. Given the very close links between two-flux theory and the diffusion approximation in homogeneous plane-parallel media, we can view the following (purely physical space calculation) as a generalization of Stephens' calculation based on "new optical parameters" that, in final analysis, we view as direct measures of Cannon's "channeling."

We will make no special assumption on the nature or the strength of the inhomogeneity yet. We simply decompose our into their "mean field" values plus a "correction" term; starting with the density field:

$$\rho(\mathbf{x}) = \bar{\rho} + \rho'(\mathbf{x}) \quad \text{with} \quad \int \rho'(\mathbf{x}) d^d\mathbf{x} = 0 \tag{2.20a}$$

We are therefore constraining the density perturbation explicitly to redistribute mass that already exists somewhere in the system. We define a similar radiation field decomposition:

$$J(\mathbf{x}) = J_h(z) + J'(\mathbf{x}) \quad \text{and} \quad \mathbf{F}(\mathbf{x}) = \mathbf{F}_h + \mathbf{F}'(\mathbf{x}) \tag{2.20b}$$

For simplicity, we have assumed our unperturbed medium has slab geometry (we generalize further on); the mean field term then obeys $\nabla^2 J_h = d^2J_h/dz^2 = 0$, and the corresponding flux is $\mathbf{F}_h = F_0 T_h \hat{\mathbf{z}}$ where F_0 is the incident flux. The precise value of the transmittance in absence of perturbation (T_h) is not important in the following. Since we will be using properties that are characteristic of the optically thick asymptotic regime (specifically, we will not attempt to distinguish Dirichlet- and mixed BCs), it should however be quite close to the estimate $T(\kappa\bar{\rho}L)$ given in (D.31') where length units that make $\kappa\bar{\rho} = 1$ were used. The geometrical vertical extent L of medium is therefore implicitly assumed much greater than $1/\kappa\bar{\rho}$. (One might add that using diffusion rather than transfer is only a good idea in quite thick systems, dominated by high orders-of-scattering, in the first place.)

For specificity only, we will take Eddington's expression for radiative diffusivity, hence the "d" factor in the following (recall that d is the dimensionality of the system). The new (inhomogeneity) term in Fick's law, $\mathbf{F} = -(\nabla J)/d\kappa\rho$, then reads:

$$\nabla J' = -\, d\kappa\, [\, \bar{\rho}\mathbf{F}' + \rho'\mathbf{F}_h + \rho'\mathbf{F}' \,] \tag{2.21}$$

where the last (higher order) term will turn out to be crucial to the final outcome. We now turn our attention to global quantities such as $T = T_h + T'$ which are horizontally extended hypersurface averages of $\mathbf{n}\cdot\mathbf{F}$, $\mathbf{n}\cdot\mathbf{F}_h$, and $\mathbf{n}\cdot\mathbf{F}'$ respectively. They are all independent of the level and the precise shape of the transection since the fluxes are all divergence free. Focussing more particularly on

$$(N^{d-1}F_0)T' = \int_{A_0} \hat{\mathbf{z}}\cdot\mathbf{F}'(x,z)\, d^{d-1}x \tag{2.22}$$

we use, for simplicity, a transection at constant geometrical depth. In the above, N is the width of the unit cell of the medium ($A_0 =]0,N[^{d-1}$), assumed to be horizontally periodic. Integrating (2.22) vertically also, we find

$$L(N^{d-1}F_0)T' = \int \hat{\mathbf{z}}\cdot\mathbf{F}'(\mathbf{x})\, d^d\mathbf{x} \tag{2.23a}$$

where, from (2.21), the integrand can be expressed as

$$\hat{\mathbf{z}}\cdot\mathbf{F}' = -\frac{1}{d\kappa\bar{\rho}}\, [\, \hat{\mathbf{z}}\cdot\nabla J' + d\kappa\rho'\mathbf{F}_h\cdot\hat{\mathbf{z}} + d\kappa\rho'\mathbf{F}'\cdot\hat{\mathbf{z}} \,] \tag{2.23b}$$

This last expression tells us that we have three different contributions to the integral in (2.23a), one for each of the terms on the r.h.s. of (2.23b).

The first two terms are easily evaluated. Using $\hat{\mathbf{z}}\cdot\nabla J' = \partial_z J'$, we obtain

$$\int \partial_z J'\, d^d\mathbf{x} = \int_{A_0} d^{d-1}x \int_0^L \partial_z J' dz = 0 \tag{2.24a}$$

since the vertical integral is simply $J'(x,z)|_{z=0}^{z=L}$ and both contributions vanish (for all $x \in A_0$) because the BCs on $J'(\mathbf{x})$ are homogeneous. We will see that this field is excited not by BCs like for $J_h(z)$ ($J_h(0)=1$, $J_h(L)=0$), but by internal sources dependent on J_h and $\nabla\rho'$, cf. eq. (2.28) below. The other linear contribution also vanishes because of the constant total mass constraint imposed on the density fluctuations, cf. (2.20a):

$$\int \rho' \mathbf{F}_h\cdot\hat{\mathbf{z}}\, d^d\mathbf{x} = F_0 T_h \int \rho'\, d^d\mathbf{x} = 0 \tag{2.24b}$$

We are therefore left with

$$(LN^{d-1})\bar{\rho} F_0 T' = -\int \rho' \mathbf{F}'\cdot\hat{\mathbf{z}}\, d^d\mathbf{x} \tag{2.24c}$$

or, equivalently,

$$T' = -\frac{\overline{\rho' F_z'}}{\bar{\rho} F_0} \tag{2.25}$$

In other words, the quantitative effect of (mass conserving) inhomogeneity on the overall flux through the system is directly proportional to the (spatial) correlation between the fluctuations in density and vertical flux. We also recall that, within the framework of diffusion theory (as applied to radiation transport), the only approximation we have made is to assume Dirichlet rather than mixed BCs.

We will now present strong evidence that the correlation term in (2.25) is likely to be negatively valued, thus making the correction T' to transmittance positive. For the moment, we will exploit diffusion theory itself and, in the upcoming sub-section, we will reconsider this question using an important numerical finding of Stephens' [1988b] within the framework of CA transfer theory. The structure of the relevant (diffusive, steady-state) radiation transport equation is quite simple; from (2.1–2), we indeed find

$$\nabla^2 J = (\nabla \ln\rho)\cdot(\nabla J) \tag{2.26}$$

and this implies, in particular, that only ratios of density are of any importance. This suggests that we should now look at

$$\ln\rho(\mathbf{x}) = \overline{\ln\rho} + (\ln\rho)' \quad \text{where} \quad (\ln\rho)' \approx \frac{\rho'(\mathbf{x})}{\bar{\rho}} \tag{2.27}$$

Only in this last step do we assume the variability to be quite weak. Substitution of (2.21) and (2.27) into (2.26) and removing the dominant term in Fick's law ($\nabla J_h=-d\kappa\bar{\rho}\mathbf{F}_h$) yields, to 1st order:

$$-\nabla^2 J' \approx d\kappa(\nabla\rho')\cdot\mathbf{F}_h \tag{2.28}$$

which, we recall from the discussion in sect. D.6, acts as a source (sink) for J' when positive (negative). If all orders of perturbation are included then $\mathbf{F}_h$, $\mathbf{F}$, hence $\mathbf{F}'$ are all divergence free; but to 1st order, taking the divergence of (2.21) allows us to write the l.h.s. of (2.28) as $d\kappa\bar{\rho}\nabla\cdot\mathbf{F}'$.

$$\bar{\rho}\nabla\cdot\mathbf{F}' \approx (\nabla\rho')\cdot\mathbf{F}_h \tag{2.29}$$

We are thus adding to the mean flux field a diverging (pseudo-source driven) flux field when $\nabla\rho'$ and $\mathbf{F}_h$ lay roughly in the same direction; otherwise, it is a converging (pseudo-sink driven) flux field. This means that the (1st order) effect of a positive density fluctuation is to decrease the total flux along the mean flux field direction, and vice-versa. In short, if the mean field flux is vertical (parallel to the z-axis), then ρ' and F_z' tend to anti-correlate; and we therefore conclude that $\overline{\rho' F_z'}$ is likely to be negative. This is essentially what the local multiplicative coupling of the radiation and the density fields has to tell us. Notice that we have implicitly assumed in the above argument that we are in higher dimensions ($d>1$). Indeed, if $d=1$, then necessarily $F' = F-F_h = 0$ everywhere; the prevailing flux passes through all density fluctuations without change (by conservation) and, in contrast, $\nabla J = J'(z)$ will change, it is only required to remain negative.

To determine not only the sign but also the magnitude of T', one must make a specific assumption on the nature of the inhomogeneity and solve the corresponding inhomogeneous PDE that would follow from (2.28). In practice however, we are more interested in systems where the variability is such that any perturbation-type approach will fail quantitatively. We will therefore retain only the qualitative features of the calculation that brought us to the "$T'>0$" or "$T>T_h$" result, most importantly, the critical roles played by higher dimensionality, on the one hand, and the nonlinear aspects of the transport process, on the other hand. We see radiation nonlinearities from the (related) viewpoints of the multiplicative nature of the matter-radiation coupling in (2.26), on the one hand, and the occurrence of very large optical thickness, hence the predominance of high orders-of-scattering (which diffusion theory takes for granted anyway, cf. sect. D.3), on the other hand.

2.3.2. *Extension from Diffusion to Transfer, Connections with Stephens' "New Optical Properties" and "Mode-Coupling" Process*

The above "$T>T_h$" result seems quite general and it is worthwhile considering the extent to which it will apply to transfer-type models of transport. Firstly, we can confidently report that, in all of our numerical DA transport (Monte Carlo) simulations, even unpublished, not a single (numerically accurate) violation of the inequality has been observed. Given their formal similarities, the above diffusive analysis could probably be adapted to such simple kinetic systems with too much effort; this goes for the rigorous general part of the argument, leading up to (2.25), as well as the perturbation-type part in (2.26–29). (This may however not be very rewarding however—except maybe in the optically thin regime—because perturbation and diffusion go hand-in-hand with weak variability, as far as truly approximating transfer goes.) The same remarks apply to our (more costly hence far less numerous) CA experiments which always use normal illumination conditions, for simplicity. Moreover, the perturbative aspects will definitely be more involved in this very (too?) general framework; we suspect however that the ideas developed by Box *et al.* [1988] are general enough to by applicable outside of their (vertically inhomogeneous) plane-parallel applications [Box *et al.*, 1989]. Secondly, very few violations of the rule were found by us in the (CA transfer) literature. One is on the thin cloud side ($\bar{\tau}<5$, with g=0.84) of Stephens' [1986] figure 7 which plots out, as a function of $\bar{\tau}$, the albedo of vertically homogeneous, and horizontally variable (y-uniform, x-Gaussian and periodic) density fields. The illumination geometry is however somewhat slant ($\cos\theta_0=13.1°$) at right angles to the striation (the Sun is in the z-x plane) so one can readily define illuminated and shadowed "sides" of the cloud, even through it does not stop abruptly. These striations being relatively well separated to consider each one as an independent cloud, we should ask ourselves which finite cloud albedo definition listed in sect. A.2–3 applies best in the circumstances. It is of course (A.36) that calls for angular integration w.r.t. a zenith that is generally distinct from the (opposite of) incidence direction. All of these angular aspects of Stephens' transfer approach contrast markedly with our diffusion approach where all angular difficulties are essentially neglected from the outset. One should therefore not be too surprized to see differences to arise, especially if $(1\text{-}g)\bar{\tau}$ is as small as 0.8 as is the case here since this is precisely the regime where diffusion is not expected to be accurate, for lack of multiple scattering (that otherwise considerably "smooths" the angular problems away). We are however reassured to see that, in the same figure, $R<R_h$ as soon as $(1\text{-}g)\bar{\tau}\gtrsim 1$ and to see that there is no more discrepancy all the way down to $(1\text{-}g)\bar{\tau}\approx 0.2$ in Stephens' [1988a] computations on the same density field, but with slightly different illumination conditions. Another exception is found in (regular or random) assemblies of individually cube-shaped clouds, but again at relatively slant illumination [e.g., Barker and Davies, 1992; and references therein]; the reason is essentially the same as above: the effective cloud surface seen by the incident light rays increases and this benefits albedo most. We suspect that the rule is applicable to CAs for any optical thickness, as long

as the illumination is sufficiently symmetric: normal or isotropic illumination will generally be required, in the case of striated media, incidence from anywhere in the "uniform" plane (at right angles to the variable direction) is probably good enough.

Rather than providing caveats for a few exceptions that lie outside of our main field of interest ($1 \gtrsim (1-g)\overline{\tau}$) anyway, it is more interesting to recall that Stephens [1988b] uses his numerical data on the Gaussian cloud model just discussed to parameterize ρ–I_u correlations as a function of $\mu = \cos(\mathbf{u}\cdot\hat{\mathbf{z}})$. In our notations and orientation conventions (the "north pole" of Ξ_3 is down, like the z-axis), he proposes

$$\overline{\rho' I_\mu'} \approx - C\, \overline{\rho}\, I_{\mu,h}\, \mu \qquad (2.30a)$$

for azimuthally-averaged radiance, where C is a positive parameter [basically the slope of the linear approximation in his fig. 6]. By further directional integration (w.r.t. μ), this directly yields

$$\overline{\rho' F_z'} \approx - C\, \overline{\rho}\, F_h < 0 \qquad (2.30b)$$

i.e., precisely the crucial inequality needed to establish that T'>0. In other words, we can propose the parameter C as a quantitative measure of "channeling" that is operationally accessible in CA transfer via (2.30a), in diffusion (or DA transfer) via (2.30b). In the case of diffusion with Dirichlet BCs, C (determined from the internal fields) can be directly compared to T', as a check for the expression in (2.25).

Interestingly, Stephens prefers to define parameters like C as "new" optical properties (beyond the usual $\overline{\tau}$, ϖ_0, and g) and uses them in a simple closure scheme. More precisely, the new parameters allow the author to accommodate (in a mean field fashion) horizontal variability within a simple 2-flux model which, unsurprisingly, yields systematically lower albedoes. (Recall that the diffusion approximation used in the above reduces to 2-flux theory when applied to plane-parallel media.) Having argued that even weak variability leads to systematic overall effects, our approach in chapters to come will be quite different from Stephens' since we will be interested in finding the new structural properties that are likely to lead to strong variability effects on the mean radiation fields and criteria in that direction are proposed at the end of chap. 4 and these are corroborated by analytical and numerical results in chap. 5 and 6 respectively. In contrast to an "optical" property, a "structural" property should make no reference to the radiation field in its definition, in Preisendorfer's [1976] jargon: only "inherent," not "apparent," properties are called for. Thus, generally speaking, a rule involving structural properties gives us predictive power whereas, in principle, a result based on optical properties could give us diagnostic power.

We have conducted our above analysis entirely in physical space and clearly that is where Cannon's expression of "channeling" has so many overtones: the original idea was to describe the tendency of the light to find the geometrical paths of least resistance (i.e., density) compatible with the laws of multiple scattering. We are however interested in finding its best Fourier space counterpart. In variability studies (e.g., turbulence), Fourier space is generally considered to be a more comfortable environment to work in (especially in perturbation studies) but, at this point in time, such is not the case when researching radiation effects. This is traceable to two complementary aspects of transfer: firstly, it is linear in its fields (hence no obvious similarity-based phenomenology arises) and, secondly, the matter-radiation coupling is nonlinear since multiplicative (hence, literally, a more convoluted description arises in Fourier space). Indeed, returning to our main culprit in diffusion theory, namely, $(\nabla\ln\rho)\cdot\nabla J$ in (2.26), we recall from app. D that it follows in direct lineage from both "$\kappa\rho(\mathbf{x})I_\mathbf{u}(\mathbf{x})$" and "$\mathbf{u}\cdot\nabla I_\mathbf{u}$" in transfer theory, i.e., the basic ingredients of the kinetic propagator, incarnated (so-to-say) by direct transmittance that we singled out as the fundamental nonlinearity of transfer in sect. A.2. Stephens [1986, 1988a] traces an elegant Fourier space picture of inhomogeneous transfer (not diffusion!), where the horizontal Fourier transform of the density field interacts via convolution with that of the radiance field, in spherical harmonic representation. If the "spectrum" of the horizontal density fluctuations is not entirely concentrated at k=0 (its spatial average) then this convolution necessarily excites non-axisymmetric modes of the radiance field. This is due to the fact that the "streaming" operator $(\mathbf{u}\cdot\nabla)$ contributes, upon Fourier transformation, a term in "$i\mathbf{u}\cdot\boldsymbol{k}$," the $i=\sqrt{-1}$ factor is in fact responsible for the coupling of the various different $\mathbf{u}$-modes. We describe[17] Stephens' symmetry-breaking mechanism as "mode-coupling" and we view it as the best Fourier space expression for "channeling." Furthermore, the expression "pseudo-source/sink" term that we use to describe $(\nabla\ln\rho)\cdot\nabla J$ is even better justified in the Fourier picture—in fact, was largely inspired from it—since its Fourier counterpart is a (convoluted but) scalar result that can be directly combined with the absorption term, when present.

In summary, we have studied the perturbation of the steady flow of radiation through a slab by the creation of internal inhomogeneity. Starting with a homogeneous, plane-parallel, vertically finite medium, we redistribute the material within some horizontally defined unit cell that is then replicated periodically. It is shown that the overall flux (or transmittance) is very likely to be systematically increased by the higher order terms but only in higher dimensions. This is traceable to the nonlinear nature of the matter-radiation coupling in the adopted (diffusion) transport equation and is indicative that the trend will not reverse for more extreme forms of inhomogeneity than perturbative-type approaches can normally accommodate. We have also argued that this finding will generalize to CA transfer if the illumination conditions are sufficiently simple (and, possibly, if the medium is effectively thick w.r.t. isotropic scattering as well). At any rate, the natural illumination geometry in the special case of (orthogonal) DA phase functions is always very simple and, accordingly, no violations have been found within that framework to date.

2.3.3. A Deterministic Narrow Band Example: Spheres with a Cavity

In the above analysis of the basic overall effect of inhomogeneity, making the medium periodic is not strictly necessary, simply easier to visualize: the homogeneous benchmark is then plane-parallel and $\mathbf{F}_h = F_0 T_h \hat{\mathbf{z}}$ applies. In the horizontally finite case, we must firstly define T according to (A.29) as always in diffusion, i.e., by finding the "(proper) terminator" set ($\partial M_=$) on the medium's boundary[18] which is always of dimension d-2. The hypersurfaces where the integration in (2.22) is performed above are now required to contain $\partial M_=$. Secondly, we must bear in mind that we are using the (usually unknown analytically but perfectly well-defined) J_h and $\mathbf{F}_h$ "mean" fields for the particular choice of M (really ∂M) under consideration. Finally, the special roles played by the horizontal and vertical coordinates in the spatial averaging can be replaced by the curvilinear coordinates defined along $J_h(\mathbf{x})$ = const. and $\mathbf{F}_h$'s field-lines, respectively (recall that $J_h(\mathbf{x})$ is harmonic). In the important result (2.25), "z" thus becomes locally defined (prior to spatial averaging) by $\mathbf{F}_h(\mathbf{x})$ but the conclusion is unchanged because it stems from the local analysis of (2.28). A prime example of T'>0 (or $T>T_h$) in this horizontally bounded case is provided below. An important implication of this generalization is that, in all fairness, one can only compare optical density fields having the same support. In particular, one can compare the qualitative differences between horizontally finite and plane-parallel media (e.g., the appearance of horizontal fluxes even for homogeneous cases). Quantitative comparison (of, say, transmittancies) is irrelevant since we would have to compare the effect of a finite to an infinite amount of material, equivalently, an extensive to an intensive quantity, or a "total amount" to a "flux." The abusive comparisons found in the literature stem from the fact that it is traditional in radiative studies to express the said total amount as an average flux, cf. definitions (A.29) and (A.38) of albedo and transmittance, one then forgets that there are no replicas in the finite case.

We now illustrate the general "$T_{inhomo}>T_{homo}$" result from §2.3.1 which applies to media that share the same support and the same total mass and generalized above to horizontally bounded cases. We will simply modify our previous (§2.2.2) analysis of the albedo problem for homogeneous spheres to accommodate spheres with a concentric spherical cavity. This will provide us with a specific example of diffusive "channeling" in a context that we understand well. Eqs. (2.8–13) as well as (2.15) apply here without modification since they concern only the in-going and out-coming radiation fields. Furthermore, since at present we are only interested in the global responses (T,R), we need only to determine the ratio $B_1^{\dagger}/2B_0^{\dagger}$ in (2.13) as a function of the cloud's external and internal geometries (i.e., radii). We must however modify eq. (2.14) which defines the spherical harmonic expansion of the radiation field. Letting r_c be the internal radius where the discontinuity in density occurs, we now have:

$$J(r,\theta) = \sum_{0}^{\infty} \beta_n' \, r^n \, P_n(\cos\theta) \qquad 0 \le r \le r_c \qquad (2.31a)$$

in the central region where we are only interested in the regular part of the solution of Laplace's equation. In contrast, we can make use of the singular solutions in the surrounding region:

$$J(r,\theta) = \sum_{0}^{\infty} [\, \beta_n r^n + \frac{\gamma_n}{r^{n+1}}] \, P_n(\cos\theta) \qquad r_c \le r \le R \qquad (2.31b)$$

Substituting (2.31b) into (2.15), we find:

$$F^{\pm}(\cos\theta) = \frac{1}{2}\sum_{0}^{\infty} \left\{ [\, 1 \mp n\frac{\chi}{R}] \, \beta_n R^n + [\, 1 \pm (n+1)\frac{\chi}{R}] \frac{\gamma_n}{R^{n+1}} \right\} P_n(\cos\theta) \quad (2.32)$$

and we recall that the coefficient of the Legendre polynomial in (2.32) is defined as $2B_n^{\pm}$ where the lower sign corresponds to known (BC-related) numerical quantities, cf. (2.9b). As in the case of homogeneous spheres (and in diffusion approximation tradition, see §D.4.2), we leave the extrapolation length χ as free parameter.

The novelty in this problem is that, by radiant energy conservation, we must require continuity across the internal boundary of the in-going and out-going hemispherical fluxes written as in (2.32) but for $r=r_c$ rather than for $r=R$. Equivalently and more simply expressed, we can require continuity, on the one hand, of the total radiance field $J(r_c{\pm}0,\theta)$ and, on the other hand, of the normal component of the net radiative flux $-D\partial J(r_c,\theta)/\partial r|_{r=r_c\pm 0}$ where D is the radiative diffusivity $(1/3(1-g)\kappa\rho)$ which has distinct values on either side of r_c.[19] Respectively, we find

$$\beta_n' = \beta_n + \frac{\gamma_n}{r_c^{2n+1}} \qquad (2.33a)$$

$$nD'\beta_n' = D[\, n\beta_n - (n+1)\frac{\gamma_n}{r_c^{2n+1}}] \qquad (2.33b)$$

For every value of n of interest, eqs. (2.32) and (2.33a,b) provide four constraints on the four unknown quantities: B_n^{+}, β_n', β_n, γ_n. Clearly the general solution will depend only on the dimensionless ratios χ/R, r_c/R, and $D'/D=\rho/\rho'$, noticing that, up to this point, we have made no specific assumption on the value of the density (or diffusivity) inside the internal boundary. At least one of our unknowns is easily determined in this quite general case: writing (2.33b) for n=0 (a value of special interest to us) we see that $\gamma_0=0$ hence $\beta_0'=\beta_0$, from (2.33a). In turn, we can use this result to see, directly from the general harmonic expansion (2.32) but truncated as previously at n=1, that the ratio of harmonic coefficients that we are seeking can be simply expressed in terms of two other ratios of the remaining unknowns:

$$\frac{B_1^+}{2B_0^+} = \frac{R}{2}\left(\frac{\beta_1}{\beta_0}\right)\left[\,(1-X) + (1+2X)\left(\frac{\gamma_1}{\beta_1}\right)\frac{1}{R^3}\right] \tag{2.34}$$

where we have let $X=\chi/R$, as in the above section on homogeneous spheres.

We now take the limit $D'/D\to\infty$ ($\rho'/\rho\to0$), i.e., we are dealing with an optical void inside a spherical shell uniformly filled with scattering material. At $n\geq1$ in (2.33b), this implies that $\beta_n'=0$. Summing up, the radiation field inside the cavity is reduced to its uniform component (corresponding to β_0') which, in this case, does not imply an absence of net flux, quite the contrary. This can be seen by noticing that $D'\beta_1'$ goes to some finite limit given ultimately by the r.h.s. of (2.33b) for n=1 and, since the l.h.s. of (2.33a) for n=1 vanishes, we know that β_1 and γ_1 are of opposite signs; therefore a non-vanishing γ_1 (creation of a cavity) in (2.33b) implies an increase in the flux ($D'\beta_1'$) at the center of the system (flux lines are converging into the cavity). In short, we are witnessing "channeling" as it was described above (and in sect. D.5); a finer analysis is bound to show that the same phenomenon will occur as soon as $D'/D>1$, i.e., long before it becomes infinite.

To finish the calculation, all we need are two independent equations to determine the two ratios (β_1/β_0, γ_1/β_1) that appear in (2.34). Eqs. (2.32) with lower signs (BCs), on the one hand, and (2.33a), on the other hand, both for n=1, provide a convenient choice. Hence

$$\begin{cases} \beta_1(1+X)R + \gamma_1(1-2X)/R^2 = 2B_1^- \\ \beta_1 r_c + \gamma_1/r_c^2 = \beta_1' \end{cases} \tag{2.35}$$

where we can readily use $2B_1^-=-1$ from (2.9b) and $\beta_1'=0$ from the above $D'/D\to\infty$ limit on the r.h.s.'s respectively. Finally, letting $v_c=(r_c/R)^3$ denote the cavity-to-sphere volume ratio ($0\leq v_c\leq1$), a little algebra leads to

$$\frac{B_1^+}{2B_0^+} = -\,\frac{(1-X) - (1+2X)v_c}{(1+X) - (1-2X)v_c} \tag{2.36}$$

and substitution into (2.13) yields

$$\frac{1}{T} - 1 = \left(\frac{1-v_c}{1+2v_c}\right)\frac{R}{\chi} \tag{2.37}$$

We find the same general form that we generally expect for homogeneous clouds with (everywhere) smooth boundary shapes. In particular, the homogeneous result (2.18) is of course retrieved at $v_c=0$ and we naturally find $T\to1$ in the opposite ($v_c\to1$) limit where the medium itself vanishes. Eq. (2.37) also implies that the radiative scaling is the same for the full and the hollow spheres. This scaling result can be considerably generalized since there is no obvious reason to not consider the hollow spheres to be representative of cloud models with arbitrary but narrow band internal variability (inhomogeneity only arises on a finite range of scales).

Returning to the verification of the general perturbation result, we wish to relate homogeneous and inhomogeneous media with the same supports and masses, i.e., in this case

$$\begin{cases} R_{\text{full}} = R_{\text{hollow}} \\ \rho_{\text{full}} = \rho_{\text{hollow}}(1-v_c) \end{cases} \tag{2.38}$$

Finally, we will assume that the numerical value of χ is the same for both media when expressed in natural (transport m.f.p.) units. In other words, $\kappa\rho\chi$, hence $\kappa\rho R$, are held constant. Writing out (2.37) for both media, taking ratios, and using relations (2.38) leads to:

$$\frac{1}{T_{\text{hollow}}(R)} - 1 = \frac{1}{1+2v_c}\left(\frac{1}{T_{\text{full}}(R)} - 1\right) \tag{2.39}$$

which means that, as predicted, as soon as a cavity is created ($v_c>0$) by redistributing the given amount the scattering material inside the external boundary, transmittance is boosted. Interestingly, the maximum ratio of 3 in the above responses is found for an infinitely thin shell ($v_c=1$) of infinite density.

We can elaborate on (2.39) in order to underscore the importance of higher dimensionality in the "channeling" process. We argued above that our analysis of homogeneous spheres (in d=3) is probably generalizable to any dimensionality (including d=1), yielding in fact the very same result! It is of interest to see why this is no longer quite true now that we have an internal cavity. We know that in d=1 the response ratio in (2.39) must be 1 for all values of v_c since we are dealing with the equivalent of slabs with (a special case of) purely vertical variability (no channeling is possible). We therefore conjecture that the factor "2" in the denominator of the ratio in (2.39) is indeed given by "d-1" (hence the above maximum ratio would be "d" in general). To see why this is likely to be true, notice that the origin of the new (v_c) terms in (2.36–37) is entirely traceable to the second kind of coefficient introduced here in (2.31b). In d=1 however, there is no need for such distinct coefficients since the most general solution of Laplace's equation is a (piecewise) linear function; in d=2, the general solution of Laplace's equation has a (logarithmic) singularity at the origin and a second set of coefficients[20] is again necessary in the region not containing the origin; in d>2, the singularity is algebraic, of order d-2.

2.3.4. A Random Broad Band Example: Uncorrelated Binary Mixtures

We now turn to the case of random optical media that are modelled by random binary mixtures that are reviewed, as simple models for inhomogeneous conductors, in §D.6.2 with sufficient detail to proceed here with a formal analogy; in particular, all of the symbols used below are defined. We recall that the individual cells in these models are given one of two density values ($\rho_\pm$); these values are distributed in a totally uncorrelated manner going from one cell to the next, with relative probabilities ($p_\pm$). However, if one considers the clusters (or "animals") made up of connected cells of one kind, then at "percolation threshold" (a "critical" value p_c of, say, $p_-=1-p_+$) the size of the cluster becomes infinite and, in this sense only, the medium has long-range correlations and we refer the reader to sect. C.2 for a brief discussion of the associated fractal aspects. We are particularly interested in the singular limit $\rho_-\rightarrow 0$ known as the "random superconducting network" (or RSN) limit where the superconducting ($\sigma_+\rightarrow\infty$) cells can simply be viewed as holes in the cloud.

To interpret the conductance results in terms of diffusive radiative transport in (horizontally periodic and) vertically finite but thick media, we only need to invoke the formal analogy ($J\leftrightarrow\phi$, $F\leftrightarrow j$ and $\kappa\rho_\pm\leftrightarrow 1/\sigma_\mp$) leading to (D.35), equivalently,

$$\frac{R}{T} = \frac{1}{T} - 1 \approx \frac{\Delta J}{\overline{F_z}} \leftrightarrow \frac{V}{\overline{j_z}} \approx \frac{L}{\Sigma} \tag{2.31}$$

for each realization of the stochastic medium. In a vast majority of cases (choices of p and $\rho_\pm$), the binary mixtures under study yield a $\langle\Sigma\rangle$ which is independent of the size L of the system, and we retrieve the standard (homogeneous-like) scaling $\langle T\rangle\propto L^{-1}$. In particular, this is true of the percolating (hence highly correlated) but non-singular case, viz. when (D.48a) applies. Nevertheless, "channeling" is already at work at the level of prefactors, as explained in the appendix, cf. the inequality in (D.49) which, interestingly, applies to average bulk conductances under average, rather than exact, conservation of mass. Normal scaling is also found for singular choices of density but when the system is not exactly at percolating threshold, viz. when (D.45) applies. And of course, the same scaling will be found in non-percolating, non-singular cases which have attracted much less attention, see however Hong *et al.* [1986].

By contrast, the percolating, singular RSN limit in (D.47) yields $\langle T\rangle\propto L^{s/v-1}$; using the numerically determined values of s/v quoted in §D.6.2, we find

$$v_T = 1 - \frac{s}{v} = \begin{cases} 0.03 & \text{in } d=2 \\ 0.2 & \text{in } d=3 \end{cases} \tag{2.32}$$

since $\langle\tau\rangle\propto L$ (if »1), see below. Notice that the "v_T" (with a subscript) refers to our usual notation for the radiative scaling exponents introduced in chap. 0–1 while the "v" (without subscript) is standard notation from the literature on percolation. The radiative analog of the "random resistor network" (or RRN) limit is not quite as interesting because of the occurrence of infinite (optical) masses: the insulating (vanishing conductance) cells are like totally opaque (i.e., very thick) individual clouds distributed, with relative probability p_+/p_-, in an otherwise normally scattering atmosphere and the transition observed at $p_+=1-p_c$ tells us that the atmosphere becomes totally reflective (no transmitted flux) long before it becomes totally cloudy, according to diffusion theory.

What does the IP approximation say about this simple stochastic cloud model? For a medium discretized on a N^{d-1}xL-sized grid, the statistics for optical thickness (τ) are obtained with a sample of N^{d-1} independent realizations of the random variable (r.v.) obtained by adding L independent r.v.'s with values $\kappa\rho_\pm l_0$ (where l_0 is the grid constant). The latter r.v.'s follow the law given by the simple Bernouilli trial in (D.40) while the former have an order L binomial distribution. The strong law of large numbers[21] tells us that this last distribution converges (in probability) towards a Gaussian distribution centered on $<\tau> = L\kappa<\rho>l_0$ ($<\rho> = \rho_+p_++\rho_-p_-$) with a relative variance of Lp_+p_-; so we are dealing with a rather narrow distribution that will produce simple scaling in its moments of all orders.[22] In particular, we will have $T_{IP} \propto <1/\tau> \propto 1/<\tau>$.

What does the transfer model of radiation transport say about these intriguing media? Not too surprisingly, Welch *et al.* [1980] find "small" differences between the radiative properties of cloud models generated with white noise and their homogeneous counterparts using Monte Carlo simulation for photon transfer; the fact that they used a continuous distribution of density values rather than binary mixture is not important, the key structural feature here is the lack of spatial correlations. The same remark applies implicitly to Boissé's [1990] numerical results for non-conservative transfer in *bone fide* binary mixtures since he finds that a single realization is sufficient to validate his own analytical mean field results from transfer calculations of media exponentially correlated on some given scale (which he naturally associates with the grid constant). More importantly, Boissé's [*ibid.*] analytical inhomogeneous formalism is becomes identical to homogeneous formalism (for the mean density) in the limit of vanishingly small correlation length, irrespective of whether the lower density value vanishes or not, whether absorption is present or not.

This major discrepancy between diffusive and transfer scaling behaviours was first anticipated by Lovejoy *et al.* [1989] who found a close connection between photons and the "skating termites" described by Bunde *et al.* [1985]. "Termites" ("ants") are special cases of particles that "diffuse" exactly on a grid in the RSN (RRN) limits; the former were originally proposed by de Gennes [1980]. A "diffusing" particle must know how to navigate in presence of any change in the local value of diffusivity D, not only going from 0 to a finite value (ants) or from there to ∞ (termites). Several versions of the termite were under study by Bunde *et al.* [*ibid.*] and the "skating" model (which had the particularity of performing ballistic flights through the superconducting cluster, like photons would in an optical void) failed to show the expected phase transition behaviour at percolation. In other words, photons poorly approximate diffusing particles (and, of course, vice-versa) but, from the above scaling results, we only expect this in presence of singular, highly correlated density fields since both of these features are *sine qua non* conditions to obtain the "anomalous" scaling in (2.32), see sect. 4.3–4 for further discussion of this point.

---

†This chapter has no published equivalent, the author is largely responsible for its content. His advisor (S. Lovejoy) was instrumental in finding a basic inconsistency in an early version of the "perturbation-like" argument in §2.3.1. He also researched the percolating conductance problem but from the point of view of "ants and termites" (see §D.6.3), rather than the formal analogy standpoint used here, and only with the singular (anomalous scaling) limit in mind; this had the effect of attracting the author's attention to binary mixtures in general (singular or not, percolating or not).

1 "Polarization" is used here in the dielectric, not radiative, sense of the word.

2 In a thermal conductance analogy, we would call these boundaries "insulating."

3 A similar argument can be made w.r.t. the insertion of conducting (ϕ_i=const.) hypersurfaces between ∂H and $\partial\Omega_0$; but this amounts to creating a number of independent capacitors in a series arrangement (the $1/C(\Omega_i)$ add) and results in an increased effective capacitance, unless the newly inserted sub-domain boundaries all coincide with equipotential surfaces of the original field.

4 In DA transfer this simply amounts to allowing for some degree of side-scattering to occur (see chap. 3).

5 The author then goes on to re-derive (and somewhat generalize) Pólya's [1948] proof of Saint Venant's conjecture that, within the framework of linear elasticity theory, maximal torsional rigidity for cylindrical cables of arbitrary section is achieved when the section is circular with one concentric hole.

6 See Le Méhauté and Crépy [1982] and Le Méhauté [1984] for a similar problem in electro-chemistry (with oscillating rather than steady-state potentials) that they treats phenomenologically with fractional (time) derivatives.

7 The author thanks P. Gabriel for attracting his attention to this early publication.

8 We will however disregard the boundary layer effects related to collimated illumination that could be incorporated by using the "direct+diffuse" formulation and internal (single-scattering) sources near the upper boundary. We assume the strictly collimated incident radiation is immediately converted into an isotropic irradiance pattern normalized to the amount dictated by (Lambert's) cosine law. The neglected effects are however partially accounted for implicitly by leaving the extrapolation length as a free parameter.

9 or Helmoltz equation, if in presence of absorption (of radiation) or multiplication (of neutrons).

10 For this, one will need $\int_0^1 xP_n(x)dx$ which is $(-1)^{n/2}n!/2^n(n-1)(n+2)(n/2)!$ for n even (in particular, -1/2 for n=0), and 0 for n odd but ≠1, 1/3 for n=1; this is adapted from Gradshteyn and Ryzhik [1980, p. 820]. The harmonic (BC) coefficients B_n^- are obtained by multiplying this expression by $-(2n+1)/2$.

11 Davison [1951] discusses these limit cases and performs numerical and analytical transfer calculations for intermediate values. Recall that these were originally intended to be used in more general but necessarily approximate diffusion calculations (such as those of Giovanelli and Jefferies [1956]) in order to increase their numerical accuracy—a very important concern in both civilian and military contemporary applications of neutronics.

12 The whole boundary is a sink for the diffuse radiation but the lower half is only a sink (no in-coming radiation, transmitted fluxes going out) while the upper half is in fact more of a source (unit in-coming) than a sink (albedo out-going).

13 This can be readily checked using standard tools from harmonic analysis in 3D cylindrical- or 2D polar coordinates, viz. Bessel's functions (of the 1st kind) and Fourier series. Note that only a cosine series will be necessary, by symmetry, just a the simple Legendre polynomials were used in d=3.

14 The integration is easily performed by using the polar angle: $l = 2R\cos\theta$ and $dP(l) = \sin\theta d\theta$.

15 In comparing the radiative properties of (say) cubes and slabs we are in fact comparing an extensive quantity (integrated flux) with an intensive quantity. This is however not immediately obvious because these quantities are always neatly normalized by the (respectively, extensive and intensive) quantities of light received.

16 The rigorous (mathematically self-contained) 2nd order perturbation theory of the complete boundary value problem at hand seems to be intractable [S. Lovejoy, p.c.].

17 See §1.5.2 for a more accurate discussion of Stephens' words.

18 The fact (pointed out in the previous section) that, for horizontally finite media, we must be more careful about mixed BCs only means that they will only be approximately verified by the total (J_h+J') radiation field in this generalization of the perturbative result.

19 This results directly from the integral form (D.2-3) of the radiant energy conservation law applied to a small volume that encloses a portion of the surface of discontinuity.

[20] These would be affected to Bessel's functions of the 2^{nd} kind that come to complement their (non-singular) counterparts of the 1^{st} kind.

[21] This is a special case of the central limit theorem, for a restricted class of random variables but with a stronger criterion for convergence.

[22] This is also basically why only the means (and no other moments) were considered in the above results for $\langle T \rangle$ and $\langle \Sigma \rangle$ as well as in §D.6.2.

Bibliography for Chapter 2

Barker, H. W., and J. Davies, "Solar Radiative Fluxes for Extensive Broken Cloud Fields," *J. Atmos. Sc.*, 1992 (in press).

Barkstrom, B. R., and R. F. Arduini, "The effect of finite size of clouds upon the visual albedo of the earth," in *Radiation in the Atmosphere*, ed. H.-J. Bolle, Science Press, Princeton, pp188–190, 1977.

Boissé, P., "Radiative Transfer Inside Clumpy Media: The Penetration of UV Photons Inside Molecular Clouds," *Astron. Astrophys.*, 228, 483–502, 1990.

Box, M. A., S. A. W. Gerstl and C. Simmer, "Application of the adjoint formulation to the calculation of atmospheric radiative effects," *Beitr. Phys. Atmosph.*, 61, 303–311, 1988.

Box, M. A., B. Croke, S. A. W. Gerstl and C. Simmer, "Application of the perturbation theory for atmospheric radiative effects: Aerosol scattering atmospheres," *Beitr. Phys. Atmosph.*, 62, 200–211, 1989.

Bunde, A., A. Coniglio, D. C. Hong, and H. E. Stanley, "Transport in a Two-Dimensional Randomly Composite Material: Scaling Theory and Computer Simulations of Termite Diffusion near Superconducting Limit," *J. Phys. A*, 18, L137–L144, 1985.

Cannon, C. J., "Line Transfer in Two Dimensions," *Astrophys. J.*, 161, 255–264, 1970.

Cushman, J. H. (Ed.), *Dynamics of Fluids in Hierarchical Porous Media*, pp. xvii+505, Academic Press, London, 1990.

Davies, R., *The three dimensional transfer of solar radiation in clouds*, Ph. D. thesis, 219pp, Univ. of Wisc., Madison, 1976.

Davies, R., "The effect of finite geometry on three-dimensional transfer of solar irradiance in clouds," *J. Atmos. Sci.*, 35, 1712–1724, 1978.

Davies, R., and J. A. Weinman, "Results from two models of the three dimensional transfer of solar radiation in finite clouds," in *Radiation in the Atmosphere*, ed. H.-J. Bolle, Science Press, Princeton, pp225–227, 1977.

Davison, B., "Influence of a Black Sphere and of a Black Cylinder upon the Neutron Density in an Infinite Non-Capturing Medium," *Lond. Phys. Soc. Proc.*, 64, 881–902, 1951.

de Gennes, P. G., "Percolation: Quelques Systèmes Nouveaux," J. Phys. (Paris) Colloq., 41, C3–17, 1980.

Giovanelli, R. G., and J. T. Jefferies, Radiative Transfer with Distributed Sources, *Lond. Phys. Soc. Proc.*, 69, 1077–1084, 1956.

Gradshteyn, I. S., and I. M. Ryzhik, *Tables of Integrals, Series, and Products*, Academic, London, 1980.

Harte, J., *Consider a Spherical Cow - A Course in Environmental Problem Solving*, William Kaufmann Inc., Los Altos (Ca.), 1985.

Hong, D. C., H. E. Stanley, A. Coniglio, and A. Bunde, "Random-Walk Approach to the Two-Component Random-Conductor Mixture: Perturbing Away from the Perfect Random Resistor and Random Superconducting Network Limits," *Phys. Rev. B*, 33, 4564–4573, 1986.

Le Méhauté, A., and G. Crépy, "Sur quelques propriétés de transferts électrochimiques en géométrie fractale," *Comptes Rendus* (Paris), 294-II, 685–688, 1982.

Le Méhauté, A., "Transfer Processes in Fractal Media," *J. Stat. Phys.*, 36, 665–676, 1984.

Lovejoy, S., P. Gabriel, D. Schertzer, and G. L. Austin, "Fractal clouds with discrete angle radiative transfer," in *IRS'88: Current Problems in Atmospheric Radiation*, eds. J. Lenoble and J. F. Geleyn, pp99–102, A. Deepak, Hampton (Va.), 1989.

McKee, T.B., and J.T. Cox, "Scattering of visible light by finite clouds," *J. Atmos. Sci.*, 31, 1885–1892, 1974.

Morse, P. M., and H. Feshbach, *Methods of Theoretical Physics*, McGraw-Hill, New York (NY), 1953.

Mossino, J., *Inégalités isopérimétriques et applications en physique*, Hermann, Paris, 1984.

Pólya, G., "Torsional rigidity, principal frequency, electrostatic capacity and symmetrization," *Quart. Appl. Math.*, 6, 267–277, 1948.

Preisendorfer, R. W., *Hydrological Optics*, vol. 1, NOAA, PMEL, Hawaii, 1976.

Preisendorfer, R. W., and G. L. Stephens, "Multimode radiative transfer in finite optical media, I: Fundamentals," *J. Atmos. Sci.*, 41, 709–724, 1984.

Stephens, G. L., "Radiative Transfer in Spatially Heterogeneous, Two-Dimensional Anisotropically Scattering Media," *J. Quant. Spectrosc. Radiat. Transfer*, 36, 51–67, 1986.

Stephens, G. L., "Radiative Transfer Through Arbitrarily Shaped Media - Part 1: General Theory," *J. Atmos. Sci.*, 45, 1818–1836, 1988a.

Stephens, G. L., "Radiative Transfer Through Arbitrarily Shaped Media - Part 2: Group Theory and Closures," *J. Atmos. Sci.*, 45, 1837–1848, 1988b.

Stephens, G. L., and R. W. Preisendorfer, "Multimode radiative transfer in finite optical media, II: Solutions," *J. Atmos. Sci.*, 41, 725–735, 1984.

Szegö, G., "Ueber einige Extremalaufgaben der Potentialtheorie," *Math. Z.*, 31, 583–593, 1930.

Welch, R. M., S. Cox, and J. Davis, "Solar Radiation and Clouds," *Meteorol. Monogr.*, 39, 1980.

Chapter Three†

DISCRETE ANGLE RADIATIVE TRANSFER, ELEMENTS AND CONNECTIONS

Preliminary Remarks and Overview: We refer the reader to app. A for a brief survey of continuous angle (CA) transfer in d-dimensional space, including all the necessary background material and (in §A.3.3) a rarely discussed interpretation of the steady-state multiple scattering (m.s.) transfer equation,

$$\mathbf{u}\cdot\nabla\, I_{\mathbf{u}}(\mathbf{x}) = -\,\kappa\rho(\mathbf{x})\,[\,I_{\mathbf{u}}(\mathbf{x}) - \oint p(\mathbf{u}'\to\mathbf{u})\, I_{\mathbf{u}'}(\mathbf{x})\, d^{d-1}\mathbf{u}'\,] \tag{3.0}$$

as a local balance between spatial variability (directional gradients of radiance field) and the angular variability (anisotropy of the radiance at a point in space). This means that we never be able to totally "decouple" these two basic aspects of the radiative transfer problem but we can reduce the level of sophistication and difficulty in the angular part. The reader is further referred to app. D for a review of the standard approach which consists in taking the hydrodynamic limit; this leads to the "diffusion" approximation which was systematically exploited in the previous chapter to investigate (largely analytically) the basic effects of spatial variability.

In this chapter, we describe a way of satisfying this same need without leaving the realm of kinetic theory: discrete angles (DAs), not a new but a previously under-exploited idea. Direction-space always has to be discretized sooner-or-later in numerical radiative transfer. "Sooner" refers to straightforward numerical solution of the transfer equation, e.g., in Chandrasekhar's [1950] discrete ordinate method that must be performed with a given number of "streams," each one associated with a pivot angle given by Gaussian quadrature formulae. "Later" refers to direct simulations, i.e., Monte Carlo techniques which call for the definition of—and computer memory allocation for—angular "bins," cf. app. B. By contrast, we do not view DA transfer as an approximation to its CA counterpart. (On the contrary, DA phase functions are limits of CA phase functions more-and-more peaked in certain directions; in this sense, CA transfer therefore can only approximate[1] its DA limit.) Being only a special (however extreme) case of CA theory, it is hoped that DA theory will share its essential features; in our view, an "essential" property is a "scaling" property and this outlook provides a way of testing this (or any other proposed simplification scheme), see chap. 4. Returning to practical (numerical) matters, DA phase functions make many new computational short-cuts available (see app. B) ... quite apart from the considerable conceptual simplification to be exploited in the present chapter.

Before proceeding and in order to accommodate future needs, we relax the steady-state assumption on the l.h.s. of (3.0) and allow for the possibility of non-m.s. sources on its r.h.s., thus

$$[\frac{1}{c}\frac{\partial}{\partial t} + \mathbf{u}\cdot\nabla]\, I_{\mathbf{u}}(\mathbf{x},t) = -\kappa\rho(\mathbf{x})\,[\, I_{\mathbf{u}}(\mathbf{x},t) - \oint p(\mathbf{u}'\to\mathbf{u})\, I_{\mathbf{u}'}(\mathbf{x},t)\, d^{d-1}\mathbf{u}' - S_{\mathbf{u}}(\mathbf{x},t)\,] \qquad (3.0')$$

will be our point of departure. (All the symbols are defined in app. A.) In the opening section, we show how (3.0') can be considerably simplified (mathematically speaking) by considering only a finite number of beams with phase function choices that only couple members of this family; we go on to show that only a countable infinity of such families exist if the phase function can only depend on relative (or "scattering") angles. The simplest of these families consist of mutually orthogonal beams and we focus on these in sect.3.2, deriving in particular their "eigenvector" representation. In sect. 3.3, we derive the 2nd order coupled PDEs obeyed by these systems and show that they have two interesting special (limiting) cases; on the one hand, systems of d uncoupled one-dimensional diffusion equations, this limit being equivalent to the "independent pixel" (IP) approximation discussed within the framework of diffusion in the previous chapter; on the other hand, d-dimensional diffusion itself is retrieved but from a very non-standard approach. The general properties of the IP approximation are discussed in sect. 3.4 and it is related to the problem of homogeneous media with random optical parameters (to which we return in chap. 5). Finally, sect. 3.5 is devoted to the two similarity theories one can develop for orthogonal DA systems, one is a straightforward transposition of its exact CA counterpart while the other is more general but only approximate w.r.t. the problem of imposing boundary conditions (BCs), not a serious concern in optically thick (and possibly also horizontally extended) systems. At any rate, the IP and diffusion limits are singular w.r.t. these similarity transformations, implying qualitatively different properties in general.

3.1. DA Phase Functions and Transfer Equations

3.1.1. The General Case where Absolute Directions are Needed

In our usual (probabilistic) transfer jargon developed in app. E (and A), we are simply going to "sample" **u**-space, Ξ_d: let $\{\mathbf{i}\}$ be a finite but otherwise arbitrary set of directions. We now simply require the radiance field and phase function be decomposable into sums of δ-functions both supported by $\{\mathbf{i}\}$:

$$I_u(x,t) = \sum_{\{i\}} I_i(x,t)\, \delta(u-i), \tag{3.1}$$

$$p(j \to u) = \sum_{\{i\}} P_{ji}\, \delta(u-i), \text{ for all } j \in \{i\}. \tag{3.2}$$

Note that DA "radiances" I_i are really coefficients in a δ-decomposition and therefore have units of flux (irradiance). Similarly, the coefficients P_{ij} can be viewed as the elements of a (dimensionless) scattering matrix $\boldsymbol{P} = \{P_{ij}\}$. Apart from this question of units, there is no intrinsic difference between the physical definitions of DA intensity I_i given by (3.1) and that of its CA counterpart, (specific) intensity I_u, given in app. A: both are conserved quantities along the beam in absence of extinction (i.e., $\kappa\rho=0$) and their respective transfer equations account for the changes that occur when $\kappa\rho>0$ (i.e., scattering in and out of the beam as well as possible absorption). However, when associating DA "intensity" (or radiance) with a CA "flux" (or irradiance), we must bear in mind that the latter is diluted by space along a bundle of rays, i.e., it obeys the "$1/r^{d-1}$" law, a basic tenet of standard transfer theory and practice.

Substitution of eqs. (3.1–2) into the CA transfer equation (3.0'), followed by **u**-integration yields the basic DA radiative transfer equation:

$$\left[\frac{1}{c}\frac{\partial}{\partial t} + j\cdot\nabla\right] I_j(x,t) = -\,\kappa\rho(x)\left\{\sum_{\{i\}} (1-P)_{ij}\, I_i(x,t) + S_j(x,t)\right\} \tag{3.3}$$

A finite, rather than infinite, system of coupled 1st order PDEs. $S_j(x,t)$ represents all of the non-m.s. DA sources, not necessarily related in any specific way to their CA counterparts. All of our CA expressions for BCs, albedoes and transmittances carry over to DAs without change. Expressions containing **u**-integrals will even simplify as did the radiative transfer equation itself. Concerning the albedo problem BCs, we must obviously choose the direction of collimated incident flux (u_0) within $\{i\}$ although we notice that, due to linearity, we can "superpose" as many $\{i\}$ families as we want (even fill all of Ξ_d!). These various families of beams will remain however mutually independent of one another.

3.1.2. The Specific Case where Only Relative Directions are Used

As in CAs, the most useful DA phase functions depend only on relative angles (equivalently, **i**·**j**) but it is important to realize, on the one hand, that relative DAs does not imply axi-symmetry and, on the other hand, that this requirement greatly restricts the number of eligible DA systems. To determine those which qualify, we note that imposing **i**·**j**-dependence is equivalent to asking that the set of transformations needed to map unit vectors $\{i\}$ onto $\{j\}$ form a non-degenerate and non-trivial finite sub-group of the corresponding rotation/reflection group O(d). By "non-degenerate," we mean a sub-group that cannot be projected unto a finite sub-group of O(d-1) and by "non-trivial," we mean a sub-group that does not reduce to the identity element[2] ($\mathbf{x} \rightarrow \mathbf{x}$) of O(d). We shall use the notation DA(d,n) for DA systems with n beams in d dimensions.

ENUMERATION IN d=1. On a line, only two directions are possible and "d-1" degeneration is not a concern; hence only one DA system that we shall denote DA(1,2) and which will prove to be formally identical to the "two-flux" model. For future (d>1) reference, we note that O(1) is itself finite as it contains only the identity and parity ($\mathbf{x} \rightarrow -\mathbf{x}$) transformations.

ENUMERATION IN d=2. In the plane, we have a countable infinity of acceptable DA systems, each one corresponding to a nondegenerate finite subgroup of O(2) generated by a rotation through $2\pi/n$ (with $n=3,4,5,\cdots$) which we shall designate by DA(2,n). Notice that the case n=1 is trivial and the case n=2 is excluded because rotation through π is equivalent to parity and DA(2,2) is therefore degenerate.

ENUMERATION IN d=3. In space, we have but five possibilities each corresponding to one of the five Platonic solids (or fully regular polyhedra): DA(3,4) for the tetrahedron, DA(3,6) for the cube, DA(3,8) for the octahedron, DA(3,12) for the dodecahedron, and DA(3,20) for the icosahedron. This indeed is the only way to divide the 4π steradians of Ξ_3 equally while maintaining the same (discrete) isotropy around every beam; this last constraint excludes the 13 semi-regular (or Archimedian) solids as well as their duals (or Catalan solids, obtained by truncation or stellation of the above), see Smith [1982] for details and Kepler [1619] for an early application to celestial mechanics[3] ... interstingly, planetary astronomy is precisely where the expression "phase function" came from in the first place (see §A.4.3).

In many applications, it is desirable that the DA system allow backscattering, that the associated sub-group of O(d) must contain parity. Eligible DA systems would then be DA(1,2), DA(2,n) (with $n=4,6,8,\cdots$) and DA(3,6), DA(3,8), DA(3,12), DA(3,20), since the tetrahedron does not have "opposite" faces. For d=1,2,3, the simplest of these are DA(d,2d) systems and they will be used extensively in the following, they correspond to mutually orthogonal beams (when d>1). An important application where DA back-scattering is prerequisite is spatial discretization of the DA transfer equations by finite differencing; in such applications, the cells are "dual" (faces perpendicular) to the direction set {i} and the associated solids must "fill" their embedding space.

ENUMERATION IN d=1. On a line, discretization poses no special problem.

ENUMERATION IN d=2. In the plane, we can exploit either one of the three well-known regular tessellations of the plane: (i) by squares, (ii) by equilateral triangles or (iii) by regular hexagons. These lattices are associated (i) with DA(2,4) systems, (ii) a sub-class of DA(2,6) systems, and (iii) all DA(2,6) systems. Consider the case of a triangular lattice where "up" and "down" triangles must be alternated: the DA(2,6) sub-class of interest corresponds to the inhibition of "transmittance" since there is no opposite face as well as "scattering" through ±120°. Thus the "transfer" of a given beam through a single cell feeds radiant energy into its opposite (at 180°) and the two others at ±60°; of course, the same source of energy will eventually feed the three other beams (including itself) upon crossing a second (or more) cell(s). For an illustration, Gabriel *et al.* [1990] used both squares and triangles.

ENUMERATION IN d=3. In space, we are interested in those Platonic polyhedra that are also (or can be combined into) parallelohedra or Fedorov solids, i.e., they fill space. These and their associated DA systems are (i) cubes and DA(3,6), (ii) "up" and "down" tetrahedra and (iii) a sub-class (cf. discussion in d=2 case) of DA(3,8), octahedra and all of DA(3,8).

Finally, we remark that in d=3, Whitney's [1974] "Dodecahedron Approach to Radiative Transfer" (DART) is closely related to the DA(3,12) system and has been used primarily to optimize radiative transfer codes; along with Chu and Churchill [1955], Siddal and Selçuk [1979], Mosher [1979], Cogley [1981], Gabriel *et al.* [1986], and Lovejoy *et al.* [1989] we favor the DA(3,6) model for its conceptual (and computational) simplicity.

3.2. The Simplest DA Systems: Orthogonal Beams

3.2.1. DA(d,2d) *in its Natural Representation, Two-Flux Theory as a Special Case*

We now turn to the simplest of DA systems where the propagation is confined to mutually perpendicular directions, conveniently oriented by the axii of a rectangular coordinate system. Writing out the DA transfer eq. (3.3) explicitly in the DA(3,6) case for which $\{\pm\hat{x},\pm\hat{y},\pm\hat{z}\}$ is the set of unit vectors for the x,y,z-axii respectively (plus their opposites), we find

$$\left[\frac{1}{c}\mathit{1}\frac{\partial}{\partial t} + A_x\frac{\partial}{\partial x} + A_y\frac{\partial}{\partial y} + A_z\frac{\partial}{\partial z}\right]\mathbf{I} = \kappa\rho(x)\left[\,(P\text{-}\mathit{1})\mathbf{I}(x,t) + \mathbf{S}(x,t)\,\right] \qquad (3.4)$$

with

$$A_x = \begin{pmatrix} 1&0&0&0&0&0\\ 0&-1&0&0&0&0\\ 0&0&0&0&0&0\\ 0&0&0&0&0&0\\ 0&0&0&0&0&0\\ 0&0&0&0&0&0 \end{pmatrix} \quad A_y = \begin{pmatrix} 0&0&0&0&0&0\\ 0&0&0&0&0&0\\ 0&0&1&0&0&0\\ 0&0&0&-1&0&0\\ 0&0&0&0&0&0\\ 0&0&0&0&0&0 \end{pmatrix} \quad A_z = \begin{pmatrix} 0&0&0&0&0&0\\ 0&0&0&0&0&0\\ 0&0&0&0&0&0\\ 0&0&0&0&0&0\\ 0&0&0&0&1&0\\ 0&0&0&0&0&-1 \end{pmatrix} \qquad (3.5a)$$

$$P\text{-}\mathit{1} = \begin{pmatrix} t\text{-}1&r&s&s&s&s\\ r&t\text{-}1&s&s&s&s\\ s&s&t\text{-}1&r&s&s\\ s&s&r&t\text{-}1&s&s\\ s&s&s&s&t\text{-}1&r\\ s&s&s&s&r&t\text{-}1 \end{pmatrix} \quad \mathbf{I} = \begin{pmatrix} I_{+x}\\ I_{-x}\\ I_{+y}\\ I_{-y}\\ I_{+z}\\ I_{-z} \end{pmatrix} \quad \mathbf{S} = \begin{pmatrix} S_{+x}\\ S_{-x}\\ S_{+y}\\ S_{-y}\\ S_{+z}\\ S_{-z} \end{pmatrix} \qquad (3.5b)$$

where t, r and s are the relative probabilities of scattering through 0, π, $\pi/2$ radians resp. The DA(2,4) model can be retrieved by making $I_{+x}=I_{-x}=0$ in (3.5b) hence $\partial/\partial x=0$ in (3.4) and reducing the order of the system accordingly; this system is the simplest where higher dimensional effects—such as "channeling" as defined in chap. 1 and described in terms of diffusion in chap. 2—can happen and it has now been extensively exploited numerically [Davis *et al.*, 1989, 1990a, 1991] (see also chap. 4 and 6). Similarly, we retrieve the DA(1,2) model by starting with $I_{+x}=I_{-x}=I_{+y}=I_{-y}=0$, $\partial/\partial x=\partial/\partial y=0$; this last system is completely equivalent to Schuster's [1905] (analytically solvable hence much used) "two-flux" model for the diffuse radiation field with **S** representing the optional single-scattering sources, see Meador and Weaver [1980] for full details. We are thus faced with a finite system of linear 1st order PDEs with all its matrices A_i (i=x,y,z) being singular[4] for d>1. We shall continue to assume that the p-matrix is constant in space, only the optical density varies, via $\rho(\mathbf{x})$. Except for notation, the full DA radiative transfer system described by (3.4–5) is identical to the "six-beam" model of Chu and Churchill [1955] and Siddal and Selçuk [1979], who seem to have worked independently. The former authors used it as an approximation to CA scattering in plane-parallel geometry (obtained by taking $\partial/\partial x=\partial/\partial y=0$ hence $\partial/\partial z=d/dz$), the latter (who incorporate internal sources) compare its performance with other solutions of the transfer problem for cuboidal enclosures (which is of importance in furnace design). Our exploitation of this idea differs substantially from theirs: we do not consider the DA case as an approximation scheme for CA transfer but rather we study it as a theoretically realizable model interesting in its own right.

Rather than the above ("natural") description of the DA scattering process in terms the elements (t,r,s) of the p-matrix, we will introduce the following equivalent parameterization when and where convenient:

$$a = 1 - t - r - 2(d-1)s \tag{3.6a}$$

$$q = 1 - t + r \tag{3.6b}$$

$$p = 1 - t - r \tag{3.6c}$$

Notice that the relative weights that multiply the various scattering matrix coefficients P_{ij} from (3.5b) in the combinations that appear in (3.5a,b,c) are simply $(\mathbf{i}\cdot\mathbf{j})^n$ with n=0,1,2 respectively. The above are therefore simply related to the 0th through 2nd coefficients of the d-dimensional spherical harmonic expansion of the DA phase function: Fourier in d=2, Fourier-Legendre in d=3 (recall that DA phase functions are not axi-symmetric). Parameters a and q are already well-known: respectively, $1-\varpi_0$ and $1-\varpi_0 g$ as can be seen from definitions (3.6a,b). Parameter p is new, from (3.6a,c):

$$p = a + 2(d-1)s \tag{3.7}$$

It can therefore be viewed as a measure of the combined effects of absorption and/or side-scattering. The (a,q,p) have natural bounds imposed by the probabilistic interpretation of the (t,r,s); namely,

$$0 \le a \le 1 \tag{3.8a}$$

$$0 \le q \le 2 \tag{3.8b}$$

$$a \le p \le 1 \tag{3.8c}$$

Equalities are obtained respectively for all/no scattering, all forward/backward-scattering, and no/all side-scattering.

3.2.2. DA(d,2d) *in Eigenvector Representation, Comparison of DA and CA Quantities*

From the definitions of sect. A.3, we can see that $1\text{-}\varpi_0$ and $1\text{-}\varpi_0 g$ are the first two harmonic coefficients of the CA scattering-extinction kernel $K(\mathbf{u}'\cdot\mathbf{u}) = \delta(\mathbf{u}'\text{-}\mathbf{u}) - p(\mathbf{u}'\cdot\mathbf{u})$ that can be used to write the whole r.h.s. of (3.0) within a single collision-type integral. We now seek a complete eigenvector characterization of the DA scattering/extinction matrix ***P-1*** in (3.4–5). Its eigenvalues are found to be:

a, q (once each)	for d=1	
a, q (twice) and 2p-a	" d=2	(3.9)
a, q (thrice) and 2p-a (twice)	" d=3	

Notice that ***P-1*** in (3.4) is (also) singular in the conservative (a=0) case; see below for what happens in d>1 when p→a and two of the eigenvalues become one. We now define the symmetric and anti-symmetric components of DA radiance along the various axii:

$$I_{j\pm} = I_{+j} \pm L_j \quad (\text{for } j=\hat{x},\hat{y},\hat{z}), \tag{3.10}$$

In d=2, we find the following association of eigenvalues and -vectors:

a:	$(1,1,1,1)^T$	(3.11a)
q:	$(1,-1,0,0)^T$ and $(0,0,1,-1)^T$	(3.11b)
2p-a:	$(-1,-1,1,1)^T$	(3.11c)

where super-script "T" denotes transposition. The projections of the (formal) radiance 4-vector **I** on the above three eigenspaces are respectively:

$$J = I_{y+} + I_{z+}, \tag{3.11a'}$$

$$\mathbf{F} = \hat{y}I_{y-} + \hat{z}I_{z-}, \tag{3.11b'}$$

$$X = -I_{y+} + I_{z+}, \tag{3.11c'}$$

i.e., total radiance (or scalar flux), net flux (2-vector), and (scalar) excess of vertically to horizontally propagating radiation. The I_{i-} terms are thus the d components of the DA flux d-vector **F** whereas the I_{i+} can be viewed as the contribution of radiation flowing along the i^{th} axis to total DA intensity J. This is the DA equivalent of using spherical harmonics to characterize radiance in CA transfer (cf. sect. A.1). Anticipating that diffusion theory only attempts to model the first two of the above, we will call the last the "non-diffusive" component of DA radiance (see below).

Similarly to (3.11a–c), we find for d=3:

a:	$(1,1,1,1,1,1)^T$	(3.12a)
q:	$(1,-1,0,0,0,0)^T$, $(0,0,1,-1,0,0)^T$ and $(0,0,0,0,1,-1)^T$	(3.12b)
2p-a:	$(-1/2,-1/2,-1/2,-1/2,1,1)^T$ and $(1,1,-1,-1,0,0)^T$	(3.12c)

Notice that the last choices are somewhat arbitrary (due to the degeneracy) and we choose to privilege the vertical axis which is usually assumed to carry the incident flux in albedo problems, hence the radiation field's main (spatial) asymmetry. We also see that, eqs. (3.11a'–c') become

$$J = I_{x+} + I_{y+} + I_{z+}, \tag{3.12a'}$$

$$\mathbf{F} = \hat{x}I_{x-} + \hat{y}I_{y-} + \hat{z}I_{z-}, \tag{3.12b'}$$

$$Z_+ = -(I_{x+} + I_{y+})/2 + I_{z+}, \text{ and } Z_- = I_{x+} - I_{y+} \tag{3.12c'}$$

The two last ("non-diffusive") components are the excesses of vertically (up- or downwards) traveling radiation over the average traveling in the $\pm$x- and $\pm$y directions (for Z_+), and the difference between $\pm$x- and $\pm$y directions (for Z_-). Alternatively, one could take $(-1,-1,0,0,1,1)^T$ and $(0,0,-1,-1,1,1)^T$, i.e., the excesses of vertically traveling radiation over that traveling in the $\pm$x- and $\pm$y directions respectively.

It is obviously important to find a operational way of comparing the CA- and DA radiation fields quantitatively and the easiest way of doing this is to consider the scalar and vectorial fluxes defined over portions of Ξ_d, the hemispheres used in (A.2'–3') providing a natural choice for comparison with the orthogonal DA(d,2d) radiances we are presently concerned with. However, the choice between the association of $I_{\pm j}$ with $J_{\pm j}$ or $F_{\pm j}$ for $j \in \{\hat{x}_j, j=1,\cdots,d\}$ cannot be made uniquely nor arbitrarily, it must be guided by general conservation principles which involve the $F_{\pm j}$, cf. eq. (D.2–3). Moreover, we can use our definitions to see that

$$\mathbf{F} = \sum_1^d \sum_\pm \pm j\, F_{\pm j}, \text{ in CAs} \tag{3.13}$$

$$\mathbf{F} = \sum_1^d \sum_\pm \pm j\, I_{\pm j}, \text{ in DAs} \tag{3.14}$$

so the adequate choice seems to be the association of $I_{\pm j}$ with $F_{\pm j}$ of (A.3'). This is particularly important when dealing with overall (boundary integrated) fluxes since $\mathbf{F}$ is the conserved (divergence-free) quantity in steady-state, non-absorbing systems. The trouble with this correspondence is that the sum of all the $F_{\pm i}$ is not J, we would have to use the $J_{\pm j}$ of (A.2') and divide by d for that to work.

Clearly, CA-to-DA comparisons are best done using their respective orthogonal function bases: spherical harmonics and formal eigenvectors, respectively. This rises the question of the CA equivalent of X, the scalar defined in (3.11c') if d=2, or of the $Z_{\pm}$, defined in (3.12c') if d=3, and a (d-1)-dimensional entity in general. The candidate(s) must be some function of the d(d-1)/2 independent components of the traceless part of the photon pressure tensor $\underline{\underline{P}}$ defined in (A.4) which, within a factor of c, is proportional to the term that follows J and **F** in the harmonic expansion of I_u. In this way, the term "non-diffusive" component still applies, see sect. D.2. We notice that, in d=2, this is again (reducible to) a scalar quantity whereas, in d=3, the appropriate two combinations of the three independent tensor components will obviously depend on the specific DA eigenvector choice (which is somewhat arbitrary due to the degeneracy, cf. above discussion). In the near future however, most inhomogeneous DA transfer calculations are most likely to be conducted in d=2 anyway, for simplicity, for numerical accuracy, and for ease of representation and/or analysis of the results (see chap. 6, for an instance).

Another aspect of the CA-DA comparison is the question of illumination geometry. In this (BC) connection, a corollary of the above "$I_{\pm j}$-to-$F_{\pm j}$" association (dictated by conservation) is that in DA transfer one is no longer able,[5] nor interested, in distinguishing between collimated (towards nadir) and diffuse illumination conditions, nor between the corresponding "zenith-Sun" and "spherical" albedoes. This may seem extraordinarily crude to those familiar with usual preoccupations of meteorological radiation studies where the primary interest is to cover the various illumination conditions on a spherical planet. However, in our view, this obsession with angular properties has diverted the overall research effort towards the only kind of system where they can be treated "properly" (i.e., with arbitrarily complicated phase functions), namely, plane-parallel 3-D slabs, often homogeneous in the vertical too, and sometimes even restricting attention to a single "typical" optical thickness.[6] We have indeed simplified the directional aspect to the extreme: we consider effectively "average" illumination conditions, somewhere between collimated (from overhead) and diffuse, "average" measures of exiting and internal radiance, somewhere between scalar and vectorial fluxes, and extremely simple phase functions. By drastically reducing the size of the functional space we operate in, we can use the same computational and analytical resources to explore systems inhomogeneous in both vertical and horizontal directions and with many different sizes, shapes and internal structures. This last remark applies fully to diffusion theory too (with the content of chap. 2 providing some relevant examples); in fact, we will now proceed to establish establish an interesting connection between diffusion and DA transfer.

3.3. The Second Order Formulation for Orthogonal DA Systems, Their Relation to Diffusion

3.3.1. *Rescaled Equations for the Symmetric and Anti-symmetric Combinations of DA Radiance*

In app. A on CA transfer, we did not look into the 2^{nd} order formulation which is mainly of use in numerical "finite element" techniques [see, e.g., Marchouk and Agochkov, 1981]; it consists essentially in the expression of the transfer equations—and (by then mixed) BCs—for the even/odd combinations of the radiance field $I_{\mathbf{u}\pm} = I_{+\mathbf{u}} \pm I_{-\mathbf{u}}$, $\mathbf{u}\in\Xi_d{}^+=\{\mathbf{u}\in\Xi_d,\ \mu=\mathbf{u}\cdot\mathbf{u}_z>0\}$. In contrast, the 2^{nd} order DA formalism leads to some analytical insight into the problem; in particular, we will discover a "route to diffusion," uncharted by Preisendorfer [1976] or anyone else, to the best of the authors' knowledge.

We introduce the following notations:

$$\delta_t = \frac{1}{c\kappa\rho(x)}\frac{\partial}{\partial t}, \qquad \delta_i = \frac{1}{q\kappa\rho(x)}\frac{\partial}{\partial x_i} \quad (\text{for } i=1,\cdots,d) \tag{3.15}$$

δ_i is a non-dimensionalized differential operator that corresponds to taking spatial gradients w.r.t. rescaled[7] ("transport") optical distance in direction $\mathbf{i}$ (recall that $q=1-\varpi_0 g$); similarly for δ_t, if one adopts units of velocity (for c) such that a m.f.p.is covered in unit time in places where $\kappa\rho=1$. Suitably generalized definitions similar to (3.10) are assumed for $I_{i\pm}$ and $S_{i\pm}$ $(i=1,\cdots,d)$.

Respectively, subtracting and adding consecutive pairs of rows in (3.4) and using definitions (3.5), (3.15) along with that of J, we obtain:

$$\delta_t I_{i-} + q\delta_i I_{i+} = -qI_{i-} + S_{i-} \tag{3.16a}$$

$$\delta_t I_{i+} + q\delta_i I_{i-} = -pI_{i+} + 2s\,(J - I_{i+}) + S_{i+} \tag{3.16b}$$

Notice that $J-I_{i+}=\sum_{j\neq i} I_{j+}$ contains d-1 terms. In connection with the validity of Fick's law, we spell out in sect. D.2 the conditions under which one can neglect the t-derivative in (3.16a); as in that diffusion situation, we will assume that these conditions are verified. We therefore drop the δ_t term in (3.16a): the response of I_{i-} to local changes in I_{i+} (and S_{i-}) is instantaneous. We however maintain it in (3.16b): temporal changes in I_{i+} can compensate for a divergence in I_{i-} and/or be forced by time dependent sources. Applying δ_i to (the remainder) of (3.16a), substituting the result into (3.16b) and using (3.7), we obtain:

$$I_{i-} = -\delta_i I_{i+} + \frac{1}{q} S_{i-} \tag{3.17a}$$

$$[\,\delta_t - q\,\delta_i^2 + p\,]\,I_{i+} = \frac{p-a}{d-1}(J - I_{i+}) + S_{i+} - \delta_i S_{i-} \tag{3.17b}$$

Essentially the same equations were obtained (for vanishing δ_t and $S_{i\pm}$) and numerically solved by Siddal and Selçuk [1979]. If we are to consider (3.17b) in isolation we must express BCs for the I_{i+}. DA transfer BCs are normally (1st order formulation) expressed in terms of the various "natural" radiances

$$I_{\pm i} = \frac{1}{2}(I_{i+} \pm I_{i-}) = \frac{1}{2}(1 \mp \delta_i)\, I_{i+} \qquad (3.18)$$

where we have used (3.17a). Conditioning the $I_{\pm i}$ on the boundaries make the BCs for the I_{i+} "mixed," which is a well-known fact of life in radiation diffusion theory that applies to 2nd order DA theory too.

In summary, we see that the system of DA equations in (3.17a,b) separate naturally into two groups: the second of which (3.17b) can, in principal, be solved for the I_{i+} independently of the first (3.17a). Given these hypothetical solutions for the I_{i+}, the remaining I_{i-} can be obtained by differentiation using (3.17a), and the various beam intensities $I_{\pm i}$ can be obtained by the linear combinations corresponding to the $I_{i\pm}$'s definitions as their even/odd combinations, cf. (3.18). In spite of this separation of (dependent) variables, this system is still difficult to handle directly since the d equations in (3.17b) are still fully coupled via side-scattering, since $(1-a/p)/(d-1)=2s$. This implies that they cannot be combined into a scalar equation for J as in diffusion theory, similarly (3.17a) is not the usual kind of Fickian relation that converts a scalar (measure of the total radiation field) into a vector (measure of the flow of radiation).

3.3.2. A New "Route to Diffusion" Using Phase Functions, Not Radiation Fields

Generally speaking, the mathematical character of the basic DA transfer eq. (3.17b) and its solutions, for given d, is determined by the values of q, p and $(p-a)/(d-1)=2s$, all of which have physical bounds set in (3.8a–c). We will however consider formally the limit $p\to\infty$ and retrieve d-dimensional diffusion, not the d independent one-dimensional diffusion equations (in effect, the IP approximation) that we find when $p\to a$. (Lovejoy *et al.* [1990] go one step further and consider $p<0$—the "unphysical" domain—in connection with the explanation of the shortcomings of the "real-space renormalization" approach to inhomogeneous radiative transport developed by Gabriel *et al.* [1990].) Notice that this way of getting from transfer to diffusion operates only on phase function parameters; specifically, we have followed a route described by CA→DA→P(t,r,s)→P(a,q,p)→$p=\infty$. We have made no *a priori* assumption on the character of the **u**-distribution as in the traditional development (reviewed in app. D). Taking the limit[8] $p\to\infty$ in (3.17b) yields

$$(d-1)I_{i+} = J - I_{i+} = \sum_{j\neq i} I_{j+} \ (\text{for } i=1,\cdots,d) \qquad (3.19)$$

This last system is easily solved for the I_{i+}: they are all equal to J/d. This limit thus imposes *a posteriori* a certain degree of isotropy on the DA distribution of radiance among the available directions. More specifically, on each axis we are given the total radiance ($I_{i+}=J/d$) and the corresponding component of the flux vector (I_{i-}); this determines the DA radiances ($I_{\pm i}$) entirely, from (3.18). In app. D, we show that CA transfer also goes to diffusion in the limit of **u**-distributions that can be represented by an isotropic (J) plus a dipole (**F**) term, i.e., a 1st order truncation in its expansion into spherical harmonics. We therefore see that the two routes from transfer to diffusion cannot wander too far apart. Conversely, assuming $I_{i+}=J/d$ in (3.17b) implies $[\delta_t - q\delta_i^2]J=0$ in absence of absorption (a=0) and non-m.s. sources ($S_{i+}=0$); so **x**-gradients and t-derivatives, on the one hand, and **u**-anisotropy, on the other hand, are in direct relation. We have thus retrieved, at 2nd order (and in the diffusion limit), this basic property of all conservative m.s. transport systems (described in CA language in §A.3.3).

The derivation of diffusion equations is now easily completed by substituting $I_{i+} = J/d$ into (3.17a), we find $I_{i-} = -\delta_i J/d + S_{i-}/q$. Hence, using various definitions:

$$\mathbf{F} = -\frac{c}{dq\kappa\rho}\nabla U + \frac{1}{q}\mathcal{S} \tag{3.20}$$

where U is the radiant energy density (J/c) and $\mathcal{S}$ is the d-vector made up the the S_{i-}; this is consistent with the notational conventions used in app. D for the anti-symmetric combination of CA non-m.s. sources found in (D.9b). The first term in eq. (3.20) expresses Fick's law for radiation if we let $D=c/dq\kappa\rho$ be radiative diffusivity, exactly as in app. D (notice that its dimensions are indeed length^2/time). Secondly, we substitute $I_{i+} = J/d$ back into (3.17b), to find $[\ \delta_t - q\ \delta_i^2 + a\ ]\ J/d = S_{i+} - \delta_i S_{i-}$ $(i=1,\cdots,d)$; hence, adding all these d equations, multiplying by $c\kappa\rho$ and using the definitions of D and of U:

$$[\ \partial_t - \nabla{\cdot}D\nabla + A\ ]\ U = \frac{1}{q}\left[\frac{c}{dD}\mathfrak{S} - \nabla{\cdot}\mathcal{S}\ \right] \tag{3.21}$$

where, on the l.h.s., $A=ac\kappa\rho=ac^2/qdD$ is the (specific) rate of destruction of radiant energy per unit of time and per unit of energy; the r.h.s., we find the corresponding rate of creation and destruction (by non-m.s. sources and sinks); $\mathfrak{S}$ is the total DA non-m.s. source function which is not different from the definition found in (D.9a), its CA counterpart (so no new notation is needed).

To summarize, we see that the parameter, p (when finite, as in physical systems of interest), is precisely what makes DA transfer an overall better approximation to CA transfer than diffusive transport, in general, but we must remember it is not trivial to relate DA radiances to experimentally accessible (3-D) CA quantities. (Standard diffusion theory's J and **F** may have a direct connection with $I_\mathbf{u}$, but it has its problems too when it comes to exiting diffuse radiation in connection with the problem of "extrapolation lengths," i.e., BCs.) Two slightly different derivations of this DA limit are given by Davis *et al.* [1990b]

for d=3 and by[9] Davis *et al.* [1991b] for d=2, both in the less general case where $\mathfrak{S}$ and ∂_t vanish. Notice that $I_{i+} = J/d$ implies that the projection of the DA radiance vector on the eigenspace with eigenvalue 2p-a vanishes identically since it is made of (d-1) combinations such as $I_{z+}-I_{i+}$ (i=1,···,d-1). In particular, we find X=0 in d=2 from (3.11c') and $Z_{\pm}=0$ in d=3 from (3.12c'); the name we coined for it, the "non-diffusive" component, is therefore fully justified. Finally, it is clear that diffusion theory will approximate transfer very well in cases were the radiance fields are quasi-isotropic ($I_{i+} \approx J/d$) and this is expected to happen in regions that are optically remote from the boundaries, e.g., throughout the bulk of homogeneous or mildly inhomogeneous media. For very inhomogeneous (e.g., multifractal) media, the question of diffusion accuracy is addressed in chap. 6.

3.3.3. Solutions for Homogeneous Plane-Parallel Media

The key result in the above derivation is the "equipartition" of the radiant energy amongst the different directions: $I_{i+} = J/d$ (i=1,···,d). There is one case where this is an exact result at finite p (hence for DA transfer proper): a homogeneous (and plane-parallel) slab of optical thickness $\tau = \kappa\rho L$. If we consider the sourceless ($S_{i+}=0$), steady-state ($\delta_t=0$) case for simplicity, we indeed find all of the I_{i+} in (3.17b) to be equal (to J/d) simply by requiring conservation (a=0), on the one hand, and $\delta_i = 0$ (i=1,···,d-1 but not i=d, for the z axis), on the other hand. Eq. (3.17a) makes the important point that $I_{i-} = 0$ (i=1,···,d-1), i.e., the net horizontal fluxes vanish. In this very special case, the above prediction about diffusion being adequate for homogeneous media is verified beyond all expectations: it is exact! The remaining equation in (3.17b), $\delta_z^2 I_{z+} = 0$, is easily solved: $I_{z+}(\tau')$ decreases linearly (using optical coordinates, $d\tau' = \kappa\rho dz$) between $I_{z+}(0) = 1+R$ and $I_{z+}(\tau) = T+0$, using definitions (3.10) and assuming unit incident flux ($F_0=1$). Finally, the last (i=d) "quasi-Fickian" law (3.17a) allows us to determine T from τ: $I_{z-}(\tau') = \text{const.} = [I_{z+}(0)-I_{z+}(\tau)]/q\tau$, which is also given by T-0 (at $\tau'=\tau$) and 1-R (at $\tau'=0$), from (3.10). Hence $T = 2(1-T)/q\tau$, or

$$\frac{1}{T(\tau)} - 1 = \frac{q\tau}{2} \tag{3.22}$$

Equivalently,[10]

$$T(\tau) = \frac{1}{1+q\tau/2} \tag{3.22'}$$

We see that p is absent from the final result—and this is precisely what makes it exactly diffusive—although it is instrumental in populating the horizontal beams: $I_{\pm i}(\tau') = I_{z+}(\tau')/2$, for i=1,···,d-1. For future reference, we note that the total DA radiance at the top of the slab is

$$J(0) = d(1+R) = d\,\frac{1+q\tau}{1+q\tau/2} \tag{3.23}$$

which naturally increases with d. The above exact solution for the case of conservative scattering complements Boissé's [1990] analysis of the absorbing/scattering case (in d=3). This author found the (completely analytical) homogeneous six-beam model to approximate quite well his (semi-analytical and Monte Carlo) results for inhomogeneous "Markovian" (i.e., exponentially decorrelating) media; we view this is a symptomatic of weakly variable media in general (see sect. 4.3–4 for further discussion).

Finally, we can define two distinct scaling (power law regimes) for $T(\tau)$ or $R(\tau)=1-T(\tau)$:

at $q\tau \ll 1$: $R(\tau) \sim \frac{q}{2}\tau$ (linear response, single-scattering) (3.24a)

at $q\tau \gg 1$: $T(\tau) \sim \frac{2}{q}\tau^{-1}$ (nonlinear response, multiple scattering) (3.24b)

Notice how (unlike the prefactor) the scaling exponents are unaffected by the phase function choice and even dimensionality. Comparing with our general definition (0.1) for F=T, we find respectively

at $\tau \ll 1/q$: $\nu_T = -1$ and $h_T = q/2$ (for $T_0 = 1$) (3.24a')

at $\tau \gg 1/q$: $\nu_T = +1$ and $h_T = 2/q$ (for $T_\infty = 0$) (3.24b')

and the same scaling parameters for R, only the fixed point changes: $R_{0/\infty}=1-T_{0/\infty}$. Using (1.2) instead, with L rather than λ (which is 1 at homogeneity), we find

at $L \ll 1/q\kappa\rho$: $K_T = +1$ (and a prefactor $q\kappa\rho/2$) (3.24a")

at $L \gg 1/q\kappa\rho$: $K_T = -1$ (and a prefactor $2/q\kappa\rho$) (3.24b")

Viewing the above as "normal" scaling, characteristic of homogeneous (and weakly inhomogeneous media in general), we will find different exponents hence "anomalous" scaling in the extremely variable (fractal and multifractal) media studied in chap. 4–5.

The detailed analysis of the non-conservative case is somewhat more involved, due to the appearance of a characteristic optical scale in (3.21) appropriately called the "diffusion length:"

$$\sqrt{\frac{D}{A}} = \frac{1}{\kappa\rho\sqrt{daq}} \tag{3.25}$$

which goes to ∞ when scattering becomes conservative. It is however quite easy to anticipate the asymptotic ($\tau = \kappa\rho L \gg 1/\sqrt{daq}$) responses in the important case of relatively weak absorption and quasi-isotropic scattering, i.e., $0 \lesssim a \ll q \lesssim 1$. In essence, we expect to find a break in the 2nd of the above scaling laws (3.24b) which becomes:

$$T(\tau) \sim \exp[-\tau\sqrt{daq}\,] \qquad (3.26a)$$

$$1 - R(\tau) \sim \sqrt{\frac{2d}{q}}\, a^{1/2} \qquad (3.26b)$$

and, of course, we have a finite bulk absorptance $A(\tau)$ as required by total energy conservation, i.e., $T(\tau)+R(\tau) = 1-A(\tau) < 1$—for a thick cloud $A(\tau)$ is roughly given by (3.26b). The last estimate in (3.26b) is obtained simply by taking $\tau \sim 1/\sqrt{daq}$ in (3.22): we schematically view the medium as non-absorbing above that depth and purely absorbing below it. Formally, we have $\nu_T = \infty$ and $\nu_R = 0$. Most importantly, (3.26b) shows that 1-R scales like $\sqrt{1-\varpi_0}$, i.e., the albedo of a very thick cloud decreases rapidly when (true) absorption sets in. It is little surprise that observed albedo discrepancies were first hypothesized to be homogeneous absorption effects rather than scattering inhomogeneous effects, cf. the discussion of the "cloud albedo paradox" in the introductory and concluding chapters.

3.4. "Independent Pixels" and/or Scattering Media with Random Optical Thicknesses

3.4.1. The IP Limit in the Framework of DA(d,2d) *Systems*

The only, but notable, exception to the characteristic coupling of the DA PDEs in (3.17b) occurs when p=a (equivalently, s=0)—or d=1 (making I_{i+}=J). In both cases, the first term on the r.h.s. vanishes identically and we recover one-dimensional diffusion equations for each of the I_{i+} separately: $[\,\delta_t - q\,\delta_i^2 + a\,]\, I_{i+} = S_{i+} - \delta_i S_{i-}$, (for i=1,⋯,d). By multiplying through with $c\kappa\rho$ and letting $\partial_i=\partial/\partial x_i$, we find one-dimensional diffusion in more traditional format:

$$[\,\partial_t - \partial_i D \partial_i + A\,]\, I_{i+} = c\kappa\rho[S_{i+} - \delta_i S_{i-}] \qquad (3.27)$$

where we have used on the l.h.s. the same definitions as in (3.21) but for d=1. Since this p→a limit implies no side-scattering,[11] a vertically irradiated medium cannot have any horizontal fluxes, net or otherwise, not even radiances (unless it is also illuminated on a side).

In other words, we are dealing with an exact DA problem which is the equivalent of the "independent pixel" (or IP) approximation to CA transfer. We have adopted this expression[12] of Cahalan's [1989] which conjures up visions of high-tech digital image processing and, indeed, the author compares the statistical properties of (Landsat) satellite imagery with those of his simulations. The inhomogeneous optical medium, confined between two horizontal planes, is first mentally fragmented into a certain number of sub-domains by vertical divides, the approximation consists in assuming each sub-division or "pixel" (as seen from above) is then homogenized and made radiatively independent of its neighbours by neglecting the net horizontal fluxes that would normally develop in the vicinity of the pixel boundaries. If the vertical division is viewed as reflecting (as a means to conserve total energy), the pixels each behave exactly like a homogeneous plane-parallel medium (in practice this means that they must be optically very thick in the horizontal). All that is left to do is to spatially average the response of interest over the whole medium, and this is easily done since we have an analytical closed-form solution (3.22) for DA transfer through each pixel-medium, call it $T_p(\tau)$ where τ is the pixel's optical thickness. The global IP transmittance is given by

$$\overline{T_p(\tau)} = \frac{1}{\mathrm{surf}(A_0)} \int_{A_0} T_p[\tau(x)]\, d^{d-1}x \tag{3.28}$$

with the notations of sect. A.2 (A_0 is the horizontal projection of M). Notice that the spatial discretization has vanished from the the final result; the theory is indeed more general (and conveniently formulated) in terms of spatial continua, as well as continuous distributions of optical thickness.

In the previous section, we obtained a total (multiply scattered) transmittance of the form

$$T_p(\tau) = \frac{1}{1 + b\tau} \tag{3.29}$$

if $a=1-\varpi_0=0$. b denotes a general purpose (phase function and/or BC parameter) which is always proportional to $q=1-g$. For instance, for DA transfer we have $b=q/2$, equivalently, we could be using the diffusion approximation to plane-parallel CA transfer (see §D.4.2) which, at best, allows for the possibility to model the effects of slant illumination geometry[13] (i.e., the appearance of a boundary layer of thickness μ_0); in this case, b can be used to represent a BC parameter (related to the "extrapolation length") which is again proportional to $q=1-g$ (thus making $b\tau$ proportional to the thickness of the slab in units of "transport" m.f.p.'s, i.e., the effective τ for isotropic scattering).

We can generally expect final DA transfer results (for, say, global transmittance) to be monotonic w.r.t. p as it goes from a to ∞; this is exactly what we already have for $a=1-\varpi_0$ as well as $q=1-\varpi_0 g$ in asymptotic diffusion theory, cf. (3.25b). We can use this fact to put bounds on either side of (say) conservative responses to external illumination for regular ($0<p<\infty$) DA transfer by using its two diffusion limits: IPs at $p=0$, on the one hand, and *bone fide* (d-dimensional) diffusion at $p=\infty$, on the other hand. This can be of use in situations where diffusion results are easier to obtain than their counterparts from DAs, let alone CAs—we recall that both of the latter transport models are in the same broad category of "kinetics," where ballistic propagation (as described in sect. A.2) is the central concept. In the context of diffusion theory proper (chap. 2), we showed that these bounds do not come in an arbitrary order; specifically, for conservative transmittance, IPs yield a lower value than d-dimensional diffusion. After IPs (which has the above closed-form final result for an arbitrary density field), the only foreseeable way the making the general albedo problem any simpler is to assume homogeneity. We can easily show that this homogeneity assumption may make the problem simpler but it also biases the result systematically, that spatial averaging, on the one hand, and radiative transport calculations, on the other hand, are operations that do not commute[14] due to the fundamentally nonlinear character of the matter-to-radiation coupling.

3.4.2. Mixing the Responses of Random Media, Relation to Jensen's Inequality

In sect. A.2, we substitute ensemble- and spatial-averages (this property defines an "ergodic" variability model) in the case of direct transmittance which, incidentally, is completely "pixel independent" by definition. We can therefore proceed using our notations for ensemble-averages and think of the above pixels simply as independent realizations of a homogeneous plane-parallel medium with a random density, equivalently, optical thickness distributed according to some given probability distribution function $P(\tau)=\mathrm{Prob}\{\tau'\leq\tau\}$. ($P(\tau)$ is readily related to the p.d.f. $p(\tau)$ by integration from 0 to τ.) We are now interested in the averages

$$\langle T_p(\tau)^h\rangle = \int_0^\infty (1+b\tau)^{-h}\, dP(\tau) \tag{3.30}$$

Unfortunately, (3.30) does not have the form of a standard integral transform, like Laplace's w.r.t. $T_d(\tau)$, cf. (A.13–14). In both cases, we are dealing with a probabilistic "randomization" or "mixing" [Feller,1971] of p.d.f.'s since $T_p(\tau)$ is itself the parameter of a Bernouilli law which has two outcomes: transmission with Prob=$T_p(\tau)$, or reflection with Prob=$R_p(\tau)$ which is $1-T_p(\tau)$, by normalization (obviously related to our usual requirement of "conservation").

Using the basic properties of the 2nd characteristic function or cumulant generating function (c.g.f.) of $P(\tau)$, we argue (sect. A.2) that the average $\langle T_d(\tau)^h\rangle$ is always greater than $T_d(\langle\tau\rangle)^h$, obtained for the average thickness, if $h>0$. This is directly related to the convexity of the exponential function and Jensen's inequality [Hardy *et al.*, 1952] which, in our notations, reads

$$\langle f(x)\rangle \begin{cases} \geq f(\langle x\rangle) \text{ if } f \text{ is convex}^{15} \\ \leq f(\langle x\rangle) \text{ if } f \text{ is concave} \end{cases} \tag{3.31}$$

Equalities are obtained for a linear $f(x)$ or for a degenerate (or "sure") x-distribution; notice that $f(x)$ must be a real (scalar) function, but x can belong to a vector space of any dimensionality. The convexity of $T_p(\tau)^h$ ($h>0$) has exactly the same consequences resulting from Jensen's inequality that we found for $T_d(\tau)^h$ and discussed at length in sect. 1.5. In particular, for h=1:

$$<T_p(\tau)> \geq T_p(<\tau>) \quad (3.32)$$

The IP transmittance is thus necessarily greater than that of the medium which (surely) has the same optical thickness under every pixel; in fact, equality is obtained only if all of the pixels have $\tau=<\tau>$. We remark that the function $T_p(\tau)$ is only used for commodity; an arbitrarily inhomogeneous medium will always have $T(\bar{\tau})\in]0,1]$ for $\bar{\tau}\in [0,\infty[$, so a decreasing, continuous $T(\bar{\tau})$ is necessarily convex. For instance, such a simple relation will arise when the given variable density field sees itself multiplied everywhere by a numerical factor (κ) which would then become the random factor in (3.32), see chap. 6 for a deterministic example.

In the literature, we have traced this kind of IP approach to atmospheric radiative variability estimation as far back as (the work performed earlier in the ex-USSR and reported by) Mullaama *et al.* [1975] who uses normal τ-distributions with careful truncation of the unphysical negative values, especially since empirical evidence suggested, unsurprisingly, the use of a variance of the same order of magnitude as the mean. Ronnholm *et al.* [1980], who seem to have worked independently, postulate log-normal variability and resort to numerical integration; nearly the same type of distribution is studied analytically by Davis *et al.* [1991a, and in chap. 5], using multifractal formalism. Their computations agree with our above (more qualitative) results even though they did not publish their figures for $(1\text{-}g)<\tau>$ greater than 4. We must however take exception to their conclusion that (spatial) variability has effects on radiative responses that are comparable to the differences that arise between various radiative transfer schemes (i.e., a few percent between, say, a δ-Eddington method and a "doubling" method). Notably, they find $\sigma_T\approx<T>$ all the way down to $(1\text{-}g)<\tau>\approx 1/4$ with reasonably broad τ-distributions, namely, where $\sigma_{\ln\tau}\approx<\ln\tau>$ (which is a specific prediction of intermittent turbulent cascade theory, cf. chap. 3). We very strongly disagree with the predicament that the direction in which ensemble-averaging changes the response is not obvious from the outset, unless some combination of undersampling of too narrow p.d.f.'s weighted by more (too?) complicated response functions has arisen. The authors also modelled "vertical" variability in plane-parallel media by "adding" ten layers up to an average total of $(1\text{-}g)<\tau>=4$ at most (in their published data) and they find much smaller deviations from the radiative response of the average medium. This is easily understandable since (for $\varpi_0=1$) "adding" several layers is like adding their scaled optical thicknesses $(1\text{-}g)\tau_i$ (i=1,10) together and ten log-normal deviates add up to an approximately normal deviate, by virtue of the central limit theorem (the variance of the log-normal distribution is finite), in turn, this is a far narrower variability model which can be expected to yield

$\langle T_p(\tau)\rangle \approx T_p(\langle\tau\rangle)$. In other words, (without saying so) Ronnholm and his co-workers also did IPs with Gaussian distributions since there is no difference in their way of modelling horizontal and vertical variability, beyond the somewhat academic distinction between IPs and random homogeneous media. This distinction can be adapted to fields (or ensembles) of clouds with horizontally finite geometry: the requirement of radiative independence translates to large inter-cloud distances. (This approach to radiation interacting with broken cloudiness is exploited by Welch and Zdunkowski [1981].) While Ronnholm *et al.* [*ibid.*] also varied ϖ_0 and g (one at a time), Mikhaylov [1982] considers the effect (via the diffusion length $1/\kappa\rho\sqrt{d(1-\varpi_0)(1-\varpi_0 g)}$) of normally distributed fluctuations of the extinction coefficient ($\kappa\rho$) in the average responses non-conservative asymptotically thick systems. Given the concavity of absorptance $A \approx 1-R$ w.r.t. $a=1-\varpi_0$ in (3.26b), systematically lesser averages are to be expected from Jensen's inequality. More recently, Pomraning [1988] discusses the general case of finite plane-parallel slabs. Finally, Stephens *et al.* [1991] present a general review the topic along with some new numerics on τ-variability.

3.5. DA Similarity Theories and the Singularity of the Diffusion Limits

In the CA formulation, the spherical harmonics of the phase function—or rather of the scattering/extinction kernel [McKellar and Box, 1981]—is particularly useful in local similarity analysis (see §A.3.2 for more details). The same is true for the eigenvector decomposition of ***1-P***: if the optical parameters (κ, a, q, p, and those that intervene in **S**) are varied but the products κa, κq, κp, and κ**S** are all left unchanged, then the corresponding solutions of (3.4) are also left unchanged. In other words, **I**=**I'** if

$$\kappa a = \kappa' a' \tag{3.33a}$$

$$\kappa q = \kappa' q' \tag{3.33b}$$

$$\kappa p = \kappa' p' \tag{3.33c}$$

and $\kappa\mathbf{S} = \kappa'\mathbf{S}'$. In particular, we see that the important class of conservative (a=0) phase functions is invariant under similarity. A good example is provided by the solution (3.22–23) to the plane-parallel DA problem for conservative scattering: it is a universal function of $q\tau=(q\kappa)\rho L$; another example can be found in the asymptotic non-conservative case (3.25–26). Furthermore, a=q=p=0 (conservative all forward scattering) is the only—and trivial—fixed point of the similarity transformation. As is the case in CAs, we must exclude the single-scattering term from **S** in order to maintain consistency since it is proportional to either t or r, not a, as would be the case for a thermal-type DA source term. The above, very simply expressed, similarity analysis concerns only the DA(d,2d) systems; it can of course be derived directly from McKellar and Box's [*ibid.*] CA similarity analysis since orthogonal DA phase functions are merely special cases.[16]

Lovejoy *et al.* [1990] develop a somewhat independent similarity theory based entirely on the 2nd order DA formulation contained in eqs. (3.17a,b) for the $I_{i\pm}$; they also assume $a=\partial_t=S_{i+}=0$ (i.e., steady-state and conservative m.s. sources only). Introducing the notation

$$\delta_i' = \frac{1}{\sqrt{pq}\ \kappa\rho(x)}\partial_i \tag{3.34}$$

for $i=1,\cdots,d$ and $0<pq<\infty$, the (readily simplified) eqs. (3.17a,b) become

$$I_{i-} = -\sqrt{\frac{p}{q}}\ \delta_i' I_{i+} \tag{3.35a}$$

$$[\ 1 - \delta_i'^2\ ]\ I_{i+} = \frac{1}{d-1}(J - I_{i+}) \tag{3.35b}$$

The second set (3.35b) no longer contains any explicit reference to the phase function values whatsoever. In other words, the I_{i+} are left invariant by changing the phase functions in such a way that $\kappa\sqrt{pq}$ remains constant, from (3.34). This time however, we proceed without requiring invariance of the I_{i-} nor of eq. (3.35a), we thus gain an extra degree of freedom. To see this, suppose we know the $I_{\pm i}^{(1)}$ fields, hence the $I_{i+}^{(1)}$, for some choice (q_1,p_1) of the (conservative) DA phase function, we now wish to obtain the original DA radiances, $I_{\pm i}^{(2)}$, for a different choice (q_2,p_2) by postulating that their corresponding I_{i+} are "similar," i.e., $I_{i+}^{(2)}(x;\kappa_2) = I_{i+}^{(1)}(x;\kappa_1)$. As usual, we take a given $\rho(x)$ field and modulate optical density via the overall multiplier κ. We now define

$$\beta = \sqrt{\frac{p_2q_2}{p_1q_1}} \qquad\qquad \alpha = \sqrt{\frac{p_2/q_2}{p_1/q_1}} = \frac{q_1}{q_2}\beta \tag{3.36}$$

where $\beta=\kappa_1/\kappa_2$, is the constant ratio of optical densities (or thicknesses). Our above postulate of course implies that $\delta_i' I_{i+}^{(2)}(x;\kappa_2) = \delta_i' I_{i+}^{(1)}(x;\kappa_1)$, and using (3.35a) and (3.36), we obtain $I_{i-}^{(2)}(x;\kappa_2) = \alpha\ I_{i-}^{(1)}(x;\kappa_1)$ where $\alpha\neq 1$ in general. Combining this with our postulate, definitions and (3.19) yields

$$I_{\pm i}^{(2)}(x;\kappa_2) = \frac{1}{2}(1\pm\alpha)\ I_{+i}^{(1)}(x;\kappa_1) + \frac{1}{2}(1\mp\alpha)\ I_{-i}^{(1)}(x;\kappa_1) \tag{3.37}$$

These "generalized" similarity relations hold for all (pairs of) conservative DA(d,2d) systems for $d>1$; otherwise ($p=a=0$), the similarity transformations (3.36) are singular. From (3.37), we see that the standard (1st order) similarity postulate (that all radiances, equivalently, both symmetric and anti-symmetric parts are invariant) is retrieved for $\alpha=1$; eqs. (3.34) then read as the "exact" DA(d,2d) similarity relations in the conservative case, namely, $\kappa_1 q_1 = \kappa_2 q_2$ and $\kappa_1 p_1 = \kappa_2 p_2$, or (3.33b,c)

In practice, the non-invariant eqs. (3.17a) or (3.35a) are important in the expression of the BCs, see the discussion around eq. (3.18). In particular, we see from (3.37) that, for $x\in\partial M$, the illumination pattern is rescaled to a different one that depends not only on the original pattern but also on the local response to it, respectively, the first and second terms in

(3.37). So, with these non-standard BCs, the above generalized (or 2nd order) DA similarity is expected to apply only "asymptotically," that is, away from boundaries. By "away" we mean out of reach of direct transmittance (for illumination or escape) but it may be quite difficult to achieve this in very inhomogeneous media, such as (multi)fractals, where radiation penetrates far deeper than in their homogeneous counterparts. Lovejoy *et al.* [*ibid.*] however go on to obtain similarity transformations for global (spatially integrated) albedoes and transmittances (applicable to media with various internal symmetries) by applying (3.37) to the corresponding BCs and by further making the approximation that the irradiation pattern can be rescaled very simply (by a constant factor). For instance, if the medium is both up/down symmetric ($T_{i,\text{"from above"}}=T_{i,\text{"from below"}}$) and cyclical in the horizontal ($R_i=1-T_i$), they find that

$$\frac{1}{T_2(\kappa/\beta)} - 1 = \frac{1}{\alpha}\left(\frac{1}{T_1(\kappa)} - 1\right) \tag{3.38}$$

Other, somewhat more involved formulae, are obtained by relaxing one or the other of the above structural constraints. As pointed out by Lovejoy *et al.* [*ibid.*], an advantage of generalized DA similarity is that, contrary to exact CA or DA similarity, it allows isotropic and 3-D Rayleigh-like ($|\varpi_2|\leq 2/5$, $\varpi_1=\varpi_i=0$, for $i\geq 3$) scattering to be related by taking $p=1-5\varpi_2$ for the latter. (Recall that $q=1-3\varpi_1$ and that, in general, we are concerned with the n^{th} Kusčer coefficient: $1-(2n+1)\varpi_n$.) This may be of some practical importance in sufficiently thick homogeneous plane-parallel Rayleigh-like atmospheres where the homogeneity hypothesis makes the constant factor rescaling assumption perfectly justified and the other (boundary-induced) shortcomings of the generalized similarity theory are unlikely to be too serious since, again due to homogeneity, boundary layers are at their thinnest (preliminary numerics seem to confirm this). We also notice, using (3.36), that unsurprisingly the (exact) plane-parallel DA transmittance in (3.22) verifies (3.38) just as well as it does the standard (exact) similarity relations.

We now recall that the motivation behind radiative similarity analysis, in both "exact" (CA or DA) and "generalized" (DA only) versions, is that the similarity transformations (of phase functions) and ensuing relations (between corresponding radiation fields) show that an understanding of the behavior of a given medium for one phase function and all possible optical thicknesses is sufficient to predict its radiative properties for other phase functions. For instance, if we restrict ourselves to the important class of conservative phase functions, either many of them (p/q=const., in "exact" DA similarity) or all of them (in "generalized" DA similarity) can be accounted for—the difference only being one in BCs. This is also the basic idea behind the above concept of "scaling" in transfer systems that we defined in the introductory chapter and it is made more precise by (tentatively) limiting the effect of phase functions to the prefactor. We can further argue for phase function independence of the scaling exponent by using the generalized DA similarity result in the asymptotic regime ($T_i \ll 1$, i=1,2). Rewriting the basic scaling relation in (0.1) but for[17] κ (i.e., $T \approx h\kappa^{\nu}$) for both T_1 and T_2. Identification of both sides of (3.38) then leads to

$$\nu_2 = \nu_1 \ (= \nu) \quad \text{and} \quad h_2 = h_1\,\alpha\beta^{\nu} \qquad (3.39)$$

Along these lines, an interesting point suggested by generalized similarity—which could be exploited numerically—is that the isotropic DA phase function (pq=1-1/d) is not the one that allows the fastest convergence to the thick cloud (scaling) limit since, taking p=q=1 (the maximum possible with r=t=0, all side-scattering), (3.36) yields $\beta=\sqrt{d/(d-1)}$ which exceeds one. Equivalently, from (2.34), the "effective" optical thickness w.r.t. this kind of non-isotropic scattering is[18] $\tau_{\text{eff}}=\tau/\sqrt{pq}<\tau$.

Finally, from sect. 3.3 above (and app. D), we see that a and q are the independent phase function parameters of diffusion theory and, as expected, its characteristic similarity relations are retrieved from our exact DA similarity relations. (Their generalized counterparts however do not really separate the rescalings of p and q, except of course when α=1.) Most importantly, we note that the two diffusion limits of DA transfer, $p \to a=0$ (dx1-D diffusion) and $p \to \infty$ (d-D diffusion) are both singular w.r.t. the (both) similarity theory(ies) since the parameter q must simultaneously remain finite as it enters the gradient rescaling in (3.15). This means that the DA transfer and diffusion radiance fields cannot be related by similarity; in particular, we can generally expect them to scale differently w.r.t. (total optical) thickness as it becomes very large. More specifically, the similarity relation (3.38) at fixed q (hence $\alpha=\beta$) predicts, as previously anticipated:

$$T_{IP} < T_{DA} < T_{dif} \qquad (3.40)$$

as represented by $\beta \ll 1$, $\beta \approx 1$, and $\beta \gg 1$, respectively. This implies

$$\nu_{IP} \geq \nu_{DA} \geq \nu_{dif} \qquad (3.41)$$

The equalities are introduced to allow for the (at least possible) case where the scaling w.r.t. κ, at constant λ (as required in the premises) is the same in all circumstances and that only prefactor differences arise. In chap. 4, we examine numerically the opposite case where κ is held constant and λ is varied but (3.41) still proves true (for both of our examples: random binary mixtures and a deterministic monofractal).

In retrospect, this difference in scaling is hardly surprising given the entirely different mathematical structure of the respective formulations of the different approaches: compare (3.30) for IPs, on the one hand, and $\nabla{\cdot}D\nabla J = 0$ (plus BCs) for diffusion, on the other hand, with (3.0) or (3.4) for CA or DA transfer (taken in the conservative steady-state case and with the appropriate BCs). However, as previously mentioned, diffusion theory is expected to provide a good approximation to transfer in "not too inhomogeneous" media. In the previous chapter that covers variability effects in diffusive transport, we find that, for a medium to be sufficiently inhomogeneous to exhibit radically different transfer- and diffusion behaviors, both a special structural property ("percolation") inducing long-range correlations <u>and</u> singular density values (the "RSN" limit) are called for. Other cases of major differences in transfer and diffusion behavior are found in monofractals (chap. 4) while multifractals (chap. 6) open very interesting questions for future investigation.

† This fundamental chapter is largely based on Lovejoy *et al.* [1990] and Davis *et al.* [1991]. S.L. and Gabriel [1988] (unknowingly) resuscitated Chu and Churchill's [1955] six-beam model and developed the basic equations, mainly on square grids (see sect. B.2); still using spatially discretized systems, they contrasted their simplified transfer model with diffusion theory. S.L. latter made the same connection in the continuous space (orthogonal beam) 2nd order formulation and he developed the "generalized" similarity theory. A.D. enumerated exhaustively the acceptable "relative scattering angle" DA systems (§3.1.2) and improved the connection with the CAs in three different ways: firstly, by establishing the flux-like nature of DA "radiance" on general grounds (§3.1.1); secondly, by completing the eigen-vector description of orthogonal DA systems which closely parallels the spherical harmonic representation of CA radiances (§3.3.2) and is likely to provide grounds for their quantitative comparison in the future; thirdly, by clarifying the simple connections between (exact) CA-, DA-, and diffusion similarity theories and how "exact" similarity relates to its "generalized" counterpart (sect. 3.5). He also considerably generalized the DA-diffusion connection in continuous space and paralleled the "new" derivation with its standard (app. D) counterpart (§3.3.2). Finally, he noticed the DA-IP connection (in the previously called "1-D" diffusion limit) and explained, on very general (Jensen's inequality) grounds, the systematic differences between homogeneous-based and IP-based—or otherwise variable optical thickness—calculations (sect. 3.4).

1 This however would be a hopeless why to proceed in practice given the very sharp angular features of a quasi-DA phase function. Indeed, Hunt [1971] is only concerned with details in Mie scattering and shows that already hundreds of spherical harmonics are necessary in single-scattering calculations, tens of streams in multiple scattering calculations.

2 Notice that the "trivial" (single-beam) DA(d,1) system is completely solved by the Bouger-de Beer law of (exponential) extinction, studied in full detail in sect. A.2.

3 Einstein was of course the one to finally succeed in bringing gravitation into the realm of geometry but Kepler's imbricated polyhedra work about as well as for the (then known) number and spacings of the planets as contemporary QCD does for the mass spectrum of (now known) particles; both approaches are based on symmetry considerations hence (consciously or not) on group theory. Were all his polyhedra chosen identical, Kepler would have predicted a structure for the Solar System with exact scaling symmetry and his "successful" combination in fact accounts for the observable discrepancies between reality and perfect scaling. The Titius-Bode law ($a_{n+1}=2a_n-0.4$) goes two planets further on, accounts for asteroids, and generalizes to the major satellite systems. Finally, von Wieszacker's turbulence-based cosmogony justifies physically this omnipresence of quasi-scaling in planetary systems.

4 In particular, this precludes a solution by characteristics for the steady-state equation.

5 Using a single orthogonal family of beams, not many independent ones as discussed in the opening section.

6 Optical thickness is often taken in the 10–30 range, with $g\approx0.85$, $(1-g)\tau$ is therefore in the range 1–4.5. These numbers are also invoked in investigations of inhomogeneous cloudiness and inhomogeneity effects are sometimes rather unclear; we strongly believe this is a consequence of the fact that we are dealing with systems that are neither thick nor thin w.r.t. isotropic scattering.

7 The notational conventions of Lovejoy *et al.* [1990] omit this rescaling which is however important in the specification of the exact (mixed) BCs for the albedo problem (at 2nd order, cf. eq. (2.18) and §3.3.3).

8 As suggested by Lovejoy *et al.* [1990], Davis *et al.* [1990b] take the $pq\to\infty$ limit but in fact q must remain finite in order to satisfy the radiative BCs of the albedo problem; see discussion around eq. (2.18). Furthermore, the extension from steady-state to time dependent problems presented here does not support their single parameter (pq) rescaling.

9 These authors consider the coupled system of 2nd order PDEs obeyed by J and X; namely,

$$[\delta_y^2+\delta_z^2]\,J=-[\delta_y^2-\delta_z^2]\,X, \qquad [\delta_y^2+\delta_z^2-4\frac{p}{q}]\,X=-[\delta_y^2-\delta_z^2]\,J.$$

10 The most interesting alternative proof of this result uses invariant imbedding [Bellman *et al.*, 1960] which transforms the linear 2-point boundary value problem (that must *a priori* be solved for the internal field) into a non-linear ODE for $R(\tau)$ which is readily integrated with initial condition $R(0)=0$. This underscores the fundamentally nonlinear nature of the radiation field (R) coupling with matter (τ), even before integrating the (Ricatti) transformed transfer equation; the special role of the BCs in revealing this nonlinearity is also emphasized. A similar proof but based on functional analysis, rather than ODEs, is given by Gabriel *et al.* [1990].

11 The radiances decouple further (w.r.t. the already decoupled mutually orthogonal families) into coupled direction pairs, i.e., one-dimensional systems.

12 The procedure comes to mind so naturally that, without having any special name, it is very often invoked. For instance, every time a radiation routine is called by a GCM and, if the notion of cloud "fraction" is diagnosed, then each grid box is itself divided into two independent pixels, one cloudy and the other not.

[13] This is done by implementing the option to use 1st order scattering sources (and associated homogeneous BCs) in the S_{i+} (or, rather, their CA equivalent $\mathcal{S}$ in eq. (D.9a)). See Meador and Weavor [1980] for an extensive review of the various "two-flux" approximations to CA plane-parallel transfer in the literature.

[14] We use the word in the same sense as in quantum theory with one important difference. In "quantics," to use Lévy-Leblond's expression that avoids the words "wave" and "mechanics," $\mathbf{x}$ and $\mathbf{p}=-i\hbar\partial/\partial\mathbf{x}$ are Hamiltonian (hence Fourier) conjugates. This is a lot worse than being nonlinear "functions" of one another: there exists a "minimal" wave packet, viz. a Gaussian; (the norm of) this wave packet is the analog of our τ- (or ρ-) distribution but there is nothing to stop us from making it degenerate. Indeed an overwhelming majority of transfer calculations in the literature apply only to this very special case.

[15] A function f is said to be convex if it satisfies $f(\frac{x_1+x_2}{2}) \leq \frac{f(x_1)+f(x_2)}{2}$ for all pairs of points (x_1,x_2) on its support. This translates to $f'' \geq 0$, if it exists, but this is not a requirement for Jensen's inequality (3.31) to be valid.

[16] Generally speaking, CA similarity theory is not limited to the axi-symmetric phase functions treated by McKellar and Box's [1981] and therefore carries over unmodified to the most general DA system as described by eqs. (3.2-3).

[17] Recall that, in general, we expect the κ- and the λ-scalings to be related via supplementary (mass or density) conservation constraints. In this case however, the similarity theory of sect. 3.5 explicitly requires a constant grid size (λ) and overall multiplication by a variable κ-factor. Furthermore, we are justified to use the notation adopted for the "mean field" exponent in (1.2–3) since, at given ρ-field (hence λ), we have $\tau \propto \kappa$.

[18] This makes intuitive sense since automatic side-scattering is certainly the most radical way of loosing track of an initial direction of propagation. Recall (from sect. D.3) that standard rescaling theory shows just how isotropy is obtained from an initially collimated beam after several scatterings if necessary.

Bibliography for Chapter 3

Bellman R., R. Kalaba, and G. M. Wing, "Invariant imbedding and mathematical physics, I: particle physics," *J. Math. Phys.*, 1, 280–308, 1960.

Boissé, P., "Radiative Transfer Inside Clumpy Media: The Penetration of UV Photons Inside Molecular Clouds," *Astron. Astrophys.*, 228, 483–502, 1990.

Cahalan, R. F., "Overview of Fractal Clouds," in *Advances in Remote Sensing (RSRM'87)*, Eds. A. Deepak *et al.*, 371–389, A. Deepak, Hampton (Va.), 1989.

Chandrasekhar, S., *Radiative Transfer*, Oxford Un. Press, 1950. (Reprinted by Dover, New York, 1960.)

Chu, M. C., and W. S. Churchill, "Numerical Solution of Problems in Multiple Scattering of Electromagnetic Radiation," *J. Chem. Phys.*, 59, 855–863, 1955.

Cogley, A. C., "Initial results for multidimensional radiative transfer by the adding/doubling method," in *Proceedings of the 4th Conference on Atmospheric Radiation*, Toronto (Ont.), June 12–16, Am. Meteorol. Soc., Boston, 1981.

Davis, A. B., P. Gabriel, S. Lovejoy, and D. Schertzer, "Asymptotic Laws for Thick Clouds, Dimensional Dependence - Phase Function Independence," in *IRS'88: Current Problems in Atmospheric Radiation*, Eds. J. Lenoble and J.F. Geleyn, pp103–106, Deepak Publ., 1989.

Davis, A., P. Gabriel, S. Lovejoy, D. Schertzer, and G. L. Austin, "Discrete Angle Radiative Transfer - Part III: Numerical Results and Atmospheric Applications," *J. Geophys. Res.*, 95, 11729-11742, 1990a.

Davis, A. B., S. Lovejoy, D. Schertzer, P. Gabriel, and G. L. Austin, "Discrete Angle Radiative Transfer Through Fractal Clouds," *Proceedings of the 7th Conference on Atmospheric Radiation*, San Fransisco (Ca.), July 23–27, Am. Meteorol. Soc., Boston, 1990b.

Davis, A. B., S. Lovejoy, and D. Schertzer, "Radiative transfer in multifractal clouds," in *Scaling, Fractals and Non-Linear Variability in Geophysics*, Eds. D. Schertzer and S. Lovejoy, Kluwer, Hingham (Mass.), 1991a.

Davis, A. B., S. Lovejoy, and D. Schertzer, "Discrete angle radiative transfer in a multifractal medium," *S.P.I.E. Proceedings*, 1558, 37–59, 1991b.

Feller, W., *An Introduction to Probability Theory and its Applications*, vol. 1, Wiley, New York, NY, 1971.

Gabriel, P., S. Lovejoy, G.L. Austin, and D. Schertzer, "Radiative transfer in extremely variable fractal clouds," in *Proceedings of the 6th Conference on Atmospheric Radiation*, Williamsburg (Va.), May 12–16, Am. Meteorol. Soc., Boston, 1986.

Gabriel, P., *Discrete angle radiative transfer in uniform and extremely variable clouds*, Ph.D. thesis, 160pp, Phys. Dep., McGill Univ., Montréal, Québec, 1988.

Gabriel, P., S. Lovejoy, A. Davis, D. Schertzer, and G. L. Austin, "Discrete Angle Radiative Transfer - Part II: Renormalization Approach for Homogeneous and Fractal Clouds," *J. Geophys. Res.*, 95, 11717–11728, 1990.

Hardy, G H., J. E. Littlewood, and G. Pólya, *Inequalities*, Cambridge University Press, 2nd ed., 1952.

Hunt, G. E., "The effect of coarse angular discretization on calculations of the radiation emerging from a model cloudy atmosphere," *J. Quant. Spectrosc. Radiat. Transfer*, 11, 309–321, 1971.

Kepler, J., *Harmonie Mundi*, Regensburg, 1619.

Lovejoy, S., P. Gabriel, D. Schertzer, and G. L. Austin, "Fractal clouds with discrete angle radiative transfer," in *IRS'88: Current Problems in Atmospheric Radiation*, eds. J. Lenoble and J. F. Geleyn, pp99–102, A. Deepak, Hampton (Va.), 1989.

Lovejoy, S., A. B. Davis, P. Gabriel, D. Schertzer, and G. L. Austin, "Discrete Angle Radiative Transfer - Part I: Scaling and Similarity, Universality and Diffusion," *J. Geophys. Res.*, 95, 11699-11715, 1990.

Marchouk, G., and V. Agochkov, *Introduction aux Méthodes des Éléments Finis*, Mir, Moscow, 1981.

McKellar, B. H. J., and M. A. Box, "The Scaling Group of the Radiative Transfer Equation," *J. Atmos. Sci.*, 38, 1063-1068, 1981.

Meador, W. E., and W. R. Weaver, "Two-Stream Approximations to Radiative Transfer in Planetary Atmospheres: A Unified Description of Existing Methods and a New Improvement," *J. Atmos. Sci.*, 37, 630–643, 1980.

Mikhaylov, G. A., *Izv. Atm. Oceanic Phys.*, 18, 993–, 1982.

Pomraning, G. C., *J. Quant. Spectrosc. Radiat. Transfer*, 38, 595–, 1988.

Stephens, G. L., P. M. Gabriel, and S.-C. Tsay, "Statistical radiative transfer in one-dimensional media and its application to the terrestrial atmosphere," to appear in *Trans. Theory and Stat. Phys.*, 1991.

Mosher, F.R., *Visible flux across finite clouds*, Ph.D. thesis, 109pp, Univ. of Wisc., Madison, 1979.

Mullaama, R. Y., M. A. Sulev, V. K. Poldmaa, H. A. Ohvril, H. J. Niylsick, M. I. Allenov, L. G. Tchubakov, and A. F. Kuusk, *Stochastic structure of clouds and radiation fields*, NASA Tech. Transl., TT F-822, 1975.

Ronnholm, K., M. B. Baker, and H. Harrison, "Radiative transfer through media with uncertain or variable parameters," *J. Atmos. Sci.*, 37, 1279–1290, 1980.

Preisendorfer, R. W., *Hydrological Optics*, vol. 3, NOAA, PMEL, Hawaii, 1976.

Schuster, A., "Radiation Through a Foggy Atmosphere," *Astrophys. J.*, 21, p1, 1905.

Siddal, R. G., and N. Selçuk, "Evaluation of a New Six-Flux Model for Radiative Transfer in Rectangular Enclosures," *Trans. Inst. Chem. Eng.*, 57, 163–169, 1979.

Smith, J. V., *Geometrical and Structural Crystallography*, ppxii+450, John Wiley, New York (NY), 1982.

Welch, R. M., and W. G. Zdunkowski, "The radiative characteristics of noninteracting cloud fields, II: Calculations for cloud fields," *Contrib. Atmos. Phys.*, 54, 273–285, 1981.

Whitney, C., "Efficient stream distributions in radiative transfer theory," *J. Quant. Spectrosc. Radiat. Transfer*, 14, 591–611, 1974.

Chapter Four†

THICK HOMOGENEOUS AND FRACTAL MEDIA, RADIATIVE SCALING PROPERTIES

Overview: In the present chapter, one of our aims is to quantitatively compare the predictions of DA transfer described in chap. 3 and those of general (CA) transfer described in app. A using, as a test, the compatibility of the exponents defined by the general asymptotic thick cloud scaling relations:

$$T \approx h_T \bar{\tau}^{-\nu_T} \tag{4.0a}$$

$$R \approx R_\infty - h_R \bar{\tau}^{-\nu_R} \tag{4.0b}$$

for transmittance (T) and albedo (R) respectively, and where $\bar{\tau}$ denotes the spatially averaged optical thickness (which is a direct measure of total LWC or optical "mass"). Notice in (4.0b) that we have naturally anticipated a non-vanishing thick cloud limit (R_∞) for albedo and we recall from our discussion in sect. A.4 that one can distinguish R and 1-T only if two conditions are met: the media are horizontally bounded, on the one hand, and very special illumination conditions, fine-tuned to non-generic boundary shapes (that allow the geometrical definition of a cloud "side") are used, on the other hand.

The other aim is to quantitatively compare these two exact kinetic theories of radiation transport with various approximate theories (IPs, diffusion and renormalization) and try to single out the important structural properties of the optical media that cause these different approaches to agree well sometimes and to disagree completely at other times. The answers are of course respectively the opposite poles of extreme homogeneity (or regularity) and extreme inhomogeneity (or singularity), but with subtleties w.r.t. the type of transport theory. Media with the former quality have been as well studied as they are unrealistic but we too will be indulging in sect. 4.1, largely motivated by the urge to wrap up some "unfinished business" concerning the scaling (actually, to a large extent, the very definition) of albedo in horizontally bounded systems. More precisely, we investigate reflection through the top only of normally illuminated square shaped two-dimensional clouds and show that this (essentially improperly defined) albedo scales trivially (ν_R=1), contrary to our previous claims based on poorer data (ν_R=3/4). One of the reasons it is important to settle this problem is that, however artificial, such simple media and responses provide a benchmark for comparing both numerical transfer methods and inhomogeneous (isolated) cloud models. For instance, in sect. 4.2, we turn to internally inhomogeneous media modelled with fractals which are far more interesting (in spite of their deterministic structure) because radiative scaling properties are totally different from their homogeneous (ν_T=1) counterparts, it is "anomalous" (ν_T<1).

In sect. 4.3, we compile all of our radiative scaling results in a comprehensive table and discuss the structural properties of the optical media that are apt to promote the anomalous scaling; according to the available data, the crucial features seem to be singular one-point statistics and long-range correlations in their two-point counterparts. The final section is more theoretical, we ask (in retrospect) whether this could have been anticipated from first principles, i.e., by looking more closely at the mathematical structure of the basic transport equations. We summarize the situation by tentatively proposing two very specific criteria, (4.9) and (4.14), for the onset of strong nonlinear effects (e.g., anomalous scaling) on which both transfer and diffusion theories agree; the former criterion implies very irregular (non-differentiable, possibly discontinuous) structures, and the latter that many scatterings are needed to build up the nonlinear effects of "channeling." These criteria have predictive (rather than diagnostic) power in the sense that they relate—in Preisendorfer's words—only the "inherent" optical (κ,g) and structural (ρ-field) properties of the medium, no "apparent" property (related directly to radiation fields, illumination geometry, etc.).

4.1. Homogeneous Squares, Cubes and Beyond

In fig. 4.1 and figs. 4.2a,b, we show numerical (Monte Carlo) results for homogeneous squares (d=2) and cubes (d=3) where the dimensionality designates not only the number of dimensions needed to describe the figure but also the number of dimensions in which the photons can propagate. In other words, the square is <u>not</u> a long 3-D square-sectioned cylinder laying parallel to its axis. Illumination is normal and transmittance is naturally defined as exit through the "bottom" (unique non-illuminated) face. Because this is a case of "terminator" pathology as described in §A.4.2 above, the way is opened to distinguishing reflectance through the (normally irradiated) "top" and through any (grazingly irradiated) "side." We will denote these responses respectively T, R and S=(1-R-T)/2(d-1) and τ is the optical length of the all the edges.

4.1.1. Standard Diffusive Rescaling Retrieved

In fig. 4.1, we find CA results for this geometry in d=2. The two-dimensional analog of the Henyey-Greenstein phase function (described in §A.3.1) was used for several values of the asymmetry factor (g). Notice that, rather than R directly, it is $\Delta R/\Delta\ln\tau$ ($\Delta\ln\tau$=0.25ln10≈0.58) that is presented on the log-log plot; it is easy to see from the basic relation (4.0b) that dR/dlnτ scales the same way as R for large (or small) τ. Furthermore, this measure of albedo, as well as transmittance, are graphed as a function of optical thickness rescaled *à la* van de Hulst and Grossman [1968], viz. $(1\text{-}g)\tau$, just as in diffusion theory. Both responses collapse onto universal curves, just as in d=1. (The discrepancies seen in the transmittance curve are entirely attributable to the numerical Monte Carlo uncertainties.) Davies [1978] as has already convincingly demonstrated that transfer and diffusion yield asymptotically similar results for homogeneous cuboidal (d=3) cloud models with various aspect ratios. The universal behavior w.r.t. $(1\text{-}g)\tau$ observed here is a strong indication that this is also true for our square media in d=2. It also implies, in particular, phase function independence in the asymptotic regimes.

Finally, we notice that $dR/d\ln\tau$ goes through a maximum, just as in d=1 (or in slab geometry) where, from (3.22),

$$\frac{dR_p}{d\ln\tau} = R_p(1\text{-}R_p) \tag{4.1}$$

which is maximal at $R_p=T_p=1/2$, i.e., $(1\text{-}g)\tau_{max}=2$. The subscript "p" stands for "plane-parallel" as in (2.28). Here, in d=2 with horizontal fluxes due to horizontal boundedness, we find a somewhat larger but still $O(1)$ value for $(1\text{-}g)\tau_{max}$. We will soon see that this type of behaviour is not specific to homogeneous media.

4.1.2. Characterization of the Phase Function Independent Scaling Regimes

Turning to figs. 4.2a,b, respectively for d=2 ($\tau\leq512$) and d=3 ($\tau\leq256$), the phase functions are either DA- or CA-isotropic (g=0) and, in d=3, the Deirmenjian "C1" ($g\approx0.85$) phase function has been added.[1] The fact that the T-curves, on the one hand, and R-curves, on the other hand, for both types of phase function become parallel in the log-log plot demonstrates that the important scaling properties (exponents) are insensitive to the phase function choice. We first focus on $T(\tau)$, in d=2, there is little doubt that this response is well into its asymptotic regime with $\nu_T=1$, unsurprisingly. More interesting is the inflection of the logT vs. $\log\tau$ curve which increases from d=2 to d=3. We note that there is none of this inflection at all in d=1 (or plane-parallel geometry[2] in d>1); indeed, from (4.1) above and $T_p=1\text{-}R_p$, we find

$$\frac{d\ln T_p}{d\ln\tau} = -R_p \tag{4.2}$$

hence, using (4.1) again, the second derivative is $-R_pT_p<0$ for all finite τ's.[3] At the same time, the value of the prefactor h_T is decreasing as d increases and, most importantly, the asymptotic regime is entered at increasingly large optical sizes. This is not too surprizing either since, from its point of injection on the top face, the typical photon "sees" the bottom face through a relative angle (on Ξ_d) that decreases constantly with d, hence increased chances of being intercepted by other sides before reaching the bottom on its RW. On the same figures, we find $\log[1\text{-}R(\tau)]$ vs. $\log\tau$ with $\nu_R=3/4$ lines indicated that seem to represent the available data adequately; we address quantitatively the question of the albedo's asymptotic behavior for d=2 in the next sub-section. In the mean time, we simply notice how the distance between T and 1-R increases with τ and, more markedly, with d. This distance is of course nil in d=1. Whatever its scaling exponent is, R also enters its asymptotic regime at optical sizes that increase with d.

These trends[4] w.r.t. increasing d are not hard to understand. First, it is easy to see that $T(\tau)$ becomes exponential in the limit $d \to \infty$ because, in ∞-D, the photons that are not directly transmitted have a vanishingly small chance of even being scattered back into the downward direction in a finite number of steps. In the same limit and for the same reasons, we expect $R(\tau)$ to vanish for all τ. This last point can be furthered by noticing that, for thick media (homogeneous or not), the fraction of all incident photons that are reflected after a single DA(d,2d) scattering is r/2 since, after reflection (with probability r), we want to know how many photons, starting at exponentially distributed optical distances from z=0 in an optically thick medium, make it back according to the same exponential optical f.p. distribution (the answer is exactly[5] 1/2). Notice how the exponential character of the distribution is not essential to the outcome. We are presently comparing, in a systematic fashion, isotropic scattering in various dimensionalities (so t=r=s=1/2d). The contribution of first order reflection is therefore 1/4d; as $d \to \infty$, this fraction vanishes identically and, since the contributions of higher orders-of-scattering necessarily go in diminishing,[6] this tells us that convergence towards a high value of R is ever slower (we need $\sim\tau^2$ scatterings, independent of d, see discussions in sect. B.1 and D.4), as d increases without bound.

4.1.3. The Evidence (and Relevance) of Non-trivial Scaling in Homogeneous Systems

Gabriel *et al.* [1990] argue that the thick cloud scaling exponent for 1-R has to be some ratio of small integers since the problem has regular BCs. In other words, the scaling may not be "trivial" (the plane-parallel result) but neither is it "anomalous" which would be the case if the exponent took on some non-rational real value. The authors in fact proposed 3/4 in d=2 and 1/2 in d=3 for ν_R; however they based their estimates on the predictions of their "real space renormalization" approach which can lead to unphysical results, as shown by Lovejoy *et al.* [1990]. Indeed, the former exponent seems to accommodate our above numerical results in both d=2 and d=3. It is clearly of interest to try to settle for some definitive understanding of these totally homogeneous (hence totally unrealistic) cloud models if we are to feel confident about our ability to understand the more interesting but more difficult case of realistically inhomogeneous clouds.

First, we recall from our discussion in §4.1.2 that, in this very special case of cloud <u>and</u> illumination geometries, there is a basic ambiguity about what we can call albedo. This ambiguity can be removed by seeking the "robust" terminator which here turns out to be the rim of the cloud's base. In this analysis of the problem there is of course only one exponent for both T and R since they add up to 1, by definition, independently of cloud geometry and even in presence of internal structure. If internal homogeneity prevails, this exponent is 1, arguably for any finite d.

Secondly, if it still appears important to separate 1-T into R, on the one hand, and 2(d-1)S, on the other hand, then we must recognize that, as d increases, the asymptotic regimes (whatever they happen to be) are ever harder to reach hence less-and-less relevant to "reasonable" optical sizes (say, in the several hundreds). For this reason, we will dwell on homogeneous squares with isotropic DA(2,4) scattering—a very simple Monte Carlo code to write—and run high quality (mega-photon) simulations that are statistically independent, not only from one photon to the next but also from one medium to the next (this inhibits certain optimization procedures used previously) for τ up to 512. The results are plotted in fig. 4.3 as they should when seeking an asymptotic scaling regime: $(1-R)\tau^{\nu_R}$ vs. $\log_2\tau$ for several test values of ν_R ranging from less than 3/4 to 1. In all cases, the numerical uncertainty is smaller than the symbol, cf. eq. (B.1b). For the right exponent, the curve levels off at an ordinate equal to the prefactor h_R. Clearly, 3/4 fails the test and a rough examination shows that ν_R can be no less than 0.8. If we believe very strongly that the two last points (τ=256,512) are in the asymptotic regime, then ν_R is slightly greater than 0.8=4/5 but 5/6≈0.83 appears to be already too big ... and the integers in the ratio that forms ν_R cannot be that small.

It seems that the easiest way to save the (perfectly valid) "small integer ratio" argument is to consider ν_R=1/1 with a very large prefactor, i.e., the log(1-R) and logT curves eventually become parallel (S and T go to 0 at the same rate ultimately). This would have the further advantage of being independent of d; otherwise, the whole exercise must be successfully repeated for all d's. Finally, there is a simple geometrical argument that predicts this behaviour, including the prefactor increasing with d (as discussed in the previous sub-section). Consider a very large homogeneous hypercubical cloud of optical size τ»1 in all d directions; only a fraction $\approx 2(d-1)\tau^{d-2}/\tau^{d-1}=2(d-1)/\tau$ of the incident photons fall within a m.f.p. of the edges and only these stand a fair chance (say, 50-50) of reaching the corresponding side, the others are generally reflected (contribute to R) and a very small number are eventually transmitted (reach the bottom) after very many scatterings. Neglecting those transmitted photons (due to the relatively small prefactor), we find $1-R\approx 2(d-1)S\approx(d-1)/\tau$. In short, sides are asymptotically unimportant, at least in these homogeneous situations. This analysis of the homogeneous cloud scene also implies that most of the top face of the large cuboidal cloud will have a quasi-plane-parallel response attached to it. In turn, this is corroborated by the simple visual experiments described by Bohren [1991]: he photographs from above (the illuminated side) horizontally finite homogeneous clouds (made of milk and water) and they indeed are featureless, except at the very edge where they naturally darken.

Finally, we note that the above argument makes use of the intuitive idea that the presence of boundaries can only be felt (in the fine directional structure of the radiation fields) up to a few photon m.f.p.'s (while the rough directional features are conditioned everywhere by the asymmetry in illumination). In turn, this leads to the idea of a "physically defined" boundary layer which, in homogeneous situations at least, would be relatively narrow (and this is essentially why the diffusion approximation can be expected to be quite accurate, see app. D). In contrast, a non-trivial albedo exponent would be an indication of the presence of a "mathematically defined" boundary layer in the sense that the required solutions of the transfer equations would behave non-analytically near the boundaries (i.e., infinite gradients would occur). Indeed, the well-studied solutions of the simplest (plane-parallel) problems are singular but they have the property of having bounded first order directional derivatives, these are the physically meaningful ones that appear in the transfer equation itself [Marchuk and Agochkov, 1981]; these derivatives can be—in fact, generally are—discontinuous across boundaries (infinite second derivatives). Exact solutions of the CA transfer problem on cuboidal media have been developed by several authors [e.g., Crosbie and Schrenker, 1982; Preisendorfer and Stephens, 1984; Stephens and Preisendorfer, 1984]; they are quite complex but, unsurprisingly, they make no use of boundary layer methods and show no evidence of singularity in the physically interesting[7] quantities.

4.2. Deterministic Monofractal Media (Sierpiński Gaskets)

4.2.1. Results for the Horizontally Infinite Cloud ("Cyclical" Boundary Conditions)

As a prototypical internally inhomogeneous medium with the kind of intermittent scale invariance that we expect from current turbulence theory (and observation), we propose to use the same $D=\log_2 3=1.585\cdots$ deterministic monofractal used as an elementary example in app. C. Fig. 4.4a shows the first three cascade steps (with $\lambda_0=2$ and $d=2$) and fig. 4.4b shows the same medium after $n=7$ cascade steps (hence $\lambda=\lambda_0{}^n=128$) while, in our numerical transfer simulations, we proceeded up to $n=9$ (cyclical BCs) and $n=12$ (open BCs), i.e., a 4096X4096 grid. In all cases, the total number of filled cells is $N_\lambda=\lambda^D$, see sect. C.2 for more details on the definition and geometrical meaning of D (including the relation to more standard ways of constructing "Sierpiński Gaskets").

The Monte Carlo simulations follow the general guidelines exposed in sect. B.1 with one difference which consists in an optimization that exploits the monofractality. Given that the individual cell is either full or empty, the (integer) array in computer memory is used to store, not directly the local value of the density, but rather the ($\log_2$ of the) size of the hole ranging from 0 (one elementary cell) to n-1 (the massive hole in the upper right corner) and a token (negative) number was used for the filled cells. This way the photon could be immediately propagated from one side of a hole to the other, with no further questions asked about the cumulative amount of scatterers encountered since it remains constant in such optical voids (hence considerable speed-up). The filled cells were maintained at one of three optical thicknesses ($\tau_0=\kappa\rho_0 l_0=1/8,1/2,2$) throughout the cascade. The total (horizontally averaged) optical thickness is thus given by

$$\bar{\tau} = \frac{\tau_0 N_\lambda}{\lambda^{d-1}} = \tau_0\lambda^{1-C} \tag{4.3}$$

where 1-C=1-(d-D)=0.585···.

The results for cyclical BCs with normal incidence and CA isotropic scattering are presented as usual ($T(\bar{\tau})$ vs. $\bar{\tau}$) in fig. 4.5 for all three adopted values of τ_0. Notice that the curve for the thickest cells lies almost entirely in its asymptotic regime, in sharp contrast with the previously discussed homogeneous media, and we find $\nu_T \approx 0.4$. Also illustrated are selected results for isotropic DA(2,4) and DA(2,6) scattering phase functions with τ_0=2 and we remark that only the DA(2,4) exponent differs significantly ($\nu_T \approx 0.5$). This is the only violation ever observed of our general rule of radiative exponent independence of phase function choice and is (probably) caused by the strong degree of anisotropy (r.h./l.h. asymmetry plus horizontal extension via cyclical BCs) somehow "resonating" with the privileged directions of propagation of the photons. Also indicated for reference on the same figure is the homogeneous plane-parallel transmittance (3.22) and we find, for T≈0.1 (not untypical of overcast conditions), an optical thickness ratio in the range 5–8 with more LWC in the inhomogeneous cloud. This agrees well with the kind of discrepancy reported in connection with the cloud "albedo paradox" [Wiscombe *et al.*, 1984] discussed in the concluding chapter.

4.2.2. Results for the Horizontally Finite Cloud ("Open" Boundary Conditions)

Fig. 4.6a shows our Monte Carlo results for the transmission through the same normally illuminated monofractal medium but without the photons being recycled if exit by a side is detected—physically, this is a very different situation (see discussion in sect. A.4 and 2.2). Again the illumination is normal and we compare CA- and DA(2,4)-isotropic phase functions. Using the data for $\tau_0 = 2$, the scaling exponent in (4.0a) is found to be $\nu_T \approx 0.5$ (not unlike the above DA exponent, but there is no reason to think this should be a rule). However, albedo (in figs. 4.6b,c) exhibits $R_\infty \approx 1/2$; its precise value will be estimated numerically along with ν_R further on. The cloud possesses a symmetry axis (at 45° clockwise from the vertical) which, combined with the isotropic phase functions used here, ensures that roughly half of the (vertically incident) photons will escape from the top and half from the r.h.s. of the cloud (if it is very thick). By the same token, we see that if the cloud were rotated 45° counter clockwise in fig. 4.4, its R_∞ would become 1, equivalently, rotate the angle of incidence 45° clockwise. Either way, we see that the boundary conditions (of illumination) have an obvious influence on the fixed point of the scale changing operation in thick cloud limit, but not on the exponents (cf. our discussion of percolation below). Notice also that, in the new configuration, the (grazingly illuminated) cloud sides are reduced to two points, one can no longer distinguish R and 1-T hence a single exponent is called for.

In order to determine the values of R_∞ and ν_R, it is convenient to graph the finite derivative of the albedo w.r.t. the (natural) log of (space-averaged) optical thickness against the albedo itself, thus avoiding a nonlinear three parameter fit. From (4.0b) one readily obtains

$$\frac{\Delta R}{\Delta \ln \overline{\tau}} = \frac{R(\overline{\tau})-R(2\overline{\tau}/3)}{\ln 3/2} = [R_\infty - R(\overline{\tau})]\ \frac{(3/2)^{\nu_R}-1}{\ln 3/2} \qquad (4.4)$$

Such a graph[8] is shown in fig. 4.7; from the linear regression coefficients one obtains $R_\infty \approx 0.53, 0.54$ in the CA and DA cases, respectively, and $\nu_R \approx 0.46$. As for the transmittance data, the exponents obtained are the same (to within numerical precision) for both phase functions, supporting the hypothesis that DA and CA are in the same "universality class" of phase functions. However this last number can be viewed as basically compatible with ν_T determined above above, given the very noisy data and the way the "asymptote" is approached (we will not stress their difference in the following). We will return to this medium in sect. 5.3 with analytical results for direct transmittance as well as IP transmittance.

4.3. The Transition from Normal to Anomalous Radiative Scaling

4.3.1. Physical Transport Theories and Model Optical Media

Table 4.1 summarizes most of our (and several other authors') findings in scaling language. Its purpose is to single out, using the available data, the structural properties of the optical medium that are necessary for obtaining anomalous radiative scaling and/or diverging predictions using different physical theories to describe radiation-matter interaction. This justifies the presence of four columns, the first three of which correspond to the three basic "general purpose" radiation transport theories, i.e., a theory that can accommodate any kind of medium, on a per realization basis when its nature is stochastic. Specifically, we have radiative kinetic theory in column #2, its hydrodynamic limit (diffusion theory) in column #3, and the "independent pixel" (IP) approximation in column #1. The above criterion excludes "mean field" theories where the average effect of some specific brand of inhomogeneity is directly modeled [e.g., Stephens, 1988; Titov, 1990; Boissé, 1990; also the brief discussion in sect. 5.1 based on our scaling results for average multifractal direct transmittance]. Also excluded *a priori* is the "real space renormalization" approach of Gabriel *et al.*, 1990] which must be redesigned more-or-less from scratch for each different (necessarily scaling) medium. "Mean field" and "renormalization" are ideas more than theories and, in fact, the quoted application of renormalization ideas to radiation transport uses a mean field idea (specifically, when across-cell gradients are neglected). *A posteriori*, there are several reasons (given below) to include this renormalization approach so it is associated with column #4. At present, we are exclusively interested in the conservative "albedo" problem (i.e., purely scattering media illuminated at a boundary) and, for completeness, we have quoted some results established (or simply discussed) elsewhere in the literature.

Transport Theory → ... DA regime:	Independent pixels $p=0$	Radiative transfer $0<p<\infty$	Diffusion approx. $p=\pm\infty$	Renorm-alization $-\infty<p<0$
Medium ↓		ν_T (ν_R)		
Homogeneous Plane-parallel:				
"rod" (d=1)	(trivial)	1	(exact)	1
(d=2)	1	1	1	1
"slab" (d=3)	1	1	1	1
Homogeneous and Bounded:				
circles		*1*	*1*	
squares		1	*1*	!
(d=2)		(1?)	(*1*?)	(3/4)
spheres		*1*	1	
cubes		1	1	!
(d=3)		(1?)	(1?)	(1/2)
Inhomogeneous and Bounded:				
Cir. Annuli (d=2)		*1*	*1*	
Sph. Shells (d=3)		*1*	1	
Binary Mixtures in Slab Geometry:				
(d=2)	1	*1*	1	
(d=3)	1	1*	1	
... same at $p=p_c$ and in the "RSN" limit:				
(d=2)	1	1†	0.03	
(d=3)	1	1	0.2	
1.58-D monofractal:				
cyclic BCs	0.71	0.4	0	0.60
open BCs		0.5		!
(d=2)		(0.5-?)		(0.16)
Multifractal-τ:				
$\langle 1/(1+r\tau)\rangle$	< 1			
$\langle \exp(-\tau)\rangle$	$< \infty$			

Table 4.1: A compilation of most known radiative scaling exponents, see text for details.

The four different transport models are not unrelated to one another and we now recall their various interconnections. The second column is reserved for radiative transfer *per se*, the fundamentally kinetic approach that models photon populations in their natural phase space (i.e., in both physical space and velocity-, or propagation direction-, space); most importantly, the photon propagation is ballistic in nature with $1/\kappa\rho(x)$ being the local m.f.p. and we will return to this aspect in the next sub-section. Based on our comparisons in the above sections, we consider the general (CA) model to be in the same class as DA(d,2d) transfer, on condition that its characteristic phase function parameter "p" remains finite. To the left, we find the IP approximation at the "$p \to 0$" DA limit and where net radiative exchanges from one (vertical) column to the next are prohibited, not by inserting internal (insulating) boundaries as described in sect. 2.1 from the diffusion viewpoint but by giving probability 0 to a sideways scattering event. To the right, we find the diffusion approximation at the (more formal) "$p \to \infty$" DA limit and where fluxes in any direction are not only allowed but given exactly by Fick's law; see sect. 3.3 and D.2 respectively for the connections with the DA- and CA transfer models. As we see, these two approximations—even DA transfer itself—can be obtained directly from CA transfer but the route via DA formalism shows how the three general models fit into a continuum parameterized by a single DA parameter; we can therefore expect systematic effects to arise when going from one transport model to the next for a given medium. For instance, it was shown (on a restricted class of inhomogeneous media) in sect. 2.1 that IPs yield smaller overall fluxes (transmittance) than diffusion theory; on the examples studied here, we will see that DA (hence CA) transfer fits neatly in between the two. Because of its close connections with DA transfer, we have provided a fourth column at the extreme right for the renormalization approach but it has entries only for those few scaling media for which it has been worked out; we note however that these connections exist at the technical level [Gabriel *et al.*, 1990] as well as at the formal level [Lovejoy *et al.*, 1990]; in the latter case, we have an association of renormalization with the "unphysical" DA regime ($-\infty<p<0$).

4.3.2. Homogeneous (but not Necessarily Plane-Parallel) Media

The rows of table 4.1 correspond to different categories of media, starting with (horizontal) homogeneity in plane-parallel geometry and there are no surprizes here since these media provide the benchmark for "normal" radiative scaling. From there, we go on to homogeneous media in some kind of bounded geometry. Entries in *italics* correspond to results that have not been established in any great detail but are nevertheless extremely plausible. For instance, we discuss circles and spheres in chap. 2 but solve the albedo problem only for the latter and only in the diffusion approximation. Because they have a well-defined terminator, only a transmittance exponent is required and it is of course unit; in sect. 2.2, it was shown that the formal equivalence to plane-parallel response goes in fact a lot further than just the exponent. In sharp contrast, squares and cubes under normal illumination have pathological terminators; in the table, we quote (with a "?" marker) our updated estimate of the "top only" reflectance exponent and hopefully put this totally academic problem to peace: either we accept that 1-R scales as for the plane-parallel medium or we use the "robust" terminator and then only the transmittance exponent is called for. It is hard to convince oneself that there is something fundamentally different between equally homogeneous spherical and cubical cloud models! We quote the diffusion result for cubes as positively known because of Davies' [1978] semi-analytical solution which agrees numerically extremely well with his Monte Carlo results. Following our discussion in §2.2.3, we omit IP estimates for all horizontally bounded media since they are basically irrelevant to that geometry. For completeness, we also quote the quantitatively poor renormalization estimates of Gabriel *et al.* [1990] for this controversial reflectance exponent and note that the authors themselves retain only the qualitative features of the approach (which borrows heavily from nonlinear dynamical systems theory): phase function independence of the radiative scaling in the "attractive" (hence stable) thick cloud limit, phase function sensitivity in the "repulsive" (hence unstable) thin cloud limit. This last method yields no information on the transmittance exponent (hence the "!" marker in the table, it is not an omission). Notice that, apart from the problematic numbers just discussed, we see only one exponent value up until now: unit.

4.3.3. Weakly Variable (but not Necessarily Smooth) Media

We now enter the realm of inhomogeneous media, starting with the deterministic case (again from chap. 2) of spherical systems with a spherical cavity. In more general terms, this example is representative of a whole class of media with inhomogeneities present only in a very narrow range of scales. "Narrow" w.r.t. the range going from overall cloud size down to some very much smaller scale, just like the inertial range in fully developed turbulence theory (cf. app. C). Unsurprisingly, the scaling is the same as for the above totally homogeneous media. This does not mean that there are no interesting and systematic effects of inhomogeneity present, only that they can affect the prefactors alone (see §2.3.2 for a very specific illustration of radiative "channeling" using hollow spheres). We now turn to very much random media, namely, "binary mixtures" where the value of (optical) density is chosen according to a simple Bernouilli trial between a lower ($\kappa\rho_-$, probability p_-) and a higher ($\kappa\rho_+$, probability $p_+=1-p_-$) value. This process is repeated in each and every cell without any correlation from one to the next. We are dealing with "on/off" or "1-bit" white noise with an offset, further discretized spatially on a grid of constant l_0 and outer size L. Its spectral density is flat from $k=2\pi/L$ to $k=2\pi/l_0$, so this is very "broad band" variability if $L \gg l_0$. In §D.6.2, we reviewed the extensive analytical and numerical diffusion studies conducted on such media and put them to radiative purposes in §2.3.4; we saw that these media have normal (homogeneous-type) diffusive scaling in general [e.g., Hong *et al.*, 1986] with exceptions discussed in the upcoming sub-section. From the transfer vantage point, Welch *et al.* [1980] report "small" differences between white noise and homogeneity using Monte Carlo simulation for photon transfer (although they did not use exactly a binary mixture, hence the "*" marker in the table). In the same vein, Boissé's [1990] analytical results the ensemble-average transfer responses of binary mixtures that are exponentially decorrelating (on a scale R) rather than uncorrelated as discussed above (and again below); the author numerically confirmed his (non-conservative) results using a white noise medium and setting $R=l_0$ in his formulae. This "mean field" theory for media that exhibit a specific scale in the structure is normally outside of the scope of this survey. However, the model has two scaling limits: $R\rightarrow\infty$ (homogeneity) and $R\rightarrow 0$ ("atomic mixture," which is an idealization of white noise on a very large grid). Interestingly, the equations in the latter limit become formally identical to those of the former limit (at the mean density).

Finally, it is important to realize that the inhomogeneous media that we have been considering are far from being "smooth" (differentiable). The hollow spheres have one major discontinuity since the density goes from some finite value to zero as the center is approached; their density field has singular values but it is almost everywhere smooth (technically speaking, it is called "piecewise constant"). We furthermore recall (from §2.3.3) that the radiation field is itself continuous across the discontinuity and we will see (in chap. 6) that multiple scattering can very powerfully smooth out very intense fluctuations in the density field. By way of contrast, the media composed of binary mixtures are nowhere differentiable although they are everywhere stochastically ("almost surely") continuous in general (i.e., as long as R remains finite). We will collectively refer to these media as "weakly variable" in spite of the possibility of vanishing density (hence of an infinite relative range in density values) because, in the cases where this happens, the optically empty regions are somehow localized and, as we will now be arguing, this is of crucial importance to the maintenance of normal transport properties ($\nu_T=1$) in presence of singularity. Indeed, it is difficult to conceive of an interesting "transport" process (e.g., "channeling") happening at a point—even Fick's law calls for a gradient (hence information from two neighboring points). Conversely, we can imagine optical media that are highly correlated and basically irregular (in the sense of non-smooth) but nowhere singular. For instance, we could mention density fields that look like Mandelbrot [1975] – Voss[1983] "fractional Brownian landscapes;" although such models have not been extensively researched[9] from the radiative point of view, we strongly suspect them to be in this category.

4.3.4. Extremely Variable (and Somehow Correlated) Media

In the statistical physics literature, binary mixtures have attracted much attention because of the "percolation" phenomenon that appears at some critical probability p_c. At this frequency of occurence, an infinite cluster of low density (ρ_-) cells appears after a stage of algebraic growth w.r.t. (p-p_c), i.e., the size of the biggest cluster $\xi \sim |p-p_c|^{-\nu}$ also known as the "correlation" length although "connectivity" length would be a better expression (see our discussion of this nomenclature in §4.4.4 below); notice that we retain the traditional notation since no confusion is possible with our radiative "νs" since the latter all carry subscripts. Furthermore, this large cluster has a characteristic fractal structure, the number of cells it contains (its "mass") grows algebraically with ξ, i.e., as ξ^D where D is the associated fractal dimension (see sect. C.2 for further details). In the above, the exponents (ν and D) are "universal" in the sense that they depend only on d (a "relevant" variable), not on the type of grid or whether we are dealing with "bond" percolation rather than (the above described) "site" percolation. In contrast, the value of p_c does depend on such so-called "irrelevant" details. For an excellent review of the geometrical aspects of percolation (and a good introduction to the transport aspects), see Stauffer [1985]. In itself, this percolation is not enough to change the diffusive nor transfer scaling, let alone IPs, but, if the limit $\rho_- \to 0$ (or $\rho_+ \to \infty$) is taken while remaining near p_c, then new and interesting transport phenomena occur, but only when diffusion is used to model it. This is the "random superconducting network" (RSN) limit where the appropriate (properly diffusing) particles to be used in simulations are de Gennes' [1980] "termites." In this limit, the incipient infinite percolation fractal cluster literally "channels" the termites and the medium becomes globally superconducting (read, totally transparent), i.e., we witness a phase change behaviour at the critical (mean) density value.[10] In table 4.1, we simply quote the diffusion RSN exponents and notice their anomaly (at last!) which is clearly related to the singular nature of the density field; for details, concerning finite size scaling in particular, we refer the reader to §D.6.2 and §2.3.4. We simply point out the fact that the RSN exponent in d=2 is the only one numerically determined to more than one significant figure (and this called for considerable computational effort—by several groups working with different techniques—motivated mainly by the eventual disproving of the "Alexandre-Orbach" conjecture). We can confidently predict normal scaling for transfer through percolating media even with null density values mainly because of Bunde *et al.* [1985] report negative results on "skating" termites (identified by a "†" in table) which, like photons, were programmed to have ballistic trajectories in the superconducting cluster. By negative, we mean that no phase transition was observed and that particular breed of termite was consequently rejected as a model for diffusion, see Lovejoy *et al.* [1990] for further discussion along these lines.

Finally, we arrive at the deterministic monofractal investigated in the previous section and, simultaneously, at a plethora of anomalous scaling exponents. The transfer entries reproduce the results obtained numerically in the previous section of this chapter. We dismiss the numerical significance of the difference between ν_R and ν_T in the case of "open" horizontal BCs (hence the "?" marker reappears). For the case of "cyclic" horizontal BCs, we use the (more universal) CA-DA(2,6) figure rather than the DA(2,4) figure which is numerically compatible with the "open" BC exponent(s). This last choice is to stress the fact that we are really dealing with two very different transfer problems, not just a minor change in BCs (in the same sense as, say, varying illumination angle is): one medium is infinite and the other not; there is no reason to believe that the exponents should be the same *a priori*, even in such simple transfer systems. The corresponding IP result is obtained analytically in the next chapter and we can confidently predict total transparency w.r.t. diffusion (T=1 hence ν_T=0) since the fractal medium is so sparse (i.e., it can by associated with an RSN medium at $p \approx 1 > p_c$). Gabriel *et al.*'s [1990] renormalization results are also quoted for completeness. What has happened? It is singularity in conjunction with long range correlations (and the appearance of a fractal structure) that caused diffusion theory to "go anomalous" in the percolating RSN limit. Here too singularity is playing a crucial role; although the worked out example is an "on/off" monofractal density field, there is no fundamental reason to restrict ourselves to this blatant type of singularity (density simply becomes exactly null here and there, as in the case of binary mixtures) but rather we can think of singularity in the sense of strong intermittency, extreme variability, i.e., the multifractal sense of the word that is encountered in turbulence theory (app. C). Here too long-range correlations are present although this time in the straightforward statistical sense of a diverging "integral scale" (cf. eqs. (4.10–13) below), not in the percolation theory usage evoked in the beginning of this sub-section. Finally, under the entry "Multifractal- τ," we quote symbolically, from the upcoming chapter, our analytical results for both total plane-parallel (IP) transmittance and direct transmittance; in both cases, the scaling is found to be non-trivial in general. Although extensive numerical radiative scaling studies have not yet been conducted for multiple scattering in multifractals of all kinds, we can anticipate anomalous exponents for both transfer and diffusion (and they will probably be different in general).[11]

In summary, non-trivial radiative scaling does not appear along with horizontal boundedness, nor inhomogeneity, nor stochasticity, not even very broad band variability of the density field. The key notions seem to be (i) wide-spread singularity, in the straightforward sense, or in that of extreme multifractal (hence intermittent) variability, and (ii) long-range correlation, in the usual statistical sense, or in that used specifically in percolation theory (see §§4.4.2–4 to come for technicalities). Singular (RSN) percolating media are associated with anomalous diffusion only and multifractals are associated with non-trivial scaling for transfer as well. In other words, it seems to take nothing short of strong (multifractal) intermittancy and the accordingly strong degree of concentration (hence correlation) for radiative "channeling" processes to affect the exponents in a transfer-type approach. In contrast, spatial correlation is of no importance to IP approaches since only 1-point statistics are needed but clearly, for anomalous behaviour to be observed in this approximation, singularity must be present not only in the d-dimensional density fields but in the associated and necessarily smoother (d-1)-dimensional optical thickness fields. It is hard to imagine how this can happen outside of multifractal models where integrals ("measures") are typically dominated by the strongest singularity present, see app. C for the basic theory and chap. 6 for a good example. We have also found that, in the cases studied, the IP- and diffusion approximations provide respectively lower and upper bounds on the scaling exponent for transmittance, as predicted in chap. 3 from their positions w.r.t. DA transfer theory.

4.4. On the Mechanisms Involved in Anomalous Radiative Behaviour

4.4.1. Transfer Theory (begin.): The Need for Singularity

The steady state radiation transport problems such as those described in sect. 4.1–2 above are described by the basic transfer equation:

$$\mathbf{u}\cdot\nabla I_{\mathbf{u}} = -\kappa\rho(\mathbf{x})\,[\,I_{\mathbf{u}} - S_{\mathbf{u}}\,] \tag{4.5}$$

The symbols are all defined in sect. A.1 and an essentially phenomenological derivation of (4.5) that emphasizes the underlying stochastic concepts is given in app. E. If the source field $S_{\mathbf{u}}(\mathbf{x})$ that appears on the r.h.s. of (4.5) is known everywhere, then it is trivially solved for the radiance field $I_{\mathbf{u}}(\mathbf{x})$:

$$I_{\mathbf{u}}(\mathbf{x}) = \int_0^\infty \exp[-\int_0^s \kappa\rho(\mathbf{x}-\mathbf{u}s')\,ds']\,\kappa\rho(\mathbf{x}-\mathbf{u}s)\,S_{\mathbf{u}}(\mathbf{x}-\mathbf{u}s)\,ds \tag{4.6}$$

as can be verified by substitution. The infinite upper bound in (4.6) simply means that we want the whole optical medium M included; M can be viewed as the region of space where optical density $\kappa\rho(\mathbf{x})$ is non-vanishing (see §A.4.1 for further details). In the albedo problems studied here, at least one boundary lies at close range and is illuminated by a distant (hence collimated) external source of radiance. Eq. (4.6) is known as the "formal" solution and, indeed, it is not of much use by itself, at least in the multiple scattering (m.s.) problems of interest to us because $S_{\mathbf{u}}(\mathbf{x})$ is also an unknown field:

$$S_{\mathbf{u}}(\mathbf{x}) = \oint p(\mathbf{u}'\rightarrow\mathbf{u})\,I_{\mathbf{u}'}(\mathbf{x})\,d^{d-1}\mathbf{u}' \tag{4.7}$$

Substitution of (4.6) into (4.7) yields the "auxiliary" integral equation of transfer which can be iterated to generate the source field $S^{(n)}_{\mathbf{u}}(\mathbf{x})$ for all orders-of-scattering ($n=0,1,2,\cdots$) by starting with the single-scattering source field given in sect. A.3; the corresponding radiance field $I_u^{(n)}(x)$ is then given by (4.6). This procedure yields the von Neumann series solution to (4.6–7).[12] The opposite substitution, (4.7) into (4.6), can also be iterated directly towards the solution $I_u(x)$ of the given transfer problem.[13]

Clearly, the most important term in the system of coupled integral equations (4.6–7) is the "integrating factor" of (4.5) that becomes the "propagation" kernel in (4.6), namely, direct transmittance from x to some other point in M, at a distance l:

$$T_d(\mathbf{x},\mathbf{x}-\mathbf{u}l) = \exp[-\int_0^l \kappa\rho(\mathbf{x}-\mathbf{u}s)\, ds] \tag{4.8}$$

In sect. A.2 on the nonlinear radiation-density field coupling encapsulated in (4.8), it is shown (i) that the geometrical photon free path statistics are directly related to T_d (viewed as a function of l), (ii) that, in homogeneous media, they are given by the well-known exponential distribution, and (iii) that, in inhomogeneous media, they can be considerably different from their homogeneous (or "optical") counterparts.[14] It is of interest to notice that the propagation kernel in (4.8) is bounded, even in presence of singular density fields. In essence, this guarantees the convergence of the above-mentioned von Neumann series and, at the same time, the convergence of the estimates of linear functionals of $I_u(x)$ based on direct Monte Carlo simulation since, by definition, Monte Carlo photons obey (4.6-7); see sect. B.1.

The above discussion makes clear that the key concept in radiative transfer is the photon free path distribution (not only the m.f.p., but all of its other moments will be of interest too, in general); we can try to use our understanding of the stochastic process associated with photon propagation in an inhomogeneous medium to anticipate criteria on this internal variability—sometimes referred to as the "disorder"—which can predict the onset of strong (highly nonlinear) effects on the overall radiative response. We start by picturing a photon taking a random walk (RW) in an infinite homogeneous medium ($\Re^d$=M). Using (optical) units of length where $\kappa\rho$=1, the average step in this RW is (the m.f.p., by definition, hence) unit and much larger steps are exponentially rare. In the transfer problems of interest here, this RW is "bounded" ($\Re^d \supset$M): it starts on an "illuminated" part of ∂M and ends as soon as it encounters any part of ∂M again, with the above step distribution, this will happen (with probability 1) in finite "time" (number of "steps," in fact, elementary scattering events). As the inhomogeneity increases, the previous (optical) free paths and their geometrical counterparts differ more and more, especially in places where $\kappa\rho(x)$ varies considerably over a (local) m.f.p.; as a standard measure of the distance over which $\rho(x)$ varies "considerably," we take the ratio of local density to its local gradient: $\rho/|\nabla\rho| = 1/|\nabla \ln\rho|$. We are thus requiring that $1/|\nabla \ln\rho| \lesssim 1/\kappa\rho$ or, equivalently,

$$\left| \nabla \frac{1}{\kappa\rho} \right| \gtrsim 1 \tag{4.9}$$

In our reasoning, we have ignored the effect of the phase function in (4.7), that is, implicitly assumed it to be constant (isotropic scattering). We can however use the simple van de Hulst–Grossman [1968] similarity relation, $\kappa \to (1-g)\kappa$, to somewhat refine the above criterion, incorporating the (1st order) effects of anisotropic scattering, via g.

We are thus conjecturing that, if (4.9) happens often enough, the cumulative effect of the difference in step values during the photon's RW is apt to become very large and we can expect interesting things to happen. What do we mean by "often enough?" On average? For the most probable density value? Or the median (i.e, half of the time)? Or on a "space-filling" (Lebesgue-measurable) set? ... This question will likely develop into a whole area of cloud radiation research with scaling concepts at the center. The term "interesting" is easier to define. For instance, if the boundaries are maintained in their positions (and, for the sake of argument, we can assume that the optical mass is redistributed around inside): (1) a different part of the boundary can be encountered first, (2) at a different number of prior steps. The first consequence can convert a reflected photon into a transmitted one or vice-versa, but the former case happens more often since (as argued in sect. A.2) geometrical path distributions are made systematically wider by the internal variability (hence upon injection at cloud top the photons start their RW closer to the cloud base). This constitutes a fundamental aspect—but only one aspect—of radiative "channeling" from the viewpoint of transfer; the other—more complex—aspect involves the angular part of the transfer process (i.e., the multiple scattering) to which we return further on. This also means that the second of the above consequences can be refined to say that the number of scatterings needed to exit an inhomogeneous medium is always (statistically speaking) less than for its homogeneous counterpart and we refer the reader to sect. 6.5 for a dramatic illustration of this. Given the importance of boundaries on the outcome of the RW, we can confidently predict that d=1 (where boundaries are always reduced to 2 points) plays a very special role in transfer theory. In other words, in (d≥2) cases where the above condition is generally met in the bulk of the medium, we expect to make quite different predictions using inhomogeneous transfer, on the one hand, and "homogenized" transfer, on the other hand. We have already seen several examples of this kind of systematic variability effect (and more will be provided) but we must first realize that, if (4.9) seems to be a necessary condition to obtain strong variability effects, it is not by itself sufficient—in essence, "channeling" can't work if we have no spatial correlations.

It is important to realize that we can use (4.9) even if the density field is non-differentiable; in fact, we can use (4.9) to argue that, in practice, $\rho(\mathbf{x})$ cannot be differentiable at least if we are interested in optically thick media. Suppose the medium is discretized on a grid (constant spacing, l_0, and linear size $\lambda=L/l_0$)—this is always necessary in computational situations anyway. Criterion (4.9) then reads

$$\frac{|\Delta\rho|}{\rho} \gtrsim \kappa\rho l_0 = \tau_0 \tag{4.10}$$

which is the optical thickness of the elementary cell. A very smooth (differentiable) medium has $|\Delta\rho|\propto l_0 \ll \rho$ (assumed to be of finite magnitude); (4.10) then calls for extremely thin cells; at finite λ, we are therefore confined to optically thin media hence trivial radiative scaling properties: the medium responds linearly to external illumination. In such quasi-homogeneous (smoothly varying) media, we can also anticipate independence w.r.t. (large enough) λ at any given optical thickness (held constant) since the decimation appears merely a computational necessity, containing no physical information on the system. In contrast to this, we can more generally define a (Hölder) exponent $|\Delta\rho|\propto l_0^H$ (H<1) that describes the "irregularity" of the density field. It is generally assumed (in the simpler models) that H is independent of the choice of origin (but it is generally not so in experimental situations). In scale invariant structures, H does not depend on l_0 either, over a large range of values (as $|\Delta\rho|$ decreases to zero), and H thus describes just how non-differentiable (fractal) the density field is, usually in a statistical sense (i.e., we are interested in $\langle|\Delta\rho|\rangle$).[15] Moving away from additive processes towards multiplicative cascade fields, one is not even interested in the "Δ" any more (to 1st order): we can directly write $\rho\propto l_0^{-\gamma}$ where the exponent γ is the "order of singularity" introduced in app. C and, very importantly, it is shown that we must then look at the "multiple" scaling of the density field (i.e., $\langle\rho^h\rangle$ will scale differently with l_0 for different values of h). Far from being differentiable, such "singular" density fields are everywhere discontinuous. At any rate, in additive (multiplicative) models, the size of the scaling range (i.e., λ) is as much a physical measure of the irregularity (singularity) as is the unique exponent H (are the various exponents γ's). We should also stress that this reading of (4.10) already imposes a strong degree of spatial correlation on the structure of the optical medium. Finally, it is worthwhile emphasizing that questions concerning the radiative properties of scaling media are essentially open (only one simple deterministic case was examined numerically in the above, a random example is studied in chap. 6, and the simplest analytical results are obtained in chap. 5).

4.4.2. Transfer Theory (cont'd): The Need for Long-Range Correlations

Viewed as a requirement on the spatial statistics of the medium, condition (4.9) applies to a local (one-point) statistic. It seems quite clear that any *bone fide* transport (hence non-local) process will be sensitive to at least the two-point statistics of the medium, say,

$$C_\rho(\mathbf{x},\mathbf{y}) = \frac{<[\rho(\mathbf{x})-<\rho(\mathbf{x})>][\rho(\mathbf{y})-<\rho(\mathbf{y})>]>}{\sqrt{<[\rho(\mathbf{x})-<\rho(\mathbf{x})>]^2>}\sqrt{<[\rho(\mathbf{y})-<\rho(\mathbf{y})>]^2>}} \tag{4.10}$$

Notice the normalization by the (local) r.m.s. deviations; implying, in particular, that $C_\rho(\mathbf{x},\mathbf{x})=1$. A random ρ-field is said to be statistically homogeneous (isotropic) if all of its n-point statistics are invariant under translation (rotation). In the homogeneous and isotropic case, C_ρ would therefore depend only on the magnitude (r) of $\mathbf{r}=\mathbf{x}-\mathbf{y}$:

$$C_\rho(r) = \frac{<[\rho(\mathbf{r})-<\rho>][\rho(\mathbf{0})-<\rho>]>}{<[\rho-<\rho>]^2>} = \frac{<\rho(\mathbf{r})\rho(\mathbf{0})>-<\rho>^2}{<\rho^2>-<\rho>^2} \tag{4.11}$$

where $<\rho(\mathbf{r})\rho(\mathbf{0})>$ is the auto-correlation function. As in the above general case, we have $C_\rho(0)=1$ (from definitions) and that we generally expect (from statistical homogeneity) that $C_\rho(\infty)=0$. The simplest example of a randomly homogeneous and isotropic field is provided by totally uncorrelated fields of density fluctuations—the spatial equivalent of "white" noise in the temporal domain—which has formally $C_\rho(\mathbf{r})\propto\delta(\mathbf{r})$ (in this special case, $C_\rho(0)=\infty$). When dealing with processes that are non-stationary[16] but do have "stationary increments," then

$$<|\rho(\mathbf{r})-\rho(\mathbf{0})|^2> = 2\,[\,<\rho^2> - <\rho(\mathbf{r})\rho(\mathbf{0})>\,] \propto 1 - C_\rho(r) \tag{4.12}$$

is used instead of $<\rho(\mathbf{r})\rho(\mathbf{0})>$, it is known as the structure function (and sometimes "variogram"). Identically null at r=0, it increases (generally monotonically) to some constant value. Given $C_\rho(r)$, one can always (tentatively) define the "integral length-scale" of the stochastic medium:

$$R_\rho = \int_0^\infty C_\rho(r)\, dr \tag{4.13}$$

This definition can not always be taken literally since, in many interesting cases, it leads (formally) to $R_\rho = \infty$ or (practically) to $R_\rho \sim L$, the overall size of the medium (where the above integral must consequently be stopped, examples to follow). For instance, in an additively scaling medium ($<|\Delta\rho|>\propto r^H$, $H<1$), $C_\rho(r)$ decays algebraically (hence quite slowly) over a large range of scales (a geophysically relevant example to follow).

Having theoretically everywhere infinite gradients, δ-correlated fields easily satisfy (4.9) but we can confidently predict very "mean field" (homogeneous-like) transfer behaviour since the mean density $\overline{\rho}$ over any finite segment, however small, is $<\rho>$, i.e., its distribution is degenerate (since a theoretically infinite number of independent ρ-values have been sampled). At any rate, Welch *et al.* [1980] indeed find very small effects in their numerical studies on such media and this is confirmed by Boissé's [1990] independent numerical and analytical results on very similar media (based, for the latter approach, on previous work by Avaste and Vainniko [1974] on binary mixtures). Even diffusion theory yields a "normal" scaling properties in uncorrelated binary mixtures, except exactly at percolation threshold and in the very special limit of vanishing density values (see §§2.3.4–5). It is important to note that, in these "white noise" studies, there is in fact a finite correlation length—equivalently, a low pass cut-off in Fourier space—imposed either by the numerical discretization (grid constant, l_0) or by the analytical model ("Poisson point fluxes" for which[17] $C(r)=\exp[-r/R]$); the δ-correlated case is approximated by (or analytically retrieved in the limit of) vanishingly small R. In a sense, this is an example of "too much," or more precisely "unstructured," rather "dull" variability. Another undesirable radiative consequence of the lack of spatial correlations is that "channeling" is essentially inhibited. We have assumed our stochastic media to be isotropic on average but this statistical symmetry is broken by every realization: at a given point, some directions lead to denser regions, others to more tenuous regions, and "channeling" tends to enhance the fluxes in these latter directions. However, in any white noise medium, no direction is special as soon as scales larger than l_0 are considered.

If we want to restore the possibility of strong variability effects via photon f.p.'s that are significantly longer than those predicted using the average density, as well as via large scale "channelling," we can tentatively require that, over and above (4.9), the ensemble-average m.f.p. $\langle E(l)\rangle$ (defined in sect. A.2) must be exceeded by R_ρ. Hence[18]

$$\langle E(l)\rangle \lesssim R_\rho \tag{4.14}$$

Returning to our examples and counter-examples, we now see that, if $C_\rho(\mathbf{r}) \propto \delta(\mathbf{r})$, then (4.13) yields $R_\rho = 0$ (since $C_\rho(0) = \infty$, in this exceptional case); consequently, media generated with white noise do violate the new condition. A radical way of satisfying (4.14) is to require $R_\rho = \infty$ (formally), that is $R_\rho \sim L$ (in practice). If indeed we have $R_\rho \sim L$, then a direct interpretation of (4.14) is that we are basically requesting that there be generous amounts of scattering involved for a typical photon history; this is necessary for the angular aspects of transfer to get to work on the "channeling" problem: the photons are individually blind, they need time (scatterings) to collectively "seek" the more tenuous parts of the medium. Recall that, in homogeneous media, τ is simply L in units of photon m.f.p.'s; so in (4.14), we are requiring, in a sense, that the medium not be too "thin," not only in the (average) "optical" sense ($\tau \gg 1$), but also w.r.t. the more relevant ensemble-averaged m.f.p.'s, and this will always call for an even greater τ (hence total mass). In app. C, we review basic turbulence theory in particular for passive scalar advection by fully developed (inertial range) three-dimensional turbulence where (Corrsin-Obukhov) phenomenology predicts $\langle|\rho(\mathbf{r})-\rho(\mathbf{0})|^2\rangle \propto r^{2/3}$ for the structure function (the associated Hölder exponent[19] is $H=1/3$), equivalently, $C_\rho(r) \approx 1-Ar^{2/3}$, i.e., a sharp but only algebraic decay over a large range of scales. The constant term dominates the integral in (4.13) and R_ρ is said to "diverge," in practice, we can state that $R_\rho \sim L$.

What do scaling media predict for the other side of (4.14), namely, $<E(l)>$? This is where additive ($<|\Delta\rho|_r> \propto r^H$, $H<1$) and multiplicative ($<\rho_r{}^h> \propto r^{-K(h)}$, $h \in \Re$ and $K(h) \in \overline{\Re}$) models are apt to differ considerably. In the additive case, average density $<\rho>$ is not defined by the stochastic model which has "stationary increments;" it is basically an independent parameter of the model that must be made large enough w.r.t. the maximum (expected) fluctuation so that ρ remains (almost surely, everywhere) positive. Optical distance (cumulative optical density) over a distance r will also have an average and a fluctuation component, respectively proportional to r and r^H ($H<1$) hence relative fluctuations are relatively small. We can therefore expect still very exponential-type photon f.p. (l) distributions; more precisely, we can anticipate (at best) "stretched" exponential distributions where the p.d.f. for l decays as $\exp[-l^H]$ ($H<1$), if the fluctuation term is somehow made to dominate at long ($l>l_0$) range, while at short range, we will of course have a linear decrease (as in the homogeneous case). The multiplicative case is somewhat more involved and it is investigated in chap. 5 in the asymptotic limit of many cascade steps (hence a very large outer-to-inner scale ratio, λ). Depending on whether this limit makes the medium optically thinner or thicker, we find respectively a linear response or an algebraic (hence very non-exponential) decay of direct transmittance with distance and correspondingly wider l-distributions.

The enhanced photon free path distributions we expect in multifractal media have an interesting—even somewhat paradoxical—consequence, especially when many orders-of-scattering are involved: clouds with such extremely variable internal density fields may look relatively featureless, like their weakly variable (possibly even homogeneous) counterparts. In homogeneous systems, radiation fields change typically on the scale of a photon m.f.p. which is the length over which radiatively pertinent information (presence of a boundary, of a source, etc.) is directly transmitted. This will still be the case in inhomogeneous systems and, as previously mentioned, radiation fields remain essentially continuous across discontinuities in density. This is especially true if many such cell boundaries are encountered along a single photon free path (on average) and this will happen everywhere (4.10) is consistently verified. Using Preisendorfer's [1976] jargon, we can therefore anticipate relatively smooth "apparent" optical properties (e.g., albedo fields) to be associated with potentially violently variable "inherent" optical properties. The paradox is that this will happen at the same time as the bulk response becomes very different from that corresponding to the (apparently and inherently) homogeneous model ... which is in turn used to explain Wiscombe *et al.*'s [1984] cloud albedo "paradox." All of this (apparent) speculation is confirmed by our detailed numerical simulations of transfer through a multifractal cloud presented in chap. 6, as well as in arctic stratus [Tsay and Jayaweera, 1984].

4.4.3. Transfer Theory (end): Long-Range Correlations, in Fourier Language

It is of interest to rephrase the above using Fourier space nomenclature. The Weiner–Khintchin theorem states that the auto-correlation function $<\rho(r\mathbf{u})\rho(\mathbf{0})>$ of a homogeneous and isotropic process is the (one-dimensional) Fourier transform of the energy spectrum of the ρ-field. The latter quantity is defined as

$$E_\rho(k) = \int_{|\mathbf{k}|=k} <\tilde{\rho}^*(\mathbf{k})\tilde{\rho}(\mathbf{k})> d^d\mathbf{k} = k^{d-1} \int_{\mathbf{u}\in\Xi_d} <|\tilde{\rho}(k\mathbf{u})|^2> d^{d-1}\mathbf{u} \qquad (4.15)$$

where $\tilde{}$ denotes a d-dimensional Fourier transformed quantity. We favour the following definition of this transformation and its inverse:

$$\tilde{\rho}(\mathbf{k}) = \int \rho(\mathbf{x})\, e^{i\mathbf{k}\cdot\mathbf{x}}\, d^d\mathbf{x} \quad \Leftrightarrow \quad \rho(\mathbf{x}) = \frac{1}{(2\pi)^d}\int \tilde{\rho}(\mathbf{k})\, e^{-i\mathbf{k}\cdot\mathbf{x}}\, d^d\mathbf{k} \qquad (4.16)$$

Mathematically, the W-K theorem then reads

$$E_\rho(k) = 2\int_0^\infty <\rho(r\mathbf{u})\rho(\mathbf{0})>\, e^{ikr}\, dr \quad \Leftrightarrow \quad <\rho(r\mathbf{u})\rho(\mathbf{0})> = \frac{1}{\pi}\int_0^\infty E_\rho(k)\, e^{-ikr}\, dk \qquad (4.17)$$

Now, from (4.11), $<\rho(r\mathbf{u})\rho(\mathbf{0})> \propto C_\rho(r)$+const. ($\mathbf{u}\in\Xi_d$) and we notice that, in the definition (4.13) of R_ρ, the integral of $C_\rho(r)$ can be related to that of $E_\rho(k)$, essentially via Percival's theorem for the Fourier transform pair in (4.17), hence any divergence of the energy integral leads to one in the correlation integral.

We now reexamine our examples (and counter-examples) of random optical media susceptible (or not) to exhibit strong variability effects. If $C_\rho(r) \propto \delta(\mathbf{r}) = \delta(r)/n_d r^{d-1}$ then $E_\rho(k) \propto k^{d-1}$, as we would expect, directly from its definition in (4.15), for (any kind of finite variance) noise that uniformly fills (d-dimensional) Fourier space. Turbulent passive scalar advection, along with (4.12), yields $<\rho^2>-<\rho(r\mathbf{u})\rho(\mathbf{0})> \propto r^{2/3}$ which translates to Kolmogorov's famous $E_\rho(k) \propto k^{-5/3}$ spectrum and the large (diverging) amount of integrated energy found at $k\approx 0$ reflects the fact that the spatial average of the ρ-field, $\bar{\rho} = \tilde{\rho}(\mathbf{0})$, fluctuates wildly—hence the necessity of reverting to increments before taking ensemble-averages. One talks about an "infra-red (large scale) catastrophy." Power law spectra with exponents in excess of -1 also have diverging integral scales, this time due to an "ultra-violet (small scale) catastrophy." Instead of large amounts of energy at the largest possible scales, used in overall spatial averaging (i.e., $k\approx k_{min}=2\pi/L$), we find large amounts of energy in the smallest possible scales, pixel-sized (i.e., $k\approx k_{max}=2\pi/l_0$, where l_0 is the grid constant) and we can expect very singular (spiky) looking fields. A good example of such a field is provided by a (conserved) multifractal cascade in ε—a "cascade quantity," as defined in app. C—has $<\varepsilon(ru)\varepsilon(0)> \propto r^{-\mu}$ with $\mu>0$ (equivalently, $E_\varepsilon(k) \propto k^{-1+\mu}$). For these multifractals, we have $|\Delta\varepsilon|\sim\varepsilon$ going from one pixel to the next and this is literally a result of their construction since, at each cascade step, we are multiplying the previous value of the field by a random number which is typically $O(1)$. Now, for lack of a satisfactory "ε-to-ρ" connection (see app. C), we currently identify ε and ρ for the purposes of numerical simulation of transfer (in sect. 4.2 above and in chap. 6 below). So (4.10) is satisfied as soon as $\kappa\rho l_0=\tau_0\lesssim 1$ (often enough), i.e., that most (not all!) cells are made optically not-too-thick. This is achieved by modulating the whole optical density field via κ and, needless to say, we find very strong inhomogeneity effects.

4.4.4. Diffusion Theory: Singular Density Values and Long-Range Correlations, Again

Recall that anomalous radiative (and, more generally speaking, transport) scaling is found for diffusion "sooner" than for transfer (or, more generally speaking, kinetics), in the sense that simple binary mixtures are sufficient ... if certain other conditions are satisfied. We will now argue that these special conditions are (again) synonymous with singularity, on the one hand, fractals and long range correlations, on the other hand, but with somewhat different meanings than (for multifractals as) used in the previous sub-section on transfer.

Compared to the coupled integral equations (4.6–7) for the transfer model of radiative transport, the steady-state conservative diffusion equation is deceptively simple:

$$\nabla^2 J = (\nabla \ln\rho)\cdot\nabla J \qquad (4.18)$$

Its most striking feature is that not only the typically diffusive phase function parameter (g) is absent but so is our customary κ factor. This means that, contrary to photons, the behaviour of diffusing particles (in unbounded media) is unaffected by an overall multiplication of the density field, only density ratios are important, see Bunde *et al.* [1985] for details. Both parameters appear however (combined) in the expression of Fick's law:

$$\mathbf{F} = -D\nabla J \qquad (4.19a)$$

with

$$D \approx \frac{1}{(1-g)\kappa\rho} \qquad (4.19b)$$

From (4.18–19a,b), we have (at various levels of approximation):

$$|\nabla \ln\rho| = \frac{|\nabla^2 J|}{|\nabla J|} \approx \frac{|\nabla J|}{J} \approx \frac{F}{J}\kappa\rho \qquad (4.20)$$

where we have taken g=0, for simplicity. Let us now recall (from sect. D.2) the condition for obtaining "normal" diffusion, defined as a case where it approximates transfer well: $F/J \lesssim 1$. Substituting this condition into (4.20), we find $|\nabla \ln\rho| \lesssim \kappa\rho$ for "normal" diffusion and, conversely, we retrieve (4.9) as a condition for "anomaly" to occur. Recalling that (4.9) must be verified "often" and that this in turn implies singular (non-differentiable, possibly discontinuous) density fields, we see that "normal" diffusion requires regularly varying density fields, which is exactly our conclusion from the above discussion of table 4.1. So the diffusion and transfer transport models agree on this (partial) answer to the question of 'what makes the radiative scaling anomalous?' which does not mean that the two theories will predict the same anomalous behaviour, quite the contrary (cf. table 4.1). This begs the question whether or not the two theories agree on the complementary criterion (4.14) which, in particular, expresses the fact that "channeling" needs some degree of spatial coherence and several scatterings get to work. Our above reasoning on photons can be transposed to diffusing particles, all known types of which move on grids from one site to one of its nearest neighbours—they have degenerate free path distributions with a m.f.p. of l_0 (the grid constant). Since R_ρ (for a discretized medium) is bounded from below by l_0, our criterion (4.14) relating the (ensemble-average) m.f.p. and the (integral) correlation length is therefore always marginally satisfied in the case of diffusion. This is a clear indication that diffusion is more (easily) perturbed by inhomogeneity than transfer, as was noted during the discussion of table 4.1: it is the first to exhibit anomalous behaviour as we make the media more inhomogeneous, and it shows the most anomalous behaviour for a given type of inhomogeneity.

In summary, the above inspection of (4.18) tells us that we can expect severe perturbation of the diffusion process if $\ln\rho$, as a random variable (one-point wise), exhibits a very wide range of values within a given medium. All the better if $\ln\rho$ exhibits, as a random field (two-point wise), long range correlations. As explained in the previous sub-sections, these two conditions basically define fractals and multifractals since their generically scale invariant structure gives them the desirable long range correlations and, for the latter, their multiplicative (cascade) nature guarantees their extreme variability (a wide singularity spectrum arises). We therefore expect diffusion on multifractals to be anomalous although we do not know of any (published) attempts to study this numerically to date.[20] In sharp contrast, a lot of effort has been invested over recent years into the topic of diffusion in binary mixtures, mainly at (or near) percolation threshold, and mainly in their singular (RRN and RSN) limits. The main results are reviewed in §2.3.4 and the outcome is that the diffusion is anomalous only if both of the above conditions are satisfied.

It is hard to imagine more diametrically opposite stochastic models as random binary mixtures (vanishing integral correlation length, only two values) and multifractals (diverging integral correlation length, large range of values). Yet, in interestingly different ways, our two "anomaly" conditions (existence of singular values and of correlated structures) are still verified. The condition of singularity is satisfied in the only straightforward way that a binary mixture possibly can: one of the allowable density values becomes infinite (RRNs) or null (RSNs). The correlation condition is satisfied in a more subtle, even somewhat paradoxical, way. We have indeed insisted in the previous sub-section that a medium generated by white noise was a vanishing "integral" correlation length R_ρ, as defined in (4.13), independently of whether its one-point statistic is a Bernouilli distribution or not. However, once discretized on a grid, we have in effect $R_\rho \sim l_0$ while $\langle E(l) \rangle = l_0$ for a diffusing particle: as noted above, (4.14) is already marginally satisfied. We will now show that, at percolation (and beyond), the criterion is in fact unambiguously satisfied on condition that we broaden our definition of what we mean by "correlation length."

In percolation studies, the term "correlation length" has taken on a rather different meaning than the one associated with eq. (4.13), a meaning in which the spatial discretization (the grid) plays a fundamental role—not the type of grid, just its existence! Letting $g(r)$ denote the probability for two sites (placed at relative distance r) to belong to the same cluster (group of connected sites having the same associated density value), the "correlation" (or "connectivity") length is defined as

$$\xi = \sqrt{\langle r^2 \rangle} = \sqrt{\Sigma r^2 g(r)} \tag{4.21}$$

but would obviously be better called the "average of all the clusters' radii of gyration," but in scaling arguments is generally interpreted as the "radius (size) of the average (typical) cluster" that (implicitly) dominates the 2nd order statistic used in (4.21) [Stauffer, 1985]. At any rate, the most prominent geometrical feature of percolation is the divergence of ξ with $(p_c\text{-}p)$ and eq. (2.43) gives the universal (grid-type independent) scaling characterization of this divergence. Furthermore, this appearance of an infinite cluster totally dominates the transport properties in the RSN (and[21] RRN) limit(s), as described in §2.4.4. In this sense, the anomalous diffusion is obtained on condition that the correlation length ξ diverges or, in practice, becomes of the order of the finite size of the medium ($\xi \sim L$). In summary, we can retain criterion (4.14) for diffusion in RSNs to become anomalous if we replace R_ρ by ξ on the r.h.s. (since we already have $\langle E(l) \rangle = l_0$ on the l.h.s.). Finally, we recall that the incipient infinite percolating cluster is a highly convoluted object that sprawls infinitely far in all directions yet it has a vanishingly small volume: it behaves like a fractal (see sect. C.2 for further details) down to scales $\approx l_0$.

4.4.5. *Summary and Discussion*

In summary, we have argued that in spatially discretized scaling media we are apt to obtain anomalous radiative scaling of their bulk properties if we have $|\Delta\rho|/\rho \gtrsim \kappa\rho l_0 = \tau_0$ "often enough," on the one hand, and $\langle E(l) \rangle \lesssim R_\rho \sim L$, on the other hand. These two criteria have been respectively interpreted to say that the media should be highly irregular and that the radiation fields of interest be dominated by relatively high orders-of-scattering.

It is important to stress that the analysis in this whole section is very qualitative and the above inequalities, indicate more a "direction to look into" than a rule (of thumb, even); in particular, they are not to be interpreted as saying "the greater the difference, the greater the expected effects." As an example of what this implies, recall that in the *ad hoc* models of "self-organized" critical phenomena first proposed by Bak *et al.* [1987] within the general framework of open, non-equilibrium systems with large scale forcing—not unlike ours (sunlight+clouds)—, the strongest effects (scaling noises in time evolution, fractal structures in space) arise at criticality and this very dynamical state of the system is attractive, stable (although obviously not in the usual sense of "static"). In our opinion, it is no accident that recent insight into the connections between self-organized criticality (s.o.c.) concepts and the idea of generic scale invariance (g.s.i.[22]) has been gained with the help of "singular" diffusion theory [Carlson *et al.*, 1990a,b; Kadanoff *et al.*, 1992] which is not unrelated[23] to the subject matter of the previous sub-section. In this context, the term "generic" refers to the scaling power spectra, diverging correlations and fractal structures that seem to dominate open systems that are far from equilibrium quite independently of the values taken by state parameters; this contrasts sharply with closed (often Hamiltonian) systems in thermal equilibrium (such as Ising models) where the scale invariant behaviour is obtained only by very finely tuning the parameters, specifically to their critical values where phase transitions occur. A simple example is provided by diffusion in singular binary mixtures where scaling anomaly kicks in exactly at the percolation threshold whereas diffusion in multifractals will (likely) be anomalous quite independently of the structural parameters of the model.

†The numerical results used in sect. 4.1–2 (except for fig. 4.3) were published in Davis *et al.* [1989, 1990]. A.D. devised the two-dimensional Henyey-Greenstein phase function and conducted the homogeneous CA simulations in d=2, as well as the DA simulations in d=2,3 and the inhomogeneous (1.585...-D fractal) in DAs and CAs. The plotting technique used in fig. 4.7 is due to S.L. The discussion in sect 4.1 is A.D.'s; responsibility is shared for that in sect. 4.2; the two last sections are essentially new.

[1]The author thanks P. Gabriel for kindly communicating these results (for $\tau \leq 200$) along with those for isotropic CAs in d=3.

[2]This lowering of transmittance (T) via horizontal fluxes does not affect our arguments (in chap. 2) about inhomogeneity always increasing T, via the same horizontal fluxes, because plane-parallel and hyper-cubic media do not have the same support, nor total mass (so they are not directly comparable in the terms clearly defined in sect. 2.3).

[3]We note incidentally that the inflection found for d>1 is entirely due to the log-log representation and does not reflect a complicated (non-convex) dependency of T on τ.

[4]Preliminary numerics confirm these trends up to d=7.

[5]More precisely, $[1-\exp(-2\tau)]/2$ where τ is the optical thickness of finite sized medium.

[6]They form a von Neumann series solution to a system of integral equations with a contracting kernel.

[7]By this we mean radiances and fluxes that are constrained by the radiative transfer equation, and not the component of the gradient at right angles to the beam.

[8]The "arches" observed here for fractal media, as well as in eq. (2.1) for their plane-parallel counterparts, are not without recalling the envelopes of Coakley and Bretherton's [1982] empirical scatter graphs of local albedo variance versus local albedo ("local" meaning a few pixels from a satellite scene). These plots are now routinely used in the "spatial coherence" method for recovering "fractional cloud cover," a parameter much used in GCM (two component IP-like) radiation calculations.

[9]Barker and Davies [1992] use such models to simulate broken but scalingly clustered cloud fields; however they use an additive constant and reduction of negative values to zero in order to modulate cloud "fraction." Moreover, the radiation is not transferred "through" the resulting two-dimensional density field which is in fact imbedded in d=3, lying flat, and illuminated from above; so most photons interact with very few cells and, unsurprisingly, relatively small inhomogeneity effects (beyond IPs) are found.

[10]In the opposite limit, $p_+ \to 0$, we find "random resistor networks" (RRNs) and de Gennes' "ants," which are of a lesser direct interest in cloud radiation studies, see discussion in §§2.3.4–5.

[11]This conjecture concerns only the highly variable cascade fields themselves. Their fractionally integrated counterparts (proposed by Schertzer and Lovejoy [1987] as a model for passive scalar fields) are much smoother and questions on their radiative properties are completely open.

[12]This procedure is however not useful in (numerical) practice: memory requirements are huge, and the convergence is slow if the scattering kernel is conservative. Monte Carlo simulation is a far more efficient way of obtaining the same order-of-scattering statistics as long as they do not need to be known everywhere; see our discussion in sect. B.1 and an illustration in sect. 6.5.

[13]In practice, this again is less efficient than Monte Carlo simulation unless the (preferably, isotropic) scattering is very non-conservative. Indeed both of these methods are used by Boissé [1990]: Monte Carlo for the different realizations of his stochastic media (composed of binary mixtures) and iteration of his mean field integral equations which are of course variable in the vertical only.

[14]Moreover, Flateau and Stephens [1988] argue that, using the appropriate transformations, the horizontally inhomogeneous plane-parallel transfer problem can be put in the one-dimensional form of (4.5), hence its the solution into that of (4.8) but with integration and exponentiation of (random) matrices rather than a simple scalar function as found here. Using two-flux theory for media with vertically variable absorption properties as an example, these authors trace the effect of the fundamental nonlinear dependence of radiance on the optical parameters (κ, p) in (4.5–8) to the non-commutation of the coupling matrices; the same remark applies to vertically variable horizontal structure, i.e., variability in both directions at once.

[15]An example (which is "close to home" w.r.t. standard radiation transport theory but) in the temporal rather than spatial domain is (a photon's) Gaussian RW in an infinite homogeneous medium: $|\Delta r| \propto t^H$ with H=1/2. See sect. D.4 for radiative details and sect. C.2 for geometrical implications (the fractal dimension of the RW is D=1/H=2, independent of the embedding dimensionality, d≥D).

[16]One should really say (statistically) non-homogeneous.

[17]The power spectrum of such a process is $\propto (1+kR)^{-2}$; i.e., flat (like for white noise) for $k \ll 2\pi/R$, which corresponds to the largest scales, and decays in k^2 (like for Brownian motion) for $k \gg 2\pi/R$, which corresponds to the smallest scales.

[18]Here again, we can somewhat refine be using "transport" m.f.p.'s which are associated with "effectively" isotropic scattering by using the standard similarity transformation $\kappa \rightarrow (1-g)\kappa$ in the calculation of $<E(l)>$.

[19]Note that the Hölder exponent H is usally defined "at a point," not as a statistic they way we use it here.

[20]Given the many potential applications of diffusion theory (cf. §2.2.1), on the one hand, and the current popularity of multifractals, on the other hand, we can also confidently predict that this will (soon) become an active area of research.

[21]In d=2 only, one could say "or" rather than "and" (because of Straley's [1977] duality).

[22]Not to be confused with Schertzer and Lovejoy's [1985] "generalized" scale invariance (GSI) which describes a formalism that can accommodate various kinds of structural anisotropy without leaving the framework of scale invariance. In this thesis, we only use the simplest (isotropic) kind of scale invariance.

[23]The fundamental difference being that diffusivity, D, is allowed to depend scalingly on the field quantity (our J), thus making the basic equation non-linear.

Bibliography for Chapter 4

Avaste, O. A., and G. M. Vaynikko, "Solar radiation transfer in broken clouds," *Izv. Acad. Sci. USSR Atmos. Oceanic Phys.*, 10, 1054–1061, 1974.

Bak, P., C. Tang, and K. Wissenfeld, *Phys. Rev. Lett.*, 59, 381–, 1987.

Barker, H. W., and J. Davies, "Solar Radiative Fluxes for Extensive Broken Cloud Fields," *J. Atmos. Sci.*, 1992 (in press).

Bohren, C. F., *What Light Through Yonder Window Breaks?*, J. Wiley & Sons, NewYork, NY, 1991.

Boissé, P., "Radiative Transfer Inside Clumpy Media: The Penetration of UV Photons Inside Molecular Clouds," *Astron. Astrophys.*, 228, 483–502, 1990.

Bunde, A., A. Coniglio, D. C. Hong, and H. E. Stanley, "Transport in a Two-Dimensional Randomly Composite Material: Scaling Theory and Computer Simulations of Termite Diffusion near Superconducting Limit," *J. Phys. A*, 18, L137–L144, 1985.

Carlson, J. M., J. T. Hayes, E. R. Grannon, and G. H. Swindle, *Phys. Rev. Let.*, 65, 2547–, 1990a.

Carlson, J. M., J. T. Hayes, E. R. Grannon, and G. H. Swindle, *Phys. Rev. A*, 42, 2467–, 1990b.

Coakley, J. A. (Jr.), and F. R. Bretherton, "Cloud cover from high-resolution scanner data: Detecting and allowing for partially filled fields of view," *J. Geophys. Res.*, 87, 4917–4932, 1982.

Crosbie, A. L., and R. G. Schrencker, "Exact expressions for radiative transfer in a three-dimensional rectangular geometry," *J. Quant. Spectros. Radiat. Transfer*, 28, 507–526, 1984.

Davies, R., "The effect of finite geometry on three-dimensional transfer of solar irradiance in clouds," *J. Atmos. Sci.*, 35, 1712–1724, 1978.

Davis, A. B., P. Gabriel, S. Lovejoy, and D. Schertzer, "Asymptotic Laws for Thick Clouds, Dimensional Dependence - Phase Function Independence," in *IRS'88: Current Problems in Atmospheric Radiation*, Eds. J. Lenoble and J.F. Geleyn, pp103–106, Deepak Publ., 1989.

Davis, A. B., P. Gabriel, S. Lovejoy, D. Schertzer, and G. L. Austin, "Discrete Angle Radiative Transfer - Part III: Numerical Results and Atmospheric Applications," *J. Geophys. Res.*, 95, 11729-11742, 1990.

de Gennes, P. G., "Percolation: Quelques Systèmes Nouveaux," J. Phys. (Paris) Colloq., 41, C3–17, 1980.

Flateau, P. J., and G. L. Stephens, "On the fundamental solution of the radiative transfer equation," *J. Geophys. Res.*, 93, 11037–11050, 1988.

Gabriel, P., S. Lovejoy, A. Davis, D. Schertzer, and G. L. Austin, "Discrete Angle Radiative Transfer - Part II: Renormalization Approach for Homogeneous and Fractal Clouds," *J. Geophys. Res.*, 95, 11717-11728, 1990.

Hong, D. C., H. E. Stanley, A. Coniglio, and A. Bunde, "Random-Walk Approach to the Two-Component Random-Conductor Mixture: Perturbing Away from the Perfect Random Resistor and Random Superconducting Network Limits," *Phys. Rev. B*, 33, 4564–4573, 1986.

Kadanoff, L. P., A. B. Chhabra, A. M. Kolan, M. J. Feigenbaum, and I. Procaccia, "Critical Indices for Singular Diffusion," *Phys. Rev. A*, 1992 (in press).

Lovejoy, S., A. B. Davis, P. Gabriel, D. Schertzer, and G. L. Austin, "Discrete Angle Radiative Transfer - Part I: Scaling and Similarity, Universality and Diffusion," *J. Geophys. Res.*, 95, 11699-11715, 1990.

Mandelbrot, B. B., "Stochastic models for the Earth's relief, the shape and the fractal dimension of the coastlines, and the number-area rule for islands," *Proc. of the Nat. Acad. of Sc.* (USA), 72, 3825–3828, 1975.

Marchuk, G., and V. Agochkov, *Introduction aux Méthodes des Éléments Finis*, Mir, Moscow, 1981.

Preisendorfer, R. W., *Hydrological Optics*, vol. 1, NOAA, PMEL, Hawaii, 1976.

Preisendorfer, R. W., and G. L. Stephens, "Multimode radiative transfer in finite optical media, I: Fundamentals," *J. Atmos. Sci.*, 41, 709–724, 1984.

Schertzer, D., and S. Lovejoy, "Generalized Scale Invariance in Turbulent Phenomena," *P.C.H. Journal*, 6, 623–635, 1985.

Schertzer, D., and S. Lovejoy, "Physically Based Rain and Cloud Modeling by Anisotropic, Multiplicative Turbulent Cascades," *J. Geophys. Res.*, 92, 9693–9714, 1987.

Stauffer, D., *Introduction to Percolation Theory*, Taylor & Francis, London, 1985.

Stephens, G. L., and R. W. Preisendorfer, "Multimode radiative transfer in finite optical media, II: Solutions," *J. Atmos. Sci.*, 41, 725–735, 1984.

Stephens, G. L., "Radiative transfer through arbitrarily shaped media, part 2: Group theory and closures," *J. Atmos. Sci.*, 45, 1836-1838, 1988.

Straley, J. P., *Phys. Rev. B*, 17, 5733, 1977.

Titov, G. A., "Statistical description of radiation transfer in clouds," *J. Atmos. Sci.*, 47, 24–38, 1990.

Tsay, S. C. and K. Jayaweera, "Characteristics of Arctic Stratus Clouds," *J. Climate Appl. Meteor.*, 23, 584-596, 1984.

van de Hulst, H. C., and K. Grossman, "Multiple Light Scattering in Planetary Atmospheres," in *The Atmospheres of Venus and Mars*, eds. J.C. Brandt and M.B. McElroy, pp. 35–55, Gordon and Breach, New York, NY, 1968.

Voss, R. F., "Fourier synthesis of Gausian fractals: 1/f noises, landscapes, and flakes," *Proc. Siggraph Conf.*, pp1–21, Detroit, 1983.

Welch, R. M., S. Cox, and J. Davis, "Solar Radiation and Clouds," *Meteorol. Monogr.*, 39, 1980.

Wiscombe, W. J., R. M. Welch, and W. D. Hall, "The effects of very large drops on cloud absorption, part 1: Parcel models," *J. Atmos. Sci.*, 41, 1336–1355, 1984.

Figure 4.1: CA transmittance and albedo for homogeneous squares with various asymmetry factors. The ordinate represents $\log_{10}$ of the photon counts (for T) or $\log_{10}$ of the differences in these counts (for R) expressed in arbitrary but similar units; the two-dimensional Heney-Greenstein phase function described in app. A–B was used (with $g = 0,\ 1/2,\ 9/11$) under normal illumination conditions. Note the constant logarithmic increments in optical size and that, if $1\text{-}R \propto \tau^{-\nu_R}$ then $dR/d(\log_{10}\tau) \propto \tau^{-\nu_R}$ also. The dispersion in the low transmittance counts is related to the characteristic noise of the adopted Monte Carlo scheme which was optimized for speed at the price of a somewhat more involved calibration (irrelevant to the slopes).

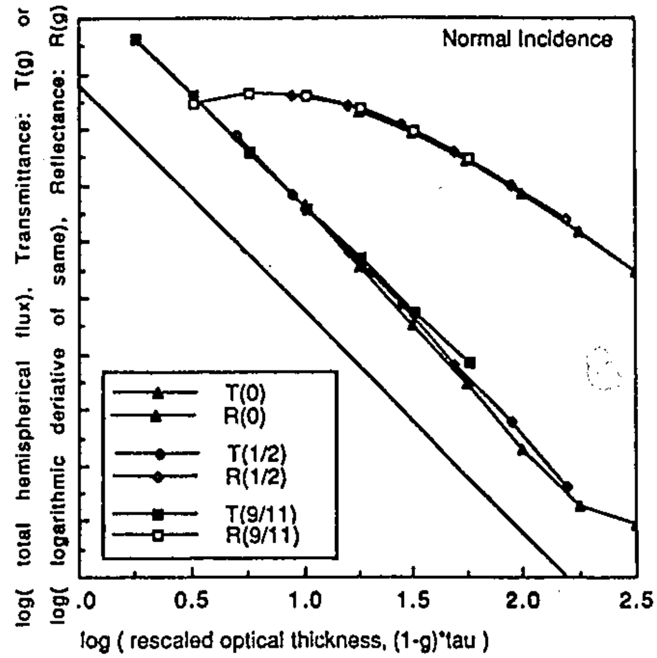

Figure 4.2a: Isotropic CA and DA transmittance and albedo for homogeneous squares. $T\times10^5$ or $(1\text{-}R)\times10^5$ versus τ for isotropic ($g = 0$) scattering in CAs and DA(2,4), obtained by Monte Carlo simulation on normally illuminated squares. The reference lines show the asymptotic slopes $\nu_R = 3/4$ and $\nu_T = 1$.

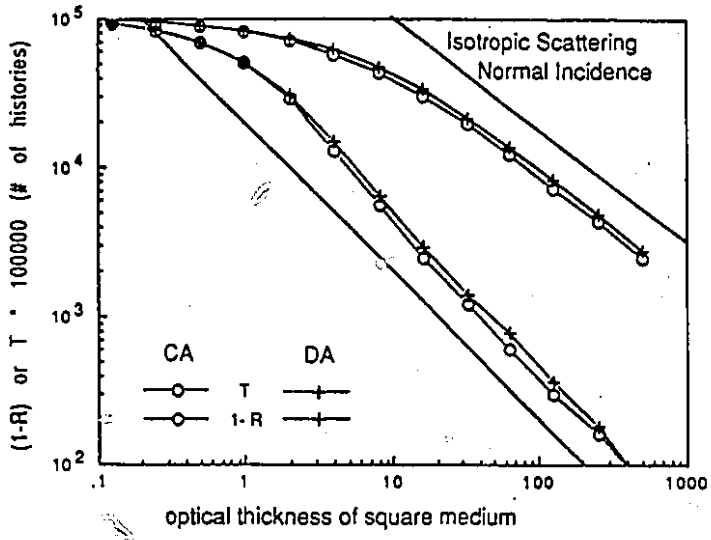

Figure 4.2b: Same Fig. 4.2a but for cubes, with the "C1" phase function added. T or $(1\text{-}R)$ versus $(1\text{-}g)\tau$ for anisotropic (Deirmenjian C1 drop size distribution, $g \approx 0.85$) and isotropic scattering in CAs—we thank P. Gabriel for this data—or DA(3,6) transfer, obtained by Monte Carlo simulation on normally illuminated cubes with 10^6 photons (except for DAs, where 10^5 histories were used).

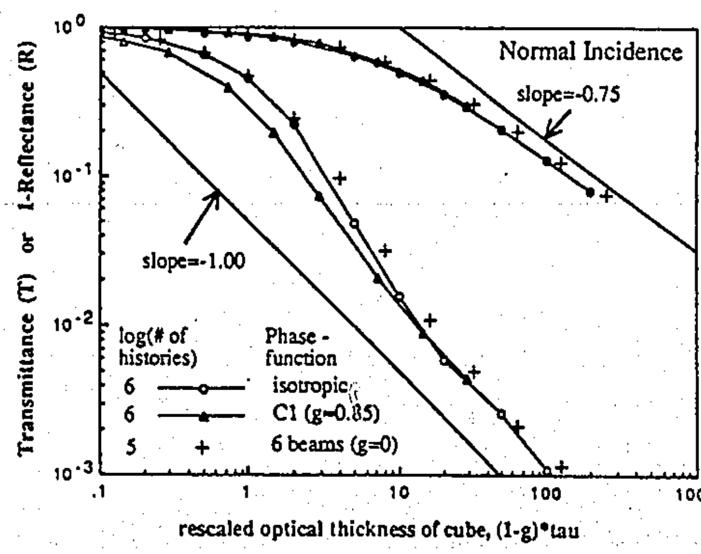

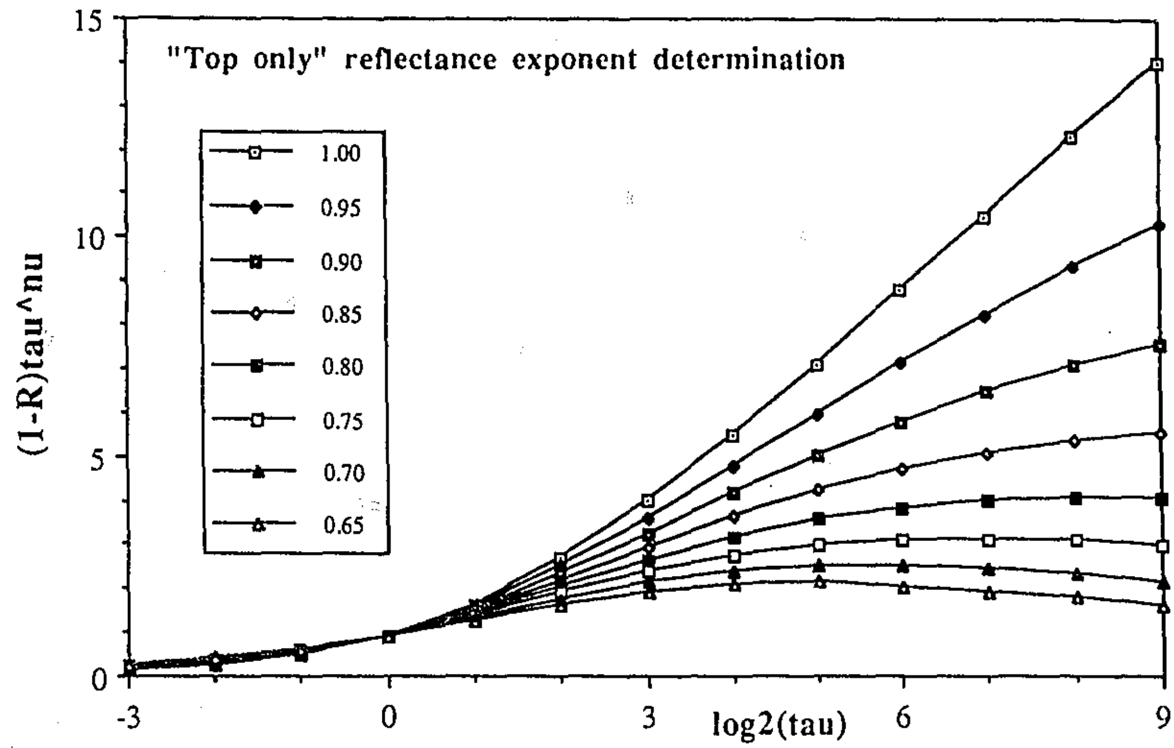

Figure 4.3: Determination of the albedo exponent for squares. The curves represent $(1\text{-}R)\tau^{\nu_R}$ for $\nu_R = 0.65(0.05)1.00$ as a function of $\log_2\tau = -3(1)9$, the optical size of the normally illuminated squares for isotropic DA(2,4) scattering. High-quality Monte Carlo data (with $N_{tot}=10^6$ histories) was used in this testing procedure. The statistical uncertanties are typically much smaller than the symbols as can be checked using

$$\Delta(1\text{-}R)\tau^{\nu_R} = \tau^{\nu_R}\Delta R \qquad \text{where} \qquad \Delta R^2 = R(1\text{-}R)/N_{tot} \qquad \text{from eq. (B.1b).}$$

The curve should become flat at the value of ν_R that we are seeking. Clearly, it cannot be less than 0.8 and, at any rate, there is no evidence that the asymptotic regime has ever been reached, even at $\tau = 512$. Note that Davis *et al.*'s [1989, 1990] claim that $\nu_R = 3/4$ is based on poorer data ($N_{tot}=10^5$) and a poorer plotting technique at least for the purposes of exponent estimation (cf. figs. 4.2a,b).

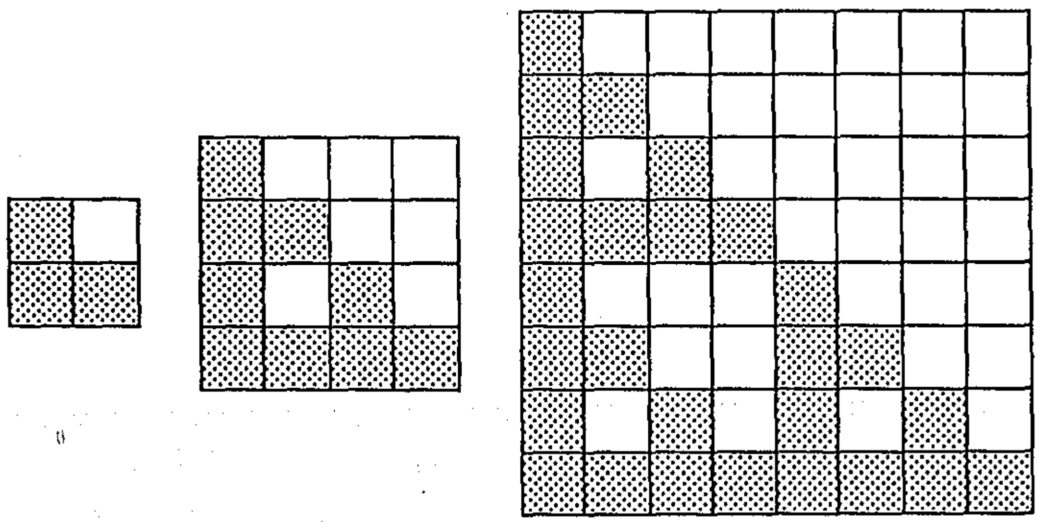

Figure 4.4a: Generation of a deterministic monofractal cloud model in d = 2 spatial dimensions (first three steps, at constant inner scale l_0) with $D = \log_2 3 = 1.585\cdots$.

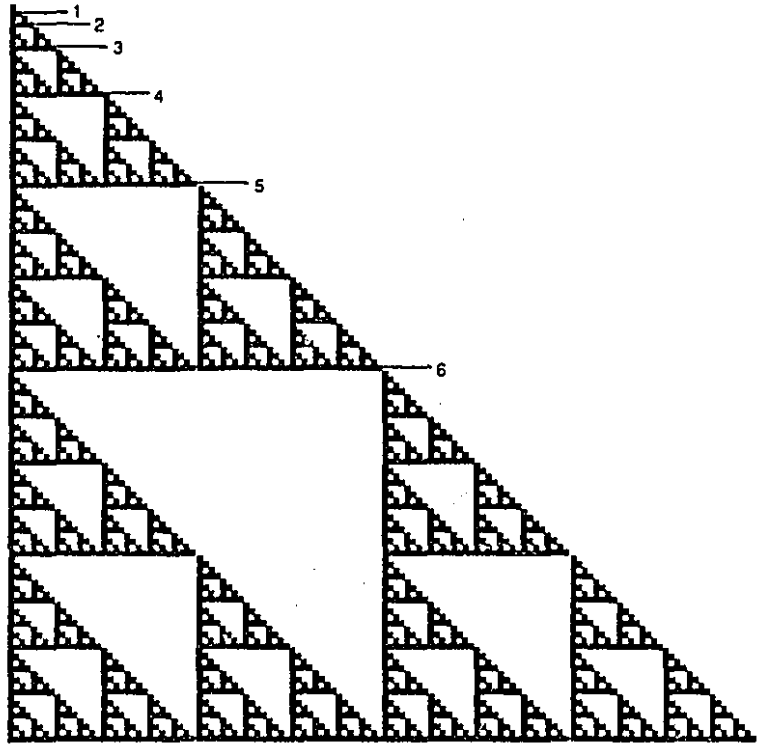

Figure 4.4b: Deterministic monofractal used as prototypical medium permeated by holes of all sizes. Illustrated are n $(0 \le n \le 7)$ successive steps into the construction procedure that can be visualized above the horizontal lines designated by n. For the purposes of all the radiative transfer calculations presented here, illumination is from the top.

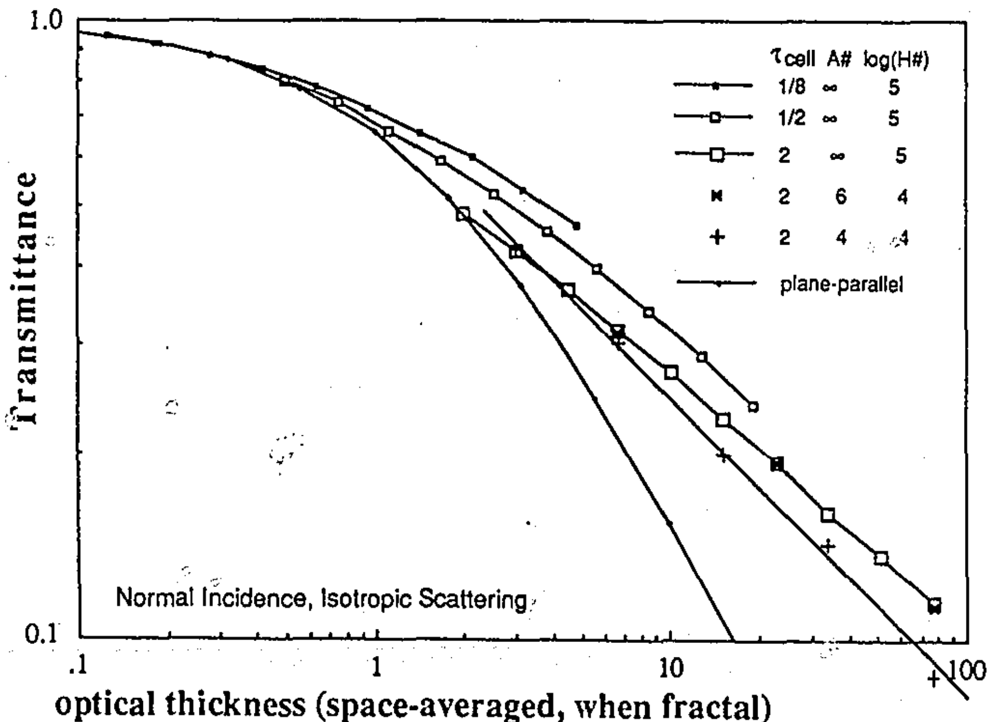

Figure 4.5: Transmittance versus spatially averaged optical thickness for the horizontally periodic cloud with a $D = \log_2 3 \approx 1.585$, $d = 2$ elementary cell. Isotropic CA, DA(2,4) and DA(2,6) Monte Carlo is used under normal illumination conditions. The data points correspond to 0 through 9 construction steps, respectively 1x1 to 512x512 grid points; three different cell optical thicknesses were used (1/8, 1/2, 2) and periodic horizontal BCs are assumed. The absolute slope for the most opaque cells is $\nu_T \approx 0.4$ for CA and DA(2,6), ≈ 0.5 for DA(2,4). The corresponding response for CA transfer through homogeneous plane-parallel media is also shown (which yields $\nu_T = 1$).

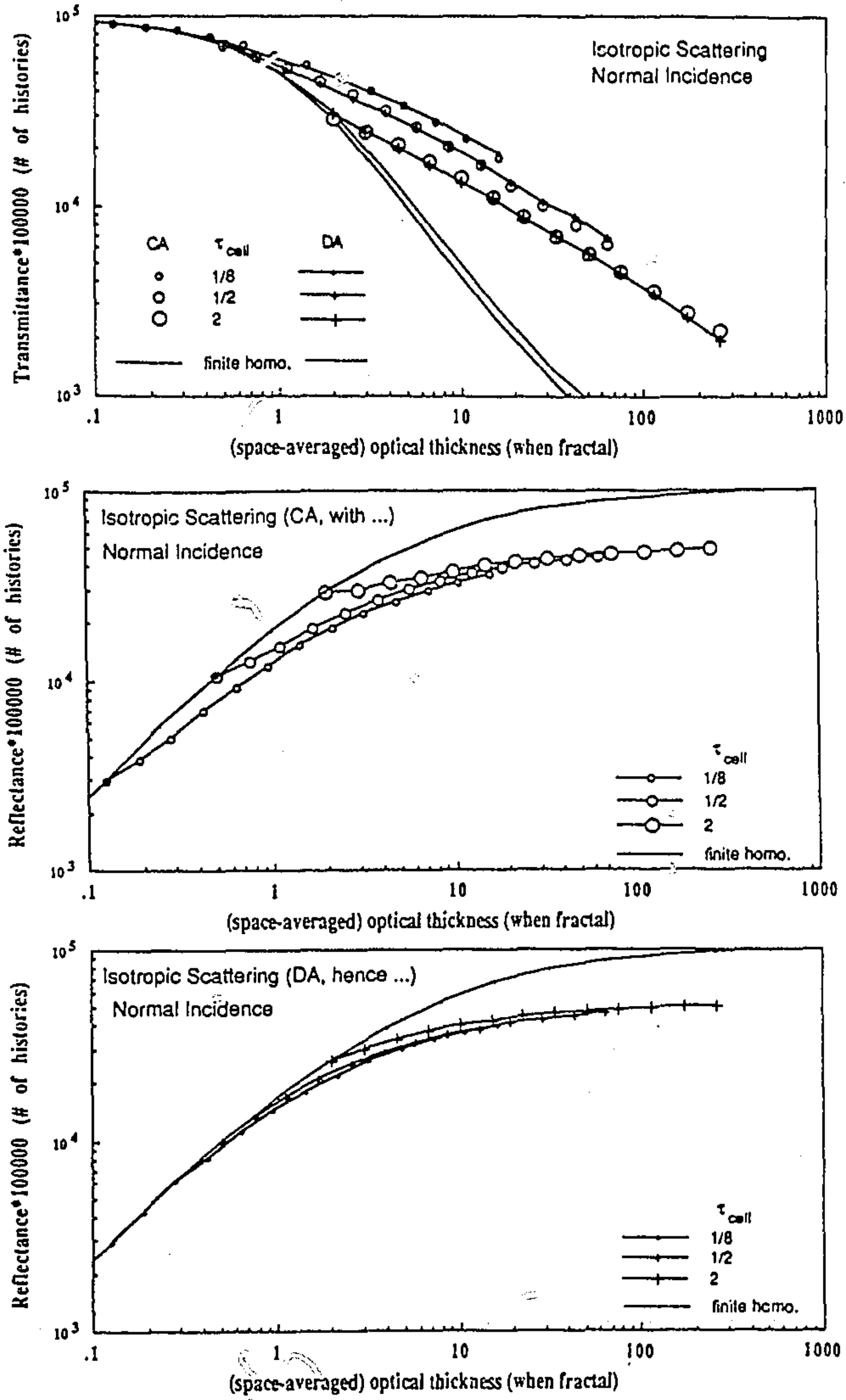

Figure 4.6: Responses for the isolated fractal cloud. (a) Same as Figure 4.5 but for CA and DA(2,4) Monte Carlo only and open horizontal BCs. The data points correspond to 0 through 12 construction steps (i.e., 1x1 to 4096x4096 grid points). The absolute slope for the most opaque cells is $\nu_T \approx 0.5$. The corresponding two transmittance curves are also shown for homogeneous squares (which both yield $\nu_T = 1$ but somewhat different prefactors for either phase function). (b) Same as Figure 4.6*a* but for reflectance (through the "top") in CA radiative transfer. Notice that $R_\infty = 1$ for the homogeneous squares and $R_\infty < 1$ for their inhomogeneous counterparts. (c) Same as Figure 4.6*b* but for DA(2,4) transfer.

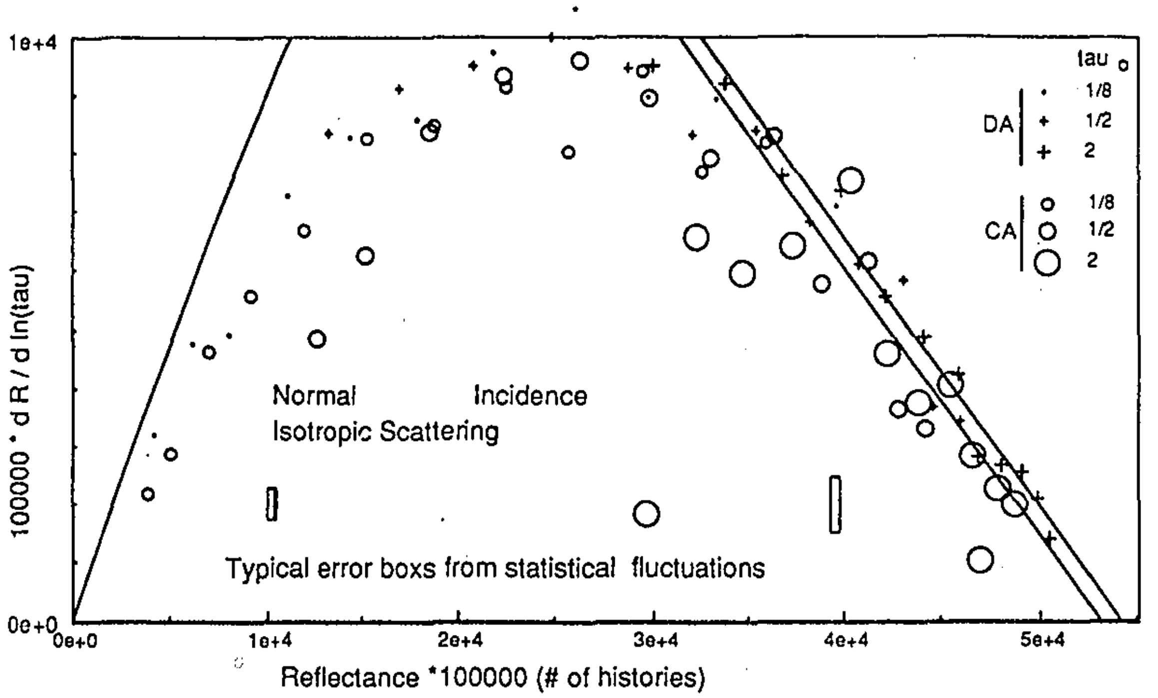

Figure 4.7: Plotting technique described in text for the objective determination of R_∞ and ν_R. Straight lines at right are linear regressions for CA and DA results, yielding $\nu_R \approx 0.46$ in both cases, whereas $R_\infty \approx 0.53$ for CAs and $R_\infty \approx 0.54$ for DA(2,4); due to the noise, the second digits cannot be considered sure in these parameters. The slightly curved line at left corresponds to plane-parallel media in the two-flux approximation or (equivalently) the DA(1,2) model.

Chapter Five†

RADIATIVE PROPERTIES OF MULTIFRACTALS, AN ASYMPTOTIC ANALYSIS

Preliminary Remarks and Overview: The atmosphere involves many nonlinearly coupled fields. If the corresponding dynamics are scale invariant over significant ranges in scale, then we generally expect that the appropriate way of relating the various fields is via their scale/resolution independent singularities and codimension functions (or, more fundamentally, the generators of the latter). For instance, let $\phi_\lambda=\lambda^{\gamma_\phi}$ denote some (conserved) cascade field quantity observed at some finite scale λ and scale invariantly characterized statistically by $c_\phi(\gamma_\phi)$ and $K_\phi(h)$, as explained in app. C. Then, say, optical thickness (or more simply, distance) τ_λ is likely to be related to ϕ_λ by

$$\tau_\lambda = \lambda^{\gamma} \approx \lambda^{a\gamma_\phi+b} \tag{5.0a}$$

hence for the orders of singularity:

$$\gamma = a\gamma_\phi+b \tag{5.0a'}$$

and for the dual scaling functions:

$$c(\gamma) = c_\phi(\gamma_\phi) = c_\phi\left(\frac{\gamma_\phi-b}{a}\right) \tag{5.0b}$$

$$K(h) = K_\phi(ah) + bh \tag{5.0c}$$

where the lack of subscript refers to the (non-conserved) quantity τ_λ. This provides a simple illustration of the types of relations we may expect.[1] In radiative transfer through multifractal clouds, we may expect relations between the orders of singularities of the cloud density and radiation fields to be statistical. However, in the cases of direct transmission and total transmission but for plane-parallel media, we have simple deterministic functional relations between the radiative response and optical thickness, and these will be exploited below to yield results analogous to (5.0a–c) above.

The formulae discussed here will be for bare cascades (a cascade constructed over only a finite range of scales λ) whereas τ is (by definition) a dressed quantity, cf. eq. (A.9) that involves an integral over a scale λ of a completed cascade. This fundamental distinction is briefly discussed in sect. C.4 [and at length in many references therein]. The $c(\gamma)$ function for the dressed quantities is the same as for the bare quantities except for the large values of γ

(where $c(\gamma)$ generally becomes linear). In the following, we ignore this complication except in the final section where it is exactly accounted for but in a rather artificial (but useful) way.

For the direct transmittance (sect. 5.1) and transmittance through (horizontally homogeneous) plane-parallel layers (sect. 5.2), the relations with τ_λ are $T_{d,\lambda}=\exp(-\tau_\lambda)$ and $T_{p,\lambda}=1/(1+r\tau_\lambda)$ respectively. In the latter (essentially 1-D) case, the parameter "r" can be used to represent either the DA phase function parameter[2] "q/2" that appears in the exact DA solution (3.22'), or the (boundary condition and phase function) related parameter "$1/2\chi$" that appears in the approximate (diffusion) CA result (D.31)—χ is the "extrapolation length" which is $\propto(1-g)$, see §D.4.2. In order to use these and obtain relations between the corresponding orders of singularity and codimensions, we introduce the following notation (dropping the λ subscript for simplicity):

$$\tau = e^{\zeta\gamma} \quad \text{where} \quad \zeta = \ln\lambda \tag{5.1}$$

We will be interested primarily in the small scale limit where $\lambda\rightarrow\infty$ (hence $\zeta\rightarrow\infty$). If this limit correspond to increasingly thick clouds, we find no longer exponential but algebraic average direct transmittance (implying much longer photon free paths) and non-trivially scaling average total "1-D" transmittance. If this limit means ever thinner clouds, the linear responses are naturally retrieved in both cases.

For convenience, all the definitions and analytical results are summarized in sect. 5.3 with the help of tables. In the same section, we also discuss some potential applications of our direct transmittance results to "mean field" approaches to radiative transport in multifractal media and, finally, we draw a parallel between the problem of total (1-D) transmittance and one of condensed matter physics. Finally, the ensemble-average results are adapted (in sect. 5.4) to a cascade model cunningly designed so that they can be interpreted as spatial averages, hence "independent pixel" (IP) estimates of the corresponding responses. Interestingly, our D=1.585··· deterministic fractal model studied in the previous chapter as well as Cahalan's [1989] random multifractal belong to this class; so new conclusions about these models can be drawn concerning, in particular, the radiative consequences of the high (and artificial) degree of anisotropy.

5.1. Simple Scaling Properties of Direct Transmittance

5.1.1. The Optically Thick Limit: Non-exponential Average Path Distributions

We will use the formula for transforming p.d.f.'s to obtain a relation between $c(\gamma)$ and $c_{Td}(\gamma_{Td})$, this will illustrate the general method employed below; namely

$$p_{Td}(\gamma_{Td}) = p(\gamma)\,\left|\frac{d\gamma}{d\gamma_{Td}}\right| \tag{5.2}$$

which, according to the definition (C.16), implies the following general relation between codimension functions:

$$c_{T_d}(\gamma_{T_d}) = c(\gamma) - \frac{\ln\left(\left|\frac{d\gamma}{d\gamma_{T_d}}\right|\right)}{\zeta} \tag{5.3}$$

Introducing

$$T_d = e^{-\tau} = e^{\zeta\gamma_{T_d}} \quad \text{with} \quad \gamma_{T_d} \le 0 \tag{5.4}$$

we obtain the following relation between the singularities in τ and T_d:

$$\gamma = \frac{\ln(-\zeta\gamma_{T_d})}{\zeta}$$

$$\gamma_{T_d} = -\frac{\exp(\zeta\gamma)}{\zeta} \qquad \gamma_{T_d} \le 0 \tag{5.5}$$

$$\left|\frac{d\gamma_{T_d}}{d\gamma}\right| = e^{-\zeta\gamma}$$

Hence in the limit as $\zeta \to \infty$, all the positive orders of singularities in τ ($\gamma>0$) are mapped onto (the infinitely) strong regularity (negative singularity) in T_d ($\gamma_{T_d} \to -\infty$). Conversely, all the regularities in τ ($\gamma<0$) are mapped onto the (single) neutral singularity in T_d ($\gamma_{T_d} = 0$). We may now use eq. (5.3) to obtain the following relation between codimension functions:

$$c_{T_d}(\gamma_{T_d}) = c(\gamma) + \gamma \tag{5.6}$$

Substituting γ_{T_d} in terms of γ in the above, and expanding $c(\gamma)$ in a Taylor series about the origin, we obtain

$$c_{T_d}(\gamma_{T_d}) = c(0) + \frac{\ln(-\zeta\gamma_{T_d})}{\zeta}\,[1+c'(0)] + \cdots \tag{5.7}$$

The first term on the r.h.s. indicates that a single codimension $c(0)$ dominates the behaviour of T_d. The second term on the r.h.s. corresponds to two prefactors in the probability density for γ_{T_d}. The first is $(-\gamma_{T_d})^{-(1+c'(0))}$, i.e., a singularity at the origin of the density of γ_{T_d} of order $(1+c'(0))$; in the probability distribution of γ_{T_d} this is of order $c'(0)$, which is regular as long as $c'(0)<0$. Conversely, when $c'(0)>0$, the probability of γ_{T_d} will be singular at the origin. The second term yields a (sub-exponential) factor $(\ln\lambda)^{-(1+c'(0))}$ in the probability distribution of γ_{T_d}; the exponent $-[1+c'(0)]$ is called a "sub-codimension." Of all the cases we discuss below, the direct transmittance problem is the only one where the detailed consideration of these higher order terms is necessary.

We may now use the Legendre transform (C.24a) to calculate $K_{T_d}(h)$ from $c_{T_d}(\gamma_{T_d})$, and hence to obtain the multiple scaling characteristics of T_d. However, relation (C.24a) is true only when exponential factors are dominant, i.e., for $c'(0)<0$ (which corresponds to $<T_d^h>\rightarrow 0$ as $\zeta\rightarrow\infty$, clouds become opaque). For $c'(0)>0$, we must consider the quantity $1-T_d$ (see next sub-section); we will find that $<T_d^h>\rightarrow 1$ (the clouds become transparent in the limit). Restricting our attention to the case $c'(0)<0$, we therefore[3] obtain:

$$K_{Td}(h) = -c(0) \quad \text{when} \quad c'(0) < 0 \tag{5.8a}$$

Eq. (5.8a) shows that the direct transmittance decreases algebraically as the cloud increases in thickness.

Following our discussion in chap. 0–1, it is often convenient to introduce another exponent which is essentially a "mean field" exponent relating $<\tau>$ to $<T_d>$, in analogy with eqs. (1.2–3), we obtain

$$<T_d> \sim <\tau>^{-v_{Td}} \tag{5.8b}$$

where

$$v_{Td} = -\frac{K_{Td}(1)}{K(1)} \tag{5.8c}$$

The above result shows that the effect of the multifractal optical density field has been to greatly enhance the mean direct transmittance which is now algebraic, not exponential. The photon free path distribution will therefore have a much longer tail. In general, from the Legendre relation, we find $-c(0) = \min[K(h)]$, hence

$$v_{Td} = -\frac{\min[K(h)]}{K(1)} \quad \text{when} \quad c'(0) < 0 \tag{5.8d}$$

This exponent is always positive since $\min[K(h)]$ is necessarily negative due to its convexity and that $K(0) = 0$. The homogeneous case ($K(h) = 0$) is indeterminate but returning to the adopted definition of $c(\gamma)$ in (C.16), we see that $c(0) = \infty$ in eq. (5.8a) for a degenerate (δ-function) p.d.f. and the exponential distribution is therefore (formally) retrieved, i.e., $v_{Td} = \infty$.

5.1.2. The Optically Thin Limit: Linear Response, Rediscovered

We saw that the exponential relation between τ and T_d mapped the continuous distribution of singularities in τ onto the two values $\gamma_{Td} = -\infty$ and 0 for $\gamma>0$, $\gamma<0$ respectively. More interesting relations (useful below) may be obtained by considering the quantity $R_d = 1-T_d$, where R_d is simply the "diffuse" radiation, i.e., the radiation that has been scattered at least once and that will end up as either transmission or reflection in the case of conservative scattering. Introducing the corresponding orders of singularity γ_{Rd}, we obtain:

$$R_d = e^{\zeta\gamma_{Rd}} = 1 - \exp(-e^{\zeta\gamma}) \quad \text{with} \quad \gamma_{Rd} \leq 0 \tag{5.9}$$

This yields

$$\gamma = \frac{\ln[\,-\ln(1-e^{\zeta\gamma_{Rd}})\,]}{\zeta}$$

$$\gamma_{R_d} = \frac{\ln[\,1-\exp(-e^{\zeta\gamma})\,]}{\zeta} \qquad \gamma_{R_d} \leq 0 \qquad (5.10)$$

$$\left|\frac{d\gamma_{Rd}}{d\gamma}\right| = \frac{e^{\zeta\gamma_{Rd}}}{(1-e^{\zeta\gamma_{Rd}})\ln[1-e^{\zeta\gamma_{Rd}}]}$$

Or, approximately,

$$\gamma_{R_d} \approx \gamma - \frac{e^{\zeta\gamma}}{2\zeta} \quad \gamma < 0; \qquad \gamma_{R_d} \approx -\frac{\exp(-e^{\zeta\gamma})}{\zeta} \quad \gamma > 0$$

$$\gamma \approx \gamma_{R_d} - \frac{e^{\zeta\gamma_{Rd}}}{2\zeta} \quad \gamma_{R_d} < 0; \qquad \gamma \approx \frac{\ln[\,-\ln(-\gamma_{Rd})\,]}{\zeta} \quad \gamma_{R_d} \approx 0 \qquad (5.11)$$

$$\left|\frac{d\gamma_{Rd}}{d\gamma}\right| \approx 1 - \frac{e^{\zeta\gamma_{Rd}}}{2} \quad \gamma_{R_d} < 0; \qquad \left|\frac{d\gamma_{Rd}}{d\gamma}\right| \approx \zeta\gamma_{Rd}\ln(-\gamma_{Rd}) \quad \gamma_{R_d} \approx 0$$

hence, as $\zeta \to \infty$, singularities in τ are mapped onto the neutral singularity in R_d, and regularities in τ are mapped onto regularities of the same order in R_d. Using these relations between γ, γ_{R_d}, and eq. (5.3), we obtain the following relation between codimension functions (valid only for $\gamma_{R_d}<0$ and ζ large enough, i.e., this formula will give information only on the regularities in τ):

$$c_{Rd}(\gamma_{Rd}) \approx c(\gamma_{Rd}) \quad \text{with} \quad \gamma_{R_d} < 0 \qquad (5.12)$$

where we have dropped the $1/\zeta$ corrections. We can now use eqs. (C.24a, 5.12) to calculate the scaling exponents of $\langle R_d^h \rangle$:

$$K_{Rd}(h) = \max_{\gamma_{Rd}<0}\,[h\gamma_{R_d} - c(\gamma_{R_d})] = K(h) > -c(0) \quad \text{with} \quad h < c'(0) \qquad (5.13a)$$

The condition $h<c'(0)$ immediately follows from the relation $h=c'(\gamma_{R_d})$, the convexity of $c(\gamma)$ hence monotonicity of $c'(\gamma)$, and the restriction $\gamma_{R_d}<0$. Furthermore, the convexity and positivity requirements on $c(\gamma_{R_d})$ ensures that $K(h)>-c(0)$, and implies that for $c'(0)>h>0$, $K(h)<0$. If $h\geq c'(0)$, the maximum in the above will depend on the limit $\gamma_{Rd}\to 0$ (i.e., the singularities in τ will dominate), and the above formula breaks down. To understand what happens, consider the two cases $c'(0)>0$, $c'(0)<0$. In the former case, for some small positive h, the above formula will hold, and $\langle R_d^h \rangle \to 0$ as $\zeta\to\infty$. This is sufficient to imply $\langle T_d^h \rangle \to 1$ for all $h>0$, in conformity with the results of §5.1.1. Conversely, when $c'(0)<0$, we expect $\langle T_d^h \rangle \to 0$, and hence $\langle R_d^h \rangle \to 1$.

Assuming that $c'(0) > 1$, we obtain $K_{Rd}(1) = K(1)$ hence

$$v_{Rd} = -\frac{K_{Rd}(1)}{K(1)} = -1 \qquad (5.13b)$$

i.e., <R_d> is a linear function of <τ>, as expected on general grounds in the case of optically thin media.

5.2. Multiple Scaling Properties of Total 1-D Transmittance

5.2.1. The Optically Thick Limit: Non-trivial Scaling by "Mixing" Trivial Responses

The plane-parallel formula (3.29) leads to particularly simple mappings between singularities, codimensions and multiple scaling exponents. To avoid ambiguity with a parameter in eqs. (5.0a–c) above, the phase function (and/or boundary condition) parameter "b" in (3.29) is replaced here by "r." Following the procedure discussed above, we obtain:

$$T_p = e^{\zeta\gamma_{T_p}} = (1 + re^{\zeta\gamma})^{-1} \qquad \text{where} \qquad \gamma_{T_p} < 0 \tag{5.14}$$

hence

$$\gamma_{T_p} = -\frac{\ln(1+re^{\zeta\gamma})}{\zeta}$$

$$\gamma = \frac{\ln(r^{-1}e^{-\zeta\gamma_{T_p}} - 1)}{\zeta} \qquad\qquad \gamma_{T_p} < 0 \tag{5.15}$$

$$\left|\frac{d\gamma_{T_p}}{d\gamma}\right| = 1 - e^{\zeta\gamma_{T_p}}$$

In the limit $\zeta \to \infty$, we obtain the following approximate formulae:

$$\gamma_{T_p} \approx -\gamma \qquad\qquad \gamma > 0 \tag{5.16}$$

$$\gamma_{T_p} \approx \frac{re^{\zeta\gamma}}{\zeta} \qquad\qquad \gamma < 0$$

The singularities in τ are thus mapped onto the corresponding regularities in T_p, and the regularities in τ are mapped onto the neutral singularity $\gamma_{T_p} = 0$. Considering only the case $\gamma_{T_p} < 0$, we therefore obtain the following relation between codimension functions:

$$c_{T_p}(\gamma_{T_p}) = c(-\gamma_{T_p}) \qquad \text{with} \qquad \gamma_{T_p} < 0 \tag{5.17}$$

Finally, using the Legendre transformation, we find the following relation between multiple scaling exponents:

$$K_{T_p}(h) = \max_{\gamma_{T_p}<0} [h\gamma_{T_p} - c(-\gamma_{T_p})] = K(-h) > -c(0) \qquad \text{with} \qquad h < -c'(0) \tag{5.18a}$$

In particular, we see that, as long as $c'(0)<0$, then the above is true for some positive h and the corresponding moments will tend to 0 as $\zeta \to \infty$. As in the above, if $h>-c'(0)$, then it is the regularities in τ that dominate ($\gamma_{T_p}=0$), and the above formula breaks down. Again, rather than attempt a complicated analysis of this case, it is much simpler to analyze $R_p=1-T_p$; i.e., the plane-parallel reflectance (see below).

It is worth mentioning that, by comparing eqs. (5.8a) and (5.18a), we have $K_{Tp}(h) \geq K_{Td}(h)$ for all h>0. This very simply follows from the fact that T_p takes into account multiple scattering, and hence $T_p \geq T_d$. We also note that the relations are all phase function (r) independent; the latter only affect the prefactors but not the exponents. If we now use eq. (5.18a) to determine

$$\nu_{Tp} = -\frac{K(-1)}{K(1)} \leq 1 \tag{5.18b}$$

where the inequality is a direct consequence of the convexity property of K(h): $K(-1)+K(1)\geq 2K(0)=0$. This is basically Jensen's inequality (3.31) for the convex function $T_p \sim \tau^{-1}$, but rephrased in scaling language. In essence, we have been "mixing" trivial (i.e., plane-parallel) responses and obtained a non-trivial average response; the term "mixing" is used here in the sense of Feller [1971], see discussions in sect. 3.4 and A.2.

5.2.2. The Optically Thin Limit: Linear Response, Again

As remarked above, we only need to consider $R_p=1-T_p$ in this case which is very easy to deal with since

$$R_p = e^{\zeta\gamma_{Rp}} = (1+r^{-1}e^{-\zeta\gamma})^{-1} \tag{5.19}$$

This is identical to eq. (5.14) for T_p except that r is replaced by r^{-1}, and γ by $-\gamma$. We therefore immediately obtain

$$\gamma_{Rp} \approx \gamma \qquad \gamma < 0 \tag{5.20}$$

$$\gamma_{Rp} \approx \frac{r^{-1}e^{-\zeta\gamma}}{\zeta} \qquad \gamma > 0$$

The regularities of τ are mapped onto the corresponding regularities of R_p, and the singularities of τ onto the neutral singularity of R_p ($\gamma_{Rp}=0$) as in the case for R_d, with comments analogous to those at the end of §5.1.2. The fact that the results for R_d and R_p are the same follows directly from the fact that both are linear functions of τ for $\tau \ll 1$.

5.3. Summary and Discussion of Multifractal Radiative Scaling Properties

Definitions
$\tau = \phi^a\lambda^b$
$T_d = e^{-\tau}$
$T_p = (1 + r\tau)^{-1}$
$R_d = 1 - T_d = 1 - e^{-\tau}$
$R_p = 1 - T_p = (1 + r^{-1}\tau^{-1})^{-1}$

Table 5.1: Summary of the definitions discussed in the text.

Regularities ($\gamma<0$)	
γ_o:	$(\gamma-b)/a$
γ_{Td}:	0
γ_{Tp}:	0
γ_{Rd}, γ_{Rp}:	γ

Singularities ($\gamma>0$)
$(\gamma-b)/a$
$-\infty$
$-\gamma$
0

Table 5.2: The mapping of singularities in τ onto the various singularities discussed in the text.

Codimension formulae
$c_o(\gamma_o) = c(a\gamma_o+b)$
$c_{Td}(\gamma_{Td}) = c(0)$
$c_{Tp}(\gamma_{Tp}) = c(-\gamma_{Tp})$
$c_{Rd}(\gamma_{Rd}) = c(\gamma_{Rd}), c_{Rp}(\gamma_{Rp}) = c(\gamma_{Rd})$

Range of validity
$-\infty \leq \gamma \leq \infty$
$\gamma_{Td} < 0$
$\gamma_{Tp} < 0$
$\gamma_{Rd} < 0, \gamma_{Rp} < 0$

Table 5.3: The codimension formulae discussed in the text.

Multiple scaling exponents
$K_o(h) = K(h/a)-bh/a$
$K_{Td}(h) = -c(0)$
$K_{Tp}(h) = K(-h)$
$K_{Rd}(h) = K_{Rp}(h) = K(h)$

Conditions of validity
$-\infty \leq h \leq \infty$
$c'(0) < 0$
$h < -c'(0)$
$h < c'(0)$

Table 5.4: The multiple scaling formulae discussed in the text.

Analogies in Condensed Matter Physics, and the Role of Algebraic Path Distributions in Radiation "Channeling"

Closely related to the algebraic (average) distributions for the photon free paths that we found in the above are the symmetric Lévy-stable distributions; these are defined by their c.g.f. (cf. sect. A.2) which is proportional to q^α ($0<\alpha<2$), hence moments of order $\geq\alpha$ diverge. Along with their Gaussian ($\alpha=2$) counterparts, symmetric Lévy deviates have the fundamental property of being invariant w.r.t. addition,[4] apart from a simple rescaling (no recentering is necessary due to the symmetry), hence self-similarity of the additive random processes based on them. Klafter *et al.* [1987] use such processes to generically obtain the "anomalous" diffusion regimes (i.e., $E(r^2|t) \sim t^k$ with $k\neq1$) observed in so many phenomena; for instance, Shlesinger *et al.* [1986] apply Lévy-flight theory to turbulent diffusion and "chaos" in Josephson junctions.

Remaining in the domain of condensed matter physics, Siebesma [1989] investigates extensively the multifractal structure of one-dimensional localized electronic wave functions in strongly disordered materials. We notice that the corresponding (quantum mechanical, not radiative) "transmission coefficient" T and conductance G in Landauer's formula $G=(2e^2/h)|T|^2/(1-|T|^2)$ are respectively equivalent to our $\sqrt{T_p}$ and $1/\tau$ in our plane-parallel result (3.29) with $b=2e^2/h$. Siebesma goes on to remark that T (hence G) will be multifractal (in the case of interest, log-normally). Consequently, the most probable value of G (viz. $e^{<\ln G>}$) is far more "typical" of the ensemble-average behavior than the average value $<G>$ itself—this kind of reasoning is akin to our use of the Legendre transform. She also points out that extreme sample dependent fluctuations are to be expected (and they are apparently observed). These ideas are made far more precise by our results from sect. 5.2.

Along the same lines but going from diffusion- to kinetic-type transport, we strongly suspect that replacing symbolically[5] $e^{-<\tau>}$ by $<e^{-\tau}>$ would lead to a far better "mean field" theory than simply replacing $\rho(x)$ everywhere by $<\rho>$. But we should not be too optimistic because we are only looking at one aspect of the transfer process (propagation) and seeing that it is seriously perturbed by inhomogeneity which allows much longer geometrical photon free paths. Just how these individual photon paths combine to form net radiative fluxes that systematically "channel" the radiation into the more tenuous regions involves the scattering (angular) part of the transfer process.[6] We examined in detail the subtle interplay of these two aspects of radiation transport within the framework of diffusion theory for arbitrary but weak variability in sect. 2.3 above, using analytical perturbation techniques; and we will return to them again but within the context of DA transfer in strong (multifractal) but particular (one single realization) variability in chap. 6 below, using purely numerical techniques. We will come to see this[7] "channeling" of the photon flow in the variable density field as the basic mechanism of inhomogeneous radiative transport in higher dimensions (i.e., modelled by transfer or diffusion, not IPs). It is largely responsible, in particular, for the systematically higher bulk transmittancies (hence exponents) observed in chap. 4.

5.4. Multifractal Independent Pixels, A Case Study

5.4.1. A Special Microcanonical α-Model for Column-wise Dressed Quantities

We are now in a position to exploit the above results to obtain the direct transmission through a simple class of "α-model" discrete microcanonical[8] cascades for the optical density. In this model, the introduction of the microcanonical constraint is really an artifice designed to avoid the problem of bare/dressed properties by ensuring that the spatial averages of τ are equal to the ensemble-averages.

We discuss only the simplest case in two dimensions (see fig. 5.1), in which each eddy is broken up into four sub-eddies, each with one half the size of the parent eddy ($\lambda_0=2$ per step). For the moment, we consider the general (non-conserved) case in which the sum of the two multiplicative factors on either side are fixed, $\lambda_0^{\gamma_1}$ and $\lambda_0^{\gamma_2}$ respectively, but do not necessarily add up to one. The factors which share a column can be randomly chosen as long as they respect this constraint; furthermore, these two factors can be distributed either left-right or right-left. This constraint is such that, as the cascade proceeds, if we are only interested in the integral of the optical density (τ) over columns, then the latter is modulated by one of the above factors at each step.

Calculating the multiple scaling for the optical thickness as for the usual α-model (C.30) with $C_\pm = 1$ (since the probabilities are both $1/2 = \lambda_0^{-1}$), we obtain[9]

$$K(h) = \frac{\log \langle\tau^h\rangle}{\log \lambda} = \log_{\lambda_0}(\lambda_0^{h\gamma_1-1} + \lambda_0^{h\gamma_2-1}) \tag{5.20}$$

hence, for a cascade that conserves τ (i.e., $K(1)=0$ so that $\langle\tau\rangle$ is independent of λ), we require that γ_1, γ_2 be constrained such that $\lambda_0^{\gamma_1}+\lambda_0^{\gamma_2}=\lambda_0$. It is straightforward to calculate the corresponding multiple scaling function for $\kappa\rho$, but to do this we must introduce the (joint) probabilities for the a,b,c,d factors.

According to our previous analysis, the two fundamental cases of interest are $c'(0)<0$, $c'(0)>0$, and we will also be interested in the value of $c(0)$. We must therefore obtain the Legendre transform of eq. (5.21) but for $\gamma=0$ only, i.e., we do not need to use the general result (C.31c). Expressions for $c(0)$, $c'(0)$ are obtained using the fact that $c(0)=K(h_0)$ where $h_0=c'(0)$ is the value that yields the minimum $K(h)$. We therefore have

$$c'(0) = h_0 = -\frac{\log_{\lambda_0}(-\gamma_1) - \log_{\lambda_0}(\gamma_2)}{\gamma_2 - \gamma_1} \tag{5.22}$$

where we have assumed $\gamma_1<0$ and $\gamma_2>0$; otherwise (0 is not in the singularity spectrum of the model), we have $c(0)=\infty$. From (5.22), it can be seen that the sign of $c'(0)$ is opposite to that of $\gamma_1+\gamma_2$. In particular, whenever $\gamma_1+\gamma_2 = 0$, we have simultaneously $c'(0)=h_0=c(0)=0$; the various cases are shown in fig. 5.2. Using the results summarized in table 5.4, we have

<u>$c'(0) > 0$, $\gamma_1+\gamma_2 < 0$:</u> This case[10] yields

$$K_{R_d}(h) = K_{R_p}(h) = K(h) \quad \text{when} \quad h < c'(0) \tag{5.23}$$

<u>$c'(0) < 0$, $\gamma_1+\gamma_2 > 0$:</u> This case yields

$$K_{T_p}(h) = K(-h) \quad \text{when} \quad h<-c'(0) \tag{5.24a}$$

$$K_{T_d}(h) = -c(0) = \min[K(h)] \tag{5.24b}$$

Here, T_p is obviously not a plane-parallel transmittance, but total transmittance in the IP approximation discussed (under various guises) in the the last three chapters. In particular, it appears as the exact solution for DA phase functions with no side scattering, only forward and backward.

We can now conveniently display the combined results for K_{T_d} and K (fig. 5.2), where we see that there are three regions corresponding to

$\langle\tau\rangle\to 0$, $\langle T_d\rangle\to 1$ (thin transparent clouds)

$\langle\tau\rangle\to\infty$, $\langle T_d\rangle\to 1$ (thick but transparent clouds)

$<\tau>\to\infty$, $<T_d>\to 0$ (thick opaque clouds)

The intersection of the curves $K_{T_d}(1)=0$ and $K(1)=0$ occurs at $\gamma_1=\gamma_2=0$ and corresponds to multiplicative factors of 1 in each column, i.e., this is the (only) non-fractal case (however $\gamma_1=\gamma_2\neq 0$ yields a non-fractal τ, whatever the make-up of a,b,c,d is).

5.4.2. Two Special Cases of Interest

As an example of the above,[11] we may consider the deterministic $D=\log_2 3\approx 1.585$ monofractal cloud in d=2 discussed in sect. 4.2 and illustrated in figs. 4.4a,b; notice that $K(1) = 1\text{-}C \approx 0.585$ since C=d-D. Within the above class of models, it corresponds to a=c=d=1, b=0 hence to $\gamma_2=1$, $\gamma_1=0$. It is interesting to see how the simple operation of column integration (which is basically a highly anisotropic form of "dressing" a cascade, using an averaging set of vertical extent L, horizontal extent l_0) can map a β-model onto an α-model, at least in this microcanonical case. Returning to our radiative preoccupations, eq. (5.22) yields $c'(0)=-\infty$ and we find $K_{T_d}(1) = -c(0) = K(-\infty) = -1$, from (5.24b), hence $\nu_{T_d} = 1/K(1) = 1/1\text{-}C \approx 1.71$. We therefore have $<T_d>\to 0$ and $<\tau>\to\infty$, i.e., the cloud is thick and opaque. For comparison, we recall that numerical multiple scattering results on this cloud are $\nu_T = 0.4$–0.5 for the case with cyclic horizontal BCs, and 0.5 for open sides. Both exponents are smaller than 1.71 as required since the direct transmittance is a lower bound on the total transmittance. We also find $K_{T_p}(1) = \log_2 3\text{-}2$, hence $\nu_{T_p} = C\nu_{T_d} \approx 0.71$ which is not only <1, it also provides an improved lower bound on ν_T. This is excatly what we expect, given the position of the IP approximation in the one parameter (p) family of transport theories going from IPs (p=0) to diffusion ($p=\infty$), via DA transfer (finite p). In order to make the model transparent in the limit, we must divide τ by at least a factor $\sqrt{2}$ (i.e., we decrease γ_1 and γ_2 by 1/2), yielding $K_{T_d}(1)=0$, and $K(1)=\log_2(3/2\sqrt{2})\approx 0.08$ which implies that τ still increases without bound.

As another example of the above model, we examine the direct transmittance properties of Cahalan's [1989] random but microcanonically conserved α-model. His model is one-dimensional, the optical density is assumed constant in vertical columns, i.e., he implicitly takes a=c, b=d. He performed extensive Monte Carlo simulations in the case where a=c=1.3 or 0.7 (with 50-50 chances), and conversely for b=d; this yields $\gamma_2=\log_2 1.3\approx 0.379$, $\gamma_1=\log_2 0.7\approx -0.575$ which, by definition, is on the curve K(1)=0 in fig. 5.2. With these parameters, we find $c'(0)\approx 0.497$, $c(0)\approx 0.017$, hence we can use formula (5.3) which will be valid for moments of R_d, R_p for h up to 0.497. We see that for the case of vertically incident radiation considered here, we expect $<T>\to 1$ as $<\tau>\to\infty$, i.e., for "overhead" illumination his cloud is transparent in the limit $\lambda\to\infty$. However, Cahalan examined the case of incidence at 60°, and obtained an increase of $<T>$ with λ, but apparently tending towards a finite (non-zero) value. This result is not too surprising since, in the limit $\lambda \to \infty$, slant incident rays will traverse an infinite number of columns before piercing the cloud base, whereas their vertically incident counterparts examined here stay in the same column. As $\lambda \to \infty$ most columns become very thin while rare, sparsely distributed columns get thicker to compensate, hence the result $\langle T \rangle \to 1$ for vertical incidence but another result for non-vertical incidence (where the "sampling" by even a single ray is infinitely more generous). This artificial dependence on angle of incidence should disappear if vertically varying $\kappa\rho$ fields—such as the slightly more general model used here—were employed.

5.4.3. Anisotropies in Cloud Models, Transport Models and Illumination Conditions

It is noteworthy that the two above models constitute a fair fraction of the strongly intermittent cloud models studied radiatively in the literature to date.[12] Both are problematic because of their high degrees of structural anisotropy that, interestingly, come from entirely different constraints imposed on them for entirely different reasons. The 1.585-D monofractal is made deterministic for simplicity, a logical step to make before adding a stochastic ingredient and, in the previous chapter, we have tried to extract as much information as possible from its simulated radiative properties. As a learning tool, its only problem is a (relatively minor) violation of the universality of the scaling exponent w.r.t. phase functions and this is (probably) due to the striking deterministic anisotropy of the model's geometry that somehow interferes with the anisotropy corresponding to the cyclical (horizontal) BCs and asymmetric illumination conditions (in the vertical); not to mention the anisotropy created by privileged (DA) propagation directions. Cahalan's model is designed to emulate the structure of marine stratocumulus as determined from one-dimensional observations, mainly power spectra of integrated LWC (which is $\propto\tau$). In absence of information on vertical structure, it is naturally neglected while the availability of Landsat (mid-morning) imagery (of territory off the Californian coast) justifies the choice of $\approx 60°$ inclination of the Sun in his simulations.

In the immediate future, we must be aware of the artificial anisotropies that we are prone to introduce into our models for many different (and perfectly good) reasons. For instance, in chap. 6 we use (for simplicity) a discrete cascade process to generate the multifractal density field of interest and that is enough to explain most of the fine (grid-like) structure found in the radiation fields. In the near future, the continuous cascade processes of Schertzer and Lovejoy [1987], which address the "grid" problem of their discrete counterparts head-on, will clearly play an important role; especially when combined with Schertzer and Lovejoy's [1985, 1987] Generalized Scale Invariance (GSI) formalism for incorporating the rotational symmetry-breaking effects of stratification, horizontal texture, etc.

†This chapter is largely based on Davis *et al.* [1991a] of which a preliminary version appeared as Lovejoy *et al.* [1990]. A.D. originated the idea of looking at the spatial statistics of direct transmittance (T_d) for the D=1.585··· deterministic monofractal cloud model (investigated at length in chap. 4), as well as looking at ensemble-averages of direct- and 1-D total transmittances (T_p) in general; he also established the connection between this deterministic "β" model in d=2 for $\kappa\rho(x,y)$ and the special microcanonical "α" model for $\tau(y)$. S.L and D.S. generalized the approach and, using multifractal formalism, obtained the exponents for the transmittancies form those of an arbitrary multifractal distribution in optical thickness. A.D. is generally responsible for the "independent pixel" applications, including to Cahalan's [1989] model; he also found the analogy of average T_p with conductance through disordered materials and insisted on the interpretation of average T_d in terms of enhanced photon (geometrical) free paths.

1 A related example is the relation between various radar rain singularities discussed in Lovejoy and Schertzer [1990].

2 Notice that, in d=1, we have $q/2 = (1-t+r)/2 = r$ in the relevant (conservative) case where $t+r = 1$.

3 Although when it holds, eq. (5.8a) doesn't involve h, there is an h dependence that enters via the correction term discussed above. This correction is estimated in Lovejoy *et al.* [1990].

4 Schertzer and Lovejoy [1987] use this property, but for negative "extremal" Lévy variables (on $\Re^-$), to define universal classes of multifractals that we briefly discussed in sect. C.5.

5 In practice, we mean replacing the exponential distribution by its (algebraic) average counterpart. For instance, extensive 1-D numerical simulations of the albedo problem using symmetric Lévy laws (with "index" $\alpha \in]0,2[$) were performed. They yield total (multiply scattered) transmittance in $L^{-\alpha/2}$, rather that the usual L^{-1}, which is retrieved of course in the Gaussian (finite variance) case at $\alpha=2$. In other words, we can generically reproduce the "anomalous" ($v<1$) transmittance laws that we expect and obtain for multiplicatively scaling (intermittent) fractal or multifractal media. See Barker [1992] for a semi-empirical application of this kind of kinetical "mean field" approach to radiation transport.

6 Putting these two aspects of transfer together, we have propagation (through inhomogeneous macroscopic density fields) subordinated to scattering (by microscopic inhomogeneities in the refractive index).

7 It is recalled that the originator of this expression is Cannon [1970] who used it when describing his numerical results on spectral line transfer in deterministic model media, varying in both vertical and horizontal directions.

8 Recall that in microcanonical cascades, there is strict conservation at each step, i.e., in fig. 5.1, a+b+c+d = constant. In canonical cascades we have the weaker restriction <a+b+c+d> = constant. Actually, the model described here is more strongly microcanonical than is usual since each column at each step is microcanonical, i.e., $a+c=W_1$ and $b+d=W_2$ where W_1 and W_2 are constants.

As noted in Schertzer and Lovejoy [1987], discrete cascades are outside the scope of the universality classes (sect. 3.5) which are obtained for continuous cascades.

9 Lovejoy *et al.* [1990] uses a quadratic approximation to (5.1) and this gives results corresponding to those below but only within this approximation.

10 In Lovejoy *et al.* [1990] a formula for $\langle T_d^h \rangle$ only valid for $c_0 = -\gamma_s/4$ was used to obtain $K_{Rd}(1)$. The latter formula is erroneous since here this special condition is not satisfied: eq. (5.3) is correct.

11 Many (but not all) random microcanonical β-models are special cases of the above: the total number of alive eddies per column must be fixed.

12 To the best of our knowledge, one can only add to the list the numerical studies of random β-models by Gabriel *et al.* [1986] and those of a single multifractal with Gaussian generators by Davis *et al.* [1991b], also chap. 6. Cahalan and Snider [1990] discuss a (smoother) variation on the α-model described here but its radiative- and even intermittancy properties remain largely unexplored. The cloud field models of Barker and Davies [1992] are additive, not multiplicative, hence not strongly intermittent in the sense we use here (furthermore, the individual cloudy "cells" are homogeneous in the vertical).

Bibliography for Chapter 5

Barker, H. W., "Radiative Transfer Through Clouds Possessing Isotropic Variable Extinction Coefficient," submitted to *Q. J. R. Meteorol. Soc.*, 1992.

Barker, H. W., and J. Davies, "Solar Radiative Fluxes for Extensive Broken Cloud Fields," to appear in *J. Atmos. Sc.*, 1992.

Cahalan, R. F., "Overview of Fractal Clouds," in *Advances in Remote Sensing (RSRM'87)*, Eds. A. Deepak *et al.*, 371–389, A. Deepak, Hampton (Va.), 1989.

Cahalan, R. F., and J. B. Snider, "Turbulence in marine stratocumulus," in *Proceedings of the 9th Symposium on Turbulence and Diffusion*, Roskilde, Denmark, April 30–May 3, Am. Meteorol. Soc., Boston, 1990.

Cannon, C. J., "Line Transfer in Two Dimensions," *Astrophys. J.*, 161, 255–264, 1970.

Davis, A. B., S. Lovejoy, and D. Schertzer, "Radiative transfer in multifractal clouds," in *Scaling, Fractals and Non-Linear Variability in Geophysics*, Eds. D. Schertzer and S. Lovejoy, Kluwer, Hingham (Mass.), 1991a.

Davis, A. B., S. Lovejoy, and D. Schertzer, "Discrete angle radiative transfer in a multifractal medium," *S.P.I.E. Proceedings*, 1558, 37–59, 1991b.

Feller, W., *An Introduction to Probability Theory and its Applications*, vol. 1, Wiley, New York, NY, 1971.

Gabriel, P., S. Lovejoy, G.L. Austin, and D. Schertzer, "Radiative transfer in extremely variable fractal clouds," in *Proceedings of the 6th Conference on Atmospheric Radiation*, Williamsburg (Va.), May 12–16, Am. Meteorol. Soc., Boston, 1986.

Klafter, J., A. Blumen, and M. F. Shlesinger, "Stocchastic pathway to anomalous diffusion," *Phys. Rev. A*, 35, 3081–3085, 1987.

Lovejoy, S., and D. Schertzer, "Multifractals, Universality Classes and Satellite and Radar Measurements of Cloud and Rain Fields," *J. Geophys. Res.*, 95, 2021–2034, 1990.

Lovejoy, S., A. B. Davis, and D. Schertzer, "Radiative transfer in multifractal clouds: observations and theory," in *Proceedings of the 7th Conference on Atmospheric Radiation*, San Fransisco (Ca.), July 23-27, Am. Meteorol. Soc., Boston, 1990.

Schertzer, D., and S. Lovejoy, "Generalized Scale Invariance in Turbulent Phenomena," *P.C.H. Journal*, 6, 623–635, 1985.

Schertzer, D., and S. Lovejoy, "Physically Based Rain and Cloud Modeling by Anisotropic, Multiplicative Turbulent Cascades," *J. Geophys. Res.*, 92, 9693–9714, 1987.

Schlesinger, M. F., J. Klafter, and B. J. West, "Levy walks with applications to turbulence and chaos," *Physica A*, 140, 212–218, 1986.

Siebesma, A. P., *Multifractals in Condensed Matter Physics*, The Cheese Press, Edam, The Netherlands, 1989.

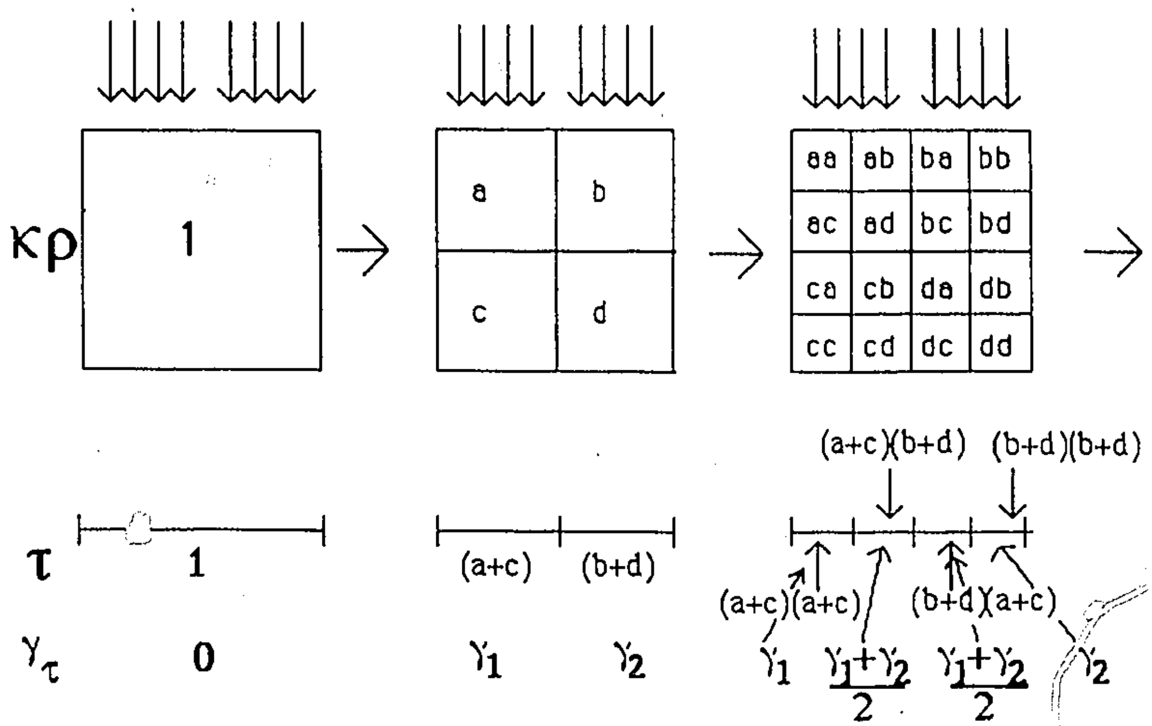

Figure 5.1: A special microcanonical cascade model for both density and optical thickness. The unit square with unit optical density (=κρ) is broken up into four sub-eddies at each step in the cascade, each sub-eddy being modulated by the factors a,b,c,d which are here deterministically arranged as shown in the middle figure (the first step of the cascade). The expressions in each box indicate the local optical density. The one-dimensional cascade shown below it shows the evolution of the vertical integral, the optical thickness (τ) with the corresponding expression for the optical density. On the line below, we indicate the corresponding orders of singularity of τ ($\gamma_\tau=\log_\lambda\tau$) with $\lambda_0^{\gamma_1}=a+c$, $\lambda_0^{\gamma_2}=b+d$, $\lambda_0=2$. Closer inspection reveals that, as far as the τ-cascade is concerned, the factors a,b,c,d can be random, as long as they are constrained so that a+c, b+d are constants. The arrows at the top indicate the incident radiation.

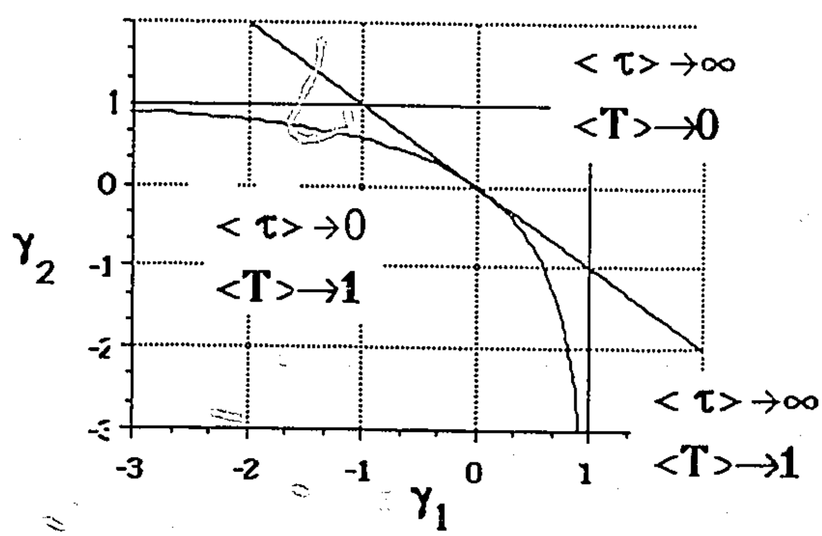

Figure 5.2: A diagram of the (γ_1,γ_2) plane showing the three different regions that characterize the scaling of the optical thickness and direct transmission. The straight line corresponds to $c'(0)=c(0)=K_{Td}(1)=0$, and the curved line to $K(1)=0$.

Chapter Six†

RADIATIVE TRANSFER IN A MULTIFRACTAL, A NUMERICAL EXPERIMENT

Preliminaries, Caveats, Overview, Summary and Outlook: In this chapter, we report on a two-dimensional numerical transfer experiment conducted on the Cray 2 of the[1] C^2VR in February 1991. The primary aim of this experiment was to show that radiation fields can be reliably calculated for extremely variable (multifractal) optical density fields (cf. app. C). This computational challenge was successfully met—the validation consists in showing that the results obtained by two quite simple and totally independent numerical techniques agree to within their expected numerical accuracies. The reader is referred to app. B for further technical details on both Monte Carlo simulation and relaxation of finite difference equations within the framework of "discrete-angle" (DA) transfer (cf. chap. 3), especially when applied to multifractals.

We have reason to believe that we are now in presence of the first complete database consisting of a fully resolved highly variable optical density field and its associated radiation fields for a conservative albedo problem. That the scattering is orthogonal and isotropic DA, not Mie, on the one hand, and that the embedding dimensionality is two, not three, on the other hand, may seem like factors that reduce the "realism" of the experiment but it must be realized that such a comprehensive experiment is impossible in Nature and that, being faced with considerable visualization problems, the "DA" and "d=2" options are in fact judicious.[2] Obviously, a countless number of statistical questions can be addressed using this database and it is hoped that the ideas discussed throughout this thesis will be helpful in formulating a reduced set of more pertinent questions. For instance, two-point statistics seem to be the minimal framework to gain physical insight into the radiation transport process (according to our discussion in chap. 4) while the notion of "channeling" (introduced as soon as chap. 2) suggests that we should attempt to quantify the anti-correlations of the deviations of the density and of the net flux vector from their local means. All of these statistics must of course be estimated at all (cloud-to-pixel) scales and characterized in scale invariant terms along the lines discussed in different parts of app. C (and with more detail in the quoted literature). We note however that all the routine scaling analyses performed to date on all kinds of geophysical signals apply to one (scalar) field at one point, not two quantities (including a 4-vector) at two points or more, although the general formalism for developing such statistics has already been described by Schertzer and Lovejoy [1991].

For the present, we will therefore limit ourselves in the following (sect. 6.3) to a rather qualitative discussion of some of the most obvious graphical renderings of the various components of the internal radiation fields. This however is not done without presenting prior and in some detail the adopted multifractal density field (in sect. 6.0), optical parameters, boundary conditions (BCs) and corresponding analytical "independent pixel" (IP) responses (in sect. 6.1). Several variants of the same cloud (ρ- or LWC distribution) are finally used, differing only by an overall multiplicative factor (κ) that determines uniquely the average optical thickness ($\bar{\tau}$) ranging from $\approx$12 to $\approx$200. The main point of this discussion is to illustrate—literally—the largest scale "channeling" event induced by the largest cluster of singularities that developed during the ten (discrete) cascade steps used to generate the multifractal. In this respect, the present numerical experiment serves us with a final (and hopefully dramatic enough) example of this very basic mechanism of inhomogeneous radiation transport which has pursued us from diffusion to transfer theories of matter/radiation interaction and from weakly variable and/or deterministic to extremely variable and/or random cloud models. Another point we will stress, in a different way from chap. 2–4, is that the rough characterization of the conditions (w.r.t. a variable density field) that make diffusion a better or a worse approximation to transfer agrees with the basic theory (reviewed in app. D), i.e., the more multiple scattering (m.s), hence the denser, the better. In sect. 6.4, we switch to a slightly more quantitative discourse in connection with the (one-dimensional) exiting radiation fields across the cloud's top (albedo) and bottom (transmittance). Indeed, we are able to determine the spectral exponents for these fields in the thinnest case which is only contaminated by numerical noise at the very smallest scales; these exponents compare favorably with their observed counterparts. The spectra of the thickest case shows (uncorrelated) Monte Carlo noise to appear precisely at the expected level and associated scale. Bearing this artefact in mind, we also witness extremely powerful smoothing of the radiation fields, both internal and exiting, by the enhanced scattering brought on by increasing the cloud's mass.

Being fully aware of the fact that we are opening more questions than we are answering (quantitatively speaking), we are content with the fact that our contributions, however modest, may well be opening the way for new vistas in theoretical, computational, statistical and, eventually, observational research into atmospheric solar radiation problems. At this point, it is however worth recalling that the main thrust of the present thesis is to account for the systematic effects of inhomogeneity that appear in the spatially unresolved radiative responses to illumination, with scaling cloud models playing an important but largely illustrative role. In our final section, we therefore revert from fully resolved fields to these simple measures of diffuse radiation and find yet another confirmation of the inequalities presented early on in chap. 2 between the transmittancies obtained using homogeneity- or transport-related hypotheses applicable to arbitrary horizontally extended media (in this case, by periodic replication). In self-explanatory notations, we expect:

$$T_{homo}(\overline{\tau}) < T_{IP} < T_{DA} < T_{dif} \tag{6.0}$$

where we have added the rightmost inequality for reference only (it is not illustrated here). We also recall that, for the leftmost inequality to apply, the amount of scattering material ($\overline{\tau}$) must be held constant. Variously restricted proofs of these inequalities were presented in chap. 2 and 3 of the thesis along with arguments for pending generalizations (and scaling examples were provided throughout), the role of nonlinearity and higher dimensionality (i.e., "channeling") was each time emphasized. Finally, the intermediate inequality is the one directly related to "channeling" and it is reconsidered here using the complete order-of-scattering decompositions of the unresolved responses that illustrate, in a specific case, our ideas about non-exponential photon free path distributions that were introduced in sect. A.2, used in sect. 4.4 and found to be scaling in sect. 5.1.

We view the inequalities in (6.0) as fundamental in the sense that they apply to every realization of a stochastic cloud model, at least for the kind of simple transport model and illumination geometry used here (and in the foreseeable future, given the ambitious program outlined in the above). Failure to see this before forging ahead with the ensemble-average properties of stochastic scale invariant cloud models will almost surely create confusion as to what systematic nonlinear radiative variability effect belongs to what cause, for at least two reasons. On the one hand, the average response of randomly thick homogeneous media can look like that of one realization of a stochastic medium (cf. chap. 4–5) and, on the other hand, the role of the scaling in the physical explanation of these effects is not fundamental (chap. 2–3), it however amplifies them (sect. 4.3–4) to a point that would soon be beyond recognition, had we not looked closely enough at the general case. An example of how we can use the information in (6.0) is easy to provide. For a (canonically conserved) stochastic model, all of the responses involved in that inequality sequence are in fact random variables.[3] Taking (positive) powers and ensemble-averages, we can add a new inequality at the left of all the others:

$$T_{homo}(\langle\tau\rangle)^h < \langle T_{homo}(\bar{\tau})^h\rangle < \langle T_{IP}{}^h\rangle < \langle T_{DA}{}^h\rangle < \langle T_{dif}{}^h\rangle \qquad (6.0')$$

where we have made the (ergodic-type) assumption that $\langle\bar{\tau}\rangle = \langle\tau\rangle$. The leftmost inequality in (6.0) is a direct consequence of Jensen's inequality (3.31) applied to the spatial average of the convex function $T_{homo}(\tau)$ that enters the definition (3.28) of T_{IP}; all we have done here is to use the same inequality again, this time for the ensemble-average w.r.t. a random $\bar{\tau}$. If an outer-to-inner scale ratio parameter (λ) enters the definition of the stochastic model as is the case below, then (6.0') will be true for all $\lambda>1$, while at $\lambda=1$ homogeneity is retrieved and all of the above inequalities become equalities.

6.0. The Structural Properties of the Optical Density Field

6.0.1. Rationale for Adopting a Cascade as a Model for Density

In order to obtain an unambiguous illustration of the radiative effects of scaling inhomogeneity, we require our model optical density field to exhibit

(i) a large range of scales,

(ii) a large range of values,

(iii) well-understood mathematical properties,

and, if possible, some degree of

(iv) physical justification.

The universal multifractal models described in sect. C.5 automatically fulfill requirements (i), (ii) and (iii) as soon as λ and C_1 (as defined in sect. C.4) are given reasonably large values within their natural ranges, respectively, $[1,\infty[$ and $[0,d[$ where d is the embedding dimensionality and either one of the lower bounds corresponds to homogeneity. In the following, we take d=2, mainly because of computer memory limitations (see app. B), also for ease of resulting radiation field visualization. Returning to the multifractal parameters, we choose

$$\boxed{\lambda = 1024} \qquad (6.1a)$$

and

$$\boxed{C_1 = 0.5} \qquad (6.1b)$$

Further justification of this last value to follow.

Concerning requirement (iv), the deep connections of multifractals with turbulence—the primary source of inhomogeneity in clouds—have now been well established (see app. C for a brief review, and the literature quoted therein for details); in particular, they have all but completely superseded the monofractal models used justifiably—for simplicity—in our previous numerical radiative studies (discussed in chap. 4). Still, item (iv) deserves a more detailed discussion. Dissipation ε is not density ρ; in particular, the spectral exponent of ε lies above -1 (see §C.4.3) whereas that of ρ is observed to be close to -5/3. Methods applicable to the concentration of scalars passively advected by fully developed turbulence—based on [Corrsin, 1951; Obukhov, 1949] phenomenology—are actively being researched [Schertzer and Lovejoy, 1987; Wilson *et al.*, 1991], but no completely satisfactory stochastic model for the fluctuations of ρ has yet been devised.

Recalling that the last[4] universal multifractal parameter to be determined is the Lévy index which can go from 0 (Bernouilli generators and monofractals) to 2 (Gaussian generators and log-normal multifractals). Having examined the radiative properties of a deterministic version of the former limit (in chap. 4), we are now tempted[5] by the opposite limit which in many respects constitutes the "ultimate" multifractal within the classification scheme proposed by Schertzer and Lovejoy [1992]; surely this extreme case of extreme variability will help our purposes in "seeing" how inhomogeneity affects the radiation fields. Hence,

$$\boxed{\alpha = 2} \tag{6.1c}$$

and consequently eqs. (C.17–18) apply. A remark of historical interest is that this model is closely related to the one proposed independently by Kolmogorov [1962] and Obukhov [1962] for the effects of intermittancy on the statistical properties of the dissipation field in fully developed turbulence, in fact two years before the prototypical monofractal model of Novikov and Stewart [1964] was introduced.

Finally, and again for simplicity, we will use the discrete cascade construction procedure illustrated graphically in fig. 6.0 with a dividing ratio λ_0=2; after n=10 cascade step, we obtain the value of $\lambda=\lambda_0^n$ quoted in (6.1a). Only λ, not the fact that the cascade is discrete, is important to the mathematical description of the model found in sect. C.2–4. The main (practical and conceptual) inconvenience of the discrete cascades w.r.t. their continuous counterparts is the persistence of the rectangular grid structure which is of course totally irrelevant to the turbulence being modelled. In our exploratory transfer experiments however, we will see that the grid structure dominates the small scale features of the radiation field (which is bad, possibly inducing scale breaks in future statistical analysis) but this provides a reference frame to the eye (which is good, but only for our present purposes of visual cross-referencing).

6.0.2. Scaling One-Point, Two-Point and Column Statistics of the Adopted Realization

The dual codimension functions corresponding to α=2 are, respectively, from eqs. (3.35) and (3.18b):

$$\begin{cases} C(h) = C_1 h \\ c(\gamma) = \frac{C_1}{4}\left(\frac{\gamma}{C_1}+1\right)^2 \end{cases} \tag{6.2}$$

and they provide the proper (scale invariant) characterization of the one-point statistics of our adopted density field.[6] Since the associated cascade is conserved, we have $<\rho>=1$ in natural units of density. In sharp contrast with our deterministic monofractal cloud model from sect. 4.2, this is an inherently stochastic model but we will focus on a single realization in the present study, being at the numerically exploratory stages of radiation applications of these kinds of model optical media.

Fig. 6.1 shows the specific realization that we adopted[7] in order of singularity representation (i.e., $\gamma(x) = \log_\lambda(\rho(x))$, with linear grey-scale) and fig. 6.2, the portion of its theoretical scale invariant histogram pertaining to a single realization (i.e., $c(\gamma) \leq d = 2$ [Lavallée *et al.*, 1991]) with remarkable values highlighted. Notice the well distributed (space-filling) intermediate shade of grey corresponding to the theoretically most probable singularity $\gamma_0 = -C_1 = -0.5$ which has $c(\gamma_0) = 0$ and is very close to our example's $\bar{\gamma} \approx -0.46$. We have also singled out the point where $c(\gamma) = C_1$; the (positive) solution, γ_1, of this equation is shown in sect. C.3 to be the order of singularity generically associated with the mean of the process, $<\rho>$. It has the remarkable property of being the point where the $c(\gamma)$ curve is tangent to the first diagonal (i.e., $c'(\gamma_1) = 1$ and $\gamma_1 = C_1$) whether the multifractal is log-normal or not, incidentally.

The overall spatial average of this realization is $\bar{\rho} \approx 1.52$ which is not a rare fluctuation from the ensemble-average $<\rho> = 1$. The individual ρ-values span a range from $\approx 10^{-7}$ to $\approx 10^{4}$. Unsurprisingly, this is quite close[8] to the theoretical fluctuation ratio of $\approx \lambda^{4\sqrt{dC_1}} \approx 10^{12}$ which is predicted from eq. (6.2) and the sampling singularity criterion discussed above (namely, $c(\gamma) \leq d$). While these huge fluctuations occur over the whole cloud, $\approx$2–4 ratios will not be rare from one cell to the next; indeed, from (C.18c), we must use $\sigma = \sqrt{2\ln\lambda_0 C_1} \approx 0.83$ in eq. (C.17a) to generate the random multiplicative weights. Letting $\tilde{\ }$ denote the (d=2) Fourier transform and **k** the wavenumber vector, we find in the isotropic power spectrum of $\rho(\mathbf{x})$, viz.

$$E_\rho(k) = \int_{|\mathbf{k}'|=k} <|\tilde{\rho}(\mathbf{k}')|^2>\, d^2\mathbf{k}' = \int_0^{2\pi} <|\tilde{\rho}(k\mathbf{u}(\theta))|^2>\, d\theta \tag{6.3a}$$

a spatial/ensemble statistic which directly generalizes the spatial and/or ensemble mean since $\bar{\rho} = \tilde{\rho}(0)$ for every realization. Since the Wiener-Khintchin theorem states that they form a one-dimensional Fourier transform pair (see sect. 4.4), the above power spectrum conveys the same information as the density field's 2-point correlation function:

$$<\rho(\mathbf{r}u)\rho(0)> \sim <\rho_\lambda^2>|_{\lambda=r/l_0} \sim \lambda^{K(2)}|_{\lambda=r/l_0} \qquad (6.3a')$$

where K(h)=(h-1)C(h); see Monin and Yaglom [1975] who however use different notations than us. Specifically, the spectrum in (6.3a) scales as $k^{-1+K(2)}$ and, in our particular case, $K(2) = 2C_1 = 1$, i.e., $E_\rho(k)$ is independent of k. (The observed spectral exponents for turbulent velocity dissipation fields are somewhat negative, corresponding to $C_1 \approx 0.2$–0.3 in this model.[9]) In short, the medium exhibits the long range correlations which, according to our discussion in sect. 4.4, are one of the prerequisites that make "interesting" radiative properties. By contrast, uncorrelated ($<\rho(\mathbf{r})\rho(0)> \sim \delta(\mathbf{r})$) noise in two dimensions, which we have often contrasted with multifractals on radiative grounds, has a constant spectral density $E_\rho(k)/n_d k^{d-1}$ hence $E_\rho(k) \sim k$ in d = 2 but totally different scaling of their probability distributions.

In order convey more directly an idea of the degree of variability of our prototypical optical medium (without referring to singularity- or power spectra), we provide in fig. 6.3a,b,c three different exceedence sets at three very different levels in density value: $1/32 \approx 0.031$, 1, and 32. These three thresholds correspond respectively to the the specially selected orders of singularity $\gamma_0 = -C_1$, $\gamma_{h_{min}} = 0$, and $\gamma_1 = +C_1$. The former is the most probable order of singularity and associated density value $\rho_{m.p.}$ (in fact, it is an order of "regularity" since $\rho_{m.p.} = \lambda^{\gamma_0} \to 0$ as $\lambda \to \infty$); it is associated (via Legendre transformation) with the 0^{th} moment of the field; finally, it fills space since $c(\gamma_0)=0$ as is clear from fig. 6.3a. The second is the "neutral" order of singularity (or regularity) corresponding to $\rho=1$ (recall that we have constrained $<\rho>$ to this value by conservation); it is Legendre associated with the order of statistical moment that minimizes K(h), i.e., $K'(h_{min})=0$ which in the $\alpha=2$ case yields $h_{min}=1/2$; finally, the exceedence set in fig. 6.3b has a theoretical codimension of $c(0)=-\min[K(h)]$ which in the $\alpha=2$ case is $C_1/4=0.125$ (in this particular case). The last is the order of singularity associated with the mean of the process $<\rho>$; indeed, the Legendre transformation associates it with the statistical moment of order 1 which implies $\gamma_1=C_1$ which is defined as K'(1); finally, the very sparse exceedence set in fig. 6.3c has a theoretical codimension of $c(\gamma_1)=C_1=0.5$ (in this particular case). Together, figs. 6.3a–c show how unsuitable "level curve" representations are for multifractals since such curves are the fractal boundaries of fractal sets.

If only to emphasize the very strong degree of concentration prevailing in the lower l.h. side of the medium, we have plotted the column-averaged densities in fig. 6.4a, namely,

$$\bar{\rho}(y) = \frac{1}{L}\int_0^L \rho(y,z)\,dz \qquad (6.3b)$$

We have proceeded similarly for row-averages and $\bar{\rho}(z)$ is illustrated in fig. 6.5a. Figs. 6.4–5a give us an idea of the difficulties[10] in properly evaluating statistics for canonically conserved multiplicative processes since each $\bar{\rho}(y)$ and $\bar{\rho}(z)$ is the overall average of a log-normal cascade in d=1; these cascades are however not mutually independent, hence the resulting one-dimensional fields are themselves multifractals. $\bar{\rho}(y)$ and $\bar{\rho}(z)$ both have minima around ≈ 0.1 and extend respectively to ≈ 40 and ≈ 20. Unsurprisingly, these maxima are reached at horizontal and vertical coordinates of the peak in the original $\rho(x)$ field. This maximum density value is ≈ 12000 which means that $\bar{\rho}(y)$ and $\bar{\rho}(z)$ acquire respectively $\approx 1/3$ and $\approx 1/2$ of their value within this single cell! This illustrates eloquently the multifractal ideas of singularity and extreme variability.

We can also define the orders of singularity associated with the column-averaged densities:

$$\gamma_{\bar{\rho}}(y) = \log_\lambda \bar{\rho}(y) \qquad (6.3b')$$

and similarly for the row-averages; both one-dimensional singularity fields have been added to figs. 6.4–5a. The corresponding ranges for the values of $\gamma_{\bar{\rho}}(y)$ and those of the statistically equivalent $\gamma_{\bar{\rho}}(z)$ are -0.35 to +0.53 and -0.27 to +0.42 respectively.

6.1. The Optical Parameters, Boundary Conditions and Independent Pixel Responses

The only physical parameters left to specify are purely optical in nature: t, r, s, and κ (with the same definitions as in chap. 2). We can view the latter as an arbitrary overall numerical multiplier of the raw density field that converts it into "optical density" or "extinction coefficient." We want a large overall optical thicknesses (as required in an opaque object such as a cloud): $\bar{\tau} = \kappa\bar{\rho}L \approx \kappa\lambda l_0 \gg 1$. At the same time, we want the medium to be optically thin at the homogeneity scale l_0 (at least on average) hence $\kappa\bar{\rho}l_0 \approx \kappa l_0 \ll 1$. This is a natural requirement in numerical applications but, in the case of multifractals (with non-negligible C_1), this constraint automatically implies the verification (on average) of the first criterion for strong radiative variability effects, i.e., inequality (4.10). When $\lambda = L/l_0 = 2^{10}$, these constraints can be fulfilled simultaneously as long as κ is kept in the range 2^{-7}–2^{-3} using natural units of length (where $l_0 = 1$). One could argue that the relevant factor for multifractals is not the average density $\langle\rho\rangle=1$ but the most probable (space-filling) density value $\rho_{m.p.}=\lambda^{-C_1}=1/32$ (here), we could thus gain five more powers of 2 in the range of κ values (up to 2^2).

Apart from constants, fig. 6.4a therefore illustrates

$$\tau(y) = \int_0^L \kappa\rho(y,z)\,dz = \kappa\,\bar{\rho}(y)\,L \qquad (6.4a)$$

As already stated, the total optical thickness is simply

$$\bar{\tau} = \frac{1}{L}\int_0^L \tau(y)\, dy = \kappa\, \bar{\rho}\, L \tag{6.4b}$$

We are left with 5 optical media by taking $\log_2\kappa$=-7,-6,-5,-4,-3. All of these are proportional to the nominal bare (log-normal) cascade field represented in figs. 6.1 and/or 6.3a,b,c; their total (or spatially averaged) optical thicknesses $\bar{\tau}$ being in the range 12.2 to 195. We will dwell mainly on the extreme values of κ (hence $\bar{\tau}$) in the remainder of this chapter. For (numerical and conceptual) simplicity, we assume conservative isotropic DA(2,4) scattering ($t = r = s = 1/4$ hence, from definitions (2.6a–c), $a = 0$, $q = 1$, $p = 1/2$); results are expected to be qualitatively the same in any other DA(2,4) system because of the similarity relations established in sect. 3.5 (that relate different values of κ).

As presented in chap. 2, transfer theory relates the optical density and radiation fields in a purely local manner; BCs are required to determine the latter completely. In early investigations using both transfer [McKee and Cox, 1974] and/or diffusion [Davies, 1978] methods, horizontal radiative fluxes were induced simply by changing the support of the (otherwise homogeneous) optical medium from an infinite slab to a finite cuboid. Since we now want to isolate variability-induced horizontal fluxes, (meteorologically) we think of our cloud as horizontally "extended" and (mathematically) we impose horizontal cyclical conditions

$$I_{\pm y}(0,z) = I_{\pm y}(L,z) \qquad (0 < z < L) \tag{6.5a}$$

in DA transfer.[11] At present, we are interested in the (DA) problem of diffuse reflection and transmittance which is defined by the following vertical BCs:

$$I_{+z}(y,0) = 1 \qquad I_{-z}(y,L) = 0 \qquad (0 < y < L) \tag{6.5b}$$

In many respects, the most important unknowns in this (so-called "albedo") problem are the exiting radiance fields which, in DA transfer, read as:

$$R(y) = I_{-z} \qquad T(y) = I_{+z}(y,L) \qquad (0 \le y \le L) \tag{6.6a}$$

for local reflectance and transmittance respectively. At the lowest level of spatial resolution (as considered in our previous studies, discussed in chap. 4), the response of the inhomogeneous medium is of course defined by[12]

$$T = \frac{1}{L}\int_0^L T(y)\, dy = 1 - R \tag{6.6b}$$

The last step equality is a global consequence of the local conservative property we assumed for the DA phase function ($a = 0$). This hypothesis makes our calculations most readily comparable to radiative transfer in the visible part of the solar spectrum where the cloud-free atmosphere is quasi-transparent and (pure) liquid water has vanishingly small absorption; the most equivalent continuous angle illumination conditions would be overhead sun, or a uniform (at least axisymmetric) distribution of diffuse radiance.

In fig. 6.4b, we have plotted the total and direct transmittances of each column for the thinnest cloud. The related fig. 6.5b is discussed in sect. 6.4 below. Total column-wise (or local IP) transmittance reads as[13]

$$T_p(\tau(y)) = \frac{1}{1 + r\tau(y)} \tag{6.7a}$$

This is the exact solution corresponding to the case of conservative ($a = 0$, $\varpi_0 = 1$) scattering in d=1 or else with no side scattering ($s = p = 0$); we then have $r = q/2 = (1-g)/2$ so, as in any standard two-flux theory, T_p is a universal function of rescaled optical thickness, $(1-g)\tau$, see the review/extension by Meador and Weaver [1980]. Recall from sect. 3.4 that total transmittance is also given by (6.7a) for any conservative DA phase function in higher dimensions but in the very restricted case of homogeneous plane-parallel media. Comparing figs. 6.4a and 6.4b, it is not hard to see the anti-correlation of T_p and τ as expected from our discussion in chap. 5: if λ and τ_λ are both »1, $\langle T_p(\tau_\lambda)^h \rangle$—with a multifractal τ_λ-distribution—was found to scale like $\langle \tau_\lambda^{-h} \rangle$ for h>0 but not too large, the result being independent of r (i.e., we again find radiative exponents independent of phase functions). A log (γ_{Tp}) plot of T_p would make this even more obvious.

Direct transmittance reads as

$$T_d(\tau(y)) = \exp[-\tau(y)] \tag{6.7b}$$

This is the exact solution corresponding to the case of transfer in a totally absorbing (ϖ_0=0) medium: $t = r = s = 0$ in orthogonal DAs, hence $a = q = p = 1$. We immediately see that $T_d(\tau(y))$ can far exceed $T_d(\bar{\tau}) = e^{-12.2} \approx 10^{-5.3}$ as well as its extreme intermittancy; neither of these features are too surprizing since our (chap. 5) analytical investigation into direct transmittance through multifractals shows it to have very simple (monofractal-like) scaling statistics in the limit $\lambda \to \infty$ and on condition that this corresponds to increasing optical thickness. We notice the relatively high levels of directly transmitted light on the r.h.s. with, in particular, $T_d(\tau_{min}) \approx 0.5$. The corresponding field for the thicker cloud model ($\kappa = 2^{-3}$) is given by the same values as illustrated here, except carried to the power 16; the maximum goes from ≈ 0.5 to $\approx 10^{-5}$! In other words, our thinner model is much like a complex (but horizontally periodic) structure of "broken cloudiness" whereas our thicker model is more like a (horizontally extended but) "single cloud" with a complex internal structure; we must however stress the arbitrariness of such a categorization in general.

We must finally settle on a numerical procedure to solve the (1st order) DA(2,4) transfer system of equations, i.e.,

$$[\,A_y\frac{\partial}{\partial y}+A_z\frac{\partial}{\partial z}\,]\,\mathbf{I}(\mathbf{x})=\kappa\rho(\mathbf{x})\,(P\text{-}1)\,\mathbf{I}(\mathbf{x}) \qquad (6.8a)$$

where

$$\mathbf{I}=\begin{pmatrix}I_{+y}\\I_{-y}\\I_{+z}\\I_{-z}\end{pmatrix}\quad A_y=\begin{pmatrix}1&0&0&0\\0&-1&0&0\\0&0&0&0\\0&0&0&0\end{pmatrix}\quad A_z=\begin{pmatrix}0&0&0&0\\0&0&0&0\\0&0&1&0\\0&0&0&-1\end{pmatrix}\quad P\text{-}1=\begin{pmatrix}t-1&r&s&s\\r&t-1&s&s\\s&s&t-1&r\\s&s&r&t-1\end{pmatrix} \qquad (6.8b)$$

with BCs (6.5a,b) and validate it. Given the novelty of the type of optical medium investigated (with its extreme variability being a particular concern), we have decided to use the most straightforward approach available: Monte Carlo simulation which can be considerably speeded up in DA transfer (see sect. B.1). Photons are tracked continuously in space and detected by digital counters at every cell boundary crossing. The validity of the code was established by applying to our thinnest medium the next most straightforward approach available, namely, (Gauss-Seidel) relaxation of the finite difference equations obtained from the above on a square lattice (see sect. B.2). The two methods are now compared using the adopted multifractal as a test case.

6.2. Validation of the Numerics, Monte Carlo and Relaxation Compared

As discussed in app. B, both methods are guaranteed to converge (they are both perfectly stable) but only the Monte Carlo method can be viewed as completely reliable, in the sense that the corresponding solution indeed obeys eqs. (6.8a,b) with BCs (6.5a,b); unfortunately the method is slow but this inconvenience is compensated by the fact that the accuracy is known *a priori* since the errors are purely statistical (i.e., we always know exactly where we stand w.r.t. the ideal case). In total contrast to this situation, the finite difference and relaxation approach can be made very accurate with enough CPU time (and far more efficiently if direct sparse matrix inversion methodology replaces our adopted relaxation solution) but its reliability—even physicality—depends somewhat on the way the finite differencing is done and very critically on the way the thick cells are dealt with (see Lovejoy *et al.* [1990], especially their appendix A). This last problem is inescapable in the framework of multifractals, it is further described in sect. B.2 along with the strategy we adopted to overcome it (namely, interpolation of the transfer coefficients from a reasonably dense tabulation generated by mega-photon Monte Carlo simulations on homogeneous squares).

The main source of numerical error when relaxation is used is the non-uniformity of the convergence which is not easily monitored during the iteration in practice. It was soon realized that, independently of the type of inhomogeneity (white noise or multifractals), the convergence of the relaxation is slowest almost throughout the thinnest row when cyclical

BCs where applied. This is easily understandable since that row is the most weakly coupled with the overall downwards flux that prevails throughout the system (due to the strongly anisotropic BCs). It is hard to say which method is really the most accurate in the absolute (neither is ideal in the long run anyway). For roughly constant CPU time (several Cray 2 CPU-hours), the relaxation technique yields results that are smoother simply because they are not contaminated with the characteristic Monte Carlo noise; to appreciate this, compare fig. 6.10a (10^4 relaxation steps) and fig. 6.8a (Monte Carlo, a run at 10^6 photons in all, $\approx 10^3$ photons/pixel).

As expected, the two methods agree to within the Monte Carlo noise level which, in the circumstances (the final run used 10,240,000 histories in all, 10^4 photons/pixel), is at the 1% level for the brighter internal/exiting fields (pixel values) and a few % for the dimmer fields. The overall (integrated) Monte Carlo responses are however reliable to a few ‰. However, this does not mean that the Monte Carlo estimate is the worse, on the contrary; the greatest discrepancies between the two methods appear in the regions of lowest overall light levels (where the Monte Carlo noise as at its maximum) but also in the regions where thick cells prevail (and where finite difference solutions are known to be more systematically biased). After $t=10^4$ iterations (see sect. B.2 for the notations), the global accuracy estimators for the relaxation were $\|I^t - I^{t-1}\|_1 \approx 2.10^{-7}$ and $R^t + T^t \approx 1.001$ (i.e., R^t and T^t appear to be slightly better estimated individually than by Monte Carlo). For our present purposes, this is all we need to proceed to the physical discussion of the results found in remainder of this chapter since we have made sure that the simulated radiation fields reflect primarily the physics, not the numerics. All of the above figures relate to the case where $\kappa=2^{-7}$ ($\bar{\tau}=12.2$) which is the only one where the thickest cell still falls within our tabulation (i.e., $\max_i \tau(i) \leq 100$). Having obtained a mutual validation of our numerical recipes in the thinnest case, the Monte Carlo method alone is retained for the thicker media. However, for $\kappa=2^{-3}$ ($\bar{\tau}=195$), only 10^3 photons could be injected per pixel (again for several hours worth of CPU-time) hence uncertainties $\approx 1\%$ for total fluxes and at the 3–10% level for the internal/exiting fields—the range being due to the greater overall gradients and extremely low fluxes are somewhat more uncertain (but relatively infrequent, they are only to be found below the major concentration visible in the lower l.h.s. of figs. 6.1 or 6.3). Finally, we note that the conceptual simplification achieved by applying cyclical horizontal BCs does carry a computation time cost in both of the methods that we implemented.

Before leaving the topic of numerical techniques, we must admit that our brute force—and overkill—approach (of using not one but two very simple methods) is only justified in the present exploratory stages of research into the radiative properties of stochastic cloud models; given that we have not even considered ensemble-averages yet, it is clearly unviable in the long run. Eventually, we will require a combination of more CPU time and improved numerical methodology (e.g., sparse matrix rather than relaxation techniques). Because of their greater flexibility and robustness (w.r.t. the thick cell problem in particular), Monte Carlo approaches are likely to be favored in future numerical transfer research, especially as more extreme kinds of inhomogeneity become the focus.[14] We must also recall that Monte Carlo algorithms can generally be adapted and optimized to target specific statistics which might be considered of special interest in future studies, using "double randomization" [Kargin *et al.*, 1985] if necessary. Other reasons to improve Monte Carlo algorithms in spite of the difficulty of accelerating them by vectorization mentioned in sect. B.1 are that (i) massively parallel supercomputers will soon become widely available and there is no limit to how many particles can be processed simultaneously in linear transfer problems, and that (ii) they have a natural by-product: the orders-of-scattering decompositions of the various flux fields (their utility is briefly discussed in sect. 6.5 and 7.3).

6.3. The Two-Dimensional Internal Radiation Vector Fields

6.3.1. General Discussion of the Visualization in Eigenvector Representation

In figs. 6.6a–c ($\bar{\tau}$ = 12.2) and figs. 6.7a–c ($\bar{\tau}$ = 195), we present grey-scale renderings of the four eigenspace projections of the DA radiance fields as defined in eqs. (2.12a–c):

J (figs. 6.6–7a)
F_y (figs. 6.6–7b) and F_z (figs. 6.6–7b')
X (figs. 6.6–7c)

This choice has proved more useful to us than the radiances themselves. Grey-scales are all linear in DA radiance (that has the same units as a flux, see sect. 3.1) and each pixel receives one unit; we have indicated the numerical min's, max's as well as means (except in figs. 6.6–7a).

Before any further discussion, it is important to "see" the amount of information contained in figs. 6.6–7; this is best done by mentally visualizing the results one would find for isotropic DA scattering in a totally homogeneous plane-parallel medium. Specifically,

figs. 6.6–7a:	J deceases linearly, hence we must picture the grey-scale key but stretched to the full frame-width of the figures.
figs. 6.6–7b,b':	$F_y = 0$, hence a blank picture appears, and $F_z = T(\bar{\tau})$ = const., hence some uniform shade of grey covers the picture.

figs. 6.6–7c: $X = 0$, diffusion applies everywhere exactly, hence we see another blank picture.

The most casual glance at figs. 6.6–7 is sufficient to see how severely this symmetry is broken by our example of internal variability. It is however important to realize that any amount of inhomogeneity will produce some perturbation by a mechanism that, inspired by Stephens' [1986, 1988] work, we have previously described as a "mode-coupling" induced by a source/sink-like term that appears on the r.h.s. of the (usual, d=3, counterpart of) transfer eq. (A.5) after harmonic analysis in **u** and Fourier analysis in (x and) y, but not in z. In sect. D.5 and 2.3, we presented arguments that show that Cannon's [1970] simple idea of "channeling" is in fact the counterpart of "mode-coupling" in physical space.

Equally striking is the fact that the huge 10^{11}-range variability of the ρ-field has been compressed into ranges of only ≈2–4 (in units of T) for the maximum absolute values of the quantities F_y, F_z and X, which are all algebraically valued *a priori* and constant (eventually null) in the homogeneous case. We have used $T = \overline{F_z}(z)$ as a convenient point of comparison since it remains constant w.r.t. the vertical coordinate by conservation of total radiant energy flux. The total range of values found for J, which is strictly positive, may seem impressive at first glance (i.e., ≈19 for the thinner- and ≈400 for the thicker cloud using max-to-min ratios) but in fact they are not much greater than the values that we predict for the corresponding homogeneous clouds: namely, from eqs. (6.9a,b), we find $J_{max}/J_{min} = (1+R)/T = 2r\overline{\tau}+1$ (i.e., ≈10 for $\overline{\tau}$=12.2 and ≈100 for $\overline{\tau}$=195, if r=1/4); so again the inhomogeneity has induced maximal change with ratios in the range 2–4.

6.3.2. Total DA Radiances

The most striking feature in fig. 6.6a is the prominence of the rectangular grid structure which has, however, almost vanished from fig. 6.7a; this provides a (first) illustration of the smoothing power of multiple scattering when boosted by an overall 16-fold increase in optical density. The artifact is of course due to the photons' propagation being restricted to the axes of the grid which are also (artificially) enhanced by the "discrete" nature of the cascade, cf. the visually obvious grid lines in fig. 6.1. For the moment, this small scale "texture" is in fact useful for tracking visually the large scale ρ(x)-I(x) connections. For instance, we notice in figs. 6.6–7a the more pronounced J-gradients in the denser regions; these come in all sizes (hence strengths) but the foremost lie in the lower l.h.s. This region is literally a (semi-isolated) cloud within the (extended) cloud and we will see it either dominate the overall picture (w.r.t. **F**(**x**), §6.3.3) or as a concentrated version of the whole picture (w.r.t. X(**x**),§6.3.4).

Returning to fig. 6.5b, we have plotted the results of three different ways of calculating the row-averaged internal total radiance (J) fields for $\overline{\tau}$ = 12.2: before (homogeneous layers) and after (IPs) applying eqs. (6.9a–c) as well as our full-blown numerical procedure. The *bone fide* (but vertically inhomogeneous) plane-parallel profile is very non-representative due to the large concentration of mass in the lower layers of the cloud which, in turn, concentrates radiation in the layers above it. It would have hardly been any better to homogenize the medium in both directions: this would have resulted in a linear decrease in J from the very same starting- and ending points and an ensuing underestimate of the amount of radiation in the lower layers. The IP approximation is much closer to reality due to the relatively low mass of this cloud (see sect. 6.5). The orthogonal grid/DA transfer-induced texture of the numerical results has survived the row-averaging to yield local increases in total radiance. These would not be present in the more relevant ensemble-averaged statistics: on average, the radiant energy will decrease with depth into the cloud but not as predicted by plane-parallel theory, if only because of inequality (6.0') above. Of course, the overall top-to-bottom gradient is due to the highly asymmetric vertical BCs that translate illumination (irradiation) from above. However indigenous to cloud-radiation interaction these BCs may be, the asymmetry they impose on the system can be viewed as problematic[15] when trying to understand the more subtle aspects of inhomogeneous transfer, some of which may be all but masked in the present situation. Analytical work is in progress on transfer (indeed, simply photon random walks) in infinite multifractals and, in this context, numerical approaches are also possible if one deals carefully with finite size effects.

6.3.3. Horizontal and Vertical Net Fluxes

In figs. 6.6–7b (F_y) and 6.6–7b' (F_z), we also notice a "smeared" texture of the net fluxes parallel to the direction they represent (stronger gradients at right angles): the photons are encouraged to stay "on track" until a major obstacle arises or more tenuous regions come within "reach" (a few locally averaged m.f.p.'s at most). This collective seeking of the most tenuous optical paths has been called "channeling" in the astrophysical literature, following Cannon [*ibid.*]. We have defined "channeling" as the the whole complex of radiative events that happen as soon as flux-lines are no longer somehow confined to the vertical; the effects caused by relaxing the vertical flux-line constraint in an inhomogeneous medium range from the global (T increases, §2.3.1 and fig. 6.14 below) to the local (the anti-correlations noted in §§2.3.1–2). The most obvious manifestation of this "channeling" can be seen in the lower half of figs. 6.7–8b where we witness divergence of horizontal flux on the l.h.s. (above the densest region) and convergence on the r.h.s.; simultaneously, in figs. 6.6–7b', we see vertical fluxes that decrease on the l.h.s. and increase on the r.h.s. (going downwards) since the two-dimensional flow of the $\mathbf{F}(\mathbf{x})$ field is divergence free due to lack of internal sources (emission) and sinks (absorption). This radiative flow pattern is clearly present at many smaller scales too. Notice that the horizontal fluxes are rather narrowly distributed around small negative means and are relatively small in absolute value: ≈0.1 (thinner) to ≈0.2 (thicker) times their mean vertical counterpart. It is remarkable that such locally small numbers can account for (up to almost) an order of magnitude difference between exact (numerical) and approximate (analytical IP) calculations of net overall flux T (see sect. 6.5 below). The vertical fluxes are distributed around a positive mean which is constrained (by conservation) to be the same in every row from top to bottom and equal to the overall transmittance (T) in eq. (6.6b). The vertical fluxes have by far the strongest fluctuations, ranging from vanishingly small values, in the densest regions, to twice T ($\bar{\tau}$=12.2) or four times T ($\bar{\tau}$=195), in the most tenuous regions.

6.3.4. Non-Diffusive Components

Finally, we turn to figs. 6.6–7c where we see the much more up/down- and y/z-symmetric "non-diffusive" component defined in eq. (2.12c). By and large, we see that it is most apt to vanish in the most opaque regions/clouds. This is indeed what we expect from standard (continuous angle) theory behind the diffusion approximation which tells us that it works best for quasi-isotropic radiation fields. In turn, we expect to find relatively isotropic radiance distributions in dense regions where lots of scattering occurs due to shorter-than-average photon f.p.'s and as (optically) far from sources/sinks as possible since these produce/cause "streaming" rather than "random walking" photon behavior; in our case, this means top/bottom boundaries. On closer examination however, we see that |X| is rarely negligible compared to T in the thin cloud. In the thick cloud however, it seems to exceed T (and even maxF_z) only very locally but, curiously, quite deep inside.

It is noteworthy that the recent *in situ* measurements of radiance in extended (marine stratocumulus) cloud decks by King *et al.* [1990] strongly suggest a predominance of diffusive behaviour although $I_u(\mathbf{x})$ was sampled exclusively in a vertical plane, hence only vertical fluxes are accessed. In essence, the authors fit (quasi-local) radiance measurements along one meridian arc to a cosine curve and claim excellent results in a majority of cases (see §D.2.2 for details). The DA(2,4) equivalent of a perfect fit is X=0 (cf. sect. 3.3); it would not be hard to find horizontal "flight paths," in our thicker cloud at least, where X(y)≈0 but this (I_{z+}≈I_{y+}) has absolutely no incidence on the value of the net horizontal fluxes (I_{y-} in figs. 6.6–7b); in particular, they need not vanish as King and his co-workers go on to assume in order to interpret their data in what we would call "IP terms." In fact, vanishing horizontal fluxes is likely to be a rare occurrence, given the variability the authors themselves find in the optical thickness[16] (compatible with the IP transport model). Our results therefore strongly suggest, on the one hand, that in future cloud radiation experimental studies, horizontal fluxes should not be overlooked due to their fundamental role in radiation "channeling" and that, on the other hand, concerted experimental and theoretical efforts should be made to better understand the transitions between the kinetic and diffusion transport regimes as well as try to characterize the situations where the IP approximation works best since, for some practical applications, it might turn out to be sufficiently accurate.

6.4. The One-Dimensional Exiting Radiation Fields

6.4.1. Simulated and Observed Power Spectra and Apparent Absorptances, Compared

In figs. 6.8a,b,c ($\bar{\tau}$ = 12.2) and figs. 6.9a,b,c ($\bar{\tau}$ = 195), we have plotted (a) R(y) and T(y) from eqs. (6.6a)—notice the separate scales in fig. 6.9a, (b) $E_R(k)$, and (c) $E_T(k)$ the (one-dimensional) power spectra of R(y) and T(y) respectively—notice the use of log/log scales. In both the physical- and Fourier space representations, it is important to distinguish the "signal" of medium's variability in this single realization experiment from the "noise" due to finite photon statistics in the numerics. This can be done by assuming a Poissonian distribution of detection events which is expected to be a very good approximation whenever the "bins" are relatively small (sect. B.1). For instance, we notice (fig. 6.9a) that the reflected flux field locally exceeds unit several times; we can focus $\max_y R(y) = R(489 l_0) \approx 1.05$ which is very likely to be a real exceedence of 1, not a Monte Carlo fluke, since the noise level for 10^3 photons is $\sqrt{10^{-3}} \approx 3\%$ (reasons for this specific location are listed below). In homogeneous media, the fluctuations in photon counts across the cloud would be spatially uncorrelated—and their spectrum flat—whereas, in variable media, weak and strong counts will tend to cluster. We have indicated on figs. 6.8–9b,c the level of Monte Carlo noise for the average response (or, in one case, the range of responses) using eq. (B.1b).[17] These *a priori* noise levels coincide with the appearance of the "whitening" trend (mainly in figs. 6.9b,c), implying that the effect of correlations in the Monte Carlo noise cannot be very important. For the rather (lower k's), we observe spectra that scale very well given that we are dealing with a single realization. The spectral exponents for reflectance are around -1, not far from the values found for satellite radiances (see Cahalan and Snider [1989] for spectra of one-dimensional sub-sets and Tessier *et al.* [1992] for full two-dimensional analyses). Transmittance spectra are somewhat steeper due to enhanced energy at the lowest frequencies; this is obviously due to the strong (cloud scale) perturbation of the radiation flow in the lowest layers of the cloud by the very dense region on the l.h.s.

We can use our simulated exiting radiation fields together in a mock cloud radiation field experiment where the albedo and transmittance fields are simultaneously probed and the (apparent) local absorptance is computed: $A(y) = 1-R(y)-T(y)$. Fig. 6.10b displays this absorptance field for the cloud with $\tau=12.2$ while, for reference, fig. 6.10a shows the the corresponding albedo and transmittance fields—these are in fact the relaxation results, not their Monte Carlo counterparts used in fig. 6.8a. Recall that we are looking at one unit cell in a periodic cloud cover. We immediately notice that $A(y)$ has a vanishing spatial average, as required by conservation, and that it exhibits spatial correlations, as one expects from the sum of two scaling noises. Apparent internal sinks ($A(y)>0$) dominate the l.h.s. due to the large concentration of synthetic LWC that prevails in that region and, consequently, apparent internal sources ($A(y)<0$) are to be found largely on the r.h.s. Again, we are seeing a direct effect of channeling within the cloud: the radiative flux-lines start, equally spaced, at cloud top and end at cloud base but non-uniformly distributed (less on the l.h.s., more on the r.h.s.). Interestingly, the range of values we find for $A(y)$, ≈ -0.3 to $\approx +0.3$. This is not at all incompatible with the range of empirically determined absorptances found in the literature, as compiled by Fouquart *et al.* [1990]: ≈ -0.1 to $\approx +0.2$ but the most negative results have probably remained unpublished because they look too suspicious [Y. Fouquart, p.c.]. To appreciate these figures, it must be recalled that the (real world) experiments are very difficult to conduct and, as in our simulations, the fluctuations are now widely believed to reflect internal variability, not true ... sorption (with the ensuing heating rates).

6.4.2. Simulated and Observed Singularity Spectra, Smoothing by Multiple Scattering

Fig. 6.11 illustrates the smoothing power of enhanced multiple scattering in another way, simply, by showing the p.d.f.'s of albedo fields for $\log_2\kappa = -7,\cdots,-3$ but they are presented in "codimension function" format: we take $c_R(\gamma_R) \approx -\log_\lambda(\Delta P_R/\Delta\gamma_R)$ from definition (C.16) where $\gamma_R(y) = \log_\lambda(R(y)/R)$ is obtained from definitions (6.6a,b) and (C.11c). Particularly obvious is the gradual narrowing of the singularity spectrum, i.e., effectively smaller C_1's are to be expected. We also see a simultaneous trend from more skewed distributions to more symmetric ones. Similar (but more thorough) analyses of remotely sensed (visible channel) cloud scenes were performed by Lovejoy and Schertzer [1990] and Tessier *et al.* [1992]. The former authors use a straightforward scaling analysis technique ("functional box counting," see §C.3.2) which focuses on the (cumulative) distribution function of the γ's (at various scales), rather than our way of plotting the p.d.f. at the finest scale only, but this finest scale dominates the log-log regression and, furthermore, the two $c(\gamma)$'s are similar when $c(\gamma)>0$ (see §C.3.2). They used synoptic scale (GOES) imagery, hence ($\approx$50% cloudy only) which is more directly comparable to our thinner cloud model and, as here, they find a relatively small $C_1 \approx 0.2$ and a Lévy index $\alpha \approx 0.6$ which indeed corresponds to a highly skewed distribution of extremal Lévy generators (see sect. C.5, for definitions of terms and parameters). The latter authors look, in particular, at almost totally ($\approx$90%) cloudy Landsat imagery which is of course more comparable with our thicker cloud model and they too find smaller C_1 values (0.05 to 0.09) and a more symmetric generator distribution ($\alpha \approx 1.4$). They also revise the above values for GOES images ($\alpha \approx 1.1$–1.5, $C_1 \approx 0.13$) but it must be realized that—being justifiably concerned with the underlying cascade process' "non-conservation," i.e., spectral exponents <-1—they analyzed not the radiance field itself but its (finite difference) gradient or Laplacian in absolute value and, furthermore, they applied the more robust "double trace moment" technique (also described in sect. C.5). Given the rough agreement before this pre-scaling analysis treatment, our data would probably yield similar results if it suffered the same fate. However, taking the gradients or Laplacians would considerably boost the numerical noise which we do not have the leisure to smooth by ensemble-averaging (yet); indeed, we would be multiplying the spectra in figs 6.8–9b by k^2 or k^4 respectively and boosting the high frequencies even more by taking the absloute values.

Being limited to this one realization, some insight into the mechanisms of radiative smoothing can be gained by pondering the reasons that make very large reflectance values not only improbable but physically impossible. On the one hand, it is not hard to identify the factors that are limiting R(y): in the IP approximation it is strictly less than 1 so any excess is necessarily due to horizontal fluxes taking energy into regions where it is already in high concentration, at the expense of regions of lower concentrations (by overall conservation); this is in outright contradiction with our general expectation from the Fickian-type (but exact) DA eq. (2.17a). On the other hand, our present maximum R(y)—merely $\approx$1.05—occurs (i) at maximum $\kappa = 1/8$ hence systematically shorter free photon paths between scatterings, (ii) at a column (#489) straddled by a more-or-less "V" shaped cluster of above-average singularities (cf. fig. 6.1 or 6.3b) that lie right at the top of the cloud, a situation where recently injected photons are likely to be "trapped" and reflected, and (iii) this structure happens to be right above the very dense region at the bottom of the cloud, hence further concentration of radiant energy; at present, it is impossible to quantify the contributions of these three factors separately but clearly occurrence (i) is perfectly natural from first principles but further enhancement of κ can only bring on still smoother fields, occurrence (ii) is certainly not exceptional in these kinds of cloud models, and occurrence (iii) is completely circumstantial.[19] Our DA reflectances obviously obey the same conservation rules as CA fluxes into the upward hemisphere while remotely sensed albedoes are really radiances expressed in terms of an equivalent

Lambertian reflector; they are therefore not physically bounded quantities but—since fluxes are bounded—very large values would call for almost Fresnelian optics (i.e., like the ocean's "glint"), unlikely and unobserved behaviour in clouds. This powerful smoothing[20] effect of multiple scattering is reminiscent of the fact that Nature produces clouds that are at once radiatively featureless and highly variable internally: arctic status [Tsay and Jayaweera, 1984] which were once viewed as potential benchmarks for homogeneous plane-parallel transfer calculations in full angular detail. Finally, we remark that the smoothing of turbulent structures by radiative transfer processes has long been recognized when the sources are thermal and the turbulent field is temperature. As explained theoretically by Spiegel [1957], this effect is traceable to the multiple scattering (hence "non-local") terms in the coupled Navier-Stokes and transfer equations [see also Simonin *et al.*, 1981; Schertzer and Simonin, 1982].

6.5. The Spatially Unresolved Radiation Fields

6.5.1. *Inequalities Amongst the Various Mean Transmittance Estimates*

Figure 6.12 summarizes many of our findings by showing $T_p(\bar{\tau})$, $\overline{T_p(\tau)}$, and T, as functions of $\bar{\tau} = \kappa\bar{\rho}L$ for $\log_2\kappa = -7,\cdots,-3$, and rises some interesting questions as well. Fundamentally, these numbers are all single samples of random variables dependent on the stochastic process that generated the optical medium but the graph leaves little doubt that there are systematic effects at work on a per realization basis. It also shows that, while spatial albedo variability diminishes (cf. fig. 6.11) with increasing $\bar{\tau}$, we see here the gradual enhancement of these systematic radiative effects of inhomogeneity as the degree of multiple scattering (hence nonlinear ρ-I coupling) increases.

We are not surprized to see that (Jensen's) general inequality $\overline{T_p(\tau)} > T_p(\bar{\tau})$ is verified since it is valid for any nonlinear—in this case, convex—function for any type of averaging over any non-degenerate p.d.f. More intriguing is the fact that, at first, most of the overall inhomogeneity effect is captured by the IP calculation, implying that most of the photons have probably not travelled very far laterally between injection and escape or, equivalently, that the net horizontal fluxes remain quite small w.r.t. their vertical counterparts (flux-lines remain quite vertical). As the density increases so is the length (and lateral extent) of the typical photon RW. At the same time, the horizontal-to-vertical net flux ratios increase, implying that the flux lines can diverge more markedly from the vertical. In short, "channeling" (as described and quantified in sect. 2.3) is continually enhanced while the IP correction to the thoroughly plane-parallel calculation goes to a constant ratio (which is not unexpected since κ, like r, only yields a prefactor term in our analytical IP calculations of sect. 5.3). Interestingly, the absolute numbers that measure the net horizontal fluxes are in fact (about twice) larger in the thinnest medium than in the thickest (cf. figs. 6.6–7b) even if their overall contribution to the channeling is lesser; so the local quantitative characterization of channeling is bound to be quite subtle in theory and in experimental situations.

At $\bar{\tau} \approx 200$, we have reached a whole order-of-magnitude ratio between plane-parallel and inhomogeneous results for total transmittance. Such ratios are in step with the worst discrepancies reported in connection with the cloud "albedo paradox:" clouds only rarely attain $R \approx 0.9$ (never 0.99!) while (rescaled) optical thicknesses approaching the hundred are not unheard of (for references and further discussion, see the introductory and concluding chapters). This alone eliminates the plane-parallel—and otherwise quasi-homogeneous—models in favour of their scaling inhomogeneous counterparts. The other inequality we observe, $T > T_p(\bar{\tau})$, can be shown to hold in general (sect. 2.3) and the sharper $T > \overline{T_p(\tau)}$ can also be proven but within a restricted class of media (sect. 2.1) but in both cases for for diffusive transport (i.e., we take $T = T_{dif}$). These inequalities are probably also exact within the framework of DA transfer; no counter-examples have been observed yet in spite of extensive (and yet unpublished) numerical experimentation. One can confidently speculate that, due to the intermediate position of DA transfer ($0 < p < \infty$) within a single parameter continuum going from IPs ($p = 0$) to diffusion ($p = \infty$), there exists a further inequality, $T_{dif} > T = T_{DA}$; this allows us to put bounds on both sides of T_{DA}. These results were summarized and applied in the introductory paragraphs of this chapter.

6.5.2. Inhomogeneity Signatures in the Order-of-Scattering Decompositions

Figs. 6.13 and 6.14a,b illustrate, for transmittance and albedo respectively, the distribution of the (otherwise) unresolved responses according to the photon's order-of-scattering upon exit from the medium (in this case $\bar{\tau}$=12.2). In both cases, we supply (as usual) the corresponding distribution for purely homogeneous media, in this case, with optical thicknesses with integer powers of 2. With this added dimension in the characterization of the radiative responses, we are able to demonstrate a systematic effect we expect of inhomogeneity in general (cf. sect. 4.4) on a particularly spectacular example that we have been analyzing in many other respects throughout this chapter.

We must first familiarize ourselves with this lesser known aspect of the homogeneous benchmarks. Notice how both transmittance ($T^{(n)}$) and reflectance ($R^{(n)}$) "after n scatterings" saturate at $n \approx \tau^2$. This is easily understandable. Indeed, for a standard (finite step size) photon's unbounded RW, a r.m.s. displacement of $\sqrt{n}$ (average) step sizes is attained in n steps and, being an additive process, this is a case of "simple" scaling, i.e., with well-behaved statistics (see sect. D.3 for further details). Conversely, a RW bounded in a region of size τ (steps) will almost surely have reached a boundary after τ^2 steps (or scatterings).[21] It is in the lower orders-of-scattering that we see an enormous difference between the two responses. Pedictably, $T^{(n)}$ scales directly with n and inversely with (large enough) τ: i.e., the graphs are linear in a log/log plot (such as fig. 6.13) and, moreover, the graphs are equidistant. Somewhat more surprisingly, the increase of $R^{(n)}$ w.r.t. n is independent of τ (again, if large enough); this is due to the fact that RWs that contribute to R all start and end at the top boundary hence those with a relatively short number of steps almost never get anywhere close to the bottom boundary and the corresponding $R^{(n)}$ statistic is insensitive to its position (namely, at relative depth τ, in average steps). Notice that fig. 6.14a is plotted in semi-logarithmic coordinates; not too surprisingly, we find a very regular scaling regime when we graph $1-R^{(n)}$, the radiation not reflected (but possibly transmitted) after n scatterings, versus n in the log-log plot used in fig. 6.14b. The well-known (Laplace transformation) connection between (in this case, homogeneous) absorption response w.r.t. ϖ_0 (or a) and the order-of-scattering distributions of course totally determine the various details of the above scalings relationships.

We see in fig. 6.13 that, compared to a homogeneous medium with $\tau=\bar{\tau}\approx12.2$, the lower[22] orders-of-scattering in transmittance for the multifractal are enhanced beyond recognition (i.e., the homogeneous cases are found way below the range of transmittancies actually illustrated in the figure). Recall from our analytical results in chap. 5 that we expect non-vanishing direct transmittance through multifractal density fields (in the optically thick regime) and that this has already been observed in fig. 6.4b. In sharp contrast to this, the multifractal has an $R^{(1)}$ very similar to the universal thick cloud value for homogeneous media, namely,[23] $r/2$ (=1/8, here). As soon as $n\geq2$, higher-dimensional, nonlinear effects become obvious in the albedo's decomposition: in essence, lesser $R^{(n)}$ values are observed for the multifractal due to the greater penetration depth at first incidence, making transmittance more likely, even for very low order scattering (in fact, as soon as the 0^{th} scattering). At the higher orders-of-scattering end of the figures, both of the multifractal's responses saturate at values that characterize a homogeneous optical medium of $\approx1/3$ the overall average density (i.e. $\tau\approx4$). In both low- and high n regimes and in both T ($n\geq0$) and R ($n\geq2$), we are witnessing different effects of "channeling" (as described and used in the Introduction and in sect. 4.4): i.e., the longer-than-homogeneously-predicted f.p.'s anticipated in sect. A.2 make the boundaries more easily (hence "sooner") reached during photon's RW. Finally and maybe most importantly, the multifractal's responses saturate at a value of n that is not significantly greater than $\bar{\tau}^2$ (as for homogeneous media) but the transition towards saturation is much slower; in other words, the n-distribution has been not only considerably displaced but also much broadened by the extreme multifractal inhomogeneity.[24]

†This chapter is largely based on Davis *et al.* [1991]. S.L. and D.S. originated the idea of looking at radiation fields associated with multifractals, A.D. is entirely responsible for the programming, the validation of the two basic codes (Monte Carlo and relaxation), most of the the data manipulation, all of the visualization work, as well as for the idea of looking at the formal eigenvector fields rather than the radiances, and virtually all of the preliminary analysis in sect. 6.3–5.

1 A partnership of *Météo-France* (whom we gratefully acknowledge) and several other french governmental scientific or technological agencies situated on the premises of the *École Polytechnique* in Palaiseau (Hauts-de-Seine).

2 To some extent, the same can be said about the use of a discrete (rather than a continuous) cascade since we will benefit visually (if not esthetically) from the persistent grid structure which provides a template that facilitates cross-referencing with the eye.

3 The proper usage would be [Titov, 1990] random "linear functionals" of the stochastic process used to generate the random optical density fields.

4 This excludes the optional order the fractional integration which is normally related to the previously mentioned passive scalar phenomenology.

5 Another reason, that has now become obsolete, is that exactly unitary centered Gaussian deviates can be efficiently generated from two independent random variables uniformly distributed on]0,1[, say ξ and ξ', by the well-known Box-Muller transformation: $\sqrt{-2\ln\xi}\cos(2\pi\xi')$. If convenient, a second (independent) Gaussian deviate is given by $\sqrt{-2\ln\xi}\sin(2\pi\xi')$. It has recently been realized [B. Watson, p.c.] that similar transformations exist for Lévy deviates [Zoltarev, 1986] hence numerically inefficient sums of algebraic (or Pareto) deviates are no longer necessary.

6 With $C_1=0.5$, the criterion for divergence of statistical moments after "dressing" the fully developed cascade field (namely, $C(h) \geq D_A$, the fractal dimension of the averaging set A) yields critical moments of order 2 and 4 respectively for averaging the unique realization over one- and two-dimensional sets.

7 There is nothing special about this realization (it was not selected for "representativeness"); we just used a very simple (easily remembered) "seed" to prime the (on line) pseudo-random number generator.

8 Although this is only one realization, part of the discrepancy can be accounted for by incorporating the extra term in the exact finite λ expression for $c(\gamma)$, quoting from app. C:

$-\log_\lambda\sqrt{\ln\lambda/2\pi\sigma^2}=-\log_\lambda\sqrt{\ln\lambda/4\pi C_1\ln\lambda_0}=-\ln(n/4\pi C_1)/2n$ (where n is the number of cascade steps).

9 Another classical way of determining C_1 uses the intermittancy corrections to the velocity (not dissipation) spectrum, i.e., the discrepancy between -5/3 and observed exponent. Again, $C_1=0.5$ is somewhat in excess of the values quoted in the literature. Schmitt *et al.* [1992], using the more sophisticated "DTM" scaling analysis techniques, find $C_1=0.2$–0.3 but for $\alpha\approx1.4$ within the universal multifractal scheme where the log-normal model used here is associated with $\alpha=2$; see sect. C.5 for further details.

10 See Stanley and Meakin [1988] for an illustration of the sampling requirements using the example of a simple multiplication of random variables.

11 In the Monte Carlo scheme, we simply "recycle" photons from one side of the medium to the opposite.

12 This overall response is denoted with a "DA" subscript in the introductory paragraphs of this chapter.

13 The notation is made less cumbersome here than in the introductory paragraphs of this chapter where the subscript "homo" was used, here we use "p" which stands for "plane-parallel" but we should always be adding horizontally homogeneous (since all of these horizontally extended media are bounded by two horizontal planes).

14 This is precisely what happened in the context of diffusion on percolation fractals where statistical (random walk) approaches based on "ants," "termites," and more general "diffusing" particles (cf. §D.6.3) supersedes, to a large extent, transfer matrix and other steady-state methods.

15 For instance, the strong vertical gradients imposed by these BCs preclude the direct statistical comparison of the J's (hence, to some extent, the radiances) at different levels in the cloud; J is not a statistically stationary field except w.r.t. purely horizontal displacements (the same remark applies to all the radiances). Removing the known linear trend corresponding to homogeneity does not help because it is not equivalent to the ensemble-average $\langle J(z)\rangle$, which is probably not even linear.

16 More precisely, the King *et al.* [1990] determine the optical altitude of the aircraft $\tau_y'(z) = \int_z^L \kappa\rho(y,z')dz'$.

[17]For these figures 10^6 photons were used in all (but for the internal field calculations, 10^4 photons/pixel were used, 10,240,000 in all). To obtain the units used in figs. 6.8–9b,c, one must divide the result by $\lambda^2=2^{20}$, equivalently, remove 20 after taking the $\log_2$'s.

[19]Here we are pushing our single realization strategy to the limit. In principal, there is no point in trying to "explain" the particular value of the radiation field at any point in a stochastic medium since it is a random functional of the density distribution and only ensemble averages are of any real significance.

[20]Barker and Davies [1992] present another example of a scaling but very smooth radiation field associated, in this case, with a Schertzer and Lovejoy [1987] passive scalar cloud model, which is already a much smoothed version of the (bare) kind of multifractal used here (via fractional integration of order 1/3).

[21]This criterion is used as a control parameter in our Monte Carlo simulations to avoid wasting a lot of computer time on exceptionally "slow"—and basically non-representative—photons (see sect. B.1).

[22]In DA the non-trivial higher-dimensional effects (i.e., the "channeling") call for at least two scatterings. We can therefore obtain analytically the 1st order scattering term in transmittance: $T^{(1)} = t\tau e^{-\tau}$ in each column (which is independent of all others for this response, as is the case of $T^{(0)}=T_d$). Notice how this expression very quickly vanishes with increasing τ, in homogeneous cases. However, in inhomogeneous cases, a spatial average must be taken and, as for T_d (cf. §5.1.1 and fig. 6.4d), we can expect very "non-average" behaviour with multifractals.

[23]The same remark as above applies to the 1st order scattering term in reflectance: $R^{(1)} = r(1-e^{-2\tau})/2$ in each column (again independently of all others w.r.t. this response). This expression very quickly becomes r/2 with increasing τ, in homogeneous cases. In inhomogeneous cases, a spatial average must again be taken but for thick multifractals $<1-e^{-2\tau}>\approx 1$, so the (thick) homogeneous $R^{(1)}$ is even representative of these.

[24]Barker [1992] presents very similar findings using a Monte Carlo simulation technique that directly uses a real cloud LWC probing rather than any specific inhomogeneity model.

Bibliography for Chapter 6

Barker, H. W., "Radiative Transfer Through Clouds Possessing Isotropic Variable Extinction Coefficient," submitted to *Q. J. R. Meteorol. Soc.*, 1992.

Barker, H. W., and J. A. Davies, "Radiative Transfer, Cloud Structure, and the Characteristics of Satellite Radiance Wavenumber Spectra," submitted to *Rem. Sens. of Environ.*, 1992.

Cahalan, R. F., and J. B. Snider, "Marine Stratocumulus Structure," *Remote Sens. Environ.*, 28, 95–107, 1989.

Cannon, C. J., "Line Transfer in Two Dimensions," *Astrophys. J.*, 161, 255–264, 1970.

Corssin, S., "On the Spectrum of Isotropic Temperature Fluctuations in Isotropic Turbulence," *J. Appl. Phys.*, 22, 469–473, 1951.

Davis, A. B., S. Lovejoy, and D. Schertzer, "Discrete angle radiative transfer in a multifractal medium," *S.P.I.E. Proceedings*, 1558, 37–59, 1991.

Davies, R., "The effect of finite geometry on three-dimensional transfer of solar irradiance in clouds," *J. Atmos. Sci.*, 35, 1712–1724, 1978.

Fouquart, Y., J. C. Buriez, M. Herman, and R. S. Kandel, "The influence of clouds on radiation: A climate modelling perspective," *Rev. of Geophys.*, 28, 145–166, 1990.

Kargin, B. A., G I. Mikhailov, M. A. Nazaraliev, and K. K. Sabalfeld, "Vector Algorithms and Randomization of Monte Carlo Methods," in *Problems of Computational Mathematics and Mathematical Modelling*, Ed. G.I. Marchuk and V.P.Dymnikov, Mir, Moscow, 1985.

King, M. D., L. F. Radke, and P. V. Hobbs, "Determination of the Spectral Absorption of Solar Radiation by Marine Stratocumulus Clouds from Airborne Measurements within Clouds," *J. Atmos. Sci.*, 47, 894–907, 1990.

Kolmogorov, A. N., "A Refinement of Previous Hypothesis Concerning the Local Structure of Turbulence in Viscous Incompressible Fluid at High Reynolds Number," *J. Fluid Mech.*, 13, 82–85, 1962.

Lavallée, D., D. Schertzer, and S. Lovejoy, "On the Determination of the Codimension Function," in *Scaling, Fractals and Non-Linear Variability in Geophysics*, Eds. D. Schertzer and S. Lovejoy, Kluwer, Hingham (Mass.), 1991.

Lovejoy, S., and D. Schertzer, "Multifractals, Universality Classes and Satellite and Radar Measurements of Cloud and Rain Fields," *J. Geophys. Res.*, 95, 2021–2034, 1990.

Lovejoy, S., A. B. Davis, P. Gabriel, D. Schertzer, and G. L. Austin, "Discrete Angle Radiative Transfer - Part I: Scaling and Similarity, Universality and Diffusion," *J. Geophys. Res.*, 95, 11699-11715, 1990.

McKee, T.B., and J.T. Cox, "Scattering of visible light by finite clouds," *J. Atmos. Sci.*, 31, 1885–1892, 1974.

Meador, W. E., and W. R. Weaver, "Two-Stream Approximations to Radiative Transfer in Planetary Atmospheres: A Unified Description of Existing Methods and a New Improvement," *J. Atmos. Sci.*, 37, 630–643, 1980.

Monin, A. S., and A. M. Yaglom, *Statistical Fluid Mechanics*, vol. 2, MIT press, Boston, Mass., 1975.

Novikov, E. A., and R. Stewart, "Intermittancy of Turbulence and Spectrum of Fluctuations in Energy Dissipation," *Izv. Akad. Naut. SSSR, Ser. Geofiz.*, 3, 408–412, 1964.

Obukhov, A., "Structure of the Temperature Field in a Turbulent Flow," *Izv. Akad. Naut. SSSR, Ser. Geogr. I Geofiz.*, 13, 55–69, 1949.

Obukhov, A., "Some Specific Features of Atmospheric Turbulence," *J. Geophys. Res.*, 67, 3011–3014, 1962.

Schertzer, D., and O. Simonin, "A theoretical study of radiative cooling in homogeneous and isotropic turbulence," in *Turbulent Shear Flow, vol. 3*, edited by L.J.S. Bradbury et al., Springer, New York, NY, pp. 262–274, 1983.

Schertzer, D., and S. Lovejoy, "Physically Based Rain and Cloud Modeling by Anisotropic, Multiplicative Turbulent Cascades," *J. Geophys. Res.*, 92, 9693–9714, 1987.

Schertzer, D., and S. Lovejoy, "Scaling Nonlinear Variability in Geodynamics: Multiple Singularities, Observables and Universality Classes," in *Scaling, Fractals and Non-Linear Variability in Geophysics*, Eds. D. Schertzer and S. Lovejoy, 41–82, Kluwer, Hingham (Mass.), 1991.

Schertzer, D., and S. Lovejoy, "Hard and Soft Multifractal Processes," *Physica A*, in press, 1992.

Schmitt, F., D. Lavallée, D. Schertzer and S. Lovejoy, "Empirical Determination of Universal Multifractal Exponents in Turbulent Velocity Fields," *Phys. Rev. Lett.*, 68, 305–308, 1992.

Simonin, O., M. F. Coantic, and D. Schertzer, "Effet du rayonnement infrarouge sur la turbulence de température dans l'atmosphère: Structure spectrale et taux de dissipation," *C.R. Acad. Sci.*, *293*, 245–248, 1981.

Spiegel, E. A., "The smoothing of temperature fluctuations by radiative transfer," *Astrophys. J.*, *126*, 202–207, 1957.

Stanley, H. E., and P. Meakin, "Multifractal phenomena in physics and chemistry," *Nature*, 335, 405–409, 1988.

Stephens, G. L., "Radiative Transfer in Spatially Heterogeneous, Two-Dimensional Anisotropically Scattering Media," *J. Quant. Spectrosc. Radiat. Transfer*, 36, 51–67, 1986.

Stephens, G. L., "Radiative Transfer Through Arbitrarily Shaped Media - Part 1: General Theory," *J. Atmos. Sci.*, 45, 1818–1835, 1988.

Tessier, Y., S. Lovejoy, and D. Schertzer, "Universal Multifractals: Theory and Observations for Rain and Clouds," submitted to *J. Appl. Meteo.*, 1992.

Titov, G. A., "Statistical Description of Radiation Transfer in Clouds," *J. Atmos. Sci.*, 47, 24–38, 1990.

Tsay, S. C. and K. Jayaweera, "Characteristics of Arctic Stratus Clouds," *J. Climate Appl. Meteor.*, 23, 584–596, 1984.

Wilson, J., D. Schertzer, and S. Lovejoy, "Continuous Multiplicative Cascade Models of Rain and Clouds," in *Scaling, Fractals and Non-Linear Variability in Geophysics*, Eds. D. Schertzer and S. Lovejoy, 185–207, Kluwer, Hingham (Mass.), 1991.

Zoltarev, V. M., *One-dimensional Stable Distributions*, Translations of Mathematical Monographs, Americ. Math. Soc., Providence, Rh.I., 1986.

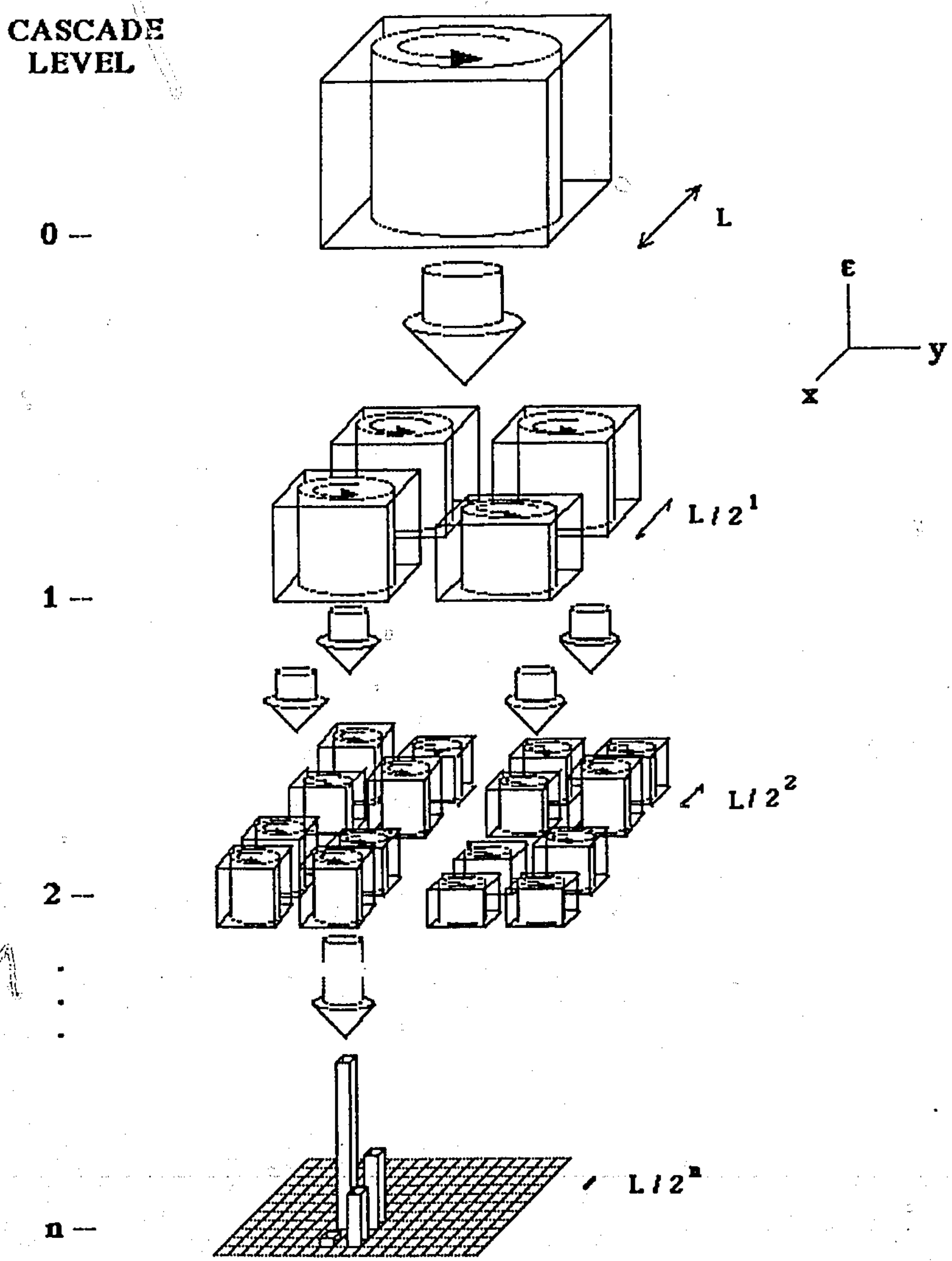

Figure 6.1: Theoretical c(γ) codimension function the (bare) cascade process illustrated in Fig. 6.2. Notice the remarkable values of γ: $\gamma_1 = +C_1$, $\gamma_{1/2} = 0$, $\gamma_0 = -C_1$ (see text and/or caption of Fig. 6.3 for a discussion of their importance).

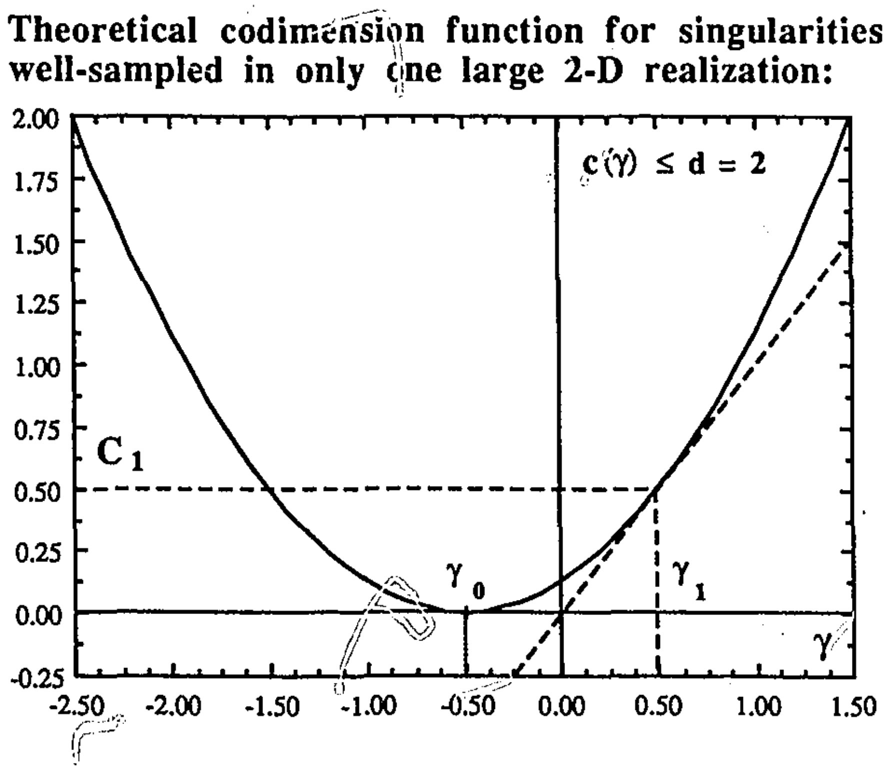

Figure 6.2: Linear grey-scale map of the orders of singularity for the adopted log-normal multifractal density field, with $C_1 = 0.5$ in $d = 2$ after $n = 10$ discrete ($\lambda_0 = 2$) cascade steps (see text for details on the highlighted γ-values).

Figure 6.2: Linear grey-scale map of the orders of singularity for the adopted log-normal multifractal density field, with $C_1 = 0.5$ in $d = 2$ after $n = 10$ discrete ($\lambda_0 = 2$) cascade steps (see text for details on the highlighted γ-values).

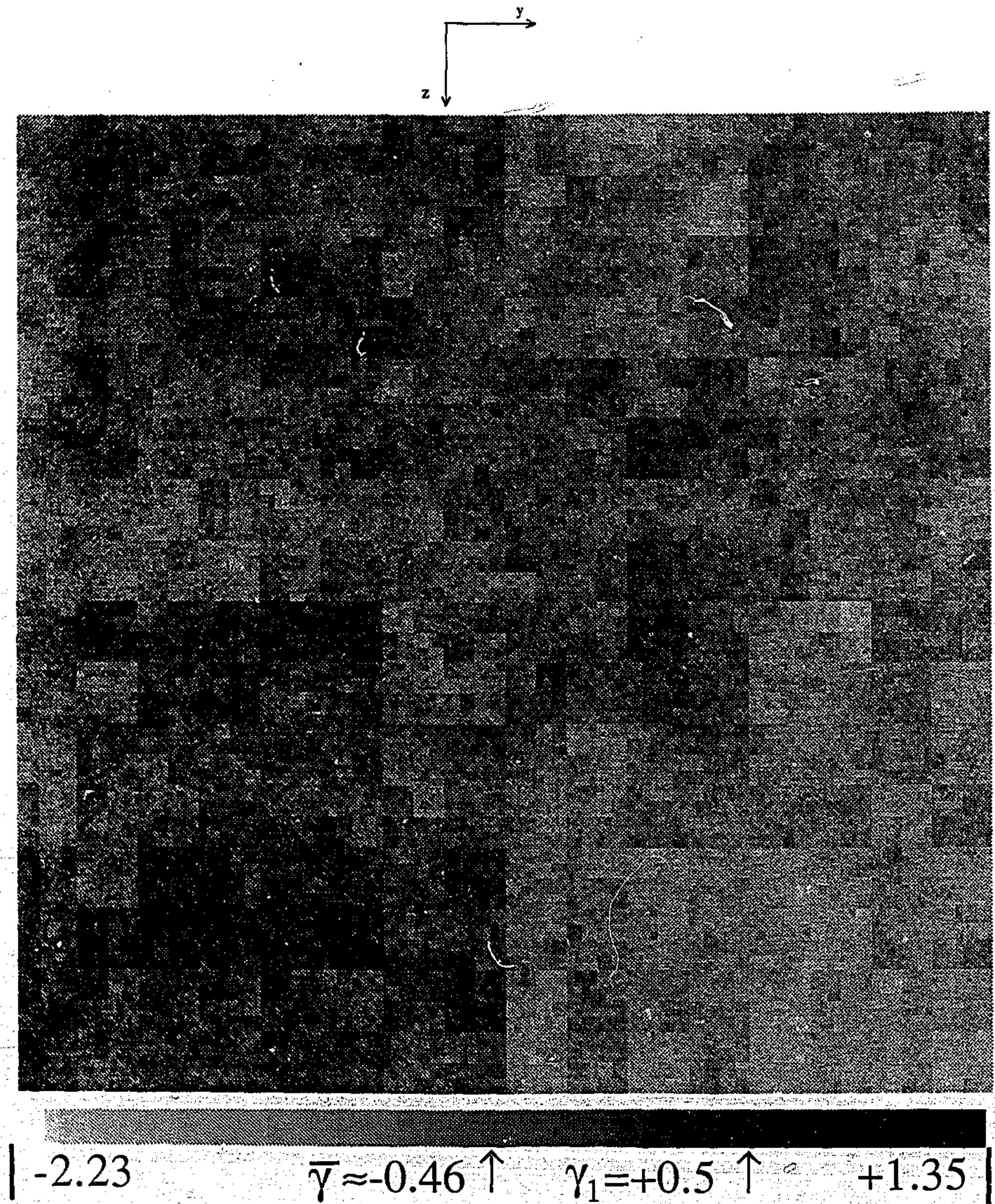

Figure 6.3a: Exceedance set for $\gamma = \gamma_1 = +C_1 = 0.5$ ($\rho = \lambda^{\gamma} = 32$), the singularity that contributes most to the average $<\rho>$); the fractal dimension is $D_1 = d\text{-}c(\gamma_1) = 2.5$ (see text for more details).

Figure 6.3b: Same as Fig. 6.3a but for $\gamma = \gamma_{1/2} = 0$ ($\rho = \lambda^{\gamma} = 1$), the neutral singularity, corresponding to the numerical value of $<\rho>$ which is 1; the fractal dimension is $D_{1/2} = d\text{-}c(\gamma_{1/2}) = 2.875$ (see text for more details).

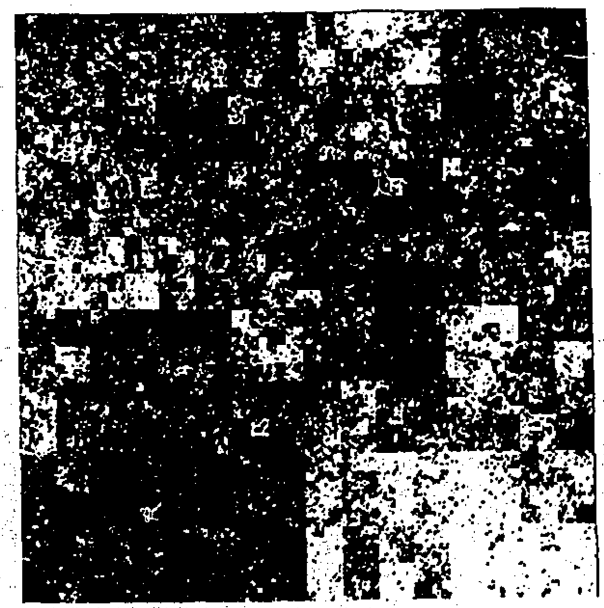

Figure 6.3c: Same as Fig. 6.3a but for $\gamma = \gamma_0 = -C_1 = -0.5$ ($\rho = \lambda^{\gamma} = 1/32$), the most probable singularity although, being of a negative order, it is in fact a "regularity;" the fractal dimension is $D_0 = d\text{-}c(\gamma_0) = 2$, this singularity fills two-dimensional space (see text for more details).

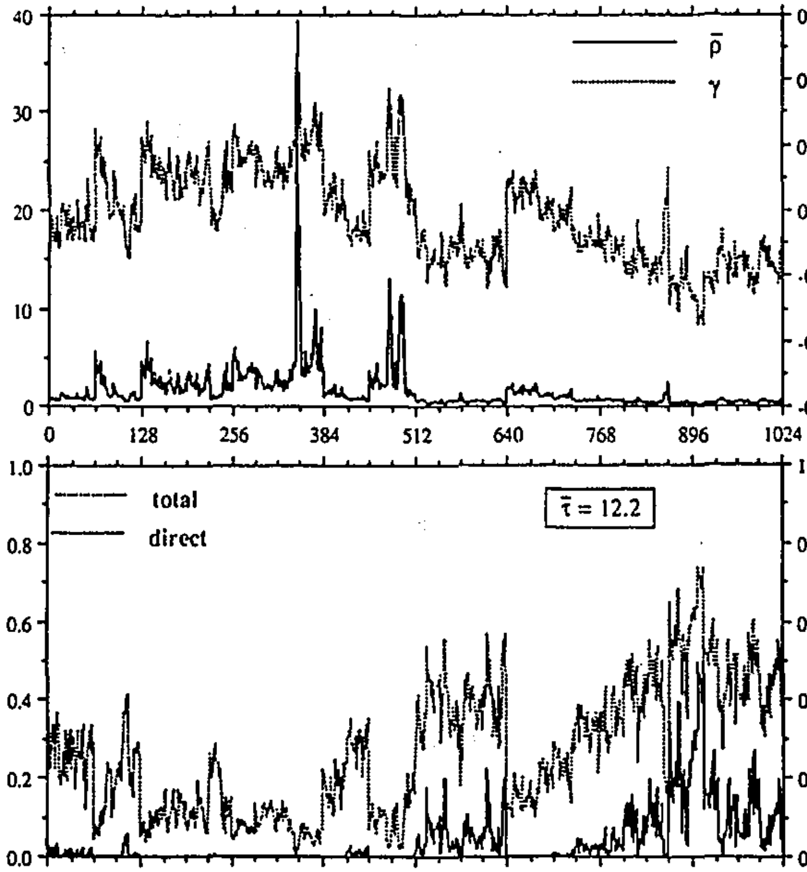

Figure 6.4: (a) Column-averaged densities and corresponding orders of singularity, (b) "independent pixel" responses (direct and total transmittances) for the thinner cloud, with $\kappa = 2^{-7}$. See text for comments, on higher κ-values in particular.

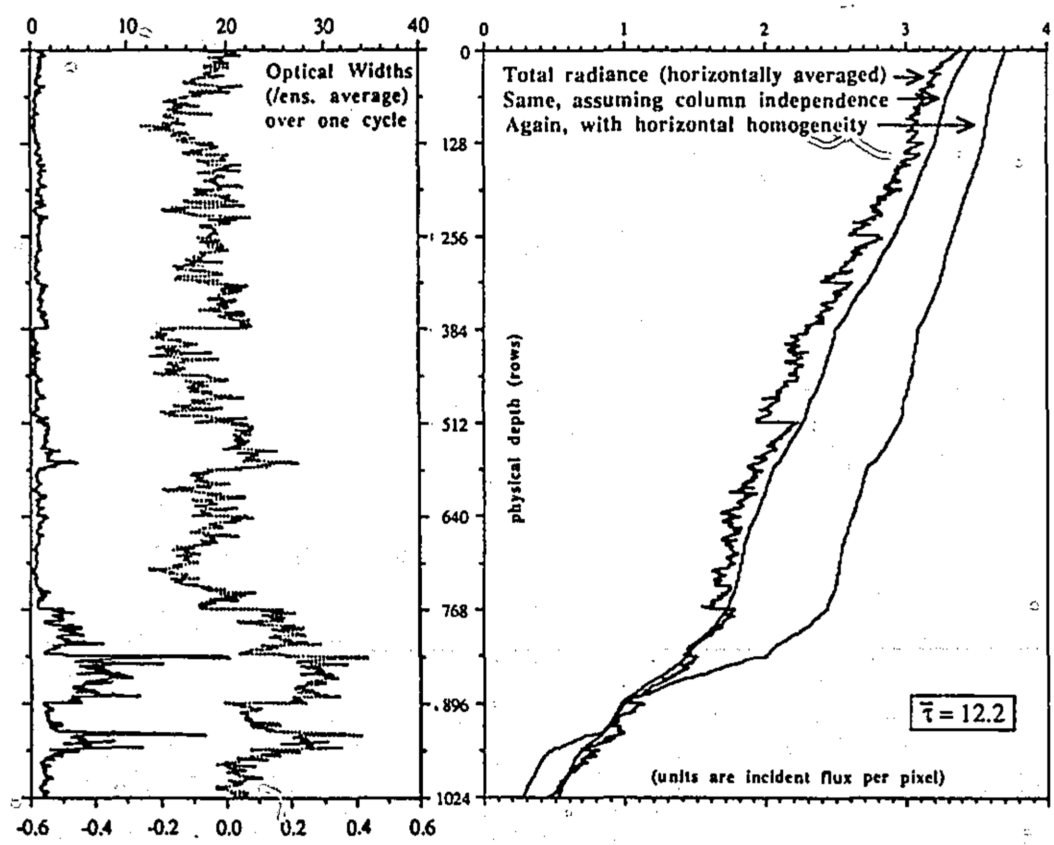

Figure 6.5: (a) Same as Fig. 6.4a but for row-averages, (b) row-averaged internal fields of total radiance(homogeneous layers, independent pixels, numerical solution).

Figure 6.6 (begin.): DA radiance fields in eigen-vector decomposition for $\overline{\tau}$ = 12.2 ($\log_2\kappa$ = -7): (a) J.

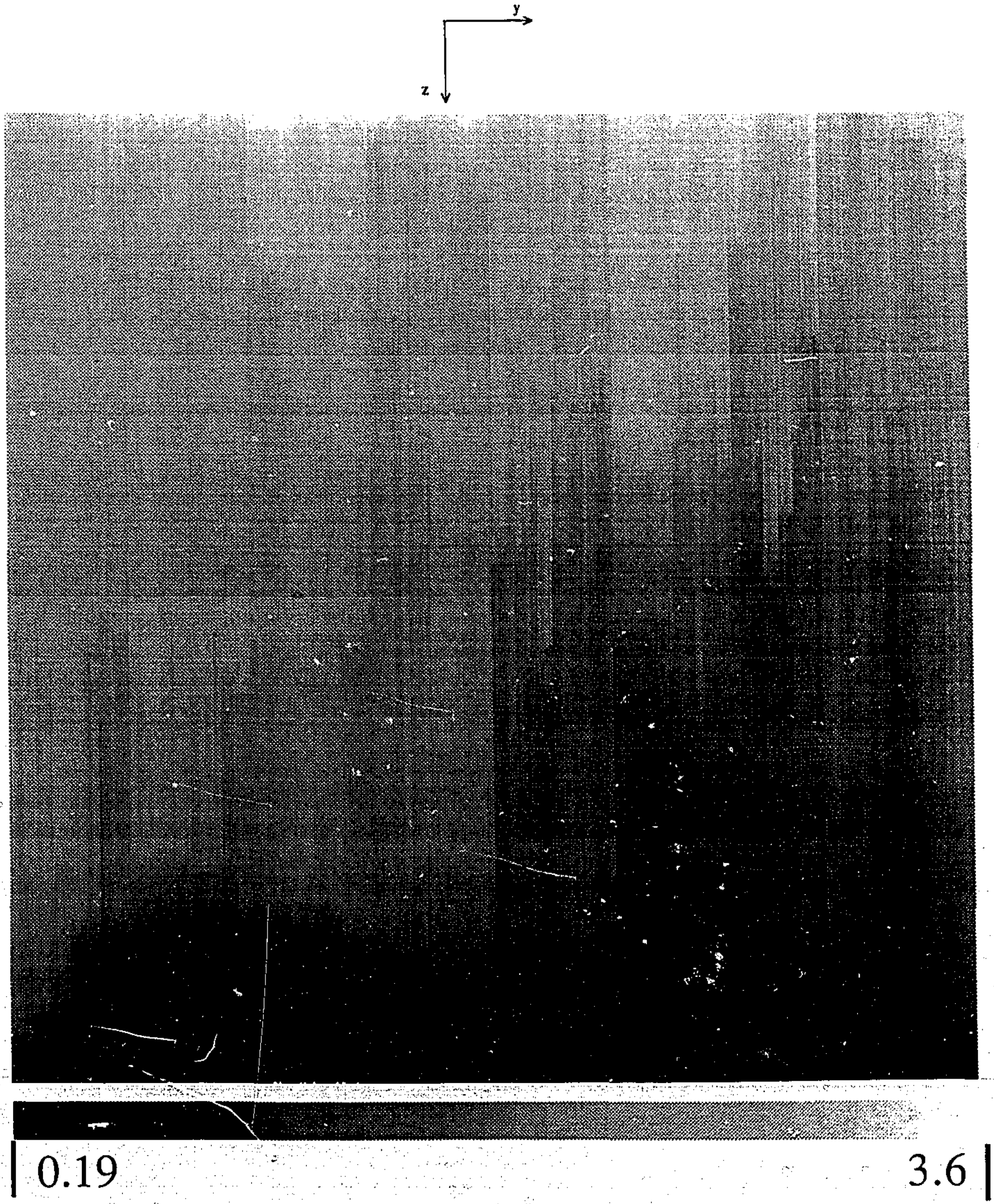

Figure 6.6 (cont'd): DA radiance fields in eigen-vector decomposition for $\overline{\tau}$ = 12.2 ($\log_2\kappa$ = -7): (b) F_y.

Figure 6.6 (cont'd): DA radiance fields in eigen-vector decomposition for $\overline{\tau}$ = 12.2 ($\log_2\kappa$ = -7): (b') F_z.

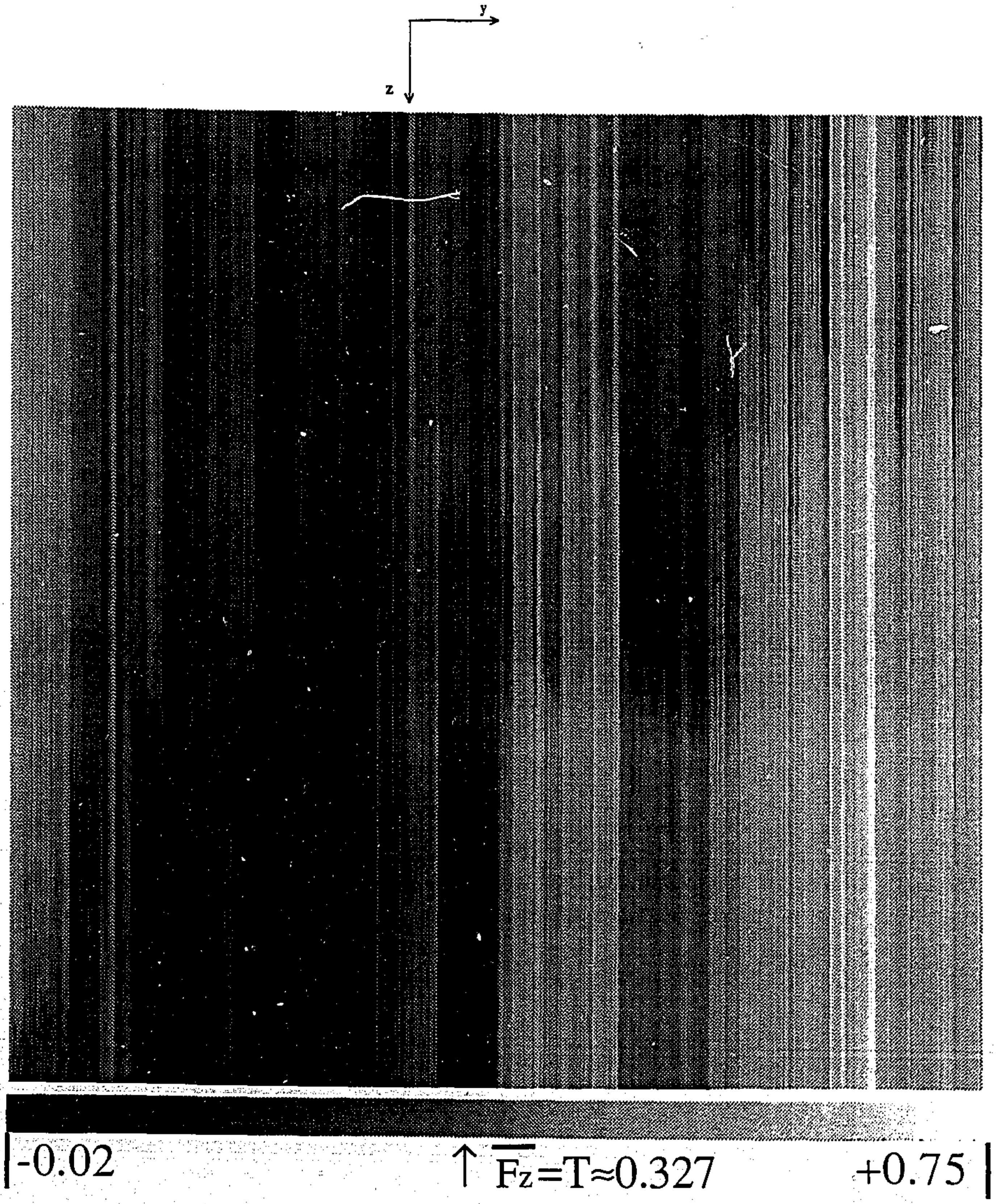

Figure 6.6 (end): DA radiance fields in eigen-vector decomposition for $\overline{\tau}$ = 12.2 ($\log_2\kappa$ = -7): (c) X.

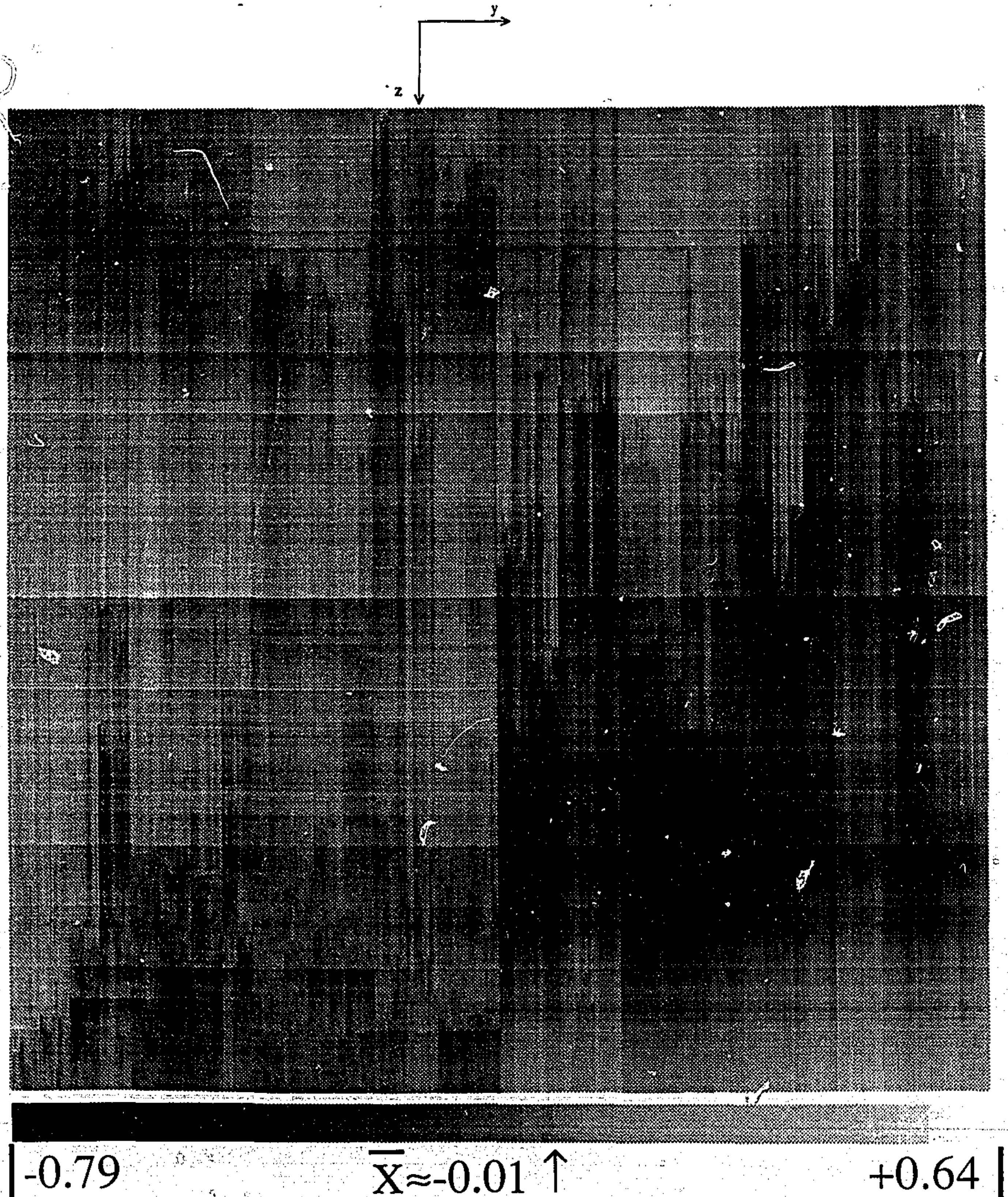

Figure 6.7 (begin.): DA radiance fields in eigen-vector decomposition for $\overline{\tau}$ = 195 ($\log_2\kappa$ = -3): (a) J.

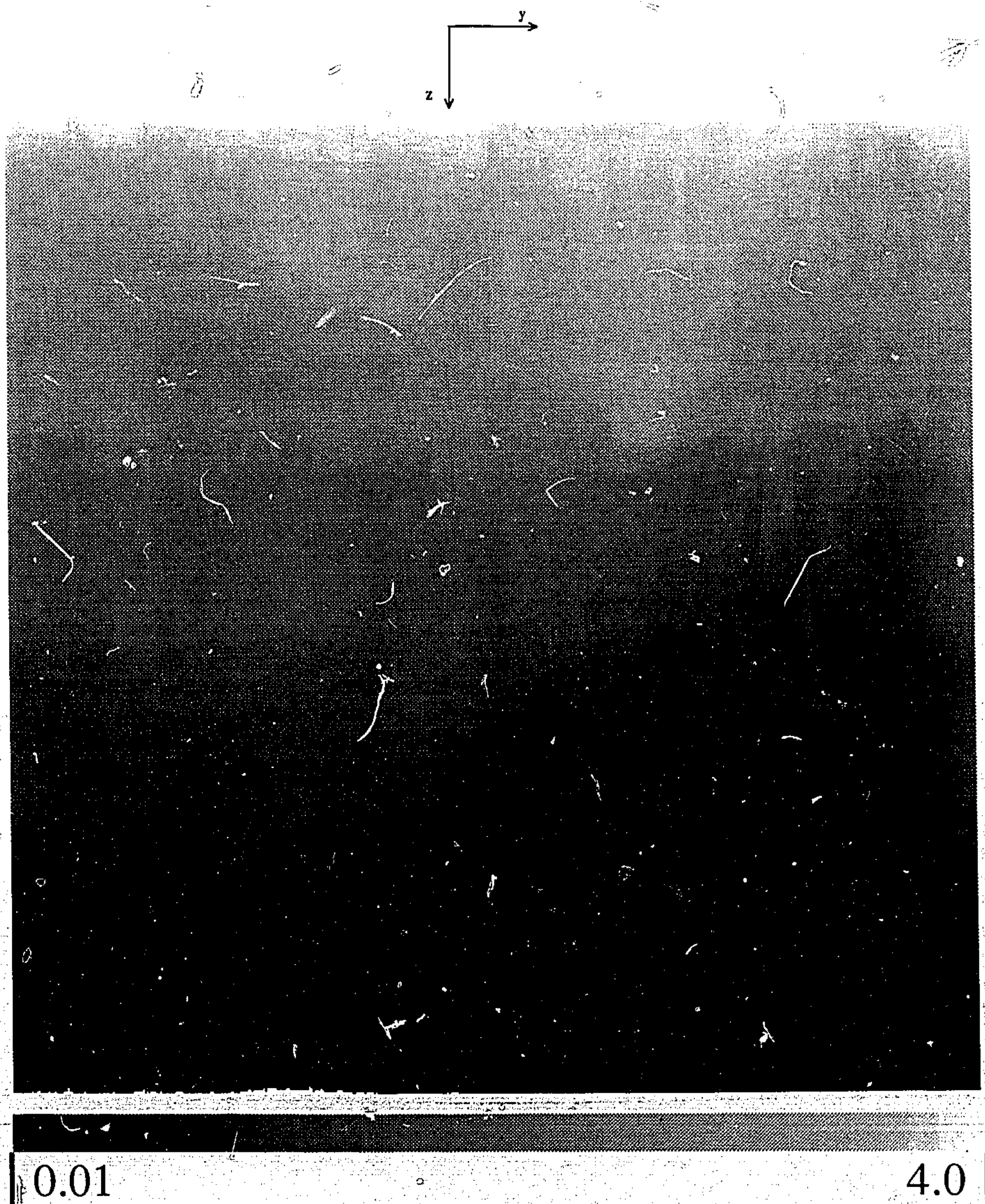

Figure 6.7 (cont'd): DA radiance fields in eigen-vector decomposition for $\overline{\tau}$ = 195 ($\log_2\kappa$ = -3): (b) F_y.

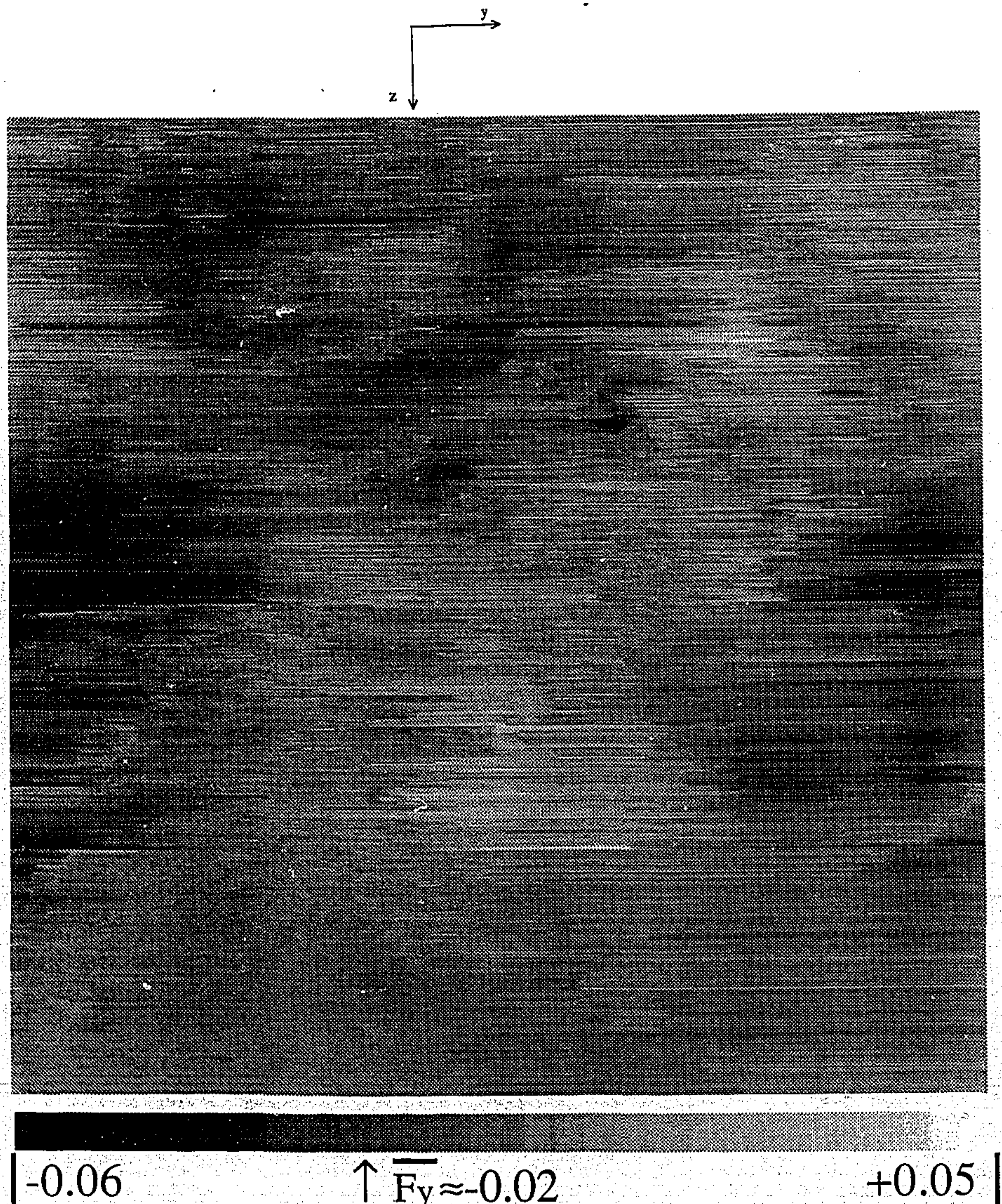

Figure 6.7 (cont'd): DA radiance fields in eigen-vector decomposition for $\overline{\tau}$ = 195 ($\log_2\kappa$ = -3): (b') F_z.

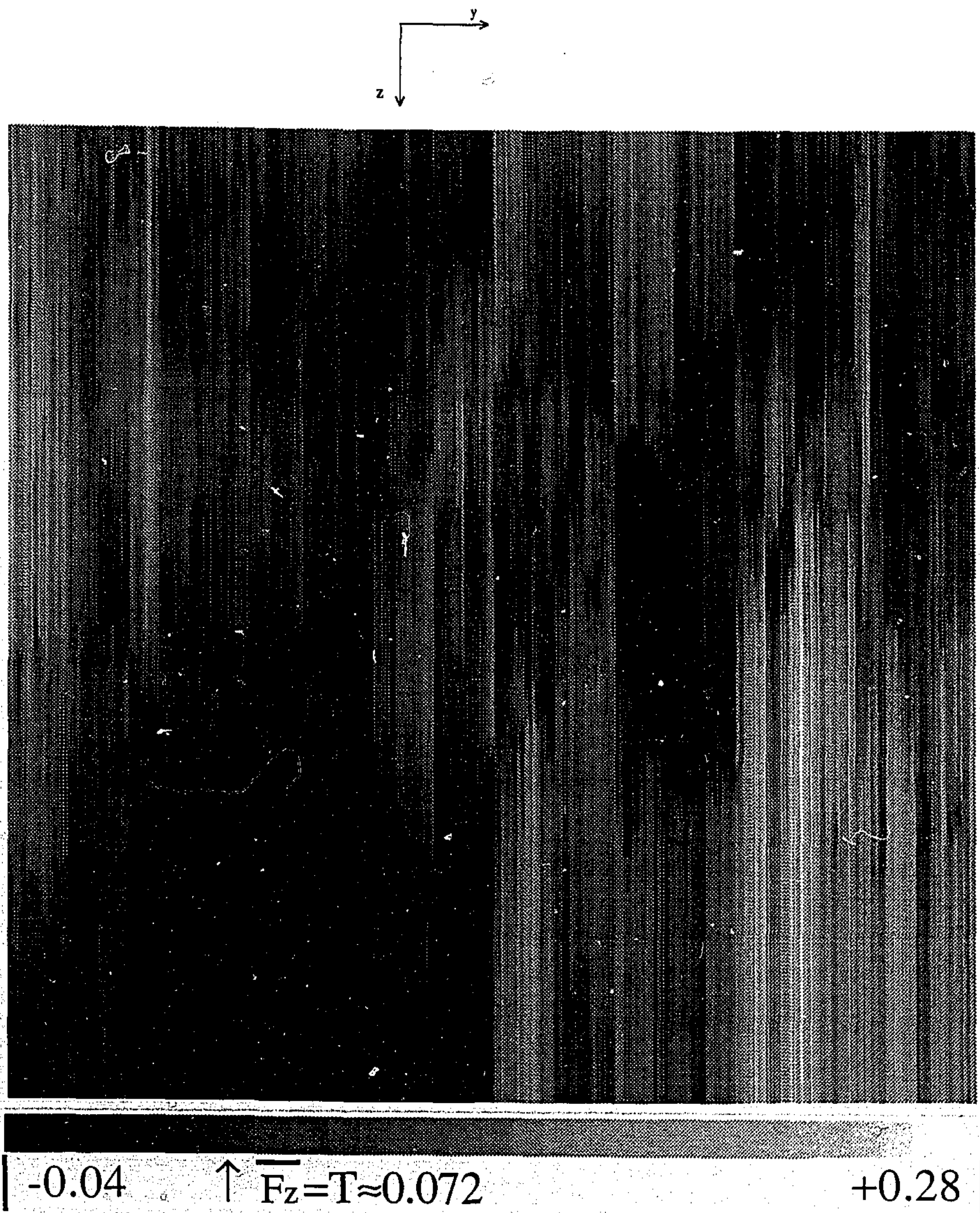

Figure 6.7 (end): DA radiance fields in eigen-vector decomposition for $\overline{\tau}$ = 195 ($\log_2\kappa$ = -3): (c) X.

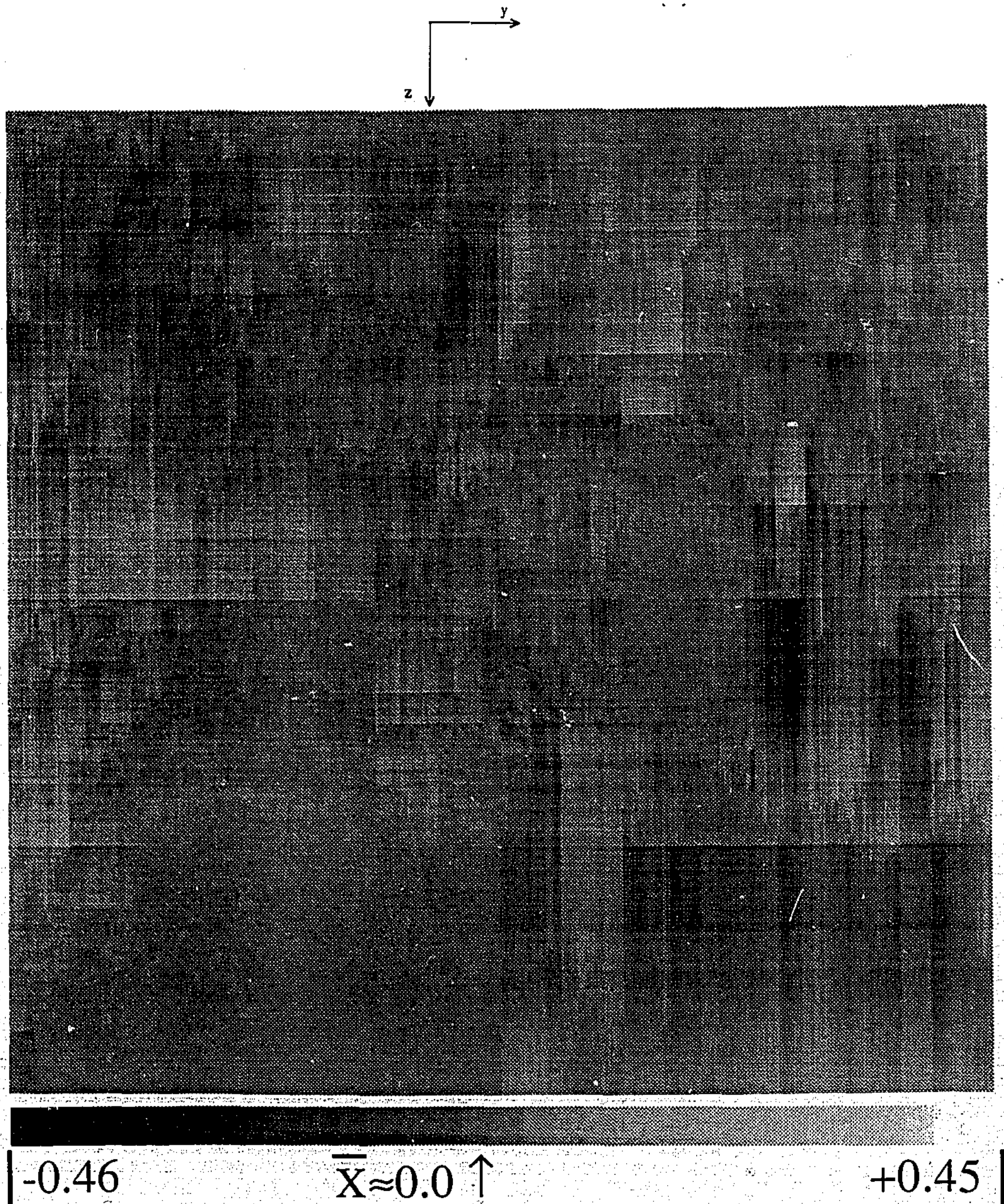

Figure 6.8: (a) Monte Carlo DA reflectance R(y) and transmittance T(y) fields and (b), (c) their respective power spectra, for $\overline{\tau} = 12.2$. Numerical noise levels are indicated for the spectra.

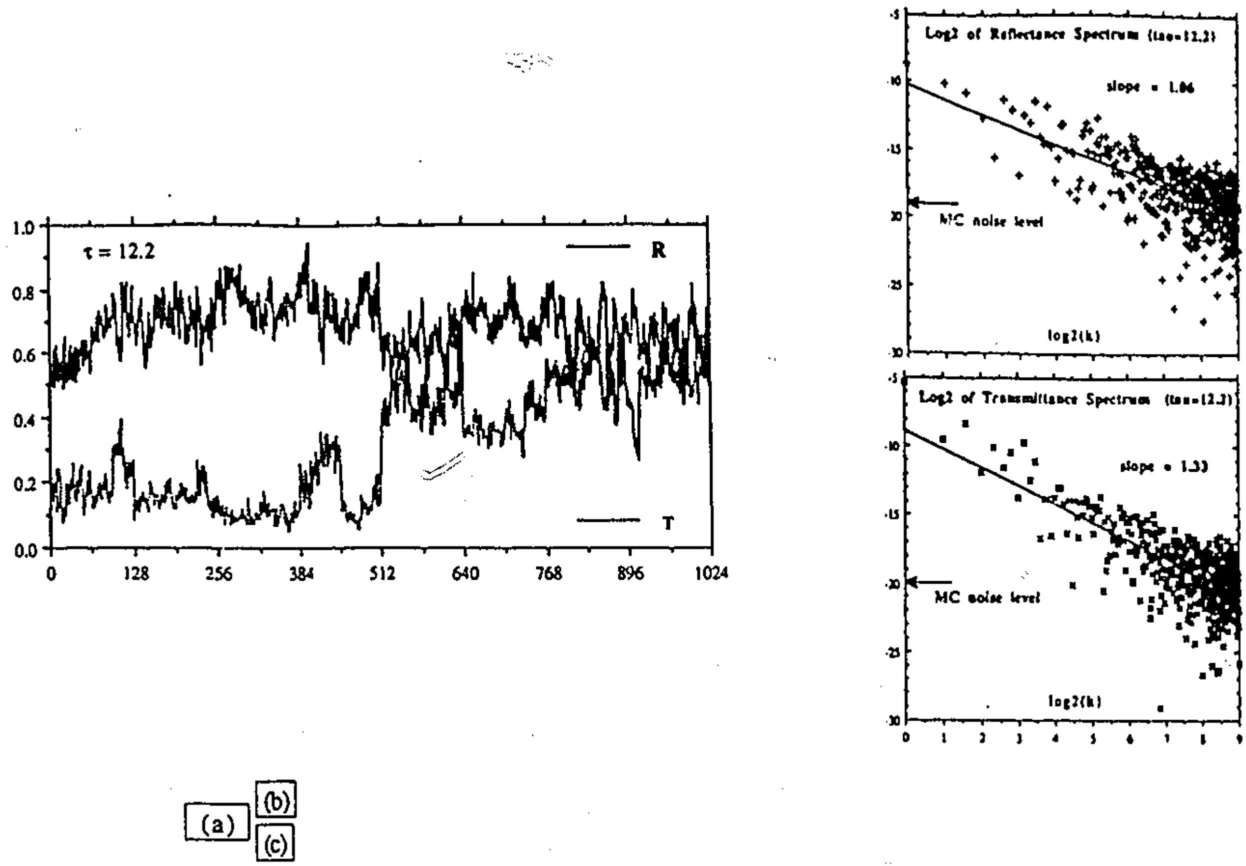

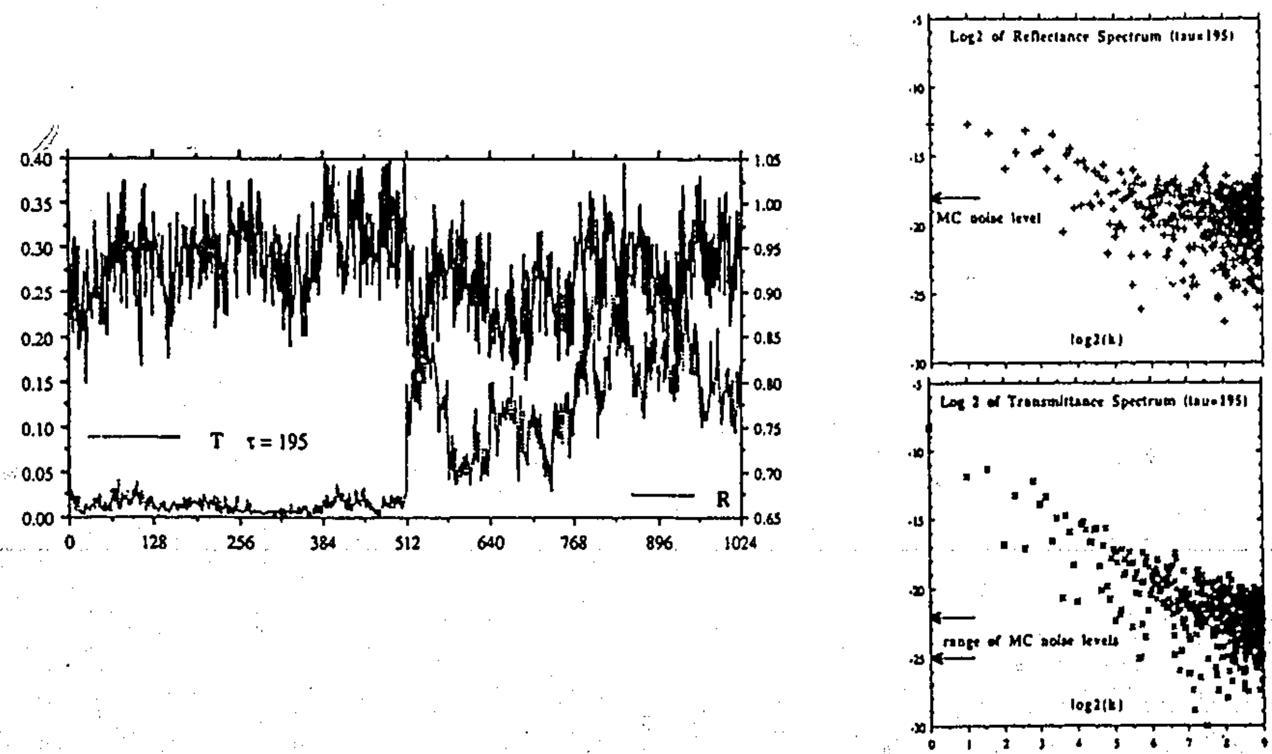

Figure 6.9: Same as Figs. 6.8a,b,c but for $\overline{\tau} = 195$. Note that for transmittance a range of Monte Carlo noise levels is indicated.

Figure 6.10a: Relaxation DA reflectance R(y) and transmittance T(y) fields, for $\bar{\tau} = 12.2$

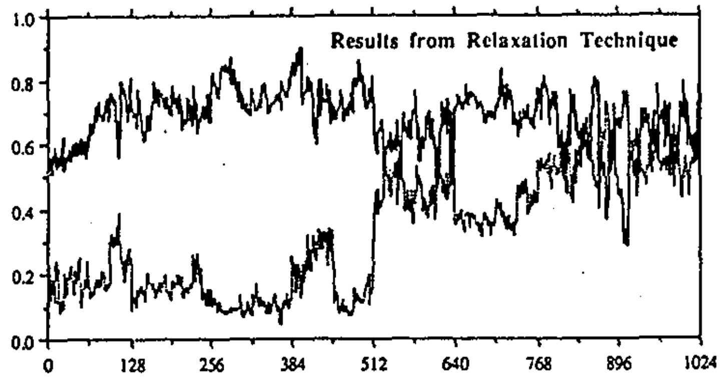

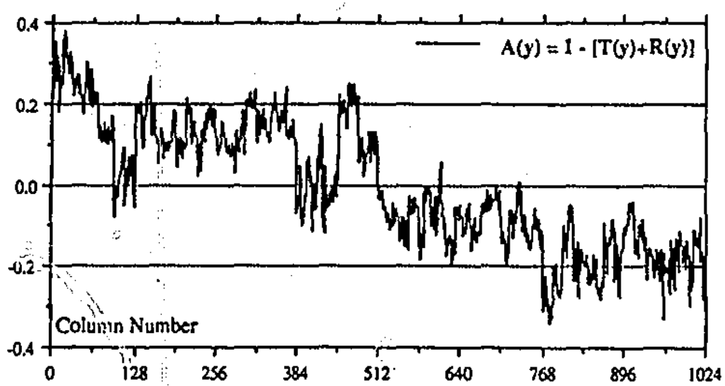

Figure 6.10b: Apparent absorptance A(y) = 1 - [R(y)+T(y)] corresponding to Fig. 6.10a.

Figure 6.11: Histograms of R(y) for the five different values of κ plotted in multifractal variables $c(\gamma_R) = \log_\lambda(\text{p.d.f.})$ versus $\gamma_R = \log_\lambda(R/\langle R\rangle)$ where $\langle R\rangle$ is taken as the spatial average for this realization. Notice the narrowing of the distribution as κ increases as well as the decrease in skewness.

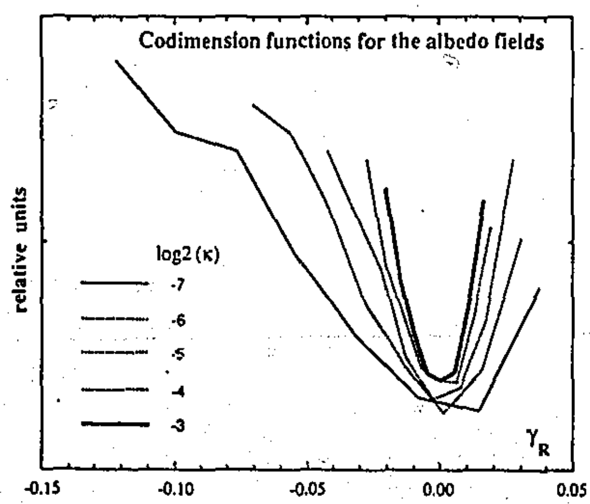

Figure 6.12: Overall transmittancies of the multifractal cloud for the five different optical thicknesses and three different methods of calculation. From bottom to top: the analytical homogeneous plane-parallel result in eq. (3.22'), the numerically evaluated average of the IP solution evaluated in the same way but for each column, and the spatially averaged DA computational results for the exiting flux across the cloud base. Notice that the curves for first two responses become parallel to one another (with the standard slope of -1), also that there is no attempt to associate a slope with the numerical results since there is no evidence of a scaling regime being reached w.r.t. κ. Finally, given the intermediate position of DA(2,4) transfer in the one-parameter (p) family of theories going from IPs to diffusion, we expect the latter to yield still large transmittancies that, moreover, approach their DA counterparts as κ (or $\bar{\tau}$) increases without bounds.

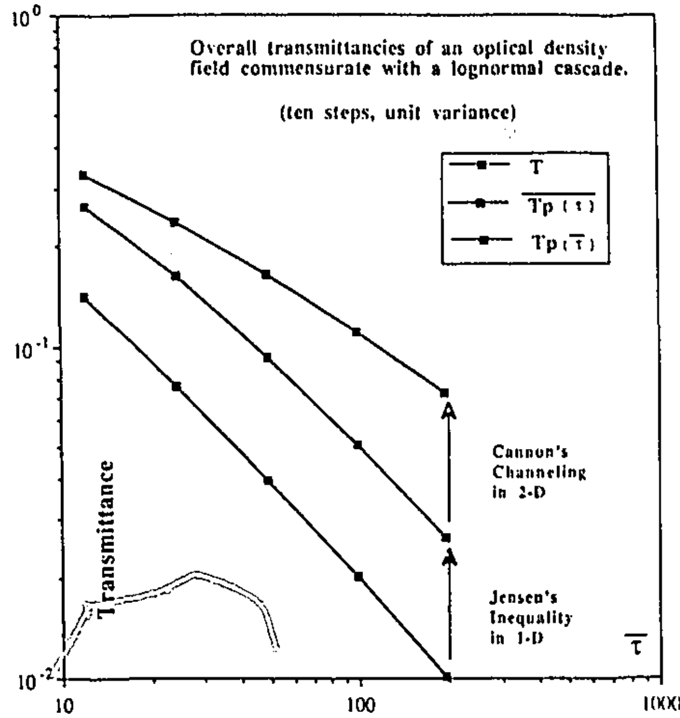

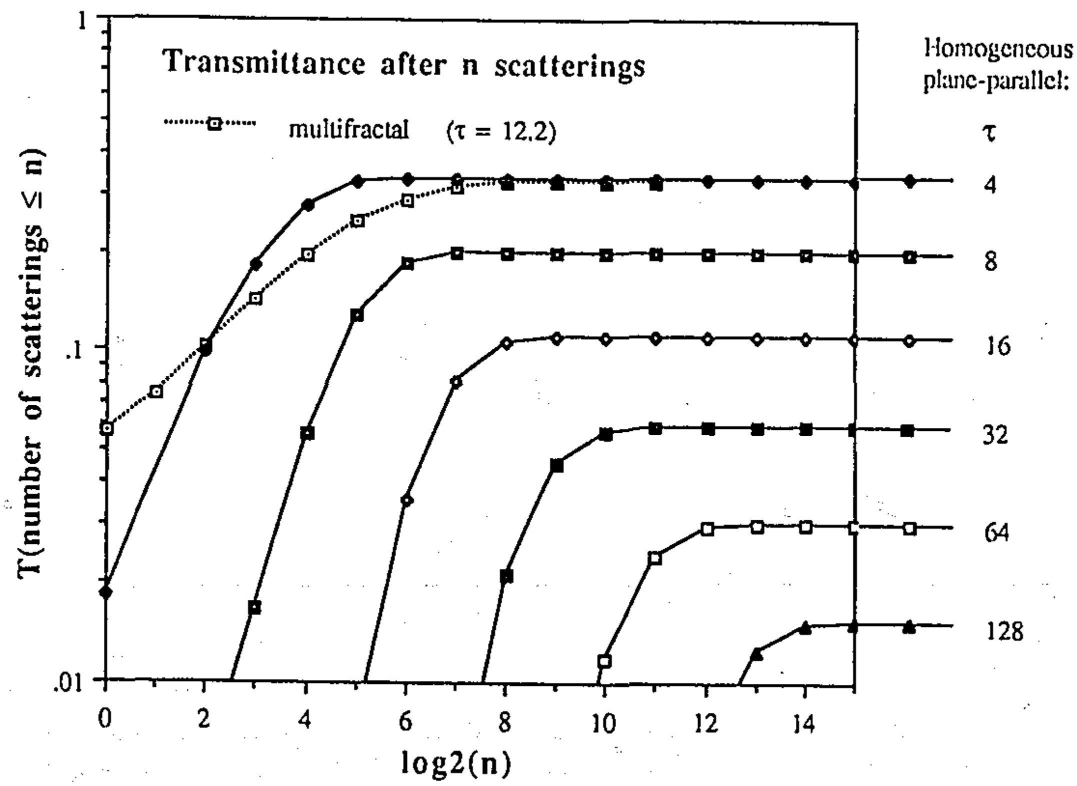

Figure 6.13: Order-of-scattering decompositions of the transmittance at $\bar{\tau}$ = 12.2. A log/log plot of overall transmittance through the thinner cloud as a function of the maximum number of scatterings involved, $T^{(n)}$.

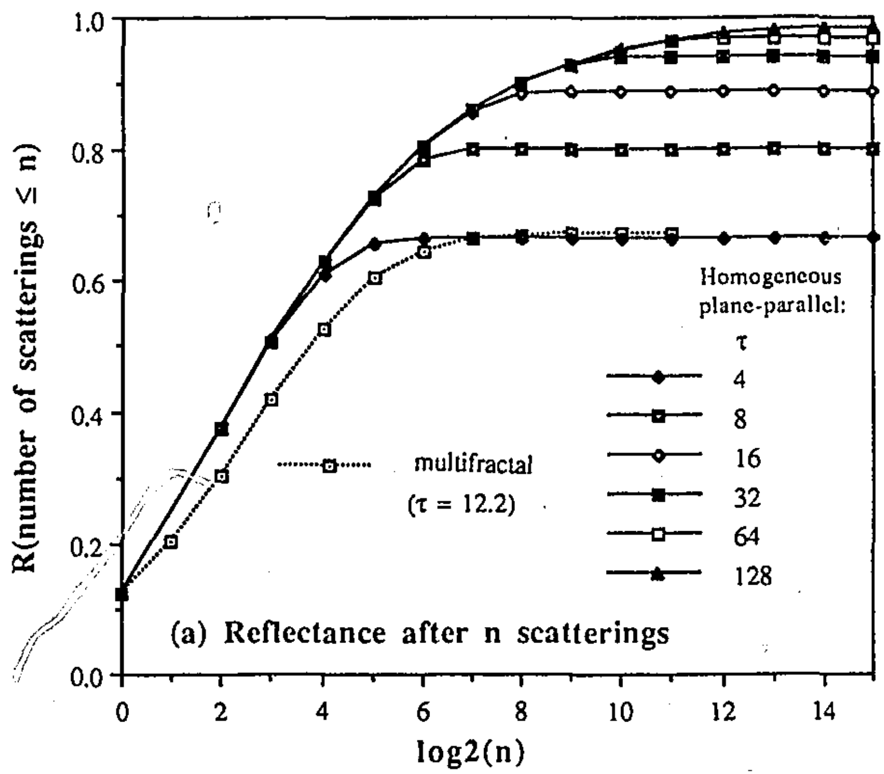

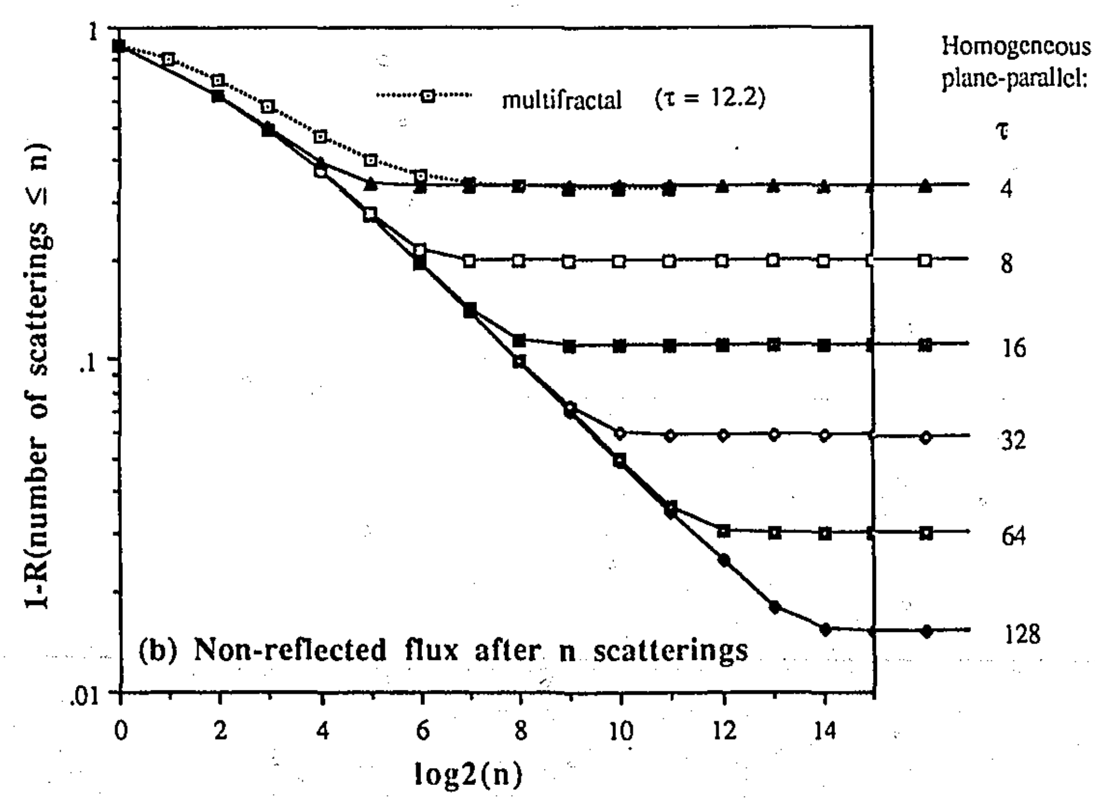

Figure 6.14: Order-of-scattering decompositions of the reflectance at $\bar{\tau}$ = 12.2. (a) Same as Fig. 6.13 but for overall albedo, $R^{(n)}$, in log/lin axes. (b) Same as (a) but for $1\text{-}R^{(n)}$, in log/log axes; recall that $1\text{-}R^{(n)} \neq T^{(n)}$, as long as $n<\infty$.

Chapter Seven

CONCLUSIONS

7.1. Physical Discussion

We can isolate four categories of results, ranging from the quite general to the very specific and, at the same time, ranging from a somewhat speculative (or "plausible") kind to straightforward computer output. The speculation, identified as such, is important in our opinion and deserves to be spelled out, if only because it provides an orientation (or simply ideas) for future research, in this case, at the more fundamental level.

7.1.1. General Results on Systems with both Vertical and Horizontal Radiative Fluxes

This is just a complicated way of describing what is known in the literature as "multidimensional" transport, a term we wish to avoid (except for cross-referencing purposes) because of the possible confusion with "multiple (fractal) dimensions" that play a very important role in the results discussed in §§7.1.2–4 below. So presently, we are interested *a priori* in any kind of radiation transport model in conjunction with any kind of medium provided it is not horizontally homogeneous and plane-parallel; this includes homogeneous media that are not of slab geometry, as well as plane-parallel media with (at the very least) horizontal inhomogeneities, and all combinations of the above, horizontally bounded or not. Many of the results in this category are clarifications of more-or-less well understood facets of inhomogeneous transport discussed in various literatures. During this process of clarification however, a persistent theme recurs: "channeling," which we therefore propose as a useful concept for future research into the radiative effects of inhomogeneity, scaling or not. We recall the radiation is "channeled" into the more tenuous regions, simply by enhanced multiple scattering in the adjacent more opaque regions. This intuitively appealing idea has first proposed by Cannon [1970] and has since gained acceptance, but mainly[1] in the astrophysical literature [Jones and Skumanich, 1980].

In the following, we will use our usual abbreviations for the different radiation transport theories: standard or "continuous angle" (CA) radiative transfer, its "discrete angle" (DA) counterpart, diffusion theory, and Cahalan's [1989] "independent pixels" (IPs); see sect. 1.3 for brief descriptions and various chapters and appendices for all the necessary details.

i: On comparing transport theories. If we wish to compare the predictions of various transport theories, we need a well-defined protocol, e.g., use a given response for given medium (or, better still, a given scaling family of media, see §7.1.2 below). As an example of a response, we can take (total) transmittance, T, which is defined as the ratio of mean-to-incident fluxes. In some cases, it might be of interest to require the chosen media to be horizontally extended, periodic and/or thick enough to avoid boundary layer effects (see item "iv" below) and/or that the variability be relatively weak. Once the specific set of rules is established and, most importantly, if the transport theories are themselves simple enough, then simple relationships can be established and these tell us about the underlying physics. After the fact, one can see whether or not the relationship (and the physical mechanisms involved) carries over to more general situations. For instance, variational arguments tell us that for homogeneous, horizontally extended (by periodic replication) but otherwise arbitrarily shaped media, we have (§2.1.1)

$$T_{\mathrm{IPs}} \leq T_{\mathrm{dif}} \tag{7.1}$$

Furthermore, IPs, DAs, and diffusion are all related (in that order) inside a one-parameter family of transport models; we naturally expect simple responses (such as T) to be monotonic w.r.t. this (phase function) parameter, hence (§3.3.2)

$$T_{\mathrm{IPs}} \leq T_{\mathrm{DAs}} \leq T_{\mathrm{dif}} \tag{7.2}$$

for the above type of media. It is important to note that the targeted media constitute a sub-class of internally inhomogeneous plane-parallel media with (simply connected) empty and full sub-domains; this of course qualifies as rather weak brand of variability. For this special class of media in particular, and inhomogeneous media in general, (7.1) and the first inequality in (7.2) is directly related to the "channeling" phenomenon (as defined w.r.t. IPs in §1.3.5).

ii: On comparing the responses of optical media. Here again, meaningful quantitative comparisons—that can teach about the internal mechanisms—call for a certain protocol. If we are interested in the effect of shape, maintain constant structure—for instance, homogeneity (for simplicity)—and constant (total) mass. In precisely this case, it can be shown (§2.1.2) that slab geometry is extremal (yields the smallest T), i.e., the "=" is attained in (7.1) at the same time as "channeling" is suppressed since the flux lines all align vertically. If we are interested in the effect of internal structure (§§2.3.1–2) then maintain a constant support and (if possible) a constant mass, then "channeling" (as defined w.r.t. diffusion in §1.3.5) automatically means a higher T, i.e., that homogeneity is the extremal situation where the "=" signs are obtained in (7.1–2). In summary, we have

$$T_{dif}(\text{uniform density}) < T_{dif}(\text{variable density}) \tag{7.3}$$

Basing ourselves on published and unpublished numerical results, this seems to generalize to DAs and, with a couple of extra constraints on the illumination, to CAs. The general idea is illustrated with the exactly solvable case of spheres with a concentric cavity (§2.3.3); further examples are provided by another exactly solvable model from the theory of regular random binary mixtures, complemented with numerical results for the singular limits (§2.3.4). A counter-example is to try to compare horizontally bounded and unbounded media (e.g., homogeneous slabs and cubes): one then gets the very wrong impression that horizontal gradients (the main difference) cause lower T's. But this is only true if we forget all the light that can bypass the cube completely (whereas it must still filter through the slab). With this kind of data, one can only draw very qualitative conclusions, e.g., that horizontal bounds induce horizontal fluxes, even at homogeneity.

iii: <u>On the roles of spatial variability and stochasticity.</u> This dichotomy may seem artificial since the most realistic variable cloud models are likely to be stochastic. It is however important to realize that the effects of internal variability and overall stochasticity are in fact quite distinct, if only because the two effects go in the same direction, viz., towards greater transmittance. More precisely, the inequalities discussed above are applicable on a per realization basis, so they allow us to better understand the effects of pure spatial variability (via the "channeling"), on the one hand, and pure randomness (via Jensen's inequality), on the other hand. For scaling examples, see respectively §7.1.2 (item "iii") and §7.1.3 (item "ii") to come. Consider a medium of given structure and we multiply the density field everywhere with a positive random variable that we will denote κ; in essence, we are modulating the total "optical" mass. We expect T to be convex w.r.t. κ since $T \in]0,1]$ and decreases with $\kappa \in [0,\infty[$. Jensen's inequality then reads

$$T(\text{average } \kappa) \leq \text{average } T(\kappa) \tag{7.4}$$

for an arbitrary κ-distribution (see §3.4.2 for more discussion). Note also that (7.4) applies also to spatial averaging (hence overall response) in the IP approximation.

In summary, there is a very definite advantage in seeking simpler transport theories like IPs, diffusion or DAs: amongst other analytical results, we can obtain quite general inequalities that are directly related to the basic radiative processes at work in inhomogeneous media, namely, the "channeling." Concerning DAs, other benefits are of course reaped at the computational level (see app. B for details).

iv: <u>On the importance of boundary conditions.</u> Even in the simplest (DA- and diffusion) transport theories, BCs can be more involved than we want to deal with; typically, do we really need the "mixed" variety, or can we satisfy ourselves with the more standard and analytically convenient "Dirichlet" type? The answer is yes, if boundary layer effects are kept to a minimum. By "boundary layer" we designate the region where escape probability (direct transmittance to any part of the boundary) is non-negligible. Unfortunately (for our systematic attempts to simplify the problem in order to cope with variability), this can include the whole medium in extremely inhomogeneous situations. Also excluded are horizontally bounded media because of the unavoidable (and physically important) presence of a "terminator," where the angle of attack of the incident flux w.r.t. the boundary becomes grazing. This also means that the IP approach becomes irrelevant since outgoing fluxes (or outer boundaries) and, in principle, internal IP fluxes (or internal boundaries) become physically (or geometrically) confused, see §2.2.3.

v: On the importance of properly defining radiative responses. The definition of albedo versus transmittance always makes some reference to the BCs. The terminator set provides a simple, spatially defined divider that we favour: albedo comes from all of the illuminated section of the boundary (grazing included), equivalently, it is the exact complement of transmittance. However, this is not always the most relevant way to proceed for the problem at hand (especially if angles are of special interest, cf. §A.4.3). It must also be realized that the terminator can become "pathological" (i.e., have a surface, hence be able support "side" fluxes of its own) in very artificial illumination-boundary geometric arrangements. Unfortunately, these are also seemingly the simplest to study, viz. normally illuminated cubes (see item "i" in upcoming §7.1.2, for an adverse effect of this kind of situation). At any rate, this whole issue is concretely illustrated by contrasting homogeneous cubical and spherical media (the latter turn out to be exactly solvable).

In summary, exact radiative BCs can be viewed as an unnecessary detail if we are careful enough but, in sharp contrast, and the presence of "sides" is definitely not a detail (the medium's support has been radically changed!) and this should not be viewed simply as "open" (versus, say, "cyclic") BCs. In this way only, we can say that BCs are not that important, nor is the precise boundary shape itself (see §7.1.2, item "i" below).

7.1.2. (Mainly) Numerical Results on the Scaling of Spatially Unresolved Responses

Let τ designate overall optical thickness; in the following, we will be using

$$T \sim \tau^{-\nu_T} \tag{7.5}$$

which is expected to apply asymptotically ($\tau \gg 1$) in scaling media with conservative scattering. The standard benchmark for radiative scaling is provided by homogeneous plane-parallel media which yield $\nu_T = 1$, independently of the phase function choice; we will call this "trivial" or "normal" scaling.

i: Homogeneous media scale trivially. We have made previous claims that the albedo R of (normally illuminated) homogeneous squares and cubes scales non-trivially (although not anomalously, the exponent being a rational). I.e., that $\nu_R < \nu_T = 1$ in

$$1\text{-}R \sim \tau^{-\nu_R} \qquad (7.6)$$

This claim relies entirely on the existence of a "pathological" terminator (made up of all the grazingly illuminated sides) and an ensuing "improper" definition of R as flux through the top only, rather than as 1-T. Most importantly, this scaling tells us nothing about horizontal boundedness in general since the far more numerous non-pathological combinations of cloud shape and illumination angle lead to trivial scaling (for instance, in the exactly solvable case of homogeneous spheres). Furthermore, even when accepting the improper definition, the numerical evidence is unsubstantiated under closer scrutiny.[2] See sect. A.4, 2.2 and 4.1 for details. In short, sides are asymptotically unimportant anyway we look at them (but this does not mean we can be careless about them, cf. §7.1.1 items "iv & v").

ii: Weakly variable media always scale trivially for transfer, usually for diffusion too. Trivial scaling is also robust against internally singular density fields as long as the range of scales where the inhomogeneity occurs is limited. Even broad band variability (white noise on a grid) yields trivial scaling in all cases for transfer, in non-singular or sub-percolating cases for diffusion. This is traceable to the lack of long-range correlations, in the sense of the "integral" correlation length, for transfer whereas diffusion reacts very strongly to the presence of the infinite (and highly auto-correlated) percolation cluster, but only if its cells are completely empty. In particular, this means that for diffusion, but not transfer, anomalous scaling is obtained but only in this special case known as the "RSN" limit in the statistical physics literature on conductance and/or diffusion (random walks) in disordered media. See §§D.6.2–3 and §2.3.4 for details.

iii: Numerical evidence for universal anomalous scaling in radiative transfer systems. We present unquestionable numerical evidence of anomalous scaling for transfer in a deterministic fractal medium and reasonably good evidence of its universality w.r.t. phase functions, in both the isolated case and the periodically replicated case (where one minor violation of universality is observed). See sect. 4.2 for more information.

iv: The roles of "channeling" and "extreme variability" in anomalous scaling. Simple arguments, based on first principles, show that strong "channeling" calls for highly singular, highly correlated media. Multifractals generically verify these criteria and the deterministic monofractal used in item "iii" above is, radiatively speaking, representative of the general case because it is of the multiplicative (cascade) type, not the (so often illustrated) additive type. For transmittance, we find

$$1 \geq \nu_{IPs} \geq \nu_{DAs} \ (= \nu_{CAs}) \geq \nu_{diff} \tag{7.7}$$

as expected from above (with "=" now obtained for weak variability, including homogeneity). This provides further evidence that "channeling," as observed in the weakly variable media used to illustrate the general principles in §7.1.1, is still at work in the extremely variable media used here. See sect. 4.3–4 for details.

7.1.3. (Strictly) Analytical Results on the Scaling of Average Multifractal Responses

We now consider the small scale limit of multifractal probability distributions of optical thickness, τ, for two important radiative properties for which we have analytical closed-form expressions: direct transmittance, $\exp(-\tau)$, and total plane-parallel transmittance for diffusion or DAs, $1/(1+b\tau)$, where b is a phase function and/or boundary condition parameter.

i: <u>Multifractal direct transmittance is scaling, not exponential, in the thick cloud case.</u> In homogeneous cases, direct transmittance decays exponentially with geometrical (and/or optical) distance; this is the famous Bouger-de Beer law which is always true w.r.t. optical distance for every realization of any kind of random medium. In weakly variable media, the average optical distance will scale like geometrical distance and the fluctuations are small, so the Bouger-de Beer law still applies very well. However, for multifractal media, the celebrated law is no longer true on average w.r.t. geometrical distance, nor w.r.t. average optical distance: the average (hence more typical) law is algebraic. In essence, this is a scaling consequence of Jensen's inequality applied to the exponential function. This also means that the geometrical f.p.'s of the photons are much longer in multifractals than in homogeneous media (of comparable average density). See §5.1.1.

ii: <u>Multifractal total transmittance mimics anomalous scaling in the thick cloud case.</u> Another consequence of Jensen's inequality expressed in scaling language is that, by averaging plane-parallel total transmittance laws (all trivially scaling) over a multifractal distribution of optical thicknesses, one finds a scaling for the average transmittance w.r.t. the geometrical size which is non-trivially related to key exponents in the multifractal hierarchy. When combined with the scaling of the average optical thickness to form a "mean field" exponent, as in eqs. (1.2–3), an anomalous-type scaling is found. An multifractal distribution of homogeneous plane-parallel media therefore behaves, on average, like a single (extremely) inhomogeneous one. This result can be interpreted directly in terms of the IP transport model for inhomogeneous scaling media. See §5.2.1.

iii: Multifractal albedo is linear w.r.t. optical thickness in the thin case. If the small scale limit of the density cascade used in the above leads to ever thinner media, rather than ever thicker, then we have a very different situation. As expected for arbitrary variability in the single-scattering approximation, we naturally retrieve a linear backscattered response w.r.t. optical thickness (average, in particular) for multifractals. The same remarks apply the whole diffuse radiation field. See §5.1.2 and §5.2.2.

7.1.4. (Preliminary) Results on the Fully Resolved Radiation Fields in Multifractals

First of all, detailed computation of multifractal transfer is feasible (but presently quite expensive). The DA radiation fields are computed everywhere in a (horizontally replicated) typical Gaussian multifractal using two totally independent numerical techniques—Monte Carlo simulation and relaxation of finite difference equations—and the results agree, to within numerical accuracy. This success is largely due to the particular care taken w.r.t. the problem posed by the thick cells in the finite difference approach. At the very least, this exercise provides us with a fully validated benchmark case of extreme variability against which any future improvements in computational transfer can—and should (if any form of spatial discretization is used)—be compared in terms of accuracy and efficiency.

Having established that the results are representative of the physics and not of the numerics, they can be discussed in terms of our previous findings, wether based on general- (including weak-) or scaling variability. With these results in mind, we ask the question "Is there anything new (when multifractals are placed) under the sun?" At this stage, it appears that the answer is no.

i: Seeing "channeling" at work (on all scales). Visualizations of these fully resolved internal radiation fields illustrate, as expected, large scale "channeling" (the fluxes literally carry the radiation around the thickest regions, through the more tenuous ones); furthermore, this kind of event seems to be present on all scales observable (to the eye). Unsurprisingly, we find $T_{IPs} < T_{DAs}$ in all cases (the basic multifractal density field is multiplied everywhere by five different numerical factors), and the difference increases with the (average) optical thickness, i.e., the overall effect of "channeling" is enhanced because of the boost in the general level (orders) of the multiple scattering which, in turn, provides a direct measure of the nonlinearity of the radiation-density field coupling.

ii: Diffusion as an approximation to transfer. The thicker the version of the cloud model, the better diffusion models the transport process (and in the thickest regions it further improves). However, there are always places with a substantial "non-diffusive" component in the DA radiation field so we cannot take diffusion as a uniformly good approximation to transfer in such extremely variable media.

iii: Smoothing out density features (by enhanced multiple scattering). The variability of the exiting albedo fields decreases with the optical thickness, thus illustrating the extremely powerful smoothing by multiple scattering of the variability present in the internal density field.

The two last items shed new light on the *in situ* radiation and microphysical measurements by King *et al.* [1990] concerning diffusion in marine stratocumulus, on the one hand, and by Tsay and Jayaweera [1984] concerning apparently uniform yet internally variable arctic stratus. Other features of the simulated emerging radiation fields also compare favorably with their observed counter parts, viz., the "apparent" absorption field and the power spectrum. Finally, order-of-scattering decompositions of the overall responses further illustrate the anticipated effects of "channeling:" these distributions are systematically lowered and broadened w.r.t. their homogeneous counterparts for the same total mass; in the upcoming sections, we will discuss the implications of this for the current issue of cloud "absorption anomaly."

The results presented in this sub-section may illustrate very well all of our previous findings, but we view still them as preliminary in the sense that it would be of considerable interest to perform elaborate statistical scaling analyses of a quantity that somehow measures "channeling." However, such analyses would normally call for many realizations since the radiation fields obtained for a single one are (vertically) non-stationary and we are ignorant of the ensemble-average profile (until the many realizations are obtained). Moreover, horizontal transections of the fields are stationary in principle but, due to their general lack of (extreme) variability, will probably be deemed "non-conserved" in the sense of multifractal cascade theory (see sect. C.3–4) which means that gradients (possibly Laplacians) should be taken, according to the "double trace moment" (DTM) recipe of Lavallée *et al.* [1992] or Tessier *et al.* [1992]. In turn, this would have the effect of boosting the numerical noise to unbearable levels (and without the many realizations needed to smooth it). Most importantly, any careful definition of a "channeling" event will necessarily call for 2-(or possibly more)-point scaling statistics for a vectorial quantity cross-correlated with a scalar one; this is far more complex than the DTM (and other) scaling analysis techniques currently in use since they apply a 1-point approach to a single scalar quantity [see, e.g., Lavallée *et al.*, *ibid.*; Tessier *et al.*, *ibid.*].

7.2. Meteorological Implications

The problem of inhomogeneous radiative transfer in presence of multiple scattering has many applications in atmospheric research and we in fact take this has our prime motivation. See sect. 0.2 [and references therein] for a discussion of three specific problems that are currently mobilizing at lot of effort: the cloud "albedo paradox" (transfer in inhomogeneous cloud in absence of absorption), the cloud "absorption anomaly" (same in presence of absorption), and problems related to global warming (inhomogeneity effects in the radiative driving of GCMs); note that in the two latter, understanding the effects of cloud liquid water content (LWC) variability is only a part of the answer (respectively, cloud microphysical and dynamical questions are also of concern). The results in this thesis pertain largely to the first of the above problems because of our focus on conservative scattering, on the one hand, and on overall responses, on the other hand. The message is clear: firstly, the albedo reducing effects of scalingly variable internal structure are strong enough to explain the observed discrepancies (w.r.t. standard plane-parallel theory) and, secondly, the effect of phase function details are minor, in comparison. Conversely, application of homogeneous models to measurements of real cloud radiation fields will lead to systematically under-estimated optical thicknesses. We will briefly speculate on the second major problem in the upcoming section.

The number and practical importance of atmospheric applications largely justifies our need for as many different radiation transport theories as we can possibly find. Each one we have used—CAs, DAs, diffusion, and IPs—has its advantages and disadvantages in terms of exactness (w.r.t. reality) and solvability (which translates directly into computer time). We have constantly compared these approaches and it is clear that the two latter (diffusion-type) theories generally do not agree with the two former (kinetic-type) theories for the more realistic scalingly inhomogeneous cloud models. This makes the simpler *bone fide* transfer theory (DAs) particularly attractive, especially in computational situations. Finally, we can reverse the previous logic and view the atmosphere not as a source of challenging theoretical problems but as a laboratory where we can validate our theoretical findings as well as put observational constraints onto future research (see below). In other words, we can ask some questions to the observationally inclined members of the cloud radiation and/or -microphysics community. For instance:

- Can we measure the radiation fluxes simultaneously in the vertical and horizontal directions (ideally, obtain complete directional distributions of radiance)? This is extremely important to decide when and where the various transport theories can be applied.
- Can we sample cloud LWC fast enough to decide what the radiatively relevant homogeneity scale is? And can we obtain more-or-less co-located LWC probings at different levels in a cloud deck? These questions are very important to the improvement of our stochastic cloud models (w.r.t. structural anisotropy in particular).

- Finally, can we investigate the statistics of directly transmitted light in real clouds? This could lead to the replacement of the Bouger/de Beer exponential law that applies in homogeneous situations by one more relevant to inhomogeneous situations; in particular, this would be of use in the context of mean field theories.

These are but a few interesting and specific questions that we would like to have answers for. Many more can be formulated, most importantly concerning the statistical properties of the spatial distribution of radiation fields; indeed, we are entering an era where these fields will be readily obtainable from theory via large-scale computer simulation; see Gabriel *et al.* [1986], Cahalan [1989] and Davis *et al.* [1991, or our chap. 6] for steady progress in this direction: respectively, on a 32X32X32 grid (and also 3D propagation in DAs), on a 4096X1X1 grid (with 3D propagation in CAs), and on a 1024X1024 grid (and also 2D propagation in DAs).

In this connection, we can suggest a new facet of Wiscombe *et al.*'s [1984] cloud "albedo paradox" (which, incidentally, also poses serious theoretical questions): namely, the simultaneous occurrence of very smooth (basically plane-parallel) looking clouds, i.e., weakly variable radiation fields, and extremely variable internal LWCs. Tsay and Jayaweera [1984] present a fully documented case of such intriguing behaviour for arctic stratus. This problem is indeed directly related to the standard formulation of the paradox (see §0.1.2) because the extreme internal variability explains the very non-plane-parallel behaviour in the overall fluxes due to strong "channeling" (nonlinear, higher-dimensional) effects.[3]

7.3. Future Directions

In the previous sections, we have already evoked some important questions that this thesis leaves unanswered. In particular (sect. 7.1), the need for a closer look at the scaling properties of the simulated radiation fields displayed and discussed on physical grounds in chap. 6. In the short run, further (e.g., DTM) scaling analyses can be performed but, in the longer run, operational definitions of "filters" that can detect "channeling events" will have to be developed. Of course, closer inter-comparison of observed and simulated cloud radiative properties is also strongly desirable (sect. 7.2), both to validate our ideas/findings based on *ad hoc* variability models and to improve the latter. In the following, we will dwell on two purely theoretical developments, one of importance to the statistical physics of transport in disordered materials in general, and the other with immediate applications to the cloud "absorption anomaly" problem in meteorology, recently reviewed by Stephens and Tsay [1990]. Interestingly, both call for a closer look at either the order-of-scattering distributions in transfer theory or their diffusion theory counterparts (viz., random walk statistics).

Firstly, we must realize that our usual way of forcing the transfer of radiation through the inhomogeneous system by applying asymmetric boundary conditions may be very natural and fully descriptive of the cloud/sunlight application but it is not the most helpful when analyzing the results. On the one hand, the mathematically simpler diffusion model attracts far more attention from the theoreticians in the physics community (it also applies very well to many laboratory situations). On the other hand, the trend is now to consider the statistics not of the bulk properties of steady-state transport systems such as ours but rather to release a large number of (diffusing) particles from a point deep inside the medium and to monitor the time evolution of this "cloud" of "light" (the quotes here are important because diffusing particles do not behave like photons in the most interesting situations). In short, we are talking about spatial δ-function as initial conditions rather than spatially uniform boundary conditions. After many realizations have been considered, we can access (the scaling of) the average (and other statistical moments) of the associated Green's function. To the best of our knowledge, this type of study has not yet been performed using multifractals to model the variability in local diffusivity. This is quite surprising given the many potential applications that can be found both in materials science and in geophysics; in particular, fluids move through bed-rock according to D'Arcy's law, hence diffusion (cf. introductory notes to chap. 2). Of course, the same kind of investigation can be done with photons too and this will certainly help us clarify the difference between diffusion and transfer and will probably help in the comparison of homogeneous to inhomogeneous situations since the basic inhomogeneity (i.e., "channeling") effects will be less masked by the strongly asymmetrical boundary conditions that we currently use.

Without shifting our attention to diffusion nor to time evolution problems, Monte Carlo simulation of conservative multiple scattering naturally produces detailed information on order-of-scattering statistics and it is well-known that this can be converted into information on the overall effects of absorption (see sect. B.1). In turn, this new information within the general framework of inhomogeneous cloud models is very important to decide whether (or to what extent) the discrepancies between observations and (homogeneous) theory in the near-IR are due to a new source of true absorption or to more inhomogeneity effects. For the moment, it can be said that inhomogeneity and absorption are basically competing with one another since "channeling" systematically reduces the number of scatterings suffered by a typical photon inside the medium (cf. §6.5.2) hence the probability of being destroyed by the occurrence of an absorption event. In scalingly inhomogeneous situations, it is quite conceivable that, on average, variability effects can "wipe out" the exponential decays that characterize (homogeneous) absorbing systems, in much the same way as we found for average direct transmittance through multifractals in chap. 5. We must recall that alternative attempts to explain the "albedo paradox" discrepancies in the strictly visible part of the spectrum called for (not extra but just) some amount of absorption[4] which is not only unnecessary in our view but unsubstantiated by direct observation in typical cloud decks [e.g., King *et al.*, 1990]. This question is important to our understanding of both remotely sensed and *in situ* cloud radiation measurements in the near-IR but it also has considerable implications for the overall radiation budget of the atmosphere-ground system since only truly enhanced absorption leads to increased local heating rates (non-vanishing divergence of the net radiative flux vector field). In short, the dynamical consequences are totally different.

Finally, we must point out that we are only beginning to understand the effects of inhomogeneity in optically simple situations, e.g., conservative scattering. Moreover, it is fair to say that even this understanding comes at the cost of further simplification, like DAs hence/or very symmetric illumination conditions; the effects of illumination angle are indeed very poorly understood (cf. §5.4.3) and must logically be approached within the framework of CA transfer. As argued in the above, the next step should be to add weak absorption to the multiple scattering processes. Also evoked above is the possibility of internal sources and, in the atmosphere, these are related to thermal emission, hence to the far-IR; as a first approximation, scattering can be neglected altogether in this region but this does not mean that inhomogeneity becomes unimportant (cf. our analysis of direct transmittance in chap. 5). In between the near- and far-IR, we find the most complicated optical situation with absorption, emission and scattering altogether ... and apparently lots of information on meteorologically relevant atmospheric constituents and state parameters—such as water vapor concentration, pressure and temperature—to extract [D. Steenbergen, p.c.]. With such an intimidating optical set-up (we can always add some oblique illumination for good measure), the net effect of the inhomogeneity is anyone's guess at this point—it shows that we are getting closer to the necessities of (the difficult "science assisted" art of) weather prediction—but we can risk a forecast. On the one hand, our experience tells us that it will non-negligible (with probability close to one) and, on the other hand, that lots of work lies ahead of us (this is the ultimate understatement concerning atmospheric radiation).

[1] In the geophysical literature, we view Stephens' [1986, 1988] analysis of horizontally inhomogeneous radiative transfer as a similar breakthrough although with less intuitive content since it is expressed in Fourier space/spherical harmonic space jargon (viz., "pseudo-source/sink terms" and "mode-coupling").

[2] This underscores one of the many difficulties in obtaining scaling exponents: large prefactors associated with a very slow approach to the asymptotic regime (Fortunately, this problem seems to be exclusive to homogeneous systems.)

[3] This leads us to speculate on another paradox, this time at the edge of the observable universe: the cosmic microwave background is observed to be far too smooth for the liking of theoretical cosmologists who believe that the inhomogeneities related to the formation of galactic clusters (or super-clusters, or else the galaxies themselves since opinions differ on what comes first) should be detectable as fluctuations in the background brightness temperature field. In this problem the sources are internal and diffuse (in fact, thermal) rather than external and collimated and the boundary (photons begin to stream rather than random walk because density decreases) is a temporal event in the expansion of the Universe rather than a simple geometrical entity. However, the bottom line is the same: we have lots of multiple scattering (and this is guaranteed prior to "decoupling," in the guise of absorption by hydrogen photo-ionization followed by re-emission at recombination) in an inhomogeneous structure that is likely to be scaling (and this is indeed the case for theoretical reasons, not to mention the ample observational evidence from the matter-dominated era). In such circumstances, our findings in chap. 6 tell us that "what you see is not necessarily what you have (especially if it looks featureless)!" And apparently the only sure way of finding out whether the medium is truly homogeneous (short of *in situ* probing which is clearly out of the question) is comparison with homogeneous theory for some response (other than the unobservable apparent variability) that reacts to the inhomogeneity. In our relatively featureless cloud albedo fields, we can look at the albedo itself if we know *a priori* the overall mass of the cloud. In the cosmological problem, we would have to look at the observed temperature itself ($\approx$2.7 K) and reassess our estimates of the current age of the Universe on the one hand, and of its average density on the other hand. Needless to say, there is already plenty of controversy and speculation on both of these issues.

[4] It is not hard to find plausible sources to incriminate: pollution by soot particles! In some very special circumstances however, these are a real factor: see Coakley *et al.* [1987] on the clouds formed in the trails of ships, thanks to their smoke effluents.

Bibliography for Chapter 7

Cahalan, R. F., "Overview of Fractal Clouds," in *Advances in Remote Sensing (RSRM'87)*, Eds. A. Deepak *et al.*, 371–389, A. Deepak, Hampton (Va.), 1989.

Cannon, C. J., "Line Transfer in Two Dimensions," *Astrophys. J.*, 161, 255–264, 1970.

Coakley, J. A. (Jr.), R. L. Bernstein, and P. A. Durkee, "Effect of Ship-Stack Effluents on Cload Reflectivity," *Science*, 237, 1020–1022, 1987.

Davis, A. B., S. Lovejoy, and D. Schertzer, "Discrete angle radiative transfer in a multifractal medium," *S.P.I.E. Proceedings*, 1558, 37–59, 1991.

Gabriel, P., S. Lovejoy, G. L. Austin, and D. Schertzer, "Radiative transfer in extremely variable fractal clouds," in *Proceedings of the 6th Conference on Atmospheric Radiation*, Williamsburg (Va.), May 12–16, Am. Meteorol. Soc., Boston, 1986.

Jones, H. P., and A. Skumanich, "The physical effects of radiative transfer in multidimensional media including models of the solar atmosphere," *Astrophys. J. Suppl.*, 42, 221–240, 1980.

King, M. D., L. F. Radke, and P. V. Hobbs, "Determination of the Spectral Absorption of Solar Radiation by Marine Stratocumulus Clouds from Airborne Measurements within Clouds," *J. Atmos. Sci.*, 47, 894–907, 1990.

Lavallée, D., S. Lovejoy, D. Schertzer, and P. Ladoy, "Nonlinear variability of landscape topography: multifractal analysis and simulation," to appear in *Fractals in Geography*, Eds. L. Decola and N. Lam, Prentice Hall, New York, NY, 1992.

Stephens, G. L., "Radiative Transfer in Spatially Heterogeneous, Two-Dimensional Anisotropically Scattering Media," *J. Quant. Spectrosc. Radiat. Transfer*, 36, 51–67, 1986.

Stephens, G. L., "Radiative transfer through arbtrarily shaped media, I: General solution, II: Group theory and closures," *J. Atmos. Sci.*, 45, 1818–1838, 1988.

Stephens, G. L., and S. Tsay, "On the Cloud Absorption Anomaly," *Q. J. R. Meteorol. Soc.*, 116, 671–704, 1990.

Tessier, Y., S. Lovejoy, and D. Schertzer, "Universal Multifractals: Theory and Observations for Rain and Clouds," submitted to *J. Appl. Meteo.*, 1992.

Tsay, S.-C., and K. Jayaweera, "Characteristics of Arctic Stratus Clouds," *J. Climate Appl. Meteor.*, 23, 584–596, 1984.

Wiscombe, W. J., R. M. Welch, and W. D. Hall, "The effects of very large drops on cloud absorption, 1: Parcel models," *J. Atmos. Sci.*, 41, 1336–1355, 1984.

CADENZA

"En France, tout finit en chanson."
(dicton français)

This thesis covered physical models of radiation-matter interaction (via multiple scattering) and physically-based (multiply scaling) cloud models. Not too surprisingly, I am still confused as to where the physics really fits in (the answer is probably multiple). I have tried my best to draw a comprehensive picture of inhomogeneous radiation transport phenomena but the subject is vast, even with a sharp focus on somehow scaling optical media. This report started off very low key with a more personal kind of work (weak disorder, diffusive transport, analytical approaches) and it ended with extremely heavy artillery and more team-like work (multifractal cascades, "DA" transfer, supercomputer simulations).

Concerning my role, as a physicist, I hear conflicting signals. Reconnecting with the musical analogy used in the Prelude, I can elaborate. Is the idea to listen carefully to enough of the music, to study enough of the scores, to experiment "hands-on" enough to figure out what the basic (truly universal) rules are? In this case, everything—starting with the very equations of radiation transport—seems to be pointing towards the concepts encompassed by "channeling" and the scale invariant models merely provide the most interesting (dramatic) variations on this theme. Or is it to actively orchestrate the facts into some greater scheme of things? In which case, it appears that everything—in the sense of geophysical observables—seems to be pointing towards the scale invariant properties (the exponents) and the fact that we are dealing with radiation is incidental, almost anecdotal, just one more instrument in the band. And (it has been decided that) the fans always want to hear the same music, the most "universal" stuff. Generally speaking, the details of a complex geophysical problem are of little interest to the inspired multifractalist and this can go as far as the equations themselves. Most often they are not even known to us in any kind of detail anyway. The equations of turbulence are known but cannot be solved, even numerically, in the most relevant situations (very high Reynolds numbers). Although he should be proficient (instrumentally literate), the band leader does not really care how the individual instruments are played, only whether they sound good all together. For the better and the worse, fast-paced technological developments have put (sound) analysis and synthesis at our finger-tips. Here is a (small) number of parameters that describe what we think resembles reality. However, the trained ear can always discriminate between a synthesizer and the real thing and, furthermore, the settings on a semi-conductor device mean nothing to the dedicated instrument artisan. Most importantly, the electronic keyboard gives no physical feed-back to the player.

In this metaphor, atmospheric radiation enjoys (?) a very special situation. Unlike so many other geophysical fields of research, its equations are not only known to us but they can be solved, at least numerically, in very interesting situations. Not only cloud images can be analyzed and synthesized with the help of fractals and multifractals, there is also the intermediate arrangement where the physical equations can be applied to the fractals and multifractals and the outcome compared to the real as well as to the purely synthetic imagery. (Basically, the radiation "instrument" player can join the band but he can also play solo.) Most importantly, we can get a feeling for how the radiation "vibrates" with the multifractals, or whatever, since the interaction can be numerically observed, analytically investigated. In final analysis, one can passively contemplate reality and try, painstakingly, to understand it from first principles, or one can by-pass the fundamental problems altogether, using a lot of creativity and even more high-tech, actively design statistical tools that target directly the appropriate parameters then imitate reality. The choice is essentially one of personal taste. And a question of rhetoric too since it can equally well be argued that a reasonably successful synthetic model must capture the most fundamental aspects of reality, especially if it provides a plausible "theory for everything" as well (in this case, cascades galore).

This thesis takes the former—more introspective—path with no further justification, otherwise it would have been called something like "Scale invariant modelling applied to radiation(-like) transport." No apologies are called for but the fact is that my advisors have adopted the opposite attitude—and it indeed sounds like so much more fun. This may partly explain why I have felt quite defensive during most of the writing exercise and, in turn, this is bound to show in the final product. I also feel slightly old-fashion because the writing is on the wall: if "virtual reality"[1] is as good as true to the mind (and all of its extensions), then clearly we should be studying its much simpler physics (that may of course be only virtual too, but then who really cares?).

Shaun, Daniel and I don't always agree on the important issues but we still have lots in common, one of those things is a strong connection with France, as a country and as a culture (but all for different reasons). French people love to use the saying in the opening quote: In France, all ends in song. I believe a PhD thesis can too, at least *au Canada Français*, at least the one I'll have to live with for the rest of my life. Daniel and myself grew up in France, Daniel as a national, myself as an alien, while Shaun grew up in New York, so I thought of

[1] Daniel and Shaun prefer the expressions "mock geophysics" or "pixel-worlds."

Jacques Brel since he is so universally admired, in part thanks to the Broadway musical that paid tribute to him, brought his sensitivity to the English speaking world. But Brel tends to make me feel nostalgic, he is no longer "live and well and living in Paris" and, besides, he's too much of an anarchistic individualist to represent a team! I then thought of Manhattan Transfer, they certainly form a real team, our discrete cascade models look strikingly like their namesake (cf. fig. 6.0) and our two-dimensional DA photons fit the bill, quite literally. But their style is not really my kind of jazz (their harmony is ... too perfect!) and, besides, neutrons obey the same basic laws as photons and, in that connection, the word "Manhattan" has highly explosive (and ultimately very sad) overtones. I finally realized that, playing only slightly with the words, the computational transfer problem that, as a team, we address in chap. 6 is conceivably one of the "wildest" and "hardest" of all (in terms of internal variability) since this is precisely how Schertzer and Lovejoy [*Physica A*, in press] classify Gaussian multifractals. I therefore feel totally comfortable with one of the best rock singer-composer-arrangers (and band leaders) that New York has ever produced. His rock may not be so "hard" but his lyrics are definitely wild and, in particular, he writes so eloquently about random walks.

Merci à tous deux,
A. D.

"Say hey babe, take a walk on the wild side!"
Lou Reed (1972),
formerly of the VELVET UNDERGROUND
(now Chevalier de l'Ordre des Arts et Lettres,
decorated by Jack Lang, Ministre de la Culture,
in Paris, the 18th of February, 1992)

APPENDICES

Appendix A

ELEMENTS OF CONTINUOUS ANGLE RADIATIVE TRANSFER THEORY

Overview: We start off by recasting the most basic concepts (quantities and equations relating them) of radiative transfer in a dimensionality independent formulation which we systematically parallel with concepts from the theory of stochastic processes. In the second section, we contrast the standard exponential distribution (with unit parameter, or average) of photon "optical" free paths (f.p.'s) with the generally unknown distribution of "real" (geometrical) f.p.'s, highlighting the fundamental role of the nonlinear radiation-to-material density field coupling; we also generalize the notion of optical thickness (viewed as a measure of the total amount of scattering material) to arbitrarily shaped and internally structured media. The third section is devoted to the fundamentally linear aspects of the multiple scattering transfer problem (i.e., sources and similarity relations); we also reinterpret the transfer equation as a local balance between the angular anisotropy and the spatial gradients of the radiance field. This complicates life in radiation transport theory to the point where we must either go "homogeneous plane-parallel" to proceed analytically with continuous angle (CA) transfer ... or contemplate ways of simplifying the angular problem in order to better explore the spatial (inhomogeneity) aspects and, being admittedly biased towards the latter option, we survey the different simplification schemes exploited and compared in various parts of the thesis. In the final section we turn to the question of boundary conditions (BCs) for the albedo problem and the related problem of defining reflectance versus transmittance which, as simple as it sounds, still needs to be clarified (mainly in the largely unexplored area of horizontally bounded media).

A.1. Radiative Transfer: A Formalism for Arbitrary Dimensionality

A.1.1. The Radiance Field and its First Three Spherical Harmonics

The basic descriptor of the macroscopic radiation field is "radiance" or "specific intensity" which we shall denote $I_{\mathbf{u}}(\mathbf{x},t)$. In the familiar 3-D context, let $\mathbf{u}$ be a unit vector that defines the direction of propagation of a geometrically definable light "beam" and $I_{\mathbf{u}}$ as the amount of radiant energy crossing a unit of area (projected) perpendicular to $\mathbf{u}$ (around $\mathbf{x}$)

within a unit of solid angle (around **u**) and a unit of time (around t). In Preisendorfer's [1976] words, radiance is an "apparent" optical property: it is measurable with a radiometric device (which could simply be the human eye), but it depends on the position, distribution and intensity of the sources of radiant energy (in our case, illumination geometry). Of course, radiance somehow reflects—the word says it all!—the "inherent" optical properties of the medium: presence of absorption, scattering cross-sections, density of scatterers (as a function of space), etc. The role of a radiative transfer theory is to describe the connection between these two types of optical quantities, how they are coupled physically.

Before characterizing this coupling of $I_u(x,t)$ with $\rho(x)$, defined as the field that models the density of optically relevant (e.g., scattering) material, we will view $I_\mathbf{u}$ as a probability distribution in direction space and look at some of its simplest properties. Define the following angular integral operator:

$$\oint (\cdot)\, d^{d-1}\mathbf{u} = \int_{\Xi_d} (\cdot)\, d^d\mathbf{u} \qquad \text{(A.1)}$$

where Ξ_d denotes the unit d-sphere $\{\mathbf{u} \in \Re^d, |\mathbf{u}|=1\}$. We now characterize the degree of **u**-anisotropy of the radiation field $I_\mathbf{u}$ in much the same way we will proceeded for the phase function in sect. A.3 below.

The first step is to define a **u**-independent measure of radiance and a natural choice is Preisendorfer's [*ibid.*] "scalar" flux which we will abusively call "total" radiance or intensity:

$$J = \oint I_\mathbf{u}\, d^{d-1}\mathbf{u} \qquad \text{(A.2)}$$

Whatever its name, J is directly related to radiant energy density: $U = J/c$ where c is the velocity of light in vacuum. Many authors prefer to use the average radiance (or specific intensity) which, in our notations, is J/n_d where $n_d = 2\pi^{d/2}/\Gamma(d/2)$ is $\oint d^{d-1}\mathbf{u}$, the d-surface (or (d-1)-volume) of Ξ_d. The proper usage for J would therefore be (not "specific," simply) "intensity." The most prominent directional feature of the radiance distribution on Ξ_d is surely indicated by (Preisendorfer's "vectorial") flux:

$$\mathbf{F} = \oint \mathbf{u}\, I_\mathbf{u}\, d^{d-1}\mathbf{u} \qquad \text{(A.3)}$$

and almost[1] everybody agrees to call it the <u>net</u> "flux" or "irradiance" vector. J and **F** are respectively equal, within d-dependent proportionality factors, to the 0^{th} and 1^{st} order coefficients of an expansion of $I_\mathbf{u}$ in spherical harmonics w.r.t. **u**.

We can also define the scalar and vectorial fluxes defined over portions of Ξ_d. The most natural choice being semi-hyperspheres on either side of a hyperplane oriented perpendicular to some $\mathbf{i} \in \Xi_d$:

$$J_\mathbf{i} = \int_{\mathbf{i}\cdot\mathbf{u} \geq 0} I_\mathbf{u}\, d^{d-1}\mathbf{u} \qquad \text{(A.2')}$$

$$F_{\mathbf{i}} = \mathbf{i}\cdot \int_{\mathbf{i}\cdot\mathbf{u}\geq 0} \mathbf{u}\, I_{\mathbf{u}}\, d^{d-1}\mathbf{u} \tag{A.3'}$$

We can obviously retrieve the complete integrals from the partial ones: $J=J_{\mathbf{i}}+J_{-\mathbf{i}}$, for any choice[2] of $\mathbf{i}$, and $\mathbf{i}\cdot F=F_{\mathbf{i}}-F_{-\mathbf{i}}$, so the components along d non-coplanar d-vectors suffice to restore **F** (the mutually perpendicular axii of a rectangular coordinate system provide a convenient choice). Preisendorfer [*ibid.*] showed how these integral transforms of $I_{\mathbf{u}}$ can be uniquely inverted. Hence there is no loss of directional information in either of the radiation field characterizations (A.2'–3') but their associated transfer equations are not independent. By contrast, the information content of (A.2–3) is patently incomplete, any intricate **u**-variation has been smoothed out by the averaging. There are several ways of showing that the deliberate choice of modelling $I_{\mathbf{u}}$ with its J and **F** components alone is congruent with the "diffusion" of "Eddington" approximation.

The next moment is best described as a 2nd order tensor and it is directly proportional the pressure tensor of the photon gas $\underline{\underline{P}}$ and the proportionality constant is simply *c*. So we will not introduce a new notation for it:

$$\oint \mathbf{u}\,\mathbf{u}\, I_{\mathbf{u}}\, d^{d-1}\mathbf{u} = c\underline{\underline{P}} \tag{A.4}$$

It essentially describes the transfer of (photon) momentum through planes of any orientation: the rate of transfer of **u**-momentum through a unit of surface perpendicular to **n** is $\mathbf{n}\cdot\underline{\underline{P}}\cdot\mathbf{u}=\mathbf{u}\cdot\underline{\underline{P}}\cdot\mathbf{n}=\underline{\underline{P}}:\mathbf{nu}$ where **nu** is the (dyadic) tensor product of d-vectors **n** and **u** (components n_iu_j in orthonormal coordinate systems). It is important to notice that not everything is new about $\underline{\underline{P}}$. Letting $\underline{\underline{1}}$ denote the (Euclidian) metric tensor with orthonormal components equal to δ_{ij}, the usual Kronecker symbols, we see (from definitions) that its trace $\underline{\underline{P}}:\underline{\underline{1}}$ is equal to[3] $U=J/c$. Moreover, the traceless (hence new) part of $\underline{\underline{P}}$ is symmetric by definition and therefore only d(d-1)/2 of its d^2 components are in fact independent.[4]

For an illustration, take a normalized purely streaming radiance distribution $I_{\mathbf{u}}=\delta(\mathbf{u}-\mathbf{u}_0)$; our definitions (A.1–4) yield respectively $J=1$, $\mathbf{F}=\mathbf{u}_0$, $J_{\mathbf{i}}=\Theta(\mathbf{i}\cdot\mathbf{u}_0)$, $F_{\mathbf{i}}=\mathbf{i}\cdot\mathbf{u}_0\Theta(\mathbf{i}\cdot\mathbf{u}_0)$ and[5] $c\underline{\underline{P}}=\mathbf{u}_0\mathbf{u}_0$ where $\Theta(\cdot)$ designates Heaviside's step function. As we will see in sect. A.3 (in connection with very peaked, $g=\pm1$, phase functions), a δ-function has spherical harmonics of equal magnitude at all orders.

A.1.2. The Radiative Transfer Equation and its Position in the Theory of Stochastic Processes

The (essentially phenomenological[6]) considerations on radiant energy (flux) conservation of app. E can be summed up in a radiative transfer equation which is sufficiently[7,8] general for our needs:

$$\left[\frac{1}{c}\frac{\partial}{\partial t} + \mathbf{u}\cdot\nabla\right] I_{\mathbf{u}}(\mathbf{x},t) = -\kappa\rho(\mathbf{x})\left[I_{\mathbf{u}}(\mathbf{x},t) - S_{\mathbf{u}}(\mathbf{x},t)\right] \tag{A.5}$$

that we have spelled out in the most traditional [Chandrasekhar, 1950] manner apart from subscript notation for u where we normally find frequency ν but one can argue that **u** and ν really belong together since both are state variables for the EM wave or photon. For a fairly rigorous connection between radiance and the constructs of EM theoretical and QED, via a coarse-graining procedure, see Wolf [1976]. In the following, we will not be adamant about the fundamentally 3-D nature of EM radiation and, by making systematic use of differential- and integral operator notation, we do not require any specific choice of embedding dimensionality[9] nor of any particular coordinate system; only the geometrical meanings of the various quantities are changed, e.g., going from d=3 to d=2, "area" translates to "length" and "solid angle" to "angle."

On the r.h.s. of (A.5), κ is the cross-section per particle (or unit of mass) which astrophysicists call "opacity." Next in line is $\rho(\mathbf{x})$, the particle (or mass) density—cloud liquid water content (LWC) in meteorology—to which we will confine (for simplicity) all spatial variability. We will denote by M the spatial "support" of $I_\mathbf{u}(\mathbf{x},t)$ and $\rho(\mathbf{x})$; this given sub-set of $\Re^d$ will be called the "(optical) medium" or simply the "cloud." $\kappa\rho(\mathbf{x})$ is the "optical" density field which can be interpreted as a (bulk) cross-section per unit of volume, its units are therefore 1/length; thus defined, optical density must be non-negative.[10] We note that $\kappa\rho(\mathbf{x})$ could also be variable in time—and in the most interesting applications (e.g., turbulence) it certainly is—but we will assume that light "sees" the $\kappa\rho$-field in a "frozen" state, i.e., light travel time is short w.r.t. the shortest dynamical time scale of the medium, even for the long optical paths that are typical of contributions to transmitted fluxes. This still leaves open the possibility of time evolution for $I_\mathbf{u}$ by imposing initial conditions (ICs) on an infinite system. The first term on the r.h.s. of (A.5) $-\kappa\rho(\mathbf{x})I_\mathbf{u}$ is a sink for (direct beam) **u**-radiance through "extinction" which can be caused by either absorption or scattering through any angle. This term controls the process of kinetic propagation and is discussed in more detail in sect. A.2 where we will see that $1/\kappa\rho(\mathbf{x})$ is the <u>local</u> value of the mean free path (m.f.p.) of the photon—the m.f.p. it would have in an extended homogeneous medium of equal density—which is non-trivially related to the real m.f.p. and its more relevant ensemble-average properties for media that are only statistically defined. The second term on the r.h.s. of (A.5) $+\kappa\rho(\mathbf{x})S_\mathbf{u}$ is a source for **u**-radiance and $S_\mathbf{u}$ is indeed known as the "source function," further discussed in sect. A.3.

It is important to realize that radiance $I_\mathbf{u}$ and the transfer eq. (A.5) are the physical (kinetic theory) counterparts of very specific concepts from the mathematical theory of stochastic processes and we refer the reader to app. E for detailed connections as well as a closer look at the phenomenological derivation of (A.5). This is particularly obvious when we are dealing with multiple scattering (m.s.) sources described in full mathematical detail in sect. A.3. In the jargon of Markov chain theory, we are characterizing an ensemble of (photons performing) continuous space, discrete time random walks (RWs) with, generally speaking, spatially inhomogeneous "transition probabilities." The random walker's "state" is given by position **x** and (nominal) velocity **u**, $I_{\mathbf{u}}(\mathbf{x})$ is commensurate with its probability density function (p.d.f.) of being in that state, (A.5) with the m.s. source function (A.17) below constitute the kinetic equivalent of the Chapman-Kolmogorov equation of the process. The hydrodynamic limit of (A.5) that we take in app. D is equivalent to the continuous time limit and we naturally find Fokker-Planck equations and "diffusion" processes. Things become a little more confusing when these "stochastic" equations, in the generally accepted mathematical sense of the term (the dependent quantity is a probability), also become "stochastic" in the sense often used in statistical physics (their coefficients are random variables or, more generally speaking, random functions of the independent variable(s), viz. space and/or time). To add to the general state confusion, the term "random" is often taken, in the atmospheric radiation literature, as synonymous with "uncorrelated fluctuations" which is in fact a very special (and rather dull) kind of randomness. This spatial equivalent of white noise is dealt with at the end of chap. 2 and, from then on, we are more interested in density fields generated by "random (cascade) processes." Interestingly, this means we will be studying additive stochastic processes (unfolding spatially as a function of time) subordinated by multiplicative stochastic processes (unfolding in density function space as a function of spatial scale).

In fact, the real difference between the two formulations (and literatures) of radiative transfer, on the one hand, and of stochastic processes, on the other hand, is that the mathematicians have shown little interest in physical problems such as reflectance and transmittance and much more in applications such as queueing theory (e.g., "what is the probability of returning to the point of departure in some given time?"). In an timely attempt to restore a semblance of clarity in questions of statistical radiative transport, we are prompted to introduce (at the very least) separate notations for ensemble-averaging over the disorder of the density field, $\langle\cdot\rangle$ ($\bar{\ }$ for spatial averages), and over all possible the photon RWs, $\mathsf{E}(\cdot)$, following the mathematicians' preference for the expression (mathematical) "expectancy." The latter form of stochasticity is of course present even in homogeneous (or otherwise deterministic) media and, furthermore, it is exploited directly for numerical purposes in Monte Carlo techniques (cf. sect. B.1). For instance, in the previous subsection, we were looking at the various statistical moments of the probability distribution of radiant energy in **u**-space: J is the normalization factor that applies and we have $\mathsf{E}(\mathbf{u}) = \mathbf{F}/J$; **F** is thus a proper measure of the mean flow of the radiation, the exact equivalent of mean velocity in gas dynamics.[11] Examples of spatial- (single realization or deterministic) and ensemble-averages are to be found in the next section along with different combinations of the various types of averaging.

This distinction would not be so important were it not for the fundamentally nonlinear coupling of the density and radiance fields in (A.5) which is at the heart of the inhomogeneous transfer problem. The two basic forms of stochasticity are therefore interacting in ways that we are interested in unraveling as best we can. This calls, in particular, for investigations of ensembles of homogeneous media or, equivalently, "independent pixel" calculations for inhomogeneous media where, in both cases, only vertical fluxes are present (see chap. 5 and 3, respectively). We will also consider radiation transport in deterministically inhomogeneous media—or their stochastic counterparts but on a single realization basis—in order to identify the important mechanisms at the most basic level, i.e., characterizing the role played by horizontal fluxes w.r.t. the spatial variations in optical density (see chap. 2, 4 and 6). Given the special role of higher dimensionality in the latter case, these two nonlinear effects of variability must not be confused and we have adopted Cannon's [1970] expression of "channeling" to describe the whole complex of phenomena that arise when going from the former to the latter type of situation. This categorization, however rough, of the fundamental processes is especially important since the systematic trends either in a (single realization) response or in an ensemble-average response go in the same direction: towards higher overall fluxes which translates to more transmittancy, lower albedo. Another reason for separating the effects of (single realization) spatial variability, on the one hand, and medium stochasticity, on the other hand, is that for scale invariant variability models (the most interesting of which are intrinsically stochastic), they are so strong that confusion of the two effects is almost bound to arise since, within that framework, only the ensemble-average properties are considered relevant. At the beginning of chap. 6, we summarize the situation and discuss ways in which the two effects are compounded.

A.2. Non-Local and Non-Linear Aspects: Direct Transmittance and Photon Propagation

A.2.1. The Standard Exponential Optical Free Photon Path Distribution

We now turn to the simple yet fundamental problem of sourceless transfer in order to focus on the "streaming" operator on the l.h.s. of the transfer equation (A.5). For simplicity, we can assume a steady-state is reached and radiance $I_u^{(0)}$ then obeys the homogeneous ($S_u=S_u^{(0)}(x)=0$) much simplified transfer equation[12]

$$u\cdot\nabla\, I_u^{(0)}(x) = -\,\kappa\rho(x)\; I_u^{(0)}(x) \qquad \text{(A.6)}$$

The superscript notation reflects the fact that we are interested in unscathed (neither scattered nor absorbed) radiation which becomes itself a local source for single-scattered radiation, $I_{\mathbf{u}}^{(1)}(\mathbf{x},t)$, and so on,$\cdots$ in the general solution procedure by successive orders-of-scattering (or von Neumann series).[13] The general solution of (A.6) is

$$I_{\mathbf{u}}^{(0)}(\mathbf{x}) = T_d(\mathbf{x},\mathbf{x}-\mathbf{u}l)\, I_{\mathbf{u}}^{(0)}(\mathbf{x}-\mathbf{u}l) \tag{A.7}$$

where the dimensionless factor $T_d(\mathbf{x},\mathbf{x}-\mathbf{u}l)$ is the "direct transmittance" between points $\mathbf{x}$ and $\mathbf{x}-\mathbf{u}l$ (a path of geometrical length l in direction $-\mathbf{u}$) in the $\rho(\mathbf{x})$-field. $T_d(\mathbf{x},\mathbf{x}-\mathbf{u}l)$ has all the usual semi-group properties of a "propagator" and is given explicitly by[14]

$$T_d(\mathbf{x},\mathbf{x}-\mathbf{u}l) = \exp[-\kappa \int_0^l \rho(\mathbf{x}-\mathbf{u}s)\, ds\,] \tag{A.8}$$

where the argument of the exponential is known as the "optical distance:"

$$\tau(\mathbf{x},\mathbf{x}-\mathbf{u}l) = \kappa \int_0^l \rho(\mathbf{x}-\mathbf{u}s)\, ds \tag{A.9}$$

between the two points of interest, i.e., a (unitless) measure of the cumulative amount of absorbing and/or scattering material encountered along a straight line between them. Notice that radiance is conserved (along the beam) in absence of matter and that $\tau(\mathbf{x},\mathbf{y})$, hence $T_d(\mathbf{x},\mathbf{y})$, are symmetric in their arguments.[15] If, in the above definition, we let $\mathbf{u}(=\mathbf{u}_z)$ be oriented vertically downward and put $\mathbf{x}$ on the "top" of the boundary ∂M of the medium, we can talk about τ as "optical depth" into M, below $\mathbf{x}$; conversely ($\mathbf{u}=-\mathbf{u}_z$ and $\mathbf{x}$ on the "bottom" of ∂M), we can legitimately talk about "optical altitude,"[16] especially since in cloud radiation studies the surface below the lower boundary is generally viewed as purely absorbing. In practice, water is a very good approximation to this situation.

Returning to the fundamentally probabilistic meaning of radiance discussed above (and in app. E), we have[17]

$$\mathrm{Prob}(l'>l \mid \mathbf{x},\mathbf{u}) = \frac{I_{\mathbf{u}}^{(0)}(\mathbf{x}+\mathbf{u}l)}{I_{\mathbf{u}}^{(0)}(\mathbf{x})} = \exp[-\tau(\mathbf{x},\mathbf{x}+\mathbf{u}l)] \tag{A.10}$$

In other words, photon <u>optical</u> free paths are always exponentially distributed (with unit mean) but their geometrical counterparts obey a similar law only in homogeneous media; this is the well-known Bouger-de Beer law of exponential extinction. If $\rho(\mathbf{x})$ is indeed uniform, then $\tau(\mathbf{x},\mathbf{x}+\mathbf{u}l) = \tau(l) = \kappa\rho l$ and $1/\kappa\rho$ is therefore the photon m.f.p., $\mathsf{E}(l)$. Recall that every detail of the exponential distribution is specified by its unique parameter (here, $\kappa\rho$); for instance, its statistical moments have the following simple scaling: $\mathsf{E}(l^m) = \Gamma(m+1)/(\kappa\rho)^m$.

One of its important properties is that its standard deviation is equal to its mean, equivalently, $\mathrm{Var}(l) = \mathrm{E}([l-\mathrm{E}(l)]^2) = \mathrm{E}(l^2)-\mathrm{E}(l)^2$ here reduces to $(\kappa\rho)^{-2}$. In this sense, the exponential distribution is by no means "narrow" amongst all possible distributions on $\Re^+$;[18] Waymire and Gupta [1981] would however classify it as "thin tailed" rather than "medium tailed" (e.g., the log-normal distribution used for ρ in chap. 6) or "fat tailed" (e.g., the algebraic law found for $<T_d>$ w.r.t. $<\tau>$ in chap. 5).

A.2.2. On the Characterization of Total Optical Mass by a Dimensionless Parameter

A most useful concept in standard (horizontally homogeneous, plane-parallel) radiative transfer is "optical thickness" τ^* which is the vertical optical distance from top to bottom boundaries. (We will drop the "*" when no confusion between distance and thickness is possible.) If ρ is constant, we can always choose units of length where $\kappa\rho = 1$, τ^* is therefore the geometrical thickness measured in photon m.f.p.'s. Depending on whether its value is much less that 1 or much greater that 1, we immediately know whether we are dealing with a system dominated by low or high orders-of-scattering, i.e., whether we are in the linear response regime or in the nonlinear domain of radiation/density field coupling respectively. Because this dichotomy is likely to be relevant in most[19] inhomogeneous systems as well, it is of interest to generalize the notion of optical thickness to these. This can be done either by averaging or by sampling.

In the latter case, we choose a "representative" 1-D transection through M. Letting A_0 be the (vertical) $\mathbf{u}_0$-projection of M and $\mathbf{x}=(x,z)$ with $x=(\mathbf{x}\times\mathbf{u}_0)\times\mathbf{u}_0$, then define (for some "typical" x)

$$\tau^*(x) = \kappa \int_{-\infty}^{+\infty} \rho(x,l')\,\mathrm{d}l' \qquad (x \in A_0) \tag{A.11}$$

where the infinite bounds simply make sure that the outer most bounds of M (viewed as the region where $\rho(\mathbf{x}) \neq 0$ *a priori*) are reached. This approach is obviously quite arbitrary. The alternative is by far preferable since the spatially averaged optical thickness is an "optical" (naturally non-dimensionalized) measure of total mass (hence total LWC, in the case of clouds). In this case, we take

$$\overline{\tau^*} = \frac{\int_{A_0} \tau^*(x)\mathrm{d}^{d-1}x}{\int_{A_0} \mathrm{d}^{d-1}x} = \frac{\kappa}{\mathrm{surf}(A_0)} \int_M \rho(\mathbf{x})\mathrm{d}^d\mathbf{x} \tag{A.12}$$

as the desired quantity. For instance, at uniform density, we find $\kappa\rho\mathcal{T}_0$ where $\mathcal{T}_0=\mathrm{vol(M)/surf}(A_0)$ is the average geometrical thickness of the medium (w.r.t. $\mathbf{u}_0$).

A.2.3. Average Geometrical Free Photon Path Distributions

As previously stated, when $\kappa\rho(\mathbf{x})$ is non-uniform, $1/\kappa\rho(\mathbf{x})$ must be interpreted as a "local" m.f.p. and the real (geometrical) m.f.p. will generally depend not only on **x**, **u** but also the actual realization of the stochastic process that generated the medium when it is only statistically defined. If such is the case, then the only well-defined quantities are the ensemble-averages, in this instance, $<T_d(\mathbf{x},\mathbf{x}+\mathbf{u}l)^h>$. In a (statistically) homogeneous and isotropic medium will only be a function of l and h, not of **x** nor **u**, all we need to know is the probability density function (p.d.f) of optical depth τ, at given l. We then have

$$<T_d(l)^h> = <\exp[-h\tau(l)]> = <\exp[-h\kappa\bar{\rho}l]> \tag{A.13}$$

where the spatial average is carried out over a segment of fixed length l. The first task is therefore to find the p.d.f. $p(\bar{\rho}|l)$ of the random variable $\bar{\rho}$ at given l and then to compute its Laplace transform or (Laplacian) "characteristic function:"

$$\phi_l(q) = <\exp[-q\bar{\rho}]> = \int_0^\infty e^{-q\bar{\rho}}\, p(\bar{\rho}|l)\, d\bar{\rho} \tag{A.14}$$

then to take $q=h\kappa l$. (Fourier counterparts, better adapted to distributions on $\Re$ rather than on $\Re^+$, are readily defined.) Notice that the non-negativeness of $p(\bar{\rho}|l)$ implies that $\phi_l(q)$ is also non-negative, as well as non-increasing, and analytic (it has derivatives of all orders). It can be shown [e.g., Feller, 1971] that $\ln[\phi(q)]$, the "2nd" characteristic function or "cumulant generating function" (c.g.f), has the general properties of being convex and, if polynomial, its order is 2 at most. We also note that a properly normalized p.d.f. has $\phi_l(0)=1$ and that the m^{th} statistical moment is given by $(-d\phi/dh)^m|_{h=0}$. In the "sure" case where p is a δ-function centered on the (ensemble-)mean $<\rho>$, one talks of a "degenerate" distribution and it is described by $\ln[\phi_l(q)]=-q<\rho>$.[20] In particular, the convexity of $\ln[\phi_l(h)]$—equivalently, Jensen's inequality (3.31)—implies that

$$<T_d(l)> = <\exp[-\kappa\bar{\rho}l]> \geq \exp[-\kappa<\rho>l] = T_{d,homo}(l) \tag{A.15}$$

In other words, we can expect deeper geometrical penetration of the photons (on average) into any kind of inhomogeneous medium than into its homogeneous counterpart (uniform density as equal to average or, equivalently, the same overall mass).

Given the information in (A.13–14), we find $<\mathrm{Prob}(l'\geq l)>$ at h=1 which could in turn allow us to calculate the ensemble-average moments of the photon f.p. distribution. Namely,

$$<E(l^m)> = \int_0^\infty l^m <dP(l)> \tag{A.16}$$

The above argument using the properties of the c.g.f. translate here to the fact that (A.16) will not lead to (A.10) with $\rho=<\rho>$ but to a "wider" distribution. In fact, $\langle T_d\rangle$ need no longer be an exponential decay at all, on average,[21] as was remarked early on in the relatively short history of inhomogeneous transfer research by Romanova [1975] and as we find in chap. 5 for multifractal distributions.

Eqs. (A.13–16) show how the different kinds of averages can interact and that the various powers and exponential functions that intervene guarantee that they do not commute. If the stochastic optical medium is reasonably "ergodic," then (by definition) the ensemble average can be obtained by using different segments within a single realization. Finally, we remark that even a deterministically variable medium has a non-degenerate $p(\bar{\rho}|l)$; in this case, we must distinguish between the spatial average over a segment of length l (bars) and looking at all possible l-segments (brackets).

A.3. Local and Linear Aspects: Sources and Similarity Theory

A.3.1. Source Functions and Phase Functions

If $S_{\mathbf{u}}(\mathbf{x},t)$ is a known quantity, then (A.5) can is simply solved with the help of an integrating factor, viz. $T_d(\mathbf{x},\mathbf{y})$, discussed in the last section. Such is the case when dealing with sources from thermal emission which (in d=3) is proportional to $B_\nu[T(\mathbf{x},t)]$, Planck's (black body) function for the local temperature $T(\mathbf{x},t)$, assuming the medium can be considered in local thermodynamical equilibrium (LTE). In most of this thesis, we are however interested in multiple scattering as a source in the transfer equation. The corresponding source function is

$$S_{\mathbf{u}}(\mathbf{x},t) = \oint p(\mathbf{u}'\to\mathbf{u})\, I_{\mathbf{u}'}(\mathbf{x},t)\, d^{d-1}\mathbf{u}' \tag{A.17}$$

where $p(\mathbf{u}'\to\mathbf{u})$ is known as the "phase function." Up to this point, we have made no assumptions on d (i.e., d≥1) but in (A.17), we implicitly assume d≥2. In other words, we are now interested in *bone fide* CA systems. (The important d=1 case fits best within the framework of DA transfer so we will resume our discussion of it in the chap. 2.) κp is simply the differential cross-section for the elementary scattering process, i.e., $d\sigma/d\Omega$ where the element of solid angle $d\Omega$ is $d^{d-1}\mathbf{u}$ in our notations. Thus the probability per unit length of the **u**-radiance to be scattered into direction **u**' is

$$\rho\, d\sigma(\mathbf{u}\to\mathbf{u}') = \kappa\rho\, p(\mathbf{u}\to\mathbf{u}')\, d^{d-1}\mathbf{u} \tag{A.17'}$$

In essence, $p(\mathbf{u}\to\mathbf{u}')$ is the transition probability density that defines the photon (beam) RW[22] on Ξ_d; accordingly, its units are 1/d-angle (i.e., inverse radians in d=2 and inverse steradians in d=3). The full mathematical complexity of continuous angle transfer is realized when we see that, together, (A.5) and (A.17) constitute an infinite system of fully coupled 1st order PDEs with variable coefficients which is subjected to BCs (for external illumination) that make it a boundary value problem in higher dimensions.

Due to linearity of the transfer eq. (A.5), the general case of (thermally) emitting, absorbing and scattering media is described by weighting $B_\nu[T(\mathbf{x},t)]$ by $(1-\varpi_0)$—only the absorbed fraction of radiant energy can be re-emitted in LTE—and combining it with (A.17). Furthermore, if external illumination is also present, the two problems of internal and external sources can be solved independently and their solutions superposed. Better still, the external sources that excite the diffuse radiation fields via BCs can equally well be viewed as internal sources by using 1st order scattering $S_{\mathbf{u}}^{(1)}(\mathbf{x}) = F_0 p(\mathbf{u}_0 \to \mathbf{u}) T_d(\mathbf{x}_0,\mathbf{x})$ where $\mathbf{x}_0(\mathbf{x},\mathbf{u}_0)$ is the (unique) intersection of the direct ($\mathbf{u}_0$) light beam passing through $\mathbf{x}$ with convex (cf. sect. A.4) ∂M. $T_d[\mathbf{x}_0(\mathbf{x},\mathbf{u}_0),\mathbf{x}]$ is known as the "escape probability" in direction $-\mathbf{u}_0$ from point $\mathbf{x}$ and is readily generalized to an arbitrary direction $\mathbf{u}$ followed by the exiting diffuse radiation. In this case, one writes a transfer equation for diffuse radiation that obeys simpler (homogeneous) BCs. We notice that, contrary to their thermal counterparts, $S_{\mathbf{u}}^{(1)}(\mathbf{x})$ sources are not distributed throughout the bulk of the medium, only within a photon m.f.p. from the upper boundary but, as argued above, inhomogeneity tends to make this geometrically deeper than in the equivalent homogeneous case. In other words, we witness a thickening of the "boundary layer" which we define loosely as the portion of M where directly transmitted, hence "streaming" (rather than diffuse) radiation prevails; in this context, direct transmittance applies equally to illumination of- and escape from the optical medium.

The most important question about a phase function is that of normalization. Let the "single-scattering albedo" be

$$\varpi_0 = \oint p(\mathbf{u}' \to \mathbf{u})\; d^{d-1}\mathbf{u}' \tag{A.18}$$

which, in principle, can still be a function of $\mathbf{u}$. $0 \le \varpi_0 < 1$ corresponds to absorption with probability $(1-\varpi_0)$ per (inelastic) scattering event, $\varpi_0 > 1$ corresponds to (neutron) multiplication with probability $(1-1/\varpi_0)$, while $\varpi_0 = 1$ is the important conservative (elastic) case.

It is often assumed that the phase function depends only on the relative scattering angle $\theta = \cos^{-1}(\mathbf{u}'\cdot\mathbf{u})$; this hypothesis is justified for all spherically symmetric scatterers (such as cloud droplets). In this case, the expansion of $p(\cos\theta)$ into spherical harmonics only contains the usual azimuth independent terms: letting the ϖ_n $(n=0,1,2,\cdots)$ designate the Fourier-cosine (for d=2) or Legendre (for d=3) coefficients for $n_d p(\theta)$, respectively:

$$2\pi p(\theta) = \sum_0^\infty \frac{2}{1+\delta_{0n}} \varpi_n \cos(n\theta) \quad \Leftrightarrow \quad \varpi_n = \int_{-\pi}^{+\pi} p(\theta)\cos(n\theta)\, d\theta \tag{A.19a}$$

$$4\pi p(\cos\theta) = \sum_0^\infty (2n+1)\varpi_n P_n(\cos\theta) \Leftrightarrow \quad \varpi_n = \frac{1}{2}\int_{-1}^{+1} 4\pi p(\cos\theta)\, P_n(\cos\theta)\, d(\cos\theta) \tag{A.19b}$$

A non-trivial consequence of the non-negativeness of p (related to its probabilistic interpretation) is that $|\varpi_n| \le 1$ (with "=" obtained for the degenerate δ-type phase functions). The 1st order harmonic coefficient is directly related to g, the famous "asymmetry factor:"

$$g = E(\cos\theta) = \frac{\oint \mathbf{u'}\cdot\mathbf{u}\ p(\mathbf{u'}\cdot\mathbf{u})\ d^{d-1}\mathbf{u}}{\oint p(\mathbf{u'}\cdot\mathbf{u})\ d^{d-1}\mathbf{u}} = \frac{\varpi_1}{\varpi_0} \tag{A.20}$$

Some natural and artificial examples are now in order.

In the familiar d=3, conservative Rayleigh scattering [Strutt, 1871, 1899] is described by[23] $\varpi_0=1$, $\varpi_2=1/10$, all others vanish (in particular ϖ_1, hence g=0). Another example relevant to meteorology is the Deirmendjian [1969] "C1" cloud droplet (size) distribution which, after Mie calculations and averaging over sizes, yields $g \approx 0.86$ but any reasonable representation of the corresponding phase function calls for a very large number of Legendre coefficients. It is therefore worthwhile to devise p-functions that are entirely determined by their g (and ϖ_0) value(s), especially in circumstances where no other scattering-related information is available. Truncation of the expansion at 1st order is sometimes used. In this case, $|g| \le 1/2$ in d=2 and $|g| \le 1/3$ in d=3 from (A.20), since the probabilistic significance of $p(\mathbf{u'}\cdot\mathbf{u})$ requires it to be non-negative. A model phase function that varies continuously away from isotropy but with no limit on g was proposed by Henyey and Greenstein [1941]:

$$p(\theta) = \left(\frac{\varpi_0}{4\pi}\right)\frac{1 - g^2}{(1 + g^2 - 2g\cos\theta)^{3/2}} \tag{A.21a}$$

The authors used it in connection with scattering by dust grains in the Milky Way galaxy—a situation where very little indeed is known about the chemistry and structure of the scatterers. It has gained much favour in atmospheric applications as a substitute for its non-analytical C1 counterpart. This is all for d=3 of course, the following two-dimensional Henyey-Greenstein type of phase function was used by Davis *et al.* [1989]:

$$p(\theta) = \left(\frac{\varpi_0}{2\pi}\right)\frac{1 - g^2}{1 + g^2 - 2g\cos\theta} \tag{A.21b}$$

This last phase function has rather simple radiation diagrams (i.e., $2\pi p(\theta)/\varpi_0$ vs. θ plotted in polar coordinates): a family of confocal ellipses[24] with semi-major axes $(1+g^2)/(1-g^2)$ and eccentricities $2g/(1+g^2)$. Both of the above phase functions have $\varpi_n/\varpi_0=g^n$ and in the limit $g \to \pm 1$ both yield the extreme (and degenerate) phase functions $\varpi_0\delta(\mathbf{u'}\mp\mathbf{u})$ respectively[25] as expected from the definition of g with "all forward" or "all backward" scattering. We also note that both of these model phase functions have closed-form (cumulative) distribution functions which is very convenient (accurate and CPU-time saving) in Monte Carlo simulations, see sect. B.1. Although important for validation purposes, we will see that even these idealizations are unnecessarily complicated in terms of radiative "scaling" where cloud structure dominates the overall picture, see chap. 4.

A.3.2. Similarity Theory in Scattering Media

Before seeking solutions of the transfer equation (or any other mathematically well-posed physical problem for that matter), it is important to see whether we can ease our task by relating solutions for one choice of optical parameters (κ and p) to another. This is the object of similarity theory. In particular, amongst the related solutions, one might be easier to obtain than all the others. For instance, isotropic scattering is far simpler to treat numerically and analytically than any other phase function choice. Even if we are not too successful with this assignment, we will at least learn about the basic scaling symmetries of our equations which, in itself, is a worthwhile exercise.

Substituting the m.s. sources (A.17) into the transfer eq. (A.5), we obtain

$$[\frac{1}{c}\frac{\partial}{\partial t} + \mathbf{u}\cdot\nabla]\, I_{\mathbf{u}}(\mathbf{x},t) = -\,\kappa\rho(\mathbf{x})\, [\, I_{\mathbf{u}}(\mathbf{x},t) - \oint p(\mathbf{u}'\to\mathbf{u})\, I_{\mathbf{u}'}(\mathbf{x},t)\, d^{d-1}\mathbf{u}' + S_{\mathbf{u}}(\mathbf{x},t)\,] \tag{A.22}$$

where $S_{\mathbf{u}}(\mathbf{x},t)$ now simply designates all non-m.s. sources. Following kinetic theory (and neutron transport) usage, we group the terms on the r.h.s. in order to define the extinction-scattering (collision) kernel :

$$[\, \frac{1}{c}\frac{\partial}{\partial t} + \mathbf{u}\cdot\nabla]\, I_{\mathbf{u}}(\mathbf{x},t) = \kappa\rho(\mathbf{x})\, [\, \oint K(\mathbf{u}'\to\mathbf{u})\, I_{\mathbf{u}'}(\mathbf{x},t)\, d^{d-1}\mathbf{u}' + S_{\mathbf{u}}(\mathbf{x},t)\,] \tag{A.23}$$

with

$$K(\mathbf{u}'\to\mathbf{u}) = p(\mathbf{u}'\to\mathbf{u}) - \delta(\mathbf{u}'-\mathbf{u}) \tag{A.24}$$

The similarity analysis of this problem is considerably simplified by the fact that it is linear: we can require, without loss of generality, that the $I_{\mathbf{u}}(\mathbf{x},t)$ fields associated with two choices of κ and p are identical[26] (up to a proportionality factor dependent on ICs or BCs). Notice that a change in κ is completely equivalent to an overall uniform change in $\rho(\mathbf{x})$,[27] hence a change in the total mass of the system that we have parameterized by average optical thickness $\bar{\tau}$, given by (A.12). For $I_{\mathbf{u}}=I_{\mathbf{u}}'$, we need only

$$\kappa K(\mathbf{u}'\to\mathbf{u}) = \kappa' K'(\mathbf{u}'\to\mathbf{u}) \tag{A.25a}$$

and

$$\kappa S_{\mathbf{u}}(\mathbf{x},t) = \kappa' S_{\mathbf{u}}'(\mathbf{x},t) \tag{A.25b}$$

One immediate consequence of this similarity relation is that it leaves the conservative ($\varpi_0=1$) property of the scattering kernel invariant, i.e., if $\|K\|=\oint K d^{d-1}\mathbf{u}=0$ then $\|K'\|=0$ too. Another consequence is that if K is expanded into d-dimensional spherical harmonics then, by orthogonality, all its coefficients must be rescaled by the same factor (κ'/κ) to yield those of K'. This implies that the only fixed point of (A.25a) is $K=0$ or $p(\mathbf{u}'\to\mathbf{u})=\delta(\mathbf{u}'-\mathbf{u})$, all forward (hence no real) scattering. As pointed out by McKellar and Box [1981] for d=3 and $K=K(\mathbf{u}'\cdot\mathbf{u})$, if the rescaling is only performed up to a finite order in the expansion then the similarity will only be approximate. Unfortunately, the coefficients of the δ-function in (A.24) are all equal to 1, so truncation carries risks. In particular, the conservative isotropically scattering kernel has 0 for first harmonic, -1 for all the others, so it is rescaled to a kernel (hence phase function) containing all the higher harmonics whereas van de Hulst and Grossmann's [1968] original similarity relations correspond to a 1st order truncation. (We will see that this is exactly what we expect from the similarity analysis of the diffusion equation obtained within Eddington's approximation, cf. sect. D.3)

Since many naturally occurring phase functions are strongly peaked in the forward direction, it is advantageous to model them with a δ component[28] which is readily grouped with the (extinction) δ already present in (A.24), in turn, this leads to the "δ-Eddington" rescaling of Joseph *et al.* [1976] and to Wiscombe's [1977] "δ-M" rescaling which, for instance, can be used to considerably reduce the computational load in a discrete ordinate scheme [Stamnes *et al.*, 1989]. While Davies [1978] applied the former method to homogeneous cuboids (in d=3), we are not aware of any application of the latter method outside of plane-parallel media. Finally, we must recognize that not all non-m.s. sources are compatible with (A.25a) and (A.25b) together: thermal sources $(1-\varpi_0)B_\nu[T(\mathbf{x},t)]$ are eligible whereas the 1st order scattering sources, $p(\mathbf{u}_0\to\mathbf{u})F_0\exp[-\tau(\mathbf{x}_0(\mathbf{x},\mathbf{u}_0),\mathbf{x})]$ applicable to the "direct+diffuse" formulation, are not. This reflects the fact that (the diffuse component of) the radiation field generally has boundary layers and is not so easily rescaled to a universal function.

A.3.3. *The Transfer Equation as a Balance Between Angular Anisotropy and Spatial Gradients*

In the remainder of this appendix (and most of this thesis), we will be interested in steady-state ($\partial/\partial t\to 0$ or $c\to\infty$) transfer problems with no internal sources beyond multiple scattering. In this case, the transfer equation (A.5) becomes

$$\mathbf{u}\cdot\nabla I_\mathbf{u}(\mathbf{x}) = -\kappa\rho(\mathbf{x})\left[I_\mathbf{u}(\mathbf{x}) - \oint p(\mathbf{u}'\to\mathbf{u})\, I_{\mathbf{u}'}(\mathbf{x})\, d^{d-1}\mathbf{u}'\right] \tag{A.26}$$

We can interpret this equation as a detailed balancing of spatial gradients (l.h.s. or "streaming" term) by angular anisotropy (r.h.s. or "source/sink" term) in the following sense: anisotropy (possibly imposed by BCs) drives the gradients of the radiation field and wherever gradients appear (possibly associated with internal density field variability) anisotropy is created. Stamnes [1986] provides a graphic illustration of the coupling of anisotropy and vertical gradients driven by illumination at a boundary in the context of homogeneous plane-parallel media, but this is in fact a universal aspect of radiation transport and we will observe the same phenomenon in our detailed numerical calculations of transfer in multifractal optical density fields. Simultaneously, and in response to the strongest positive density fluctuations, we will also see the creation of large scale horizontal fluxes via changes in the local angular distribution of (DA) radiance, see chap. 6.

To see how this coupling arises, we first suppose $I_{\mathbf{u}} = I$: it is independent of $\mathbf{u}$. Using the normalization condition (A.18), the r.h.s of (A.26) becomes $-\kappa\rho(1-\varpi_0)I$ which vanishes identically in the conservative case. Conversely, anisotropy implies generally non-vanishing directional gradients. (We expect this picture to remain qualitatively true for the many interesting cases where $\varpi_0 \approx 1$.) The reciprocal of this statement is easily proven in the case of isotropic (but not necessarily conservative) scattering, i.e., $p = \varpi_0/n_d$. We now suppose that the l.h.s. of (A.26) vanishes, i.e., $\mathbf{u}$ and $\nabla I_{\mathbf{u}}$ are perpendicular; this happens, for example, in plane-parallel atmospheres when $\mathbf{u}$ lies in the horizontal, at right angles to the only allowed gradients. In general, when $\mathbf{u}\cdot\nabla I_{\mathbf{u}} = 0$, the transfer eq. (A.26) implies that either

(1) $I_{\mathbf{u}} = S_{\mathbf{u}}$ and using the definition of m.s. sources (A.17) for $S_{\mathbf{u}}$ and our isotropic phase function, we find $S_{\mathbf{u}} = S = (\varpi_0/n_d)\oint I_{\mathbf{u}} d^{d-1}\mathbf{u}$, i.e., the radiation field is (locally) isotropic. Conversely, gradients that do not vanish (in all directions) promote some kind of anisotropy w.r.t. $\mathbf{u}$. In summary, the spatial and angular parts of the m.s. transfer problem are intimately intertwined by the transfer equation itself. In chap. 3 and app. D, we will be seeking different ways of simplifying the angular part in order to better study the spatial part. This is of course the exact opposite of the strategy implicit in the staggering amount of literature available on the homogeneous plane-parallel problem.

(2) $\kappa\rho(\mathbf{x}) = 0$ which reminds us of the simple fact that $I_{\mathbf{u}}$ is constant (along any $\mathbf{u}$) over an expanse of (optical) vacuum whether it lies inside or outside the boundaries of the overall optical medium under consideration. The (optically) empty medium is clearly the only one that can support simultaneously arbitrarily anisotropic $I_{\mathbf{u}}$ fields and vanishing directional gradients. A prime example of this is provided by the starry skies of cloud-free nights: $I_{\mathbf{u}}$ is composed of many δ-functions (of various magnitudes[29]) scattered—if not scattering—on Ξ_3 and a witness to the fact that interstellar space is by-and-large optically thin.[30]

A.3.4. The Various Ways of Simplifying the Angular Problem

In summary and in spite of our attempts at independent discussion of the properties of the nonlinear, propagation (hence non-local) aspects, on the one hand, and of the linear, scattering (hence local) aspects, on the other hand, as well as our (somewhat **u**-minimizing) notational efforts, the spatial ($\Re^d$) and angular (Ξ_d) parts of the m.s. problem remain closely related via the transfer equation itself. We will be presenting and comparing two very different ways of simplifying the angular part in order to better study the spatial part ... which is of course the exact opposite of the strategy implicit in the staggering amount of literature available on the horizontally homogeneous plane-parallel problem. Since in essence we a dealing with a distribution of radiant energy on Ξ_d, the required simplifications can proceed either by sampling **u**-space or by averaging the I_u-distribution.

In app. D, we explore the latter approach by taking the hydrodynamic limit of the kinetic transfer equation (A.26) with a 1st order truncation of the spherical harmonic expansion; this is (one of) the standard (and equivalent) route(s) to diffusion theory with, in particular, its characteristic "constitutive" Fickian law (which is a direct result of the above anisotropy-gradient coupling). It is, at best, an approximation of transfer which works best in very homogeneous media (chap. 4) but it is certainly an interesting physical model of transport phenomena in its own right and there is a staggering amount of literature on diffusion processes with applications in many fields; some of this literature is revisited in app. D and chap. 2 and the main results are translated into radiation language and some new results are obtained. The approximation is however not so poor that diffusion theory cannot help us to considerable insight into the mechanisms of "channeling," as tentatively defined in the introductory chapter. We have come to view this as the basic mechanism of inhomogeneous transport in higher dimensions since the simple picture drawn in chap. 2 (for weakly variable media) does not vanish from the scene in chap. 6 (for extremely variable media). This leads us to conjecture that extreme variability amplifies the effects—and the mechanisms by which they arise—already present in weakly variable media, rather than induce totally new physical transport phenomena.

In chap. 3, the former approach is exploited by using discrete angle (DA) phase functions in (A.26); the end result is a *bone fide* transfer theory that is exact in the limit of δ-type CA phase functions. This original idea of Chu and Churchill [1955] was left largely unexploited until Lovejoy *et al.* [1990], Gabriel *et al.* [1990], and Davis *et al.* [1990a] showed how it can be used both analytically and numerically to considerable advantage in inhomogeneous situations. Using a combination of analytical and numerical arguments, they show that, generally speaking, DAs are in the same class as CA transfer w.r.t. the way the predicted radiative properties scale with the size and/or mass of the system in eqs. (1.1–2). Furthermore, Davis *et al.* [1990b] show that diffusion, on the one hand, and "independent pixels" (IPs, see below), on the other hand, are retrieved as limiting cases of DA transfer, simply by further manipulating the phase function. However, the corresponding similarity relations are singular in these two limits hence IPs and diffusion are not expected to be in the same class as CAs; this prediction turns out to be true in more relevant case of extremely variable media (chap. 4).

If one is reluctant to abandon sophisticated phase functions and/or the comfort of well-understood plane-parallel media, there is a third possibility—definitely an approximation—were "channeling" is explicitly inhibited by neglecting (net) horizontal fluxes: the medium is divided into (radiatively) "independent pixels" (or columns), an expression coined by Cahalan [1989] for a procedure used already in very many circumstances for its sheer simplicity. The expression is precise and better appreciated by recalling that the author was interested in recreating (statistically speaking), by numerical simulation (and this simpler approach), what he sees in satellite imagery of typical cloud fields. Both in terms of the computational effort invested and w.r.t. the final result, IPs turn out to be a compromise between full-fledged (numerical) inhomogeneous transfer and using a (closed-form analytical) homogeneous model of equal mass. How happy this compromise is depends largely on the degree of inhomogeneity (chap. 4 and 6) and whether or not it can be used in reducing real data, as do King *et al.* [1990] will doubtless become the focus of future research. In the meantime, we indulge in IP calculations in chap. 5, using multifractal distributions of optical thickness.

A.4. Diffuse Reflection/Transmission Problem: Boundary Conditions and Overall Responses

A.4.1. Boundaries and Boundary Conditions for External Collimated Sources of Radiance

The steady-state m.s. transfer eq. (A.26) is of course only a local constraint on the radiance distribution $I_\mathbf{u}(\mathbf{x})$, $\mathbf{x} \in M$ and $\mathbf{u} \in \Xi_d$, and its directional gradients $\mathbf{u}\cdot\nabla I_\mathbf{u}$ in combination with the phase function $p(\mathbf{u}'\to\mathbf{u})$ and the local value of optical density $\kappa\rho(\mathbf{x})$. The entire radiance field is completely determined only after setting BCs. In absence of internal sources, these BCs are the only way to get radiant energy into the system. Eq. (A.26) then describes a boundary value problem (in higher dimensions) for an infinite set of (generally coupled, 1st order) PDEs.

In the above, M can be quite general; in essence, it is the support of $I_\mathbf{u}(\mathbf{x})$ and will be called the "optical medium" or, more simply, the "cloud." There is a standard topological feature of the support of $I_\mathbf{u}(\mathbf{x})$ worth mentioning: in order to define partial derivatives in all directions, M must contain a neighborhood around each of its points, it is an "open" set. In contrast to this, the boundary of M (∂M, in traditional topological notation) is a "closed" set: it contains all of its limit points.[31] In particular, this makes ∂M eligible to be fractal (hence non-rectifiable). This is in fact an attractive prospect when modelling natural clouds given (i) the non-integer dimensions found by many authors, starting with Lovejoy [1982], for (the most obvious radiometric definition of) cloud boundaries as viewed from satellite imagery, (ii) the striking realism of purely synthetic images based on renderings of stochastic scale invariant models [e.g., Lovejoy and Mandelbrot, 1985; Lovejoy and Schertzer, 1985, 1986] and (iii) that we know their dynamics to be highly turbulent and it is now well established that turbulence is generically related to fractal and multifractal structures [very many references, see app. C for a few]. We only need to think of the billowing in strongly convective ("cauliflower") clouds that generates surface features at all observable scales, but this reflects internal inhomogeneity on all scales as well; see aircraft LWC probings by Tsay and Jayaweera [1984], Stephens and Platt [1987] for fully documented examples, and Durouré and Guillemet [1990] for a simple scaling analysis.

In m.s. problems, BCs can be used to specify illumination of the medium by external sources of radiance; this class of problems is known as diffuse "reflection/transmission-" or "albedo" problems. The necessary data to be specified is $I_{\mathbf{u}}(\mathbf{x})$ for $\mathbf{x}\in\partial M$ and $\mathbf{u}\cdot\mathbf{n}(\mathbf{x})\leq 0$ where $\mathbf{n}(\mathbf{x})$ is the outward pointing normal to ∂M at $\mathbf{x}$—this assumes that ∂M is (almost everywhere) smooth, hence rectifiable (blatantly excluding the fractals just discussed, but we will soon see how to reconciliate the mathematical and physical requirements). A complete set of BCs for collimated illumination coming from direction $-\mathbf{u}_0$ with flux F_0 is

$$\left.\begin{array}{ll} I_{\mathbf{u}}(\mathbf{x}) = F_0\delta(\mathbf{u}-\mathbf{u}_0) & \text{for } \mathbf{x} \in \partial M_{\leq} \\ I_{\mathbf{u}}(\mathbf{x}) = 0 & \text{for } \mathbf{x} \in \partial M_{>} \end{array}\right\} \text{ and } \mathbf{u}\cdot\mathbf{n}(\mathbf{x}) < 0 \tag{A.27}$$

where we have defined the complementary "directly illuminated" and "shadowed" parts of ∂M

$$\begin{array}{l} \partial M_{\leq} = \{\mathbf{x}\in\partial M,\ \mathbf{u}_0\cdot\mathbf{n}(\mathbf{x})\leq 0\} \\ \partial M_{>} = \{\mathbf{x}\in\partial M,\ \mathbf{u}_0\cdot\mathbf{n}(\mathbf{x})>0\} = M\backslash\partial M_{\leq} \end{array} \tag{A.28}$$

These sub-sets of ∂M are "simply connected" if M is convex; as explained below, this property can always be assumed (at least within the framework of inhomogeneous media). We notice, incidentally, that the mere fact that M is finite in the horizontal direction (considering $\mathbf{u}_0$ to define the vertical) is sufficient to induce horizontal gradients (hence fluxes, cf. §A.3.3 above) in the radiation field, even when $\kappa\rho$ is constant within M.

If M is required to be convex then no part of ∂M "sees" (is illuminated by) any other part of ∂M; we therefore avoid the complication of explicit specification of re-entering direct- and diffuse beams. These requirements of smoothness and convexity on M only constitute real limitations—either that or complications—in the very restricted class of internally homogeneous media. Within the general framework of internally variable media, one can study non-smooth (nor even rectifiable) and/or non-convex sub-domains M' of an otherwise acceptable M simply by allowing for null values of $\rho(\mathbf{x})$, e.g., we simply can take $\rho(\mathbf{x})=\rho 1_{M'}(\mathbf{x})$ to obtain the above-mentioned homogeneous cases. ($1_S(\mathbf{x})$ denotes the indicator function of set S which is 1 if $\mathbf{x}\in S$, 0 otherwise.) The above remarks on M and ∂M make it clear that the whole program of investigation of the radiative properties of inhomogeneous cloudiness is more easily implemented within the framework of (hydrodynamically driven) variable optical density "fields" than that of (geometrically defined) cloud "shapes."

A.4.2. Horizontally Bounded Media I: The "Terminator" Definitions of Albedo

Viewing radiative transfer as a theory of remotely sensed measurement, the most important feature of the radiation field excited by external illumination is the "outgoing" radiance field, namely, $I_{\mathbf{u}}(\mathbf{x})$ for $\mathbf{x}\in\partial M$ and $\mathbf{u}\cdot\mathbf{n}(\mathbf{x}) \geq 0$. In view of the general BCs (A.27) of the diffuse reflectance/transmittance problem, the most natural definitions of (global) reflectance R_0 and transmittance T_0, are surely

$$\begin{cases} R_0 = \dfrac{1}{F_0 S_0} \displaystyle\int_{\partial M_{\leq}} F^+(\mathbf{x})\, d^{d-1}\mathbf{x} \\ T_0 = \dfrac{1}{F_0 S_0} \displaystyle\int_{\partial M_{>}} F^+(\mathbf{x})\, d^{d-1}\mathbf{x} \end{cases} \tag{A.29}$$

where

$$S_0 = \int_{\partial M_{\leq}} |\mathbf{u}_0\cdot\mathbf{n}(\mathbf{x})|\, d^{d-1}\mathbf{x} = \int_{\partial M_{>}} \mathbf{u}_0\cdot\mathbf{n}(\mathbf{x})\, d^{d-1}\mathbf{x} \tag{A.30}$$

is the (d-1)-measure of the geometrical shadow ($\mathbf{u}_0$-projected area) of M, $A_0=\{(\mathbf{x}\times\mathbf{u}_0)\times\mathbf{u}_0,\ \mathbf{x}\in M\}$, and

$$F^+(\mathbf{x}) = F_{\mathbf{n}(\mathbf{x})}(\mathbf{x}) = \int_{\mathbf{u}\cdot\mathbf{n}(\mathbf{x})\geq 0} \mathbf{u}\cdot\mathbf{n}(\mathbf{x})\, I_{\mathbf{u}}(\mathbf{x})\, d^{d-1}\mathbf{u}, \quad \text{for } \mathbf{x}\in\partial M \tag{A.31}$$

is the local outgoing flux where we used definition (A.3'). (The incoming flux, $F^-(\mathbf{x})$, is not of interest here since it is entirely determined by the said BCs.) In essence, we are saying that "transmittance starts where illumination (grazing included) stops, irrespective of direction of propagation upon escape from the medium," hence the sub-script "0" notation that is traditionally associated with external illumination. In (planetary) astronomical applications, the natural delimiting (boundary-on-a-boundary) set we have just used is called the "terminator:" $\partial M_= = \partial(\partial M_{\leq}) = \partial(\partial M_>)$, the sub-set of ∂M with exactly grazing incidence. Using this definition and assuming the Sun is at zenith, we can see—even from ground level—light "reflected" off clouds in all directions (except directly overhead) and this indeed is the proper way of defining the bright (white) parts of a typical (relatively isolated) fair weather cumulus (FwCu). At high Sun, this operational definition of the reflecting parts of a cloud coincides with that of cloud "top" but, at very slant Sun, it can include large portions of what would otherwise be viewed as a cloud "side."

Global absorptance A is, from first principles, given by

$$(F_0S_0)\,A = \int_M (\nabla\cdot\mathbf{F})\,d^d\mathbf{x} = \int_{\partial M} \mathbf{n}(\mathbf{x})\cdot\mathbf{F}(\mathbf{x})\,d^{d-1}\mathbf{x} \tag{A.32}$$

We also have

$$(F_0S_0)\,(T_0+R_0) = \int_{\partial M} F^+(\mathbf{x})\,d^{d-1}\mathbf{x} \tag{A.33}$$

Of course the divergence theorem applied to (A.26), guarantees that $A = 1\text{-}T_0\text{-}R_0$; in particular, $T_0+R_0=1$ and $A=0$ when $\varpi_0=1$, cf. (D.2).

A variation on definitions (A.29) that may appear quite subtle is to replace $\partial M_\leq$ by $\partial M_<$ and R_0 with R_0'. Subtle because R_0-R_0' vanishes with the (d-1)-measure of $\partial M_=$ which is normally 0. Following Davies [1978] and other authors, we will be considering (in sect. 4.1) the case of cubes under normal illumination ($\mathbf{u}_0$ is parallel to the "side" faces) and, sure enough, we will find that 1-R_0' is considerably larger than T_0 (even at $\varpi_0=1$) simply because surf($\partial M_=$)>0. The ensuing side "losses" have of course nothing to do with absorption even if their apparent effect on the radiative balance of the cloud is analogous ($T_0+R_0'<1$) since there is no associated heating rate ($\nabla\cdot\mathbf{F}=0$). This conclusion is unchanged even in view of the formal analogy, pointed out by Davies [*ibid.*], between new terms due to horizontal gradients that appear after horizontally Fourier-transforming the transport equation[32] and the usual absorption terms. To see how this analogy fails, recall that the presence of (true) absorption implies the existence of a characteristic optical length scale hence exponential type solutions to the transfer equation. Conversely (and apart from eventual boundary layers[33]), its absence dictates algebraic behavior to these solutions although this feature might be masked by the infinite sums of exponential (Fourier) terms and this is indeed the final format of Davies' (semi-)analytical diffusion results for R_0' or T_0 [cf. his eq. (63)].

In summary, our claim is simply that escape through sides is really just more reflectance. Although one could ask 'Why we are sub-dividing reflectance, not transmittance?' True enough, this choice is hinges entirely on the position of the "=" sign (along with "<") in definitions (A.29). This position is not arbitrary since grazing incidence is a valid choice for illumination geometry. Nor is the choice of "<," not "≤," in the conditioning of $\mathbf{u}$ in the BCs (A.27) arbitrary since outgoing grazing ($\mathbf{u}\cdot\mathbf{n}=0$) diffuse radiance is determined by the transfer equation. For instance, vanishingly thin plane-parallel media always have reflectance (and transmittance) 1/2 at grazing incidence, at least for axi-symmetric phase functions. To see this, consider a small (but finite) τ, the diffuse radiation field here reduces to its singly scattered component $I_{\mathbf{u}}^{(1)}$—which is proportional to $p(\mathbf{u}_0 \cdot \mathbf{u})$, by its very definition—for horizontal $\mathbf{u}_0$, half of this $\mathbf{u}$-distribution lies in the upper hemisphere. At $\tau=0$, this situation must persist and indeed, from BCs (A.27), we see that only 1/2 of the light gets "into" M (to be immediately transmitted) while the other 1/2 carries on to be immediately "reflected," from definitions (A.29–31). Finally, we notice that media for which surf($\partial M_{=}$) can be finite must have edges and then surf($\partial M_{=}$)>0 can only happen for particular choices of $\mathbf{u}_0$ (and their number is, at any rate, finite). We therefore suggest "collapsing" the ill-defined terminator to a properly defined one by requiring it to be stable (or "robust") w.r.t. a slight perturbation in $\mathbf{u}_0$, in all cases this should remove any ambiguity about what is transmitted versus reflected radiation. All of the above complications of course disappear as soon as we leave the rather pathological class of media that have a terminator with a surface. This is done as soon as chap. 2 where homogeneous spheres are examined and, in retrospect, a much simpler overall picture of the effect of horizontal boundedness (on the radiative properties' scaling) will be drawn in the final section of chap. 4.

A.4.3. Horizontally Bounded Media 2: The "Zenith" Definitions of Albedo

It can be argued that the choice of starting by averaging over angles really reflects our eagerness to get to a simpler (scalar) function of x to study (scalingly, of course) and that the decision to separate T from R at the terminator is just another bias towards spatial properties. But $\mathbf{u}$ is an argument of $I_{\mathbf{u}}(\mathbf{x})$ in its own right (no matter how small and low we make it look!). Hence a totally opposite approach to the definition of albedo is possible: let the light ray's direction of propagation upon escape from the medium, irrespective of the position of its "piercing point" on ∂M, decide whether it is a contribution to albedo or to transmittance.

We can define $P(\mathbf{u}_0 \rightarrow \mathbf{u})$ as the normalized radiance produced by multiple scattering within M. This constitutes a genuine return to the origins of the expression "phase function" which, in planetary astronomy, is the properly normalized measure of the (specific) "luminosity," i.e., the total flux per unit of apparent size (in steradians), measured in units of total (area-integrated) flux of incident sunlight (F_0S_0). In a sense, this is the "unresolved" radiance of an angularly resolvable celestial body, such as the Moon or Venus. If the body is sufficiently symmetric and uniform, then this ratio depends only of the object's "phase" (angle), viz. $\cos^{-1}(-\mathbf{u}_0 \cdot \mathbf{u}) = \pi - \cos^{-1}(\mathbf{u}_0 \cdot \mathbf{u})$, the angle subtended by the Earth and the Sun at the planet. The knowledge of $P(\mathbf{u}_0 \cdot \mathbf{u})$ allows the astronomer to compute the planet's brightness from F_0 which, along with $\mathbf{u}_0 \cdot \mathbf{u}$, can be predicted from celestial mechanics (and S_0 is of course tabulated); conversely, $P(\mathbf{u}_0 \cdot \mathbf{u})$ can be obtained from photometry, and celestial mechanics.

As in the case of our (transfer) phase function, we will not assume such symmetry *a priori*:

$$P(\mathbf{u}_0 \rightarrow \mathbf{u}) = \delta(\mathbf{u}-\mathbf{u}_0) + \frac{1}{F_0 S_0} \int_{\partial M} \mathbf{u} \cdot \mathbf{n}(\mathbf{x}) \, I_\mathbf{u}(\mathbf{x}) \, d^{d-1}\mathbf{x} \tag{A.34}$$

where the $\delta(\mathbf{u}-\mathbf{u}_0)$ term is introduced to cancel the incoming contributions to the integral term (from $\partial M_\leq$) and which are not to be confused with the outgoing contributions (from $\partial M_>$). Using, the definitions (A.3) of $\mathbf{F}$ and (A.32) of A, we see that angular integration of (A.34) yields

$$\oint P(\mathbf{u}_0 \rightarrow \mathbf{u}) \, d^{d-1}\mathbf{u} = 1 - A, \ \text{for all } \mathbf{u}_0 \in \Xi_d \tag{A.35}$$

as expected from global conservation considerations. In planetary applications (M is a 3-sphere), this is basically the "spherical" (planetary, or Bond) albedo.[34] Letting $-\mathbf{u}_z$ denote some "zenithal" direction (not necessarily $-\mathbf{u}_0$ but, in principle, such that $\mu_0 = \mathbf{u}_0 \cdot \mathbf{u}_z \geq 0$), we are tempted to redefine reflectance and transmittance simply by partitioning the angular integral in (A.35), i.e.,

$$\begin{cases} R_z = \displaystyle\int_{\mu \leq 0} P(\mathbf{u}_0 \rightarrow \mathbf{u}) \, d^{d-1}\mathbf{u} \\ T_z = \displaystyle\int_{\mu > 0} P(\mathbf{u}_0 \rightarrow \mathbf{u}) \, d^{d-1}\mathbf{u} \end{cases} \tag{A.36}$$

In essence, R_z and T_z are (proportional to) the leading terms in the expansions in spherical harmonics of $\Theta(-\mu)P(\mathbf{u}_0 \rightarrow \mathbf{u})$ and $\Theta(\mu)P(\mathbf{u}_0 \rightarrow \mathbf{u})$ respectively, with the "north pole" lying at $\mathbf{u}_z$. Following McKee and Cox [1974], Davies [1978] also applies this alternative definition to his cuboidal cloud models of variable aspect ratio, illuminated under various incidences. Here again, on could sub-divide R_z into its "$\mu<0$" part (R_z') and "$\mu=0$" part ($1-T_z-R_z'$) which, generally speaking,[35] vanishes along with the (solid) angle subtended by a great circle on Ξ_d. This is however just as artificial as in the "terminator" option of the previous sub-section although, unlike for that option, there is no clear reason for associating the "$\leq$" relation with albedo in (A.36) rather that a "$\geq$" relation with transmittance beyond a duality argument w.r.t. the definitions (A.29) of R_0 and T_0 (faces are associated with their normals).

We can illustrate the differences between albedo and transmittance definitions (A.29) and (A.36) qualitatively by returning to the planetary analogy. Taking $\mathbf{u}_z = \mathbf{u}_0$ for simplicity, we witness (from Earth) contributions to the Moon's "T_z-transmittance" from new moon to first quarter and the Moon's "R_z-reflectance" from then to full moon (and similarly in its waning phases); respectively, from inferior conjunction to greatest elongation and from then to superior conjunction, in the case of Venus. Using the previous (terminator-based) definition, the Moon has of course no "T_0-transmittance" at all whereas that of Venus is entirely contained in her (atmospherically-induced) "horns."

The above multiple definitions (and eventual complications) concern media with a finite S_0 (hence bounded M): R_0 and T_0 are more appealing to our intuitive idea of reflectance and transmittance from an isolated cloud whereas R_z and T_z seem more relevant to the contribution of the said cloud to (say) the surface radiation budget. (In the latter case however, we are certainly even more interested in the contribution of all the clouds, in full radiative interaction with each other, and this is really a problem to be modelled within the framework of unbounded media discussed below.) So there is no unique answer to the question of which is the most appropriate definition but there is always one which we are more interested in—furthermore, one can conjure up yet other definitions.[36] Our rule of thumb will therefore be, if clouds must be viewed in isolation, then we favour the former definitions because of their conceptual simplicity (and generally drop the "0" subscripts); if not, then there is nothing to stop us from moving the (potentially problematic) terminator set $\partial M_=$ to infinity at right angles to the vertical direction $\mathbf{u}_z$, we then obtain a horizontally extended "atmosphere."

A.4.4. Horizontally Unbounded Media: A Unique Definition of Albedo

When emulating the horizontal extension of Earth's atmosphere (as well as its relative flatness) using the procedure just suggested, cyclical horizontal BCs are used consistently in the literature, as they will be here. Recall that, if defined in discretized Fourier space, then the medium is automatically periodic as soon as Fourier space has itself been discretized, see Stephens [1986] for a direct application to CA transfer. Without loss of generality (because of the possibility of internal null ρ-values), we can take $M=]0,N[^{d-1}\otimes]0,L[$ (with $N=L$, if necessary), i.e., $\mathbf{x}=(\boldsymbol{x},z)$ with $\boldsymbol{x}=(\mathbf{x}\times\mathbf{u}_z)\times\mathbf{u}_z$ where $\mathbf{u}_z$ denotes the vertical unit vector (oriented downwards). The vertical component of $\mathbf{u}$ is traditionally denoted $\mu=\mathbf{u}\cdot\mathbf{u}_z$ and we can assume (again without loss of generality) that $\mathbf{u}_0$ lies in the 1st horizontal coordinate hyper-plane, i.e., its components are $\{\eta_0,0,\cdots,\mu_0\}$ with $\mu_0=\mathbf{u}_0\cdot\mathbf{u}_z$ (assumed ≥ 0) and $\eta_0=\sqrt{1-\mu_0^2}$. BCs then become

$$\left.\begin{array}{ll} I_\mathbf{u}(\boldsymbol{x},0) = \mu_0 F_0 \delta(\mathbf{u}-\mathbf{u}_0) & \text{for } \mu > 0 \\ I_\mathbf{u}(\boldsymbol{x},L) = 0 & \text{for } \mu < 0 \end{array}\right\} \text{ and } \boldsymbol{x} \in [0,N]^{d-1} \tag{A.37a}$$

in the vertical, and

$$I_\mathbf{u}(\cdots,0,\cdots,z) = I_\mathbf{u}(\cdots,N,\cdots,z) \text{ for } z\in[0,L],\ \mathbf{u}\in\Xi_d, \text{ and in all the (d-1) horizontal coordinates} \tag{A.37b}$$

which enforces periodicity in the horizontal, instead of

$$\left.\begin{array}{ll} I_\mathbf{u}(0,\cdots,z) = \eta_0 F_0 \delta(\mathbf{u}-\mathbf{u}_0) & \text{for } \mathbf{u}\cdot\mathbf{u}_1 > 0 \\ I_\mathbf{u}(N,\cdots,z) = 0 & \text{for } \mathbf{u}\cdot\mathbf{u}_1 < 0 \\ I_\mathbf{u}(\cdots,0,\cdots,z) = I_{-\mathbf{u}}(\cdots,N,\cdots,z) = 0 & \text{for } \mathbf{u}\cdot\mathbf{u}_i > 0\ (i=2,\cdots,d-1) \end{array}\right\} z\in[0,L] \tag{A.37b'}$$

which would apply for the same medium with "open" (or "absorbing") sides.

We are again primarily interested in the outgoing radiation fields at the "top" and "bottom" of the medium, i.e., $I_u(x,0)$ and $I_u(x,L)$, respectively for $\mu \le 0$ and $\mu \ge 0$. If BCs (A.37a,b) are adopted, then the above definitions of albedo and transmittance merge:

$$\begin{cases} R = \dfrac{1}{F_o\mu_o N^{d-1}} \int_0^N \ldots \int_0^N F^+(x,0)\, d^{d-1}x = \int_{\mu \le 0} R(u_o \to u)\, d^{d-1}u \\ T = \dfrac{1}{F_o\mu_o N^{d-1}} \int_0^N \ldots \int_0^N F^+(x,L)\, d^{d-1}x = \int_{\mu \ge 0} T(u_o \to u)\, d^{d-1}u \end{cases} \tag{A.38}$$

The first expressions are based on (A.29–31) with $n(x,L)=-n(x,0)=u_z$ and $S_o=\mu_o N^{d-1}$, not $(\mu_o N+\eta_o L)N^{d-2}$ which would be the case if the (cuboidal) cloud were isolated, and they call for the (local) outgoing hemispherical fluxes:

$$\left.\begin{array}{l} F^+(x,0) = \int_{\mu \le 0} |\mu|\, I_u(x,0)\, d^{d-1}u \\ F^+(x,L) = \int_{\mu \ge 0} \mu\, I_u(x,L)\, d^{d-1}u \end{array}\right\} \text{ for } x \in [0,N]^{d-1} \tag{A.39}$$

The second expressions in (A.38) are based on (A.36) and they call for the (spatially unresolved) bi-directional reflectance and transmittance defined (here) as:

$$\left.\begin{array}{l} R(u_o \to u) = \dfrac{|\mu|}{\mu_o F_o N^{d-1}} \int_0^N \ldots \int_0^N I_u(x,0)\, d^{d-1}x \text{ for } \mu \le 0 \\ T(u_o \to u) = \dfrac{\mu}{\mu_o F_o N^{d-1}} \int_0^N \ldots \int_0^N I_u(x,L)\, d^{d-1}x \text{ for } \mu \ge 0 \end{array}\right\} \text{ and } \mu_o \ge 0 \tag{A.40}$$

Like $P(u_o \to u)$, these have units of [(solid) angle]$^{-1}$. R and T in (A.38) can of course be viewed as the leading terms in the expansions of $R(u_o \to u)$ and $T(u_o \to u)$ in spherical harmonics. One can also define the spherical albedo of a plane parallel medium as its response to isotropic illumination and it is obtained by integrating over the residual u_o-dependence in the expression for R in (A.38).[37]

In principle, the former quantities in (A.39) can be sampled along a 1-D transection by flying a (transparent) aircraft just above cloud top with a downward looking pyranometer (resp., below cloud base, looking up) and the first in (A.40) by a radiometer on an orbiting platform programmed to keep looking at the same portion of atmosphere during fly-by (this is not feasible with the usual electro-optical scanning imagers). We notice that the information content of both types of measurement is only redundant with respect to our definition of "overall" albedo R in (A.38), the local fluxes can be used to estimate the effects of sub-pixel variability on satellite data whereas the bi-directional properties of cloud cover seem unavoidable for the inter-comparison and quantitative exploitation of satellite imagery.

---

[1]Net flux is denoted "πF" in the astrophysical (d=3) literature, the advantage of this definition is that "astrophysical" flux F and I_u share the same units hence it is easier to compare spherical (Bond) albedoes with 3-D Lambertian surfaces (uniform reflected radiance, F/π). To be consistent with this convention, one should require the phase function to be dimensionless (and $d^{d-1}u \to d^{d-1}u/n_d$, in our notations).

[2]One should subtract, a term that vanishes in general since the surface of a great circle, i.e., $\int_{l\cdot u=0} d^{d-1}u$ is null. In certain DA systems with certain choices of l, this correction can however be finite; for instance, any one of the DA(d,2d) cases in higher dimensions and with l chosen among the orthogonal directions.

[3]In other words, the isotropic component of the pressure field, trace($\underline{P}$) averaged over all d directions, is $p=\underline{P}:\underline{1}/d=U/d$, as expected from elementary kinetic theory for any ultra-relativistic ($p=E/c$) gas in d spatial dimensions.

[4]Given that diffusion theory (examined in detail in app. D) makes no attempt to model the radiance field beyond J and F, we can confidently predict it to be an exact model for transport in d=1. To see this more plainly, notice that, since $cP=J$ in d=1, thus we have not introduced any new unknowns, as is the case in d>1. They are $J=I_+ + I_- \in \Re^+$ and $F=I_+ - I_- \in \Re$ for the two independent equations (D.1) and (D.7).

[5]hence $p=U$, i.e., the maximal pressure-to-energy density ratio, just what we expect for a 1-D photon (or otherwise ultra-relativistic) gas.

[6]The derivation of (A.5) presented in app. E cannot be considered physically rigorous since it relies heavily on a questionable analogy between light- and material particles such as neutrons. It does however clarify the deep connections between radiative transfer and the theory of stochastic processes, as well as further justify the numerous analogies we make throughout this thesis with various other transport phenomena involving matter.

[7]Various states of polarization could be added making each I_u a formal 4-vector (in Stoke's representation) where only three components are independent: the two above mentioned angles and an amplitude. We refer to Chandrasekhar [1950] for details, including remarkable agreement of strictly plane-parallel calculations with observations (of the positions of "neutral" points) of multiple scattering in our ($\tau \approx 0.1$ vertically, but horizontally ∞) Rayleigh atmosphere. In the remainder of this thesis, we will ignore this complication since it has negligible effects in thick systems such as clouds where high orders of scattering dominate, hence vigorous mixture of the different polarizations. Furthermore, this simplification will allow us to explore lower and higher dimensionalities without any preconceived ideas about the fundamental 3-D nature of light and collect benefits on both conceptual and computational levels.

[8]Another refinement that we ignore, is spatial variation in the medium's dispersivity; see Harris [1965], Pomraning [1968], Zhelenznyakov [1971; and references therein] for the controversy about the proper way of modifying the transfer equation (A.5) to accommodate the effects of refraction in the limit of ray optics which are apparently important in the study of microwave transfer in plasma.

[9]Normally d = 1, 2, or 3, but in sect. 4.1 we briefly consider even higher values (in fact up to ∞).

[10]Alternatively, using (A.5) as an operational definition of κ can lead to its being effectively negative in the special case of lasing media. In our notations, the emission coefficient is $\kappa\rho S_u$ with lasing corresponding to S_u/I_u = const. > 1, i.e. more "out" than "in," due to stimulated emission (and inverted atomic populations) hence $\kappa_{eff} = -(u\cdot\nabla I_u)/\rho I_u < 0$.

[11]As defined in the hydrodynamic limit of Boltzmann's equation (E.5) which yields the Navier-Stokes eq. (C.1).

[12]Flateau and Stephens [1988] argue that the most general transfer equation can be transformed into the same simple form but with vector-like fields and matrix-like coefficients multiplying them. They work out the two-flux model in detail using invariant imbedding which demonstrates eloquently the nonlinearity of the radiation- to scattering material density field couplings. Much of the following discussion therefore applies to more general circumstances with an interesting complication (due to the fundamental nonlinearity) that appears in higher dimensions (with variability in both vertical and horizontal directions): the arising of non-commuting (generally random) matrices.

[13]This calls for the iteration of the so-called "auxiliary" integral equations which are equivalent to the transfer equation, plus BCs. These are obtained by substituting the "formal" solution of (A.5)—where radiance is expressed in terms of the source function and $T_d(x,y)$—into the definition of the multiple scattering source function (A.17), so these integral equations are fully coupled (see Dave [1965] for an application to plane-parallel systems).

[14]In order to see that (A.7–8) indeed verify (A.6), notice that we have considered $\mathbf{x}$ as a constant and that $\mathbf{u}\cdot\nabla$ is simply the (directional) derivative d/dl in direction $\mathbf{u}$ which is also held constant since we do not consider any

macroscopic refraction effects here; they only become appreciable at grazing incidence and/or long paths hence through (optically) thin, stratified and/or spherical atmospheres.

[15] At this level (a specific photon's track), the propagation process is symmetric under time reversal and very general reciprocity relations can be obtained [e.g., Lenoble, 1977]. It is equally clear that, from the point of view of photon gas thermodynamics (many photon tracks), the transfer eq. (A.5) is entropy producing even in conservative steady-state conditions; indeed, we have much more information on the photon's whereabouts (in phase space) before than after scattering (especially when multiple). In other words, (A.5) has its "H-theorem" just like any other kinetic equation such as Boltzmann's. Considerable problems however arise when hydro- and thermodynamical coupling with matter (hence the basic nonlinearity) is taken into account [Essex, 1984; and references therein].

[16] Either of these quantities provides a convenient independent variable in either 1-D transport or in horizontally homogeneous plane-parallel media in higher dimensions where $\rho(\mathbf{x})=\rho(z)$ and the optical distance between two arbitrary points is $\Delta\tau/\mu$ where $\Delta\tau=|\kappa\int_z^{z+\Delta z}\rho(z)dz|$ is the absolute difference in (say) optical depth and μ is the vertical cosine of $\mathbf{u}$. In general, such optical coordinates are of little use outside of these well-studied plane-parallel media. An exception is found in the optimization of "DA(d,2d)" Monte Carlo code (for rectangular grids) by pre-calculation of the cumulated densities along this grid lines, cf. sect. B.1.

[17] A straightforward probabilistic derivation would start with the elementary probabilities for no scattering nor absorption event to occur in the segment $[\mathbf{x},\mathbf{x}+\mathbf{u}\Delta s[$ (viz., $1-\kappa\rho(\mathbf{x})\Delta s=1-\Delta\tau$) then take the limit of optically thin segments. Hence

$$\mathrm{Prob}(l'>l\,|\mathbf{x},\mathbf{u}) = \lim_{\max_i(\Delta\tau_i)\to 0} \prod_i(1-\Delta\tau_i) = \lim_{\max_i(\Delta\tau_i)\to 0} \exp[-\Sigma_i\Delta\tau_i] = \exp[-\kappa\int_0^l \rho(\mathbf{x}+\mathbf{u}s)ds]$$

and (A.8–9) follows. Notice that the above reasoning remains valid in the limit of very singular density fields such as (fully developed) multifractals since we only deal with integrated (dressed) quantities or "measures" which are finite.

[18] A good example of a "narrow" distribution (on $\Re^+$) is the binomial distribution encountered in §2.3.4 in connection with the optical thickness field for random binary mixtures models where the density can take only one of two values (the sum of several such Bernouilli variables is binomially distributed).

[19] But not all! An exception is presented at the end of chap. 5, within the framework of multifractals.

[20] Another useful property of $\phi(q)$ is that sums of independent random variables imply convolution of their p.d.f.'s hence products of their $\phi(q)$'s or sums of their c.g.f.'s; this makes characteristic functions an essential tool in the theory behind "central limit" theorems. In particular, they have been extensively exploited in the establishing the (universal) mathematical properties of multifractals constructed by stochastic cascade processes (see app. C, for a review).

[21] This "non-exponential" behaviour is well-known in the context of (direct) gaseous transmittance for large spectral bands where one must average over many frequencies with very diversified values of κ; various more-or-less *ad hoc* models (such as the above) have been proposed and their parameters fit either to experimental data or to "line-by-line" transfer calculations [e.g., Goody, 1952].

[22] By way of contrast, it is easy to imagine that it is a kernel dependent on $\kappa\rho(\mathbf{x})$–indeed $T_d(\mathbf{x},\mathbf{y})$–that controls the more important RW in $\Re^d$ (or M, when bounded).

[23] Recall that the 2^{nd} order Legendre polynomial is $P_2(x) = (3x^2-1)/2$ and, in our notations, Rayleigh's phase function is $(3/16\pi)[1+\cos^2\theta]$.

[24] While on the topic of ellipsis (an unforeseen jump in logic), this turns out to be a rather uncanny return to Keplerian "sources" since the very name "phase function" happens to find its origins in planetary (or lunar) astronomy but in the field of radiometry, over and above celestial mechanics (see sect. A.4 for precisions). In sect. 3.1 on DA phase functions, we will find an even weirder parallel with Kepler's geometrical theory for the discrete distribution of planetary orbits via (quantum-like) group theory. A typical Keplerian "premonition" [Koestler, 1959] of discrete atomic orbitals ... hence phase function calculation (in the case of molecules, at least). Our attitude towards phase functions however is closer to Keplerian practice: we will postulate them *ex nihilo* (chap. 3) and find physical justification for them after (eq. (A.20–21), sect. 3.5 and chap. 6–7). The unifying concept in all of the above is of course spherical harmonic analysis, "harmony of the spheres" in Kepler's jargon and more synthetic outlook on the greater scheme of things.

[25]Notice that the upper sign ($g=+1$) trivializes the whole m.s. problem: what isn't transmitted directly is scattered forward! The lower sign ($g=-1$) makes the problem 1-D but certainly not trivial: the position of a (non-random) walker after an infinite number of unit steps in alternate directions starting at the origin is $\Sigma_0^\infty(-1)^n = 1/(1-(-1)) = 1/2$.

[26]In general, similarity analysis is more involved. For instance, with Navier-Stokes equations (C.1) in mind, we make the following transformations $x \to \lambda x$ (hence $\nabla \to \lambda^{-1}\nabla$) and $v \to \lambda^H v$ (hence $t \to \lambda^{1-H} t$), an independent rescaling of the dependent variable is required because of nonlinearity. Here, we must impose a $I_n \to I_n$ transformation in order to accommodate the linearity of transfer w.r.t. its sources. Moreover, we must impose $t \to \lambda t$, since c must remain constant.

[27]Thus any rescaling of density, such as that required by the (Corrsin-Obukhov) phenomenology of passive scalar advection by turbulence ($\Delta\rho \to \lambda^H \Delta\rho$), can be absorbed into a change in κ as long as the average density is rescaled in the same way. (This is required by the linearity of the mass continuity equation anyway.)

[28]As pointed out by McKellar and Box [1981], the weighting of this component seems to be a matter of personal taste.

[29]In the context of transfer, we should really be say "fluxes" (in astronomical usage) or "irradiances" (in geophysics). Specific intensity or radiance can only be defined (observationally) in terms of the surface brightness of an angularly resolved object such as the Sun, planets or the sky itself. Note that the astronomer's "magnitude" is flux on a log (or "order of singularity") scale.

[30]The geometrical distance to the stars may be huge but the optical distance is tiny and, as a matter of fact, is almost entirely accumulated in the last 10 km or so after following the light ray through vast expanses of optical void. Indeed, one airmass-worth of Rayleigh scattering brings in ≈ 0.1 in optical path (at "visible" wavelengths). This is indeed a prerequisite for obtaining reliable direct information by any means of remote sensing and applies to any other "visible" objet whether celestial and viewed from the ground, or terrestrial and viewed from orbit, whether the wavelength is "visible" or not, *strictu sensu*.

[31]This results directly from its formal definition: $\partial M = \overline{M} \cap (\Re^d \backslash M)$ where $\overline{M}$ is the "closure" of M (M plus all of its limit points) and $\Re^d \backslash M$, its complement in $\Re^d$ (the elements of $\Re^d$ which are not in M). Both these sets are of course themselves closed and closure is obviously preserved by intersection.

[32]In this [Davies, 1978] case, an approximate diffusion equation, but the same comment applies to the exact transfer equation, cf. Stephens [1986]. In both cases, the difference between the *bone fide* absorption (or multiplication) sink (or source) term and the "pseudo-source/sink" term is a very important factor of $\sqrt{-1}$, cf. discussion in sect. D.5.

[33]These boundary layers are related to the penetration of direct radiation hence, even in absence of absorption, they will be exponential (on a $1/\mu_0$ scale) in quasi-homogeneous cases but algebraic in scalingly inhomogeneous cases.

[34]It intervenes, for instance, in the calculation of the equilibrium planetary temperature in the approximation of no thermal, greenhouse- nor atmospheric circulation effects: $((1-A)F_0/\sigma_B)^{1/4}$ for the sub-solar point (F_0 is the solar constant and σ_B, the Stephan-Boltzmann constant), to be divided by $\sqrt{2}$ for the average on a slow rotator, and by $\sqrt[4]{2}$ for a fast rotator.

[35]An obvious exception is provided by orthogonal DA(d,2d) systems with $d \geq 2$ where the incidence direction must be along one of the axes (hence a finite amount of radiant energy is found propagating at $\mu = 0$).

[36]For instance, one could define a second (pseudo-)terminator with the help of $u_z \neq u_0$ and integrate spatially the fluxes up to either side of it.

[37]This is equivalent to seeking the planetary albedo of a hypothetical planet covered with small (unresolved but still radiatively independent) pixels, each made of many replicas of the same medium (if the cyclical BCs are to make any sense), and relaxing the (non-essential) constraint on u_0 that it lies in a horizontal coordinate plane.

Bibliography for Appendix A

Cahalan, R. F., "Overview of Fractal Clouds," in *Advances in Remote Sensing (RSRM'87)*, Eds. A. Deepak *et al.*, 371–389, A. Deepak, Hampton (Va.), 1989.

Chandrasekhar, S., *Radiative Transfer*, Oxford University Press, 1950. (Reprinted by Dover, New York, NY, 1960.)

Chu, M. C., and W. S. Churchill, "Numerical Solution of Problems in Multiple Scattering of Electromagnetic Radiation," *J. Chem. Phys.*, 59, 855–863, 1955.

Cannon, C. J., "Line Transfer in Two Dimensions," *Astrophys. J.*, 161, 255–264, 1970.

Dave, J. V., "Meaning of succesive iteration of the auxiliary equation in the theory of radiative transfer," *Ap. J.*, 140, p1292, 1965.

Davies, R., "The effect of finite geometry on three-dimensional transfer of solar irradiance in clouds," *J. Atmos. Sci.*, 35, 1712–1724, 1978.

Davis, A. B., P. Gabriel, S. Lovejoy, and D. Schertzer, "Asymptotic Laws for Thick Clouds, Dimensional Dependence - Phase Function Independence," in *IRS'88: Current Problems in Atmospheric Radiation*, Eds. J. Lenoble and J.F. Geleyn, pp103–106, Deepak Publ., 1989.

Davis, A. B., P. Gabriel, S. Lovejoy, D. Schertzer, and G. L. Austin, "Discrete Angle Radiative Transfer - Part III: Numerical Results and Atmospheric Applications," *J. Geophys. Res.*, 95, 11729–11742, 1990a.

Davis, A. B., S. Lovejoy, D. Schertzer, P. Gabriel, and G. L. Austin, "Discrete Angle Radiative Transfer Through Fractal Clouds," *Proceedings of the 7th Conference on Atmospheric Radiation* (San Fransisco, July 23–27), A.M.S., Boston, 1990b.

Deirmendjian, D., *Electromagnetic Scattering on Spherical Polydispersions*, 290pp, Elsevier, Amsterdam, 1969.

Durouré, C., and B. Guillemet, "Analyse des Hétérogenéités Spatiales des Stratocumulus et Cumulus," *Atmos. Res.*, 25, 331–350, 1990.

Essex, C., "Minimum entropy production in the steady state and radiative transfer," *Ap. J.*, 285, 279–293, 1984.

Feller, W., *An Introduction to Probability Theory and its Applications*, vol. 1, Wiley, New York, NY, 1971.

Flateau, P. J., and G. L. Stephens, "On the fundamental solution of the radiative transfer equation," *J. Geophys. Res.*, 93, 11037–11050, 1988.

Gabriel, P., S. Lovejoy, A. Davis, D. Schertzer, and G. L. Austin, "Discrete Angle Radiative Transfer - Part II: Renormalization Approach for Homogeneous and Fractal Clouds," *J. Geophys. Res.*, 95, 11717–11728, 1990.

Goody, R. M., "A statistical model for water-vapor absorption," *Quart. J. Roy. Meteor. Soc.*, 78, 165–169, 1952.

Harris, E. G., "Radiative Transfer in Dispersive Media," *Phys. Rev. B*, 138, 479–485, 1965.

Henyey, L. C., and J. L. Greenstein, "Diffuse radiation in the Galaxy," *Astrophys. J.*, 93, 70–83, 1941.

Joseph, J. H., W. J. Wiscombe, and J. A. Wienman, "The delta-Eddington approximation for radiative flux transfer," *J. Atmos. Sci.*, 33, 2452–2459, 1976.

King, M. D., L. F. Radke, and P. V. Hobbs, "Determination of the Spectral Absorption of Solar Radiation by Marine Stratocumulus Clouds from Airborne Measurements within Clouds," *J. Atmos. Sci.*, 47, 894–907, 1990.

Koestler, A., *The Sleepwalkers*, Hutchinson, 1959.

Lenoble, J. (Ed.), *Standard Procedures to Compute Radiative Transfer in a Scattering Atmosphere*, NCAR, Boulder, Colo., 1977. (Reprinted by A. Deepak, Hampton, Va., 1985.)

Lovejoy, S., "The area-perimeter relation for rain and clouds," *Science*, 216, 185–187, 1982.

Lovejoy, S., and B. Mandelbrot, "Fractal properties of rain and a fractal model," *Tellus*, 37A, 209–232, 1985.

Lovejoy, S., and D. Schertzer, "Generalized scale invariance in the atmosphere and fractal models of rain," *Water Resour. Res.*, 21, 1233–1250, 1985.

Lovejoy, S., and D. Schertzer, "Scale invariance, symmetries, fractals and stochastic simulation of atmospheric phenomena," *Bull. Am. Meteorol. Soc.*, 67, 21–32, 1986.

Lovejoy, S., A. Davis, P. Gabriel, D. Schertzer, and G. L. Austin, "Discrete Angle Radiative Transfer - Part I: Scaling and Similarity, Universality and Diffusion," *J. Geophys. Res.*, 95, 11699-11715, 1990.

McKee, T.B., and J.T. Cox, "Scattering of visible light by finite clouds," *J. Atmos. Sci.*, 31, 1885–1892, 1974.

McKellar, B. H. J., and M. A. Box, "The Scaling Group of the Radiative Transfer Equation," *J. Atmos. Sci.*, 38, 1063-1068, 1981.

Pomraning, G. C., "Radiative Transfer in Dispersive Media," *Ap. J.*, 153, 321–324, 1968.

Preisendorfer, R. W., *Hydrological Optics*, vols. 1–2, NOAA, PMEL, Hawaii, 1976.

Romanova, L. M., "Radiative transfer in a horizontally inhomogeneous scattering medium," *Izv. Acad. Sci. USSR Atmos. Oceanic Phys.*, 11, 509–513, 1975.

Stamnes, K., S. C. Tsay, W. J. Wiscombe, and K. Jayaweera, "A general-purpose numerically stable computer code for discrete-ordinate-method radiative transfer in scattering and emitting layered media," in *IRS'88: Current Problems in Atmospheric Radiation*, edited by J. Lenoble and J. F. Geleyn, pp448–453, A. Deepak, Hampton, Va., 1989.

Stamnes, K., "The Theory of Multiple Scattering of Radiaiton in Plane Parallel Atmospheres," *Rev. of Geophysics*, 24, 299–310, 1986.

Stephens, G. L., and C. M. R. Platt, "Aircraft observations of the radiative and microphysical properties of stratocumulus and cumulus cloud fields," *J. Climate Appl. Meteor.*, 26, 1243–1269, 1987.

Stephens, G. L., "Radiative Transfer in Spatially Heterogeneous, Two-Dimensional Anisotropically Scattering Media," *J. Quant. Spectrosc. Radiat. Transfer*, 36, 51–67, 1986.

Strutt, J. W. (Lord Rayleigh), "On the Light from the Sky, its Polarization and Colour," *Phil. Mag.*, XLI, p107, and "On the Scattering of Light by Small Paricles," *Ibid.*, p274, 1871.

Strutt, J. W. (Lord Rayleigh), "On the Transmission of Light through an Atmosphere containing Small Particles in Suspension, and on the Origin of the Blue of the Sky," *Phil. Mag.*, XLVII, p375, 1899.

Tsay, S. C. and K. Jayaweera, "Characteristics of Arctic Stratus Clouds," *J. Climate Appl. Meteor.*, 23, 584–596, 1984.

van de Hulst, H. C., and K. Grossman, "Multiple Light Scattering in Planetary Atmospheres," in *The Atmospheres of Venus and Mars*, ed. J.C. Brandt and M.B. McElroy, pp. 35–55, Gordon and Breach, New York, NY, 1968.

Waymire, E., and V. J. Gupta, "The Mathematical Structure of Rainfall Representations, Parts 1–3," *Water Resour. Reas.*, 17, 1261–1294, 1981.

Wiscombe, W. J., "The delta-M method, Rapid yet accurate radiative flux calculations for strongly anisotropic phase functions," *J. Atmos. Sci.*, 34, 1408–1422, 1977.

Wolf, E., "New Theory of Radiative Energy Transfer in Free Electromagnetic Fields," *Phys. Rev. D*, 13, 869–886, 1976.

Zhelenznyakov, V. V., "On the correct form of the equation of radiative transfer in a nonuniform magnetoactive plasma," *Ap. J.*, 168, 281–282, 1971.

Appendix B

TWO SIMPLE TECHNIQUES IN NUMERICAL TRANSFER, APPLICATIONS TO MULTIFRACTALS AND ORTHOGONAL BEAMS

Overview: We summarize the two most straightforward numerical procedures for solving transfer problems in arbitrary geometry and for arbitrary optical density fields: Monte Carlo simulation, on the one hand, and relaxation of finite difference equations, on the other hand. The first two sections are devoted to each one of these approaches and special attention is paid to their application to DA(d,2d) systems (i.e., orthogonal beams). There is only one source of error in Monte Carlo simulation and it is well-understood: finite photon statistics. In particular, it can accommodate arbitrarily thick cells which are bound to arise in multifractal media. In sharp contrast, thick cells pose a fundamental problem for finite difference approaches where cross-cell gradients are neglected; the only reliable solution is to imbed finer meshes that ultimately make the sub-cells thin, but then the method can no longer be viewed as "simple." For the purposes of the numerical experiment presented in chap. 6, we adopt a hybrid solution for the thick cell problem which proves satisfactory in the case study but has its limitations (alternatives are briefly discussed).

In short, Monte Carlo simulation provides a reliable solution of the real transfer problem (there equations are identical) but accuracy comes at a very high cost in CPU time. Finite difference equations may by derived from those of the transfer problem in various ways but they take on a life of their own; in other words, they can be solved efficiently and accurately (the relatively slow relaxation procedure can eventually be replaced by a direct sparse matrix technique) but they are only guaranteed to be reliable—even physical—if the "thin-cell" rule-of-thumb is strictly enforced. Since this is impossible for multifractals in practical situations, some compromise must be settled upon but, in turn, this makes it mandatory that finite difference techniques be carefully calibrated with the "fool-proof" Monte Carlo method. In particular, the scaling behaviour of the fully relaxed solutions must reproduce that obtained with high quality Monte Carlo simulations. For a specific report on how well the two numerical techniques compare when applied to the multifractal density field, see chap. 6 and, having satisfied the numerical reliability tests, the results are also discussed on physical grounds.

B.1. Direct Monte Carlo Simulation

B.1.1. Safe-Guards, Bins and Associated Uncertainties

The simplest possible way of obtaining a reliable answer to a radiative transfer problem with multiple scattering is to simulate the photon's random walk (RW), starting at the source and, in a conservative[1] simulation, ending as soon as the boundary (∂M) is encountered. This is known the "Monte Carlo" method. Given the vast amount of technical literature available on the subject, we will discuss it only enough to underscore the aspects where DA transfer allows a degree of conceptual simplification in the numerical procedure (which can often be "optimized" at the level of FORTRAN encoding as well). Before proceeding however, it is important to stress that, as long as one excepts the validity[2] of the radiative transfer equation (w.r.t. Maxwell's equations), Monte Carlo photons are simply the digital analogs of their real counterparts and the only fundamental difference is in the numbers involved. This contrasts sharply with other Monte Carlo particles designed to solve other types of equations. For instance, the propagation rules for "diffusing" particles (of which "ants" and "termites" are special cases [see, e.g., Bunde *et al.* [1985]) are dictated by the <u>spatially discretized</u> diffusion equation whereas the propagation rules for Monte Carlo photons are based on the very same premises as the <u>continuous space</u> transfer equation (whether in DAs or CAs).

For the albedo problem, the photon starts its journey at a random point on the illuminated part of the boundary ($\partial M_{\leq}$), in the specified ($\mathbf{u}_0$, inward) direction. In the case of conservative scattering, (it can be shown that) this event will happen—with probability 1—in a finite number of "steps." In practice however, it can take a large amount of CPU-time, too much for a single realization of the photon RW which is sometimes called a "history." Moreover, this is eventually within a single realization of the stochastic optical medium. So, at any rate, one must always set some maximum number of steps (n_{max}), stop the RW if it is reached before exit and "bin" the photon as "lost." For the simulation to be valid, the total number of lost photons (N_{lost}) should be very small compared to the grand total injected (N_{tot}), otherwise, one has in effect a spurious absorption (that, unlike real absorption, only affects highly scattered radiation). Thick homogeneous media are the worst offenders w.r.t. the loss of photons since the photon free paths are at their absolute minimum in such media (see sect.5.1). Fortunately, the scaling of the RW statistics for that case is well-known and very simple: $E(r^m|n) \sim n^{m/2}$ (any d) where r is the distance (in units of m.f.p.'s) covered after n steps (sect. D.4); hence a criterion (not necessarily optimal but) that works well enough in the homogeneous case is $\log_2 n_{max} \approx 2\log_2 \tau$ where τ is the (greatest) optical size. The same criterion has never failed to work in reasonably inhomogeneous cases. If a simulation yields $N_{lost}>0$, the tolerance (N_{lost} w.r.t. N_{tot}) will depend largely on the desired accuracy in all of the other "bins" (see discussion below). Of course, the problematic simulation can always be restarted with different n_{max} and N_{tot}, the existing photon statistics are not wasted.

Having dealt with this practical problem, we now assume the photon has reached ∂M in n steps (scatterings). It is then "binned" according to predefined spatial- and/or angular criteria which can be further subdivided into orders-of-scattering ($0 \leq n \leq n_{max}$).[3] The final subdivision is not always possible, in terms of the available memory and/or CPU time, nor is it necessarily desirable. For instance, one can be interested in estimating simultaneously albedo and transmittance flux (angularly integrated) fields (N spatial bins), on the one hand, and order-of-scattering decompositions by powers of 2 for the spatially integrated fluxes, on the other hand; this can be done with $\approx 2N+2\log_2 n_{max}$ integer bins (+1, for unscattered transmittance) over and above the $N \mathrm{x} L$ (usually real[4]) values needed to define the optical density field. In the following, a "bin" can be anything from a global response (e.g., "transmittance," defined as exit from any non-illuminated part of the boundary, into any direction and after any number of scatterings) to a narrowly defined radiance (e.g., exit out of top pixel #3904, into zenith angles in the range 21°–20° after precisely 6 scatterings).

By returning literally to the kinetic origins (app. E) of radiative transfer theory, the Monte Carlo method directly yields an "estimator" of the flux going into the bin

$$F^*_{bin} = \frac{N_{bin}}{N_{tot}} \tag{B.0a}$$

which (by construction) converges to the required radiative flux F_{bin} as $N_{tot} \to \infty$. Equivalently, on can think of many independent experiments conducted for some finite $N_{tot} \geq 1$, then

$$F_{bin} = \mathrm{E}(F^*_{bin}) = \frac{\mathrm{E}(N_{bin})}{N_{tot}} \tag{B.0b}$$

However, N_{bin} is then only a r.v. but its *a priori* variance is well-understood [e.g., Spanier and Gelbard, 1969]:

$$\mathrm{var}(N_{bin}) = \frac{N_{bin}(N_{tot}-N_{bin})}{N_{tot} - 1} \tag{B.1a}$$

is an unbiased estimator for $N_{tot}>1$. This is totally independent of the specific nature of the problem, merely a question of finite discrete statistics. Notice that N_{bin} behaves like a Poissonian r.v. when $N_{bin} \ll N_{tot}$ but, when $N_{bin} \lesssim N_{tot}$ (e.g., total albedo for a thick medium), then the 2nd factor on the r.h.s. makes use of the (certain) fact that N_{bin} will never be greater than N_{tot}, i.e., it is then N_{tot}-N_{bin} that is approximately Poissonian. This tells us that

$$\mathrm{var}(F^*_{\mathrm{bin}}) \approx \frac{F^*_{\mathrm{bin}}(1-F^*_{\mathrm{bin}})}{N_{\mathrm{tot}}} \quad \text{(B.1b)}$$

for $N_{tot} \gg 1$. In other words, Monte Carlo r.m.s. errors, $\sqrt{\mathrm{var}(F^*_{bin})}$, decrease relatively slowly with $1/\sqrt{N_{tot}}$ (and CPU-time of course increases directly with N_{tot}).

Finally, there is no reason to keep the digital "detectors" on the boundaries only. It is relatively straightforward to set up (in RAM, digital) flux measuring devices on either side of all the boundaries of all the cells. In CAs, they are incremented at the same time as the end point of the photon's current step is sought. In general, periodic horizontal BCs require more attention and, furthermore, in DAs special care must be taken to account for those long horizontal steps in optically thin rows where one or more cycles are crossed (in which case, the same photon activates the some of the counters more than once). Eqs. (B.0–1a,b) apply to bins for "exiting" fluxes where the histories are necessarily terminated. As far as we know, the question of Monte Carlo uncertainties on internal fluxes has not yet been thoroughly researched. Generally speaking, we expect that, if some N_{tot} is considered sufficient for resolving the exiting fields, then the accuracy of the statistics for the internal fields will be intermediate between those obtained for the (local) albedo and transmittance fields.

B.1.2. Numerical Simulation of the Propagation and Scattering Processes

In order to proceed, all we need to know is how to propagate and how to scatter the "digital" photon. Propagation is trivially simple in the homogeneous case where each step length is an independent exponentially distributed random variable (using optical units):

$$l = -\ln\xi \quad \text{(B.2)}$$

where ξ designates a random number uniformly distributed on [0,1]. Isotropic scattering is hardly more involved:

$$\theta = 2\pi\xi \qquad \text{in d=2} \quad \text{(B.3a)}$$

$$\theta = \cos^{-1}(1-2\xi),\ \varphi = 2\pi\xi \qquad \text{in d=3} \quad \text{(B.3b)}$$

in CAs, where the direction cosines (μ_i, $i=1,\cdots,d$) are obtained as usual. In DA(d,2d), we have simply

$$\mu_i = 1-2\mathrm{int}(2\xi) \quad \text{(B.4)}$$

and we remark that, if one opts for the case of "all-side" scattering ($t=r=0$, $s=1/2(d-1)$), then one less call to the(pseudo-)random number generator is needed. We also notice the the calculation of the "piercing points" where the ray encounters the various boundaries (which are necessary to determine whether the photon is still in M or not) is considerably simplified in the DA case. Anisotropic scattering is again a lot simpler in the orthogonal DA systems, using the probabilistic meanings of the basic phase function parameters (t,r,s). For CAs, we refer the reader to the literature for d=3 and, for d=2, we provide the formula for the scattering angle according to the 2-D Henyey-Greenstein phase function proposed and used by Davis *et al.* [1989]:

$$\theta = 2\tan^{-1}\left[\left(\frac{1-g}{1+g}\right)\tan\frac{\pi}{2}(1-2\xi)\right] \tag{B.5}$$

In this volume, it is described in sect. A.3, eq. (A.21b) and exploited in sect. 4.1. Eqs. (B.3b) and (B.5) are written with inverse trig functions only for clarity, it is never necessary to actually compute them since the the basic operations call only for the direction cosines: propagation along the various axes and angular addition (using products and sums of direction sines and cosines, not via trigonometric function calls).

We now turn to the more numerically challenging case of inhomogeneous media. All of the above applies without modification except that, after drawing the exponentially distributed optical distance to cover using (B.2), one must determine the corresponding geometrical distance by solving

$$\kappa \int_0^l \rho(\mathbf{x}+\mathbf{u}s)\, ds = -\ln\xi \tag{B.6}$$

for l; see fig. B.1 for a schematic. So, on the one hand, our particles follow the stochastic rules in (B.6) for spatial propagation, and on the other hand, any one of those associated with a phase function choice; examples being provided in (B.3–5). It is not hard to see that the histories (tracks) of such particles are Markov chains, with "transition probabilities" determined by the said rules. In steady-state injection conditions, the relative probability of finding a particle in a "state" $(\mathbf{x},\mathbf{u})$ is in direct proportion to radiance $I_\mathbf{u}(\mathbf{x})$, as constrained by the coupled integral equations spelled out in (4.6–7) which play the role of Kolmogorov-Chapman equations for the stochastic process associated with the photon random walk.[5]

Returning to the numerical solution of (B.6) can only be done by viewing each elementary cell as a homogeneous medium of optical thickness $\tau(\mathbf{i}) = \kappa\rho(\mathbf{i})l_0$, where l_0 is the grid constant (usually taken to be 1) and $\mathbf{i}=\mathrm{int}(\mathbf{x}+\mathbf{u}s)$ is the integer coordinate vector of the current position of the photon and $\rho(\mathbf{i})$, the discretized density value. In general CA (hence DA) transfer, this means obtaining "entering" and "exiting" piercing points and for each and every cell on the way and using their distance to increment the l.h.s. of (B.6)—there are however various ways of optimizing this calculation. When enough scattering material has been encountered, a simple interpolation within the last cell determines the end point of that step (and scattering angles can be reckoned). Assuming the grid is aligned with the propagation axes, this step can be considerably speeded up in DA transfer, not only because the piercing points are known *a priori* from the direction of propagation, but also because all the cumulated amounts can be pre-computed (say, from the boundary at coordinate 0) in all d directions. This carries a cost in terms of memory requirement but allows the end point's cell to be found in far less operations by doing a binary search for the readily known optical coordinate. For this to be worthwhile, we have put ourselves in the more interesting cases where $\log_2 L$ and $\log_2 N$ are both relatively large integers; we are indeed comparing these numbers of operations to anywhere from ≈ 1 to $\approx L$ or N itself with a bias towards the higher end of that range since the cells are usually made thin on average.

Note on vectorization: From the above, it is clear that the computation of a RW is so full of contingencies that it seems impossible to be—even conditionally—"pipe-lined" through a vector processor. This applies to the binary search in DAs too, but the internal DA field bins' incrementation is readily vectorized. The two remedies left to explore are: (1) to propagate a whole batch of photons unconditionally and periodically ask if they are still in M, and then to consolidate the sub-batchs that qualify [W. Ridgway, p.c.], and (2) to fill the machine's RAM with independent realizations of the stochastic medium and inject one photon per medium, making the inner most loop—inside the binary search for DAs—cover the media [P. Gauthier, p.c.]. Both solutions have relatively minor inconveniences: the former calls for more "book-keeping" code, the second heavily taxes the memory allocation, which usually carries a cost in priority. We expect that as very fast massively parallel facilities become available, and more "user friendly," Monte Carlo techniques will become very popular, since they are too simple conceptually to introduce serious "bugs" that cannot be immediately eradicated.

B.2. Finite Differencing Followed by Relaxation

B.2.1. General Principles and the Problem Posed by Thick Cells

Before even contemplating the idea of computing ensemble-average properties, it is important to apply a stringent quality control on our product at the level of single realizations. Recall that we are attempting to determine a whole slew of (linear) functionals of a (potentially violently) random density field. In spite of the proverbial robustness of the above Monte Carlo technique, it is hard to "believe" the resultant fields by visual inspection since they look very random, as they should. We are, after all, using an intrinsically statistical method to determine the value of a very large number of random variables. To probe the accuracy of our results, it is desirable to reduce to a minimum the methodological source of uncertainty—at least on one "typical" case. The traditional procedure of numerical code validation in transfer studies is to retrieve results published in the literature, for the same BCs, phase functions, illumination geometry and, most importantly, optical density field [e.g., Lenoble, 1977, for plane-parallel media]. This is of course not possible when dealing with DA phase functions and multifractal density fields. We have therefore decided to focus on one "benchmark" realization of the log-normal cascade and invoke a numerical methodology that is completely different (i.e., that is prone to go wrong in a very different way) from the Monte Carlo simulation technique, and to see how well the results agree; it should theoretically be within the known—or rather, anticipated—accuracies. This is the strategy behind the numerical work that lead up to the results confidently presented and discussed on physical grounds in chap. 6.

We have naturally opted for the next simplest technique (after Monte Carlo): finite difference equations[6] solved by straightforward (Gauss-Seidel) relaxation, no over-relaxation or under-relaxation parameter is used, for simplicity (otherwise it must be carefully turned). Here again, there is abundant literature on the topic, so we will focus on the specific application to DA transfer. The easiest way to visualize this method is to use the framework of time-dependent DA(d,2d) transfer in the presence of multiple scattering (m.s.), i.e., the fully coupled finite system of linear 1st order PDEs in eqs. (3.4–5a,b). We will take d=2 for specificity and drop the non-m.s. sources (this is the situation of practical interest described in the above anyway):

$$[\mathcal{I}\frac{\partial}{\partial t} + A_y\frac{\partial}{\partial y} + A_z\frac{\partial}{\partial z}]\ \mathbf{I}(\mathbf{x},t) = \kappa\rho(\mathbf{x})\ (\mathcal{P}-\mathcal{I})\ \mathbf{I}(\mathbf{x},t) \tag{B.7}$$

where we use time units such that c=1, let $\mathbf{I} = (I_{+y}, I_{-y}, I_{+z}, I_{-z})^T$, and

$$A_y = \begin{pmatrix} 1 & 0 & 0 & 0 \\ 0 & -1 & 0 & 0 \\ 0 & 0 & 0 & 0 \\ 0 & 0 & 0 & 0 \end{pmatrix} \qquad A_z = \begin{pmatrix} 0 & 0 & 0 & 0 \\ 0 & 0 & 0 & 0 \\ 0 & 0 & 1 & 0 \\ 0 & 0 & 0 & -1 \end{pmatrix} \tag{B.8a}$$

$$\mathcal{P} = \begin{pmatrix} t & r & s & s \\ r & t & s & s \\ s & s & t & r \\ s & s & r & t \end{pmatrix} \qquad \mathcal{I} = \begin{pmatrix} 1 & 0 & 0 & 0 \\ 0 & 1 & 0 & 0 \\ 0 & 0 & 1 & 0 \\ 0 & 0 & 0 & 1 \end{pmatrix} \tag{B.8b}$$

We are seeking the steady-state solution $\mathbf{I}(\mathbf{x})$ of the horizontally cyclical albedo problem BCs:

$$\begin{aligned} &I_{+z}(y,0) = 1,\ I_{-z}(y,L) = 0 \quad (0 \le y \le N) \\ &I_{\pm z}(0,z) = I_{\pm z}(N,z) \qquad\quad (0 \le z \le L) \end{aligned} \tag{B.9}$$

This solution is of course unknown to us but we can make a initial (educated) "guess," $\mathbf{I}^0(\mathbf{x})$, and this provides us with initial conditions, $\mathbf{I}(\mathbf{x},0)$, for the t-dependent problem. Since the (boundary) sources are constant, we know there exists an equilibrium asymptotic solution $\mathbf{I}^\infty(\mathbf{x})=\mathbf{I}(\mathbf{x},\infty)$ which is none other than to our unknown radiance field; at the same time, this guarantees the (absolute) numerical stability of the relaxation method [Press *et al.*, 1986]. Clearly the proximity of $\mathbf{I}^0(\mathbf{x})$ and $\mathbf{I}^\infty(\mathbf{x})$ in function space is the determining factor for the convergence of the method and we return to this issue in the next sub-section.

The discretization of (B.7) on the same rectangular grid as used in the previous section, leads to

$$[\, \mathbf{I}^{t+1}(\mathbf{i}) - \mathbf{I}^{t}(\mathbf{i})\,] + \sum_{1}^{d} A_j \Delta_j \mathbf{I}^{t}(\mathbf{i}) = \kappa\rho(\mathbf{i})l_0\, (P\text{-}I)\, \mathbf{I}^{t}(\mathbf{i}) \tag{B.10a}$$

where $\kappa\rho(\mathbf{i})l_0$ is the optical thickness $\tau(\mathbf{i})$ of the cell at the grid point of (integer) coordinates $\mathbf{i}$. In practice, one would normally take l_0=1 for simplicity in coding. Δ_j is the finite difference operator in the j[th] direction:

$$\Delta_j \mathbf{I}^{t}(\mathbf{i}) = \mathbf{I}^{t}(\mathbf{i}+\mathbf{u}_j) - \mathbf{I}^{t}(\mathbf{i}) \tag{B.10b}$$

Rearranging (B.10a,b), we find the simple iteration rule[7]

$$\mathbf{I}^{t+1}(\mathbf{i}) = \Big[P_{\text{cell}}(\mathbf{i}) - \sum_{1}^{d} A_j \Delta_j \Big]\, \mathbf{I}^{t}(\mathbf{i}) \tag{B.11}$$

and we are seeking its fixed point $\mathbf{I}^*(\mathbf{i})$; see fig. B.2 for an illustration. $P_{\text{cell}}(\mathbf{i})=P_{\text{cell}}(\tau(\mathbf{i}))$ is the 2dX2d "transfer matrix" of the i[th] cell, of optical thickness $\tau(\mathbf{i})$, and which is necessarily block-symmetric; for instance, in d=2, it reads

$$P_{\text{cell}}(\tau) = \begin{pmatrix} T & R & S & S \\ R & T & S & S \\ S & S & T & R \\ S & S & R & T \end{pmatrix} \tag{B.12}$$

Lovejoy *et al.* [1990] establish the connection between the steady-state, $\mathbf{I}^{t+1}(\mathbf{i})=\mathbf{I}^{t}(\mathbf{i})=\mathbf{I}^*(\mathbf{i})$, version of (B.11–12) and Preisendorfer's [1965] fundamental "Interaction Principle" which is the natural postulate for radiative transfer on discretized space—the basic transfer equation (B.7) with $\partial/\partial t=0$ being its "local" (DA) version. We should also mention that the steady-state system of finite difference equations can, in principle, be solved directly by some optimized inversion procedure for the corresponding sparse matrix problem (rather than the above iteration which not considered to be an efficient way of solving linear systems, large or small).

It is important to realize that $\mathbf{I}^*(\mathbf{i})$ is the solution of the large coupled system steady-state finite difference equations, and not the spatially discretized representation of $\mathbf{I}^\infty(\mathbf{x})$, the exact solution of the corresponding continuous space equations which is what we are really after. Even in ideal circumstances (absence of numerical round-off errors and using some non-approximate method, e.g., sparse matrix rather than relaxation algorithms), $\mathbf{I}^*(\mathbf{i})$ and $\mathbf{I}^\infty(\mathbf{i}/l_0)$ are only as close as the fineness of the grid can make them, over and beyond the homogeneity scale in principle. This is a fundamental difference between the two techniques presented in this appendix, the Monte Carlo method is totally insensitive to the spatial discretization which is only used in practice for storing an image of the medium in computer memory, with no impact whatsoever on its performance. The method of statistical simulation respects the physics of the problem completely: below the discretization (or "homogeneity") scale, the medium is treated as homogeneous, while f.p.'s that cover several cells account for the variations in density exactly.

At this point, we must consider the practical determination of the coefficients (T,R,S) in (B.12). Comparing (B.9–11), one finds

$$P_{cell} = [1-\tau(i)]I + \tau(i)P \tag{B.13}$$

where the 1st term expresses (linearized) extinction, i.e., direct transmittance for a very small optical thickness, and the 2nd expresses single-scattering contributions.

We are now in a dilemma because, on the one hand, (B.13) makes no sense if $\tau(i)$ is not very small (w.r.t. unity) and, on the other hand, $\tau(i)$ can easily change by a very large factor within one realization of the kind of "extremely" variable density field models we are interested in (cf. sect. 4.4), e.g., the "conserved" multifractals described in app. C. In practice (chap. 6), for a grid of size $\lambda = L/l_0 \approx 10^3$, the thickest cell can be $\lambda^{\gamma_{max}} \approx 10^4$ times denser than the average cell ($<\rho>=1$) and therefore cannot be made thin (via κ) without making the whole cloud optically thin! Indeed, if $\tau_{max} \approx \kappa\lambda^{\gamma_{max}} \ll 1$, then $<\bar{\tau}> = \lambda<\tau(i)> = \kappa\lambda \ll \lambda^{1-\gamma_{max}}$. In the "typical" case studied in chap. 6, this yields $\approx 1/10$; in general, the maximum order of singularity to be observed in a single realization (γ_{max}) is already $\approx$d for "microcanonical" conservation [Schertzer *et al.*, 1991] hence >1, forcing $<\bar{\tau}>$ to go to zero as λ increases. This is an unescapable consequence of the singular nature of a multifractal field: its maximum (and even the typical contributions to the mean, cf. app. C) increase faster than λ^d, so we are guaranteed to obtain thick cells sooner or later.

The most obvious fixes for this practical problem are (1) imbedded sub-grids (hence far more complicated code) or, (2) interpolation using a tabulation of (at least two of) P_{cell}'s coefficients (say, T and R) for the chosen DA phase function and optical thicknesses that range from the end of the strictly linear regime ($(1-g)\tau \approx 1/4$) to the anticipated τ_{max} (≈ 100). The disadvantage (danger?) of the latter approach is that, in the spirit of (1st order) finite differences, all gradients that might otherwise arise across a side of a single cell are neglected. A third avenue is currently being investigated, using a "semi-implicit" approach in the finite differencing from the outset [D. Schertzer and R. Borde, p.c.]. Of course, being another finite difference technique, it will also have to pass the reliability test before being adopted, i.e., favorable comparison to high quality Monte Carlo simulations for various benchmarks, including the multifractal used in chap. 6 (along the lines of the discussion in sect. 6.2) as well as some of the scaling results found in table 4.1.[8]

For the moment, we have adopted the second and simplest solution and applied it with great caution. Naturally, the (logarithmic) interpolation is done before the iteration was initiated. Using mainly optically thick cells (R≈1, T≈0) can obviously have devastating effects on the final numerical results; Lovejoy *et al.* [1990] discuss this in connection with their criticism of the the "real space renormalization" approach developed by Gabriel *et al.* [1990]. This is not a major concern here since the cells are explicitly required to be mainly thin, only exceptionally will they be quite thick; this requirement does however put an upper bound on the overall multiplier of the density field (κ). In this sense, the finite difference technique is more limited than the Monte Carlo technique because, although they are not resolved by the method, gradients on the scale of a single cell are (like everything else) exactly accounted for (in the limit of very many photons).[9] Generally speaking, the problem of thick cells must be carefully addressed whatever the numerical approach (other than Monte Carlo), e.g., the invariant imbedding formulation (followed by "adding/doubling") described by Stephens [1986].

B.2.2. Beginning and Ending: Initialization Strategy and Convergence Criterion

There are only two remaining questions but they are quite important (CPU-time is involved). What is the best initial field $\mathbf{I}^0(\mathbf{x})$? And when do we stop iterating (B.11)? As in Monte Carlo simulation, one must set an arbitrary upper bound to the number of iterations (if only, for safety) but the question of tolerance is more of an art than a science. We can start by computing the "L^p-norm" of $\Delta\mathbf{I}=\mathbf{I}^\iota-\mathbf{I}^{\iota-1}$ on our function space from its definition:

$$\| \Delta\mathbf{I} \|_p = \Sigma_{\{j\}}\int_M |\Delta I_j(\mathbf{x})|^p \, d^d\mathbf{x} \approx \Sigma_{\{j\}}\Sigma_i |\Delta I_j(i)|^p \tag{B.14}$$

The most popular of these are[10] $p=1,2,\infty$ but any one can be used to define the "distance" between $\mathbf{I}^\iota(i)$ and $\mathbf{I}^{\iota-1}(i)$ which is used as an estimator of "where we are" w.r.t. $\mathbf{I}^*(i)$, the discrete counterpart of $\mathbf{I}^\infty(\mathbf{x})$. We used our "artistic licence" to choose p=1 and used $\|\mathbf{I}^\iota-\mathbf{I}^{\iota-1}\|_1$ to monitor the situation but, in fact, we stopped the iteration when roughly the same amount of CPU time was consumed as for the Monte Carlo simulation; this gave relaxation a slight edge in terms of accuracy (see below). This strategy is obviously not optimal but satisfies our present needs which is basically to compare the two methods.

Concerning $\mathbf{I}^0(\mathbf{x})$, any choice will do (the relaxation method is "absolutely stable") but some are obviously better than others. It was initially hoped that, in the case of multifractals, the previous steps in the cascade would do well. Such is not the case, unless all the intermediate radiation fields are in fact required (e.g., to visualize the development of the "radiative cascade"). During the preliminary runs on multifractals (at n=5 for $\lambda_0=2$, hence $\lambda=32$), it became apparent that decimating the (DA) radiation fields on a finer ($N=L=4\lambda$) grid than the density field did not improve the accuracy significantly. Nor did it help (in terms of overall convergence time) to use the radiation fields associated with previous ($n = 1,\cdots,4$) cascade steps; the optimal initialization strategy seems to be to use the analytically known solution for the internal radiation fields corresponding to the "independent pixel" approximation (see sect. 3.4). Specifically, we have

$$I^0_{z+}(y;z) = I^0_{z+}(y;0) - \left(\frac{dI^0_{z+}}{d\tau'}\right)_y \tau'(y;z) \quad \text{(B.15)}$$

with

$$\begin{cases} I^0_{z+}(y;0) = 1+R_p(\tau(y)) \\ \left(\frac{dI^0_{z+}}{d\tau'}\right)_y = \dfrac{2R_p(\tau(y))}{\tau(y)} \end{cases} \quad \text{(B.16)}$$

where $R_p(\tau(y)) = 1-T_p(\tau(y))$ and $T_p(\tau)=1/(1+r\tau)$ and

$$\tau'(y;z) = \kappa\int_0^z \rho(y,z')\,dz' \quad \text{(B.17)}$$

We also have $I_{z-}(y;z) = T_p(\tau(y))$ for all z. Definitions $I_{z\pm}(y;z) = I_{+z}(y;z) \pm I_{-z}(y;z)$ finally yield the four required DA radiances: $I_{\pm z}(y;z) = [I_{z+}(y;z) \pm T_p(\tau(y))]/2$ and $I_{\pm y}(y;z) = I_{z+}(y;z)/2$.

<u>Note on vectorization and general comparison of the two methods</u>: The time consuming step in relaxation is of course the iteration of (B.11) above but it vectorizes spontaneously on condition that $I^{t+1}(i)$ and $I^t(i)$ are stored in distinct arrays, otherwise "recurrences"[11] will arise. Moreover, we need memory for T(i), R(i) and, preferably S(i) too; note however that one of these can take the place of $\tau(i)$ once the pre-computations are finished. In all, a DA(d,2d) relaxation calculation on a λ^d-grid calls ideally for a memory allocation of $(4d+4)\lambda^d$ times the number of words per real variable whereas an optimized DA Monte Carlo simulation with fully resolved internal fields calls for only $2d\lambda^d$ integers plus $3\lambda^d$ reals, i.e., as much as four times less. This last estimate assumes that orders-of-scattering statistics are not required everywhere; this would probably be unrealistically time consuming anyway; such decompositions should be limited to average fluxes or, if absolutely necessary, exiting fields in which case another $(2\log_2 n_{max}+1)\lambda^{d-1}$ integers are needed. In the end, the somewhat more accurate relaxation experiment took roughly twice the amount of time than the directly comparable (fully optimized DA) Monte Carlo. Recalling that Monte Carlo accuracy increases only as $\sqrt{\text{CPU-time}}$, this means that the two methods have roughly the same accuracy per unit of CPU-time yield, but Monte Carlo has several advantages over relaxation hence finite differences, at least at present. For instance, the statistical method naturally yields order-of-scattering statistics which contain valuable information on inhomogeneous transfer effects (see sect. 6.5) as well as on the potential effects of absorption.

[1] When non-conservative scattering is being investigated, usually several cases are needed (a range of ϖ_0 values); it is then always more efficient to compile the conservative order-of-scattering statistics and then to compute the absorptive responses:

$$N_{\text{bin},\varpi_0} = \sum_{n=0}^{n=\infty} \varpi_0{}^n N_{\text{bin},1}(n)$$

By dividing through by N_{tot} and noticing that $N_{\text{bin},1}(n)/N_{\text{bin},1} = \text{prob}_{\text{bin}}(n)$, we see that

$$F_{\text{bin},\varpi_0} = F_{\text{bin},1} \sum_{n=0}^{n=\infty} \varpi_0{}^n \,\text{prob}_{\text{bin}}(n) = F_{\text{bin},1}\, g_{\text{bin}}(\varpi_0)$$

where $g_{\text{bin}}(\cdot)$ is the "(moment) generating function" of the discrete probability distribution of the orders-of scattering in the given bin. The other—more straightforward but less efficient—option is to allow for the possibility of actually stopping the RW inside M (by calling the machine's random number generator and comparing the result to a single value of ϖ_0, unchanged for the whole simulation). In computational applications, the above summations will of course have to be truncated (at n_{max}).

[2] The status of our understanding of the connections between radiative transfer and mainstream optics formalisms is briefly reviewed (in a footnote) at the beginning of app. E; to the best of our knowledge, the most recent contribution to this effort is by Wolf [1976] who defines radiance explicitly in terms of coarse-grained quantities in the frameworks of both classical- and quantum EM theory.

[3] Other statistics can also be obtained, e.g., the horizontal distance covered between entry and exit (this is of interest in the "environment" effect in problems of inhomogeneous ground under thin aerosol atmospheres [Tanré *et al.*, 1981]). Furthermore, if the outcome is a random quantity (as in the above example), there is no obligation to always use a decimated histogram approach, one could equally well focus directly on statistical moments or even the characteristic function. Such is the flexibility of the Monte Carlo method.

[4] It is possible to use an integer in those cases where the density field can only take on a finite number of values (e.g., the "α-model" multifractals).

[5] The equivalent integral equation of (steady-state) transfer is of course readily obtained from the standard "integro-differential" equation of transfer given, e.g., in (A.29). Proof of the equivalence of the two formulations—obtaining (A.29) from (4.6–7), or simply (4.5) from (4.6)—hinges entirely on the existance of the directional derivatives $\mathbf{u}\cdot\nabla I_{\mathbf{u}}(\mathbf{x})$. This existance is certainly guaranteed if both density values and sources are finite but remains an open question for media (such as fully developed multifractals) with singular density values. The results presented in chap. 6 are however very encouraging in this respect; notice, in particular, the smoothness of the flux components in the direction of the beam in figs. 6.6–7b,b'.

[6] The question as to whether we can expect *a priori* quantitative agreement between a method based on the integro-differential formulation of transfer (such as finite differencing) and one based on the purely integral formulation (such as Monte Carlo simulation) is breifly addressed in the opening discussion of §4.4.1.

[7] Notice that the procedure in (B.11) reads somewhat like a cellular automaton rule with nearest neighbor interactions but where the state of the lattice gas is described by $\mathbf{I}(\mathbf{i})$, i.e., a 2d-vector that can assume continuous real values.

[8] Preliminary results using this approach yield different exponents than ours for the deterministic monofractal and even the albedo of homogeneous square [Borde, 1991]: exactly the same symptoms as in previously attempted finite difference approaches [Gabriel, 1988] for the same media. So, not too surprisingly, this technique will need further refinement.

[9] The Monte Carlo method may not have any fundamental problem with thick cells, but there is a practical one: if ever a photon wanders too far into a thick cell, it will only get out again at the expense of copious amounts of CPU time (scatterings)!

[10] Note that $\|\Delta \mathbf{I}\|_\infty = \text{Max}_{j\in\{j\},\mathbf{x}\in M}\, [|\Delta I_j(\mathbf{x})|]$.

[11] Due to its presence in the "pipe-line," the value of a variable in the CPU register can differ from the copy taken from RAM; final scalar and vector results generally differ and (at default settings) the compiler inhibits vectorization.

Bibliography for Appendix B

Borde, R., *Rayonnement dans les Nuages Multifractals*, Rapport de Stage de D.E.A., 28pp, LAMP, Université Blaise Pascal (Clermont-Ferrand), Juillet, 1991.

Bunde, A., A. Coniglio, D. C. Hong, and H. E. Stanley, "Transport in a two dimensional randomly composite material: Scaling theory and computer simulations of termite diffusion near superconducting limit," *J. Phys. A*, 18, L137–L144, 1985.

Davis, A. B., P. Gabriel, S. Lovejoy, and D. Schertzer, "Asymptotic Laws for Thick Clouds, Dimensional Dependence - Phase Function Independence," in *IRS'88: Current Problems in Atmospheric Radiation*, Eds. J. Lenoble and J.F. Geleyn, pp103–106, Deepak Publ., 1989.

Gabriel, P., *Discrete angle radiative transfer in uniform and extremely variable clouds*, Ph.D. thesis, 160pp, Phys. Dep., McGill Univ., Montréal, Québec, 1988.

Gabriel, P., S. Lovejoy, A. Davis, D. Schertzer, and G. L. Austin, "Discrete Angle Radiative Transfer - Part II: Renormalization Approach for Homogeneous and Fractal Clouds," *J. Geophys. Res.*, 95, 11717–11728, 1990.

Lenoble, J. (Ed.), *Standard Procedures to Compute Radiative Transfer in a Scattering Atmosphere*, NCAR, Boulder, Colo., 1977. (Reprinted by A. Deepak, Hampton, Va., 1985.)

Lovejoy, S., A. Davis, P. Gabriel, D. Schertzer, and G. L. Austin, "Discrete Angle Radiative Transfer - Part I: Scaling and Similarity, Universality and Diffusion," *J. Geophys. Res.*, 95, 11699-11715, 1990.

Preisendorfer, R.W., *Radiative Transfer on Discrete Spaces*, 460 pp, Pergamon, New York, 1965.

Press, W. H., B. P. Flannery, S. A. Teukolsky, and W. T. Vetterling, *Numerical Recipes*, Cambridge, London, 1986.

Schertzer, D., S. Lovejoy, D. Lavallée and F. Schmitt, "Universal Hard Multifractal Turbulence: Theory and Observations," in *Non-linear Dynamics of Structures*, Eds. R. Z. Sagdeev *et al.*, pp213–235, World Scientific, Hong Kong, 1991.

Spanier, J., and E. M. Gelbard, *Monte Carlo Principles and Neutron Transport Problems*, Addison-Wiley, 234pp, 1969.

Stephens, G. L., "Radiative transfer in spatially heterogeneous, two-dimensional anisotropically scattering media," *J. Quant. Spectrosc. Radiat. Transfer*, 36, 51–67, 1986.

Tanré, D., M. Herman, and P. Y. Deschamps, "Influence of the background contribution upon space measurements of ground reflectance," *Appl. Opt.*, 20, 3676–3684, 1981.

Wolf, E., "New Theory of Radiative Energy Transfer in Free Electromagnetic Fields," *Phys. Rev. D*, 13, 869–886, 1976.

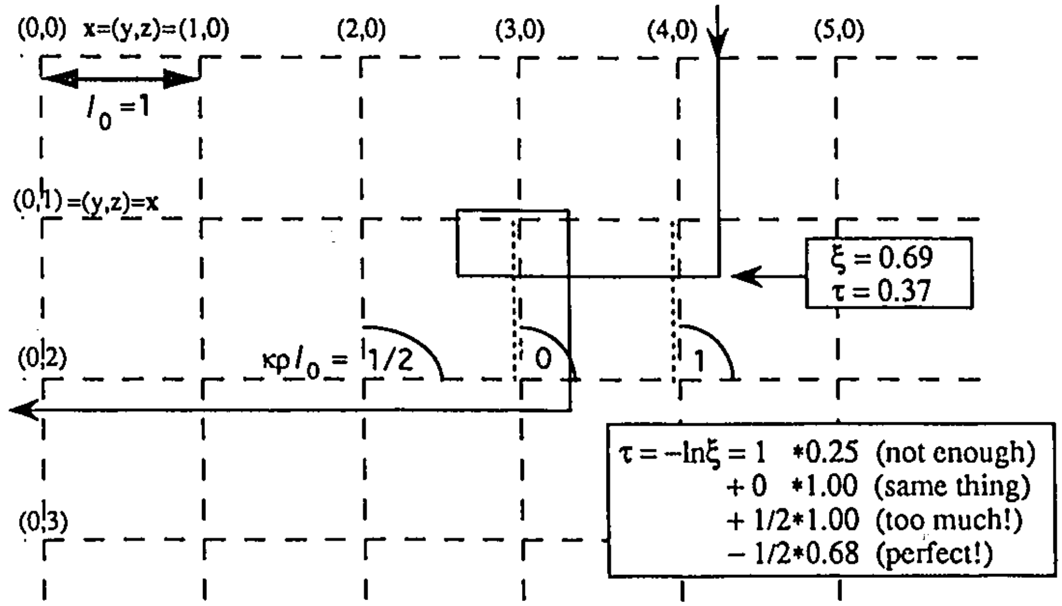

Figure B.1: Propagation in an inhomogeneous DA(2,4) Monte Carlo simulation. A short photon history with 5 scatterings is illustrated. The determination of the geometrical length of the second step is detailed; notice that fluxes in the -y direction through the interfaces between (4,1) and (4,2) on the one hand, and between (3,1) and (3,2) on the other hand, are incremented (in that order). See text for definition of the symbols.

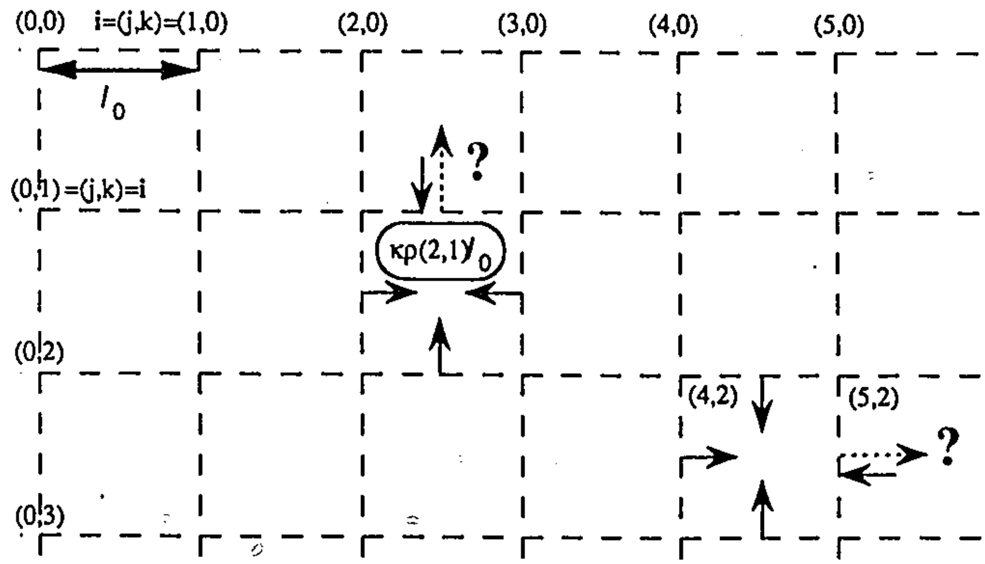

Figure B.2: Iteration in a simple DA(2,4) finite difference scheme. The density field $\rho(i)=\rho(j,k)$ is first used to determine the cell's bulk responses: $T(\tau_0)$, $R(\tau_0)$, ans $S(\tau_0)$, where $\tau_0=\kappa\rho(i)l_0$. In this case, we used logarithmic interpolation in a look-up table based on high quality (megaphoton) Monte Carlo simulations of isotropic ($t=r=s=1/4$) DA(2,4) transfer in homogeneous squares with pivot points at $\log_{10}\tau_0$=-2.0(0.1)+2.0; for $\tau_0<10^{-2}$, linear response was used and no cells cells with $\tau_0>10^{+2}$ were called for. The improved estimates of two typical fluxes are illustrated; explicitely, we have (using $l_0=1$):

$$I^{t+1}_{-z}(2.5,1) = T(2,1)\, I^{t}_{-z}(2.5,2) + R(2,1)\, I^{t}_{+z}(2.5,1) + S(2,1)\,[I^{t}_{+y}(2,1.5)+I^{t}_{-y}(3,1.5)]$$

$$I^{t+1}_{+y}(5,2.5) = T(4,2)\, I^{t}_{+y}(4,2.5) + R(4,2)\, I^{t}_{-y}(5,2.5) + S(4,2)\,[I^{t}_{+z}(4.5,2)+I^{t}_{-z}(4.5,3)]$$

The weakness of this method is the assumption of constant fluxes (sampled nominally at semi-integer coordinates) along the cell interfaces interfaces (placed nominally at integer coordinates in the perpendicular direction).

Appendix C

SCALE INVARIANT MODELLING TOOLS IN TURBULENCE THEORY

Overview: In this appendix, we survey the development of scale invariant concepts in the context of statistical fluid mechanics, from Kolmogorov's landmark contributions (sect. C.1) to recent insight into the general properties of multifractal cascades. The basic ideas of stochastic scale invariant modelling are systematically illustrated with three examples: the "β," "α," and "log-normal" models of intermittancy in turbulence. These three models are of direct use in chapters 4, 5 and 6 respectively. Moreover, we illustrate fractal geometry (sect. C.2) with several examples including Brownian motion tracks and percolation in random binary mixtures, the former are relevant to standard photon transport in homogeneous media and the latter are used to model optical media in chap. 2. Multifractals are introduced (sect. C.3), as usual, with the help of a straightforward but specific generalization of the (mono)fractal "β" model, namely, the "α" model and the concept is further illustrated with the "log-normal" model. With these examples in mind, the general multifractal formalism, centered on the Legendre transformation, is presented (sect. C.4) and it too is used in the main body of the thesis—most notably in chap. 5. The field of multifractal modelling is in rapid growth and the chosen examples are already somewhat antiquated compared to the family of "universal" multifractals (sect. C.5) that are generically related to continuous cascades. This last family of models contain the "β" and "log-normal" models as special (extreme) cases but specifically excludes "α" models for which the cascade is necessarily discrete. As in the realm of the living, energetic growth generically causes defects; in this case, multiple—somtimes conflicting—definitions, not to mention different notation schemes that have been developed independently in the literature, reflecting the multiplicity of possible applications of multiple scaling theory in physics (pure and applied). We will use our examples to show how these different definitions sometimes conflict and sometimes agree. Pictures are very important to all aspects of fractal research whereas this review is more technically oriented and therefore cannot really stand by itself; basically, the essential needs of this thesis—$c(\gamma)$, $K(h)$, $E_\varepsilon(k)$, $E_\rho(k)$—are covered in sufficient detail and we refer the reader to Lovejoy and Schertzer [1990] for visual compensation.[1]

In geophysical applications, all of the above mentioned models are motivated by turbulence theory (sect. C.1) and, accordingly, they primarily target the velocity (and related dissipation) field(s) but they can in fact be applied to any geophysical field that is shaped by reasonably nonlinear processes, i.e., in which cascade-like dynamics are expected to arise. To boot, fractals (sect. C.2) and multifractals (sect. C.3–5) can be used not only for the purposes of computer simulation (e.g., chap. 4 and 6 resp.) but also to characterize statistically empirical datasets (e.g., acquired remotely from satellite platforms). We therefore briefly discuss, at different places, several different multifractal analysis techniques currently available, as well as the results directly relevant to clouds interacting with solar radiation; in particular, this calls for a distinction between the "bare" (theoretical) and "dressed" (observable) quantities, the latter are more variable and prone to exhibit divergence of their statistical moments. Finally, we comment (sect. C.6) on the far more difficult problem of passive scalar advection by turbulence, a problem directly related to that of internal cloud structure.

C.1. Turbulent Cascade Processes, Power-Law Structure Functions and Spectra

C.1.1. Kolmogorov's Theory of Homogeneous and Isotropic Turbulence

Macroscopic velocity (and pressure) field(s) **v** (and p) obey the Navier-Stokes equation:

$$[\frac{\partial}{\partial t} + \mathbf{v}\cdot\nabla\,]\;\mathbf{v} = \nu_a\,\nabla^2\,\mathbf{v} - \frac{1}{\rho_a}\nabla p + f \tag{C.1}$$

where ν_a (10^{-5} m^2/s) and ρ_a (1.3 kg/m^3) are respectively, the (kinematic) viscosity and density of the fluid (numbers refer to air at STP) while f represents a forcing term that can partially account for the effects of BCs. Eq. (C.1) expresses the conservation of momentum in the system and must be complemented by energy and mass conservation law (not to mention BCs). Meteorologically significant motions happen in the lower atmosphere which, as a fluid, can be considered almost incompressible. Hence **v**(**x**,t) is divergence-free to a high degree of precision:

$$\nabla\cdot\mathbf{v} = 0 \tag{C.2}$$

which is sufficient to close the problem, as long as the specific acceleration term f(**x**,t) is a given quantity, no new variables have been added.[2]

We are interested in highly turbulent regimes where the nonlinear term on the l.h.s. of (C.1) dominates the viscous dissipation term. If L is the overall size of the system and V_L the characteristic velocity at that scale, then we require $V_L{}^2/L \gg \nu_a V_L/L^2$ or, equivalently, that the overall dynamical time scale (L/V_L) is much shorter than the dissipation time scale (L^2/ν_a); either way, we obtain

$$\mathrm{Re}_L = \frac{V_L L}{\nu_a} \gg 1 \tag{C.3}$$

In the atmosphere ($L \approx 10^3$–10^4 km and $V_L \approx 0.1$–100 km/h), the above Reynolds number is in the range 10^8–10^{12}. At scales somewhat smaller than L, boundary effects become negligible and those of viscosity are also negligible down to the scale (l_0) at which the flow becomes laminar ($\mathrm{Re}_{l_0} \approx 1$). In the atmosphere η can generally be put in mm–cm range. The range of scales ($L \gg l \gg l_0$) where (C.3) (with l instead of L) remains true is known as the "inertial range." Within this (vast) range of scales, the turbulent flow can be viewed, for simplicity, as (statistically) stationary in time and homogeneous in space (as well as isotropic, but only with much smaller ranges of scale in mind[3]). One talks about "fully developed" turbulence which obviously needs to be maintained by continuous external forcing. In the atmosphere, this forcing is of course guaranteed by its state of radiative non-equilibium (with clouds playing a very important role).

In his seminal "1941" paper, Kolmogorov defines a fundamental (scale invariant) quantity "ε," using a similarity argument with strong phenomenological overtones. To see how this works, we make the following substitutions

$$\begin{cases} \mathbf{x} \to \lambda \mathbf{x} & \text{hence } \nabla \to \lambda^{-1}\nabla \\ \mathbf{v} \to \lambda^{H}\mathbf{v} & \text{hence } t \to \lambda^{1-H} t \end{cases} \tag{C.4}$$

which implies, in particular, $\nu_a \to \lambda^{1+H}\nu_a$. Viewed a simple independent change of units of length and time, this naturally leaves the dimensionless Re in (C.3) unchanged for any choice of H. We however prefer to view (C.4) as a change in scale, a "zoom," simultaneously in space and in time. We then expect to see different (increasing) Re's as we zoom away from the homogeneity scale l_0 into the inertial range where the flow becomes more-and-more chaotic and, sure enough, we will come to see Re_l as a scaling function of λ, cf. (C.10) below. If the natural dimensionless number is scale dependent, is there a physical quantity that is not?

Let ε be the rate of removal of turbulent kinetic energy from the system (per unit mass):

$$\varepsilon(\mathbf{x},t) = \frac{\partial}{\partial t}\left(\frac{v^2}{2}\right) \tag{C.5}$$

The similarity transformation in (C.4) implies $\varepsilon \to \lambda^{3H-1}\varepsilon$ and Kolmogorov argues that ε cannot depend on scale within the inertial range where the dissipative effects of viscosity are too small (its time scale l^2/ν_a is much less than "eddy turn over time" v_l/l). This requires that H=1/3. The associated phenomenological picture is that of a "cascade" of turbulent kinetic energy which is injected into the system at the largest possible scales ($\approx L$) but removed only by dissipation processes only at the smallest possible scales ($\approx l_0$, often called the "Kolmogorov" scale). An "ε-flux" is thus established across the inertial range but the "transport" phenomenon is best viewed in Fourier space: a (steady-state) "ε-source" is placed in a small region (radius, $k_{min}=2\pi/L$) around the origin and all the concentric k-shells contained in the inertial range are crossed (i.e., up to $k_{max}=2\pi/l_0$) before the kinetic energy is efficiently transformed into internal heat by viscosity.

Essentially the same idea was conveyed—although more poetically[4]—by Richardson [1922]. This inspired and influential author describes the mechanism of the above flux of kinetic energy from one scale to the next as the breaking up of larger eddies into smaller ones by hydrodynamical instabilities. This "break up" is directly traceable to the intrinsically destablizing nonlinear term on the l.h.s of (C.1) where the only stabilizing term is the viscous term on the r.h.s, so the turbulent cascade stops when dissipation comes into the picture. The basic mechanism involved is "vortex stretching:" incompressible advection alone (without viscosity or diffusion) does not allow material to cross the boundaries of vorticity ($\Omega=\nabla\times\mathbf{v}$) tubes since vorticity lines are also material lines [e.g., Tritton, 1977]; so, as their length increases, their width decreases and the velocity (perpendicular to the tube's axis) increases, enhancing the nonlinear effects until break-up occurs after considerable distortion and wandering. This stretching (and its irreversible outcome) happens far more often than the opposite which would call for an unlikely cooperation of fluid particles all around the vortex tube (hence at relatively large distances). There is one notable exception where this "coherence" is guaranteed and that is when the flow is confined to two spatial dimensions where, in fact an inverse (small-to-large scale) cascade develops.[5]

By applying the divergence theorem to the scalar product of (C.1) with $\mathbf{v}$, it is readily shown that the nonlinear term on the l.h.s. makes only boundary contributions which can be made negligible in a very large volume (the velocity vanishes at ∞). We are left with the volume integrals

$$\int \varepsilon(\mathbf{x},t)\, d^3x = -\frac{\nu_a}{2}\int \left(\frac{\partial v_i}{\partial x_j}+\frac{\partial v_j}{\partial x_i}\right)^2 d^3x \qquad \text{(C.6)}$$

where the usual implicit summation of repeated indices is used. The r.h.s. is the net work of the internal stresses, i.e., heating by the friction of fluid particles one against another. This flux of kinetic energy from the macroscopic (fluid level) to the microscopic (molecular level) will be approximately true for volumes that are simply large w.r.t. l_0^3. For averages over such (inertial range) scales, we can say that $\varepsilon\sim\nu_a(\partial v/\partial x)^2$ hence ε is generally referred to simply as the (local) "dissipation" field.

In the above sense, the nonlinear term "conserves" ε during the complicated break up process (tentatively) described above, i.e., the sub-eddies each carry away their share of the total energy flux. There is however no need for this "conservation" to be exact, except for the whole system but then again the most interesting systems (such as the atmosphere) are never energetically closed anyway—otherwise the turbulence would simply decay and the fluid would end up in hydrostatic equilibrium (and slightly warmer). At best, homogeneity and isotropy are statistical symmetries of the turbulence and, accordingly, we will only require a statistical conservation of ε. In particular, only ensemble-average conservation will be required in (most of) our stochastic models for the spatial distribution of ε, i.e., explicit recipes for generating ε(x) fields using random numbers (several examples are provided in the following sections).

Kolmogorov's similarity hypothesis allows us to relate all the main quantities to the fundamentally scale invariant quantity ε, basically via dimensional analysis. For instance, the experimentally relevant structure function of the velocity field $<|\mathbf{v}(\mathbf{x}+l\mathbf{u})-\mathbf{v}(\mathbf{x})|^2>$ ($|\mathbf{u}|=1$) which, from homogeneity and isotropy, is only a function of l, the distance between the two sampling points. The scaling of the structure function can only be

$$<\Delta v^2(l)> \approx \varepsilon^{2/3}\, l^{2/3} \tag{C.7}$$

This can be rephrased in spectral terms (see §4.4.3, for definitions) to obtain Kolmogorov's famous (and ubiquitously observed) "-5/3" law,

$$E_v(k) \approx \varepsilon^{2/3}\, k^{-5/3} \tag{C.8}$$

which is expected to extend over the the full inertial range ($k_{min} \ll k \ll k_{max}$). The Kolmogorov scale itself can be estimated from $Re_{l_0} = v_{l_0} l_0/\nu_a \approx 1$ using (C.7) to evaluate the typical velocity at scale l_0 (v_{l_0}) by formally extending the spectral inertial range up to k_{max}. Hence

$$l_0 \approx \varepsilon^{-1/4}\, \nu_a^{3/4} \tag{C.9}$$

This allows us to estimate ε numerically for typical atmospheric conditions; using the numbers quoted at the opening of this section, we find 10^{-7}–10^{-3}J/kg/s which converts to 10^{-5}–10^{-1} °/day, a relatively small figure compared to typical radiative heating rates of several °/day. This does not mean that turbulence is energetically unimportant however, quite the contrary and for the following reason. Because it is solar radiation that ultimately drives the turbulent atmospheric dynamics, the above calculations underscore the importance of obtaining accurate estimates for the various contributions to the radiative budget. Now, the effect of clouds in this balance is probably the most poorly understood, largely due to their inhomogeneity which, in turn, is closely related to the atmosphere's state of turbulence (including convection) and how that affects the hydrological budget. Incidentally, the fate of water (in all phases) a major source of uncertainty in current dynamical modelling efforts, again largely due to the extreme spatial variability.[6]

Finally, by extending (C.6) down to k_{min}, (C.7) up to L, we can relate the (outer) Reynolds number in (C.3) to the outer-to-inner scale ratio $\Lambda = L/l_0$:

$$\mathrm{Re}_L = \frac{\mathrm{V}_l L}{\mathrm{v}_{l_0} l_0} \approx \Lambda^{4/3} \tag{C.10}$$

In turn, this allows us to make a rough estimate of the number of degrees of liberty that the system enjoys, namely $\mathrm{Re}_L^{3/4}$ in each of the three dimensions. We can use the above quoted values for L and l_0 to obtain an estimate of Re_L using (C.10), i.e., without making use of the known value of v_a nor any assumption about the range of wind speeds that prevails in the atmosphere: $\Lambda \approx 10^8$–10^{10} thus yields $\mathrm{Re}_L \approx 10^{12}$, in good agreement with the independent empirical estimate. This constitutes a simple validation of Kolmogorov's "2/3" (hence "-5/3") law(s). The fact that the upper end of the empirical range is more consistent with the semi-theoretical values reminds us that strong (10–100 km/h) average winds are certainly more apt to sustain fully developed turbulence than (0.1–1 km/h) breezes.

C.1.2. The Necessity of Corrections for the Intermittancy of Turbulence

The above theory of "homogeneous" turbulence can be improved by incorporating the spatial variability of ε while retaining the basic ideas of scale invariance as we will now see. Returning to the historical development, Kolmogorov's [1941] theory of homogeneous and isotropic turbulence was soon attacked, in spite of its successes, by Batchelor and Townsend on observational grounds (real turbulence exhibits "spottiness": a turbulent signal is characterized by short periods of extreme activity separated by relatively long periods of calm) and by Landau and Lifchitz [1953] on theoretical grounds (the dissipation field cannot be spatially uniform on all scales). In response to these criticisms, two competing scale invariant models were developed in the early '60s to account for the strongly "intermittent" character of the inhomogeneity in turbulence: the "fractally" homogeneous (or monofractal) model [Novikov and Stewart, 1964], on the one hand, and the log-normal model [Kolmogorov, 1962; Obukhov, 1962] which turns out to be the prototypical "multifractal," on the other hand. Of course, the terms "fractal" and "multifractal" were coined in the '70s and '80s respectively [Mandelbrot, 1975; Frisch and Parisi, 1985].

These models fall into two broader categories (next two sections) which can now be viewed as the extreme forms of a family of universal multifractals (penultimate section). The two basic multiplicative models are illustrated by two figures that can be found in the main part of this thesis, namely, fig. 4.4a and fig. 6.0. In both cases, we can see cascade processes developing in d = 2 with, on the one hand (figs. 4.4a,b), the daughter "eddies" becoming either "dead" (for once and for all) or remaining "alive" (for the moment) or, on the other hand (fig. 6.0), the daughter eddies becoming simply "weaker" or "stronger." Both examples are illustrated using a "discrete" cascade (for pedagogical purposes), i.e., the scale dividing ratio is chosen to be $\lambda_0 = 2$ for simplicity. For contrast, fig. 4.4a uses a deterministic construction (for simplicity) and a grid of increasing physical size; the latter choice is arbitrary and the overall size of the system is maybe best viewed as constant, as in fig. 6.0 where the energy flux in the (ever smaller) sub-eddies are randomly boosted or decreased. In both cases, we are dealing with a multiplicative process which is intuitively more consistent with the fundamentally nonlinear nature of the underlying dynamics.

After some relatively large number (n) of these cascade "steps," the total range of scales is $\lambda = \lambda_0^n$. In the remainder of this appendix, we will be using the following notation: let $\mu\varepsilon_i$ be the i^{th} random multiplicative increment[7] of the dissipation field. This choice of notation is based on an analogy with the usual idea of "δr" being an additive increment in, say, a standard random walk process developing in (ordinary) space as a function of time. Here, it is the random field as a whole that is developing into function-space (or rather measure-space) as a function of the scale ratio λ. We then find, at some point on the d-dimensional grid

$$\varepsilon_n = \varepsilon_\lambda = \varepsilon_0 \prod_1^n \mu\varepsilon_i \tag{C.11a}$$

for the n^{th} iterate of ε. We can think of ε_0 as Kolmogorov's uniform ε; in particular, it carries the appropriate physical dimensions (i.e., length^2/time^3). As usual, one can always choose "natural" units for which $\varepsilon_0 = 1$, without any loss of generality. Eq. (C.11a) then reads, after taking log's

$$\log_\lambda \varepsilon_\lambda = \frac{1}{n} \sum_1^n \log_{\lambda_0}(\mu\varepsilon_i) \tag{C.11b}$$

The choice of the base λ for the logarithms is arbitrary but we will soon see that the grid size—more generally speaking, the outer-to-inner scale ratio—provides the best choice (at any rate, more "natural" than e=2.718···). In a sense, the choice of a large base for the logarithms "tames" the extreme variability of the dissipation field: we are more interested in the rate at which ε_λ goes to ∞ (or 0) with ever larger λ than its actual value, i.e.,

$$\varepsilon_\lambda \sim \lambda^\gamma \tag{C.11c}$$

where γ is its associated "order of singularity (or regularity)." In the same vein, $\log_{\lambda_0}(\mu\varepsilon)$ is more interesting than $\mu\varepsilon$ itself and, borrowing from semi-group theoretical jargon, is called a "generator."

C.2. Fractal Sets as Models for the "Support" of Turbulence

C.2.1. The Two Basic Ways of Constructing Fractals and Determining their Dimensions

As an operational definition of a set A's "fractal" dimension D(A), we will simply take the exponent that replaces d (the dimensionality of space) in the mass-size relation. By "mass," we mean the number of "boxes" needed to cover A using a grid (of some large size

λ); we are therefore working at some "resolution" (box "size," or simply "scale," in the cartographical sense) $1/\lambda$ w.r.t. to the outer scale of A (taken to be 1). Let this number be

$$N_\lambda(A) \propto \lambda^{D(A)} \tag{C.12a}$$

and not the usual $N_\lambda \propto \lambda^d$ *a priori*. Equivalently,

$$D(A) = \lim_{\lambda\to\infty} \log_\lambda N_\lambda(A) \tag{C.12b}$$

In the above, $D(A) \leq d$ is justifiably known as the "box-counting" dimension of A. Notice that the d-measure of such a set is generally vanishingly small for large λ; indeed, the total number of boxes in the grid is λ^d, and $\lambda^{D(A)} \ll \lambda^d$ as soon as $D(A)<d$. It can be shown [Falconer, 1990] that the above algorithm will generally converge to the Haussdorf dimension of the set A which, roughly speaking, is defined as follows (with no need for a grid). Let $N_r(A)$ be the minimal number d-balls of maximum size r that are necessary to cover the set A (i.e., the most efficient covering), then there is a unique "critical" exponent D(A) such that $N_r(A)r^{D'}$ goes to 0 for $D'>D(A)$ and to ∞ for $D'<D(A)$ as r goes to 0 (hence $N_r(A)$ to ∞). Moreover, the limit (not necessarily finite) towards which $N_r r^{D(A)}$ converges is the Haussdorf measure of A, denoted $\int_A d^{D(A)}x$ in straightforward generalization of the Lebesgue measure we have (implicitly) used up until now, viz. $\int_A d^d x$. In (C.12–13), $1/\lambda$ plays the role of r and the grid provides an expedient way of estimating (if not determining exactly) N_r.

We can illustrate the definition in (C.12b) with the example found in fig. 4.4a which uses $\lambda_0=2$ and $d=2$. By inspection, we see that $\lambda=2^n$ and $N_\lambda=3^n$ (whereas the total surface goes as $4^n=\lambda^2$) hence

$$D = \frac{\log 3^n}{\log 2^n} = \log_2 3 = 1.585\cdots \tag{C.13}$$

Numerous other examples can be found in Mandelbrot's [1975, 1977, 1983] "essays." A majority of the constructions he presents use one of two basic strategies; another of his favorite procedures, iteration of nonlinear (complex) mappings, is not unrelated to the idea of Poincaré phase space maps that are used in dynamical systems research (briefly discussed in §3.2.2).

The simplest way to proceed is by recursively removing points from a d-dimensional set. The prototypical fractal of this category is the famous Cantor set, which is the d=1 and $\lambda_0=3$ counterpart of the above fig. 4.4a where the middle section is systematically removed; in other words, its "generator" is "——— → — —" and we see that the "mass" (in fact, total length) is reduced by a factor of 2/3 at each iteration. The recursivity guarantees that the limiting set is self-similar: every part of it is a smaller image of the whole. The end product is isomorphic with the set of all points on [0,1] with a coordinate that contains no 1's when expressed in base 3 which is clearly very sparse w.r.t. the full segment. The above box-counting algorithm would yield $D=\log_3 2=0.631\cdots$ which is indeed less than 1. In Mandelbrot's pictural description, it is less than a line and more than a point, a "dust."

The most numerous examples however proceed in the opposite direction, i.e., by recursively adding new points to some lower ($d'<d$) dimensional set. The deterministic prototype of this category is the well-known Koch "snowflake" or "island" where we are focussing on the ever more convoluted shape of the boundary, i.e., $d'=1<d=2$ (d' is the "topological" dimension of the Koch "curve"). In this case, we again have $\lambda_0=3$ but the generator is "____ → _/_" for each of the three sides of an equilateral triangle, the "mass" (in fact, length of the perimeter) is increased by a factor of 4/3 at each iteration. In such examples, the shrinking boxes (of dimension $d=2$) of the box-counting algorithm in (C.12a,b) can be replaced by ever smaller segments (of dimension $d'=1$) linking ever closer points on the curve—this is known as Richardson's "yardstick" algorithm. With this difference in mind, definition (C.12b) still applies and we find $D=\log_3 4=1.262\cdots$, as intuitively expected, we find $d'<D<d$; had we applied box-counting to the "island" as whole rather than its "coastline," we would have of course found $D=d=2$—it is a so-called "fat" fractal.

Interestingly (from the radiative transfer viewpoint), the prototypical random counterpart of the above additive procedure is provided by the trace of standard Brownian motion, e.g., a photon's random walk (RW) in an infinite homogeneous medium, as a function of time (or number of scatterings) in $\Re^d$ has $D = \min(2,d)$. To see this, notice that the "large parameter" is Δt, the number of steps, and the "field quantity," is the total displacement $|\Delta r|$ from $t=0$ to $t=\Delta t \gg 1$. Now the scaling of uncorrelated, finite step (variance) RWs is $\langle \Delta r_t{}^h \rangle \sim (\Delta t^H)^h$ with $H = 1/2$ (see §D.4.1) which is known, in general, as the "Hölder" exponent and measures the irregularity of the process ($H \geq 1$ can be associated with smooth, ballistic motion); notice the simple scaling w.r.t. h, the order of the statistical moment. However, the "size" of the object (equivalent to scale ratio λ) is Δr, and its "mass," the analog of $N_{\Delta r}$, is $\propto \Delta t$ (in higher dimensions); so, using $h=1$ in the above, we find $N_{\Delta r} \sim \Delta r^{1/H}$ and, according to (C.12a,b), we obtain $D=1/H=2$ (if $d>1$). This of course generalizes to other values of H which correspond to correlated ($1 \geq H > 1/2$) or anti-correlated ($0<H<1/2$) steps and the associated processes are known as "fractional" Brownian motion; they are indeed readily generated by fractionally integrating (to order $H+1/2$) a sample of purely white noise (this is conveniently done by applying a scaling low-pass filter in Fourier space, the final spectral exponent is $2H+1$). A related example is provided by the graph of any one of the Brownian particle's coordinates as a function of t, say x(t). Viewed as a curve, this graph is self-affine rather than self-similar (i.e., the scale changes are different for the space and time variables) and it has D=3/2 while its intersection with the time axis (or "zero-crossing set") has D=3/2-1=1/2, by virtue of the fractal intersection theorem; see Falconer [*ibid.*] for details, including many proofs as well as generalizations to $H \neq 1/2$ as well as to Lévy processes which are characterized by steps with infinite variance. We will briefly discuss spatial generalizations in §C.4.2, in connection with Mandelbrot's [1974] (monofractal) model for the "support" of turbulence (in fact, the dissipation field).

Finally, we remark that fractal sets are uniquely defined by their construction procedure but not vice-versa. For instance, apart from an affine transformation than brings an equilateral- to a right-angled isosceles triangle, we arrive at the same limiting set as in fig. 4.4a starting by with an equilateral triangle made up of 4 half-sized images of itself and recursively removing the central one; the result is known as the Sierpiński gasket. More intriguingly, on can also build a Sierpiński gasket additively: starting with the unit segment, we replace it with half of a regular hexagon, and so on (cf. Mandelbrot's [e.g., 1983] discussion of the "arrowhead" curve).

C.2.2. (Many) Other Geometrical, Computational and Physical Ways of Obtaining Fractals

It is important to realize that we have not exhausted the ways of obtaining fractals in the previous sub-section. Not even for Sierpiński gaskets! They indeed arise as the result of playing the "chaos game," as well as in the time evolution of simple one-dimensional cellular automata starting with only one "live" cell [e.g., Peterson, 1988]. These last ways of producing a Sierpiński gasket are quite interesting because they have a dynamical, rather than purely geometrical flavor to them. Remaining in the context of strictly deterministic behaviour that "looks random," the interest in "strange" (i.e., fractal) attractors in nonlinear dynamical systems seems to be growing with no foreseeable bounds. In our opinion however, the most interesting systems consist of physical models that are generally described by analytically intractable equations, rather than the above mathematical models that basically postulate their equations in a form that facilitates their manipulation; the latter approach leads to "deterministic chaos" whereas the former spontaneously develop fractal patterns that are characterized by *bone fide* randomness. Examples abound [e.g., Pietronero and Tosati, 1986; Pietronero, 1989; Aharony and Feder, 1990], many provided by laboratory- or computational situations: growth phenomena such as diffusion limited aggregation (or "DLA"), statistical physics tools and/or phenomena such as spin glasses, "roughening" in phase transitions, lattice gas simulations, models of self-organized critical systems, etc. Many other examples [e.g., PAGEOPH, 1989; Schertzer and Lovejoy, 1991] come from natural (geophysical) situations. As a general rule, we are dealing with systems that are characterized by very many degrees of freedom.

For our final example, we nevertheless return to geometry—but with a distinctly stochastic ingredient added—and describe an extraordinarily simple system which has attracted a lot of attention from physicists (during the late '70s and early '80s): fields of randomly distributed "live" and "dead" cells, "0s" and "1s," or whatever. The relative probabilities are p and 1-p (respectively), and no correlations are introduced from one cell to the next (i.e., spatially discretized binary white noise in higher dimensions). The huge amount of interest generated by this model hinges entirely on the purely geometrical phenomenon of "percolation." In turn, this phenomenon dominates the transport properties of such systems that we will discuss in some detail in §§D.6.2–3 and use in §2.3.4 to illustrate the basic mechanisms of inhomogeneous (e.g., radiation) transport within the framework of diffusion which, in well-defined cases, contrasts markedly with radiative transfer through the same medium (see sect. 4.3–4). For the moment, we dwell on the purely structural aspects, taking just the material we will eventually need from Stauffer's [1985] highly recommended review. The term "percolation" relates to the fact that, at $p=p_c$ (some "critical" value), a cluster of connected live cells (almost always) spans the whole system, no matter how big it is!

If $g(r)$ is the probability for two sites (at some distance r apart) to belong to the same cluster, then the "correlation" (or "connectivity") length[8] is defined as $\xi = \sqrt{<r^2>}$ where $<r^2>=\sum r^2 g(r)$ and it is found that $\xi \sim (p_c-p)^{-\nu}$, i.e., it diverges algebraically as $p \to p_c^-$, at percolation "threshold." The exponent "ν" is universal in the sense that it is independent of the grid's geometry and of the type of percolation ("site" or "bond"); in contrast, p_c will generally depend on such (so-called "irrelevant") details. Many other universal exponents arise. For instance, the probability of a cell to belong to the infinite cluster is $P \sim (p-p_c)^\beta$, i.e., it vanishes as $p \to p_c^+$; this means, in particular, that the volume (Lebesgue measure) of the infinite cluster is zero at $p=p_c$, which does not stop it from dominating the transport properties! Finally and most interestingly for our present purposes, the live clusters (sometimes called percolation "animals") are statistically self-similar to one another and upon degrading the spatial resolution (box-counting) on a given individual: they are fractal. Eliminating $|p-p_c|$ between the above scaling relations and using the fact that $\xi = \lambda$ (the overall size of the system, this is known as a scaling "ansatz"), we find $P_\lambda \sim \lambda^{-\beta/\nu}$. In other words ($P_\lambda = N_\lambda/\lambda^d$), $D = d-\beta/\nu$ is the fractal dimension of the infinite cluster, according to the definition (C.12a,b). As an example in d=2, it is found that $\nu=4/3$ and $\beta=5/36$, hence D=91/48 whereas p_c is ≈ 0.59275 on square lattices, 1/2 on triangular ones and ≈ 0.6962 on hexagonal ones (for site percolation, other values for bond percolation).

C.2.3. The "β-Model" of Dissipation in Fully Developed Turbulence Theory

The random version of the fractal in fig. 4.4a is the so-called "β-model" and corresponds to the following two parameter Bernouilli law for the $\mu\varepsilon_i$:

$$\mu\varepsilon = \begin{cases} \lambda_0^{\gamma_+} & \text{Prob} = \lambda_0^{-C} \\ 0 & \text{Prob} = 1-\lambda_0^{-C} \end{cases} \qquad \text{(C.14a)}$$

Notice that this probability distribution has been properly normalized from the outset. From (C.14a), we see that $C \geq 0$, with homogeneity retrieved at equality; in the non-trivial ($C>0$) case, ε_λ will also have a Bernouilli distribution with only two possible values but the non-zero value ($\lambda_0^{\gamma_+ n}=\lambda^{\gamma_+}$, with $\gamma_+>-\infty$) is found more-and-more rarely as λ increases. The parameter C is called the "codimension" of the limiting ($\lambda=\lambda_0^n\to\infty$) fractal set; to see why, we ask 'how many of the $(\lambda_0^d)^n=\lambda^d$ cells are still "alive" after n cascade steps?' and find

$$N_\lambda(\,\varepsilon_\lambda > 0\,) = (\lambda^d)(\lambda_0^{-C})^n = \lambda^{d-C} \qquad \text{(C.14a')}$$

although only on average. We are therefore dealing with a very sparse fractal set and $D = d-C$ is its fractal dimension according to definition (C.12). Eq. (C.14a') is more simply written as a probability

$$\text{Prob}(\,\varepsilon_\lambda = \lambda^{\gamma_+} > 0\,) = \lambda^{-C} \qquad \text{(C.14a'')}$$

We remark the formal similarity with (C.14a). The base λ logarithms occur naturally when we turn (C.14a'') into an operational definition of C (and of γ_+):

$$C = -\log_\lambda[\,\text{Prob}(\,\log_\lambda\varepsilon_\lambda = \gamma_+\,)\,] \qquad \text{(C.14a''')}$$

In case there is a transient regime for small λ (large boxes), a "$\lambda\to\infty$" limit can be taken on the r.h.s. of (C.14a'''), cf. (C.12b); in some cases, $\lim_{\lambda\to\infty}(\log_\lambda[\cdot])$ is best replaced by $\lim_{\lambda\to\infty}(d\log[\cdot]/d\log\lambda)$ to eliminate the uninteresting prefactors in (C.12–13).

The two basic parameters in (C.14a) can in fact be equated to C as soon as the constraint of (turbulent cascade flux) conservation is imposed. Indeed, we have

$$\log_{\lambda_0}\langle\mu\varepsilon\rangle = \gamma_+ - C = 0 \qquad \text{(C.14b)}$$

We recall that "conservation" means that we want to have $\langle\varepsilon_\lambda\rangle = 1$ at all steps in the cascade, (C.14b) and (C.11b) guarantees that this will indeed be the case since the $\mu\varepsilon_i$ are chosen independently. This strategy was justified in the previous section, further justification comes from the fact that we will often want to model only some section of a much larger system (e.g., when $d<3$: we can think of fig. 6.0 as a two-dimensional cut through an idealized three-dimensional dissipation field).

The ancestor of the β-model is Novikov and Stewart's [1964] model of "pulses-in-pulses" for the "support" of the dissipation field (i.e., where $\varepsilon\neq 0$); no grid is necessary here (the relative positions of the sub-pulses are random) but there is always the same number of sub-pulses, the model therefore has "microcanonical" conservation, i.e., $\overline{\varepsilon}_\lambda = 1$ for every realization. (For instance, in d=2 with λ_0=2, we could start by drawing three of the four random weights according to (C.14a), the fourth weight is determined by the requirement[9] $\overline{\varepsilon}_\lambda = 1$.) The model has since been proposed in different guises, primarily by Mandelbrot [1974] who first argued for the idea of "canonical" conservation that we favour and Frisch *et al.* [1978] who coined the term "β-model."

C.3. Multifractal Measures as Models for Turbulent Dissipation Fields

C.3.1. The "α-Model" and the Scaling of the Singularities' Probability Density Function

An apparently subtle variation on the theme of the β-model was originally proposed by Schertzer and Lovejoy [1983, 1984] who called it the "α-model." We now consider the three parameter Bernouilli law:

$$\mu\varepsilon = \begin{cases} \lambda_0^{\gamma_+} & \text{Prob} = \lambda_0^{-C_+} \\ \lambda_0^{\gamma_-} & \text{Prob} = 1-\lambda_0^{-C_+} \end{cases} \tag{C.15a}$$

where one normally assumes $\gamma_+ > \gamma_- > -\infty$ (respectively, stronger and weaker sub-eddies, not alive and dead as in the β-model). Homogeneity is retrieved at $\gamma_+ = \gamma_-$ (or for C_+=0,∞). From (C.11a,b), we see that a "log-(nth order) binomial" law is to be expected for ε_λ, i.e., the order of singularity $\gamma=\log_\lambda\varepsilon_\lambda$ (a sum of n Bernouilli i.r.v.'s) can take on n+1 different values $\{\gamma_i, i=0,\cdots,n\}$ equally spaced between γ_- and γ_+ included.

To see how much richer the model in (C.15a) is compared to that in (C.14a), we only have to ask 'what is the (average) number of boxes where we find ε_λ equal to λ^{γ_i}?'. Letting C_- denote $-\log_{\lambda_0}(1-\lambda_0^{-C_+})$ in order to make the notation more symmetric, the answer is

$$N_\lambda(\,\varepsilon_\lambda = \lambda^{\gamma_i}\,) = \lambda^d \binom{n}{i} \lambda_0^{-[iC_+ + (n-i)C_-]} \tag{C.15a'}$$

where $\binom{n}{i}$ designates the binomial coefficient. We take i as the number of times a boost (by λ^{γ_+}) was hit in the trial set up in (C.15a). In general, we will get a different answer for each different value of γ_i (at given C_+ and n). By contrast, the β-model has only one characteristic exponent (its codimension C) and it is in fact retrieved here in the limit $\gamma_-\to-\infty$; in this limit, only i=n ($\gamma_n=\gamma_+$) survives (ε_λ>0) in (C.15a') since $i\gamma_+-(n-i)\infty=-\infty$, if i<n. In this extreme case, we can equate C_+ with C and thus retrieve the simple scaling relation (C.14a'). So, not only the field has a range of orders of singularity but also the codimension (say, c_i) is now going to be a function of i (or γ_i). Indeed, in analogy with (C.14a",a'"), we can write down the following definition of c_i:

$$\text{Prob}(\,\varepsilon_\lambda = \lambda^{\gamma_i}\,) = \binom{n}{i} \lambda_0^{-[iC_+ + (n-i)C_-]} = \lambda^{-c_i} \tag{C.15a"}$$

at any finite number of cascade steps. A complete description of the γ's p.d.f. is then given by $p_\lambda(\gamma) = \Sigma_i\lambda^{-c_i}\delta(\gamma-\gamma_i)$.

Taking the small scale limit, we find a (countably) infinite number of orders of singularity, all in the range $[\gamma_-,\gamma_+]$, and we can define

$$c(\gamma) = \lim_{n\to\infty} c_{i_\gamma(n)} \quad \text{where} \quad i_\gamma(n) = \mathrm{int}\left(n\frac{\gamma-\gamma_-}{\gamma_+-\gamma_-} \right) \tag{C.15a'''}$$

The above "codimension function" $c(\gamma)$ will be estimated for the α-model further on using an indirect method (see eq. (C.20b) below). For the moment, we can only anticipate that $c(\gamma_+)=c_n=C_+$ and that $c(\gamma_-)=c_0=C_-$ (since $\binom{n}{0}=\binom{n}{n}=1$, independently of n); also, from our knowledge of p.d.f.'s, it is clear that these limits will be approached from below. In the standard development of probability theory, it is customary to seek a Gaussian approximation to the binomial p.d.f. by using Stirling's formula to approximate $\binom{n}{i}=n!/(n-i)!i!$ and expand (C.15a") around its most probable value ($\approx n\lambda_0^{-C_+}$). This would of course yield a log-normal multifractal which we will be discussing independently in the next sub-section. For the moment, let it be said that this may be a good idea w.r.t. the additive process defined by (C.11b) for the generators ($\gamma=\Sigma_i \log_{\lambda_0}\mu\varepsilon_i$) but the subsequent operation in (C.11c) is so highly nonlinear ($\varepsilon_\lambda=\lambda^\gamma$) that the extreme Gaussian events will completely dominate the statistical behavior in ways we will discuss in the next section.

The conservation constraint associated with the α-model is expressed by

$$\langle\mu\varepsilon\rangle = \lambda_0^{\gamma_+-C_+} + \lambda_0^{\gamma_--C_-} = 1 \tag{C.15b}$$

and we recall the p.d.f. normalization constraint: $\lambda_0^{-C_+} + \lambda_0^{-C_-} = 1$ (where $C_\pm \geq 0$). These equations can be readily solved for two (remaining) parameters, given at least one of the $\gamma_\pm$ and either the other or one of the two $C_\pm$ parameters. Notice that conservation is possible only if both orders of singularity and orders of regularity co-exist in a particular model (i.e., that $\gamma_+>0>\gamma_-\geq-\infty$). These will be the two free parameters of the conserved cascade model which makes only one more parameter than for the conserved β-model monofractals yet the α-model can generate up to an infinite number of fractal dimensions!

In the literature, the microcanonical version of the α-model is known as the "p-model" of Meneveau and Sreenivasan [1987]. Just like our deterministic monofractal in fig. 4.4a, deterministic multifractals are a possibility that offers some pedagogical advantages (they are of course microcanonical by construction); for instance, Feder [1988] considers the case with $\lambda_0=3$ (in d=1) where he boosts the first sub-portion, somewhat less the second, and leaves the third empty; this amounts to the generation of a log-binomial multifractal measure supported by the Cantor set rather than by the full unit segment. The resulting field has all the mathematical attributes of a multifractal, albeit of a rather mild variety according to the classification scheme of Schertzer *et al.* [1991] and/or Schertzer and Lovejoy [1992]. Moreover, their [1987a,b] "universal" multifractals provide, rather than the above straightforward hybridization of the β-model and the (inherently discrete valued) α-model, a continuous variation away from monofractals towards (continuously valued) multifractals, specifically, the log-normal model described below.

In summary, we have shown that only one exponent is necessary to characterize all of the β-model's statistical properties, this limiting case is therefore called a <u>mono</u>fractal; all other cases clearly call for a whole family of exponents, they are better called <u>multi</u>fractals. Mathematically speaking, the former models are defined by sets (of d-measure zero), hence they are "geometrical" in nature, whereas the latter are defined in the (weak) limit of singular measures, they have a more "dynamical" flavor.[10] Furthermore, we can define a scaling characterization of the the p.d.f. of the various orders of singularity (γ) present with the help of the codimension function $c(\gamma)$:

$$p_\lambda(\gamma)\, d\gamma = \mathrm{Prob}(\, \lambda^{\gamma} \le \varepsilon_\lambda < \lambda^{\gamma+d\gamma}\,) = \lambda^{-c(\gamma)}\, d\gamma \tag{C.16}$$

The β-model has an infinite $c(\gamma)$ everywhere except at a single value γ=C while the α-model's $c(\gamma)$ is infinite everywhere except on (a countable infinite number of values on) a segment $[\gamma_-,\gamma_+]$, see eqs. (C.14a''') and (C.15a''') respectively.

C.3.2. The "α=2" Model and the Scaling of the Singularities' Probability Distribution Function

The title for this sub-section is deliberately chosen as close as possible to that of the previous one in order underscore simultaneously two possible sources of confusion that we wish to clarify immediately. Firstly, the "α" in the chosen name[11] of the prototypical multifractal model for the dissipation field (briefly discussed above) is not to be confused, on the one hand, with the "α" of the formalism that prevails in the dynamical systems[12] (strange attractor) literature and discussed briefly in upcoming sect. C.4 nor, on the other hand, with the "α" of Lévy index[13] fame, discussed in sect. C.5 on "universal" multifractals (as well as in sect. 5.1, with a totally different application—and Lévy's "β" parameter for that matter[14]—in mind). Within the context of universal multifractals, "α=2" designates log-normal model which we discuss here and use (radiatively speaking) in chap. 6, hence the above title. Secondly, we have chosen to define the codimension function $c(\gamma)$ in terms of the γ's p.d.f. (cf. (C.16) above), not its integral which is the γ's (complementary) distribution function (cf. (C.19) below); however, in the multifractal literature, both definitions are in usage and, in practice, a third—based on the Legendre transformation—can be singled out.[15] This choice of using the p.d.f. is made in order to meet our specific needs (in chap. 5–6), so we will clarify this source of ambiguity as best as possible before closing this sub-section by listing the rationales behind each definition and illustrating the differences with specific examples.

Compared to the α-model developed in the '80s, a far more violent type of multifractal had already existed in the literature for some time as a result of the very first attempts to address the problem of intermittancy quantitatively (i.e., with an explicit model in mind): Kolmogorov [1962] and Obukhov [1962] independently proposed the following log-normal law for the $\mu\varepsilon$:

$$\mu\varepsilon = e^{\Gamma}, \quad dP(\Gamma) = \frac{1}{\sqrt{2\pi}}\, e^{-\frac{(\Gamma-\mu)^2}{2\sigma^2}}\, \frac{d\Gamma}{\sigma} \qquad \text{(C.17a)}$$

Like for the β-model, this model has only two parameters (mean μ and variance σ^2) and there exists a simple conservation constraint between them:

$$\ln\langle\mu\varepsilon\rangle = \tfrac{1}{2}\sigma^2 + \mu = 0 \qquad \text{(C.17b)}$$

Homogeneity is retrieved in the limit $\sigma \to 0$ while at finite σ^2 we can see that the log-normal model is very different from both of the dissipation models described in the two previous sub-sections: its singularity "spectrum" is not narrowed down to a single value like the β-model's, nor is it restricted to a (countable infinity on a) bounded segment of the real axis as is the α-model's. It is every where dense and indeed encompasses all of the real axis. In this very basic sense, the above "α=2" model is more multifractal than the "α-model" and we will see further on (sect. C.5) that this carries over to almost every imaginable case.

The "extreme" multifractality of the log-normal model can be further underscored by evaluating its codimension function $c(\gamma)$. Using the same definition (C.16) as for the α-model, the $c(\gamma)$ for the log-normal model in eq. (C.17a) is readily obtained by invoking the well-known properties of sums of n independent, identical distributed Gaussian (μ,σ^2) deviates. More precisely, we make the substitutions $\mu \to n\mu$ and $\sigma^2 \to n\sigma^2$ while the definitions (C.11b,c) and (C.16) dictate the change of variable $\Sigma_i\Gamma_i \to n(\ln\lambda_o)\gamma$. Hence, collecting results, we obtain

$$c(\gamma) = \frac{\ln\lambda_o}{2\sigma^2}\left(\gamma - \frac{\mu}{\ln\lambda_o}\right)^2 \qquad \text{(C.18a)}$$

Notice that the additive normalization constant for $\log_\lambda[p_\lambda(\gamma)]$, namely $\log_\lambda[\sqrt{\ln\lambda/2\pi\sigma^2}]$, vanishes when the small scale ($\lambda \to \infty$) limit is taken because it is $O(\log n/n)$, for large n. In practice (finite λ) however, this term will be non-negligible if the variance σ^2 is not itself $O(1)$. Using the conservation relation (C.17b), (C.18a) reads

$$c(\gamma) = \frac{C_1}{4}\left(\frac{\gamma}{C_1} + 1\right)^2 \qquad \text{(C.18b)}$$

where we have defined

$$C_1 = \frac{\sigma^2}{2\ln\lambda_o} \qquad \text{(C.18c)}$$

This choice of notation will be fully justified in the next section, for the moment, we see that $-C_1$ is the most probable order of singularity and that the "width" of the singularity spectrum can, in a sense, be measured by $1/c''(\gamma)|_{\gamma=-C_1}=2C_1$; as expected, increasing the variance increases the probability of obtaining large deviations in the γ's hence extremely variable (very large ratios in) ε_λ's.

Before leaving the topic of codimension functions, we can show how much simpler things become in the asymptotic limit ($\lambda\to\infty$). Unfortunately, this simplification opens the way for some notational ambiguity. Indeed, in the small scale limit, $c(\gamma)$ determines not only the fractal dimensions of the level sets of the ε_λ field but also that of its exceedence sets for all thresholds λ^γ, but only if γ is greater than its most probable value. To see this, imagine that the ε-field has been generated down to some resolution $1/\lambda$ on a d-dimensional grid with λ boxes on a side; the number of boxes required to cover an exceedence set is then

$$N_\lambda(\varepsilon_\lambda \geq \lambda^\gamma) = \lambda^d \,\mathrm{Prob}(\varepsilon_\lambda \geq \lambda^\gamma) = \lambda^d \int_\gamma^\infty \lambda^{-c(\gamma')}\, d\gamma' \sim \lambda^{d-c(\gamma)} \tag{C.19}$$

where the "~" relation is introduced, as usual, to absorb both prefactors (e.g., $c'(\gamma)$) and slowly varying scale dependent terms (e.g., $\ln\lambda$). Of course, using (C.19) as a definition of $c(\gamma)$ yields a non-decreasing function so it can only agree with definition (C.16) for the higher, hence more interesting, orders of singularity for which $c'(\gamma)>0$. Yet another definition of $c(\gamma)$ is possible, namely, by using the Legendre transform of some (postulated) "K(h)" function. This definition will always yield a convex codimension function; in the next two sections, we will see examples obtained from this third and last (?) definition that are non-decreasing $c(\gamma)$'s and others that give negative $c'(\gamma)$ branches also.

To illustrate the difference between the three definitions of $c(\gamma)$, we consider the somewhat caricatural β-model. The definition contained in (C.19) yields

$$c(\gamma) = \begin{cases} 0 & \text{for } \gamma = -\infty \text{ (an almost sure event)} \\ C & \text{for } -\infty < \gamma \leq \gamma_+ \\ +\infty & \text{for } \gamma > \gamma_+ \text{ (an impossible event)} \end{cases} \tag{C.20}$$

The Legendre definition is the same except for $c(-\infty)$ which has to be $+\infty$, not 0, to make the result convex. Finally, the definition (C.16) is consistent with a very much "defective" (sub-normalized) p.d.f. entirely concentrated at $\gamma=\gamma_+$ plus a huge complementary peak placed (formally) at $\gamma = -\infty$; the intensities of (i.e., integrals under) these peaks are respectively λ^{-C} and $(1-\lambda^{-C})$; at these two points, $c(\gamma)$ is formally $-\infty$ (the log of the inverse of a δ-function!), everywhere else it is $+\infty$ (since the p.d.f. vanishes identically). Fortunately, $c(\gamma)$'s are much better behaved for multifractals and the three definitions agree at least two-by-two. For the log-normal model and the α-model, the first (C.16) and last

(Legendre) definitions agree, but only in the limit of infinitely many cascade steps.[16] Finally, for universal multifractals (sect. C.5), the $c(\gamma)$'s can only be obtained analytically by Legendre transformation which yields only the leading term; if $0<\alpha<2$ (i.e., *bone fide* log-Lévy multifractals), this term is non-decreasing.[17] In this case, it is therefore definition (C.19) that agrees with the Legendre estimate but all information about the $c'(\gamma)<0$ branches is lost.

The agreement in the log-Lévy case is basically circumstantial and, if we are looking for a better rationale for using (C.19), we should briefly consider the problems posed by data analysis. Now definition (C.19) can be readily used in straightforward box-counting techniques of empirically determined ε-fields made available, say, on a Λ-sized grid. Some threshold (simply denoted Λ^{γ}) is chosen and used to define the exceedence set which is then covered with Λ/λ-sized boxes and $c(\gamma)$ is determined from (C.14a") or via (C.12b), using d. Having done this for several values of γ, one can plot $c(\gamma)$ as a function of γ. This is the basic idea of Lovejoy *et al.*'s [1987] "functional box counting" (FBC) technique which Gabriel *et al.* [1988] apply it to GOES satellite imagery, finding very log-normal looking $c(\gamma)$'s in both VIS and IR channels. In the above, the fundamental reason to use (C.19) rather than (C.16) is that better statistics are obtained for a semi-infinite range of γ's than for a finite (let alone infinitesimal) range.

For the same reasons, definition (C.19) is also favored by Lavallée *et al.* [1991] in their "Probability Distribution/Multiple Scaling" (PDMS) technique which has now superseded FBC. To see how the two methods differ, recall that FBC uses only the ε_Λ-field, viewed as a theoretical (or "bare") quantity that we have implicitly been modelling by proceeding "down" the cascade (from large to small scales), whereas the PDMS approach uses the observed (or "dressed") $\bar{\varepsilon}_\lambda$-field which is obtained by proceeding back "up" the cascade, spatially averaging the fully developed ε_∞-field. In practice, we assume $\varepsilon_\infty \approx \varepsilon_\Lambda$ and average over boxes of size Λ/λ. In the following section, we will only briefly discuss the differences between the statistics of ε_λ and those of $\bar{\varepsilon}_\lambda$ that Lavallée [1991] studies in full detail. He also compares the PDMS technique not only with FBC but also with two others, namely, "Trace Moments" and "Double Trace Moments" (that we will briefly describe, respectively, in the next two sections); he concludes in favour of the last which is geared specifically towards finding the best fit by a "universal" multifractal (as described in sect. C.5). Some of the problems encountered by the PDMS technique are traceable to the (weakly λ-dependent) normalization constant which is not accounted for in the scaling characterizations (C.16) or (C.19) and, as pointed out above, it can become quite important—even for the bare quantities—if the parameter C_1 that controls variability (or, more precisely, intermittancy) is quite small and/or the useful range of scales is not huge. By "useful" range, we mean the range (usually smaller than [1,Λ]) where the the log-log plots of the cumulative histograms (or moments) are reasonably linear w.r.t λ. Unsurprisingly, when the intermittancy is relatively weak (e.g., satellite imagery, topography) the different methods tend to disagree but when it is quite strong (e.g., rain, wind, earthquakes) better agreement is achieved.

C.3.3. (Many) Other Situations where Multifractals Arise Naturally

Much like fractals themselves (§3.2.1–2) there are many ways of obtaining multifractals, not only cascade processes deliver them. In fact more-or-less at the same time as Schertzer and Lovejoy [1983, 1984] were realizing that the basic concept (of multiple scaling, sect. 3.4) had been around for some time in turbulence theory [Kolmogorov, 1962; Obukhov, 1962; Mandelbrot, 1974], Hentchel and Procaccia [1983] and Grassberger [1983] were using very similar concepts ("generalized" dimensions) within the context of chaotic dynamical systems. The multiplicity of exponents arises as soon as the distribution of points on the strange attractor is considered: viewed as a set, the attractor is only the support of an interesting p.d.f. which is naturally to be "weighed" by integration (of different moments, see below) over different scales.

It was only after these pioneering studies that, on the one hand, the notations were stablized, with phase space and strange (but deterministic) attractors in mind [Halsey *et al.*, 1986], and that, on the other hand, the expression "multifractal" proposed, with turbulence and (random) cascades in mind [Frisch and Parisi, 1985]. Of course applications of multifractal concepts does not stop there! Every time there is a field quantity involved in a physical system with no characteristic scale, scaling p.d.f.'s and scale-invariant measures (sect. 3.4) will arise. For instance, we can mention current (or potential) in conductance through percolating binary mixtures [e.g., Rammal *et al.*, 1985], electronic wave-functions of localized states in disordered materials [e.g., Siebesma, 1989], p.d.f.'s of RWs on a fractal [e.g., Havlin and Bunde, 1989], rate of growth in DLA and other systems in statistical physics [e.g., Derrida, 1986; Stanley and Meakin, 1988]. All of the above examples from physics involve diffusion-like equations but that is not an absolute necessity, the equations of general relativity, QCD, or those of radiative transfer (i.e., linear transport theory) would do just as well ... if only they were more tractable, but theoretical (numerical simulation) and/or observational progress can be reported on all of these fronts.[18]

Note on notation #1: From eq. (C.16), it can also be seen that, in our notations, the fractal dimension $d-c(\gamma)$, when positive, corresponds to the "$f(\alpha)$" used by many authors, mainly involved in strange attractor studies, following Halsey *et al.* [*ibid.*]; at the same time, their "α" is to be equated with our $d-\gamma$ since, in dynamical systems theory, the focus is on the "measure" $\varepsilon_\lambda \lambda^d$ itself—rather than its "density" ε_λ—as a function of the size of the averaging set $(1/\lambda)$—rather than λ. Our multifractal notation is independent of d, as are the notations we use in (most of) the sections of the thesis devoted to radiative problems; this is an important advantage in stochastic modelling since the very large sample-space will be formally related to the limit $d\to\infty$ in the next section. In "$f(\alpha)$" notations, which rely heavily on a specific d, the purely statistical effects, such as under-sampling by using a single realization, are felt in the negative—or "latent"—$f(\alpha)$'s which are associated with rare events.

C.4. Multiple Scaling of the Statistical Moments and the Dual Codimension Function

C.4.1. General Properties of the "Bare" Moments and the Divergence of "Dressed" Moments

An alternative—in fact, complementary—approach to the statistical characterization of turbulent dissipation fields is possible, based on the moments of ε_λ. From the scaling of the p.d.f.'s, we expect *a priori* these averages to scale with λ also:

$$\langle\varepsilon_\lambda{}^h\rangle = \lambda^{K(h)} \tag{C.21}$$

From this definition, $K(0) = 0$ if the p.d.f. is properly normalized and, if the cascade process is conserved, then $K(1) = 0$ too. In essence, $K(h)$ is the 2nd characteristic (or cumulant generating) function (c.g.f.) of the probability distribution of the γ's:

$$\langle\varepsilon_\lambda{}^h\rangle = \int_0^\infty \varepsilon_\lambda{}^h\, dP(\varepsilon_\lambda) = \int_{-\infty}^{+\infty} \lambda^{h\gamma}\, p_\lambda(\gamma)\, d\gamma = \int_{-\infty}^{+\infty} e^{i(h\ln\lambda/i)\gamma}\, p_\lambda(\gamma)\, d\gamma \tag{C.22a}$$

If $\phi_\lambda(t)$ is the Fourier transform of $p_\lambda(\gamma)$, then $K(h)=\log_\lambda\phi_\lambda(h\ln\lambda/i)=\ln\phi_n(nh\ln\lambda_0/i)/n\ln\lambda_0$. Now γ is the running average of n identically and independently distributed (i.i.d.) random generators, $\log_{\lambda_0}(\mu\varepsilon)$, cf. (C.11b,c). From the discussion below eq. (A.14) on the properties of the c.g.f., we recall that the c.g.f. of a sum of n i.i.d.r.v.'s is n times the c.g.f. of just one of them, hence $\log_{\lambda_0}\phi_n(t/n)=n\log_{\lambda_0}\phi_1(t/n)$ and, finally, dropping the subscript "1":

$$K(h) = \frac{1}{\ln\lambda_0}\ln[\phi(h\ln\lambda_0/i)] \tag{C.22b}$$

Thus $K(h)$ inherits all of the general properties of the (Laplacian) c.g.f. In particular, it is convex and, if $K(h)$ is polynomial, its degree is 2 at most. Furthermore, a degenerate $\mu\varepsilon$-distribution (homogeneous ε_λ) has a linear c.g.f.: $K(h) = h\ln\langle\mu\varepsilon\rangle$, which vanishes identically if conservation is required.

The two fundamental multifractal functions $c(\gamma)$ and $K(h)$ are therefore in the same dual relationship as $p(\mu\varepsilon)$ and its Fourier transform $\phi(t)$, except translated into exponent language. Frisch and Parisi [1985] realized that in the asymptotic small scale limit ($\lambda\gg1$) one can do away with the (integration part of the) Fourier transformation altogether:

$$<\varepsilon_\lambda{}^h> = \int_{-\infty}^{+\infty} \lambda^{h\gamma - c(\gamma)}\, d\gamma \sim \lambda^{\max[h\gamma - c(\gamma)]} \qquad \text{(C.23)}$$

where the last step makes use of the method of steepest descents. Hence, comparing with the definition (C.21) of K(h),

$$K(h) = \max_\gamma [\, h\gamma - c(\gamma)\,] \qquad \text{(C.24a)}$$

i.e., the Legendre transformation which is known to be involutive; thus

$$c(\gamma) = \max_h [\, h\gamma - K(h)\,] \qquad \text{(C.24b)}$$

This is very convenient because, in many interesting cases, it is K(h) that is known *a priori* (e.g., the universal multifractals, presented in the next section) or else it is more simply expressed than the $c(\gamma)$ and is independent of λ even if it is finite (e.g., the α-model, as shown below). The only limitation of (C.24b) is related to the fact that the Legendre transform of a convex function is necessarily convex also. So the $c(\gamma)$ estimated from K(h) in (C.24b) is will be convex on all of its domain even though the p.d.f. $p_\lambda(\gamma)$ can be bi-modal (β-model) or multi-modal (α-model) and, from its definition (C.16), these attributes carry over to $c(\gamma)$. The above Legendre transform estimate of $c(\gamma)$ is therefore the convex envelop of $c(\gamma)$ as defined by (C.16), not (C.19) since we explicitly need the p.d.f. in (C.22a,b–23).

There is a well-known geometrical interpretation to the Legendre transformation. We see that, if the $c(\gamma)$ curve is given, the K(h) curve is defined parametrically by

$$\begin{cases} h_\gamma = c'(\gamma) \\ K(h_\gamma) = \gamma h_\gamma - c(\gamma) \end{cases} \qquad \text{(C.25a)}$$

i.e., slope and (negative) intercept of the tangent with the vertical axis, respectively. Of course, the same applies conversely:

$$\begin{cases} \gamma_h = K'(h) \\ c(\gamma_h) = h\gamma_h - K(h) \end{cases} \qquad \text{(C.25b)}$$

An alternative characterization of the scaling of the statistical moments of conserved (K(1)=0) cascade processes is given by the "dual" codimension function C(h) where

$$K(h) = (h-1)C(h) \qquad \text{(C.26)}$$

From K(h)'s general properties, we have C(0) = 0 and C(h) is necessarily non-decreasing. C(h) is useful in specifying the statistical differences that arise between the theoretical ("bare") cascade quantities used (here) in simulation and the observable ("dressed") quantities. The latter are spatial averages of the former taken to their ultimate singular expression obtained in the small scale limit. The bare (ε_λ) and the dressed ($\bar{\varepsilon}_\lambda$) dissipation fields are best compared at the same resolution (λ) and the difference between the two is that the statistical moments of the former are always well defined (hence convergent) whereas those of the latter are apt to diverge at high order. This phenomenon is due to the singularities that remain "untamed" by the averaging either because they are too frequent (recall that there are infinitely many cascade steps below the averaging scale) or, equivalently, because the averaging set is too sparse to sense these singularities on a regular basis and they appear only as statistical flukes (that would probably be dismissed as "outliers" in more standard approaches). More specifically, it can be shown [e.g., Schertzer and Lovejoy, 1987a] that the h^{th} order moment of the average flux through a set A of (generally fractal) dimension D(A) diverges if

$$C(h) \geq D(A) \tag{C.27}$$

hence the often used term of "hierarchy of critical (fractal co)dimensions." The inequality in (C.27) will always happen sooner or later if C(h) is unbounded ("wild" singularities are present): taking the maximum D(A)=d, moments of order greater than $C^{-1}(d)$ will diverge for almost any realization. They can however be tamed by averaging over N_r realizations, but only up to order $C^{-1}(d+\log_\lambda N_r)$ [Lavallée *et al.*, 1991]—as expected, we see that increasing d by 1 is equivalent to studying λ realizations (each on a grid of size λ in each direction). In this sense, the probability space containing all possible realizations of the given stochastic multifractal model has infinite dimensionality.

In practice, "divergence" in the above discussion means that the dressed statistic is completely dominated by a single singularity γ_c which (C.25b) associates with h_c, the critical moment that verifies the equality in (C.27) for the given dimension of the averaging set. This singularity will fluctuate from one realization to the next but, for a given realization, $\langle\bar{\varepsilon}_\lambda{}^h\rangle$ will scale approximately like $\langle\varepsilon_\lambda{}^h\rangle = \lambda^{K(h)}$ for $h<h_c$ and like $(\lambda^{\gamma_c})^h\lambda^{-c(\gamma_c)} \approx \lambda^{hK'(h_c)-c(\gamma_c)}$, for $h \geq h_c$. In other words, the K(h) for the dressed quantity simply follows the tangent of the bare K(h) curve beyond h_c since, from (C.25b), $-c(\gamma_c)$ is the the intercept of the tangent at h_c. By Legendre transformation, the same applies for the $c(\gamma)$ for the dressed quantities, beyond γ_c: i.e., for the dressed quantities, we have $p(\gamma) \approx \lambda^{-c(\gamma)}$ for $\gamma<\gamma_c$ and $p(\gamma) \approx \lambda^{-\gamma c'(\gamma_c)+K(h_c)}$ for $\gamma \geq \gamma_c$.

As described by Lavallée *et al.* [*ibid.*], "Trace Moments" (TMs) can be readily evaluated from "data," i.e., some ε-field on a grid of maximal size Λ. This is done by degraded the field over boxes (D(A)=d) of size $1/\lambda$ w.r.t. the overall system, reckoning the average flux in them ($\bar{\varepsilon}_\lambda$), carrying it to the power h, and finally averaging these over all available boxes ($\langle\bar{\varepsilon}_\lambda{}^h\rangle$). Apart from the above (eventual) divergence of the higher moments, logarithmic regression of these TMs w.r.t. λ yields an estimate of K(h), equivalently, of C(h). This empirical K(h) can then be nonlinearly fitted to any particular model for K(h) such as those presented below, eqs. (C.30) for the α-model or (C.34) for the log-normal model, or else those of the universal multifractals of sect. C.6 in (C.38a). This method is not plagued with the problems of the PDMS approach that are related to the unknown normalization constants of continuously distributed generators, e.g., the Γ's in (C.17a).

The single most important exponent in the whole C(h) hierarchy is the "codimension of the singularities (γ_1) associated with of the mean ($<\varepsilon_\lambda>$) of the process," that we will denote by C_1. Although $<\varepsilon_\lambda> = 1$ by conservation, γ_1 is generally quite different from the "neutral" order of singularity (γ=0) which is associated with $\varepsilon_\lambda = 1$. The most important order of singularity in the whole spectrum is certainly the most probable of all, and we will denote it by γ_0. Now recall that for conserved cascades, K(0) = K(1) = 0 hence, from the convexity of K(h), we necessarily have $K'(0) \leq 0$ and $K'(1) \geq 0$, with equalities obtained simultaneously at homogeneity. On the one hand, the most probable order of singularity γ_0 is given by K'(0) since $c'(\gamma_0) = h_{\gamma_0} = 0$, from (C.25a), and is therefore negatively valued; moreover, $c(\gamma_0) = \gamma_0 h_{\gamma_0} - K(h_{\gamma_0}) = 0$, i.e., this order of singularity has the remarkable property of filling space. On the other hand, from (C.25b) with h = 1, we find $\gamma_1 = K'(1)$ and $c(\gamma_1) = \gamma_1 - K(1)$ where K(1) = 0 hence $C_1 = c(C_1)$, i.e., C_1 is a fixed point of $c(\gamma)$ and is found at the intersection of the $c(\gamma)$ curve with the first diagonal. Another remarkable property of γ_1 is obtained from (C.25a): $c'(\gamma_1) = 1$ and the intercept of this tangent to $c(\gamma)$ is K(1) = 0, i.e., the first diagonal is in fact tangent to the $c(\gamma)$ curve at $\gamma_1 = C_1$, the fixed point is unique. This property can be used to determine C_1 from an empirically determined $c(\gamma)$ curve [e.g., Lovejoy and Schertzer, 1990]. Furthermore, we have

$$C_1 = C(1) \tag{C.28}$$

since K'(1) = C(1) from the definition in (C.26), hence the adopted notation. Using this with the divergence criterion in (C.27), we notice that, in practice, the cascade process can only be properly conserved if $C_1 < d$ since $<\varepsilon_\lambda>$ itself must obviously converge, if it is to be equated with 1; more precisely, the average of the process (ε_λ=1) should be well sampled in almost every realization. Stochastic cascade processes with $C_1 \geq d$ are said to be "degenerate," for almost every realization the set where ε_λ>1 is sparse even in probability space (all realizations combined); rare realizations contain extremely strong events (since the ensemble-average is still unit).

Note on notation #2: The more standard [Halsey *et al.*, 1986] multifractal notation is "τ(q)" for our (h-1)d-K(h) and "D(q)" for our d-C(h), with "q" equated to our h; the differences are mainly due to the fact that, in phase-space portraits of chaotic attractors, the focus is on the moments of the measure $<(\varepsilon_\lambda \lambda^d)^h>$ as a function of $1/\lambda$). Apart from the conceptual advantages of our notations when dealing with stochastic processes, we wish to avoid undesirable ambiguity with our DA- and general radiative transfer notations, for "q" and "τ," respectively.

C.4.2. Illustrations with Monofractals, α-Models and Log-Normal Multifractals

The three intermittancy models discussed in the previous two sections can be used to illustrate different aspects of the multiple scaling of statistical moments examined above in the general case.

We start at level zero on the multifractality scale with the monofractal ß-model (C.14a) with its log-Bernouilli statistics. Its K(h) is easily obtained directly from its (Bernouilli) p.d.f. in (C.14a): first taking (positive) h^{th} powers and then ensemble-averaging yields $<\varepsilon_\lambda{}^h> = (\lambda^{h\gamma_+})(\lambda^{-C}) = \lambda^{h\gamma_+-C}$ and, otherwise ($h < 0$), $<\varepsilon_\lambda{}^h>$ is infinite because of the (very numerous) null values dominate. In summary,

$$K(h) = \begin{cases} h\gamma_+ - C & h > 0 \\ 0 & h = 0 \\ \infty & h < 0 \end{cases} \tag{C.29}$$

The conserved case yields

$$K(h) = (h-1)C \qquad (h > 0) \tag{C.29'}$$

hence $C(h) = C$ and, in particular, $C_1 = C$. Moreover, if $C<d$, all the positive order moments will always converge for this model. Recall that a homogeneous ε-field also has a linear K(h) but for all h, not just positive; we are therefore fully justified in calling these simple fractal models "fractally homogeneous."

Finally, we note that $<\varepsilon_\lambda{}^h> = \lambda^{h\gamma_+-C}$ is as close as we can (formally) get, within the context of multiplicative processes, to the simple scaling obtained for their additive counterparts such as the spatial analogs of RWs discussed in §C.2.1 where we have $\Delta x \to \Delta f$ and $\Delta t \to \Delta x$ hence $<|\Delta f|_{\Delta x}{}^h> \sim (\Delta x^H)^h$ and this applies, like for homogeneity, to all real values of h (and that makes all the difference!). These spatial generalizations of Brownian motion (viz. Mandelbrot [1975] - Voss[1983] "fractional Brownian landscapes") could be used to model (optical) density $(\kappa)\rho(x)$ fields in any dimensionality. They must then be viewed as functions of position that fluctuate around some mean that is large enough to avoid unphysical negative values in every realization. Such models would totally lack the intermittancy and corresponding extreme variability of multifractals, including simple—but multiplicatively generated—monofractals, thanks to the diverging negative ordered moments of the latter. To obtain a degree of intermittancy using this kind of additive model in the context of turbulence, Mandelbrot [1974] considers the "support" of three-dimensional turbulence to be the "zero-crossing set" (no additive constant is called for, as in the above) of such a process embedded in (3+1)-dimensional space. A combination of these ideas (an additive constant, followed by truncation of negative values) was recently used by H. Barker [p.c.] in d=2 to obtain the optical thicknesses $\tau(x,y)$ of individually homogeneous clouds that cluster scalingly in an attempt to model "realistic" broken cloud fields.

We now turn to the prototypical multifractal α-model (C.15a) with its log-binomial statistics. It yields by direct calculation, $\langle\varepsilon_\lambda{}^h\rangle = [(\lambda_0{}^{h\gamma_+})(\lambda_0{}^{-C_+}) + (\lambda_0{}^{h\gamma_-})(1-\lambda_0{}^{-C_+})]^n$ with n designating the (finite) number of cascade steps, by virtue of the binomial theorem; hence, for all values of n and of h (as long as $\gamma_- > -\infty$):

$$K(h) = \log_{\lambda_0}[\,\lambda_0{}^{h\gamma_+-C_+} + \lambda_0{}^{h\gamma_--C_-}\,] \qquad \text{(C.30)}$$

where we use the same notations as in §C.3.1. In particular, proper normalization ($K(0)=0$) requires $\Sigma_\pm\lambda_0{}^{-C_\pm} = 1$, and conserved ($K(1)=0$) α-models must have $\Sigma_\pm\lambda_0{}^{\gamma_\pm-C_\pm} = 1$ also; this leaves only two of the parameters unconstrained but does not make (C.30) any simpler to write. In the previous section, we were able to describe the (finite n) p.d.f. of the γ's as a sum of n+1 δ-functions centered on the n+1 distinct orders of singularity generated between γ_- and γ_+ (included), cf. (C.15a"). The intervening δ-functions however make the corresponding $c(\gamma)$ ill-defined, as remarked in our discussion of the β-model's $c(\gamma)$ under eq. (C.20). This inconvenience vanishes however in the small scale limit since the γ's fill (countably) the segment $[\gamma_-,\gamma_+]$ and the associated $c(\gamma)$ can be obtained by computing the Legendre transform (C.25b) for the K(h) in (C.30). After a little algebra, we find

$$h_\gamma = \frac{1}{\Delta\gamma}\log_{\lambda_0}(\,r(\gamma)\,\lambda_0{}^{\Delta C}) \qquad \text{(C.31a)}$$

where we have set $\Delta C = C_+ - C_-$, $\Delta\gamma = \gamma_+ - \gamma_-$ and

$$r(\gamma) = \frac{\gamma-\gamma_-}{\gamma_+-\gamma} \qquad \text{(C.31b)}$$

maps $[\gamma_-,\gamma_+]$ onto $\overline{\Re^+} = \Re^+ + \{\infty\}$. With these notations,

$$c(\gamma) = \log_{\lambda_0}\left(\frac{[\,r(\gamma)\,\lambda_0{}^{\Delta C}\,]^{\gamma/\Delta\gamma}}{\Sigma_\pm\, r(\gamma)^{\gamma_\pm/\Delta\gamma}\,\lambda_0{}^{-C_\pm}}\right) \qquad \text{(C.31c)}$$

As expected, the $c(\gamma)$ in (C.31c) is finite only on $[\gamma_-,\gamma_+]$ and (formally) infinite elsewhere.

At any rate, $c(\gamma)$ may be convex but its graph is not a parabola as for the log-normal model in (C.18a), except possibly perceived as a rough approximation around the minimum at γ_0 (given below). In other words, and contrary to what one might have expected, the log-binomial model (C.15a) does not converge to the log-normal model (C.17a) in the limit of many cascade steps even though their respective binomial and Gaussian generators do (i.e., their "non-log" counterparts, due to the strong law of large numbers). One could try to remedy this situation by extending the range of singularities to all of $\Re$ by taking the limits $\gamma_\pm \to \pm\infty$. Recall however that we only have a countably infinite number of γ's at our disposal and they cannot cover $\Re$ densely, their distribution will be no more continuous than the indicator function of all integers. So we still do not retrieve Gaussian behavior in spite of the fact that in the limit $\gamma_\pm \to \pm\infty$, the proper algebra may allow us to make (C.31c) formally identical to (C.18a); we must remember that (C.31c) is only the ($\lambda \to \infty$ limit) of the convex envelop of the very singular $c(\gamma)$'s for finite λ. We return to this important point further on for a closer look (w.r.t. the statistical moments) and, in the following section, we argue that the fundamental problem comes from the discrete nature of the cascade.

In the conserved case, the corresponding C(h) does not simplify but the important C_1 reads

$$C_1 = \gamma_+\lambda_0^{\gamma_+-C_+} + \gamma_-\lambda_0^{\gamma_--C_-} = \Sigma_\pm\gamma_\pm\lambda_0^{\gamma_\pm-C_\pm} \tag{C.32a}$$

which also expressible as $<\mu\varepsilon\log_{\lambda_0}\mu\varepsilon>$ and is necessarily greater than $<\mu\varepsilon>\log_{\lambda_0}<\mu\varepsilon> = 0$ because of Jensen's inequality (3.31) applied to the convex function $f(x) = x\log x$; so $\gamma_1 = C_1$ is indeed positive. We can also obtain the most probable γ:

$$\gamma_0 = \gamma_+\lambda_0^{-C_+} + \gamma_-\lambda_0^{-C_-} = \Sigma_\pm\gamma_\pm\lambda_0^{-C_\pm} \tag{C.32b}$$

which is also expressible as $<\log_{\lambda_0}\mu\varepsilon>$ and is necessarily less than $\log_{\lambda_0}<\mu\varepsilon>=0$ because of the same inequality applied to the concave function $f(x)=\log x$. The α-model's K(h) and C(h) can also be studied in the asymptotic regions:

$$K(h) \approx h\gamma_\pm - C_\pm \quad \text{at} \quad h \to \pm\infty \tag{C.33a}$$

In other words, K(h) becomes asymptotically linear in both directions. This means that the corresponding C(h) levels off in both directions and takes all of its values in $]\gamma_-,\gamma_+[$, increasing steadily from the former to the latter. Being upwardly bounded by

$$C_\infty = C(\infty) = \gamma_+ \tag{C.33b}$$

the singularities generated by the α-model can always be tamed by dressing, given big enough averaging sets and/or a sufficient number of realizations. We are dealing with "soft" multifractals in the general classification of Schertzer *et al.* [1991], also described by Schertzer and Lovejoy [1992].

Finally, we discuss the log-normal model (C.17a). Up until now, we have been able to obtain our K(h) directly from definitions, without using the c.g.f. connection established in (C.22b), by exploiting the discrete nature of the γ-distributions. Here, we no longer have this advantage but the c.g.f. of the normal distribution is well-known: viz., for the Γ's in (C.17a), $\ln[\phi(t)] = i\mu t - \sigma^2 t^2/2$. Hence, from (C.22b) with the natural change of variables $\Gamma = \gamma\ln\lambda_0$:

$$K(h) = \frac{1}{\ln\lambda_0}\left(\frac{1}{2}\sigma^2h^2 + \mu h\right) \tag{C.34}$$

which is also the result obtained by Legendre transformation of (C.18a). Using the conservation constraint (C.17b) this yields

$$K(h) = C_1h(h-1) \tag{C.34'}$$

with $C_1 = \sigma^2/2\ln\lambda_0$, as previously defined in (C.18c). The corresponding dual codimension function is simply

$$C(h) = C_1 h \tag{C.35}$$

for any h. Since the C(h) in (C.35) increases beyond all bounds, high enough order moments will diverge no matter how many realizations are sampled. In the characterization by Schertzer *et al.* [*ibid.*], we are dealing with "hard" multifractals. In a sense, log-normal multifractal are the "hardest" of all since polynomial K(h)'s are of degree 2 at most, the corresponding C(h)'s cannot increase faster than predicted in (C.35).

Comparing (C.30) and (C.34), we see that the binomial law may converge to the normal law "almost surely" (in probability, or p.d.f.'s) when $n \to \infty$ (strong law of large numbers), and so do their log- counterparts in the same sense, but they fail to converge "stochastically" (in moments, or c.g.f.'s). This is entirely traceable to the rare Gaussian events that deviate strongly from the mean, i.e., more than the binomial approximation can account for accurately, at any order. Their effect does not dominate (the statistics of) the sum of random generators in (C.11b) but the strong nonlinearity of the exponentiation in (C.11c) causes them to dominate in (sufficiently high order moments of) the product of random "weights" in (C.11a). In short, "rare" does not mean "unimportant" when dealing with multiplicative processes; on the contrary, these rare events are the cause such violent effects as the divergence of moments because they are nonlinearly amplified (by exponentiation) but not beyond recognition. So, unlike what might have been expected, log-binomial cascade models do not provide a valid interpolation between Bernouilli monofractals and log-normal multifractals. This task is to be fulfilled by the "universal" multifractals that we will now be turning our attention to. Furthermore, the above lack of stochastic convergence is endemic in multiplicative processes and has lead some authors to believe that their is no universality classes in multifractals, each law for $\mu\varepsilon$ has its particular and unique properties. We will argue that this is only true within the very artificial framework of discrete (integer λ_0) cascades and that universal properties appear naturally within the broader framework of "continuous" cascades.

C.4.3. The Dissipation Spectrum and the Intermittancy Correction for Velocity Spectrum

Although K(h) and $c(\gamma)$ are only one-point statistics, they convey plenty of spatial information because of the cascade procedure used to generate the ε-field and that either function specifies completely. This fact can be used to determine the ε-field's correlation properties which are of course scaling and related, by the Wiener-Khintchine theorem, to the (scaling) energy spectrum $E_\varepsilon(k)$ of the stochastic process. Specifically, one finds [Monin and Yaglom, 1975] in our notations

$$E_\varepsilon(k) \sim k^{-1+K(2)} \tag{C.36}$$

for the (conserved) dissipation field itself. Furthermore, the velocity and ε-fields are related by (C.7) which yielded the famous "-5/3" spectrum for homogeneous ε. This exponent must now be corrected for the scale dependence of ε, the so-called "intermittancy correction" arises. This leads to [Monin and Yaglom, *ibid.*]

$$E_v(k) \sim k^{-5/3-K(2/3)} \tag{C.37}$$

Using $K(h) = C_1 h(h-1)$, i.e., the conserved Gaussian generator model (C.34–35), in (C.36–37) yields values of C_1 in the range 0.2–0.5 given the experimentally determined spectral exponents of either kind—we will use this upper bound in our simulations of radiative transfer in chap. 6.

C.5. Continuous Cascades and Universal Multifractals

Throughout the above discussion, we have tried to not overemphasize the role of the "dividing" ratio, λ_0, in the cascade process. We usually think of it as an integer $(2,3,4,\cdots)$ and this allows us to relate it to the final grid size (or, more precisely, inner-to-outer scale ratio) λ after some finite number of cascade steps. There is however nothing fundamental about any one of these integers and, all things considered, the original idea of turbulent kinetic energy transport through concentric shells in Fourier space implies, if anything, a dividing ratio of 1^+, or a whole continuum of dividing ratios. In practice (i.e., before the small scale limit), we are looking at λ-1 steps of ratio $1+(\lambda-1)^{-1}$ to obtain the same final grid size as n λ_0-steps getting us to $\lambda=\lambda_0^n$. Notice that, if such is the case, we have $\approx\lambda$, not $n\approx\ln\lambda$, random numbers that participate in each and every value of the final ε-field. With so many random numbers participating, we can expect that central limit theorems are somehow going to intervene making the final results quite simple. The main difference will be that amount of multiplicative "noise" involved in each infinitesimal cascade step must be carefully filtered to yield the proper multiple scaling. In essence, a discrete cascade process (with λ_0=2) very simply distributes one unit of multiplicative noise (i.e., a single generator $\mu\varepsilon$) per "octave" in frequency or, more precisely, wavenumbers. In order to retain this essential property of energy equipartition[19] amongst the generators, we want the same total amount in every octave. In other words, the infinitesimal generators must have an exactly "1/k" energy spectrum, they are no longer totally independent (spatially uncorrelated).

Along these lines, Schertzer and Lovejoy [1987a,b] develop (in equations) the formal theory of continuous cascading in Fourier space which, on quite general grounds, calls for a very specific kind of "sub-generator," the continuous cascade equivalent of Γ in our discrete cascade prescription (C.17a) for the log-normal model. These previously unexplored Γ's are negatively extremal Lévy-stable r.v.'s. In this context, "stability" means "sums are distributed like their components, apart from a simple rescaling." Gaussian deviates are the only stable r.v.'s with finite variance and, for infinite variance but finite moments of order less than α, one finds Lévy deviates which have various amplitude-, skewness- and centering parameters; because we are interested in generating log-Lévy variables, only the most negatively skewed can be retained if (at least some) positive order moments are to exist. The concept of stability is related to the notion of attraction in probability theory as in general. For instance, the standard central limit theorem tells us that by summing/rescaling independent r.v.'s, all of finite variance, one eventually obtains a normal deviate. Equivalent theorems exist for r.v.'s of infinite variance and Lévy-stable deviates [Feller, 1971]. This attractive property entails a strong degree of universality to the multifractals based on such generators.

Since Lévy-stable r.v.'s are defined in terms of their c.g.f.'s, the corresponding "universal" multifractals are defined from their K(h)'s:

$$\left.\begin{array}{ll} 0<\alpha<2\ (\alpha\neq 1): & K(h) = \dfrac{C_1}{\alpha-1}\,(h^{\alpha}-h) \\ \alpha=1: & K(h) = C_1\, h \ln(h) \end{array}\right\} \ h\geq 0 \text{ and } K(h)=\infty \text{ for } h<0 \qquad \text{(C.38a)}$$

The two basic "universal" multifractal parameters are (C_1,α). On the one hand, the parameter C_1 has been adopted quite naturally as a measure of the degree of inhomogeneity (in the sense of intermittancy) since homogeneity is found in the limit $C_1\to 0$. On the other hand, α (the Lévy "index") measures the degree of multifractality since monofractals and (C.29) are retrieved at $\alpha\to 0^+$, the lower bound, as is the log-normal model and (C.34) at $\alpha\to 2^-$, the upper bound. Notice that $K''(0)=\infty$ (infinite-Γ-variance), except in this $\alpha\to 2^-$ limit where $K''(0)<\infty$ (finite Γ-variance) and analytic continuation to $h<0$ is possible.

From our above discussion on the divergence of moments, we are particularly interested in

$$C_\infty = \begin{cases} \infty & 1\leq\alpha\leq 2 \\ \dfrac{C_1}{1-\alpha} & 0\leq\alpha<1 \end{cases} \qquad \text{(C.38b)}$$

So, according to the classification proposed by Schertzer *et al.* [1991], "wild" singularities are present in all $\alpha\geq 1$ universal multifractals, they are "hard."

The above K(h)'s can be analytically Legendre-transformed to yield the associated $c(\gamma)$'s, at least to first order:

$$\left.\begin{array}{l} c(\gamma) \approx C_1 \left[\dfrac{\gamma}{\alpha' C_1} + \dfrac{1}{\alpha}\right]^{\alpha'} \quad \left(\dfrac{1}{\alpha'} + \dfrac{1}{\alpha} = 1\right) \\ c(\gamma) \approx C_1 \exp\left[\dfrac{\gamma}{C_1} - 1\right] \quad (\alpha' = \pm\infty) \end{array}\right\} c'(\gamma)\geq 0 \qquad \text{(C.39a)}$$

but, since $K(h)=\infty$ for $h < 0$, no $c'(\gamma)<0$ information is conveyed by Legendre transformation, the above $c(\gamma)$'s are therefore expected to be good approximations for the cumulative probabilities in (C.19). The only, but notable, exception is found in the limit $\alpha\to 2^-$ ($\alpha'\to 2^+$), where analytic continuation of the $K(h)$ to $h<0$ yields a $c'(\gamma) < 0$ branch in the corresponding $c(\gamma)$ and it therefore models a p.d.f. according to our adopted definition (C.16).[20] In connection with the possibility of divergence of moments, we are interested in the order of singularity corresponding to the root of the argument of the power/exponential law in (C.37a), i.e.,

$$\gamma_0 = \begin{cases} \dfrac{-C_1}{\alpha-1} & 1\leq\alpha\leq 2 \\ \dfrac{C_1}{1-\alpha} & 0\leq\alpha<1 \end{cases} \tag{C.39b}$$

In the former case, we have (a first order estimate of) the most probable order of singularity which (to the same order) fills space. In the latter case, we retrieve C_∞ and it represents the maximum possible order of singularity; Schertzer *et al.* [1991] would classify these $0\leq\alpha<1$ universal multifractals (monofractals at α=0) as "soft."

Lavallée *et al.* [1992] have recently modified the "Trace Moment" (TM) data analysis technique, briefly described in the previous section, simply by starting not with the given ε-field as such but with that same field carried to some power η and then spatially degraded. The ensuing scaling analysis then yields not a $K(h)$ but a $K(h,\eta)$, hence the name "Double Trace Moment" (DTM). One can see that

$$K(h,\eta) = K(h\eta,1) - hK(\eta,1) = K(h\eta) - hK(\eta) \tag{C.40}$$

where, by definition, $K(h)=K(h,1)$. Indeed, using $\varepsilon_\lambda{}^\eta$ instead of ε_λ in (C.21–22) is like considering the $(h\eta)^{\text{th}}$ order moment—hence the first term in (C.40)—except that the $\varepsilon_\lambda{}^\eta$ field is not conserved since $\langle\varepsilon_\lambda{}^\eta\rangle\approx\lambda^{K(\eta)}$—hence the second term in (C.40). Equivalently, we are looking at the very same cascade with generators all multiplied by factor η and recentered by $-K(\eta)$; and the Legendre transform of $c'(\gamma')=c(\gamma)|_{\gamma=(\gamma'+K(\eta))/\eta}$ is $K'(h)=K(\eta h)-hK(\eta)$. If there is no difference between "dressed" and "bare" moments of order h and $h\eta$, then we can substitute (C.38a) into (C.40) yielding

$$K(h,\eta) = \eta^\alpha K(h) \tag{C.41}$$

for $h\geq 0$ only, except if α=2, and where $K(h)$ is given by (3.38a). Having determined $K(h,\eta)$ for a few h's and as many η's as possible, α (and C_1) are obtained by a simple logarithmic regression of $K(h,\eta)$ w.r.t. η. This is a substantial improvement over the kind of nonlinear fitting (and/or graphical methods) necessary to obtain α (and C_1) using the

PDMS or TM techniques. Recent DTM analyses [Schmitt *et al.*, 1992] of wind (tunnel) data yield $\alpha \approx 1.3$, i.e., in between the β- and log-normal models which have been used most often to date.

A third universal parameter is reserved for directly measuring the <u>degree of non-conservation</u> of the multiplicative process; on general grounds, this amounts to an extra linear term in K(h) or, equivalently, a translation (by γ_t) along the γ-axis, depending on whether a moment- or a histogram method is used. Many geophysical signals have been analyzed in terms of α, C_1 and (say) γ_t with the various techniques described above. Included, and of particular interest to us, are the Earth's radiation fields as measured by GOES (geostationary meteorological) satellite imagery (8 km resolution for 1024 km sized scenes) in the VIS and (thermal) IR channels: $\alpha \approx 0.6, 1.7$ and $C_1 \approx 0.2, 0.3$ for $c(\gamma\text{-}\gamma_t)$, with $\gamma_t \approx 0.15, 0.19$, respectively, from PDMS analyses [Lovejoy and Schertzer, 1990]. These values have been updated with the introduction of the DTM technique [Tessier *et al.*, 1992] with even smaller C_1's but $\alpha \approx 1.3$ for the visible channel that we are more concerned with, hence closer to the α=2 class obtained from the FBC analysis of Gabriel *et al.* [1988]. It should finally be mentioned that in all of our discussions of data analysis, it is taken for granted that the empirical field is of the "ε-type," i.e., it is (at the very least) non-negative and "conserved" (i.e., ensemble-average is unit) which, in particular, implies a spectral exponent in excess of -1, see (C.36). To achieve this, a certain amount of "pre-treatment" is sometimes necessary; its description is totally beyond the scope of this review but an example relevant to radiation is discussed in some detail in §6.4.2.

C.6. Passive Scalar Advection by Homogeneous Turbulence

We have gone full circle with turbulence, starting at a spectral exponent of -5/3 and ending at -[5/3+B] with B≈0.15 which may not seem like a big difference but we must realize that, on the one hand, spectral exponents are very robust statistics (almost insensitive to intermittancy, in particular) and that, on the other hand, we have elaborated very general modelling tools for extreme nonlinear variability in the meantime. We will finish this appendix with a few comments on the highly non-trivial problem of passive scalar advection by turbulence. This will give us an opportunity to appreciate the fact that Kolmogorov-type spectra are not specific to the turbulent velocity field.

Let $\rho(x,t)$ be the instantaneous density field of some contaminant (or admixture or "scalar") introduced into the fluid, the velocity field of which is $v(x,t)$ at time t; furthermore, the contaminant is assumed to be dynamically passive, hence $v(x,t)$ is still described by the Navier-Stokes eqs. (C.1–2). Conservation of the total amount of admixture is locally guaranteed by the continuity equation

$$[\frac{\partial}{\partial t} + \mathbf{v}\cdot\nabla\ ]\ \rho = D_a\,\nabla^2\rho + f' \tag{C.42}$$

where D_a is the diffusivity of the admixture in (say) air and $f'(\mathbf{x},t)$ represents a new (scalar) forcing term that partially accounts for boundary- and/or initial conditions. Alone, the l.h.s. of (C.42) is responsible for the advection of the scalar quantity ρ by the velocity field which we continue to assume is homogeneously and isotropically turbulent with a well developed inertial range first without and then (next sub-section) with intermittancy. The r.h.s. accounts for any amount of contaminant that leaves or enters the moving fluid particle and we have spelled out explicitly the effect of molecular diffusion, all other sources and sinks are incorporated into the forcing term. We have put ourselves in the context of passive scalar advection-diffusion for the sake of specificity; indeed, (potential) temperature obeys an similar equation with κ_a (thermal conductivity) replacing D_a and, in particular, a contribution proportional to $\varepsilon\sim\nu_a(\partial v/\partial x)^2$ entering f' as a source of heat from the viscous dissipation of (turbulent) kinetic energy, see eq. (C.48) below. In purely mathematical terms, (C.42) reads as a three-dimensional Fokker-Planck equation with $\mathbf{v}$ representing the "drift" term. This is not unfamiliar to those versed into inhomogeneous diffusive transport—radiative, in particular, where the main particularity is that the analogs of $\mathbf{v}$ and D_a are not unrelated to each other, cf. eq. (D.32).

Compared to the Navier-Stokes equations in (C.1–2) and the many unsolved problems of turbulence, equation (C.42) and the problems of passive admixtures look trivially simple being scalar rather than vectorial and linear in the field quantity. However, being coupled (in one direction at least), the problems are compounded as soon as turbulent velocity fields are involved. Some simple questions can be addressed within the framework of "K41" turbulence theory nevertheless; for instance 'How do the passive scalar fluxes fluctuate in space?' As in the case of the velocity field, we turn to similarity-based phenomenology for ideas. We start by adding

$$\rho \to \lambda^{H'}\rho \tag{C.43}$$

to the operations already present in (C.3). Viewed as a simple change of units for the scalar quantity (density or temperature), this leaves the Prandtl number

$$\mathrm{Pr} = \frac{\nu_a}{D_a} \tag{C.44}$$

unchanged if and only if H' = H.

Corrsin [1951] and Obukhov [1949] independently developed a natural extension of Kolmogorov's [*ibid.*] cascade phenomenology of the velocity field (sect. C.1) to the temperature field in homogeneous, isotropic turbulence. Recall that λ in (C.3) and (C.43) is then viewed a zoom ratio, they are scale changes. Given the fundamental scale invariant quantity ε which is related to $\mathbf{v}$, we need an analog related to ρ. A choice that is consistent with the similarity constraint (H'=H=1/3) is given by

$$\chi(\mathbf{x},t) = \frac{\partial}{\partial t} (\Delta\rho)^2 \qquad \text{(C.45)}$$

i.e., the flux (rate of change) of scalar "variance." The "Δ" is not called for in the case of $\varepsilon(\mathbf{x},t)$ w.r.t. velocity $\mathbf{v}(\mathbf{x},t)$, cf. eq. (C.5), since $\mathbf{v}^2/2$ is a well-defined and physically meaningful quantity and the nonlinear term in the Navier-Stokes eq. (C.1) is important to its Galilean invariance (adding a constant and uniform velocity to the whole field). The passive scalar eq. (C.42) is of course also invariant under a Galilean transformation (the presence of a total derivative on the l.h.s. guarantees this), however it is linear in ρ and additive constants are irrelevant to the dynamics. As in the case of velocity, the most easily obtained empirical statistic for scalar density is the structure function $\langle|\rho(\mathbf{x}+l\mathbf{u})-\rho(\mathbf{x})|^2\rangle$ ($|\mathbf{u}|=1$) which is only a function of l in statistically homogeneous and isotropic fields. From dimensional arguments, the scaling of the structure function can only be

$$\langle\Delta\rho^2(l)\rangle \approx \chi\, \varepsilon^{-1/3}\, l^{2/3} \qquad \text{(C.46)}$$

hence another "-5/3" law:

$$E_\rho(k) \approx \chi\, \varepsilon^{-1/3}\, k^{-5/3} \qquad \text{(C.47)}$$

Since temperature (T) obeys an equation formally identical to (C.42), the same analysis applies and another Kolmogorov spectrum is obtained, only the definition of χ is adapted in (C.45).

In summary, $\mathbf{v}$, ρ and T all have Kolmogorov-type spectra (and phenomenologies). Yet there are fundamental differences between them which are bound to show themselves in the answer to the next most logical question to ask: 'How does the inhomogeneity of turbulence—its intermittancy—affect the fluctuations $\Delta\rho$ and ΔT?' Unfortunately, no completely satisfactory model has yet been provided in spite of intense theoretical [e.g., Schertzer and Lovejoy, 1987a,b; Wilson *et al.*, 1991] and experimental [e.g., Sreenivasan and Prasad, 1989] research. This is largely why we have used dissipation-type fields to model the spatial variations of optical density throughout this thesis and, therefore, even a cursory review of this research is totally outside of its scope.

[1]Better still, the ultimate in multifractal teaching tools: Lovejoy and Schertzer [1992].

[2]The 1^{st} order effects of compressibility come hand-in-hand with those of gravity to generate convective heat transport across the system when it is submitted to a temperature gradient (or, more generally, heat sources and sinks on different parts of its boundary); this breaks the *a priori* rotational symmetry of (C.1–2). If necessary, these effects can be accommodated by directly incorporating a buoyancy term into f in (C.1) within the Boussinescq approximation and the new field quantity (potential temperature or specific entropy) will be constrained by a continuity equation that balances advection by the velocity field and molecular dissipation (via diffusion processes).

[3]Otherwise, rotational symmetry-breaking effects must be taken into account, most notably those of gravity and of the Coriolis force. This is an important aspect of scale invariant modelling and analysis that we will totally leave aside: Generalized Scale Invariance or "GSI" [Schertzer and Lovejoy, 1985; Lovejoy and Schertzer, 1985; Pflug *et al.*, 1990; Lovejoy *et al.*, 1992].

[4]"Big whorls have little whorls that feed on their velocity,
and little whorls have smaller whorls and so on to viscosity
—in the molecular sense." This summary of atmospheric dynamics is based on a equally compact summary by J. Swift of the dynamics of 18^{th} century english society using an appropriate biological analogy: (parasitic) fleas!

[5]This is related to the fact that, in d=2, the (surface) integral of "enstrophy" Ω^2 is conserved. In d=3, the circulation of "helicity" $v \cdot \Omega$ (along closed paths) plays a similar role in the currently very active research on "coherent structures" in three-dimensional turbulence.

[6]It is no accident that the first (and very simple) applications of scaling analysis techniques to atmospheric fields were concerned with cloud cover and rain regions [Lovejoy, 1982]. There are now scores of researchers worldwide engaged in scaling studies of atmospheric, oceanic and internal geophysical phenomena ranging from the geometry of lightning strokes to the shape of the sea's surface to the frequency and distribution of earthquakes [Schertzer and Lovejoy, 1991].

[7]Some authors prefer to talk about random multiplicative "weights," W_i.

[8]This "correlation length" is not to be confused with the "integral" (correlation) length discussed in sect. 4.4. The latter is defined in terms of the auto-correlation function of the field which, in this context, vanishes beyond l_0 (the grid constant).

[9]Since this is repeated in every subdivision at every scale, it leads to conservation at every point: "picocanonical" conservation according to Schertzer and Lovejoy [1989].

[10]From the point of view of cloud modelling for the purposes of radiative transfer calculations, multifractals provide *bone fide* (potentially extremely) variable density fields (cf. ch. 6) whereas monofractals can be viewed as homogeneous clouds with very convoluted "internal" boundaries (cf. ch. 4).

[11]In original (but now obsolete) α-model notations: $C_+ = C$, $\gamma_+ = C/\alpha$ and $\gamma_- = -C/\alpha'$ hence the β-model is retrieved at $\alpha \to 1$ and $\alpha' \to 0$.

[12]In the literature on strange attractors in phase space, with the notational standards set by Halsey *et al.* [1986], α designates the Hölder exponent which is related to our γ (order of singularity), see §C.3.2.

[13]In Lévy-stable (infinite variance) random variable theory, $\alpha \in]0,2[$ designates the order of the moment that first diverges; moreover α', such that $1/\alpha + 1/\alpha' = 1$, plays an important role. Gaussian (finite variance) generators—hence log-normal (bare) multifractals—are retrieved at $\alpha \to 2^-$ and $\alpha' \to 2^+$, and the β-model monofractals at $\alpha \to 0^+$ and $\alpha' \to 0^-$, cf. sect. C.5.

[14]In Lévy-stable random variable theory, $\beta \in [-1,+1]$ designates the "skewness" parameter. At $\beta = \pm 1$, the r.v.'s are extremal with algebraic tails in either positive or negative directions, not both; apart from a recentering by translation, the support is $\Re^{\pm}$, not $\Re$. At $\beta = 0$, we find symmetric r.v.'s. The former are called for in the design of universal multifractals and the latter in the theory of additive Lévy processes where standard RWs with finite (variance) "steps" are replaced by "flights" with infinite variance, possibly even infinite mean in the absolute (if $\alpha \le 1$), i.e., the fundamental m.f.p. of kinetic theory fame is divergent.

[15]With three definitions for the codimension function in the physical literature, we are still far behind the number definitions of fractal dimension that can be found in the mathematical literature which is currently twelve [C. Tricot, manuscript].

[16]This condition arises for different reasons in the two cases. For the log-normal model, the many cascade steps are necessary to reduce to zero the contribution of the normalization constant of the p.d.f. and which the Legendre transform does not restore. For the α-model, the same necessity arises from the discrete distribution of singularities which becomes dense only in the limit.

[17] This is related to the fact that this leading term is responsible for the exponential approach to the strict positive cut-off of the generators in these "extremal" log-Lévy models. Only negatively large deviations (associated with Lévy "holes" in the ε-field) are allowed.

[18] Multifractal analyses of rapidity in elementary particle "cascades" in high energy physics have been performed [Bialas and Peschanski, 1988], similarly in the realm of the nebulae [Atmanspacher *et al.*, 1989]

[19] This expression from (equilibrium) statistical mechanics is chosen deliberately. There are many formal analogies between multifractal formalism and thermodynamics [Chhabra *et al.*, 1989]. In this context, the analog of a generator is an degree of freedom in the system. The usefulness of these analogies becomes more debatable when 2^{nd} order phase transitions are included as they play a role analogous to the divergence of high order moments discussed in sect. C.4; see Schertzer and Lovejoy [1989] for a discussion in our notations.

[20] Another, somewhat fortuitous, exception is found at $\alpha=1/2$ ($\alpha'=-1$) where we find inverse squared Gaussian deviates to be exactly extremal Lévy deviates (of index 1/2). Correspondingly, we have not only a Legendre transform estimate of $c(\gamma)$ for very large λ's but also an exact inverse Fourier-Laplace transform of $<\varepsilon_\lambda{}^h>$ in the form of a $p_\lambda(\gamma)$, viz.

$$p_\lambda(\gamma) = \sqrt{\frac{\ln\lambda}{\pi C_1}}\left[2-\frac{\gamma}{C_1}\right]^{-3/2}\lambda^{-C_1/(2-\gamma/C_1)}$$

hence

$$c_\lambda(\gamma) = -\log_\lambda p_\lambda(\gamma) = \frac{1}{2}\log_\lambda\left[\frac{\pi C_1}{\ln\lambda}\right] + \frac{3}{2}\log_\lambda\left[2-\frac{\gamma}{C_1}\right] + \frac{C_1}{2-\gamma/C_1}$$

before taking the small scale limit. Notice how the $c_\lambda'(\gamma)<0$ branch which corresponds to the essential algebraic "tail" in $p_\lambda(\gamma)$ appears as a "slowly varying" logarithmic function of γ in the above whereas the normalization constant becomes a straightforward "log-correction" to the first order (Legendre) term from (C.37a) which, in turn, appears last in the above expression for $c_\lambda(\gamma)$. It is also clear that $c_\lambda(\gamma)$ is not convex on all of its domain $]-\infty,2C_1[$. The above exact formulae (also available for $\alpha=2$) can be useful in the calibration of computational synthesis or analysis tools by eliminating one source of uncertainty, namely, finite-size effects.

Bibliography for Appendix C

Aharony, A., and J. Feder (Eds.), *Fractals in Physics*, Noth-Holland, Amsterdam, 1990.
Atmanspacher, H., H. Scheingraber, and G. Weidenmann, *Phys. Rev. A*, 40, p3945–, 1989.
Bialas, A., and R. Peschanski, *Nucl. Phys. B*, 308, p857–, 1988.
Chhabra, A. B., R. V. Jensen, and K. R. Sreenivasan, "Extraction of underlying muliplicative processes from multifractals via the thermodynamic formalism," *Phys. Rev. A*, 40, 4593–4611, 1989.
Corssin, S., "On the Spectrum of Isotropic Temperature Fluctuations in Isotropic Turbulence," *J. Appl. Phys.*, 22, 469–473, 1951.
Derrida, B., *J. Phys. (Paris)*, 48, p1154–, 1986.
Falconer, K. J., *Fractal Geometry - Mathematical Foundations and Applications*, pp.xxii+288, J. Wiley, New York, 1990.
Feder, J., *Fractals*, Plenum, New York, NY, 1988.
Feller, W., *An Introduction to Probability Theory and its Applications*, vol. 2, Wiley, New York, NY, 1971.
Frisch, U., P.L. Sulem, and M. Nelkin, "A simple dynamical model of intermittent fully developed turbulence," *J. Fluid Mech*, 87, 719–724, 1978.
Frisch, U., and G. Parisi, "A Multifractal Model of Intermittancy," in *Turbulence and Prdicability in Geophysical Fluid Dynamics and Climate Dynamics*, 84–88, Eds. M. Ghil, R. Benzi, and G. Parisi, North-Holland, 1985.
Gabriel, P., S. Lovejoy, D. Schertzer, and G. L. Austin, "Multifractal Analysis of Resolution Dependence in Satellite Imagery," *Geophys. Res. Lett.*, 15, 1373–1376, 1988.
Grassberger, P., "Generalized dimensions of strange attractors," *Phys Rev. Lett. A*, 97, p227, 1983.
Halsey, T. C., M. H. Jensen, L. P. Kadanoff, I. Procaccia, and B. Shraiman, "Fractal Measures and their Singularities; The Characterization of Strange Sets," *Phys. Rev., A 33*, 1141–1151, 1986.
Hentschel, H. G. E., and I. Procaccia, "The infinite number of generalized dimensions of fractals and strange attractors," *Physica D*, 8, 435–444, 1983
Havlin, S., and A. Bunde, "Probability densities of random walks in random systems," *Physica D*, 38, 184–191, 1989.
Kolmogorov, A. N., "Local Structure of Turbulence in an Incompressible Liquid for Very Large Reynolds Numbers," *Dokl. Akad. Nauk SSSR*, 30 (4), 299–303, 1941.
Kolmogorov, A. N., "A Refinement of Previous Hypothesis Concerning the Local Structure of Turbulence in Viscous Incompressible Fluid at High Reynolds Number," *J. Fluid Mech.*, 13, 82–85, 1962.
Landau, L., and E. M. Lifchitz, *Fluid Mechanics*, 1st Russian Edition, 1953. (English translation: Pergamon, London, 1962)
Lavallée, D., *Multifractal Analysis and Simulation Techniques and Turbulent Fields*, Ph.D. thesis, McGill U., Physics Dept., Montréal, 132pp, 1991.
Lavallée, D., D. Schertzer, and S. Lovejoy, "On the Determination of the Codimension Function," in *Scaling, Fractals and Non-Linear Variability in Geophysics*, Eds. D. Schertzer and S. Lovejoy, Kluwer, Hingham (Mass.), 1991.
Lavallée, D., S. Lovejoy, D. Schertzer, and P. Ladoy, "Nonlinear variability of landscape topography: multifractal analysis and simulation," to appear in *Fractals in Geography*, Eds. L. Decola and N. Lam, Prentice Hall, New York, NY, 1992.
Lovejoy, S., "The Area-Perimeter Relation for Rain and Clouds," *Science*, 216, 185–187, 1982.
Lovejoy, S., D. Schertzer, and A. A. Tsonis, "Functional box-counting and multiple elliptical dimensions in rain," *Science*, 235, 1036–1038, 1987.
Lovejoy, S., and D. Schertzer, "Multifractals, Universality Classes and Satellite and Radar Measurements of Cloud and Rain Fields," *J. Geophys. Res.*, 95, 2021–2034, 1990.
Lovejoy, S., and D. Schertzer, "Generalized Scale Invariance in the Atmosphere and Fractal Models of Rain," *Wat. Resour. Res.*, 21, 1233–1250, 1985.
Lovejoy, S., and D. Schertzer, "Our multifractal atmosphere: A unique laboratory for non-linear dynamics," *Physics in Canada*, 46 (#4), 1990.
Lovejoy, S., D. Schertzer, and K. Pflug, "Generalized Scale Invariance and differential rotation in cloud radiances," *Physica A*, in press, 1992.
Lovejoy, S., and D. Schertzer, *Turbulence, Cascades, Multifractals and Atmospheric Applications*, course notes to be published by World Scientific, Hong Kong, 1992.
Mandelbrot, B. B., "Intermittant turbulence and self-similar cascades: Divergence of high moments and dimension of the carrier," *J. Fluid Mech.*, 62, 331–350, 1974.
Mandelbrot, B. B., *Les Objets Fractals: Forme, Hasard et Dimension*, Flammarion, Paris, 1975.
Mandelbrot, B. B., *Fractals - Form, Chance, and Dimension*, Freemann, New York, NY, 1977.
Mandelbrot, B. B., "Stochastic models for the Earth's relief, the shape and the fractal dimension of the coastlines, and the number-area rule for islands," *Proc. of the Nat. Acad. of Sc.* (USA), 72, 3825–3828, 1975.
Mandelbrot, B. B., *The Fractal Geometry of Nature*, Freemann, New York, NY, 1983.

Meneveau, C., and K. R. Sreenivasan, "A simple multifractal cascade model for fully developped turbulence," *Phys. Rev. Lett.*, 59(13), 1424–1427, 1987.
Monin, A. S., and A. M. Yaglom, *Statistical Fluid Mechanics*, vol. 2, MIT press, Boston, Mass., 1975.
Novikov, E. A., and R. Stewart, "Intermittancy of Turbulence and Spectrum of Fluctuations in Energy Dissipation," *Izv. Akad. Naut. SSSR, Ser. Geofiz.*, 3, 408–412, 1964.
Obukhov, A., "Structure of the Temperature Field in a Turbulent Flow," *Izv. Akad. Naut. SSSR, Ser. Geogr. I Geofiz.*, 13, 55–69, 1949.
Obukhov, A., "Some Specific Features of Atmospheric Turbulence," *J. Geophys. Res.*, 67, 3011–3014, 1962.
PAGEOPH, Vol. 131, Special Issue, 1989.
Peterson, I., *The Mathematical Tourist*, Freemann, New York, NY, 1988.
Pflug, K., Lovejoy, S., and D. Schertzer, "Generalized Scale Invariance and differential rotation in cloud texture," in *Non-linear Dynamics of Structures*, Eds. R. Z. Sagdeev *et al.*, 213–235, World Scientific, Hong Kong, 1991.
Pietronero, L. (Ed.), *Fractals' Physical Origin and Properties*, Plenum, New York, NY, 1989.
Pietronero, L., and E. Tosati (Ed.), *Fractals in Physics*, North-Holland, Amsterdam, 1986.
Rammal, R., C. Tannous, P. Breton, and A.-M. S. Tremblay, "Flicker (1/f) Noise in Percolation Networks: A New Hierarchy of Exponents," *Phys. Rev. Lett.*, 54, 1718–1721, 1985.
Richardson, L. F., *Weather Prediction by Numerical Process*, Cambridge Un. Press, 1922. (Reprinted by Dover, New York, NY, 1965.)
Schertzer, D., and S. Lovejoy, "The dimension of atmospheric motions," preprint volume of the IUTAM Symposium on *Turbulence and Chaotic Phenomena in Fluids*, 141–144, Kyoto Un., Japan, 1983.
Schertzer, D. and S. Lovejoy, "On the dimension of atmospheric motions," in *Turbulence and chaotic phenomena in fluids*, ed. T. Tatsumi, Elsevier North-Holland, New York, NY, pp505–508, 1984.
Schertzer, D., and S. Lovejoy, "Generalized Scale Invariance in Turbulent Phenomena," *P.C.H. Journal*, 6, 623–635, 1985.
Schertzer, D., and S. Lovejoy, "Physically Based Rain and Cloud Modeling by Anisotropic, Multiplicative Turbulent Cascades," *J. Geophys. Res.*, 92, 9693–9714, 1987a.
Schertzer, D., and S. Lovejoy, "Singularités anisotropes et divergence de moments en cascades multiplicatives," *Ann. Math. Qué.*, 11, 139–181, 1987b.
Schertzer, D., and S. Lovejoy, "Nonlinear variability in geophysics: Multifractal simulations and analysis," in *Fractals' Physical Origin and Properties*, pp49–79, Pietronero, L. (Ed.), Plenum, New York, NY, 1989.
Schertzer, D., and S. Lovejoy (Eds.), *Non-Linear Variability in Geophysics*, Kluwer, Dordrecht, 1991.
Schertzer, D., S. Lovejoy, D. Lavallée and F. Schmitt, "Universal Hard Multifractal Turbulence: Theory and Observations," in *Non-linear Dynamics of Structures*, Eds. R. Z. Sagdeev *et al.*, 213–235, World Scientific, Hong Kong, 1991.
Schertzer, D., and S. Lovejoy, "Hard and Soft Multifractal Processes," *Physica A*, in press, 1992.
Schmitt, F., D. Lavallée, D. Schertzer and S. Lovejoy, "Empirical Determination of Universal Multifractal Exponents in Turbulent Velocity Fields," *Phys. Rev. Lett.*, 68, 305–308, 1992.
Siebesma, A. P., *Multifractals in Condensed Matter Physics*, The Cheese Press, Edam, The Netherlands, 1989.
Sreenivasan, K. R., and R. P. Prasad, "New results on the fractal and multifractal structure of the large Schmidt number passive scalars in fully turbulent flows," *Physica D*, 38, 322–329, 1989.
Stanley, H. E., and P. Meakin, "Multifractal phenomena in physics and chemistry," *Nature*, 335, 405–409, 1988.
Stauffer, D., *Introduction to Percolation Theory*, pp. vii+124, Taylor & Francis, London, 1985.
Tessier, Y., S. Lovejoy, and D. Schertzer, "Universal Multifractals: Theory and Observations for Rain and Clouds," submitted to *J. Appl. Meteo.*, 1992.
Tritton, D. J., *Physical Fluid Dynamics*, Cambridge Un. Press, London, 1977.
Voss, R. F., "Fourier synthesis of Gausian fractals: 1/f noises, landscapes, and flakes," *Proc. Siggraph Conf.*, pp1–21, Detroit, 1983.
Wilson, J., D. Schertzer, and S. Lovejoy, "Continuous Multiplicative Cascade Models of Rain and Clouds," in *Scaling, Fractals and Non-Linear Variability in Geophysics*, Eds. D. Schertzer and S. Lovejoy, pp185–207, Kluwer, Hingham (Mass.), 1991.

Appendix D

DIFFUSIVE TRANSPORT, THE RADIATION CONNECTION

Preliminary Remarks and Overview: One of the main messages contained in app. A is that the major source of difficulty, and subtlety, in general (continuous angle, or "CA") radiative- or neutron transfer is the angular part of the problem. Moreover, the complexity is traceable to the presence of multiple scattering (m.s.); the problem at hand is epitomized by equation (A.5) and source function (A.17):

$$\left[\frac{1}{c}\frac{\partial}{\partial t} + \mathbf{u}\cdot\nabla \right] I_{\mathbf{u}}(\mathbf{x},t) = -\,\kappa\rho(\mathbf{x}) \left[I_{\mathbf{u}}(\mathbf{x},t) - \oint p(\mathbf{u}'\to\mathbf{u})\, I_{\mathbf{u}'}(\mathbf{x},t)\, d^{d-1}\mathbf{u}' \right] \quad \text{(D.0)}$$

i.e., an infinite set of fully coupled PDEs constrained by BCs that make it a boundary value problem in higher dimensions, with highly variable coefficients in the most interesting cases. The hope for analytical progress in such a situation is very slim and we are confined in practice to numerical methods.

In this appendix, we review the most traditional way of coping with the angular problem which however carries a cost, in terms of subtlety. The traditional route of the "diffusion approximation" (d.a.) is to assume that the angular (**u**) distributions of radiance are everywhere smooth enough to be well represented by a small number of average quantities (in fact, statistical moments). This amounts to taking the hydrodynamic limit of the above kinetic equation for the photon gas dynamics which, at least, is linear in radiance since, rather than interacting with each other, the photons interact with ambient scattering material. In chap. 2, we will systematically exploit this approximate theory of transfer—but an interesting transport theory in its own right—to gain insight into a (the?) basic mechanism of transport in inhomogeneous and/or non-plane-parallel media: flux-lines are attracted by negative fluctuations of optical density, including (non-illuminated) boundaries, and repelled by positive fluctuations, including isolated clouds. This is clearly an aspect of "channeling," according to Cannon's [1970] definition (the light seeks the lesser optical paths through the medium).

In chap. 3, we re-examine Chu and Churchill's [1955] original idea of arbitrarily reducing the order of the coupled system in (D.0) as another means of reducing the level of angular complexity. This discrete angle (or "DA") transfer—which is a simply a special, more tractable, case of exact (CA) transfer—is systematically exploited numerically in chaps. 4 (where it is compared with CAs) and 6 (where it is used to ease an exceptionally heavy computational task). We are basically faced with photon populations distributed on the angular part of their characteristic phase space and the perennial choices of averaging versus sampling lead us (respectively) the d.a. and to DAs. Not too surprisingly, the latter approach turns out to be not only a better model of inhomogeneous transfer processes (w.r.t. their scaling characterization, see sect. 4.3) but also a more encompassing theoretical framework since an entirely new "route to diffusion" is unearthed in sect. 3.3 by formally pushing DA phase function parameters beyond their physical limits, not by manipulating the radiance field as we do here.

We consider, in sect. D.0, the (beginning of the) hierarchy of exact angular moment equations derived from the above CA transfer equation; each one corresponds to a fundamental radiative conservation law that is briefly discussed. In sect. D.1, we close this hierarchy at 1st order by introducing Eddington's approximation, closely examining its conditions of validity from the theoretical standpoint whereas, in sect. D.2, we adopt a more empirical point of view. In connection with the latter approach, we discuss some recent radiometric measurements by King *et al.* [1990] inside a marine stratocumulus cloud deck; these observations are extremely interesting although, in our opinion, incomplete (and this prompts us to describe the ideal *in situ* cloud radiation transport experiment). In sect. D.3, we briefly look at the similarity properties of diffusion theory which can be readily interpreted in terms of the photon's generally correlated random walks (RWs). Section D.4 is devoted to the diffusive scaling properties of homogeneous media (our standard benchmarks) either with vertical bounds and external excitation or infinite but with a focus on the dispersion of a cloud of diffusing particles. Formal analogy is a powerful tool in diffusion theory (used mainly in chap. 2) and the only concern, going from one application of diffusion to another, arises from differences in the boundary conditions (BCs). These problems undergo close scrutiny in sect. D.5 and the method is illustrated by the following two examples: (vertically inhomogeneous, horizontally homogeneous) plane-parallel media behave like resistors in series, on the one hand, while inhomogeneous media treated in the "independent pixel" (IP) limit behave like resistors in parallel, on the other hand, and there is a well-known inequality between the two situations. Finally, we look at inhomogeneous situations in sect. D.6 and introduce "channeling" as the basic mechanism by which the radiation reacts to density fluctuations (thus providing a qualitative introduction to the somewhat more quantitative approach developed in chap. 2). The simple class of inhomogeneous media consisting of uncorrelated random binary mixtures, viewed as a variable conductivity problem, attracted a lot of attention in the statistical physics literature (in the early '80s); the (typically numerical) results of these studies provide us with a perfect illustration of the bulk effects of "channeling" and, moreover, they will be of use in chap. 2.

D.0. Radiative Energy and Momentum Flux: Conservation Equations for Scattering Media

By applying $\oint(\cdot)d^{d-1}\mathbf{u}$ to both sides of the m.s. transfer eq. (D.0), inverting the order of the angular integrations and using normalization (A.18) along with the definitions (A.2-3), we find the well-known exact relation

$$\frac{\partial U}{\partial t} + \nabla\cdot\mathbf{F} = -\kappa\rho(\mathbf{x})\,(1-\varpi_0)\,cU(\mathbf{x},t) \tag{D.1}$$

where we have reintroduced the radiant energy density $U=J/c$. This is simply the continuity equation for U, in particular, we find it to be locally conserved when $\varpi_0=1$. Consider a regular closed hyper-surface $\Sigma=\partial V$; the difference between outgoing and incoming energies (per unit of time) is

$$\oint_\Sigma F_{\mathbf{n}(\mathbf{x})}d^{d-1}\mathbf{x} - \oint_\Sigma F_{-\mathbf{n}(\mathbf{x})}d^{d-1}\mathbf{x} = \oint_\Sigma \mathbf{F}(\mathbf{x},t)\cdot\mathbf{n}(\mathbf{x})\,d^{d-1}\mathbf{x} \tag{D.2}$$

where $\mathbf{n}(\mathbf{x})$, $\mathbf{x}\in\Sigma$, is the running outwardly oriented normal unit vector. Notice that the l.h.s. calls for the hemispherical fluxes (A.3') whereas the r.h.s. uses net fluxes (A.3). Using (D.1–2) and the divergence theorem, we find this difference to become:

$$\int_V \nabla\cdot\mathbf{F}\,d^d\mathbf{x} = -\frac{\partial}{\partial t}\int_V U(\mathbf{x},t)\,d^d\mathbf{x} - c\kappa(1-\varpi_0)\int_V \rho(\mathbf{x})U(\mathbf{x},t)\,d^d\mathbf{x} \tag{D.3}$$

In steady-state, conservative systems such as clouds (at visible wavelengths) both terms on the r.h.s. of (D.3) vanish identically:[1] what goes in must come out, either as "transmittance" or as "reflectance" although there are at least two natural definitions of these as discussed at length in sect. A.4. Another important consequence of (D.3) is that, in absence of optically active material ($\kappa\rho=0$), radiance and flux have very different behavior: radiance is conserved whereas flux is diluted in space[2] according to a law in $1/r^{d-1}$.

By applying this time $\oint\mathbf{u}(\cdot)d^{d-1}\mathbf{u}$ to both sides of the m.s. transfer eq. (D.0), we enter the classical hierarchy of equations starting with

$$\frac{1}{c}\frac{\partial\mathbf{F}}{\partial t} + \nabla\cdot c\underline{\underline{P}} = -\kappa\rho(\mathbf{x})\left\{\mathbf{F}(\mathbf{x},t) - \oint\mathbf{u}\oint I_{\mathbf{u}'}(\mathbf{x},t)\,p(\mathbf{u}'\to\mathbf{u})\,d^{d-1}\mathbf{u}'d^{d-1}\mathbf{u}\right\} \tag{D.4}$$

Recall from sect. A.1, that $\underline{\underline{P}}(\mathbf{x},t)$ is the pressure tensor field of the photon gas.

In the second term on the r.h.s. of (D.4), we now revive the assumption $p(\mathbf{u}'\to\mathbf{u}) = p(\theta)$ where $\theta = \cos^{-1}(\mathbf{u}'\cdot\mathbf{u})$ and, as in sect. A.3, we can expand $p(\theta)$ into (azimuth-independent) spherical harmonics; the double integral in (D.4) is then readily evaluated by using the appropriate orthogonality relations. As we have not gone beyond 1st order in the $\mathbf{u}$-moments of $I_{\mathbf{u}}$, only the 0^{th} and 1^{st} harmonics of the phase function are called for, i.e., (A.19a,b) can be truncated at n=1.[3] From the definition (A.20) of g, we see that

$$\oint \mathbf{u}' \, p(\mathbf{u}' \cdot \mathbf{u}) \, d^{d-1}\mathbf{u}' = \varpi_0 g \, \mathbf{u} \tag{D.5}$$

We therefore obtain a simple expression for the r.h.s. integral in (D.4):

$$\oint I_{\mathbf{u}'}(\mathbf{x},t) \oint \mathbf{u} \, p(\mathbf{u}' \cdot \mathbf{u}) \, d^{d-1}\mathbf{u} \, d^{d-1}\mathbf{u}' = \varpi_0 g \, \mathbf{F}(\mathbf{x},t) \tag{D.6}$$

and (D.4) itself becomes

$$\frac{1}{c}\frac{\partial \mathbf{F}}{\partial t} + \nabla \cdot c\underline{\underline{P}} = -\kappa\rho(\mathbf{x}) \, (1-\varpi_0 g) \, \mathbf{F}(\mathbf{x},t) \tag{D.7}$$

Like (D.1), this is an exact relation and it too can be integrated over a given d-volume.[4] Equations (D.1) and (D.7), as laws of radiative energy and momentum conservation, can be viewed as (an integral part[5] of) those of radiative "hydrodynamics." This is a perfectly good analogy since the continuity and Navier-Stokes and mass conservation equations (C.1–2) can be obtained from Boltzmann's equation (E.5) by the very same averaging procedure although the derivation is more involved due to the nonlinearity of the collision term (see, e.g., Chapman and Cowling [1970]). More importantly for our systematic interest in general purpose physical models of inhomogeneous radiative transport, (D.1) and (D.7) are the traditional point of departure of the diffusion approximation which we will now derive. We will eventually draw fluid dynamical (and other) analogies within this framework that will help us clarify the basic workings of inhomogeneous transport, mainly in chap. 2.

Before proceeding, we restate our expressions for the conservation of radiant energy and momentum:

$$\frac{1}{c}\frac{\partial J}{\partial t} + \nabla \cdot \mathbf{F} = \kappa\rho(\mathbf{x}) \left[-(1-\varpi_0) J(\mathbf{x},t) + \mathfrak{S}(\mathbf{x},t) \right] \tag{D.8a}$$

$$\frac{1}{c}\frac{\partial \mathbf{F}}{\partial t} + \nabla \cdot c\underline{\underline{P}} = \kappa\rho(\mathbf{x}) \left[-(1-\varpi_0 g) \, \mathbf{F}(\mathbf{x},t) + \mathcal{S}(\mathbf{x},t) \right] \tag{D.8b}$$

where have simply added to their r.h.s.'s the contributions of non-m.s. sources that were dropped from the above derivations for simplicity. They are related to their CA counterpart $S_{\mathbf{u}}$ by

$$\mathfrak{S}(\mathbf{x},t) = \oint S_{\mathbf{u}}(\mathbf{x},t) \, d^{d-1}\mathbf{u} \tag{D.9a}$$

$$\mathcal{S}(\mathbf{x},t) = \oint \mathbf{u} \, S_{\mathbf{u}}(\mathbf{x},t) \, d^{d-1}\mathbf{u} \tag{D.9b}$$

For instance, $\mathbf{u}$-isotropic thermal (hence d=3) sources yield $\mathfrak{S}(\mathbf{x},t) = 4\pi(1-\varpi_0)B_\nu(T(\mathbf{x},t))$ and $\mathcal{S} = \mathbf{0}$. Their (very much non-thermal) single-scattering counterparts for uniform steady-state illumination at a boundary, collimated in direction $\mathbf{u}_0$, yield $\mathfrak{S}(\mathbf{x}) = \varpi_0 F_0 T_d(\mathbf{x}_0(\mathbf{x},\mathbf{u}_0),\mathbf{x})$ and $\mathcal{S}(\mathbf{x}) = \varpi_0 g \mathbf{u}_0 F_0 T_d(\mathbf{x}_0(\mathbf{x},\mathbf{u}_0),\mathbf{x})$, if the phase function is axisymmetric (only a function of $\mathbf{u}_0 \cdot \mathbf{u}$), the latter will vanish only in the case of isotropic ($g=0$) scattering. Recall (from sect. A.3) that $T_d(\mathbf{x}_0(\mathbf{x},\mathbf{u}_0),\mathbf{x})$ represents the escape probability from position $\mathbf{x}$ into the direction opposite to that of incidence.

D.1. The Radiative Hydrodynamic Limit: Eddington's Approximation as a Closure in Direction Space

Although solving the angular problem that is presently our preoccupation was not the purpose of the exercise that lead to the transport problem underlying (D.8a,b), we have certainly not made any progress on it. On the contrary, since (thanks to $c\underline{\underline{P}}$) the said equations contain more unknowns than constraints between them: $[1+d+d(d-1)/2]$ and $(1+d)$, respectively. We are $d(d-1)/2$ equations short, the number of independent components of $c\underline{\underline{P}}$ that were enumerated in sect. A.1. Notice that this "closure" problem does not affect $d=1$ where vectors and 2^{nd} order tensors are isomorphic with scalars; in particular, $cP=J/d$, from their respective definitions (A.4) and (A.2). The way around this problem in higher dimensions is the introduction of a closure scheme, and this is where Eddington's approximation enters: $\underline{\underline{P}} = (U/d)\underline{\underline{1}}$ (i.e., as in hydrodynamics, the pressure exerted by the photon gas is the same in every direction, even if it has a non-vanishing mean flow direction $\mathrm{E}(\mathbf{u}) \propto \mathbf{F}$). In terms directly applicable to eqs. (D.8a,b), we have

$$c\underline{\underline{P}} = \frac{J}{d}\underline{\underline{1}} \tag{D.10}$$

Equivalently, we can say that we have decided to neglect the traceless part of $c\underline{\underline{P}}$, in particular, all of its off-diagonal components are set to 0. This means that the radiance field can be described by its two first spherical harmonics, namely, J and $\mathbf{F}$:

$$I_{\mathbf{u}} \approx \begin{cases} \frac{1}{2\pi} J + \frac{1}{\pi} \mathbf{F}\cdot\mathbf{u} & (d=2) \\ \frac{1}{n_d} J + \frac{3}{2n_{d-1}} \mathbf{F}\cdot\mathbf{u} & (d>2) \end{cases} \tag{D.11}$$

This can be verified directly by substitution, using[6]

$$\oint \mathbf{u}\mathbf{u}\, d^{d-1}\mathbf{u} = \underline{\underline{1}} \begin{cases} \pi & (d=2) \\ \frac{2n_{d-1}}{3} & (d>2) \end{cases} \tag{D.12}$$

The next term in (D.11) would be proportional to $(c\underline{\underline{P}}-\underline{\underline{1}}J/d):\mathbf{uu}$, viz. the traceless part of $c\underline{\underline{P}}$ doubly contracted with the dyadic product of $\mathbf{u}$ with itself (recall that $\underline{\underline{1}}:\underline{\underline{1}}=d$). This is indeed the only way to maintain the orthogonality between the various terms of the expansion in monopoles, dipoles, quadrupoles, etc.

Conversely, it is a simple matter to deduce Eddington's closure (D.10) from the truncated radiance distribution given in (D.11).[7] This makes them equivalent to each other and, to some extent, this equivalence validates Eddington's hypothesis in meteorological applications because of the recent [King *et al.*, 1990] observation of dipolar **u**-distributions as in (D.11) in quite typical cloud; this evidence is closely re-examined in the next sub-section. In the meantime, it is easy to provide an example of conditions where the hypothesis in (D.11) becomes very poor: those where the photon gas is best viewed as a well collimated stream (of flux F_0, along direction $\mathbf{u}_0$), yielding $c\underline{\underline{P}}=F_0\mathbf{u}_0\mathbf{u}_0$ which is far from being traceless; such conditions are also often observed, granted, mainly in between the clouds and near their boundaries.

Substituting (D.10) into (D.8b) yields

$$\frac{d}{c}\frac{\partial \mathbf{F}}{\partial t} + \nabla J = d\,\kappa\rho(\mathbf{x})\,[\,-(1-\varpi_0 g)\,\mathbf{F}(\mathbf{x},t) + \mathcal{S}(\mathbf{x},t)] \tag{D.13}$$

In principle, $\mathbf{F}$ can now be eliminated between (D.13) and the continuity equation (D.8a). In practice, this yields an integro-differential equation in J (or U) alone which is only of interest in cases where energy densities and fluxes vary on the same time-scale.[8] We can neglect the troublesome first term on the l.h.s, in steady-state of course but also, more generally speaking, in situations where the flux reacts instantaneously and locally to changes in J rather than with the time-lag and non-locality implicit in (D.13). Hence

$$\mathbf{F}(\mathbf{x},t) = -D(\mathbf{x})\,\nabla U(\mathbf{x},t) + \frac{1}{(1-\varpi_0 g)}\,\mathcal{S}(\mathbf{x},t) \tag{D.14}$$

where the first term is the contribution to radiative flux from Fick's law for photons, and

$$D(\mathbf{x}) = \frac{c}{d(1-\varpi_0 g)\kappa\rho(\mathbf{x})} \tag{D.15}$$

is the (local) radiative diffusivity. $1/(1-\varpi_0 g)\kappa\rho$ is known as the "transport" m.f.p. and it corresponds to the "effective" m.f.p. for an "effectively" isotropic scattering (see upcoming section for details). D is therefore the exact radiative equivalent of molecular diffusivity which is always on the order of (thermal) velocity multiplied by the m.f.p.

To avoid the complications evoked above in connection with t-dependence, we can require specifically that

$$\frac{F}{|\partial F/\partial t|} \gg \frac{D(\mathbf{x})}{c^2} = \frac{1}{cd(1-\varpi_0 g)\kappa\rho(\mathbf{x})} \tag{D.16}$$

i.e. that changes in flux occur over periods of time much longer than light-travel time across a transport m.f.p.[9] There is another implicit constraint, this time on the norm of the flux, that comes from the fact that we must enforce positive values for $I_{\mathbf{u}}$ in (D.11). Hence, without being too specific about the constants involved, we can simply require that

$$F(\mathbf{x},t) = \frac{D(\mathbf{x})}{c}\,|\nabla J(\mathbf{x},t)| \lesssim J(\mathbf{x},t) \tag{D.17}$$

i.e., the transport m.f.p. must be relatively small w.r.t. the scale on which J changes considerably. The (D.17) is carefully written so that it does not exclude one-dimensional transport *per se* (even at the lower boundary where F=J); this is important since diffusion is known to be exact in d=1. At the same time, (D.17) makes a steaming ($J=|F|=||c\underline{\underline{P}}||=\cdots$) u-distribution look at least suspicious in higher dimensions.[10] We also note that (D.17) has no direct incidence on the variation of $D(\mathbf{x})$ itself. Even if D becomes infinite ($\rho=0$), F can remain finite if ∇J vanishes; an example of this situation is provided in §2.3.3. In §§2.3.4–5, we will also consider very disorderly (white-noise) media where transfer and diffusion give either very comparable or very different results, depending on whether or not and how often D takes on infinite values. This is already quite understandable since, when density vanishes (making D and the photon m.f.p. infinite), streaming in the photon gas is radically promoted, as argued in §A.3.3 directly from the properties of the transfer equation. Generally speaking (§4.4.3), the singularity condition is needs to be complemented by a high degree of correlation to yield "anomalous" diffusion.[11]

In all atmospherical- and many physical applications, (D.16) is well verified. As argued above, (D.17) is impossible to justify on general grounds. In sect. 4.4–5, we will (tentatively) define the favorable property of the optical medium as "regularity" in the sense of lack of "singularity," itself taken in a sense broader than the limit $\rho \to 0$ evoked above (specifically, we incorporate the multifractal concept of singularity developed in app. C). In chap. 6, things become more subtle because we will see that deep inside a very singular medium, diffusion can be relatively accurate if the optical thickness is large enough (i.e., there is plenty of scattering going on). We will also return to this question with an empirical frame of mind in the upcoming sub-section.

At any rate, by substituting (D.14) into (D.13), we obtain the following prototypical diffusion-type equation for energy density U:

$$\left\{\left[\frac{\partial}{\partial t} - \nabla\cdot D(\mathbf{x})\nabla\right] + \frac{c^2}{dD(\mathbf{x})}\left(\frac{1-\varpi_o}{1-\varpi_o g}\right)\right\} U = \frac{1}{(1-\varpi_o g)}\left[\frac{c}{dD(\mathbf{x})}\mathfrak{S}(\mathbf{x},t) - \nabla\cdot\boldsymbol{S}\right] \quad \text{(D.18)}$$

In the following two last sections we will be describing the specific role of each one of the three terms on the above l.h.s. Notice that divergence of the (vectorial) flux of the non-m.s. sources in (D.9a,b) acts as sink for U as it should.[12] Eq. (D.18) can be transposed into the more familiar terms of $J(\mathbf{x},t)$ and $\rho(\mathbf{x})$:

$$\left\{\left[\left(\frac{d(1-\varpi_o g)}{c}\right)\frac{\partial}{\partial t} - \nabla\cdot\frac{1}{\kappa\rho(\mathbf{x})}\nabla\right] + d(1-\varpi_o)(1-\varpi_o g)\kappa\rho(\mathbf{x})\right\} J$$
$$= d(1-\varpi_o g)\kappa\rho(\mathbf{x})\mathfrak{S}(\mathbf{x},t) - d\nabla\cdot\boldsymbol{S} \quad \text{(D.19)}$$

while bearing in mind the vector- and scalar fluxes are related by

$$\mathbf{F}(\mathbf{x},t) = -\frac{1}{d(1-\varpi_o g)\kappa\rho(\mathbf{x})}\nabla J(\mathbf{x},t) + \frac{1}{(1-\varpi_o g)}\boldsymbol{S}(\mathbf{x},t) \quad \text{(D.20)}$$

The first r.h.s. term defines a Fickian "constitutive" relationship and it is clearly diffusion theory's way of saying that, in absence of the non-m.s. sources (in the second term), spatial gradients (∇J) and angular anisotropy (**F**) are directly related, one driving the other, just as find in CA (sect. A.3) and DA (sect. 3.3) transfer.

D.2. The "Diffusion Domain" of Real Clouds: Recent Observations by King, Radke and Hobbs

Before leaving the topic of the accuracy of diffusion as a model of radiation transport, we must have another look at our most basic premise, namely, the radiance **u**-distribution (D.11) but from the empirical viewpoint. Eq. (D.11) is telling us that I_u is made up of a isotropic (monopole) term modulated by a dipole term with its axis oriented by **F**. Hence sampling I_u in any plane yields a cosine law in "azimuth," understood as relative to the direction normal of the sampling plane; if this normal is horizontal, then we are sampling in a meridian plane w.r.t. the vertical (an example to follow). Furthermore, this law has maximum amplitude (peak-to-peak variation) when the sampling plane contains **F** and vanishing amplitude when the plane lies perpendicular to **F**. In general, we do not expect (D.11) to be a very good representation of I_u, and indeed we have often argued that the number of harmonic terms required to describe I_u depends largely on the proximity of boundaries and/or non-thermal sources which can be either highly directional or well localized or both. (Recall that a localized source implies strong gradients, hence strong anisotropy according to the argument presented in §A.3.2, potentially stronger than (D.11) can allow for.) In clouds, this certainly happens within a few optical m.f.p. values of the open and/or illuminated boundaries (for even the mildest forms of inhomogeneity) and—according to the arguments presented in §A.2.2 (based on arbitrary variability)—it is quite conceivable that, in some cloud types at least, this can translate to geometrical m.f.p.'s that permeate the whole cloud.

In spite of these potentially severe shortcomings, there is strong evidence that (D.11) is an accurate representation of radiation fields in at least one situation of particular interest to us: deep inside marine stratocumulus (StCu) which typically form horizontally extensive cloud fields. This is a most remarkable finding of King *et al.* [1990] who flew horizontally through a 50 km wide cloud deck off the coast of California with a scanning radiometer oriented at right angles to the line of flight in the nose of a Convair C-131A aircraft during the First ISCCP (International Satellite Cloud Climatology Project) Regional Experiment (FIRE) on July 10 1987 between 09:22 and 09:55 PDT [their sect. 4, figs. 5, 6 and 8a, in particular]. Their prime objective was to quantify spectral absorption features in the near-IR but we will dwell mainly on their observations at 0.503 μm wavelength where they posit

$\varpi_0=1$. We agree with their (widely accepted) first conclusion that the observed albedo reduction at strictly visible wavelengths ($\lesssim 0.7\mu m$) cannot be due to "anomalous" absorption since it is unobserved, leaving spatial inhomogeneity as the prime candidate, and we can only wonder why they rely so heavily on a homogeneous model to draw their second conclusion about the reality of "anomalous" absorption in the 1.6–2.2μm region before this question is seriously re-examined within the context of inhomogeneous transfer in presence of (normal) absorption. (This is well within the reach of our present computational resources: simply by keeping accurate account of the orders-of-scattering in a conservative Monte Carlo simulation, one can reproduce after the fact responses for any amount of absorption.)

Interestingly, the authors find considerable variability in radiance amplitude, $(3/2\pi)|\mathbf{F}\times\mathbf{v}|/v$, where $\mathbf{v}$ is the aircraft's (almost horizontal and constant) velocity vector, and much less in midpoint radiance, $J/4\pi$. According to the raw data [presented in their fig.7], $J\approx 240$ ($\pm 15\%$) and $|\mathbf{F}\times\mathbf{v}|/v\approx 35$ ($\pm 50\%$), both in units of mW/cm^2/μm whereas their fig.8a shows that the residuals of $I_\mathbf{u}$ w.r.t. the cosine that barely reach 0.1 mW/cm^2/μm/sr. We of course think of these numbers as spatial averages. As expected from our often mentioned counter-example (w.r.t. diffusion theory) of "streaming" (δ-like) radiance, the authors report some instances of scans being "contaminated" by direct sunlight or that otherwise deviate from the ominous cosine behavior [cf. their fig.8b] but there are apparently very few of these. Clearly, a streaming radiation flow would often be observed in "broken" (non-stratiform) cloud fields, e.g., in (between) fair weather cumulii. Of course, all the intermediate cases are bound to occur too.

King and his co-workers define the part of the cloud where (their relatively selective sampling of) $I_\mathbf{u}$ obeys eq. (D.11) as the "diffusion domain," we accept this definition of the on condition that the criterion is extended to all of Ξ_3. Unfortunately, no attempts have been made yet to directly measure any non-vertical components of $\mathbf{F}$. This is mainly due to hardware limitations: for instance, King's apparatus uses opto-mechanical scanning technology which is now essentially superseded by CCD devices at the focus of telemetric lenses [M. Herman, p.c.]. There are also software limitations: current transfer models can only accommodate a vertical $\mathbf{F}$ since they rely heavily on their postulates of plane-parallel geometry and horizontal homogeneity—this applies in particular to King's [1981] asymptotic theory which uses diffusion ideas within the framework of transfer [and is used in their sect. 2 and 5].

The authors do constrain their "theoretical" cosines to be in phase w.r.t. maximum radiance being detected at zenith viewing ($\mathbf{u}$ pointing vertically downwards) and still find many scans to be well fit. At the same time, one of the poorer fits [their fig. 8b] shows a cosine slightly out of phase hence indication of an $\mathbf{F}$-component in the horizontal direction contained in the sampling plane, plus a hint of higher harmonics. Furthermore, the criterion does not exclude a case where **F** has a horizontal component, even substantial, at right angles to the sampling plane. We can only conclude that the observations tend to indicate that **F** does not deviate very much nor very often from the vertical. Equivalently, the vertical fluxes are not dominated by their horizontal counterparts on average which is very different from saying it never happens. This in no way justifies the plane-parallel assumption that the authors implicitly use further on [in their sections 2 and 5] and there is in fact no serious incompatibility between their (empirical) findings and our extensive (chap. 6) model calculations based on a scaling multifractal cloud. Recall that the data only pertains to a single 1-D transection through one specimen of a 3-D stochastic optical medium. (This kind of limitation is of course precisely what makes satellite imagery so attractive compared to such *in situ* radiometry.) Furthermore, it is illusory to try to interpret the internal radiation fields—quantitatively speaking—on a pixel-per-pixel basis, given the stochastic nature of the cloud. The same remark applies to the remotely sensed exiting (albedo) fields. In app. C, we will refer to more meaningful (turbulence-based) statistical alternatives which have been successfully applied to synoptic scale reflectance data [Gabriel *et al.*, 1988; Lovejoy and Schertzer, 1990; Tessier *et al.*, 1992] and the basic ideas can surely be adapted to the internal ("diffusion" domain) fields as well. At any rate, these scaling analysis techniques call for the maximum attainable spatial resolution; given v=80 m/s and the stated sampling rate, we are presently talking about 24 m (between zenith and nadir viewings). This can be reduced to ≈3 m simply by reducing the number of spectral channels to one,[13] without restricting the above-mentioned (CCD-based) bi-directional sampling of Ξ_3.

For these reasons, we are of the opinion that the authors' reduction of the data to physical parameters of the cloud can be largely disregarded, except in terms of a kind of IP hypothesis. Most interestingly, they do find a factor of two in the variability of their optical "altitude" (cumulative $\kappa\rho$ below the aircraft) hence a probable factor of four in (total) optical "thickness," assuming the aircraft is at mid-cloud level. A consistency check would be to perform 3-D Monte Carlo calculations on the horizontally variable retrieved 1-D (vertically extended) optical density field showing negligible horizontal fluxes, but this outcome is doubtful given the sharp gradients apparent in their probing, cf. their fig.10.[14] Furthermore, only 611 out of 3133 eligible (quasi-vertically oriented quasi-cosine) scans were reduced, apparently due to aircraft roll in excess of 5°, hence vignetting of either zenith or nadir views. In other words, the "pixels" in the horizontal probing are of variable width, averaging around 80 m rather than the theoretically attainable 24 m (and possibly only 3 m). This provides another argument in favor of future bi-directional sampling strategies. This also biases the selection procedure in favor of the more vertical fluxes since roll, strong up (down) drafts and horizontal LWC variability all occur together due to both shear-enhanced turbulent passive advection and cloud droplet condensation (evaporation) provoked by admixture of saturated (dry) air from cloud base (top).

In sect. 2.1, we argue on theoretical grounds that, on the one hand, homogeneous plane-parallel media are an extremal $\kappa\rho$-distribution w.r.t. the amount of diffuse radiation (e.g., albedo) generated and that, on the other hand, pixel-wise 1-D calculations provide only lower bounds to full 3-D transport when interpreted in terms of an apparent (or "effective") optical thickness. We can therefore take the authors' estimate of overall variability in optical thickness as a lower bound: a factor 2 at mid-cloud, 4 in all for the vertically integrated (hence smoothed) $\kappa\rho$. Durouré and Guillemet [1990] perform simple scaling analyses of cloud droplet counts in both StCu and (precipitating) cumulus congestus which prove to be extremely variable, see also Malinowski and Zawadski [1992]. (Apparently, King *et al.* use their cloud droplet size spectra only for the purpose of Mie calculations in order to relate the measurements in absorbing to non-absorbing wavelengths [in their sections 3 and 5].) The ideal experiment should obviously collect both reliable LWC and (directionally and spatially generous) radiance samples, this would provide the basis for extensive "cloudy atmosphere truthing," the equivalent of "ground-truthing" in the remote-sensing of the environment. With such a comprehensive data-base, one could simultaneously address the questions of which radiation transport model best applies (e.g., diffusion or transfer? when and where?) and of which cloud LWC variability model best applies (e.g., fractal or multifractal? when and where? and what kind?). Furthermore, since we can theoretically predict that certain variability models are incompatible with certain transport models, we will have a way of checking our grasp of the problem of inhomogeneous transport in a context of practical (meteorological) importance.

D.3. The Classical Similarity Relations: Their Interpretation in Terms of Correlated Random Walks

In essence, it is the truncated representation of radiance in (D.11) that makes diffusion theory insensitive to the higher harmonics of the phase function. Accordingly, its (exact) similarity relations are a first order truncation of those of full-fledged radiative transfer (see §A.3.2). This can also be seen by direct inspection of (D.19–20). Recall that the aim is to leave J and **F** invariant while rescaling the optical density field via κ. Independently of the non-m.s. sources, $\kappa(1-\varpi_0)$ and $\kappa(1-\varpi_0 g)$ must remain independently constant, equivalently

$$\begin{cases} 1-\varpi_0' = \dfrac{\kappa}{\kappa'}(1-\varpi_0) \\ 1-\varpi_0'g' = \dfrac{\kappa}{\kappa'}(1-\varpi_0 g) \end{cases} \tag{D.21}$$

These relations were heuristically derived by van de Hulst and Grossman [1968] from the radiative transfer equation itself. Notice that King's [1981] "similarity parameter" $\sqrt{(1-\varpi_0)/(1-\varpi_0 g)}$ is invariant whereas the "inverse (optical) diffusion length" $\sqrt{d(1-\varpi_0)(1-\varpi_0 g)}$ is rescaled by a factor κ/κ' along with the overall optical mass of the system. Finally, the same remarks as for CA and DA transfer apply to the two above-mentioned contributions to the non-m.s. source term.

In essence, the (axisymmetric) phase function in, say, (D.5) describes the probability distribution on Ξ_d of the new direction of propagation (**u**) w.r.t. the old (**u'**); equivalently, we have a p.d.f. of scattering angle $\theta=\cos^{-1}(\mathbf{u}'\cdot\mathbf{u})$ on $[0,2\pi]$ in d=2 and, in d=3, a p.d.f. for $\cos\theta$ itself on $[-1,+1]$ given that relative azimuth is uniformly distributed on $[0,2\pi[$. In this respect, the spherical harmonic coefficients ϖ_i defined in (A.19a,b) are closely related (in both cases) to the statistical moments of the $\cos\theta$-distribution. Clearly, ϖ_0 tells us about normalization: a conservative ($\varpi_0=1$) phase function is a properly normalized distribution; otherwise ($\varpi_0<1$), it is "defective" and the probability of survival (w.r.t. absorption) after n scatterings is ϖ_0^n, hence rapidly decreasing if ϖ_0 is not very close to 1. Focussing exclusively on the RW on Ξ_d for a moment, let $\mathbf{u}_0$ be the initial direction and take $\varpi_0=1$. This will also be the average position of the Ξ_d-RWer after any number of steps (scatterings). Letting $\mathbf{u}_n$ denote this position, we have $E(\mathbf{u}_n)=\mathbf{u}_0$, and definition (A.20) of the asymmetry factor tells us that $E(\mathbf{u}_{n+1}\cdot\mathbf{u}_n)=g$ for all $n\geq 0$. If $\theta_n=\cos^{-1}(\mathbf{u}_n\cdot\mathbf{u}_0)$ designates the (great circle) distance on Ξ_d between the points of departure and arrival, it is clear that

$$E(\theta_n) = 0 \tag{D.22a}$$

(by symmetry) and easy to show (by induction[15]) that

$$E(\cos\theta_n) = g^n \tag{D.22b}$$

Once familiar with characteristic function theory in probability, the simplicity of this result is no surprise since spherical harmonics are the equivalent in Ξ_d of Fourier transforms in $\Re^d$ and addition of independent random variables translates to products of characteristic functions which, here, are replaced by the (discrete) ϖ_i coefficients. Relations similar to (D.22b) can be obtained for higher order moments of $\cos\theta_n$, but they will not be as simple since "addition" theorems for the spherical harmonics intervene; in other words, it is better to stay within the spherical harmonic functional basis on Ξ_d: they constitute the "right" combination of powers of $\cos\theta$ to work with. Their orthogonality rules guarantee that

$\varpi_i=(g^i)^2$ for all the coefficients of the p.d.f. of θ_2 with (D.22b) for n=2 corresponding to the 1st order result; this makes g^2 is the "effective" asymmetry factor after two scatterings.[16]

A further consequence of (D.22b) is that $\mathbf{u}_n$ can be almost anywhere on Ξ_d (say, $E(\cos\theta_n)\approx 1/e$) as soon as $n\approx 1/\ln(1/g)$. If $g\approx 1$, this reads as $n\approx 1/(1-g)$ which yields $n\approx 7$ scatterings for the C1 phase function and $n\approx 1$ for Rayleigh scattering which is correct for such a quasi-isotropic phase function.[17] This trend towards **u**-isotropy of multiply scattered radiation is in fact applicable to all (non-degenerate) phase functions since, recalling that $|\varpi_i|<1$, the i^{th} harmonic coefficient after the n^{th} scattering is ϖ_i^n which goes to 0 with n (except for $\varpi_0=1$). Turning to the spatial consequences of the above, we remark that

$$E\Big(\sum_0^\infty \cos\theta_n\Big) = \sum_0^\infty g^n = \frac{1}{1-g} \tag{D.23}$$

is also the average position of the "correlated" [Renshaw and Henderson, 1981] random walking light particle in a $\kappa\rho$-homogeneous d-space, projected along $\mathbf{u}_0$ and measured in m.f.p.'s, after an infinite number of steps. Summarizing, an isotropic RWer loses track of its direction of propagation at every step but it takes the **u**-correlated spatial RWer about $n\approx 1/(1-g)$ scatterings for its current direction of propagation ($\mathbf{u}_n$) to become effectively independent of its original direction of propagation ($\mathbf{u}_0$). However, this has caused it to travel roughly (on average, precisely) that much further in that initial direction than its uncorrelated (g=0) counterpart. Everything is happening approximately as if the photon where scattering isotropically in a medium with 1-g times (less) the original optical density.

This is exactly the prediction of diffusion theory's similarity relations (D.22) but, generally speaking, it can only be an approximation in transfer theory. The rescaling would be exact if, instead of an exponential (photon-like) f.p. distribution, they were always unit valued (and this is indeed the case of "diffusing" particles such as P.G. de Gennes' "ants" and "termites," briefly discussed at the end of this appendix). From this vantage point, we see that the above homogeneity assumption on the density distribution is paramount to make this diffusion approximation a more accurate model for transfer since we need the photon f.p.'s to be as similar as possible; in other words, their (average) p.d.f. must be as close as possible to the standard exponential case, in sharp contrast to our analytical (multifractal) results presented in sect. 5.1. Conversely, this constitutes a strong indication that diffusion and transfer will predict radically different radiative behaviors in "extremely" variable media (where photon f.p.'s are far from exponential); this will be confirmed in the case of the "singular" density fields discussed in chap. 4 and 6.

In practice, the similarity relations (D.21) can be exploited to yield solutions for all possible (κ,ϖ_0,g) values corresponding to a given $\rho(\mathbf{x})$-field and BCs from three basic cases: ϖ_o is 0, finite (and less than 1), or 1. Notice that ϖ_o=0,1 are fixed points of the similarity transformation. For our immediate heuristic purposes, we wish to bear in mind the fourth possibility of multiplying media (hence applications in neutronics): ϖ_o is finite, but greater than 1. Thanks to the above similarity analysis, we can take g=0 without any loss of mathematical generality; physically, this corresponds to rescaling all m.f.p.'s, or densities, by their corresponding "transport" ratio, $1-\varpi_o g$. With these notational simplifications in mind, we will proceed in the two last sections of this appendix to make various assumptions that allow us to single out the qualitative effect of the various terms on the l.h.s.'s of (D.18-19).

D.4. Diffusion in Homogeneous Media: The Standard Scaling Properties

D.4.1. Initial Conditions and Diffusive Random Walks in Unbounded Media

We now start by postulating homogeneity, the all-too-standard assumption; this will give us a point of reference for the discussion of inhomogeneity effects in the upcoming final section. We will also see how this framework just about exhausts the resources offered by the standard curriculum in mathematical physics. In this case, we can always work in natural units of length where $(1-\varpi_o g)\kappa\rho=1$ (i.e, the transport m.f.p. is unit). Finally, we will also adopt the natural time units for our problem which make c=d, i.e., light travels a (transport) m.f.p. in each available direction in unit time and this makes the radiative diffusivity unit (within Eddington's approximation). Now (D.19) reads simply as

$$\left[\frac{\partial}{\partial t} - \nabla^2 \pm m^2 \right] J(x,t) = 0 \tag{D.24}$$

with $m^2 = d|1-\varpi_o|$.

If we furthermore consider only steady-state ($\partial/\partial t=0$) problems, we find a classical Helmoltz equation: $(-\nabla^2 \pm m^2)J=0$. The qualitative features of its solutions are dictated by the remaining choice of sign. In the radiative (+) case, where we should view $1/m=1/\sqrt{d(1-\varpi_o)}$ as the above-mentioned "diffusion" length scale (expressed here in transport m.f.p. units) and we expect exponential decays in space to occur on that scale. It is notable that the extreme case of pure absorption ($\varpi_o=0$, $m=\sqrt{d}$) does not yield the proper exponential decay expected from standard radiative transfer theory (i.e., with the m.f.p. as e-folding distance, except of course in d=1 where diffusion is not an approximation). This reminds us that, although $\kappa\rho$ appears explicitly in the expression for D, diffusion is insensitive to phenomena on the scale of the m.f.p. Turning to the multiplying (–) case, we see that the constant and the Laplacian operator have the same sign, as in the (hyperbolic) wave equation after separation of variables, and we expect spatially oscillating solutions which become unstable at the "critical" threshold in ϖ_o (or system size, by similarity). In the important conservative (m=0) case, the diffusion length becomes infinite and we find the (elliptical) Laplace equation, so the entire body of harmonic analysis applies. This fact will be exploited, via general theorems (in sect. 2.1) and via standard techniques of variable separation (in spherical coordinate systems, in sect. 2.2 and 2.3).

Still at m=0, but now relaxing the steady-state assumption, (D.24) becomes the prototypical (parabolic) diffusion equation with its characteristic t-irreversible, entropy-producing solutions which, at best, are functions of scaling (algebraic) combinations of the space and time variables.[18] For initial conditions $J(\mathbf{x},0)=\delta(\mathbf{x})$, we find the classical isotropic Gaussian distribution in $\Re^d$:

$$J(\mathbf{x},t) = J(r,t) = \frac{1}{(2\pi t)^{d/2}} \exp(-r^2/2t) \tag{D.25}$$

where $r=|\mathbf{x}|$ and from which we can estimate the moments of the "diffusing" particle's position which preform standard RWs in this homogeneous case. We find the following simple scaling w.r.t. t:

$$E(r^q|t) = \int r^q J(r,t)\, d^d x = \frac{\Gamma(\frac{d+q}{2})}{\Gamma(\frac{d}{2})} (2t)^{q/2} \tag{D.26}$$

By "simple," we mean that the knowledge of one moment is sufficient to define all the other moments; in app. C, we will see that this is related to the monofractal nature of the RW. In particular, (D.26) gives us the variance

$$E(r^2|t) = dt \tag{D.26'}$$

i.e., a factor t is contributed by every direction, as expected from the definition of Euclidian distance ($r^2=x_1^2+\cdots+x_d^2$) and the stability property of Gaussian distributions under repeated convolution (variances of sums of r.v.'s add). Restoring dimensionalized variables, but still for isotropic (g=0) scattering, the above reads

$$E(r^2|t) = \frac{ct}{\kappa\rho} \tag{D.26''}$$

For $E(r^2|t) \sim t^k$, we talk about "normal" or "standard" diffusion if $k=1$, otherwise it is deemed "anomalous" and an example of anomalous diffusion is briefly discussed in sect. 5.1 in connection with our finding of algebraic, not exponential, average direct transmittance laws for multifractal media. Finally, we notice that, after Laplace transformation of (D.24) in time, the absorption and time-derivative terms combine so, in a sense, time evolution and dependence on absorption contain the same information[19] on the system. (This last remark is in fact totally independent of the homogeneity hypothesis and we will make use of it further on.)

D.4.2. Bounded Media, Boundary Conditions and the "Extrapolation Length" Problem

We now return to steady-state systems and face one of the more annoying yet fundamental idiosyncrasies of diffusive radiation transport: its "mixed" BCs[20] that also plague DA(d,2d) transfer, in its 2^{nd} order guise. Our usual (transfer) BCs are expressed in terms of radiance; in principle, we must therefore start by expressing I_u in terms of J alone using (D.11) and Fick's law in (D.20):

$$I_u \approx \frac{1}{n_d} [\, 1 - \frac{1}{(1-\varpi_0 g)\kappa\rho(x)} \mathbf{u}\cdot\nabla \,]\, J \tag{D.27}$$

in d = 1, 2, 3 (curiously, but not 4, nor more). The diffusion approach is intrinsically incapable of accommodating a δ-radiance distribution as required in the specification of the BCs (A.27) for the (steady-state but otherwise) general albedo problem. We can however specify any given entering (–) or exiting (+) hemispherical flux w.r.t. the running normal to the surface of the medium we are interested in:

$$F^{\pm}(\boldsymbol{x}) = F_{\pm\mathbf{n}(\boldsymbol{x})}(\boldsymbol{x}) \approx \frac{1}{2} [\, 1 \mp \chi\, \mathbf{n}(\boldsymbol{x})\cdot\nabla \,]\, J(x)\, |_{x=\boldsymbol{x}\in\partial M} \tag{D.28}$$

where χ is known as the "extrapolation length" and we prefer to view its as an unspecified, free parameter of $O(1)$ (when expressed in transport m.f.p. units). This was indeed the tradition in the early investigations of diffusion approximations to exact transfer in homogeneous media since the fitting of the BCs was soon recognized to be its main weakness. Notice that χ is the only (free) parameter left in the steady-state conservative (m=0) problem in (D.24).[21] The practice was therefore to determine χ from exact transfer calculations, numerical if necessary, and then to use it in the diffusion solution.[22] At least in d=3, the well understood cases are, on the one hand, the semi-infinite medium (in connection with the Milne problem) that yields χ=0.7104··· and, on the other hand, the (optically) very thin case where $\chi \to 4/3^-$. The exact dependance of χ on size between these two extremes being a function of the precise geometry of the medium, see Davison [1951, and references therein]. Finally, we notice that we can formally retrieve at χ=0 the more standard Dirichlet BCs (although they apply to J/2) and, since we intend to exploit analogies with such problems quantitatively, it is of interest to see just how seriously we err by reverting to them.

We notice that a direct consequence of diffusion theory's commitment to fluxes (rather than radiances) is that only the definitions (A.29) of transmittance and albedo are of any use here; recall that these require the definition of a "terminator" on ∂M. Eq. (D.28) therefore tells us that, at a non-irradiated boundary point (contributing to transmittance) where $F^-(\boldsymbol{x})=0$ (with $\boldsymbol{x}\in\partial M_>$), we can use

$$T(\boldsymbol{x}) = \mathbf{n}(\boldsymbol{x})\cdot\mathbf{F}(\boldsymbol{x}) = F^+(\boldsymbol{x}) - F^-(\boldsymbol{x}) = -\chi\mathbf{n}\cdot\nabla J(x)\, |_{x=\boldsymbol{x}\in\partial M_>} \tag{D.29}$$

where Fick's law predicts $-(\mathbf{n}\cdot\nabla J)/d$ hence $\chi_{Fick}=1/d$, i.e., a systematic underestimate (except in d=1). From the DA equivalent (3.18) of (D.28), we see that all DA(d,2d) systems yield the reasonable (intermediate) value of $\chi_{DA}=1$.

Returning to the expression of steady-state diffusion BCs in (D.28), we see that—as is the case for DA transfer in chap. 3—no distinction between collimated and isotropic (or otherwise diffuse) illumination can be made. A substantial improvement on the problem of representing collimated irradiation, especially in relatively thin media, is made possible by using single-scattering sources in the definition of $\mathfrak{S}$ and S; in this case, still mixed but simpler (homogeneous) BCs are applied. This improvement comes however at a cost that makes the whole of diffusion theory much less attractive. Moreover it only affects the layers that are touched by directly transmitted radiance (i.e., only the first few in mildly inhomogeneous media), which is precisely why this complication is mainly of importance in extending the accuracy of diffusion towards thin media. The bulk properties of thick media are unaltered and, turning to very inhomogeneous media, we will see (chap. 4) that it is not a good idea to think of diffusion as an approximation to transfer anyway but rather as a theory of transport in its own right; in both cases, using the simplest possible BCs (or ICs) is therefore fully justified.

We can further illustrate the effect of χ by considering the conservative transport problem in a d-dimensional homogeneous slab problem, assuming it is illuminated by an incident flux F_0 at z=0 and is of total thickness L (or $(1-g)\tau$, since we are using transport m.f.p. units). Net flux is a constant vertical vector of magnitude $F=|\nabla J|/d$ (from Fick's law) and Laplace's equation $\nabla^2 J=0$ is satisfied in rectangular coordinates by $J(\mathbf{x})=J(z)=J_0-(dF)z$. The two BCs (D.28) allow the determination of J_0 and F in terms of L and χ: $J_0+\chi dF=2F_0$ and $(J_0-dFL)-\chi dF=0$. Hence

$$J_0 = F_0\frac{\chi+L}{\chi+L/2} \qquad\qquad F = F_0\frac{1/d}{\chi+L/2} \tag{D.30a}$$

and, for $L \gg \chi$ (or, equivalently, at $\chi\to 0$)

$$\frac{J_0}{F_0} \approx 2\left(1-\frac{\chi}{L}\right) \qquad\qquad \frac{F}{F_0} \approx \frac{2}{dL} \tag{D.30b}$$

Since χ vanishes from the dominant terms, it can be viewed as largely irrelevant to the asymptotic scaling properties of the system. Consequently, we generally need not be too meticulous about the enforcement of the mixed BCs.

This however does not mean that we can systematically take χ to be 0, even in terms of scaling. To see why, we first compute the transmittance of the slab from (D.29–30a,b):

$$T = \frac{F^{+}(L)}{F_0} = d\chi \frac{F}{F_0} = \frac{1}{1+L/2\chi} \tag{D.31}$$

Since L represents $(1\text{-}g)\kappa\rho L$ in our present units, this result is identical to (3.22') for DA transfer in homogeneous slabs if we take $\chi=1$ (as anticipated above), recalling that $1\text{-}g=q$ in conservative systems and that $\tau=\kappa\rho L$. We now take the limit $L \gg \chi$:

$$T \approx 2\chi L^{-1} \tag{D.31'}$$

Apart from notations (stemming from different ways of non-dimensionalizing the problem), the only difference we find between the complete DA transfer result (3.22'–23) and above diffusion solutions is a factor of d in (3.23) for the total DA radiance at the top which is absent from (D.30a). Comparing (D.31') with the scaling relation (1.2) with λ replaced by L (due to the prevailing homogeneity assumption, $\lambda=1$), we see that[23] $K_T=-1$ (with a prefactor[24] 2χ), independent of d—inasmuch as χ is (e.g., as in orthogonal DA systems); equivalently, from (0.1) with $\bar{\tau}=\tau=L$ (in the units presently in use), we find $\nu_T=1$, $h_T=2\chi$. The remarkable success of diffusion in reproducing *bone fide* transfer results—up to prefactors—in this example is entirely traceable to the ultra-symmetric geometry of the slab's boundaries. In chap. 2, we introduce formal analogies with electrostatics and -dynamics that we will then use to show, in particular, that the homogeneous plane-parallel assumption is "extremal" in other important respects also.

Finally, we remark that an equivalent form for the general (any L) result (D.31) is:

$$\frac{1}{T} - 1 = \frac{L}{2\chi} \tag{D.31''}$$

which seems to be canonical for diffusive responses, cf. (2.18) and (2.37) for spherical systems—a case where the mixed BCs are of considerable importance to the final result—and the discussion in §2.2.3 about its generalization to other shapes. The same form also arises in DA transfer, cf. (3.22) for homogeneous slabs of course but also (3.38) for the ("generalized") similarity relation between not-necessarily-homogeneous slabs.

D.5. The Power of Formal Analogy: Transposing Results to/from Another Field

D.5.1. The Importance of Mixed Boundary Conditions in Horizontally Extended, Weakly Variable Media is Minimal

Radiation (or neutron) transport is just one instance were diffusion equations arise (all we need is a conservation law plus a constitutive law); several instances are listed at the beginning of chap. 2. A perfect equivalence in the local physics may however be marred by different boundary conditions (BCs). Typically, we must compare solutions for the two extreme cases of Dirichlet (given field) and von Neumann (given normal gradient) with those for the "mixed" variety which will arise in any 2nd order formulation of radiation transport (see, e.g., sect. 3.3. for DA transfer). We will therefore closely examine their effect and find them to be (relatively) unimportant as long as the medium is somehow horizontally extended and not too inhomogeneous. This latter constraint is necessary for diffusion and transfer to yield quantitatively similar results anyway (cf. sect. 4.3).

We only need to consider one example in detail and the most obvious choice of an analog of diffusive "photon" transport is diffusive "charge carrier" transport, i.e., steady-state electrodynamics (in the following, we will simply say "conductance"). Consider the problem of conductance through a homogeneous (d-dimensional) "wire" of length L (extending vertically) and width N (extending in all d-1 horizontal directions). The "insulating" side BCs ($\mathbf{n}\cdot\mathbf{j}=0$) make the wire equivalent to a finite portion of a slab of infinite horizontal extent since $\mathbf{j}$ (current density) is a constant vector in the wire. All we need to do is to find the equivalents of our physical quantities, continuity equation and constitutive laws. In this case, Fick's ($\mathbf{F}=-[1/d(1-g)\kappa\rho]\nabla J$) becomes Ohm's law ($\mathbf{j}=\sigma\mathbf{E}$, where $\mathbf{E}=-\nabla\phi$, with the usual meanings for the symbols[25]) and the conservation rule for radiant energy ($\nabla\cdot\mathbf{F}=0$) becomes that for electrical charge[26] ($\nabla\cdot\mathbf{j}=0$). Hence the substitutions

$$\begin{cases} \dfrac{1}{d(1-g)\kappa\rho} \to \sigma \text{ (with } (1-g)\kappa\rho=1 \text{ in homogeneous media)} \\ \mathbf{F} \to \mathbf{j} \\ J \to \phi \text{ (hence } F_0 \to \dfrac{V}{2}) \end{cases} \tag{D.33}$$

where V is the potential drop and the division by 2 compensates the "1/2" in the mixed BCs (D.28), with lower signs.[27] Our homogeneous radiative result in (D.30a,b) therefore applies with vanishing extrapolation length ($\chi=0$) since we now want Dirichlet BCs and, with (D.33), reads

$$j=\frac{\sigma}{L}\,V \tag{D.34}$$

exactly as we expect from elementary considerations (viz. $V/L=E$). We are now interested in doing the opposite: obtain a radiative result from conductance theory or experiment.

Generally speaking (inhomogeneous situations, $\sigma=\sigma(\mathbf{x})$), "bulk" conductivity or "inverse resistance" is defined from macroscopically measurable quantities—such as the current I (or its spatial average density $\overline{j_z}$)—by

$$\Sigma=\frac{I/N^{d-1}}{V/L}=\frac{\overline{j_z}}{V/L} \tag{D.35}$$

which is equal to σ in the above homogeneous case. One might expect Σ to be independent of L as it is of N since these are simply geometrical constants, there is nothing physical about them *a priori* but such is not the case in "extremely" inhomogeneous media. We will be examining a well-known instance of this kind of anomaly (in §D.6.2), namely, singular (0 or ∞) σ-valued binary mixtures at "percolating" threshold (cf. sect. C.2). We can also confidently anticipate anomalous bulk conductance properties for materials (local conductivity fields) modeled by multifractals as described in sect. C.3–5, they too are "singular" although in a sense we define more precisely in the corresponding appendix.

Going from the trivial conductivity result (D.33) to its radiation counterpart is somewhat more subtle. Clearly we cannot recuperate any information on χ directly, being a dimensionless number of $O(1)$ related to precise BCs. We are simply interested in finding the closest possible radiative analog for Σ in (D.34), if only for future reference. We know that the above substitutions work in the reverse direction, namely, $\phi \rightarrow J$ and $\mathbf{j} \rightarrow \mathbf{F}$ where (letting $F_0=1$) we can take F=T=1-R, $J(0) \approx 1+R$ and $J(L) \approx T+0$ (these last two relations are exactly true in d=1). We can therefore use $\overline{j_z} \rightarrow T$ and $V \rightarrow \Delta J = J|_L^0 \approx (1+R-T) = 2R$ in (D.34) to yield

$$\frac{\Sigma}{L} \approx \frac{T}{2R} \tag{D.35}$$

Using the $\Sigma = \sigma \rightarrow 1/d$ substitution (that can be obtained by direct comparison of the Eddington-Fick and Ohm laws), we find

$$\frac{1}{T} - 1 \approx \frac{d}{2} L \tag{D.36}$$

When compared to (D.31") this yields precisely the Eddington-Fick estimate for the extrapolation length ($\chi_{Fick}=1/d$). Of course, this attempt to determine T for all possible values of L is an overkill: for the purposes of scaling alone, $\overline{j_z} \rightarrow F = T$ (hence $T \sim L^{-1}$) would have been perfectly sufficient. The success brought on by the careful use of formal analogy however does encourage us to use it in more general cases, namely, (weakly) non-planar geometry and inhomogeneous media (both generalizations are used in chap. 2, respectively in sect. 2.1 and 2.3). The BC problem should however be re-examined whenever qualitative changes are made: e.g., horizontal bounded media (equivalent to non-insulated sides in the above) which are considered in sect. 2.2, using spheres as an (exactly solvable) example that is likely to be generic.

D.5.2. The (Well Known) Radiative Equivalents of Resistors Mounted in Series and in Parallel

Finally, the above conductance analogy serves us with an elementary interpretation of plane-parallel radiative transport (with inhomogeneity confined to the vertical coordinate), on the one hand, and of the "independent pixel" (IP) approach to inhomogeneous radiative transport (where horizontal transport is explicitly inhibited), on the other hand. Consider a (hyper-)cube of size L^d filled with some kind of inhomogeneous (imperfectly) conducting material at a constant potential across the top, grounded at the bottom, and with insulating sides. We first insert n perfectly conducting (constant potential) planes, laying horizontally at various levels, and then homogenize the material in between them leading to some conductance σ_i for the i^{th} layer; no matter how we subdivide, we end up with a number or resistors in a series arrangement that add up to a total effective resistance equal to that of a homogeneous cube of equal mass. In this case, we have a constant (unit) current crossing all layers and are adding the various potential drops (hence the depths):

$$\frac{1}{\Sigma_{series}} = \sum_{1}^{n} \frac{1}{\sigma_i} = \frac{1}{\Sigma_{homo}} \qquad \text{(D.37a)}.$$

where we have assumed (for simplicity) regular decimation at l_0 spacings (with $\lambda l_0 = L$=const.). The last equality in (D.37a) comes from the required conservation of total mass (recall that density ρ_i is $\propto 1/\sigma_i$).

We now repeat the operation but with some number (n) of insulating ($\mathbf{F}\cdot\mathbf{n}=0$) vertical planes, oriented at right angles to all the different horizontal directions; this is the diffusive way of making the different columns ("pixels") independent of one another. We are of course now dealing with a certain number of resistors in a parallel arrangement and it is well known that this leads to a smaller "effective" resistance (and higher total current). In this case, we have a constant (unit) potential drop and are adding the various currents (hence the sections):

$$\Sigma_{parallel} = \sum_{1}^{n^{d-1}} \sigma_i \leq \Sigma_{homo} \qquad \text{(D.37b)}$$

The last inequality in (D.37b) comes from Jensen's inequality (3.31) for $f(x)=1/x$ along with the mass conservation constraint expressed in (D.37a). The equality in (D.37b) is obtained only if all the σ_i are equal. The minimum is attained with an infinitesimal horizontal mesh, i.e., IPs as in (3.30) but with Dirichlet BCs (this does not make much difference if most of the pixels are at least several m.f.p.'s long).

We will argue on quite general grounds in §2.3.1 that still smaller bulk resistance is obtained by leaving the inhomogeneous material as it was in the first place, before introducing any king of internal boundary. In §D.6.2 below we will see (on an example) that, if we are free to move the mass around inside the cube as much as we please, then there are conditions in which we can indeed reduce the bulk resistance to zero, simply by creating perfectly conducting (null density) regions at random, the relative probability of creating a hole need only be above a certain threshold. There are no spatial correlations (beyond the elementary cell size) are introduced during the construction of the medium. However, near the "percolation threshold" the clusters made of connected empty (infinite conductance!) cells are highly correlated (see sect. C.2): they extend throughout the medium and its bulk conductivity becomes infinite, being basically "short-circuited" by the sprawling percolation "animals." In chap. 5, we will argue that the same result can be obtained by using extremely singular (multifractal) distributions which, in contrast, have long-range spatial correlations built into them, by construction. So, in both cases, singularity and correlation seem to be key factors; this can also be argued from first principles (sect. 4.4).

D.6. Diffusive "Channeling" in Inhomogeneous Media: Examples of Normal and Anomalous Scaling

D.6.1. The "Pseudo-Source/Sink" Term and its Role in "Channeling"

Having duly considered homogeneous cases, we return to (D.18) and look at the inhomogeneous but <u>conservative</u> case by taking ϖ_0=1 and we again ignore the non-m.s. sources. Invoking the operator identity $\nabla\cdot(\phi\nabla)=\phi\nabla^2+(\nabla\phi)\cdot\nabla$ and re-arranging the terms, we find

$$\frac{\partial U}{\partial t} = D(\mathbf{x})\ \nabla^2 U + (\nabla D)\cdot\nabla U \tag{D.38}$$

which is a standard Fokker-Planck equation for a diffusion process which sports a variable diffusivity and a variable "drift" velocity $\nabla D(\mathbf{x})$.[28] In this case, the latter just happens to be related to the diffusivity itself or, more precisely, its spatial variability; in general, the coefficients of ∇^2U and ∇U in Fokker-Planck equations are not related to each other.

In view of (D.38), we can better explain how inhomogeneous transport works at the most basic level by noticing that only the first term on the r.h.s. of (D.38) helps the radiant energy (local density, U) to enter low D (high ρ) regions but not very well since, on the one hand, diffusion is notoriously slow anyway (w.r.t. ballistic motion) and, on the other hand, diffusion is only as fast as D will make it (and D is already relatively low). In contrast to this, the second term advects the energy carriers efficiently into high D (low ρ) regions on essentially ballistic trajectories, in absence of the diffusion term proper. This is a diffusion theoretical way of describing the "channeling" phenomenon that will be discussed elsewhere in this thesis (chap. 4 an 6) in kinetic (transfer) terms, namely, the systematic enhancement of geometrical photon f.p.'s by inhomogeneity which, aided by spatial correlations in the density field, induce systematic effects in the bulk radiative responses.

Next, we return to almost the same point of departure as above, namely, eq. (D.19) in order to examine the inhomogeneous but <u>steady-state</u> assumption, still ignoring the non-m.s. sources on the r.h.s. Using the same vector identity, we find

$$\nabla^2 J = \{\ (\nabla \ln\rho)\cdot\nabla \pm [m\kappa\rho(\mathbf{x})]^2\ \}\ J(\mathbf{x}) \tag{D.39}$$

using the same definition for the non-negative parameter "m" and the same sign affectation as in sect. D.4 above: "+" refers absorption (of photons), "–" refers multiplication (of neutrons). This equation has first obtained by Giovannelli [1959] who also considered the possibility of emission by internal sources, our $\mathfrak{S}(\mathbf{x})$ in (D.19). He then performed 1st order perturbation on it using small amplitude horizontal sine-wave variations in ρ (and/or emission) but he had different geometry and BCs in mind than us, corresponding to a flux emerging from deep inside a semi-infinite medium (with, for instance, applications to the solar atmosphere). The more interesting effects w.r.t bulk transport properties in vertically finite media appear however at higher order, as we show in chap. 2.

Since D and ρ vary in opposite directions, eqs. (D.38–39) will tell us the same qualitative story about the effect of inhomogeneity but different images come to mind to illustrate it; as observed at the end of §D.4.1, absorption (here) and t-dependence (above) contain the same information, but different aspects of "channeling" become apparent. For constant ρ, Laplace's equation is retrieved at m=0 and we see that the r.h.s. behaves as a sink in the radiative (+) case, a source in the fission (–) case, just as we expect intuitively. Now consider the "pseudo-source/sink" term $(\nabla \ln\rho)\cdot\nabla J \propto -(\nabla \ln\rho)\cdot\mathbf{F}$ in (D.39) that characterizes the ρ-variability. By comparison with the above "real" source/sink term, we see that it acts like a source (the streamlines of the **F**-field diverge) when **F** and $\nabla \ln\rho$ are roughly oriented in the same direction, as a sink in the opposite case (the streamlines of the F-field converge). This is more or less what happens when a given mean flow of radiation collides head-on with an "obstacle," i.e., a more-or-less localized increase in the density field—a "singularity," in multifractal jargon. Such a "mean" radiative flow is present in all the physical and geophysical applications we will be considering: either the particles are leaving a localized internal source and going (on average) towards the sinks at infinity or else, leaving the illuminated boundaries and going (on average) towards the simply absorbing ones.[29]

We can therefore say that, much like a material fluid, radiation tends to flow around obstacles using, on average, paths of lesser optical length. The radiative "fluid" can also be funnelled into the relatively tenuous regions that lay on the path of the mean flow. Again we see that both of these possibilities describe exactly what "channeling" is all about; a stunning example of it is illustrated (literally speaking) in chap. 6 and we will witness its effects everywhere else. The role of higher dimensionality is clearly essential: neither of the above phenomena can happen in d=1 nor in horizontally homogeneous plane-parallel media in d>1 (since there is no way "around" nor "through" an obstacle consisting of a denser intervening layer). In d=1, gradients in J already tend to steepen where ρ reaches a peak, as required by Fick's law (since the flux F is constant in absence of absorption). In d≥2, **F** cannot be made to stagnate no matter how fast ρ increases since $\nabla \cdot \mathbf{F}=0$, but the flux lines will "spread out" considerably, and they will "collect" if a negative fluctuation in ρ occurs. In slightly different words, (D.39) is implying that the fluctuations of ρ and F tend to anti-correlate, a fact we will make use of to obtain a perturbation-like estimate of the effect of inhomogeneity on the overall flux (see sect. 2.3).

D.6.2. Some Useful Results from the Theory of Conductance in Uncorrelated Binary Mixtures

We now provide an interesting example to illustrate the systematic effect of inhomogeneity in the bulk diffusive transport properties that are induced by "channeling," viewed as the internal phenomenon described below eq. (D.38). Consider internally variable media that consist of binary mixtures of cells that are either thinner or thicker than some average value and where the values are distributed randomly, with no correlation from one cell to the next. More precisely,

$$\begin{cases} \sigma = \sigma_+ & \text{Prob} = p \\ \sigma = \sigma_- & \text{Prob} = 1\text{-}p \end{cases} \tag{D.40}$$

hence the ensemble-average conductance

$$<\sigma> = p\sigma_+ + (1\text{-}p)\sigma_- \tag{D.41}$$

which will will be very close to the spatial-average $\bar{\sigma}$ as soon as the total number of cells in the discretized ($N^{d-1}xL$) d-dimensional medium is relatively large. In the above we have used the conductance notations introduced in §2.1.1 since we will be largely following the discussion in that context found in Stauffer's [1985] excellent review before establishing the appropriate radiative analogies using the guidelines traced out in the same sub-section. We recall that density ρ (or resistivity) is inversely proportional to conductivity σ; this means that the "homogenized" medium conductance

$$\sigma_{\text{homo}} = \left\langle \frac{1}{\sigma} \right\rangle^{-1} = \frac{1}{p/\sigma_+ + (1\text{-}p)/\sigma_-} \tag{D.42}$$

differs systematically from the above "mean" conductance $<\sigma>$.

Random binary mixtures are by far the simplest possible model for a disordered medium and it attracted much attention in the (condensed matter) physical literature when it was realized that, in spite of its simplicity, it exhibits many interesting structural properties mainly centered on the phenomenon of "percolation," extensively reviewed by Stauffer [*ibid.*] and of which we briefly discuss the fractal aspects in sect. C.2. The geometrical aspect of percolation that we will be concerned with is the appearance, at percolation "threshold" ($p = p_c$), of an infinite cluster of connected σ_+-cells. More precisely, using the definition discussed in sect. C.2, the (average) size ξ of the "incipient" infinite cluster at $p \lesssim p_c$ scales as

$$\xi \sim (p_c - p)^{-\nu} \tag{D.43}$$

p_c is dependent on many details of the problem, e.g., type of grid (rectangular or triangular) and type of percolation (bond or site)—these are called a "irrelevant" variables.[30] In contrast, the exponent ν is "universal" in the sense that it depends only on the embedding dimensionality (for instance, ν is equal to 4/3 and 0.9 in d=2,3, respectively); other universal exponents are discussed in sect. C.2. Notice that there is no subscript for this "ν" and no confusion with our radiative counterparts form chap. 1 should ensue. We note that ξ is also known as the "correlation length" but this is not to be taken in the sense based on the auto-correlation properties of the (conductance) field, i.e., that of "integral" correlation length, cf. eq. (4.13).

Interest in these systems increased dramatically as their transport properties were systematically explored, mainly in the limits

$$\begin{cases} \sigma_-=1 \text{ and } \sigma_+\to\infty: \text{ "random superconducting network" (RSN) limit} \\ \sigma_+=1 \text{ and } \sigma_-\to 0: \text{ "random resistor network" (RRN) limit} \end{cases} \tag{D.44}$$

with analytical, numerical and even experimental methods. Again qualitative (phase-change type) transitions are observed at p_c for (ensemble-average) bulk conductivity and new (transport) exponents arise, namely,[31]

$$\begin{cases} \langle\Sigma\rangle \sim (p_c - p)^{-s} \text{ in the RSN limit for } p\lesssim p_c \text{ (and } \infty \text{ beyond)} \\ \langle\Sigma\rangle \sim (p - p_c)^{\mu} \text{ in the RRN limit for } p\gtrsim p_c \text{ (and 0 before)} \end{cases} \tag{D.45}$$

where the signs are chosen so as to leave s and μ positive. Many attempts—culminating in the Alexander-Orbach [1982] conjecture—were made to relate the transport exponents in (D.45) to their structural counterparts: generally speaking, d and/or ν and/or β (see sect. C.2 for a definition of this last exponent). As we will see below on an example, this (A–O) conjecture eventually failed and, more recently, the interest in these systems has shifted from the bulk properties to the multifractal aspects of the internal fields [e.g., Rammal *et al.*, 1985].

So, as p increases away from 0,$\langle\Sigma\rangle$ becomes infinite for RSNs at $p=p_c$ (i.e., long before the medium is totally superconducting) and, similarly, $\langle\Sigma\rangle$ remains null for RRNs up to $p=p_c$ (i.e., only at point when the insulating substrate has been considerably doped with conducting material). In both cases, we see that $\langle\Sigma\rangle$ obviously has nothing to do with $\langle\sigma\rangle$ nor σ_{homo} in (D.41–42) but its position w.r.t. these quantities is foreseeable given the role played by "channeling." In particular, $\langle\sigma\rangle=\infty$ but $\sigma_{homo}=\sigma_-/(1-p)$ remains finite for all p<1 in the RSN limit as expected: we obtain greater overall fluxes than in the homogenized case.

In the RRN limit we have $<\sigma>=p\sigma_+$ which is finite for all $p>0$ but $\sigma_{homo}=0$ since the mass of the whole system is effectively infinite as soon as a single cell is made totally insulating by increasing its "density" without bounds;[32] in spite of this infinite "mass," we obtain a finite $<\Sigma>$ as soon as percolation is achieved, again thanks to channeling by the infinite cluster of connected conducting sites.

In fact, eqs. (D.45) refer to idealized infinite systems and therefore cannot be used directly in conjunction with the definition of Σ in (D.34) which we can rewrite (on a per realization basis)

$$\frac{\Sigma}{L} = \frac{\overline{I_z}}{V} \tag{D.46}$$

for more convenience. Below we will briefly describe how this problem can be overcome by using the statistics for random walks by "diffusing" particles that are constrained by the density fluctuations; for the moment, we must first understand the finite size scaling properties. This can be done (exactly) at $p=p_c$ by taking $L\sim\xi$ (a "scaling *ansatz*") and eliminating $(p-p_c)$ between (D.43) and (D.45), hence

$$\begin{cases} <\Sigma> \sim L^{s/\nu} & \text{in the RSN limit} \\ <\Sigma> \sim L^{-\mu/\nu} & \text{in the RRN limit} \end{cases} \tag{D.47}$$

i.e., we assume the system is dominated by the largest cluster. Several authors using several different methods [Stauffer, *ibid.*; and references therein] have determined μ/ν numerically to a relatively high degree of precision using the second of the above relations as an operational definition. This considerable computational effort proved necessary to disprove the A–O conjecture. For instance, in d=2, the (carefully determined) numerical values for $s/\nu=\mu/\nu$ are in the range 0.97–0.98, while the A–O conjecture predicts $91/96\approx0.95$ so it was numerically disproved. (The equality of s and μ is due to a duality argument by Straley [1977].) In d=3 (where the duality argument no longer applies), the numerics yield $s/\nu\approx0.8$ and $\mu/\nu\approx2.2$.

The "anomalous" scaling described in (D.47) in the two singular limits (D.44) can be contrasted with the perfectly "normal" scaling observed when σ_- and σ_+ are both finite, viz. $<\Sigma>$ is also finite at a value which is function of the $\sigma_\pm$ and of p. We refer to Hong *et al.* [1986] for the determination of these dependencies in the special cases $p\approx p_c$ but $0<\sigma_\pm<\infty$, on the one hand, and $1=\sigma_-\ll\sigma_+<\infty$ $(0<\sigma_-\ll\sigma_+=1)$ at $p<p_c$ $(p>p_c)$, on the other hand. Using $s=\mu$ (hence in d=2 only), the authors are able to show, in particular, that (when our notations are used)

$$<\Sigma> = (\sigma_+\sigma_-)^{1/2} \tag{D.48a}$$

for bond percolation ($p=p_c=1/2$) on a square lattice. This is an exact result and it provides us with a means to further illustrate the systematic effect of channeling. In this special case, we have

$$<\sigma> = \frac{\sigma_+ + \sigma_-}{2} \tag{D.48b}$$

and we know that the above (arithmetic) average is always greater[33] than the harmonic average that appears in (D.48a). More importantly, we have $\sigma_{homo} = 2\sigma_+\sigma_-/(\sigma_+ + \sigma_-)$ from its definition (D.42) or, equivalently, we can write

$$\frac{\sigma_{homo}}{<\Sigma>} = \frac{<\Sigma>}{<\sigma>} \leq 1 \tag{D.48c}$$

where equality is of course obtained for $\sigma_+=\sigma_-$. Hence,

$$\langle\sigma\rangle \geq \langle\Sigma\rangle \geq \sigma_{homo} \tag{D.49}$$

and we note that the last inequality is in the direction that we anticipate in sect. 2.3. It is important to realize that the argument in chap. 2 works on a per realization basis but, in principle, for a stochastic model that conserves the total mass (recall that density $\rho \propto 1/\sigma$, here). This is reminiscent of the rules of "microcanonical" conservation used in thermodynamical systems (as well as in multifractal theory, cf. sect. C.2). The model used here has only "canonical" conservation of mass, yet the basic inequalities presented in chap. 2 still apply; this is possibly due to the well-behaved (simple-scaling) nature if the statistics of binary mixtures which, in particular, allow us to consider only means, throughout the discussion.

D.6.3. From the Steady-State (Finite-Size) Scaling to the Random Walk (Space-Time) Scaling using Einstein's Relation

Before leaving the topic of diffusive transport through percolating systems, we must note that considerable conceptual and computational progress was made when de Gennes [1980] suggested a connection between the above infinite medium bulk conductances in (D.45) and the problems of "ants" and "termites" in "labyrinths" (respectively, associated with the RRN and RSN limits). These designations refer to particles that move on a lattice according to various sets of probabilistic rules that are carefully chosen so that the particles "diffuse" in the inhomogeneous medium: always one cell per step in a random direction (the relative jump probabilities being proportional to the diffusivity ratios) while time increments are dictated by the local value of the diffusivity. We refer the reader to Bunde *et al.* [1985] for a discussion of the general case as well as of the (singular) "termite" limit. The colorful expression "labyrinth" was chosen by de Gennes to convey an idea of the convoluted—indeed, fractal—structure of the infinite percolation cluster which defines the maze in which the animal's motion is (eventually) confined.

In the homogeneous case (all directions are equally probable and constant t-increments), the statistics of the RWs of above particles are given by (D.26) and eqs. (D.26'–26") suggest that, in general, bulk diffusivity can be defined as $<E(r^2|t)>/(dt)$. Furthermore, we know (Einstein's relation) that it must be proportional to $<\Sigma>$, i.e., in natural units, we will have

$$<E(r^2|t)> \approx <\Sigma>t \tag{D.50}$$

when $<\Sigma>$ is finite, e.g., when the $\sigma_\pm$ are (both) finite in the random binary mixture model in (D.40). In the singular (D.44) limits of the same model at $p=p_c$, scaling arguments yield $<E(r^2|t)> \sim t^k$ with

$$k = \begin{cases} \dfrac{1}{1-s/(2\nu-\beta)} > 1 & \text{in the "termite" (RSN) limit} \\ \dfrac{1}{1+\mu/(2\nu-\beta)} < 1 & \text{in the "ant" (RRN) limit} \end{cases} \tag{D.53}$$

i.e., "super-diffusive" and "sub-diffusive" behaviours, respectively [see, e.g., Hong *et al.*, 1986; or Stauffer, 1985]. The latter relation was directly exploited by Pandley *et al.* [1984] to numerically estimate μ in d=2,3.

Lovejoy *et al.* [1990]—who were presenting transfer as an approximation to diffusion, rather than vice-versa for the sake of argument—discuss the formal equivalence that exists between the "skating" termites of Bunde *et al.* [1985], a faulty model for RSN diffusion (since the above transition is not observed at $p=p_c$), and photons, a proper model for transfer (by definition, see sect. B.1). This observation provides another—more qualitative—explanation of the difference in bulk conductive/radiative behaviour as predicted by (termite) diffusion, on the one hand, and (photon) transfer, on the other hand, that arise when the density field is allowed to become singular.

[1] When present, the first term can be balanced by steady-state internal sources, not included in the calculation (they do however play an important role in nuclear reactor- and stellar cores). The second term describes the bulk effect of absorption (or multiplication). The condition for overall radiative equilibrium is obtained by further integrating (D.3) over all the relevant photon frequencies (neutron energies) and taking $V \supseteq M$ (the whole system) whereas the stronger constraint of local radiative equilibrium is expressed by ν-integrating (D.1).

[2] This leads to the Olbers ("blazing sky") paradox in stationary homogeneous universes either infinite and filled with point-like sources or simply large enough and filled with finite-sized sources. The two obvious ways out of this problem are (i) the universe is not stationary, as in the standard (big-bang) model, or (ii) it is not homogeneous but hierarchically structured, as in Charlier-Mandelbrot (scaling) models; clearly both capture an aspect of reality but are hard to reconcile one with the other at early epoches, since there is no observational evidence of inhomogeneity (via anisotropy) in the 3K cosmic background. It is noteworthy that, over two centuries prior to Olbers' (the early 19^{th}), Kepler described and resolved the problem correctly: in his view, the stellar universe just isn't that big; by contrast, Olbers' solution—the ether is absorbant—is wrong (since it would then heat up to stellar surface temperatures in finite time). Given the well known close relation between absorption and t-dependence, there is an interesting parallel to be made with the more recent "cloud albedo" paradox [Wiscombe *et al.*, 1984] for which the two ways out are again basically homogeneous absorption and scaling inhomogeneity, resp., wrong and right at visible wavelengths (but in the near IR it is anybody's guess, at present).

[3] Since this truncation is merely for convenience, not by necessity, this does not imply any d-dependent limit on $|g|$ in order to keep $p(\theta)$ positive as any well-defined p.d.f. should be.

[4] This yields an equation for the conservation of the momentum transferred from the photons to the scattering/absorbing material, i.e., an expression for the radiative bulk forcing (by direct mechanical transfer, not via heating as in the Earth's atmosphere) which would enter the Navier-Stokes equations for the radiating fluid as a specific acceleration term. This is of paramount importance in the theory of radiatively driven stellar winds that prevail in early-type (hotter, younger) stars, Wolf-Rayet stars being a prime example.

[5] Pomraning's [1973] "radiative hydrodynamics" are concerned with the global conservation of mass, energy, and momentum for the combined and interacting photon- and particulate fluids.

[6] All of the off-diagonal elements vanish identically upon integration, by anti-symmetry. For a diagonal element, use $\mathbf{u}\mathbf{u}d^{d-1}\mathbf{u} = n_{d-1}\mu^2 d\mu$ $(1\geq\mu\geq-1)$ in $d>2$, and $2\cos^2\theta d\theta$ $(0\leq\theta\leq\pi)$ in $d=2$.

[7] Eddington's [1916] ideas were originally expressed in scalar terms because he was dealing with full-fledged radiance fields but only in 3-D plane-parallel stellar atmospheres (or spherically stratified interiors) hence axisymmetric distributions on Ξ_3. Using spherical harmonics to model an arbitrary radiance distribution, Giovanelli [1959] seems to be the first to generalize them to density fields and/or sources spatially variable in all (3) directions. Independently, Unno and Spiegel [1966] reckoned directly on the pressure tensor and Wilson [1968] demonstrated the equivalence of the two approaches. The compact tensor notation used here is inspired, in particular, from Mihalas [1978] and Preisendorfer [1976]. The later also discusses the two main paths to these equations described above (but takes Fick's law as a premise rather than a consequence); he also outlines more sophisticated closure schemes.

[8] For instance, in presence of rapidly evolving sources and/or media, i.e., $D=D(\mathbf{x},t)$ too. The problem is maybe best left as a system of PDEs which is already of more manageable proportions than full m.s. transfer systems. Zachmanoglou and Thoe [1976] shows the homogeneous case in d=1 (of importance in "transmission line" theory) to be tractable and finds damped wave-like behavior for the solutions.

[9] Using Fick's law in (D.14), in spite of its condition of validity (D.16) not being verified, leads unsurpisingly to violations of causality; amongst other reasons, this prompted Levermore and Pomraning [1981] to develop "flux limited" diffusion (FLD) theory which is easier to use than the PDE-system in d>1 (not to mention t-dependent transfer) Indeed, Bethe and Brown [1985] and their co-workers have performed detailed numerical calculations based on FLD applied to both the neutrino- and the photon yield of Super-Nova explosions using as initial input the (dynamically unstable) core obtained at the end point of stellar evolution models (themselves, a sequence of hydrostatic equilibrium configurations); their predicted fluxes where amazingly close to those observed for SN1987a in the Larger Magellanic Cloud, discovered by young Canadian astronomer I. Shelton while stationed at U. of Toronto's facility in Chile. (The last SN in our galactic neighborhood, observable from Earth, was recorded by J. Kepler in 1604.)

[10] The diffusion approximation is widely used in reactor design neutronics, and this is easily understood since violation of either the conditions (D.16–17) spells big trouble. Very fast flux variations will be hard to control by moving macroscopic objects in or out of the core, so there is a risk of melt-down if they start to occur; in the worst case scenario, this leads to major radiation leakages—streaming (long m.f.p.) neutrons—into remote places where they probably do not belong (e.g., in human beings).

[11]The radiative equivalent of the opposite limit of vanishing D is an infinitely dense region, completely impossible for the photons to penetrate: they must go around it if possible (otherwise, they are trapped); clearly, the structure of the medium will again play a key role in the outcome.

[12]It can be shown that the single-scattering contribution to S is divergence-free if $\varpi_0=1$, in which case, the thermal contribution to $\mathfrak{S}$ vanishes identically; so, for the purposes of substitution into the continuity equation (D.8a), it could equally well be left out of (D.14) or (D.20).

[13]A radical improvement, allowing multispectral observation at high spatial/directional resolution, would of course be achieved (at a modest cost) by using a tethered balloon [R. Davies, personal communication].

[14]King *et al.* [1981]—not the same group—find a $\sim k^{-s}$ spectrum, with $s\approx 1.7$ (hence very Kolmogorov-like), for density (LWC) fluctuations. We recall that processes with spectral slopes $s\leq 2$ are almost surely nowhere differentiable and that we argued (in sect. 4.4) that this is one of the cases where we can expect *a priori* strong radiative inhomogeneity effects.

[15]Indeed, we have $\cos\theta_{n+1} = \cos\theta_n\cos\theta - \sin\theta_n\sin\theta$ in d=2 and the only difference in d>2 is another (zero-average) azimuth factor in the second term, hence $E(\cos\theta_{n+1}) = E(\cos\theta_n)E(\cos\theta)$ in all cases.

[16]This leads us to conjecture that the Henyey-Greenstien phase functions (A.21a,b), considered as a 1-parameter class, are in fact closed under convolution in u-space with $g_{1*2}=g_1g_2$. This makes these p.d.f.'s the Ξ_d analogs of Γ-distributions on $\Re^+$ as well as of (centered) Gaussian, Cauchy (or otherwise symmetric Lévy-stable) distributions on $\Re$.

[17]Curiously, the formula even works for the non-random g=-1 case since only "1/2" of a single backward scattering is enough to get half way across Ξ_d!

[18]Interestingly, an apparently innocuous change, $t\to t/i$, transforms (D.24) into Schrödinger's equation for a free particle (m=0) or one in a region of constant potential energy (m≠0); this equation is however t-reversible, although not trivially: $J(\mathbf{x},t)$ is to be interpreted as the wave-function and probability density $|J|^2=J^*J$ is unaffected by the phase change that follows $t\to -t$. This constitutes another opto-mechanical "analogy-with-a-contrast" which at least explains the resemblance of the eigenvalue problems associated with scattering by square potential wells in quantum mechanics, on the one hand, and Davies' [1978] cuboidal cloud models in meteorology, on the other hand.

[19]This is the diffusion theory equivalent of the well-known close connection between absorptive responses and the orders-of-scattering decompositions of conservative responses in general transfer theory, not necessarily homogeneous plane-parallel.

[20]Mixed BCs are sometimes referred to as "radiative," not so much because of their association with the present albedo problem, but rather because of their appearance in heat conduction problems when the boundary is neither in contact with a heat bath ($\delta T(\mathbf{x})=$ const.) nor thermally insulated ($\mathbf{n}\cdot\mathbf{F}\propto \mathbf{n}\cdot\nabla\delta T=0$), but allowed to emit thermally into the environment ($\mathbf{n}\cdot\mathbf{F}=\varepsilon\sigma_B T^4 \approx (3\varepsilon\sigma_B T^3)\delta T$ where ε is emissivity and σ_B, the Stephan-Boltzmann constant).

[21]Apart from the diffusion length (when m≠0), the non-m.s. source term can be used to specify single-scattering as an internal source with homogeneous BCs ($F^-(\mathbf{x})=0$, $\mathbf{x}\in\partial M$) in (D.28) and this creates another length scale (namely, μ_0 in m.f.p. units), see Meador and Weaver [1980] for a detailed study of "two-flux" theory which is formally equivalent to diffusion in plane-parallel media, both with and without this boundary layer activated.

[22]This solution is more useful than its transfer counterpart since it is usually analytical and known everywhere in M. Numerical accuracy is of course a very major concern when dealing with nuclear reactor (or A-bomb) design.

[23]This scaling is characteristic of homogeneous media in general, as is the simple scaling w.r.t. time found in (D.26). It is however not trivial to relate the types of scaling two together in a general enough way to accommodate anomalously scaling RWs, e.g., with infinite variance Lévy-flights replacing the finite variance steps implicit in (D.26), cf. discussion in sect. 5.3.

[24]This is an "irrelevant" variable in the jargon of dynamical systems, "relevant" variables influence the exponent.

[25]Recall that in cgs-es units, those of conductance σ are length^2/time. In fact, $\sigma \sim v_{\text{thermal}} \times$ (carrier) m.f.p. in standard plasma theory; so, in a complete analogy, the velocity of light in vacuum is to be replaced by the thermal velocity of the charge carriers.

[26]This applies strictly to steady-state problems, otherwise we need a $\partial\rho/\partial t$ term (where ρ is the density of charge). This however does not imply that the radiative analog of ρ is $U=J/c$ as we would tend to conclude by direct comparison of charge conservation with eq. (D.1) for radiant energy conservation. The proper framework is of course Maxwell's complete set of equations and the diffusion-conductance analogy fails in general—electro-

magnetism is not entirely reducible to diffusion problems! Somewhat paradoxically, this does not stop us from determining (steady-state) bulk conductivities by solving time-dependent diffusion problems, as briefly described at the end of this chapter.

[27]It may seem paradoxical that a dissipation phenomenon such as bulk resistivity can be modelled within the framework of conservative multiple scattering processes. More precisely, there is a local production of heat ($\mathbf{j}\cdot\mathbf{E} = j^2/\sigma$, by Ohm's law) in conduction yet no local heating rate ($\nabla\cdot\mathbf{F} = 0$) in the corresponding radiation problem. The paradox disappears when we recall that, in conduction, charge is conserved ($\nabla\cdot\mathbf{j} = 0$) as are the photons whereas, in radiative transport, the is entropy (hence "heat") creation simply by the continuous conversion of collimated radiation into a diffuse radiation field ($\mathbf{F}\cdot\nabla J = dF^2$ is a direct measure of the system's steady-state entropy production since it is a straightforward measure of the "distance" from thermal equilibrium, hence maximal entropy, where J alone represents the radiation field.)

[28]Bunde *et al.* [1985] used the above interpretation of (D.38) to devise propagation rules for particles that "diffuse" exactly (on a grid).

[29]Illuminated boundaries are also "absorbing" but for diffuse radiation only which is of course precisely what contributes to "reflectance," according to the definition (A.29) based on the existence of a (proper) terminator.

[30]For instance in d=2, $p_c \approx 0.59277$ for site percolation on a rectangular grid whereas bond percolation is obtained at $p_c = 1/2$.

[31]The bulk properties of these systems fluctuate little from one realization to the next (see §2.3.4), so only mean quantities need to be considered in the following.

[32]Note that, in reality, it is not the (mass) density that becomes infinite but the m.f.p. of the charge carriers that vanishes in insulating material. In our radiative analogs, the scattering cross-sections become very large ($\kappa \rightarrow \infty$), the photon m.f.p.'s vanish but the "optical" mass diverges.

[33]This is a straightforward consequence of Jensen's inequality (3.31) when applied to the concave function log(x).

Bibliography for Appendix D

Alexander, S., and R. Orbach, "Density of states on fractals: fractons," *J. Phys. (Paris) Lett.*, 43, 625, 1982.

Bethe, H. A., and G. E. Brown, *Sci. Am.*, 252, p60, 1985.

Bunde, A., A. Coniglio, D. C. Hong, and H. E. Stanley, "Transport in a Two-Dimensional Randomly Composite Material: Scaling Theory and Computer Simulations of Termite Diffusion near Superconducting Limit," *J. Phys. A*, 18, L137–L144, 1985.

Cannon, C. J., "Line Transfer in Two Dimensions," *Astrophys. J.*, 161, 255–264, 1970.

Chapman, S., and T. G. Cowling, *The Mathematical Theory of Non-Uniform Gases*, 3rd ed., Cambridge, London, 1970.

Chu, M. C., and W. S. Churchill, "Numerical Solution of Problems in Multiple Scattering of Electromagnetic Radiation," *J. Chem. Phys.*, 59, 855–863, 1955.

Davies, R., "The effect of finite geometry on three-dimensional transfer of solar irradiance in clouds," *J. Atmos. Sci.*, 35, 1712–1724, 1978.

Davison, B., "Influence of a Black Sphere and of a Black Cylinder upon the Neutron Density in an Infinite Non-Capturing Medium," *Lond. Phys. Soc. Proc.*, 64, 881–902, 1951.

de Gennes, P. G., "Percolation: Quelques Systèmes Nouveaux," J. Phys. (Paris) Colloq., 41, C3–17, 1980.

Durouré, C., and B. Guillemet, "Analyse des Hététrogenéités Spatiales des Stratocumulus et Cumulus," *Atmos. Res.*, 25, 331–350, 1990.

Eddington, A. S., "On the radiative equilibrium of stars," *Mon. Not. Roy. Ast. Soc.*, 77, 16–35, 1916.

Gabriel, P., S. Lovejoy, D. Schertzer, and G. L. Austin, "Multifractal Analysis of Resolution Dependence in Satellite Imagery," *Geophys. Res. Lett.*, 15, 1373–1376, 1988.

Giovanelli, R. G., "Radiative Transfer in Non-Uniform Media," *Aust. J. Phys.*, 12, 164–170, 1959.

Hong, D. C., H. E. Stanley, A. Coniglio, and A. Bunde, "Random-Walk Approach to the Two-Component Random-Conductor Mixture: Perturbing Away from the Perfect Random Resistor and Random Superconducting Network Limits," *Phys. Rev. B*, 33, 4564–4573, 1986.

King, M D., "A Method for Determining the Single-Scattering Albedo of Clouds Through the Observation of the Internal Scattered Radiation Field," *J. Atmos. Sci.*, 38, 2031–2044, 1981.

King, M. D., L. F. Radke, and P. V. Hobbs, "Determination of the Spectral Absorption of Solar Radiation by Marine Stratocumulus Clouds from Airborne Measurements within Clouds," *J. Atmos. Sci.*, 47, 894–907, 1990.

King, W. D., C. T. Maher, and G. A. Hepburn, "Further performance tests on the CSIRO liquid water probe," *J. Atmos. Sci.*, 38, 195–200, 1981.

Levermore, C. D., and G. C. Pomraning, "A Flux-Limited Diffusion Theory," *Ap. J.*, 248, 321–334, 1981.

Lovejoy, S., and D. Schertzer, "Multifractals, Universality Classes and Satellite and Radar Measurements of Cloud and Rain Fields," *J. Geophys. Res.*, 95, 2021–2034, 1990.

Lovejoy, S., A. Davis, P. Gabriel, D. Schertzer, and G. L. Austin, "Discrete Angle Radiative Transfer - Part I: Scaling and Similarity, Universality and Diffusion," *J. Geophys. Res.*, 95, 11699-11715, 1990.

Malinowski, S., and I. Zawadski, "On the Surface of Clouds," preprint, 1992.

Meador, W. E., and W. R. Weaver, "Two-stream approximations to radiative transfer in planetary atmospheres: A unified description of existing methods an a new improvement," *J. Atmos. Sci.*, 37, 630–643, 1980.

Mihalas, D., *Stellar Atmospheres*, 2nd ed., pp. xvii+632, Freeman, San Francisco, CA, 1979.

Pandley, R. B., D. Stauffer, A. Margolina, and J.G. Zabolitzky, "Diffusion on random systems above, below and at their percolation threshold in two and three dimensions," *J. Stat. Phys.*, 34, 427–450, 1984.

Pomraning, G., *Radiation Hydrodynamics*, Pergamon, London, 1973.

Preisendorfer, R. W., *Hydrological Optics*, vol. 3, NOAA, PMEL, Hawaii, 1976.

Rammal, R., C. Tannous, P. Breton, and A.-M. S. Tremblay, "Flicker (1/f) Noise in Percolation Networks: A New Hierarchy of Exponents," *Phys. Rev. Lett.*, 54, 1718–1721, 1985.

Renshaw, E., and R. Henderson, "The Correlated Random Walk," *J. Appl. Probab.*, 15, 403–414, 1981.

Stauffer, D., *Introduction to Percolation Theory*, Taylor & Francis, London, 1985.

Straley, J. P., *Phys. Rev. B*, 17, 5733, 1977.

Tessier, Y., S. Lovejoy, and D. Schertzer, "Universal Multifractals: Theory and Observations for Rain and Clouds," submitted to *J. Appl. Meteo.*, 1992.

Unno, W., and E. A. Spiegel, *Pub. A. S. Japan*, 18, p85, 1966.

van de Hulst, H. C., and K. Grossman, "Multiple Light Scattering in Planetary Atmospheres," in *The Atmospheres of Venus and Mars*, ed. J.C. Brandt and M.B. McElroy, pp. 35–55, Gordon and Breach, New York, NY, 1968.

Wilson, P. R., "On the Three-Dimensional Form of the Eddington Approximation," *Ap. J.*, 151, 1019–1028, 1968.

Wiscombe, W. J., R. M. Welch, and W. D. Hall, "The Effects of Very Large Drops on Cloud Absorption, Part 1: Parcel Models." *J. Atmos. Sci.*, 41, 1336-1355, 1984.

Zachmanoglou, E. C., and D. W. Thoe, *Introduction to Partial Differential Equations with Applications*, Williams and Wilkins, Baltimore (MD), 1976. (Reprinted by Dover, New York (NY), 1986.)

Appendix E

THE STATISTICAL APPROACH TO RADIATIVE TRANSFER

Preliminary remarks: It is important to realize that the status of radiative transfer within the edifice of theoretical physics is unclear, to say the least. From Schwartzchild's [1914] pioneering of radiative transfer in continuous angles to Chandrasekhar's [1950] treatise and well beyond, the radiative transfer equation is derived from purely phenomenological considerations of radiant energy (flux) conservation. Attempts to improve this situation, to derive the transfer equation from first principles, have met only partial success.[1] A troublesome consequence of this lack of grounding in mainstream optics is that we know rather little *a priori* about the conditions of validity of transfer theory, although nobody doubts they are generally met as soon as we deal with macroscopic quantities of natural (incoherent) light. The main difficulty lies in the fact that in rigorous EM theory, in both classical or quantum (QED) guises, as well as in scalar wave theory, one views propagation and scattering in a unified[2] way whereas in radiative transfer the two phenomena are clearly separated. This can be traced by "coarse-graining" the spatio-temporal features of the wave field: at the scales of interest to us, light can be described by geometrically defined beams (hence several wavelengths wide) with a constant flux (hence very incoherent phase mixtures must be present and/or we are considering time scales of many pulsation periods).

Fortunately, there is an alternative route from the micro- to the macrophysics of radiation in interaction with bulk matter that borrows heavily from kinetic theory. The approach we are about to embark on lacks consistency in several places that we will point out but it has the advantage of putting the numerous analogies between radiative- and mass-, charge-, etc.- transport problems on a more solid footing. If used carefully, mechanical/radiative parallels can be quite helpful and we will draw on them in chap. 2. (Some of our findings may thus be reflected back to these other transport phenomena although their respective specialists will have to look into that.) Interestingly, this approach starts with a probabilistic characterization of flows in phase space, and this is precisely where one of the earliest and still one of the more common applications of multifractal formalism is found: quantifying the "strangeness" of the "attractor." It was more-or-less simultaneously realized that multifractal concepts had in fact been used in connection with cascade models of (intermittancy in) fully developed turbulence [see references in app. C]. Moreover, there is a recent trend in the literature to apply multifractal analysis techniques directly to the Earth's radiation fields themselves [more references in app. C], and these are of course precisely what radiative transfer theory is all about in the first place. We will therefore invest in this inter-connectedness of all things (important to us) and introduce, within a familiar radiative transfer context, some less familiar but very useful mathematical, mainly probabilistic, concepts. In the process, we partially fulfill Preisendorfer's [1965] program according to which modern integration- and measure theory should be used to clarify the foundations of radiation transport theory.

E.1. Phase Space Flows and Boltzmann's Equation

Consider a gas of N point-like material particles in d-dimensional space $\Re^d$ ($\Re$ denotes the set of all real numbers) which can be be described within the framework of classical Hamiltonian mechanics, i.e., by their positions $\mathbf{x}_i(t)$ and momenta $\mathbf{p}_i(t)$ ($i=1,\cdots,N$ and $t\in\Re$). Now recall Liouville's theorem which states that the flow in phase space is incompressible:

$$(\nabla_\mathbf{x},\nabla_\mathbf{p})\cdot(\dot{\mathbf{x}},\dot{\mathbf{p}}) = \nabla_\mathbf{x}\cdot\dot{\mathbf{x}} + \nabla_\mathbf{p}\cdot\dot{\mathbf{p}} = \frac{\partial}{\partial \mathbf{x}}\left(\frac{\partial H}{\partial \mathbf{p}}\right) + \frac{\partial}{\partial \mathbf{p}}\left(-\frac{\partial H}{\partial \mathbf{x}}\right) = 0 \tag{E.0}$$

A (non-trivial) corollary of Liouville's theorem is Poincaré's: a conservative Hamiltonian system will eventually return arbitrarily close to its initial state—mainly because the motion is confined to a surface of constant energy in the N-body phase space $[\Re^d\otimes\Re^d]^N$ (see, e.g., Zaslavsky [1985]). This will happen in spite of the almost invariably strong (exponential) divergence of trajectories starting from arbitrarily close states, the so-called "sensitivity to initial conditions." No matter how complicated—we now say "chaotic"—the phase space orbit is (recall the possibility of many-body interactions), no information is intrinsically lost, no entropy is produced.

We now define a sub-set (S) more or less centered around a point $(\mathbf{x},\mathbf{p})$ of the 1-body (2d-dimensional) phase space. For instance, this "neighborhood" could be $[\mathbf{x},\mathbf{x}+\Delta\mathbf{x}[\otimes[\mathbf{p},\mathbf{p}+\Delta\mathbf{p}[$ or else $B_d(\mathbf{x},\Delta x)\otimes B_d(\mathbf{p},\Delta p)$ where $B_d(\mathbf{x}_0,r)=\{\mathbf{x}\in\Re^d, |\mathbf{x}-\mathbf{x}_0|<r\}$ is the d-sphere of radius r, centered on $\mathbf{x}_0$. Given such a sub-set S, we find $N_S(t)=\iint\Sigma_i\delta(\mathbf{x}-\mathbf{x}_i(t))\delta(\mathbf{p}-\mathbf{p}_i(t))1_S(\mathbf{x},\mathbf{p})d^d\mathbf{x}d^d\mathbf{p}$ of the N particles in it, at a given time t. In this expression, we recognize Dirac's familiar (generalized) δ-function and the "indicator" function of the set S:

$$1_S(\mathbf{x},\mathbf{p}) = \begin{cases} 1 \text{ if } (\mathbf{x},\mathbf{p})\in S \\ 0 \text{ otherwise.} \end{cases} \tag{E.1}$$

It can be used, in particular, to define the (Lebesgue-)integral over the given (Lebesgue-)measurable set S, i.e.,

$$\iint_S (\cdot)\, d^d x d^d p = \iint (\cdot)\, 1_S(x,p)\, d^d x d^d p \qquad \text{(E.2)}$$

For instance, the d-volume (Lebesgue measure) of the set S is $vol(S)=\iint 1_S(x,p) d^d x d^d p$. We will breifly discuss other measures in app. C.

An independent discussion of Lebesgue's (L-)integral is in order to remove some of the circularity in the above definitions. The main difference between Lebesgue's and the more familiar Riemann (R-)integral is that the latter is defined as the limit of an ever finer decimation along the axis (axii) of the independent variable(s) where the function is readily sampled whereas the former proceeds along the axis of the dependent variable. The L-integral was cunningly devised to have the following enormous advantage over Riemann's: the operations of taking limits of (stepwise constant) functions and L-integration commute whereas there is no guarantee that a limit of R-integrals will converge towards the R-integral of the limit. Its practical evaluation requires however the knowledge of how often a given functional value occurs within the set where its arguments take their values, the "support" of the function but this apparent disadvantage in fact makes L-integration the perfect tool for probability theory on which we will be drawing extensively. For instance, one could view $\Sigma_{i=1}^{i=N} \delta(\mathbf{x}-\mathbf{x}_i(t))\delta(\mathbf{p}-\mathbf{p}_i(t))/N$ as the properly normalized (instantaneous) probability density function for the whereabouts of any one of our particles. For more rigorous axiomatics and proofs, the reader is referred to one of the many available mathemetical reference texts although only intuitively understandable results will be used in the following.

A direct consequence of Liouville's theorem is that the phase space particle density function

$$f(\mathbf{x},\mathbf{p},t) = \lim_{\substack{vol(S)\to 0 \\ N\to\infty}} \frac{N_S(t)}{vol(S)} \qquad \text{(E.3)}$$

remains constant along any past or future trajectory of the system since any given set (S) that encloses the corresponding number (N_S) of particles at t=0 has constant volume as it moves (*à la* Lagrange) through phase space. Therefore, the continuity equation for the current density driven by the dynamics of the system, i.e.,

$$\partial f/\partial t+(\nabla_{\mathbf{x}},\nabla_{\mathbf{p}})\cdot[(\dot{\mathbf{x}},\dot{\mathbf{p}})f] = 0, \qquad \text{(E.4)}$$

reduces to (Vlasov's equation), $Df/Dt = 0$, where D/Dt denotes the total (Lagrangian, or convective) derivative $\partial/\partial t + \dot{\mathbf{x}}\cdot\nabla_{\mathbf{x}} + \dot{\mathbf{p}}\cdot\nabla_{\mathbf{p}}$. Recalling that in N-body phase space the system is represented by a single point, we see from definition (E.3), without $N\to\infty$, that the corresponding density function $f(\mathbf{x}_1,\cdots,\mathbf{x}_N, \mathbf{p}_1,\cdots,\mathbf{p}_N, t)$ is, and remains, a δ-function.

In practice (macroscopic measurement devices are used in systems with large but finite N), all we can hope to access is a coarse-grained (small but finite S) version of the usual (1-body) phase space in (E.3) which is an incomplete description of the system and the amount of (Shannon's) information it contains will fluctuate before returning to its initial level, after one Poincaré cycle which is however a strongly increasing function of N. Moreover, when N»1, we proceed—still on heuristic grounds—to separate the motion of our N particles into one under an external force field (no interaction terms in the Hamiltonian) plus (2-body) collisions; the latter act as a source/sink term that balances exactly (locally) any non-continuity in the (Hamiltonian) evolution of the phase space density function, hence (Boltzmann's equation) :

$$\left[\frac{\partial}{\partial t} + \dot{\mathbf{x}}\cdot\nabla_{\mathbf{x}} + \dot{\mathbf{p}}\cdot\nabla_{\mathbf{p}}\right] f(\mathbf{x},\mathbf{p},t) = \frac{Df}{Dt}\Big|_{\text{collisions}} \tag{E.5}$$

which in general is a fierce nonlinear integro-differential equation since typical collision terms are quadratic in f and involve convolution-type integrals in **p**-space. In this case, we systematically loose whatever information we had in the initial coarse-grained density function: on average, collisions can only broaden f(**x**,**p**,t) by taking the particles into the more remote regions of phase space accessible to the them.

E.2. Linear Transport Theory 1, The Case of Neutrons

The problem of transport in presence of collisions simplifies considerably as soon as the particles are decoupled from the external force field ($\dot{\mathbf{p}}$=0) and, even more importantly, they do not interact together, only with some ambient material via bulk collisional cross-sections which can depend on t, **x** and **p** but not on the values of f (whether local or not). This guarantees the linearity of the collision term, hence of the whole equation, with respect to f. Such is the case for neutrons penetrating some (moderating or multiplying) medium. The most general "1-body" (linear) collision term can be expressed as

$$\frac{Df}{Dt}\Big|_{col}(\mathbf{x},\mathbf{p},t) = \int K(\mathbf{x},t;\, \mathbf{p}'\to\mathbf{p})\, f(\mathbf{x},\mathbf{p}',t)\, d^d\mathbf{p}' \tag{E.6}$$

where K is the scattering kernel. $K(\mathbf{x},t;\,\mathbf{p}'\to\mathbf{p})d^d\mathbf{p}'d^d\mathbf{p}$ is the probability that a particle (which happens to be in position **x** at time t) will suffer a collision (within the next unit of time) that takes its momentum from **p**' to **p**, to within $d^d\mathbf{p}'$ and $d^d\mathbf{p}$ respectively.

By now the phase space trajectories ($\mathbf{x}_i(t),\mathbf{p}_i(t)$) of our individual ($i=1,\cdots,N$) particles have become highly convoluted random walks (RWs) each of which are different realizations of a Markovian stochastic process in time; the Markov property expresses the fact that the particle's future is (statistically) determined by it present state $(\mathbf{x},\mathbf{p})_t$, it has no "memory" of its past history. From now on, the system's only well-defined (deterministic) properties are probability distributions—such as f itself—and average quantities that depend on these.

Within this framework, eqs. (E.5–6) are equivalent[3] to the Chapman-Kolmogorov equations of the system. Furthermore, it is a "homogeneous" Markov process if K is independent of t, irrespective of its **x**-dependence. (In chap. 4 and app. C, we will discuss spatial generalizations of Markov- and other stochastic processes as methods for generating random optical media.) Notice that a direct consequence of the irreversibility acquired from the collision term is that the largest support for f(x,p,t) is now effectively $\Re^d \otimes \Re^d \otimes \Re^+$, no physically meaningful predictions can be made about negative times when the density function is entirely specified at t=0.

Now turning to neutrons in d=3 (neutron-like particles otherwise), let us suppose they suffer collisions that are not necessarily elastic, i.e. there is a possibility of absorption or multiplication, but we assume the kinetic energy of all the neutrons (old and new) to be the same, i.e., there is only one velocity "group" (and we let v=p/m). If we further assume the scattering to be isotropic, then the kernel in (E.6) becomes

$$K(\mathbf{v}'\to\mathbf{v}) = v\sigma_t\rho \left[\frac{\varpi_0}{s_d(v)} 1_{S_d(v)}(\mathbf{v}') - \delta(\mathbf{v}'-\mathbf{v}) \right] \qquad \text{(E.7)}$$

where σ_t is the total (scattering, absorption or multiplication) d-dimensional cross-section per particle in the medium, ρ being their (d-)density. This makes $\sigma_t\rho$ the (bulk) cross-section per unit of d-volume, which has units of 1/length, hence $v\sigma_t\rho$ is the event probability per unit of time and per neutron. The second term on the r.h.s. of (E.7) describes the depletion of neutrons from the "**v**-beam" by any of the above-mentioned elementary processes whereas the first term describes the (isotropic) creation of **v**-neutrons with ϖ_0 designating the "single-scattering albedo." This is a measure of the relative probability of absorption ($1-\varpi_0$, when >0) or multiplication ($1-1/\varpi_0$, when >0). For $\varpi_0=1$, we find the important case of elastic scattering. In principle, all of these parameters could be functions of t and **x**. We have also used the d-surface of a hypersphere of radius r: $s_d(r) = \mathrm{surf}[S_d(r)] = n_d\, r^{d-1}$ where $n_d = 2\pi^{d/2}/\Gamma(d/2)$. In the present case, the sphere is centered on the origin: $S_d(r)=\{\mathbf{x}\in\Re^d, |\mathbf{x}|=r\}=\partial B_d(0,r)$ which is of course a (d-1)-dimensional manifold being the boundary (∂) of a d-domain. In the expression for n_d, $\Gamma(\cdot)$ is Euler's gamma function whereas the prefactors in front of r^{d-1} are defined as $n_d=s_d(1)$, the d-surface—(d-1)-volume—of the unit sphere $\Xi_d=S_d(1)$ and worth 2 (points), 2π (radians), 4π (steradians), respectively in d = 1, 2, 3.

Given that the ∇_p-term has already vanished from the l.h.s. of (E.5), by lack of coupling of the neutrons with external force fields, the above example provides justification for a simplification in notation rarely exploited in the literature. Since the collision term on the r.h.s. of eq. (E.5) can only couple the various directions of motion, we are justified in viewing $f(\mathbf{x},\mathbf{v},t)=f(\mathbf{x},\mathbf{p},t)/m^d$ as an infinite dimensional vector field $\{f_{\mathbf{v}}, \mathbf{v}\in S_d(v)\}$ defined on $\Re^d\otimes\Re^+$ rather than a scalar field defined on the (infinitely) vaster support

$\Re^d \otimes S_d(v) \otimes \Re^+$. Notice that the units of f_v are now particles per unit of d-volume (in ordinary space) and per unit of d-surface (in velocity space). A further justification of this departure from traditional notation becomes obvious as we realize that the fundamental nature of RWs in the $\Re^d$ and $S_d(v)$ components of the mono-kinetic neutron's phase space is likely to be very different, given their radically different topologies, sizes and geometries : open, infinite and Euclidian versus closed (and disjoint if d=1), finite and cyclical (even Riemannian for d>2). It is not too surprising then that the spatial and angular aspects of transfer will take on entirely different importances in our final analysis, especially since the effects of inhomogeneity, on which we focus primarily, necessarily hinge on the spatial part. From this vantage point, we can already anticipate the very special role played by d=1 which is perfectly representative of plane-parallel geometry in d>1.[4]

E.3. Linear Transport Theory 2, Generalization to Photons

Viewing photons as point-like Hamiltonian particles is totally inconsistent with the teachings of special relativity and second quantization. Nevertheless, photons do not couple with external force fields[5] nor do they interact with each other.[6] We are therefore tempted to treat them kinetically as we do neutrons; moreover, relativity's fundamental postulate of constancy of c, the velocity of light in vacuum, tells us that the photon gas is mono-kinetic (but of course not mono-energetic). In a frame of reference where their frequency is ν and where they propagate in direction $\mathbf{u}$ ($|\mathbf{u}|=1$), their momentum is given by $\mathbf{p}=(h\nu/c)\mathbf{u}$ where h is Planck's constant. An acceptable notation for the (number) density of photons is therefore $f_{\mathbf{p}}(\mathbf{x},t)=(h/c)^3 f_{\nu,\mathbf{u}}(\mathbf{x},t)$.

In the case of photons at least, we can make the distinction between the $\mathbf{p}$-argument and $\mathbf{p}$-subscript notations less academic by anticipating that, on the one hand, the space-time coordinates and, on the other hand, the state variables of the EM-wave or photon will always be well separated within the ideal—but not yet formulated—radiative kinetic theory based on EM- or quantum field theory, both being intrinsically 3-D. In contrast, the strong $\mathbf{x}$-$\mathbf{p}$ connection in the adopted derivation is a by-product[7] of our non-rigorous analogy with Hamiltonian mechanics. A complete set of state variables inherited from EM theory could be $\omega=2\pi\nu$, $\mathbf{k}$ (wavenumber, $k=\omega/c$) and two scalars—usually (phase) angles—to define the wave's state of polarization (e.g., in r.h.-l.h. circular decomposition[8]); whereas, in a QED (second quantization) approach, we are more likely to use $E=\hbar\omega$, $\mathbf{p}=\hbar\mathbf{k}$ ($\hbar=h/2\pi$) and two scalars to define the state of spin $\mathbf{s}$ of the photon, namely, $s=\hbar$ and $\mathbf{s}\cdot\mathbf{k}=\pm\hbar$ (0 is not an option since the spin must be is longitudinal for a massless particle). Notice that the first scalar and the 3-vector are the Fourier- (resp., Hamiltonian-) conjugates of t and $\mathbf{x}$, this gives radiation transport theory a rather peculiar status amongst physical theories, having independent variables in both physical- and Fourier space. These sets of variables are however of a quite different nature: the Fourier variables retain their original (EM- or quantum-) meanings whereas we recall that the physical space variable has been "coarse-grained"—we therefore talk about "macroscopic" radiation fields—and, on occasions, these too will be the object of Fourier transformation [e.g., Stephens, 1986]. As usual in such non-equilibrium thermodynamical theories, time plays a special role.

In "coherent" radiative transfer, it is assumed that the scattering processes redistributes the photons in direction space (Ξ_d), leaving their frequency unchanged. (This is in fact only an approximation w.r.t. energy-momentum conservation[9] that is valid in the limit of infinitely massive scattering centers.) In particular, this framework does not allow the consideration of sharp spectral features, such as atomic or molecular resonance lines, in moving media where Doppler- and aberration effects introduce ν,**u**-dependencies in the (bulk) cross-sections related to the macroscopic velocity fields; otherwise, we must also consider RWs in ν-space as well. In short, the only parameter in the photon's expression for momentum $(h\nu/c)\mathbf{u}$ that can change in a scattering event is the direction of propagation $\mathbf{u}\in\Xi_d$ so we can now denote the density of photons $f_\mathbf{u}(\mathbf{x},t)$ which has units of particles per d-volume per d-angle. All that is lacking now is a link between $f_\mathbf{u}(\mathbf{x},t)$ and the standard descriptor of the radiation field, namely "radiance" or "specific intensity" that we will denote $I_\mathbf{u}(\mathbf{x},t)$ and will designate by either name since both are widely used, sometimes abusively omitting the "specific." (Many others exist, each in a specific field of application, e.g., in the biomedical literature, one talks about "fluence.") $I_\mathbf{u}$ is defined (in the familiar d=3) as the amount of radiant energy crossing a unit of area (projected) perpendicular to **u** (around **x**) within a unit of solid angle (around **u**) and a unit of time (around t). Comparing with definition (E.3) of $f_\mathbf{u}$, we find $I_\mathbf{u}=h\nu c f_\mathbf{u}$. Multiplying (E.5) by $h\nu$, we find, the radiative transfer equation:

$$\left[\frac{1}{c}\frac{\partial}{\partial t}+\mathbf{u}\cdot\nabla\right] I_\mathbf{u} = -\kappa\rho\,[\,I_\mathbf{u} - S_\mathbf{u}\,] \tag{E.8}$$

where the r.h.s. (Boltzmann collision term) has been recast as a general source/sink term. The first term is the amount of radiant energy lost by the **u**-beam in an infinitesimal volume and it is proportional to the intensity $I_\mathbf{u}$ of the beam (due to linearity), to the local density ρ of scattering and/or absorbing material, and to cross-sections that determine κ. $\kappa\rho S_\mathbf{u}$ is a general purpose source term which will be given in app. A for multiple scattering, single scattering and thermal emission.

[1] It is not too difficult to establish close analogies between the mean field equations for wave propagation in random media and the multiple scattering transfer equation but only within the small angle approximation [e.g., Ishimaru, 1978], the general case is much more involved. Within the framework of scalar wave theory, Ishimaru [1975] builds on earlier results [e.g., Barabanenkov, 1969] and obtains a formal correspondence between radiance and the directional auto-correlation function of the wave field. Independently, Wolf [1976] is able to define radiance rigorously in both classical- and quantum EM theoretical terms but only in vacuum (where it is conserved). Starting with Maxwell's equations, Harris [1965] had already obtained the streaming and extinction terms of the transfer equation (but no scattering sources). The common characteristic of all of these approaches is the need for a spatial average of the wave quantity over some domain (this is known as "coarse-graining"); this physical size of this domain will depend on the density of the medium and, at any rate, this defines the smallest scale that radiative transfer has anything meaningful to say about, even in theory.

[2] For instance, in the classical picture, the scattering pattern (phase function) is shaped by interference in the far field hence propagation delay from the various parts of the object ; in the quantum picture, scattering results from the perturbation of the (electronic) state of the object by the passage (propagation) of the (quantized) EM wave.

[3] The exact analogs of the Chapman-Kolmogorov equations would be the integral equations that are equivalent to (E.5–6) plus BCs. Things would be quite different if we were dealing with N-body interactions: the Chapman-Kolmogorov equations could be related to the N-body "master equations" which are formulated in N-body phase space (or "Γ-space") whereas the Boltzmann formulation is fundamentally linked to 1-body phase space (or "μ-space").

[4] $d=2$ is also special but to a much lesser extent : several instances of "$d=2$" versus "$d>2$" dichotomies will appear in the following ; in particular, the diffusion equation resolvant (Green's function) has a logarithmic, rather than algebraic, decay in $d=2$. This, in turn, is not unrelated to the fact that the standard (uncorrelated, finite variance) RW has fractal dimension $D=2$.

[5] Indeed in the QED picture, (virtual) photons "are" the EM force field. In general-relativistic environments, photons follow null geodetics but an inertial frame observer can interpret this motion (change in energy-momentum) as a "gravitational" deflection and/or Doppler shift.

[6] Excluding purely formal diagrammatic interactions in QED, photon-photon scattering is expected to happen only at GUTs energies.

[7] This can be seen as a typical drawback in such opto-mechanical parallels (of which we will see many in the thesis), the corresponding advantage being the natural generalization to any number of dimensions (and that we will be keen to exploit, capitalizing on the conceptual and computational simplifications).

[8] Along with the two corresponding amplitudes, we can readily construct the four "Stoke's parameters," cf. Chandrasekhar [1950].

[9] A previously stationary scatterer must recoil to some extent and, doing so, carries some of the photon's energy away which, in turn, implies a change in (lab) frequency. This direct mechanical effect of the radiation field sustains (and maybe accelerates) the violent stellar winds of the hotter stars. We can generally neglect them here since, typically, we are dealing with a solar (μm-wavelength) photon impinging on a (μm-sized) cloud droplet ; we are therefore comparing an eV or so with the energy equivalent of a small but macroscopic object, so laser beam type fluxes are needed to balance the difference. Interestingly, planetary winds are also radiatively driven but via a very different mechanism, namely, absorption (hence heating) somewhere in the surface-atmospheric system.

Bibliography for Appendix E

Barabanenkov, Y. N., "On the Spectral Theory of Radiation Transport Equations," *Sov. Phys. JETP*, 29, 679–684, 1969.

Chandrasekhar, S., *Radiative Transfer*, Oxford University Press, 1950. (Reprinted by Dover, New York, NY, 1960.)

Harris, E. G., "Radiative Transfer in Dispersive Media," *Phys. Rev. B*, 138, 479–485, 1965.

Ishimaru, A., *Wave Propagation and Scattering in Random Media*, vol. II, Academic, New York, NY, 1978.

Ishimaru, A., "Correlations Functions of a Wave in a Random Distribution of Stationary and Moving Scatterers," *Radio Science*, 10, 45–52, 1975.

Preisendorfer, R. W., *Radiative Transfer on Discrete Spaces*, Pergamon, London, 1965.

Schwartzchild, K., "Diffusion and Absoption in the Sun's Atmosphere," *Sitzungsberichte der Köninglichen Preussichen Akademie der Wissenschaften*, pp1183–1200, 1914. (Reprinted in *Selected Papers on the Transfer of Radiation*, Ed. D.H. Menzel, Dover, New York, NY, 1966.)

Stephens, G. L., "Radiative Transfer in Spatially Heterogeneous, Two-Dimensional Anisotropically Scattering Media," *J. Quant. Spectrosc. Radiat. Transfer*, 36, 51–67, 1986.

Wolf, E., "New Theory of Radiative Energy Transfer in Free Electromagnetic Fields," *Phys. Rev. D*, 13, 869–886, 1976.

Zaslavsky, G. M., *Chaos in Dynamic Systems*, Harwood, London, 1985.